frontiers

RESEARCH TOPICS

VISUAL PERCEPTION AND VISUAL COGNITION IN HEALTHY AND PATHOLOGICAL AGEING

Topic Editors
Mark W. Greenlee and Allison B. Sekuler

frontiers in PSYCHOLOGY

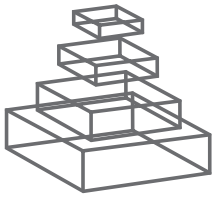

frontiers

ISSN 1664-8714
ISBN 978-2-88919-253-3
DOI 10.3389/978-2-88919-253-3

ABOUT FRONTIERS

Frontiers is more than just an open-access publisher of scholarly articles: it is a pioneering approach to the world of academia, radically improving the way scholarly research is managed. The grand vision of Frontiers is a world where all people have an equal opportunity to seek, share and generate knowledge. Frontiers provides immediate and permanent online open access to all its publications, but this alone is not enough to realize our grand goals.

FRONTIERS JOURNAL SERIES

The Frontiers Journal Series is a multi-tier and interdisciplinary set of open-access, online journals, promising a paradigm shift from the current review, selection and dissemination processes in academic publishing.
All Frontiers journals are driven by researchers for researchers; therefore, they constitute a service to the scholarly community. At the same time, the Frontiers Journal Series operates on a revolutionary invention, the tiered publishing system, initially addressing specific communities of scholars, and gradually climbing up to broader public understanding, thus serving the interests of the lay society, too.

DEDICATION TO QUALITY

Each Frontiers article is a landmark of the highest quality, thanks to genuinely collaborative interactions between authors and review editors, who include some of the world's best academicians. Research must be certified by peers before entering a stream of knowledge that may eventually reach the public - and shape society; therefore, Frontiers only applies the most rigorous and unbiased reviews.
Frontiers revolutionizes research publishing by freely delivering the most outstanding research, evaluated with no bias from both the academic and social point of view.
By applying the most advanced information technologies, Frontiers is catapulting scholarly publishing into a new generation.

WHAT ARE FRONTIERS RESEARCH TOPICS?

Frontiers Research Topics are very popular trademarks of the Frontiers Journals Series: they are collections of at least ten articles, all centered on a particular subject. With their unique mix of varied contributions from Original Research to Review Articles, Frontiers Research Topics unify the most influential researchers, the latest key findings and historical advances in a hot research area!
Find out more on how to host your own Frontiers Research Topic or contribute to one as an author by contacting the Frontiers Editorial Office: researchtopics@frontiersin.org

VISUAL PERCEPTION AND VISUAL COGNITION IN HEALTHY AND PATHOLOGICAL AGEING

Topic Editors:
Mark W. Greenlee, University of Regensburg, Germany
Allison B. Sekuler, McMaster University, Canada

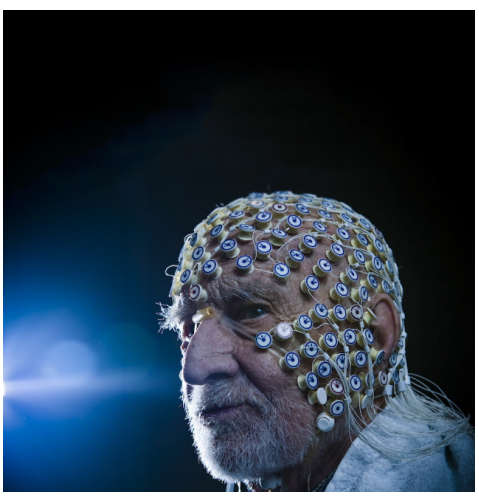

A senior participant in the Vision and Cognitive Neuroscience Lab at McMaster University. Photo credit: JD Howell. Permission for use given by Allison Sekuler.

Our understanding of visual perception and visual cognition has advanced considerably over the last decades. The effects of ageing on visual perception and visual cognition are less well understood. This Research Topic features state-of-the-art approaches to determining the effects of ageing on visual perception, visual attention, visual memory and visually guided behaviour. Studies using methods that incorporate psychophysics, eye movements, electrophysiology, structural and functional neuroimaging, as well as computational modelling are included. In addition to the focus on how ageing effects normal vision, the topic also includes studies on the effects of pathological ageing in the retina (e.g., age-related macular degeneration) and the brain (e.g., neurodegenerative disorders) on vision and visual cognition.

Table of Contents

frontiers in PSYCHOLOGY

EDITORIAL
published: 06 May 2014
doi: 10.3389/fpsyg.2014.00348

Visual perception and visual cognition in healthy and pathological ageing

Mark W. Greenlee[1]* and Allison B. Sekuler[2]

[1] *Institute for Experimental Psychology, University of Regensburg, Regensburg, Germany*
[2] *Department of Psychology, McMaster University, Hamilton, ON, Canada*
**Correspondence: mark.greenlee@psychologie.uni-regensburg.de*

Edited and reviewed by:
Philippe G. Schyns, University of Glasgow, UK

Keywords: ageing, vision, visual cognition, central scotoma, age-related macular degeneration, Alzheimer's disease, mild cognitive impairment, functional MRI

This volume features state-of-the-art approaches to determining the effects of ageing on visual perception, visual cognition, and visually guided behavior. They incorporate psychophysics, eye movements, electrophysiology, and neuroimaging to determine how ageing affects vision in health and pathology.

Brockmole and Logie (2013) present behavioral findings on the visual working memory (VWM) abilities of over 55,000 individuals, aged 8 and 75 years, who were studied on-line to provide an analysis of age-related change in VWM. The results showed that VWM varies over the lifespan, peaking at age 20, to be followed by a sharp linear decline. By the age 55 years, adults possess poorer immediate visual memory than 8 and 9 year olds. Allard et al. (2013) present their work on age-related deficits on second-order motion processing at all temporal frequencies including the ones for which no age-related effect on first-order motion processing has so far been observed. They conclude that aging affects the ability to track moving features. Van der Stigchel et al. (2013) tested four macular degeneration (MD) patients in a visual search paradigm and contrasted their performance with that of healthy controls with and without a simulated scotoma. Saccadic search latencies for the MD group were significantly longer in both conditions compared to controls. Legault et al. (2013) report the results of a study on the capacity of older participants to improve their tracking-speed thresholds in a dynamic, virtual reality environment. Their results show that this capacity is significantly affected by healthy aging but that perceptual-cognitive training can significantly reduce age-related effects in older individuals. Bower et al. (2013) show how perceptual learning can improve motion discrimination for older, compared to younger, individuals under high- and low-contrast conditions. Both older and younger subjects exhibited lower duration thresholds after training. Graham et al. (2013) focus on patients with early Alzheimer's dementia with respect to the temporal stability of their aesthetic judgments of paintings. They find that the stability of aesthetic judgments for portrait paintings, landscape paintings, and landscape photographs is not different from those of controls, whereas the aesthetic stability for portrait photographs was significantly impaired in the AD group. Hamel et al. (2013) use a driving simulator paradigm with eye- and head-movement recordings in young and old subjects to assess age-related changes in visual exploratory behavior. No significant age effects were found regarding saccadic parameters. In the older subjects head movements increasingly contributed to gaze amplitude. Interestingly, video game-experienced subjects revealed larger saccade amplitudes and a broader distribution of fixations. They conclude that it is essential to consider video game experience in all testing methods using virtual media.

Hutchison et al. (2013) investigated the origin of age-related differences in the BOLD signal by comparing its blood flow and oxygen metabolic constituents. Using MR dual-echo arterial spin labeling and CO_2 ingestion, they observed age-equivalent fractional cerebral blood flow (ΔCBF) in the presence of age-related increases in fractional cerebral metabolic rate of oxygen ($\Delta CMRO_2$). Reductions in ΔCBF responsiveness to increased $\Delta CMRO_2$ in elderly participants led to paradoxical age-related BOLD decreases. Age-related $\Delta CBF/\Delta CMRO_2$ ratio decreases were associated with increases in behavioral reaction times, suggesting that age-related slowing resulted from less efficient neural activity. Alichniewicz et al. (2013) used functional magnetic resonance imaging (fMRI) to reveal the neural correlates of saccadic inhibition in young participants, in elderly participants and in patients with amnestic mild cognitive impairment (aMCI). The results indicate decreased activation in parietal lobe in healthy elderly persons compared to young persons and decreased activation in frontal eye fields in aMCI patients compared to healthy elderly persons during the execution of anti-saccades. The study by Rosengarth et al. (2013) examined the effects of oculomotor training on the fMRI response in patients with AMD. During a 6-month eccentric-fixation training period the AMD subjects and the control group took part in three functional and structural magnetic resonance imaging sessions. Oculomotor training improved fixation stability, visual acuity and reading speed. Positive correlations were evident between brain activation changes and improvements in fixation stability in the visual cortex during training. Brewer and Barton (2014) present fMRI results on visual field map (VFM) organization and population receptive fields (pRFs) between young adults and healthy aging subjects for occipital VFMs in early visual areas. Healthy aging subjects do not show major VFM organizational deficits, but do have reduced surface area and increased pRF sizes in the foveal representations of V1, V2, and hV4 relative to healthy, young controls, consistent with behavioral deficits seen in healthy aging. Results from two patients with mild Alzheimer's dementia (AD) are presented, which reveal potential changes in visual cortex.

Bieniek et al. (2013) investigated the effects of aging, luminance and individual differences on early event-related potential (ERP) components in healthy participants (aged 18–79). In two experiments they recorded EEG while participants viewed faces or noise textures at different luminance levels. They found a 1 ms per year slowdown in visual processing that was independent of luminance. Their results suggest that early ERPs to faces are delayed by aging and that these delays are of cortical, rather than optical origin. Roudaia et al. (2013a)varied contour and distracter inter-element spacing, collinearity, and stimulus duration in multiple Gabor displays. Their findings indicate that contour discrimination accuracy was lower in older subjects, but the effect of aging did not vary with contour spacing or orientation jitter. Stimulus duration had a greater effect on older subjects' performance, but only for less salient contours. Roudaia et al. (2013b) studied age-related changes in the integration of multiple inter- and intra-modal cues in the perception of moving objects that are either perceived to collide or bounce off each other. The findings indicate that a sharp sound coincident with the disks' overlap increased both groups' perception of bouncing, but did so significantly less for older subjects. The results point to a weakened inter- and intra-modal integration with aging.

It is our hope that these studies contribute to a better understanding of the effects of ageing on visual perception and visual cognition.

REFERENCES

Alichniewicz, K. K., Brunner, F., Klünemann, H. H., and Greenlee, M. W. (2013). Neural correlates of saccadic inhibition in healthy elderly and patients with amnestic mild cognitive impairment. *Front. Psychol.* 4:467. doi: 10.3389/fpsyg.2013.00467

Allard, R., Lagacé-Nadon, S., and Faubert, J. (2013). Feature tracking and aging. *Front. Psychol.* 4:427. doi: 10.3389/fpsyg.2013.00427

Bieniek, M. M., Frei, L. S., and Rousselet, G. A. (2013). Early ERPs to faces: aging, luminance, and individual differences. *Front. Psychol.* 4:268. doi: 10.3389/fpsyg.2013.00268

Bower, J. D., Watanabe, T., and Andersen, G. J. (2013). Perceptual learning and aging: improved performance for low-contrast motion discrimination. *Front. Psychol.* 4:66. doi: 10.3389/fpsyg.2013.00066

Brewer, A. A., and Barton, B. (2014). Visual cortex in aging and Alzheimer's disease: changes in visual field maps and population receptive fields. *Front. Psychol.* 5:74. doi: 10.3389/fpsyg.2014.00074

Brockmole, J. R., and Logie, R. H. (2013). Age-related change in visual working memory: a study of 55,753 participants aged 8–75. *Front. Psychol.* 4:12. doi: 10.3389/fpsyg.2013.00012

Graham, D. J., Stockinger, S., and Leder, H. (2013). An island of stability: art images and natural scenes – but not natural faces – show consistent esthetic response in Alzheimer's-related dementia. *Front. Psychol.* 4:107. doi: 10.3389/fpsyg.2013.00107

Hamel, J., De Beukelaer, S., Kraft, A., Ohl, S., Audebert, H. J., and Brandt, S. A. (2013). Age-related changes in visual exploratory behavior in a natural scene setting. *Front. Psychol.* 4:339. doi: 10.3389/fpsyg.2013.00339

Hutchison, J. L., Shokri-Kojori. E., Lu, H., and Rypma, B. (2013). A BOLD perspective on age-related neurometabolic-flow coupling and neural efficiency changes in human visual cortex. *Front. Psychol.* 4:244. doi: 10.3389/fpsyg.2013.00244

Legault, I., Allard, R., and Faubert, J. (2013). Healthy older observers show equivalent perceptual-cognitive training benefits to young adults for multiple object tracking. *Front. Psychol.* 4:323. doi: 10.3389/fpsyg.2013.00323

Rosengarth, K., Keck, I., Brandl-Rühle, S., Frolo, J., Hufendiek, K., Greenlee, M. W., et al. (2013). Functional and structural brain modifications induced by oculomotor training in patients with age-related macular degeneration. *Front. Psychol.* 4:428. doi: 10.3389/fpsyg.2013.00428

Roudaia, E., Bennett, P. J., and Sekuler, A. B. (2013a). Contour integration and aging: the effects of element spacing, orientation alignment and stimulus duration. *Front. Psychol.* 4:356. doi: 10.3389/fpsyg.2013.00356

Roudaia, E., Sekuler, A. B., Bennett, P. J., and Sekuler, R. (2013b). Aging and audio-visual and multi-cue integration in motion. *Front. Psychol.* 4:267. doi: 10.3389/fpsyg.2013.00267

Van der Stigchel, S., Bethlehem, R. A. I., Klein, B. P., Berendschot, T. T. J. M., Nijboer, T. C. W., and Dumoulin, S. O. (2013). Macular degeneration affects eye movement behavior during visual search. *Front. Psychol.* 4:579. doi: 10.3389/fpsyg.2013.00579

Conflict of Interest Statement: The authors declare that the research was conducted in the absence of any commercial or financial relationships that could be construed as a potential conflict of interest.

Received: 15 March 2014; accepted: 02 April 2014; published online: 06 May 2014.
Citation: Greenlee MW and Sekuler AB (2014) Visual perception and visual cognition in healthy and pathological ageing. Front. Psychol. ***5****:348. doi: 10.3389/fpsyg.2014.00348*
This article was submitted to Perception Science, a section of the journal Frontiers in Psychology.

frontiers in
PSYCHOLOGY

ORIGINAL RESEARCH ARTICLE
published: 29 January 2013
doi: 10.3389/fpsyg.2013.00012

Age-related change in visual working memory: a study of 55,753 participants aged 8–75

James R. Brockmole[1]* and Robert H. Logie[2]

[1] *Department of Psychology, University of Notre Dame, Notre Dame, IN, USA*
[2] *Philosophy, Psychology, and Language Science, University of Edinburgh, Edinburgh, UK*

Edited by:
Mark W. Greenlee, University of Regensburg, Germany

Reviewed by:
David Kane, University College London, UK
Joseph Schmidt, University of South Carolina – Columbia, USA

****Correspondence:***
James R. Brockmole, Department of Psychology, University of Notre Dame, 127 Haggar Hall, Notre Dame, IN 46556, USA.
e-mail: james.brockmole@nd.edu

Visual working memory (VWM) abilities of 55,753 individuals between the ages of 8 and 75 were assessed to provide the most fine-grain analysis of age-related change in VWM to date. Results showed that VWM changes throughout the lifespan, peaking at age 20. A sharp linear decline follows that is so severe that by age 55, adults possess poorer immediate visual memory than 8 and 9 year olds. These developmental changes were largely explained by changing VWM capacity coupled with small short-term visual feature binding difficulties among children and older adults.

Keywords: visual working memory, ageing, binding, objects, internet

INTRODUCTION

Visual objects are defined by a range of basic visual features such as color, shape, luminance, size, orientation, and texture. Therefore, accurate recall of objects depends not only on the amount of information that can be retained in memory, but also on each individual's ability to bind or properly associate these various features in memory. Recent investigations have considered whether this binding ability, in addition to memory capacity, varies as a function of age. For example, one's ability to remember object location bindings in visual working memory (VWM)[1] appears to be susceptible to the aging process. Both children and senior citizens seem to have more difficulty maintaining memory for object location than do young adults in their twenties (e.g., Mitchell et al., 2000; Cowan et al., 2006). This inverted-*U* shaped trend in binding ability perhaps parallels growth and decline in several memory-based abilities in childhood and old age (e.g., Logie and Maylor, 2009; Maylor and Logie, 2010).

Age-related binding deficits, however, may not be universal. After reaching adulthood, bindings between surface features such as color and shape seem to be generally unaffected by normal aging (Brockmole et al., 2008; Parra et al., 2009; Brown and Brockmole, 2010). This result is somewhat surprising given that age-related feature-based binding deficits exist in long-term memory (Chalfonte and Johnson, 1996; Naveh-Benjamin, 2000; Naveh-Benjamin et al., 2004). Given this contrast, at least one recent result suggesting an age-related surface-feature binding deficit in VWM (Brown and Brockmole, 2010), and the relative lack of data on such binding abilities in childhood, the present study revisits the issue with a sample size large enough to detect even very small age-related changes in binding abilities from childhood to very old age.

MATERIALS AND METHODS

Data were collected from 160,405 volunteer participants who spontaneously accessed the Science pages on the British Broadcasting Corporation (BBC) website between May 2006 and March 2007 and completed a set of tests of different aspects of memory[2]. Here, we focus on results from the test of visual feature binding from this set. Results from the other tests in the set, and additional data from the same source, are reported elsewhere (e.g., Logie and Maylor, 2009; Johnson et al., 2010; Maylor and Logie, 2010). Participants reported 138 different countries of residence, but the vast majority reported residing in the United Kingdom or United States. Initial data analysis revealed no differences between those reporting residence in English language-dominated countries and those that did not. Although participants were not specifically asked to indicate fluency in English, we considered it reasonable to assume that they had a high level of English fluency because they had to find and to choose to access the study through English language web pages maintained by the BBC.

For this study, we made use of a subset of the data records collected. We excluded all those under the age of 8, over the age of 75, and those who did not provide age, gender, education, country

[1] In the literature on visual attention, visual perception, and feature binding, the terms "visual short-term memory" and "visual working memory" tend to be used interchangeably. We view visual short-term memory as comprising a temporary store that is one of a range of functions of visual working memory, which in turn is a set of functions within a broader, multi-component working memory (Logie, 2011), and we use the terms in this way throughout the manuscript. This issue is outside the scope of the present paper and the adopted term "visual working memory" (VWM) is intended to be theoretically neutral here with respect to models of working memory, and how these models account for feature binding. See Logie and van der Meulen (2009) for a review and detailed discussion.

[2] At the time of writing this report, the complete set of tests was available at: http://www.bbc.co.uk/science/humanbody/mind/surveys/memory/flash/one_show_test.shtml. However, the continued availability of these tests is under the control of the BBC, and they might not be available indefinitely.

of residence, or a general health rating of "Good" or "Excellent." In an effort to include only serious attempts to complete the task, we additionally excluded participants who did not provide at least one correct response. Finally, because it was impossible to ascertain how many times a particular individual completed the tests, we made use of only the first data record from each computer in order to minimize the frequency of repeated attempts in the data set(cf. Logie and Maylor, 2009; Johnson et al., 2010). This left a total of 55,753 data records for analysis (see **Figure 1**).

Observers were presented with displays containing one to four colored objects(an example trial is illustrated in **Figure 2**). Approximately half of the observers (28,171) were shown geometric shapes (circle, square, triangle, diamond) with the remaining observers (27,582) shown line drawings of animals (camel, penguin, elephant, pig). Preliminary analyses showed that there were no reliable differences in the data across the two stimulus types, and analyses were collapsed across this design factor. Objects were red, yellow, green, and blue. Colors and shapes were combined without replacement. Displays of 1, 2, 3, and 4 objects were shown for 2, 4, 6, and 8 s, respectively.

Following object offset, four color patches and four shape outlines appeared along the top and left edges of the screen respectively. All four possible object locations were marked with *x*'s. Observers recalled objects by clicking on a color patch, then clicking on a shape, and then clicking on a location. Observers were shown up to two trials per set size, beginning with a set size of 1, and progressively increasing. The test stopped if a participant failed to recall all three features for all the objects in the study display on two successive trials. Performance was scored as the number of objects for which color, shape, and location were reported correctly and thus ranged from 1 to 20. While additional trials would have allowed finer grain measurement of memory both within and across individuals, the difficulty, and duration of the task were of greater concern in a set of tests that were offered online for the purpose of both research and community engagement in science. This level of task demand helped ensure task completion by a

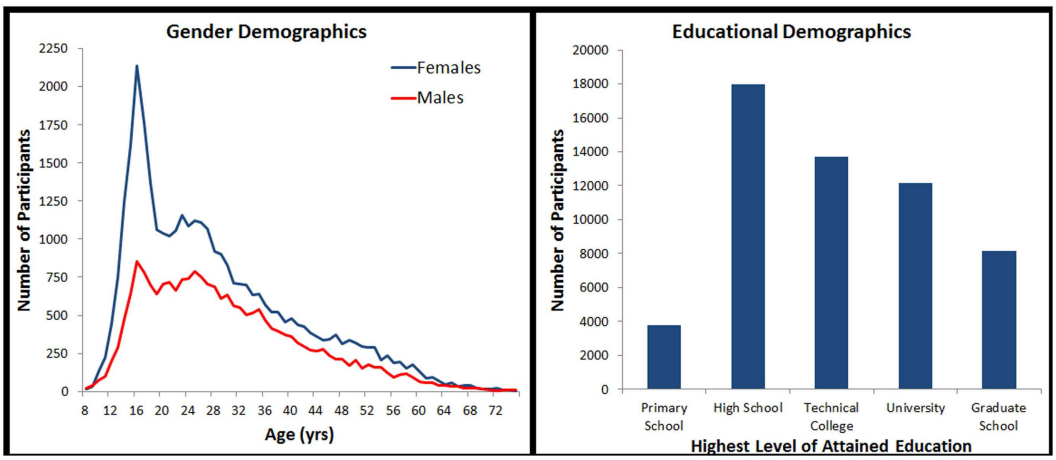

FIGURE 1 | Sample demographics broken down by age, gender, and education.

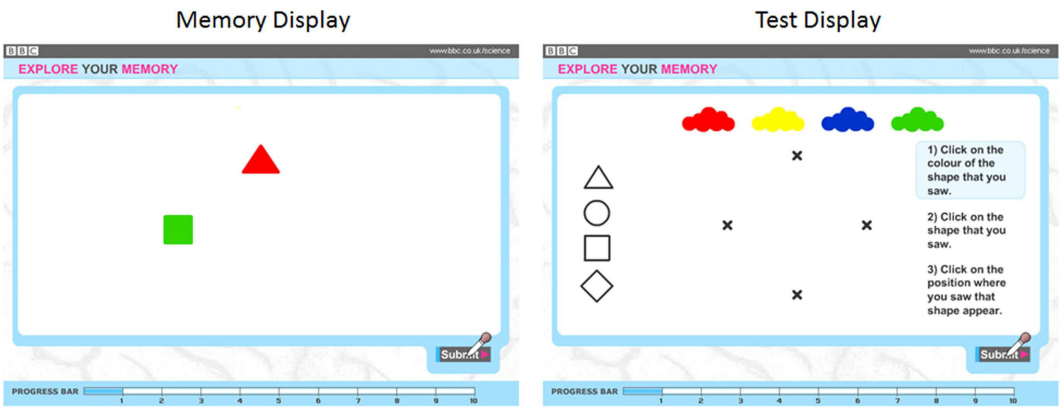

FIGURE 2 | Sample memory (left) and test (right) displays used during the experiment. In this example, the observer is to remember the color, shape, and location of two objects.

substantial number of individuals, and the resulting number of participants yielded substantial statistical power.

RESULTS

The results of a one-way ANOVA indicated that object memory varied as a function of age, as measured on a year-by-year basis [$F(67, 55{,}752) = 43.4$, $p < 0.0001$, $\eta_p^2 = 0.05$]. Two clear trends emerged (**Figure 3** green line): memory improved from age 8 to 20, while from age 21 to 75, a steady linear decline was observed. Performance observed for participants aged 42–55 was statistically indistinguishable from that of the 8 and 9-year-olds, and statistically poorer performance was observed for those participants aged 56 and over. No differences in performance were observed between males and females throughout the entire age range. Although treating education as a covariate showed a direct relationship between VWM ability and education [$F(1, 55{,}684) = 31.4$, $p < 0.0001$, $\eta_p^2 = 0.0001$], it did not completely temper age-related memory decline [$F(67, 55{,}684) = 43.9$, $p < 0.0001$, $\eta_p^2 = 0.05$].

To investigate binding abilities *per se*, we re-scored performance in two ways (see blue and red lines in **Figure 3**). A *color feature score* considered any response as correct if a color was placed in the correct location irrespective of the correspondingly selected shape. A *shape feature score* considered a response correct if the shape was placed in the correct location irrespective of the paired color. These scores reveal the quality of memory for individual feature-location bindings because a correct response does not require the proper binding of color to shape.

We first examined memory differences in color and shape memory, controlling for education. A main effect of feature score was reliable [$F(1, 55{,}685) = 215$, $p < 0.0001$, $\eta_p^2 = 0.004$]. Color feature scores ($M = 13.35$) were, on average, slightly higher than shape feature scores ($M = 12.99$), a finding that parallels much of the existing lab-based literature. Trends in color and shape memory were similar across age, however [$F(67, 55{,}685) = 1.22$, $p = 0.12$]. We therefore simplified our remaining analyses by averaging each participant's color and shape feature scores to create a single *general feature score* which represents an observer's ability to remember the identities of individual features irrespective of whether those features are assembled correctly.

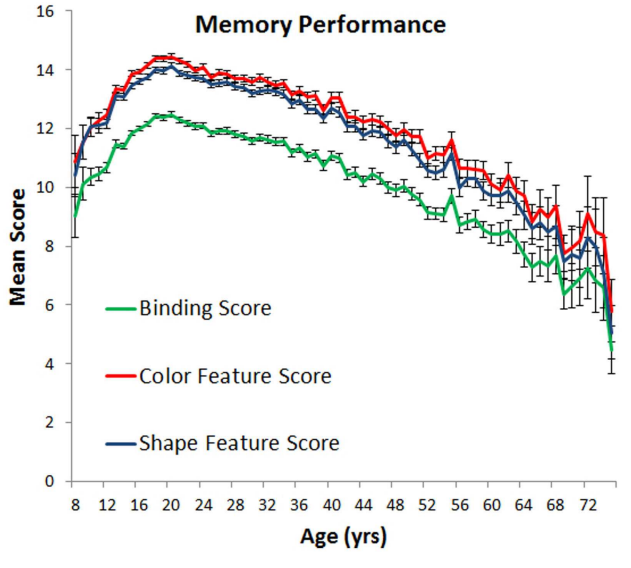

FIGURE 3 | Mean number of objects remembered (with standard error) as a function of age.

We contrasted general feature scores with our original scoring system which considered a response to be correct only if the observer reproduced the precise combinations of features (i.e., bindings between color and shape in the correct location). If memory for bindings is differentially affected by age relative to memory for features, then the effects of age on trends in the two scoring systems should likewise differ. We considered these interactions for both children (age 8–19) and adults (age 20–75). For children, age affected feature memory and binding memory differently [$F(11, 15{,}601) = 2.48$, $p < 0.01$, $\eta_p^2 = 0.002$]. Although quadratic trends were noted, we used linear regression models to estimate the average rate of change in binding scores across the ages tested[3]. On average, feature memory increased at a rate of 0.241 features per 1 year increase in age while binding memory increased at a lesser rate of 0.232 objects per 1 year increase in age. For adults, feature memory and binding memory also had different trajectories [$F(55, 40{,}084) = 4.05$, $p < 0.0001$, $\eta_p^2 = 0.006$]. Linear regression analyses indicated that, on average, feature memory declined at a rate of 0.100 features per 1 year increase in age while binding memory declined at a slower rate of 0.095 objects per 1 year increase in age.

The differential rates of change in feature and binding memory suggest that the relative proportion of bound and unbound features in VWM may also vary as a function of age(see **Figure 4**). To assess this possibility, we calculated the number of colors and shapes that were correctly remembered to co-occur (i.e., that were properly bound) and the number of remembered colors and shapes that were not correctly paired in memory (i.e., that were not properly bound). On average, unbound features accounted for 14% of all remembered features in children (ages 8–19) and 16% of all remembered features in adults (ages 20–75). In both cases, the percentage of unbound features varied as a function of year-over-year differences in age [children: $F(11, 15{,}601) = 2.733$, $p < 0.05$, $\eta_p^2 = 0.002$; adults: $F(55, 40{,}084) = 7.02$, $p < 0.001$, $\eta_p^2 = 0.01$]. For children, linear regression analyses indicated that, on average, the percentage of unbound features declined at a rate of 0.14% per 1 year increase in age. For adults, the percentage of unbound features increased at a rate of 0.06% per 1 year increase in age.

To summarize the data, VWM improves throughout adolescence with peak performance observed around age 20. The

[3]Quadratic trends are described as follows:

$$Y_{CB} = 4.234 - 0.018x^2 + 0.771x \quad (1)$$

$$Y_{CF} = 5.114 - 0.021x^2 + 0.881x \quad (2)$$

$$Y_{AB} = 12.852 - 0.001x^2 - 0.004x \quad (3)$$

$$Y_{AF} = 14.423 - 0.001x^2 + 0.012x \quad (4)$$

where Y refers to performance, x refers to the age of the participant and the subscripts c, a, b, and f refer to children, adults, binding score, and feature score, respectively.

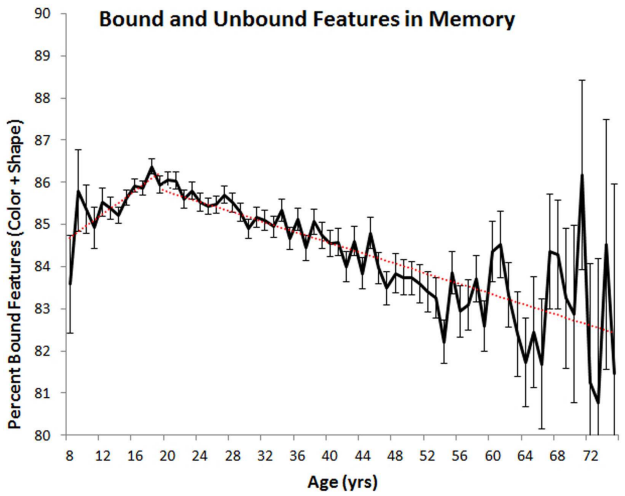

FIGURE 4 | Mean percentage of remembered colors and shapes that were correctly bound together (with standard error) plotted as a function of age. Red lines indicate best-fit linear trends.

following decline across adulthood is characterized by a linear trend, with adults in their late 50s and older displaying poorer VWM than 8 and 9 year olds. No difference in performance was observed between men and women and the effects of aging were equivalent across the genders. Higher education was associated with some sparing of visual working memory, but did not completely temper the effects of aging. In terms of feature binding, the proportion of features in memory that are properly bound increases across childhood, with the reverse trend observed in adults.

DISCUSSION

Using a common metric consistently measured across most of the lifespan on a year-by-year basis, we have shown, like many studies before ours, that VWM abilities change across the lifespan. Regarding children, previous results have shown that performance on VWM tasks improves from birth to at least 11 or 12 years of age. Our study now shows that this improvement continues throughout adolescence, reaching a peak in one's early twenties whereupon steady declines are observed (see Cornoldi and Vecchi, 2003; Reuter-Lorenz and Sylvester, 2005; Park and Payer, 2006 for reviews). What is more, we have shown that short-term feature memory and short-term binding memory are differentially affected by aging. In childhood, the proportion of properly bound features in memory improves with age, a result which suggests that as children and adolescents get older they are better at remembering feature combinations. In adulthood, the opposite trend is observed, indicating that older adults may have more difficulty remembering bindings. That said, these shifts in binding abilities are very small in comparison to shifts in memory capacity. For example, at age 20, observers remembered, on average, 12.47 of the 20 possible objects they could have viewed. At age 75, they remembered only 4.47 objects, representing a nearly two-thirds drop in capacity. In comparison, 85% of remembered features were properly bound at age 20 compared to 82% for those aged 75. The relative importance of VWM capacity changes are also substantiated by observed effect sizes (see above), with changes in capacity explaining at least five times the variance in performance compared to changes in binding ability.

Aside from the inherent limitations of cross-sectional (as compared to longitudinal) experimental designs, one potential concern with the interpretation of these trends is that the display durations that we used, coupled with a lack of articulatory suppression, might have allowed use of verbal coding of the stimuli, thereby undermining the test as a pure measure of VWM. However, our analyses of the larger dataset from this study (Johnson et al., 2010) have revealed that verbal working memory shows a much slower rate of decline across the adult age range than do measures of VWM. Indeed a test of verbal short-term memory (digit span) showed no age-related decline between the ages of 20 and 65. Therefore, it seems unlikely that the rapid rate of decline in performance across adult aging in the data reported here could be interpreted as reflecting extensive use of verbal codes for colors, shapes, and locations.

Our results, then, are consistent with previous findings (Brockmole et al., 2008) suggesting that age-related decline in short-term color-shape binding memory is driven largely by a decline in capacity for retaining individual features. Short-term color-shape binding shows somewhat different age-related trajectories than individual feature-location binding throughout childhood and appears relatively insensitive to adult aging. This last result is in contrast with the well-established age-related decline in associative learning across the adult lifespan. This possible distinction between temporary feature binding and associative learning is consistent with other findings demonstrating that temporary memory for color-shape bindings may be relatively automatic (e.g., Allen et al., 2006; Gajewski and Brockmole, 2006). The results also suggest that there is considerable merit in further exploring differential changes in binding and feature memory through childhood and adolescence.

ACKNOWLEDGMENTS

We are grateful to the British Broadcasting Corporation Science Division, especially Becky Palmer and Stephen Mather, for their collaboration on this project, and to Annelinde Vandenbroucke for her assistance with data analysis.

REFERENCES

Allen, R. J., Baddeley, A. D., and Hitch, G. J. (2006). Is the binding of visual features in working memory resource-demanding? *J. Exp. Psychol. Gen.* 135, 298–313.

Brockmole, J. R., Parra, M. A., Della Sala, S., and Logie, R. H. (2008). Do binding deficits account for age-related decline in visual working memory? *Psychon. Bull. Rev.* 15, 543–547.

Brown, L. A., and Brockmole, J. R. (2010). The role of attention in binding visual features in working memory: evidence from cognitive ageing. *Q. J. Exp. Psychol. (Hove)* 63, 2067–2079.

Chalfonte, B. L., and Johnson, M. K. (1996). Feature memory and binding in young and older adults. *Mem. Cognit.* 24, 403–416.

Cornoldi, C., and Vecchi, T. (2003). *Visuo-Spatial Working Memory and*

Individual Differences. New York: Psychology Press.

Cowan, N., Naveh-Benjamin, M., Kilb, A., and Saults, J. S. (2006). Life-span development of visual working memory: when is feature-binding difficult? *Dev. Psychol.* 42, 1089–1102.

Gajewski, D. A., and Brockmole, J. R. (2006). Feature bindings endure without attention: evidence from an explicit recall task. *Psychon. Bull. Rev.* 13, 581–587.

Johnson, W., Logie, R. H., and Brockmole, J. R. (2010). Working memory tasks differ in factor structure across age cohorts: implications for dedifferentiation. *Intelligence* 38, 513–528.

Logie, R. H. (2011). The functional organisation and the capacity limits of working memory. *Curr. Dir. Psychol. Sci.* 20, 240–245.

Logie, R. H., and Maylor, E. A. (2009). An internet study of prospective memory across adulthood. *Psychol. Aging* 24, 767–774.

Logie, R. H., and van der Meulen, M. (2009). "Fragmenting and integrating visuospatial working memory," in *The Visual World in Memory*, ed. J. R. Brockmole (Hove: Psychology Press), 1–32.

Maylor, E. A., and Logie, R. H. (2010). A large-scale comparison of prospective and retrospective memory development from childhood to middle-age. *Q. J. Exp. Psychol.* 63, 442–451.

Mitchell, K. J., Johnson, M. K., Raye, C. L., Mather, M., and D'Esposito, M. (2000). Aging and reflective processes of working memory: binding and test load deficits. *Psychol. Aging* 15, 527–541.

Naveh-Benjamin, M. (2000). Adult age-differences in memory performance: tests of an associative deficit hypothesis. *J. Exp. Psychol. Learn. Mem. Cogn.* 26, 1170–1187.

Naveh-Benjamin, M., Guez, J., Kilb, A., and Reedy, S. (2004). The associative memory deficit of older adults: further support using face-name associations. *Psychol. Aging* 19, 541–546.

Park, D. C., and Payer, D. (2006). "Working memory across the adult lifespan," in *Lifespan Cognition: Mechanisms of Change*, eds E. Bialystock and F. Craik (New York: Oxford University Press), 128–142.

Parra, M. A., Abrahams, S., Logie, R. H., and Della Sala, S. (2009). Age and binding within-dimension features in visual short-term memory. *Neurosci. Lett.* 449, 1–5.

Reuter-Lorenz, P. A., and Sylvester, C.-Y. C. (2005). "The cognitive neuroscience of working memory and aging," in *Cognitive Neuroscience of Aging: Linking Cognitive and Cerebral Aging*, eds R. Cabeza, L. Nyberg, and D. Park (New York: Oxford University Press), 186–217.

Conflict of Interest Statement: The authors declare that the research was conducted in the absence of any commercial or financial relationships that could be construed as a potential conflict of interest.

Received: 22 August 2012; accepted: 07 January 2013; published online: 29 January 2013.

Citation: Brockmole JR and Logie RH (2013) Age-related change in visual working memory: a study of 55,753 participants aged 8–75. Front. Psychology ***4****:12. doi: 10.3389/fpsyg.2013.00012*

This article was submitted to Frontiers in Perception Science, a specialty of Frontiers in Psychology.

frontiers in PSYCHOLOGY

ORIGINAL RESEARCH ARTICLE
published: 15 July 2013
doi: 10.3389/fpsyg.2013.00427

Feature tracking and aging

Rémy Allard**†, Sarah Lagacé-Nadon† and Jocelyn Faubert

Visual Psychophysics and Perception Laboratory, School of Optometry, Université de Montréal, Montréal, QC, Canada

Edited by:
Allison B. Sekuler, McMaster University

Reviewed by:
Allison B. Sekuler, McMaster University
Mark W. Greenlee, University of Regensburg, Germany

****Correspondence:***
Rémy Allard, Visual Psychophysics and Perception Laboratory, School of Optometry, École D'optométrie, Université de Montréal, 3744 Rue Jean-Brillant, QC H3t 1b9, Canada
e-mail: remy.allard@umontreal.ca
† These authors have contributed equally to this work.

There are conflicting results regarding the effect of aging on second-order motion processing (i.e., motion defined by attributes other than luminance, such as contrast). Two studies (Habak and Faubert, 2000; Tang and Zhou, 2009) found that second-order motion processing was more vulnerable to aging than first-order motion processing. Conversely, Billino et al. (2011) recently found that aging affected first- and second-order motion processing by similar proportions. These three studies used contrast-defined motion as a second-order stimulus, but there can be at least two potential issues when using such a stimulus to evaluate age-related sensitivity losses. First, it has been shown that the motion system processing contrast-defined motion varies depending on the stimulus parameters. Thus, although all these three studies assumed that their contrast-defined motion was processed by a low-level second-order motion system, this was not necessarily the case. The second potential issue is that contrast-defined motion consists in a contrast modulation of a texture rich in high spatial frequencies and aging mainly affects contrast sensitivity at high spatial frequencies. Consequently, some age-related sensitivity loss to second-order motion could be due to a lower sensitivity to the texture rather than to motion processing *per se*. To avoid these two potential issues, we used a second-order motion stimulus void of high spatial frequencies and which has been shown to be processed by a high-level feature tracking motion system, namely fractal rotation (Lagacé-Nadon et al., 2009). We found an age-related deficit on second-order motion processing at all temporal frequencies including the ones for which no age-related effect on first-order motion processing was observed. We conclude that aging affects the ability to track features. Previous age-related results on second-order and global motion processing are discussed in light of these findings.

Keywords: aging, motion, feature tracking, fractal rotation, second-order motion

INTRODUCTION

Healthy aging induces several physiological, perceptual and cognitive changes. At the level of the visual system, several visual functions are found to decrease with advancing age, such as contrast sensitivity (Owsley et al., 1983), visual acuity (Weale, 1975; Owsley et al., 1983) and perceptual processing (Faubert, 2002). Visual perception is classically looked at in terms of low or high level perceptual functions. These would require different level of cognitive processing and hence, could be altered differentially by healthy aging of the visual system. Interestingly, Faubert (2002) suggested that the underlying physiological processes involved in both low and higher level perceptual functions are probably altered with aging, but that these age-related deficits should be more functionally apparent when processing higher level information. This explanation has been referred to as the "processing complexity hypothesis of aging" (Faubert, 2002). The rationale here is that when there are diffuse subtle neurobiological changes as a result of aging, some perceptual functions may still be performed at similar levels by the elderly because of the recruitment of alternate neural networks (e.g., McIntosh et al., 1999; Della-Maggiore et al., 2000; Bennett et al., 2001). However, when processing implicates larger neural machinery or requires larger simultaneous networks, performance breaks down. On this basis it is expected that higher-order processing will be more affected as it was shown for symmetry perception, inter-attribute spatial frequency discrimination and other functions.

From the complexity hypothesis perspective, it is interesting to study the effect of aging on two similar perceptual tasks that differ in processing complexity such as first- and second-order motion processing. First-order motion stimuli are defined by local variations of luminosity (Anstis and Mather, 1985; Chubb and Sperling, 1988, 1989; Cavanagh and Mather, 1989; Wilson et al., 1992), which can be processed directly by the well-known first-order motion system, that is, low-level energy-based spatiotemporal filtering. In contrast, second-order stimuli are those defined by other properties than luminance, such as contrast, polarity and orientation, presumably making them "invisible" to the first-order motion system. To perceive second-order motion, a given property (e.g., contrast) of a texture (i.e., the "carrier") must first be locally estimated before its modulation can be globally integrated over space and time. This integration can either be performed by a low-level energy-based spatiotemporal filter (i.e., a second-order motion system) or by an actively tracking position shift of the texture (i.e., a feature tracking motion system). The second-order motion system would be low-level and analogous to the first-order motion system (i.e., motion

extraction by energy-based spatiotemporal filtering). However, as opposed to first-order motion system, it would first require an extra processing step consisting in rectifying the texture modulation introducing energy at the spatiotemporal frequency of the texture modulation (Wilson et al., 1992; Lu and Sperling, 1995, 2001). Conversely, the feature tracking motion system would be high-level and would consist of a different processing strategy: identify the position of the texture modulation and attentively track the position shift over time (Cavanagh, 1992).

Three studies have evaluated the effect of aging on first- and second-order motion processing and found diverging results. Two of those (Habak and Faubert, 2000; Tang and Zhou, 2009) found that second-order motion processing was more vulnerable to aging than first-order motion processing, which is consistent with Faubert's complexity hypothesis. Conversely, Billino et al. (2011) found that aging affected first- and second-order motion processing by similar proportions, which suggests "more direct associations between functional decline and differential ageing of critical brain areas" (p. 3160). These three studies used contrast-defined motion as second-order stimuli. There are at least two potential issues when using such a stimulus to evaluate age-related sensitivity losses. The first issue pertains to the fact that the motion system processing contrast-defined motion varies depending on the stimulus parameters, such as interstimulus interval (Smith, 1994), texture contrast (Ukkonen and Derrington, 2000), modulation contrast (Seiffert and Cavanagh, 1999) and temporal frequency (Holliday and Anderson, 1994; Seiffert and Cavanagh, 1999; Allard and Faubert, 2008a). The three studies assumed that their contrast-defined motion was processed by a low-level second-order motion system. However, this was not necessarily the case. Furthermore, besides the fact that the motion system processing contrast-defined motion depends on many parameters, even the existence of a second-order motion system remains controversial. Some (Ukkonen and Derrington, 2000; Allard and Faubert, 2008a) have argued that contrast-defined motion can either be processed by the low-level first-order motion system due to non-linearities (which could explain the same age-related effect for first- and second-order motion processing found by Billino et al., 2011) or by a high-level feature tracking motion system (which could explain the specific age-related effect to second-order motion processing observed by Habak and Faubert, 2000 and Tang and Zhou, 2009), which questions the existence of a second-order motion system. The second potential issue is that contrast-defined motion requires the modulation of a texture rich in high spatial frequencies, such as noise or a high spatial frequency sine wave grating, and aging mainly affects contrast sensitivity to high spatial frequencies (Kline et al., 1983; Owsley et al., 1983; Morrison and McGrath, 1985; Crassini et al., 1988) Consequently, motion perception that requires the processing of high spatial frequencies could artificially induce an age-related sensitivity loss to second-order motion attributable to a lower sensitivity to the texture (i.e., carrier), rather than to the motion processing *per se*. As such, Billino et al. (2011) suggested that part of the previously reported age-related sensitivity loss specific to the second-order motion processing could be explained by age-related changes to the optics of the eye, which changes mainly affect contrast sensitivity at high spatial frequencies. However, high spatial frequencies are essential for the processing of contrast-defined motion.

To avoid these two potential issues, the current study used a second-order motion stimulus proven to be processed by a high-level feature tracking motion system (Lagacé-Nadon et al., 2009), namely fractal rotation. This stimulus was originally introduced by Benton et al. (2007). We modified the stimulus (Lagacé-Nadon et al., 2009) to eliminate all high spatial frequency components from its composition. It is composed of successive noise frames rich in orientation cues changing over time resulting in a rotating percept (**Figure 1**). Since the noise is resampled at every frame (i.e., dynamic noise), there is no local luminance correlation between frames resulting in no net local luminance translation cue. As a result, fractal rotation is "invisible" to the first-order motion system, which is sensitive to luminance translation cues. Note that contrast-defined motion (the second-order stimuli used in the previous aging studies cited above), as fractal rotation, does not contain any net local luminance translation cues and should therefore be "invisible" to the first-order motion system. However, early non-linearities within the stimulus or the visual system can easily introduce luminance variations (Smith and Ledgeway, 1997), making such a second-order stimulus "visible" to the first-order motion system. As opposed to most second-order stimuli, fractal rotation does not consist in the modulation of a texture, so that even strong early non-linearities would not introduce any net luminance translation cues. This robustness to early non-linearities guaranties that fractal rotation cannot be processed by the first-order motion system. Indeed, to perceive rotation from fractal stimuli, one needs to track changes in orientation over time, rather than local luminance translations. As a result, fractal rotation is processed by the high-order feature tracking motion system (Lagacé-Nadon et al., 2009). We therefore chose fractal rotation as our second-order motion stimulus because (1) it is robustly "invisible" to the first-order motion system and, (2) it can be composed exclusively of low spatial frequencies, which are not or little affected by aging (Owsley et al., 1983), thereby minimizing visibility difference between younger and older adults.

Feature tracking requires observers to attentively track changes of a given property (e.g., position or orientation) and is therefore attention-based. Another attention-based motion task widely studied is multiple-object tracking (MOT). Performance to MOT tasks has been found to decline with age (Trick et al., 2005; Sekuler et al., 2008; Kennedy et al., 2009), which could reflect a decline of

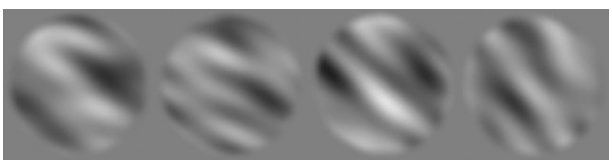

FIGURE 1 | Fractal rotation stimulus example. Stimulus is rotating clockwise. From this 4-frames sequence, it can be seen that a noise frame is resampled at every frame. An example movie of these stimuli can be viewed in Lagacé-Nadon et al. (2009; Movie 2).

attention-based processing. However, it is difficult to determine precisely which process is affected by aging since the performance to a MOT task depends on many factors, such as working memory, the observer's strategy (e.g., eye gaze) and the ability to divide attention and maintain it over a long period of time. Conversely, feature tracking has the advantage of probing attention without directly soliciting all these factors. Thus, feature tracking appears to be relatively simple for an attention-based task and if there is a general age-related decline of attention, then this simple attention-based task should also be affected.

EXPERIMENT 1: DISCRIMINATION OF DIRECTION OF FIRST-ORDER AND FRACTAL ROTATION

Contrast sensitivities to motion direction discrimination of first-order and fractal rotation (Benton et al., 2007) were measured for two age groups. The use of a band-pass spatial filter to keep only spatial frequencies ranging between 0.125 and 0.5 cycles per degree (cpd) ensured that the observed decline in contrast sensitivity to motion direction is attributable to the effect of age on motion processing *per se*, rather than to diminished visibility of the noise pattern.

Contrast sensitivity was measured over a large range of temporal frequencies to reflect the band-pass and the low-pass sensitivity function of first-order and feature tracking motion processing. Measuring sensitivity over a large range of temporal frequencies is particularly relevant because aging affects motion sensitivity differently at different temporal frequencies. As such, Habak and Faubert (2000) reported a significant age-related decrease in motion sensitivity of first-order stimuli presented at low (2 Hz) and high (8 Hz) temporal frequencies, but not at a medium temporal frequency (4 Hz). These results underline the importance of looking at motion perception over a large range of temporal frequencies.

MATERIALS AND METHODS

Subjects

Participants have been divided into two groups, the younger and the older adults groups. Ten individuals aged between 18 and 32 years of age (mean age 23.8 ± 5.01 years) and 12 individuals between 65 and 75 years old (mean age 68.46 ± 2.65 years) participated in the study. All participants needed to have a best corrected monocular visual acuity of at least 6/6. Subjects were required to have a good ocular health to be included and any subject with strabismus, amblyopia, cataract, age-related macular degeneration, glaucoma, cerebral vascular accident history or visual field dysfunctions was excluded. Subjects from the older adult group all had a complete visual examination done by an optometrist at the School of Optometry of Université de Montréal within the year before the experiment. Our protocol was approved by the university's research ethics board. Informed consent was given by each participant upon evaluation.

A Mini-Mental State Examination (MMSE) was administered to older participants prior to psychophysical evaluation. Average score on the MMSE for the older adult population was 29.5/30 ± 0.1946 (range: 28–30/30). All subjects were located in the 75th percentile or above for their age and educational level, except for two subjects who were located between the 50 and 75th percentiles (Crum et al., 1993). Ametropias, astigmatism and presbyopia were all corrected, after which measures of monocular and binocular acuity was performed to ensure optimal correction was obtained for the testing distance.

Apparatus and stimuli

Stimuli were generated by a Pentium 4 computer. Images were presented on a ViewSonic E90FB.25CRT computer screen using a Matrox Parhelia 512 graphic card. The Noisy-Bit method (Allard and Faubert, 2008b) implemented with the error of the green color gun inversely correlated with the error of the two other color guns made the 8-bit display equivalent to an analog display having a continuous luminance resolution. Mean luminance of the screen was 47 cd/m^2 and refresh rate was 60 Hz. Each pixel possessed 1/32 degrees of visual angle at the viewing distance of 57 cm. The monitor was the only source of light in the room. A Minolta CS100 photometer interfaced with a homemade program calibrated the output intensity of each gun. Presentation time was 1 s to ensure optimal temporal integration for the older adult group (Raghuram et al., 2005; Bennett et al., 2007).

In the present study, two types of stimuli were presented: first-order and fractal rotation (Benton et al., 2007; Lagacé-Nadon et al., 2009). Stimuli were composed of 1/f noise that was filtered as a function of the spatial frequency and orientation. The filtering in the spatial frequency dimension was done to minimize the visibility difference of the stimulus between young and old observers. Given the well-known age-related contrast sensitivity losses to high spatial frequencies (Owsley et al., 1983; Morrison and McGrath, 1985; Crassini et al., 1988; Tulunay-Keesey et al., 1988; Elliott et al., 1990), each noise frame was band-pass filtered to keep only low spatial frequencies ranging from 0.125 to 0.5 cpd. A 10 degrees wide orientation filter was applied to each presented noise frame, such that the image spatial structure was rich in orientation cues. A rotating stimulus was composed of successive noise frames that were rotated after being filtered in the spatial and orientation dimensions. The rotating direction (clockwise or counterclockwise) and initial orientation were randomized on each trial. The only difference between the first-order and fractal rotations stimuli was that a different noise sample was used at each frame (refreshed at 60 Hz) for the fractal stimulus and the same noise sample was used for the first-order stimulus. Thus, the first-order stimulus corresponded to a rotating noise image (**Figure 2**) and the fractal rotation corresponded to dynamic noise in which the orientation varies over time (**Figure 1**). Hence, for the first-order stimulus, the local motion direction could

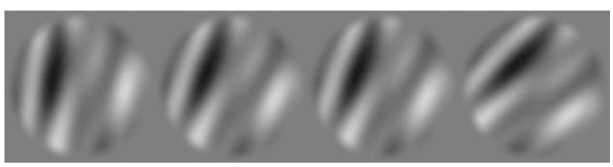

FIGURE 2 | First-order rotation stimulus. Stimulus is rotating clockwise. From this 4-frames sequence, it can be seen that a single noise frame is rotated in time. An example movie of these stimuli can be viewed in Lagacé-Nadon et al. (2009; Movie 1).

be determined by local luminance translation cues, which can be detected by the low-level first-order motion system. But for the fractal stimulus, the direction of local luminance translation cues was random due to the noise resampling at every frame. So to perceive fractal rotation, one needs to track changes in spatial structure (i.e., orientation) over time, rather than local luminance translations, so fractal rotation is processed by the high-order feature tracking motion system (Lagacé-Nadon et al., 2009). Both stimuli were presented within a circular aperture, subtending 8 degrees of visual angle and were displayed on a gray background.

Procedure

Before each session, subjects were adapted to room luminance testing condition for 20 min (Jackson et al., 1999). A single-interval, two-alternative forced-choice procedure was used in combination with a direction discrimination task (clockwise or counterclockwise). A 2-down-1-up staircase protocol was used to measure contrast thresholds (Levitt, 1971). Each staircase consisted of 10 reversals and thresholds corresponded to the geometric mean of the last 6 reversals. Each trial started with the apparition of the fixation bull's-eye to which participants were asked to maintain fixation. A feedback sound was provided to participants. Temporal frequencies of presented stimuli were 0.25, 0.5, 1, 2 circle rotations (360 degrees) per second (or r/s) for fractal rotation and 0.25, 0.5, 1, 2, 4, 6, 8 r/s for first-order rotation. Speeds of presented stimuli were determined based on the temporal frequency functions of both first-order and fractal rotation stimuli, as established in a previous study (Lagacé-Nadon et al., 2009). Each participant completed fifteen blocks of trials. The first four blocks consisted of practice trials to familiarize subjects with first-order and fractal rotation stimuli. The presentation order of the 11 block conditions (4 fractal and 7 first-order rotation speeds) was randomized. Trials and practice trials were divided into two equal testing sessions, which were conducted on separate days. Stimuli were viewed binocularly.

RESULTS AND DISCUSSION

Contrast thresholds for discrimination of direction of first-order and fractal rotation stimuli were obtained for each participant as a function of temporal frequencies. Group results for both younger and older adults are presented in **Figure 3**. Results are expressed in terms of contrast sensitivity, which was defined as the reciprocal of the contrast threshold. Consistent with our previous findings (Lagacé-Nadon et al., 2009), contrast sensitivity functions of first-order and fractal rotations were band-pass and low-pass in nature, respectively, which is consistent with our interpretation that first-order and fractal rotation stimuli are analyzed by the first-order and feature tracking motion systems, respectively.

As can be seen in **Figure 3**, different age-related sensitivity losses were observed with the two stimuli. Age-related sensitivity losses for the first-order rotation were not uniform, with sensitivity losses observed only at low (i.e., 0.25, 0.5, 1 r/s) and very high temporal frequencies (6, 8 r/s). As such, contrast sensitivity thresholds for first-order rotation at medium temporal frequencies (2, 4 r/s) were comparable between the younger and older adult group. These results are consistent with those obtained by Habak and Faubert (2000) who found an age-related sensitivity loss to first-order motion processing at low (2 Hz) and high (8 Hz) temporal frequencies, but not at a medium temporal frequency (4 Hz). Conversely, contrast sensitivity to fractal rotation was reduced at all temporal frequencies for the older adult as compared to the younger adult group. Importantly, an age-related sensitivity loss to fractal rotation was observed at a temporal frequency (2 r/s) at which first-order motion processing was unaffected. This shows that aging affects the feature tracking motion processing *per se*, and that the results cannot simply be explained by another general factor not directly related to the task.

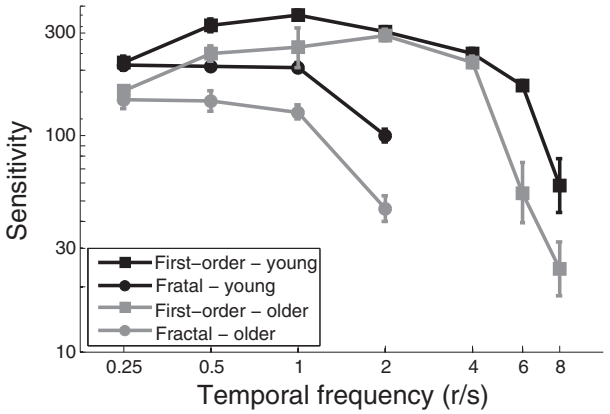

FIGURE 3 | Mean contrast sensitivity to first-order and fractal rotation as a function of temporal frequency. Error bars represent the standard error of the mean.

These findings were statistically confirmed by performing a three-way repeated measure ANOVA (age × stimulus type × temporal frequency) on logarithmic contrast sensitivity values with stimulus type (2 levels: first-order and fractal rotation) and temporal frequency (4 levels: 0.25, 0.5, 1, and 2 r/s) as within-subject factors and age as between-subject factors (2 levels: younger and older adults). Analysis revealed a significant three-way interaction [$F_{(2.043,\ 40.852)} = 5.399$, $p = 0.002$]. Further two-way ANOVA were performed to examine interactions between age and stimulus type for each temporal frequency. At 0.25, 0.50, and 1 r/s, there was no interaction [$F_{(1,\ 20)} = 0.390$, $p = 0.539$ for 0.25 r/s, $F_{(1,\ 20)} = 0.295$, $p = 0.593$ for 0.50 r/s and $F_{(1,\ 20)} = 0.292$, $p = 0.595$ for 1 r/s], but a significant main effect of age was found [$F_{(1,\ 20)} = 16.839$, $p = 0.001$ for 0.25 r/s, $F_{(1,\ 20)} = 11.258$, $p = 0.003$ for 0.50 r/s and $F_{(1,\ 20)} = 9.600$, $p = 0.006$]. Consequently, it is not possible to determine whether the age-related sensitivity loss to fractal rotation was specific to fractal rotation motion processing at these temporal frequencies. At 2 r/s, however, a significant age x stimulus type interaction was identified [$F_{(1,\ 20)} = 21.897$, $p < 0.001$]. Independent samples t-test revealed significant effect of age for fractal rotation [$t_{(20)} = 4.915$, $p < 0.001$] but not for first-order rotation [$t_{(20)} = 0.543$, $p = 0.593$]. This shows an age-related impairment specific to fractal rotation motion processing at this medium frequency.

To evaluate age-related impairment to first-order rotation at higher temporal frequencies, another two-way repeated measures ANOVA has been performed with the temporal frequency as the within-subjects factors (3 levels: 4, 6, and 8 r/s) and age as the between-subjects variable (2 levels: younger and older adults). A significant interaction between age and speed of presented stimuli was found [$F_{(2,\ 40)} = 3.313$, $p = 0.047$]. Independent sample t-test revealed significant effect of age at 6 and 8 r/s for first-order motion [$t_{(20)} = 3.588$, $p = 0.004$ for 6 r/s and $t_{(20)} = 2.149$, $p = 0.044$ for 8 r/s) such that thresholds for discrimination of direction were higher for the older individuals. However, no significant effect of age was observed for first-order motion presented at 4 r/s [$t_{(20)} = 0.996$, $p = 0.331$].

To evaluate if there were common factors affecting the sensitivity to both first-order and fractal rotation motion processing, we evaluated the correlation between these thresholds for both age groups. The Spearman's correlation coefficients with variables independently ranked for each temporal frequency were 0.41 and 0.46 for young and older adults, respectively. These moderate correlations between first-order and fractal rotation thresholds can be explained by factors that affect both thresholds but vary between subjects. These factors could be low-level (e.g., contrast gain due to light scattering) or high-level (e.g., motivation or fatigue).

In sum, the main findings indicate significant effect of age on direction discrimination thresholds of fractal rotation at all temporal frequencies, and first-order rotation at low and high temporal frequencies, but not at medium temporal frequencies.

EXPERIMENT 2: CONTROLLING FOR THE STIMULUS VISIBILITY

The first experiment showed age-related sensitivity loss to direction of all fractal rotation temporal frequencies using a stimulus composed of only low spatial frequencies to avoid the known age-related sensitivity loss to high spatial frequencies. Using such a stimulus, we assumed that the age-related effect to fractal rotation was due to motion processing *per se*, not to a lower visibility of the noise. The goal of the second experiment was to confirm this empirically. To differentiate between an age-related sensitivity loss to feature tracking motion processing *per se* from a visibility loss, we measured the sensitivity to a stationary (i.e., not rotating) noise pattern.

MATERIALS AND METHODS

Subjects

The same subjects as in the first experiments participated in the second experiment.

Stimuli

Replicas of first-order and fractal rotation stimuli used in the first experiment were presented to subjects, except that the orientation did not change over time. Hence, a single noise frame was generated for first-order rotation control condition resulting in a static noise pattern rich in orientation cues. For the fractal rotation control stimulus, noise frames were refreshed at every frame (60 Hz), resulting in dynamic noise rich in orientation cues. For both stimuli, the mean orientation of the spatial filter was randomly assigned a value of 0 or 90°. Importantly, both stimuli used in this control condition are accessible to first-order sensitive mechanisms. Examples of presented stimuli are given in **Figures 4**, **5**.

Procedure

A single interval, two-alternative-forced choice procedure was used in combination with an orientation discrimination task (horizontal or vertical). As in the first experiment, contrast thresholds were measured using a 2-down-1-up staircase protocol (Levitt, 1971).

RESULTS AND DISCUSSION

For each observer, contrast sensitivity for first-order and fractal rotation controls was obtained from logarithmic transformed contrast sensitivity values. Average contrast sensitivity for discrimination of orientation of first-order and fractal rotation was then calculated. Results show similar log contrast sensitivities between both age groups for first-order (younger adult $= 2.17 \pm 0.031$, older adult $= 2.16 \pm 0.032$) and fractal rotation (younger adult $= 2.44 \pm 0.030$, older adult $= 2.39 \pm 0.032$) control conditions. Independent samples t-tests indicate no significant effect of age on log sensitivity to both static [$t_{(20)} = 0.063$, $p = 0.950$] and dynamic [$t_{(20)} = 1.078$, $p = 0.294$] noise pattern. In other words, the visibility of the static and dynamic noise was similar for both age groups so the age-related sensitivity losses to first-order and fractal rotation observed in the previous experiment must be due to motion processing *per se*, not to some other factor affecting stimulus visibility.

GENERAL DISCUSSION

The temporal sensitivity functions to first-order and fractal rotation were band-pass and low-pass in nature, which is consistent with our previous findings (Lagacé-Nadon et al., 2009) that led us to conclude that first-order and fractal rotation stimuli are

FIGURE 4 | Example of a vertical stimulus presented in the first-order control condition. A sequence of four presented frames on a single interval is shown. The same noise image is presented at all frames.

FIGURE 5 | Example of a vertical stimulus presented in the fractal control condition. A sequence of four presented frames on a single interval is shown. Noise is resampled on every presented frame. As can be seen, a flickering pattern is obtained.

analyzed by the first-order and feature tracking motion systems, respectively. Because fractal rotation can be designed to solicit the feature tracking motion system in the absence of high spatial frequency content, it constitutes an appropriate stimulus to study high-order motion processing in the elderly (who are less sensitive to high spatial frequencies). Results indicate an age-related sensitivity loss to fractal rotation at all temporal frequencies and an age-related sensitivity loss to first-order motion at low and high temporal frequencies but not at medium temporal frequencies. As confirmed in the second experiment, the sensitivity loss to fractal rotation was not attributable to a lower visibility of the noise pattern, which implies that this age-related sensitivity loss was due to feature tracking motion processing *per se*. To our knowledge, the current study is the first to provide direct evidence of an age-related sensitivity loss to feature tracking motion processing.

The age-related sensitivity loss to feature tracking observed here is in accordance with the results of two other studies (Habak and Faubert, 2000; Tang and Zhou, 2009). As such, Habak and Faubert (2000) found a sensitivity loss at all temporal frequencies for second-order motion processing, but only at low and high temporal frequencies for first-order motion processing. Age had no significant impact on first-order motion sensitivity at a medium temporal frequency (4 Hz). More recently, Tang and Zhou (2009) found that age-related sensitivity loss to second-order motion processing began earlier and was more pronounced than the sensitivity loss to first-order motion processing. As mentioned in the introduction, the existence of a second-order motion system remains controversial. The results from these two studies have shown a particular age-related sensitivity decline to second-order motion processing which could be reflecting a deficit to the feature tracking motion system rather than the second-order motion system as assumed by the authors. The current findings that age affects feature tracking are also compatible with this alternate hypothesis. Consequently, if there is a second-order motion system, the question of whether it is particularly sensitive to aging remains open.

Our results diverge from the ones obtained by Billino et al. (2011) who found similar age-related sensitivity loss to first- and second-order motion processing. However, it is likely that their second-order motion stimulus was processed by the first-order motion system. First, they tested at a relatively high temporal frequency (∼7 Hz) and it has been argued that the second-order motion at high temporal frequencies can be processed by the first-order motion system (Holliday and Anderson, 1994; Ukkonen and Derrington, 2000; Allard and Faubert, 2008a, 2013a) Second, they tested in the peripheral visual field and there is some evidence suggesting that there is no motion system other than the first-order motion system under such conditions (Allard and Faubert, 2013b). And more critically, Billino and collaborators have used a motion *detection* task that did not require any second-order motion processing. Subjects had to indicate which of the four simultaneously presented stimuli contained motion. Since adding contrast-defined motion (i.e., a second-order stimulus) to a static texture introduces drift-balanced first-order motion (i.e., the same amount of expected first-order motion drifting in the same and opposite directions as the second-order motion, Chubb and Sperling, 1988), subjects could perform the task simply by detecting the first-order motion. Other studies have generally used a motion *discrimination* task, which requires second-order motion processing since although such a stimulus contains first-order motion, it is drift-balanced and therefore is not informative of the drifting direction of the second-order motion. Consequently, for any of these three reasons it is likely that Billino et al. (2011) second-order motion stimuli were processed by the first-order motion system, which would explain their findings of similar age-related deficits to first- and "second-order" motion processing.

Another way to probe the first-order and feature tracking motion systems is with short- and long-range apparent motion, respectively (Braddick, 1974). As such, Roudaia et al. (2010) have looked at the effect of aging on motion processing using random-dot kinematograms in a two-frame apparent motion paradigm and systematically varied the spatial step-size and the interstimulus interval between the two frames. They found that the elderly were less accurate than their youth at discriminating the motion direction when the spatial or temporal spacing was high (>0.3 degrees or >40 ms). At such high spacing, apparent motion was found to be process by a correspondence-based (i.e., feature tracking) motion system (>0.25 degrees, Braddick, 1974; and >40 ms, Georgeson and Harris, 1990). Thus, although Roudaia et al. (2010) claimed that they were investigating the low-level (first-order) motion system, the age-related effects they found for long-range apparent motion are more likely due to high-level motion processing. This is compatible with the current findings of an age-related sensitivity loss due to the feature tracking motion system.

The current study shows that aging affects high-level, feature tracking motion processing. Previous studies evaluating the effect of aging on "high-level" motion processing other than second-order have generally focused on MOT and global motion processing. As mentioned in the introduction, MOT is sensitive to aging (Trick et al., 2005; Sekuler et al., 2008; Kennedy et al., 2009), but since MOT probes various high-level processes (e.g., divided attention, observer's strategy) it is difficult to determine which of these is specifically affected by aging. Conversely, feature tracking has the advantage of being a high-level, attention-based task without directly soliciting all these factors. Thus, the feature tracking appears to be relatively simple for a high-level attention-based task and the fact it is affected by aging supports the hypothesis of a general age-related decline of attention-based processing.

Global motion processing requires the integration of local (typically first-order) motion over a large area. A recent review by Hutchinson et al. (2012) concludes that aging impairs global motion processing only under some conditions: when the visual field is very large, at low and high (but not medium) velocities and at low contrast. There are at least two reasons that could suggest that age-related sensitivity loss to global motion processing may not reflect a deficit to high-level *global motion* processing *per se*. The first issue relates to the size of the visual field stimulated. As suggested by Faubert (2002) integrating information over larger visual field areas may require the solicitation of larger neural networks and by its very nature could show age-related defects not seen for smaller integration zones. A good example of this is the

study by Legault et al. (2012), where they demonstrated that biological motion perception for increasingly larger stimuli became more and more difficult for the elderly while the young observer generally maintained a stable level of performance. There is also evidence from the dual-task paradigms, such as the useful field of view, that visual field size matters in aging (Ball et al., 1988; Sekuler et al., 2000). Hence, the age-related sensitivity loss to global motion, when using a very large stimulus, could depend on integration over a critical field size and not on the global *motion* processing *per se*. Another reason why age-related global motion sensitivity loss may not necessarily reflects an impairment to global motion processing *per se* is that global motion consists in integrating local first-order motion. Thus, lower sensitivity to local first-order motion processing may result in a lower sensitivity to global motion. As mentioned above, age-related global motion sensitivity loss was observed at low and high velocities, but not at medium velocities. In the current study and another by Habak and Faubert (2000), analogous results for local first-order motion processing were observed: aging caused an age-related sensitivity loss at low and high temporal frequencies, but not at medium temporal frequencies. Consequently, it is possible that age-related sensitivity loss to global motion at low and high velocities could be due to a sensitivity loss to local first-order motion processing rather than *global* motion processing *per se*. Note that this could also explain the different age-related effects observed by Billino et al. (2008) for various high-level motion tasks requiring the integration of moving dots (i.e., translational global motion, radial global motion and biological motion). Indeed, these different age-related effects (for instance, aging was found to affect translational but not radial global motion) could be due to the fact that different dot speeds were used for different tasks and that aging affects differently local motion processing at different speeds. Conversely, the current study found an age-related sensitivity loss that must be due to a high-level motion processing (i.e., feature tracking) at all temporal frequencies, including the ones at which first-order motion processing was spared. Thus, compared to global motion processing studies, our study clearly shows an age-related sensitivity loss to *high-level motion* processing *per se*.

Faubert (2002) proposed the complexity hypothesis to explain visual perceptual impairments observed with healthy aging. According to this hypothesis, aging would create subtle diffuse neurobiological alterations. These would have little impact on simple tasks requiring small neural network, but would result in a measurable age effect for complex tasks requiring integration over a broader neural network or for those requiring many processing steps (e.g., inter-attribute spatial frequency discrimination or symmetry perception). The previously observed age-related selective effect on second-order motion processing has been interpreted as evidence in favor of the complexity hypothesis (Habak and Faubert, 2000; Tang and Zhou, 2009). However, the current findings of an age-related impairment to feature tracking and partial sparing of the first-order motion processing does not confirm nor infirm this complexity hypothesis. Nevertheless, there is no doubt that feature tracking is more complex, requires more processing steps and involves larger neural networks than first-order motion processing. Thus, the selective age-related impairment to feature tracking is compatible with the complexity hypothesis. On the other hand, the fact that first-order motion processing and feature tracking involve qualitatively different motion systems implies that the current results are also compatible with the selective deficit hypothesis. For instance, feature tracking involves attentional resources to track features (Cavanagh, 1992). Therefore, the choice of first-order and feature tracking is not optimal for directly addressing the complexity hypothesis for motion *per se*. Given that aging affects attention (Kramer and Kray, 2006; Kramer and Madden, 2008), the effect of aging on feature tracking could relate to a selective attentional deficit.

CONCLUSIONS

The present study confirms previous studies (Habak and Faubert, 2000; Tang and Zhou, 2009) showing selective second-order motion sensitivity losses. However, what was particularly relevant in the present study is that: (1) the motion system (feature tracking) processing this second-order motion stimuli was known and not controversial, and (2) the stimuli were void of high-spatial frequency components known to be affected by aging. We found an age-related deficit on second-order motion processing at all temporal frequencies including the ones for which no age-related effect on first-order motion processing was observed. We conclude that aging affects the ability to track features.

ACKNOWLEDGMENTS

This work was supported by the NSERC-Essilor Industrial Research Chair and an NSERC discovery grant to Jocelyn Faubert.

REFERENCES

Allard, R., and Faubert, J. (2008a). First- and second-order motion mechanisms are distinct at low but common at high temporal frequencies. *J. Vis.* 8, 1–17. doi: 10.1167/8.2.12

Allard, R., and Faubert, J. (2008b). The noisy-bit method for digital displays: converting a 256 luminance resolution into a continuous resolution. *Behav. Res. Methods* 40, 735–743. doi: 10.3758/BRM.40.3.735

Allard, R., and Faubert, J. (2013a). No second-order motion system sensitive to high temporal frequencies. *J. Vis.* 13, 1–14. doi: 10.1167/13.5.4.

Allard, R., and Faubert, J. (2013b). "No dedicated second-order motion system in the periphery," in *Conference Proceedings and Abstracts* (Naples, FL).

Anstis, S. M., and Mather, G. (1985). Effects of luminance and contrast on direction of ambiguous apparent motion. *Perception* 14, 167–179. doi: 10.1068/p140167

Ball, K. K., Beard, B. L., Roenker, D. L., Miller, R. L., and Griggs, D. S. (1988). Age and visual-search-expanding the useful field of view. *J. Opt. Soc. Am. A* 5, 2210–2219.

Bennett, P. J., Sekuler, A. B., McIntosh, A. R., and Della-Maggiore, V. (2001). The effects of aging on visual memory: evidence for functional reorganization of cortical networks. *Acta Psychol. (Amst.)* 107, 249–273. doi: 10.1016/S0001-6918(01)00037-3

Bennett, P. J., Sekuler, R., and Sekuler, A. B. (2007). The effects of aging on motion detection and direction identification. *Vision Res.* 47, 799–809. doi: 10.1016/j.visres.2007.01.001

Benton, C. P., O'Brien, J. M., and Curran, W. (2007). Fractal rotation isolates mechanisms for form-dependent motion in human vision. *Biol. Lett.* 3, 306–308. doi: 10.1098/rsbl.2007.0056

Billino, J., Bremmer, F., and Gegenfurtner, K. R. (2008). Differential aging of motion processing mechanisms: evidence against general perceptual decline. [Research Support, Non-U.S. Gov't]. *Vision Res.* 48, 1254–1261. doi: 10.1016/j.visres.2008.02.014

Billino, J., Braun, D. I., Bremmer, F., and Gegenfurtner, K. R. (2011). Challenges to normal neural functioning provide insights into separability of motion processing mechanisms. [Research Support, Non-U.S. Gov't]. *Neuropsychologia* 49, 3151–3163. doi: 10.1016/j.neuropsychologia.2011.07.009

Braddick, O. J. (1974). A short-range process in apparent motion. *Vision Res.* 14, 519–527. doi: 10.1016/0042-6989(74)90041-8

Cavanagh, P. (1992). Attention-based motion perception. *Science* 257, 1563–1565. doi: 10.1126/science.1523411

Cavanagh, P., and Mather, G. (1989). Motion: the long and short of it. *Spat. Vis.* 4, 103–129. doi: 10.1163/156856889X00077

Chubb, C., and Sperling, G. (1988). Drift-balanced random stimuli: a general basis for studying non-Fourier motion perception. *J. Opt. Soc. Am. A* 5, 1986–2007. doi: 10.1364/JOSAA.5.001986

Chubb, C., and Sperling, G. (1989). Two motion perception mechanisms revealed through distance-driven reversal of apparent motion. *Proc. Natl. Acad. Sci. U.S.A.* 86, 2985–2989. doi: 10.1073/pnas.86.8.2985

Crassini, B., Brown, B., and Bowman, K. (1988). Age-related changes in contrast sensitivity in central and peripheral retina. *Perception* 17, 315–332. doi: 10.1068/p170315

Crum, R. M., Anthony, J. C., Bassett, S. S., and Folstein, M. F. (1993). Population-based norms for the Mini-Mental State Examination by age and educational level. *JAMA* 269, 2386–2391. doi: 10.1001/jama.1993.03500180078038

Della-Maggiore, V., Sekuler, A. B., Grady, C. L., Bennett, P. J., Sekuler, R., and McIntosh, A. R. (2000). Corticolimbic interactions associated with performance on a short-term memory task are modified by age. *J. Neurosci.* 20, 8410–8416.

Elliott, D., Whitaker, D., and MacVeigh, D. (1990). Neural contribution to spatiotemporal contrast sensitivity decline in healthy ageing eyes. *Vision Res.* 30, 541–547. doi: 10.1016/0042-6989(90)90066-T

Faubert, J. (2002). Visual perception and aging. *Can. J. Exp. Psychol.* 56, 164–176. doi: 10.1037/h0087394

Georgeson, M. A., and Harris, M. G. (1990). The temporal range of motion sensing and motion perception. [Research Support, Non-U.S. Gov't]. *Vision Res.* 30, 615–619. doi: 10.1016/0042-6989(90)90072-S

Habak, C., and Faubert, J. (2000). Larger effect of aging on the perception of higher-order stimuli. *Vision Res.* 40, 943–950. doi: 10.1016/S0042-6989(99)00235-7

Holliday, I. E., and Anderson, S. J. (1994). Different processes underlie the detection of second order motion at low and high temporal frequencies. *Proc. R. Soc. Lond. B Biol. Sci.* 257, 165–173. doi: 10.1098/rspb.1994.0111

Hutchinson, C. V., Arena, A., Allen, H. A., and Ledgeway, T. (2012). Psychophysical correlates of global motion processing in the aging visual system: a critical review. [Review]. *Neurosci. Biobehav. Rev.* 36, 1266–1272. doi: 10.1016/j.neubiorev.2012.02.009

Jackson, G. R., Owsley, C., and McGwin, G. Jr. (1999). Aging and dark adaptation. *Vision Res.* 39, 3975–3982. doi: 10.1016/S0042-6989(99)00092-9

Kennedy, G. J., Tripathy, S. P., and Barrett, B. T. (2009). Early age-related decline in the effective number of trajectories tracked in adult human vision. *J. Vis.* 9, 21.1–21.10. doi: 10.1167/9.2.21.

Kline, D. W., Schieber, F., Abusamra, L. C., and Coyne, A. C. (1983). Age, the eye, and the visual channels: contrast sensitivity and response speed. *J. Gerontol.* 38, 211–216. doi: 10.1093/geronj/38.2.211

Kramer, A. F., and Kray, J. (2006). "Aging and attention," in *Lifespan Cognition: Mechanisms of Change*, eds E. Bialystok and F. I. M. Craik (Oxford; Toronto: Oxford University Press), 57–69. doi: 10.1093/acprof:oso/9780195169539.003.0005

Kramer, A. F., and Madden, D. J. (2008). "Attention," in *The Handbook of Aging and Cognition*, 3rd edn, eds F. I. M. Craik and T. A. Salthouse (New York, NY: Psychology Press), 189–249.

Lagacé-Nadon, S., Allard, R., and Faubert, J. (2009). Exploring the spatiotemporal properties of fractal rotation perception. [Comparative Study Research Support, Non-U.S. Gov't]. *J. Vis.* 9:3. doi: 10.1167/9.7.3

Legault, I., Troje, N. F., and Faubert, J. (2012). Healthy older observers cannot use biological-motion point-light information efficiently within 4 m of themselves. *Iperception* 3, 104–111. doi: 10.1068/i0485

Levitt, H. (1971). Transformed up-down methods in psychoacoustics. *J. Acoust. Soc. Am.* 49(Suppl. 2:467+). doi: 10.1121/1.1912375

Lu, Z.-L., and Sperling, G. (1995). The functional architecture of human visual motion perception. *Vision Res.* 35, 2697–2722. doi: 10.1016/0042-6989(95)00025-U

Lu, Z.-L., and Sperling, G. (2001). Three-systems theory of human visual motion perception: review and update.[see comment][erratum appears in *J. Opt. Soc. Am. A Opt. Image. Sci. Vis.* 2002;19, 413]. *J. Opt. Soc. Am. A Opt. Image Sci. Vis.* 18, 2331–2370. doi: 10.1364/JOSAA.18.002331

McIntosh, A. R., Sekuler, A. B., Penpeci, C., Rajah, M. N., Grady, C. L., and Sekuler, R. (1999). Recruitment of unique neural systems to support visual memory in normal aging. *Curr. Biol.* 9, 1275–1278. doi: 10.1016/S0960-9822(99)80512-0.

Morrison, J. D., and McGrath, C. (1985). Assessment of the optical contributions to the age-related deterioration in vision. *Q. J. Exp. Physiol.* 70, 249–269.

Owsley, C., Sekuler, R., and Siemsen, D. (1983). Contrast sensitivity throughout adulthood. *Vision Res.* 23, 689–699. doi: 10.1016/0042-6989(83)90210-9

Raghuram, A., Lakshminarayanan, V., and Khanna, R. (2005). Psychophysical estimation of speed discrimination. II. Aging effects. *J. Opt. Soc. Am. A. Opt. Image Sci. Vis.* 22, 2269–2280. doi: 10.1364/JOSAA.22.002269

Roudaia, E., Bennett, P. J., Sekuler, A. B., and Pilz, K. S. (2010). Spatiotemporal properties of apparent motion perception and aging. *J. Vis.* 10, 1–15. doi: 10.1167/10.14.5

Seiffert, A. E., and Cavanagh, P. (1999). Position-based motion perception for color and texture stimuli: effects of contrast and speed. *Vision Res.* 39, 4172–4185. doi: 10.1016/S0042-6989(99)00129-7

Sekuler, A. B., Bennett, P. J., and Mamelak, M. (2000). Effects of aging on the useful field of view. *Exp. Aging Res.* 26, 103–120. doi: 10.1080/036107300243588

Sekuler, R., McLaughlin, C., and Yotsumoto, Y. (2008). Age-related changes in attentional tracking of multiple moving objects. [Research Support, N.I.H., Extramural]. *Perception* 37, 867–876. doi: 10.1068/p5923

Smith, A. T. (1994). Correspondence-based and energy-based detection of second-order motion in human vision. *J. Opt. Soc. Am. A Opt. Image Sci. Vis.* 11, 1940–1948. doi: 10.1364/JOSAA.11.001940

Smith, A. T., and Ledgeway, T. (1997). Separate detection of moving luminance and contrast modulations: fact or artifact? *Vision Res.* 37, 45–62. doi: 10.1016/S0042-6989(96)00147-2

Tang, Y., and Zhou, Y. (2009). Age-related decline of contrast sensitivity for second-order stimuli: earlier onset, but slower progression, than for first-order stimuli. [Research Support, Non-U.S. Gov't]. *J. Vis.* 9, 18. doi: 10.1167/9.7.18

Trick, L. M., Perl, T., and Sethi, N. (2005). Age-related differences in multiple-object tracking. [Comparative Study Research Support, Non-U.S. Gov't]. *J. Gerontol. B Psychol. Sci. Soc. Sci.* 60, P102–P105. doi: 10.1093/geronb/60.2.P102

Tulunay-Keesey, U., Ver Hoeve, J. N., and Terkla-McGrane, C. (1988). Threshold and suprathreshold spatiotemporal response throughout adulthood. *J. Opt. Soc. Am. A* 5, 2191–2200. doi: 10.1364/JOSAA.5.002191

Ukkonen, O. I., and Derrington, A. M. (2000). Motion of contrast-modulated gratings is analysed by different mechanisms at low and at high contrasts. *Vision Res.* 40, 3359–3371. doi: 10.1016/S0042-6989(00)00197-8

Weale, R. A. (1975). Senile changes in visual acuity. *Trans. Ophthalmol. Soc. U.K.* 95, 36–38.

Wilson, H. R., Ferrera, V. P., and Yo, C. (1992). A psychophysically motivated model for two-dimensional motion perception. *Vis. Neurosci.* 9, 79–97. doi: 10.1017/S0952523800006386

Conflict of Interest Statement: The authors declare that the research was conducted in the absence of any commercial or financial relationships that could be construed as a potential conflict of interest.

Received: 26 October 2012; accepted: 22 June 2013; published online: 15 July 2013.

Citation: Allard R, Lagacé-Nadon S and Faubert J (2013) Feature tracking and aging. Front. Psychol. ***4****:427. doi: 10.3389/fpsyg.2013.00427*

This article was submitted to Frontiers in Perception Science, a specialty of Frontiers in Psychology.

frontiers in PSYCHOLOGY

ORIGINAL RESEARCH ARTICLE
published: 03 September 2013
doi: 10.3389/fpsyg.2013.00579

Macular degeneration affects eye movement behavior during visual search

Stefan Van der Stigchel[1]*, Richard A. I. Bethlehem[1], Barrie P. Klein[1], Tos T. J. M. Berendschot[2], Tanja C. W. Nijboer[1,3] and Serge O. Dumoulin[1]

[1] Experimental Psychology, Helmholtz Institute, Utrecht University, Utrecht, Netherlands
[2] University Eye Clinic Maastricht, Maastricht, Netherlands
[3] Rudolf Magnus Institute of Neuroscience and Centre of Excellence for Rehabilitation Medicine, University Medical Centre Utrecht and Rehabilitation Centre De Hoogstraat, Utrecht, Netherlands

Edited by:
Mark W. Greenlee, University of Regensburg, Germany

Reviewed by:
Jens Schwarzbach, Trento University, Italy
William Seiple, Lighthouse International, USA

***Correspondence:**
Stefan Van der Stigchel, Experimental Psychology, Helmholtz Institute, Heidelberglaan 2, 3584 CS Utrecht, Netherlands
e-mail: s.vanderstigchel@uu.nl

Patients with a scotoma in their central vision (e.g., due to macular degeneration, MD) commonly adopt a strategy to direct the eyes such that the image falls onto a peripheral location on the retina. This location is referred to as the preferred retinal locus (PRL). Although previous research has investigated the characteristics of this PRL, it is unclear whether eye movement metrics are modulated by peripheral viewing with a PRL as measured during a visual search paradigm. To this end, we tested four MD patients in a visual search paradigm and contrasted their performance with a healthy control group and a healthy control group performing the same experiment with a simulated scotoma. The experiment contained two conditions. In the first condition the target was an unfilled circle hidden among c-shaped distractors (serial condition) and in the second condition the target was a filled circle (pop-out condition). Saccadic search latencies for the MD group were significantly longer in both conditions compared to both control groups. Results of a subsequent experiment indicated that this difference between the MD and the control groups could not be explained by a difference in target selection sensitivity. Furthermore, search behavior of MD patients was associated with saccades with smaller amplitudes toward the scotoma, an increased intersaccadic interval and an increased number of eye movements necessary to locate the target. Some of these characteristics, such as the increased intersaccadic interval, were also observed in the simulation group, which indicate that these characteristics are related to the peripheral viewing itself. We suggest that the combination of the central scotoma and peripheral viewing can explain the altered search behavior and no behavioral evidence was found for a possible reorganization of the visual system associated with the use of a PRL. Thus the switch from a fovea-based to a PRL-based reference frame impairs search efficiency.

Keywords: visual search, macular degeneration, eye movements, preferred retinal location, saccades

INTRODUCTION

Macular vision is important for tasks that involve high spatial acuity, such as reading and recognizing faces. When central vision is damaged, e.g., due to macular degeneration (MD), people will miss this location of high visual acuity and therefore experience problems with these high-acuity tasks. Both juvenile and age-related MD exist. The juvenile form of MD occurs in 1 out of 10,000 people (Bither and Berns, 1985), whereas age-related MD is the main cause of diminished visual acuity in the elderly (Leibowitz et al., 1980). In its advanced stage, MD creates a central visual field scotoma. Therefore, MD patients typically adopt a strategy to direct the eyes such that the image falls onto a peripheral location on the retina to compensate for their impairment: a location on the retina which is not part of the scotoma and which functions as a "pseudo-fovea" (Timberlake et al., 1986, 1987; Whittaker et al., 1988; Fletcher et al., 1999). Currently, there is a debate whether this strategy coincides with a reorganization of the visual system (Baker et al., 2005, 2008; Masuda et al., 2008).

Similarly, the oculomotor system needs to adapt to this PRL as well. Eye movements bring regions of interest toward the fovea. In MD a PRL-based reference frame replaces the fovea-centered reference frame. Therefore, eye movements in MD patients might be expected to be less effective than in normally sighted people. Although previous studies have indicated that a shift of oculomotor reference to a non-foveal location is indeed possible, eye movements using this new oculomotor reference are generally associated with prolonged initiation latencies and decreased accuracy (White and Bedell, 1990; Whittaker et al., 1991). Furthermore, the fixation ability is known to be impaired when a new oculomotor reference frame is adopted, although this ability can be trained resulting in improved reading abilities (Tarita-Nistor et al., 2009).

Whereas previous studies have examined the oculomotor behavior of the PRL in reading tasks in detail (McMahon et al., 1991; Fletcher et al., 1999; Lingnau et al., 2008; Chung, 2011; Nguyen et al., 2011), very little is known about the characteristics

of oculomotor behavior in other tasks such as visual search. Reading is a specific oculomotor task, which includes numerous constraints such as the horizontal lay-out of a text and the small saccades associated with foveating words. We suggest that visual search can be considered a more naturalistic viewing task, which requires more exploratory oculomotor behavior. Knowledge about the oculomotor behavior of the PRL, such as saccade amplitude and search times, in visual search tasks might therefore unravel the characteristics of the eye movement pattern in daily life situations that do not require reading. Although previous studies have revealed that visual search is impaired in persons with a visual impairment, including age-related MD (Kuyk et al., 2005; MacKeben and Fletcher, 2011), the underlying oculomotor behavior specific to the PRL remains unclear.

The aim of the current study was to examine the oculomotor search behavior of MD patients with a new oculomotor reference frame. To this end, four patients with a stable PRL due to juvenile MD participated in a search task while their eye movements were recorded. The performance of this group during visual search was quantified in terms of search time, saccade amplitudes and number of saccades needed to bring the target to the PRL. This performance was compared to the search behavior of a group of normally sighted participants and a group of normally sighted participants who performed the task with a simulated central scotoma (and therefore viewed the search array with their peripheral vision, Henderson et al., 1997). This way, we were able to compare the PRL-based reference frame with a fovea-based reference frame either using the fovea or a peripheral location. Previous studies have revealed that inducing a simulated central scotoma in normally sighted participant induces impairments in visual search tasks, such as increase in search time and fixation duration (Bertero, 1988; Cornelissen et al., 2005; McIlreavy et al., 2012) and a decrease of search facilitation for repeated displays (Geringswald et al., 2012). To compare the search behavior in different types of visual search, the experiment contained two conditions: in the first condition the target was an unfilled circle hidden among c-shaped distractors of equal size (serial condition) and in the second condition the target was a filled circle (pop-out condition). These two search conditions are associated with different search behavior in that the serial condition will result in slow and serial search, whereas the pop-out condition will result in rapid, parallel search (Van der Stigchel et al., 2009). This pop-out condition will unravel whether fast parallel visual search is still possible when a new oculomotor reference frame is adopted.

METHODS

PARTICIPANTS

Four patients with central vision loss participated in the experiment: Cases 1, 2, 3, and 4 (**Table 1**). Ten healthy controls (age 29.9 ± 10.0, 4 males) participated in the visual search task. Five healthy controls (age 25.2 ± 1.3, 3 males) were recruited to perform a visual search task with an online scotoma simulation. The participants gave informed consent and this study was approved by the ethical committee of the University Medical Center Utrecht.

EQUIPMENT

We used a Iiyama CRT display monitor (subtending $36.83 \times 27.62°$; refresh rate 60 Hz), driven by a Dell Precision PWS390 computer for all experiments. The contrast was kept as high as possible to enhance visibility. Eye movements of the dominant eye were registered with a sampling frequency of 1000 Hz using the Eyelink 1000 infrared eye-tracker (Desktop Mount; SR Research Ltd.). Thresholds for detecting the onset of a saccadic movement were acceleration of $8000°/s^2$ and a velocity of 30°/s.

STIMULUS AND PROCEDURE

Prior to the experiment, the participants' dominant eye was determined using a visual alignment task (Porac and Coren, 1976). Participants sat in front of the computer monitor with their eyes at a distance of 57 cm from the screen, while their chin rested in a chin rest. Each participant was given a verbal explanation of the tasks they were about to perform. The experiment started directly after calibration of the eye-tracker. Using a nine-point grid calibration participants were asked to fixate on the calibration dots. In the case of the MD-group, participants were explicitly instructed to try and see the dot as clear as possible. During the calibration procedure the calibration was validated by presenting the nine calibration points again. The calibration was only successful with a small error between the two presentations for each calibration point ($<1°$). This procedure ensures that patients were using the same retinal location during calibration for a specific calibration point. Because patients were viewing a calibration point consistently with the same retinal location, we assume that patients were fixating with their PRL.

Before each experimental procedure started, participants were given eight practice trials. Each trial started with a drift check. Only trials with an oculomotor drift smaller than 2° were

Table 1 | Patient descriptives.

Patient	Gender	Diagnosis	Age (year)	Age diagnosis (year)	Dominant eye	PRL Eccentricity
Case 1	Female	Stargardt	29	12	Left	15.5°
Case 2	Male	Stargardt	23	9	Left	2.3°
Case 3	Male	Stargardt	47	40	Right	10.9°
Case 4	Female	Stargardt	21	8	Left	
Case 5	Female	Stargardt	31	15	Right	
Case 6	Female	Stargardt	29	9	Left	
Case 7	Female	Stargardt	19	17	Right	

accepted. Directly after the drift check, the trial started[1]. The targets and distractors in all tasks were black and projected on a white background (80.9 cd/m^2). The Michelson contrast was 98%.

VISUAL FIELD AND SLO MEASUREMENT

A visual field test was used to check if participants in the MD group indeed suffered from a central scotoma. In this visual field test, only one target at a time was shown and a fixation cross was used which remained on screen during presentation of the target. The target was a 1.5° circle and could appear at 33 possible stimulus locations. The 33 locations were organized in five rows; three rows consisted of seven locations and two rows of six locations, corresponding to the target locations used in the visual search paradigm discussed later. Participants were instructed to remain fixated on the fixation cross and report, using the "z" and "/" keys, whether they had seen a target or not. After their response a confirmation of their choice was presented on screen. Target present trials were mixed with "catch" trials in which no target was presented. All target locations were presented four times along with 16 catch trials, making for 148 trials in total. The visual field test confirmed that all MD patients suffered a partial scotoma; all patients reported to have not seen a target for certain locations tested in the visual field test. No patient reported false positives. In one case (Case 3) the visual field test was not useful in clearly determining the scotoma, because the loss of vision was not limited to a specific quadrant (see **Figure 1**).

Furthermore, in order to gain information about fixation stability and absolute locus of the PRL, the MD patients were invited for a Scanning Laser Ophthalmoscope (SLO) measurement at the University Eye Clinic Maastricht. We used a home build SLO with the ability to modulate the laser intensity (Ossewaarde-Van Norel et al., 2002) which enabled us to project a fixation cross in the raster pattern. To determine the absolute location of the PRL at the retina and its stability, 60 SLO images per patient were acquired with the use of a frame grabber, having a 1 sec interval in between. The SLO measurement showed clear peripheral fixation. One case (Case 4) was unable to participate in an SLO measurement due to technical difficulties. For the three remaining cases, fixation stability was, on average, within 1.2° standard deviation of the fixation point. **Figure 1** shows the results from the visual field test and SLO measurement.

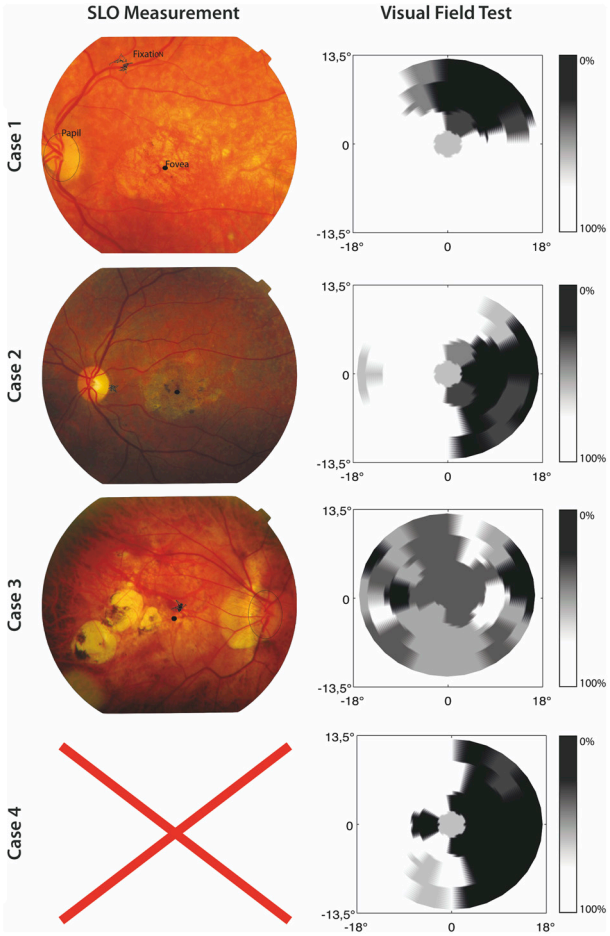

FIGURE 1 | SLO Measurement and results of the visual field test for the included MD patients. The left panel shows SLO pictures where fixation, fovea, and papilla are marked. No SLO measurement was possible for Case 4. For the results of the visual field test the gray scale indicates the percentage correctly identified targets.

VISUAL SEARCH TASK

The stimulus for the visual search task consisted of a visual search field with 32 c-shaped distractors and one target. There were two conditions, the target being either a circle or a dot, see **Figure 2**. Both the location of the target and the orientation of the opening of the C's varied for each trial. The openings of the C's could be oriented toward the top (0°), right (90°), bottom (180°), or left (270°). The objects were organized in the same manner as the visual field paradigm. The target could appear at all locations except the center location and the six locations around the center. The target could therefore appear at 26 locations. The objects were 1.5° wide, and the C's and the target circles' rim size was 0.1°. The target dots had the same size as the C's and the target circles, but were filled. The size of the gaps of the C's was 0.93°. The objects were placed at a center-to-center distance of 5°. This was the case within the rows as well as between the rows. The search field was presented 100 ms after the drift correction. During the 100 ms interval a white screen was presented. Participants were instructed to find the target as soon as possible. They were explicitly instructed to fixate on the target as soon as they found it. When they had found the target, participants pressed the space bar to continue to the next trial. Every target-type was used two times on every target location. In total the visual search task contained 110 trials.

A separate group of healthy controls participated in a scotoma simulation version of the visual search task. In this version of the visual search task the center of the visual field was occluded online

[1]Although the drift check failed more frequently in the MD group than the other groups (17 vs. 2%, respectively), search latency in the MD group did not differ between trials in which the drift check failed and trials in which the drift check was immediately successful (p's > 0.25).

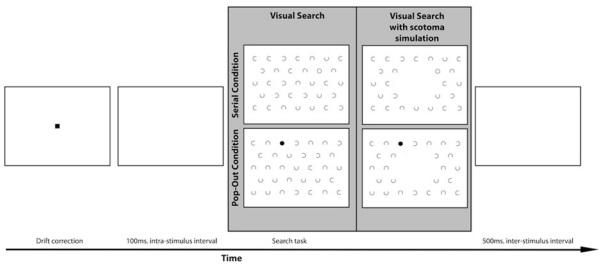

FIGURE 2 | Lay-out of the visual search paradigm with an example of a trial in both the serial and the pop-out condition. The gray panel shows an example of a search display for the MD and the control group on the left. Participants in the simulation group performed the visual search task with a simulated central scotoma, as indicated on the right of the gray panel.

with a 10° disc that had the same luminance and color as the background to simulate a central scotoma. Targets could also appear inside the area of simulated scotoma with equal probability as the other areas in the search array. After calibration of the eye-tracker this dot "followed" the participant's eye movement in real-time continuously occluding their center of vision, see **Figure 2**.

DATA ANALYSIS

Saccades were detected off-line and only saccades larger than 0.5° were accepted. In the visual search analysis, saccades larger than 40° were excluded from the analysis, because this is larger than the search field. Only trials were accepted in which a saccade was made onto the target. A saccade on the target was defined as a saccade that ended on a location within a radius of 1.97° of the center of the target. Trials on which a saccade was made within 80 ms after stimulus presentation were also excluded from further analysis. Trials for which the total search latencies exceeded two standard deviations from the subject mean were also excluded. This led to an average exclusion of 4.0% of the trials in the control group, 6.7% in the MD group and 14.4% in the simulation group. For the remaining trials search latency was analyzed as the primary measure. Search latency is defined as the time between stimulus onset and the moment the eye landed on the target. In addition to search latency, saccade amplitudes, number of saccades, and inter-saccade-interval of all saccades until the target was found were analyzed.

One-Way repeated measures ANOVA was used to determine main group (Control × Simulation × MD) effects for both conditions separately. Where Levene's test for homogeneity of variances indicated that homoscedascity was violated, Brown–Forsythe robust test for equality of means was used instead. *Post-hoc t*-tests with Bonferroni correction for multiple comparisons were used to make *post-hoc* group comparisons.

RESULTS

SEARCH LATENCY

Results show that search latency, defined as the time required to find a target, was longer in the MD group. Brown–Forsythe robust test for equality of means indicated a trend level effect of group on search latency in the *serial condition*, $F_{(2,\ 3.074)} = 8.733$, $p = 0.054$. *Post-hoc* tests revealed that the control group had significantly shorter response latencies in the serial condition compared to the MD group ($p < 0.001$), see **Figure 3**. Individual subjects are shown in **(C,D)**. The group that performed the scotoma simulation test also indicated faster responses compared to the MD group ($p < 0.01$). There were no differences in search latency in the serial condition between the control group and simulation group. Brown–Forsythe robust test for equality of means also indicated a significant main effect of group on search latency in the *pop-out condition*, $F_{(2,\ 7.711)} = 20.365$, $p < 0.01$. *Post-hoc* tests revealed that the controls were significantly faster than the MD group ($p < 0.001$) and also faster than people that performed the simulation ($p < 0.05$). Additionally the MD group was significantly slower than the simulation group ($p < 0.01$).

The search latency of the MD group was longer than the control group and simulation group. Based on signal detection theory this may be caused by either a decreased sensitivity or a change in response bias. The latter case may be interpreted as the MD subjects being more "careful" to compensate for their loss in visual acuity. To make sure that these differences in search latency did not originate from a change in response bias a second experiment was performed. In this second visual search paradigm a condition without any target was added to the experimental design and participants were asked to press "z" or "/" on a keyboard to indicate whether the target was present or absent, respectively. Cases 4, 5, 6, and 7 (listed in **Table 1**) participated in this experiment. Signal detection theory measures were calculated for this second experiment. These indicated that there were no significant differences between the control group (mean $d' = -0.21$; st. dev. $= 0.23$) and the MD group (mean $d' = -0.05$; st. dev. $= 0.15$) on choice sensitivity [paired samples *t*-test: $t_{(6)} = 1.196$, $p = 0.277$] nor on bias [$t_{(6)} = 1.036$, $p = 0.340$]. This control experiment indicated that there was no change in response bias, and that the differences in search latency between the control and the MD group can be attributed to decreased sensitivity.

Given that the differences in search latency could not be explained by a selection bias, the oculomotor search behavior was explored to reveal which characteristics caused the increased search latency in the MD group. Here, we examined saccade amplitude, number of saccades needed to foveate the target and the intersaccadic interval.

SACCADE AMPLITUDE

The amplitude of saccades for the MD group was similar to both control groups in the *serial* condition, but not in the *pop-out* condition. Brown–Forsythe indicated no main group effect on average saccade amplitude in the *serial condition*. There was a main effect of group on average saccade amplitude in the *pop-out condition* as apparent from One-Way repeated measures ANOVA, $F_{(2,\ 17)} = 4.210$, $p < 0.05$, see **Figures 4A,B**. *Post-hoc* tests indicated a trend that the control group made larger saccadic movement than the MD group in the *pop-out condition* ($p = 0.068$). There was no significant difference between the control and the simulation group in the *pop-out condition*. There was a trend level difference between the MD group and the simulation group, revealing that the MD group made, on average, smaller saccadic movements ($p = 0.056$).

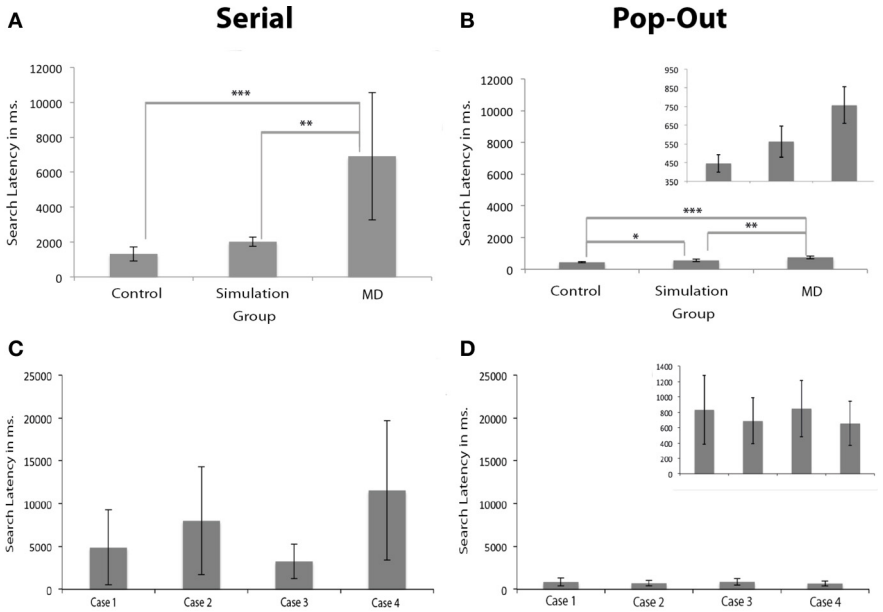

FIGURE 3 | Search latencies in visual search. (A,B) Show the search latencies for the *serial* and *pop-out* condition. Error bars represent the groups standard deviation. **(C,D)** Show the individual search latencies for Cases 1 to 4 (here, error bars represent individual standard deviations). The figures for the pop-out condition are presented twice: once with the same range as the serial condition and once with an adapted range for visibility of the differences between the groups and the individual subjects. The MD group had longer search latencies than the simulation and the control group, irrespective of whether the target was presented in the scotoma. Significant differences are marked (± meaning a trend level *p*-value, $^{*}p < 0.05$, $^{**}p < 0.01$, and $^{***}p < 0.001$).

NUMBER OF SACCADES TO TARGET

MD patients needed a higher number of saccades to find the target. Brown–Forsythe tests indicated a significant effect of group on number of saccades to a target $F_{(2,\ 3.354)} = 9.243$, $p < 0.05$ in the *serial condition*, see **Figure 4C**. *Post-Hoc* tests indicated that the control and the simulation group needed significantly fewer saccades than the MD group ($p < 0.001$ and $p < 0.01$ respectively). One-Way repeated measures ANOVA also revealed a main effect of group on number of saccades to target in the *pop-out condition*, $F_{(2,\ 17)} = 23.713$, $p < 0.001$, see **Figure 4D**. *Post-hoc* tests indicated that the MD group needed more saccades to find a target compared to the control group ($p < 0.001$) and the simulation group ($p < 0.01$).

INTER SACCADIC INTERVAL

Compared to the control group, the inter saccadic interval was significantly longer in the simulation group in both conditions. In the *serial* condition the MD group also showed longer saccadic intervals. Brown–Forsythe tests indicated a significant main effect of group on inter-saccadic-interval $F_{(2,\ 4.795)} = 9.373$, $p < 0.05$ in the *serial condition*. *Post-Hoc* tests reveal that in the *serial condition* the simulation group had significantly longer inter-saccadic-intervals compared to the control group ($p < 0.01$), see **Figure 4E**. Compared to the control group, the MD group also had a significantly longer inter-saccadic-interval ($p < 0.01$). In the *pop-out condition* One-Way repeated measures ANOVA indicated a significant effect, $F_{(2,\ 17)} = 37.470$, $p < 0.001$, **Figure 4F**. *Post-Hoc* tests revealed that in this condition the simulation group used longer intervals than the control ($p < 0.001$) and the MD group ($p < 0.01$).

SACCADE DIRECTION

In addition to the measures described above we also set out to analyse if the saccade amplitude was different for saccades directed toward the scotomous area compared to saccades moving away from the scotoma. In three patients we could clearly and reliably define one or two quadrants of the visual field as scotomous (see **Figure 5**). Within each participant and each condition we compared saccades toward and away from the scotomous area. For saccade amplitude, both Case 1 and Case 4 had larger saccade amplitudes away from the scotoma compared to saccades towards the saccade amplitude in the *serial condition* [for Case 4; $t_{(1376)} = -3.34$, $p < 0.001$, for Case 1; $t_{(580)} = -4.66$, $p < 0.001$]. There were no significant differences in the *pop-out condition* for any of the patients.

DISCUSSION

The aim of the present study was to examine the oculomotor behavior of MD patients who developed a stable PRL to explore the visual world. To this end, four MD patients participated in a visual search experiment. Their performance was compared to a control group and a control "simulation" group in which a central scotoma was simulated. Search performance was impaired for MD patients: the search latency, the time necessary to locate and foveate the target, was longer for the MD group than for the control group. This was observed for both the serial and the pop-out

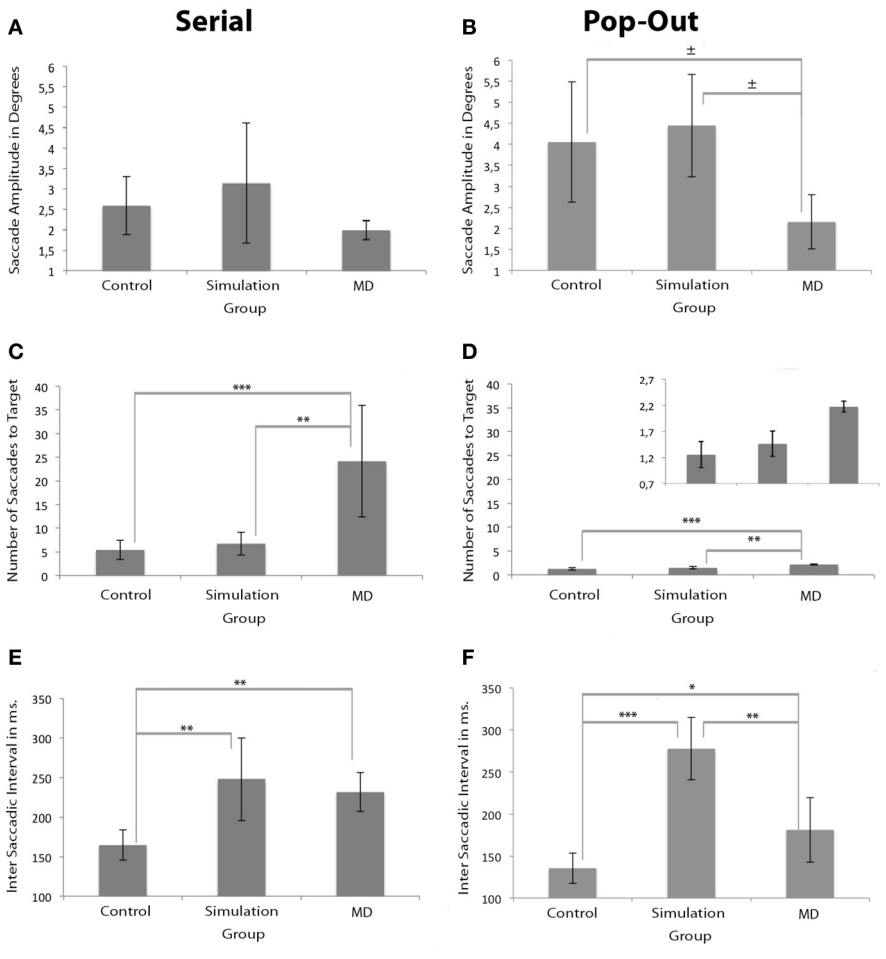

FIGURE 4 | Measurements of oculomotor characteristics. Left and right panels show the results for the serial and pop-out conditions. **(A,B)** Show saccade amplitudes. **(C,D)** Show the number of saccades before the eye landed on the target for both conditions. The figure of the number of saccades for the pop-out condition is presented twice: once with the same range as the serial condition and once with an adapted range for visibility of the differences between the groups. **(E,F)** Show the inter-saccade-interval in milliseconds for both conditions. Significant differences are indicated ($^{*}p < 0.05$, $^{**}p < 0.01$, and $^{***}p < 0.001$; $^{\pm}0.05 > p < 0.07$).

search conditions. Although participants in the simulation group were somewhat slower than the control group, this group outperformed the MD group in both the serial and the pop-out search conditions. Control experiments indicated that the differences in search latency between the control and the MD group were not caused by a difference in selection bias.

To investigate the source of the slowing in visual search in MD patients, oculomotor behavior in the search task was divided in three separate measures: saccade amplitude, the number of saccades needed to foveate the target and the intersaccadic interval (i.e., the time in between fixations). With respect to saccade amplitude, no differences were observed in the serial condition between the different groups. However, when taking saccade direction into account relative to the scotoma, saccades toward the scotoma had a smaller amplitude than saccades away from the scotoma. This effect was observed in two of the three cases in which this analysis was possible. Thus saccade amplitude seems affected in a direction-specific manner, an effect lost when pooling over all directions. In the pop-out condition, MD search behavior was also associated with smaller saccadic amplitudes. No effect of saccade direction was found, but this might have been a power issue as the total number of saccades in the pop-out search condition was much lower than in the serial search condition. In short, MD search behavior is associated with smaller saccade amplitudes.

When examining the number of saccades, the results indicated that the MD group made more saccades, both in the pop-out and the serial condition. Finally, the intersaccadic interval was longest in the MD and the simulation group compared to the control group. These results were most reliable in the serial condition, as the pop-out search condition only indicated a main effect at a trend level. In short, we attribute the increased search latencies in MD to decreased saccadic amplitudes, increased number of saccades and increased saccadic intervals.

The simulation group cannot be considered the ideal comparison to the behavior observed in the MD group. Firstly, the

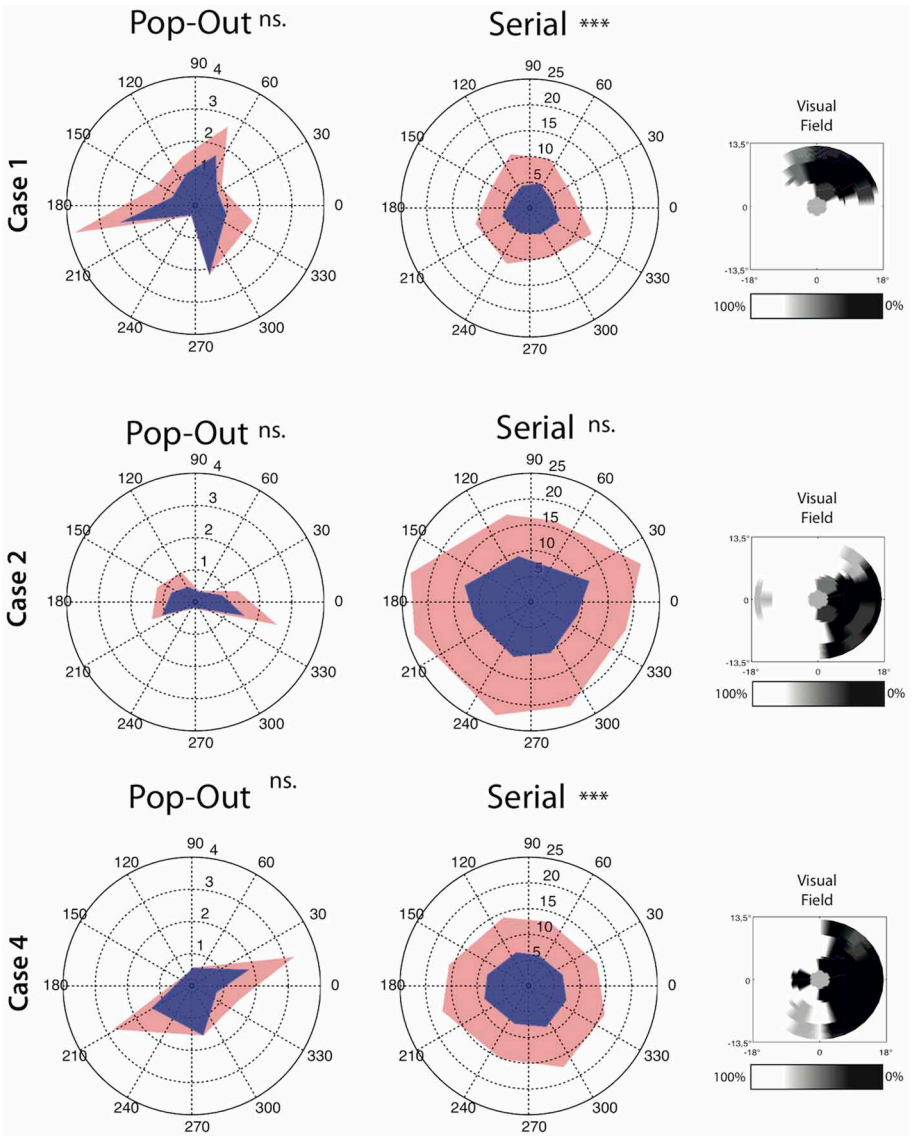

FIGURE 5 | Average angle by direction characteristics for all saccades for each condition separately. Saccade amplitude is depicted as the radius whereas the angle represent the direction of the saccades. Upper confidence interval is plotted in light-red on top of the average saccade amplitude. Note that the left and middle panel have a different range. The right panel for each case depict the interpolated scotoma based on measurements from the visual field test. Cases 1 and 4 show lower saccade amplitude toward the scotoma than away from the scotoma in the serial search condition. Significant differences are indicated (***$p < 0.001$, ns. = non-significant).

scotoma is always visible to control subjects which might influence oculomotor programming. Secondly, MD is not only associated with a central scotoma (absolute scotoma), but will also affect regions beyond the scotoma to various degrees (relative scotoma). Thirdly, the location of the PRL might not be the location of highest acuity on the residual retina (Shima et al., 2010). This was also reflected in the oculomotor behavior of the MD group: although they have developed a new oculomotor reference frame, search latency was longer than the simulation group. If the sole difference between the simulation and the MD group was the central scotoma, one might expect the MD group to outperform the simulation group, because the MD group has more experience with viewing the visual world with a central scotoma than the simulation group. As this was not observed, we suggest that part of the overall slowing in search performance is due to more diffuse impairments of retinal functions. Besides the diffuse loss of retinal function, the search time is also increased by the presence of a central—absolute—scotoma: the simulation group was slower than the control group, most prominently in the pop-out condition.

In line with the previous observation that the absolute scotoma affects search performance, some of the MD participants made saccades with shorter amplitudes toward the scotoma than away from the scotoma. This can be explained by the fact that

visual information projected to the scotomous region is not being transferred to the oculomotor system. The "selection for-action" view (Schneider and Deubel, 1995, 2002) argues that the function of spatial attention is to provide a spatial code to the eye movement system to program the subsequent eye movement. As spatial attention cannot be allocated to the scotomous region, a bias might therefore develop to not make eye movement toward the scotomous region, resulting in saccades with shorter amplitudes which still land outside the region of the visual field previously subserved by the scotoma. The shorter amplitudes in the MD group might also be related to the increased number of eye movements necessary to find the target; with shorter eye movements, it takes more saccades to make a complete search of the visual field.

The idea that spatial attention cannot be allocated to the scotomous region is reminiscent of a study in which normal-sighted participants performed a visual search task while vision was restricted to a gaze-contingent viewing window (Lingnau et al., 2010). This study varied the location of the viewing window and found no specific part of the visual field or gaze direction for which performance on the visual search task was most beneficial. Interestingly, however, performance on the visual search task was directly related to the location of the viewing window and the direction of visual attention: there was an impaired performance when visual attention and gaze had to be moved in opposite directions. In line with our results, this appears to indicate that there is a direct interplay between the direction of visual attention and the location of the scotoma.

As our eye tracker was calibrated with respect to the macula in the simulation group and they did not have a stable PRL, a similar analysis could not be performed for the simulation group and it was impossible to disentangle between eye movements toward and away from the scotoma. However, as no overall decrease in saccade amplitude was observed in the simulation group compared to the control group, it is possible that this decrease in saccade amplitude is restricted to the MD group. We speculate that it could be beneficial to make saccades with a higher amplitude toward the scotoma, because this will bring more visual information from the scotoma to the region with detailed vision. Future studies focusing on training oculomotor behavior in MD patients might include this factor to investigate whether this is truly beneficial or whether the observed shorter saccades is the most optimal solution.

The intersaccadic interval observed in the MD group was similar to the interval observed in the simulation group, whereas both groups had longer intervals compared to the control group. This result therefore seems to be specific to peripheral processing of the target. The periphery may need more time to process the stimulus information than the fovea. Interestingly, the overall decrease in visual acuity in the MD group is expected to result in an even longer interval as it is expected to take longer to process visual information when visual acuity in the periphery is low than when visual acuity is high, like in the simulation group. The comparable interval between the MD and the simulation group might therefore be the result of a large amount of experience using the PRL for MD patients.

Our results reveal no evidence for the claim that the use of a PRL coincides with a reorganization of the visual system (Baker et al., 2005, 2008; Masuda et al., 2008). Presumably, if the adult visual system has compensatory mechanisms to cope with adventitious loss, its ultimate goal would be to have beneficial behavioral consequences. Reorganization and in particular access of the PRL to fovea-based cortical processing units might have resulted in an improved search performance of the MD patients with respect to the simulation group, who have no experience with a central scotoma. This was not observed. This conclusion should be regarded with caution, however, as the simulation group had no peripheral retinal impairments, in contrast to the MD patients. Thus any possible benefit from a reorganization of the visual system was not able to overcome the impaired performance associated with the loss of retinal function.

To conclude, search behavior is impaired in MD patients and is associated with saccades with decreased amplitudes toward the scotoma, an increased intersaccadic interval and an increased number of eye movements necessary to locate the target. This suggests that the switch from a fovea-based to a PRL-based reference frame comes at the cost of search efficiency.

ACKNOWLEDGMENTS

This research was funded by a grant from the Dutch MD-foundation.

REFERENCES

Baker, C. I., Dilks, D. D., Peli, E., and Kanwisher, N. G. (2008). Reorganization of visual processing in macular degeneration: replication and clues about the role of foveal loss. *Vis. Res.* 48, 1910–1919. doi: 10.1016/j.visres.2008.05.020

Baker, C. I., Peli, E., Knouf, N., and Kanwisher, N. G. (2005). Reorganization of visual processing in macular degeneration. *J. Neurosci.* 25, 614–618. doi: 10.1523/JNEUROSCI.3476-04.2005

Bertero, J. H. (1988). The effect of simulated scotomas on visual search in normal subjects. *Invest. Ophthalmol. Vis. Sci.* 29, 470–475.

Bither, P. P., and Berns, L. A. (1985). Stargardt's disease: a review of the literature. *J. Am. Optomol. Assoc.* 59, 106–111.

Chung, S. T. L. (2011). Improving reading speed for people with central vision loss through perceptual learning. *Invest. Ophthalmol. Vis. Sci.* 52, 1164–1170. doi: 10.1167/iovs.10-6034

Cornelissen, F. W., Bruin, K. J., and Kooijman, A. C. (2005). The influence of artificial scotomas on eye movements during visual search. *Optom. Vis. Sci.* 82, 27–35.

Fletcher, D. C., Schuchard, R. A., and Watson, G. (1999). Relative locations of macular scotomas near the prl: effect of low vision reading. *J. Rehabil. Res. Dev.* 36, 356–364.

Geringswald, F., Baumgartner, F., and Pollmann, S. (2012). Simulated loss of foveal vision eliminates visual search advantage in repeated displays. *Front. Hum. Neurosci.* 6:134. doi: 10.3389/fnhum.2012.00134

Henderson, J. M., McClure, K. K., Pierce, S., and Schrock, G. (1997). Object identification without foveal vision: evidence from an artificial scotoma paradigm. *Percept.Psychophys.* 59, 323–346. doi: 10.3758/BF03211901

Kuyk, T. K., Liu, L., and Fuhr, P. S. W. (2005). Feature search in persons with severe visual impairment. *Vision Res.* 45, 3224–3234. doi: 10.1016/j.visres.2005.07.019

Leibowitz, H. M., Krueger, D. E., Maunder, L. R., Milton, R. C., Kini, M. M., Kahn, H. A., et al. (1980). The framingham eye study monograph: an ophthalmological and epidemiological study of cataract, glaucoma, diabetic retinopathy, macular degeneration, and visual acuity in a general population of 2631 adults. *Surv. Ophthalmol.* 24, 355–610.

Lingnau, A., Schwarzbach, J., and Vorberg, D. (2008). Adaptive strategies for reading with a forced

retinal location. *J. Vis.* 8:6. doi: 10.1167/8.5.6

Lingnau, A., Schwarzbach, J., and Vorberg, D. (2010). (un-)coupling gaze and attention outside central vision. *J. Vis.* 10, 1–13. doi: 10.1167/10.11.13

MacKeben, M., and Fletcher, D. C. (2011). Target search and identification performance in low vision patients. *Invest. Ophthalmol. Vis. Sci.* 52, 7603–7609. doi: 10.1167/iovs.10-6728

Masuda, Y., Dumoulin, S. O., Nakadomari, S., and Wandell, B. A. (2008). V1 projection zone signals in human macular degeneration depend on task, not stimulus. *Cereb. Cortex* 18, 2483–2493. doi: 10.1093/cercor/bhm256

McIlreavy, L., Fiser, J., and Bex, P. J. (2012). Impact of simulated central scotomas on visual search in natural scenes. *Optom. Vis. Sci.* 89, 1385–1394. doi: 10.1097/OPX.0b013e318267a914

McMahon, T. T., Hansen, M., and Viana, M. (1991). Fixation characteristics in macular disease. *Invest. Ophthalmol. Vis. Sci.* 32, 567–574.

Nguyen, N. X., Stockum, A., Hahn, G. A., and Trauzettel-Klosinski, S. (2011). Training to improve reading speed in patients with juvenile macular dystrophy: a randomized study comparing two training methods. *Acta Ophthalmol.* 89, e82–e88.

Ossewaarde-Van Norel, J., van den Biesen, P. R., van de Kraats, J., Berendschot, T. T., and van Norren, D. (2002). Comparison of fluorescence of sodium fluorescein in retinal angiography with measurements *in vitro*. *J. Biomed. Opt.* 7, 190–198. doi: 10.1117/1.1462034

Porac, C., and Coren, S. (1976). The dominant eye. *Psychol. Bull.* 83, 880–897.

Schneider, W. X., and Deubel, H. (1995). "Visual attention and saccadic eye movements: Evidence for obligatory and selective spatial coupling," in *Eye Movement Research: Mechanism, Processes and Applications*, eds J. M. Findlay, R. Walker, and R. W. Kentridge (Amsterdam: Elsevier Science B. V), 317–324. doi: 10.1016/S0926-907X(05)80027-3

Schneider, W. X., and Deubel, H. (2002). "Selection-for-perception and selection-for-spatial-motor-action are coupled by visual attention: A review of recent findings and new evidence from stimulus-driven saccade control," in *Attention and Performance xix: Common Mechanisms in Perception and Action*, eds W. Prinz and B. Hommel (Oxford: Oxford University Press), 609–627.

Shima, N., Markowitz, S. N., and Reyes, S. V. (2010). Concept of a functional retinal locus in age-related macular degeneration. *Can. J. Ophthalmol.* 45, 62–66. doi: 10.3129/i09-236

Tarita-Nistor, L., Gonzales, E. G., Markowitz, S. N., and Steinbach, M. J. (2009). Plasticity of fixation in patients with central vision loss. *Vis. Neurosci.* 26, 487–494. doi: 10.1017/S0952523809990265

Timberlake, G. T., Mainster, M. A., Peli, E., Augliere, R. A., Essock, E. A., and Arend, L. E. (1986). Reading with a macular scotoma. I. Retinal location of scotoma and fixation area. *Invest. Ophthalmol. Vis. Sci.* 27, 1137–1147.

Timberlake, G. T., Peli, E., Essock, E. A., and Augliere, R. A. (1987). Reading with a macular scotoma: Ii. Retinal locus for scanning text. *Invest. Ophthalmol. Vis. Sci.* 28, 1268–1274.

Van der Stigchel, S., Belopolsky, A. V., Peters, J. C., Wijnen, J. G., Meeter, M., and Theeuwes, J. (2009). The limits of top-down control of visual attention. *Acta Psychologica* 132, 201–212. doi: 10.1016/j.actpsy.2009.07.001

White, J. M., and Bedell, H. E. (1990). The oculomotor reference in humans with bilateral macular disease. *Invest. Ophthalmol. Vis. Sci.* 31, 1149–1161.

Whittaker, S. G., Budd, J., and Cummings, R. W. (1988). Eccentric fixation with macular scotoma. *Invest. Ophthalmol. Vis. Sci.* 29, 268–278.

Whittaker, S. G., Cummings, R. W., and Swieson, L. R. (1991). Saccade control without a fovea. *Vis. Res.* 31, 2209–2218. doi: 10.1016/0042-6989(91)90173-3

Conflict of Interest Statement: The authors declare that the research was conducted in the absence of any commercial or financial relationships that could be construed as a potential conflict of interest.

Received: 16 November 2012; accepted: 12 August 2013; published online: 03 September 2013.

*Citation: Van der Stigchel S, Bethlehem RAI, Klein BP, Berendschot TTJM, Nijboer TCW and Dumoulin SO (2013) Macular degeneration affects eye movement behavior during visual search. Front. Psychol. **4**:579. doi: 10.3389/fpsyg.2013.00579*

This article was submitted to Perception Science, a section of the journal Frontiers in Psychology.

frontiers in
PSYCHOLOGY

ORIGINAL RESEARCH ARTICLE
published: 06 June 2013
doi: 10.3389/fpsyg.2013.00323

Healthy older observers show equivalent perceptual-cognitive training benefits to young adults for multiple object tracking

Isabelle Legault*, Rémy Allard and Jocelyn Faubert

Visual Psychophysics and Perception Laboratory, School of Optometry, Université de Montréal, Montreal, QC, Canada

Edited by:
Allison B. Sekuler, McMaster University, Canada

Reviewed by:
Natasha Sigala, University of Sussex, UK
Karla K. Evans, Harvard Medical School, USA
Patrick J. Bennett, McMaster University, Canada

****Correspondence:***
Isabelle Legault, Visual Psychophysics and Perception Laboratory, School of Optometry, Université de Montréal, 3744 Jean-Brillant, 210-01, Montreal, QC H3T 1P1, Canada
e-mail: isabelle.legault.3@umontreal.ca

The capacity to process complex dynamic scenes is of critical importance in real life. For instance, traveling through a crowd while avoiding collisions and maintaining orientation and good motor control requires fluent and continuous perceptual-cognitive processing. It is well documented that effects of healthy aging can influence perceptual-cognitive processes (Faubert, 2002) and that the efficiency of such processes can improve with training even for older adults (Richards et al., 2006). Here we assess the capacity of older participants to improve their tracking speed thresholds in a dynamic, virtual reality environment. Results show that this capacity is significantly affected by healthy aging but that perceptual-cognitive training can significantly reduce age-related effects in older individuals, who show an identical learning function to younger healthy adults. Data support the notion that learning in healthy older persons is maintained for processing complex dynamic scenes.

Keywords: aging, perceptual-cognitive training, learning, 3D-MOT, attention

INTRODUCTION

In our daily activities, we constantly interact with our environment. This environment is dynamic and requires the integration of various objects, motions, speeds, locations etc. There is ample evidence that the healthy aging process affects visual perceptual processing. Age-related deficits are particularly noticeable when the cognitive processes involved in the integration of information are more complex and require simultaneous assimilation of many aspects of the environment (Faubert, 2002). For example, in order to avoid collisions and be efficient in our displacements while driving, walking down a busy street, or through a crowded shopping center, we must process rapid movement and react quickly. In addition, our attention is distributed to encompass numerous elements simultaneously; for example, crossing the street requires an evaluation of traffic and pedestrian movement dynamics while maintaining a navigational goal. To conduct this efficiently, all the information available in our visual field must be integrated. Researchers report that older adults have difficulty with dividing their attention between a central stimulus and another stimulus simultaneously presented in the peripheral visual field (Ball et al., 1988; Richards et al., 2006) along with processing of complex motion (Habak and Faubert, 2000; Bennett et al., 2007; Tang and Zhou, 2009). This is generally consistent with verbal reports by older individuals that getting older has repercussions on their daily life (Kosnik et al., 1988).

A perceptual-cognitive task of particular relevance for exploring multifocal attention and complex motion information is multiple object tracking (MOT). MOT is a task where the observer is required to simultaneously track multiple moving items among many. The ability of the observer is typically evaluated by the number of elements that can be tracked successfully (Pylyshyn, 1989), and performance decreases with the number of targets (Pylyshyn and Storm, 1988; Yantis, 1992). Furthermore, a recent study has demonstrated that speed is a critical factor that is independent of other events in the scene, such as collisions, number of distractors, and distance between target and distractor (Feria, 2013). Pylyshyn and Storm (1988) proposed the FINST model to explain how people track items. Their model, based on primitive vision mechanisms, suggests that the visual system assigns preattentive indices to each element that works independently (Pylyshyn, 1994). On the other hand, Yantis (1992) proposed that targets are grouped together to form a higher-order perceptual representation or a virtual polygon, which requires a single attentional channel; this grouping is maintained during motion and facilitates tracking. However, more recent work has proposed that the visual system deploys a multifocal attention mechanism to keep track of the moving items (Cavanagh and Alvarez, 2005).

Regardless of the models to explain how people track multiple objects, older observers are less efficient at tracking multiple objects (Trick et al., 2005; Sekuler et al., 2008). Trick et al. (2005) have demonstrated that performance of older observers declines with an increasing number of objects being tracked. In their conditions, the maximum number of items that older adults could track was around three, whereas younger adults could track up to four. They suggested an age-related deficit in either the ability to report item position or to follow the position of multiple items. On the other hand, Sekuler et al. (2008), have suggested that age-related deficits are associated with tracking time, where longer tracking time and higher displacement speed reduce performance in older observers.

A number of questions remain, however, in regards to the perceptual-cognitive abilities of older observers. Some obvious questions are whether older observers' capacity and learning rate differ from that of younger adults. Previous studies on divided attention with the useful field of view (UFOV) have shown that older adults could benefit from training (Ball et al., 2002; Richards et al., 2006; Edwards et al., 2009). However, the UFOV task, although useful for assessing dual attention throughout the visual field, does not directly assess dynamic scene processing. Faubert and Sidebottom (2012) demonstrated that remarkable improvements on the 3D-MOT task can be achieved with younger adults in a relatively short time. As argued by Faubert and Sidebottom, the potential for transferability of training on a perceptual-cognitive task to real-life situations like sports, navigation and driving, depends on a number of factors including visual field size, the necessity for tracking multiple dynamic objects, the presence or absence of stereoscopy (Viswanathan and Mingolla, 2002; Tinjust et al., 2008), and the use of speed. In a recent study we showed the relevance of 3D-MOT training by demonstrating that it can effectively transfer to a socially relevant percept such as biological motion, under conditions that are critical for collision avoidance (Legault and Faubert, 2012). We had previously demonstrated that the distance of a walker in virtual space impacted older observers' abilities to determine walking direction (Legault et al., 2012). In the following study (Legault and Faubert, 2012) we tested three groups of older observers. One group was trained on the 3D-MOT task, another was trained on a visual task for the same duration, and a third was a control with no training. When the groups were subsequently assessed on the biological motion task, only the group trained on the 3D-MOT showed improvements.

The purpose of the present study was therefore to address these questions directly with two experiments. The goal of the first experiment was to determine if older observers have lower limits in their capacity to track multiple moving objects when compared to young adults (Trick et al., 2005). The second experiment addressed the training capacity of older observers compared to younger adults. If one assumes that aging reduces learning functions, then older observers should not progress at the same rate as younger observers. On the other hand if learning is maintained, then a similar progression rate as a function of training would be observed. Yet a third outcome is possible. If training can reverse age-related impairments, then older observers may show an even better learning rate.

EXPERIMENT 1

In a MOT-type task where the dependent measure used was the maximum number of elements that could be tracked, Trick et al. (2005) suggested that older adults' tracking ability was probably lower then young adults (three items in their conditions). Faubert and Sidebottom (2012) proposed that speed thresholds may be a more relevant and controllable measure of MOT demands than using the total number of items as a dependent measure. To redress the proposed limitation of three items for older observers, Experiment 1 compared the speed thresholds of younger and older observers tracking three and four targets. If older observers are truly limited to three targets then we should not be able to obtain thresholds regardless of the speed of the elements. If on the other hand older observers can track four targets and the difference between tracking three and four targets is purely quantitative then we should find no group by target condition interactions. A group by target interaction would indicate both a capacity to track elements yet with greater relative difficulty for the older group.

METHODS

Participants

Ten younger adults (mean age 27 years old, range: 22–34 years old) and 10 older adults (mean age 66 years old, range: 61–74 years old) participated in this study. All participants were naïve to the purpose of the experiment. All subjects had normal or corrected-to-normal vision (6/6 or better) with normal stereoacuity as measured by the Frisby test (40 s of arc or better) (Sasieni, 1978; Frisby, 1980). Viewing was binocular. Younger adults had their most recent eye exam within the last year. Older adults were recruited at the school of optometry of Université de Montréal and had their most recent eye exam within the last 6 months. This eye exam included refraction, binocular vision evaluation, tonometry, visual field, retinal exam under pupil dilatation. Only subjects without ocular pathology or other abnormality were included in the study. Older observers completed the Mini-Mental State Examination, a screening measure for cognitive impairment and all scores were within the normal range (range, 26–30/30; subject mean was 28/30) (Crum et al., 1993). Therefore, they were all considered cognitively healthy. Ethical approval was obtained from the University's ethics board.

Apparatus

The 3D-MOT task was assessed using a fully immersive virtual environment: the Cave Automatic Virtual Environment (CAVE) system. The CAVE was an $8 \times 8 \times 8$ feet room that includes three canvas walls (one frontal and two laterals) and an epoxy floor that all serve as surfaces for image projection (Faubert and Allard, 2004). Four high-resolution projectors were synchronized and the image was updated in real-time to maintain the true viewing perspective of the observer (no false parallax). A magnetic motion tracker system (Flock-of-Birds) was used to measure head position, which was used to correct for the viewing perspective of the observers in real-time. The CAVE was under the computer control of an SGI ONYX 3200 (two Infinite Reality 2 graphics cards) generating a stereoscopic environment. The stereoscopy was generated with Crystal Eyes 2 active shutter glasses synchronized at 96 Hz (48 Hz per eye).

Stimuli and procedure

Before testing, participants were familiarized with the virtual environment and the stimulus. They were then asked to wear the stereoscopic goggles, which allowed them to perceive the 3D characteristics of the environment. Each participant sat at 177 cm from the central wall of the CAVE with eye height set at 160 cm from the ground. They were asked to stare at the fixation point, located straight ahead. Stimuli consisted of nine spheres projected into a virtual cube having transparent virtual light blue walls. The anterior side of the cube measured 42 ° of visual angle and was seen at 57 cm. The spheres followed a linear trajectory in the 3D virtual space but were bouncing on one another and on the walls when collisions occurred (see **Figure 1**).

We used the 3D-MOT speed threshold protocol (Faubert and Sidebottom, 2012). There were two conditions: three or four targets to track. Each block (i.e., staircase) lasted about 10 min. In one session, participants ran three staircases per condition (three or four spheres), for a total of 60 min. Each trial had five phases (see **Figure 2**). *Phase 1, presentation phase*: nine yellow static balls were presented for 2.5 s in random positions. *Phase 2, indexation phase*: three or four spheres turned red for 2 s for target identification, before turning back to yellow. *Phase 3, tracking phase*: all spheres started moving in random directions at a speed defined by the staircase procedure (see below) and bounced off of one another and off the virtual walls for 10 s. *Phase 4, identification phase*: the spheres stopped moving and each had a unique identification label from 1 to 9. The participants' task was to report, verbally, the 3 (or 4) numbers corresponding to the three (or four) target spheres that had been indexed. *Phase 5, feedback phase*: feedback was given, showing the observer the spheres that were initially indexed. Speed thresholds were then evaluated using a one up one down staircase procedure (Levitt, 1971) that is, after a correct response, ball speed displacement was increased by 0.05 log units and decreased by the same proportion after each incorrect response, resulting in a threshold criterion of 50%. The staircase was interrupted after eight inversions and the threshold was estimated by the geometric mean speed of the last four inversions. The initial virtual speed was fixed at 3.75 cm/s. To obtain a correct answer, participants had to correctly report all the targets.

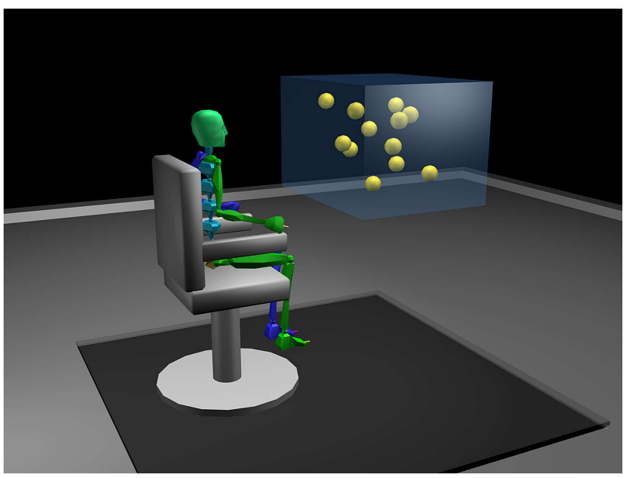

FIGURE 1 | Illustration of the experimental 3D-MOT set-up in the CAVE environment. The walls of the virtual cube are shown here for illustration purposes. They were not visible in the actual set-up.

RESULT AND DISCUSSION

From the 10 older participants, only nine were included in the analysis. One could not perform the task even for three targets at very low speeds (e.g., 1 cm/s). This participant was considered as an outlier since he was the only one from 30 (including 20 in Experiment 2) that could not complete the task. A 2×2 split-plot ANOVA on log speed thresholds revealed a significant Age (between variable) $\times$ Number of targets (3 or 4, within variable) interaction, $F(1, 17) = 6.45$, $p = 0.021$. Subsequently, paired t-test showed significant differences for number of targets; younger adults: $t(1, 9) = 3.480$, $p = 0.007$, older adults: $t(1, 8) = 8.204$, $p < 0.001$.

Results show that older adults can successfully follow three and four targets, but at significantly lower speeds (**Figure 3**). Healthy aging clearly reduces the ability to track many objects. Performance for younger adults with four targets is similar that with three targets for older adults. Furthermore, as shown by a significant interaction, performance decline between three and four spheres is more pronounced for older adults, suggesting that they have difficulty managing more information and require more time to process it. Our results show that older observers are not limited to tracking three targets. However, we do show greater relative difficulty for tracking four targets in this population as evidenced by the significant interaction, which partially supports the conclusion of the Trick and colleague study that healthy older observers have more difficulty tracking four targets.

EXPERIMENT 2

In the second experiment we trained younger and older adults during five consecutive weeks on the 3D-MOT task to determine the performance progress for younger and older adults. Here we wanted to determine which of the three possible outcomes prevails for 3D-MOT: either (1) they have a slower learning rate than younger adults; (2) they still have equivalent learning functions; or (3) training can reverse some age-related impairment, in which case training should reduce the performance difference between both age groups.

METHODS

Participants

Two new experimental groups participated in this experiment. One group was composed of 20 young observers (mean age

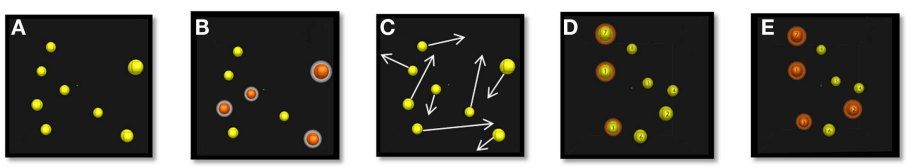

FIGURE 2 | Illustration of the five critical phases: (A) presentation of randomly positioned spheres in a virtual volumetric space, (B) identification of the spheres to track during trial, (C) removal of identification and movement of all spheres with dynamic interactions, (D) observer's response by identifying the spheres, (E) feedback was given to the observer.

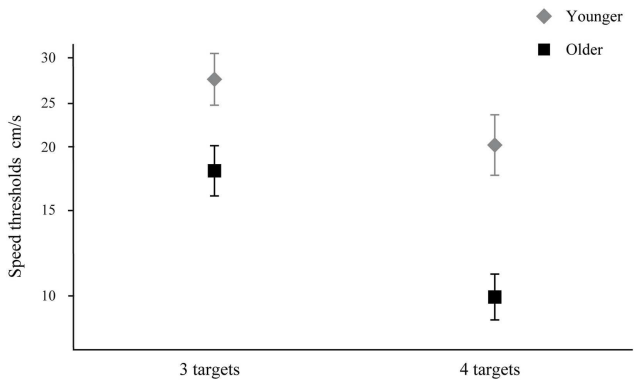

FIGURE 3 | Ten younger and nine older adults speed thresholds (±SEM) for three and four targets.

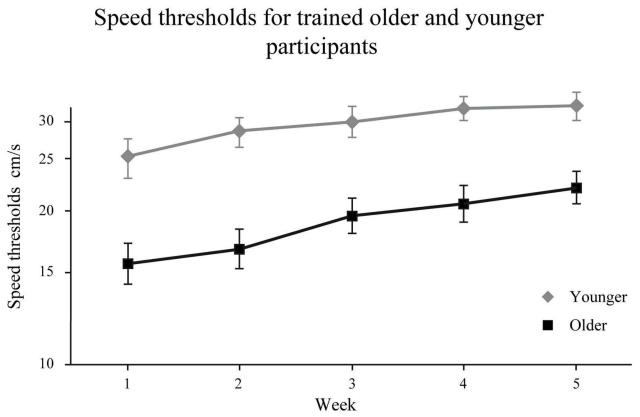

FIGURE 4 | Twenty younger and 20 older adults speed thresholds (±SEM) for five consecutive weeks.

24 years old, range: 18–35 years old) and another consisted of 20 older observers (mean age 67 years old, range: 64–73 years old). All observers came to the lab once a week for five consecutive weeks. The same inclusion and exclusion criteria were used as for Experiment 1. Again, the older observers' scores on the Mini-Mental State Examination were all within the normal range (range, 28–30/30; subject mean was 29/30) (Crum et al., 1993). Therefore, they were all considered cognitively healthy. All participants completed a short survey on video game habits. The survey questions are listed below.

Name of the game
Electronic game device
Number of hours per session
Number of sessions per month

Stimuli and procedure

The same set-up, stimuli and procedure as in Experiment 1 were used. We used the three-target protocol and for every session, participants ran three blocks (three thresholds) for a total of a 30-min session per week.

RESULTS AND DISCUSSION

A split-plot ANOVA on log speed thresholds comparing post-training condition (week 5) versus the initial scores (week 1) revealed a significant group effect, $F(1, 41) = 18.250$, $p < 0.001$ and a significant training effect $F(1, 41) = 65.747$, $p < 0.001$. Specifically, younger adults obtained higher thresholds compared to older adults and thresholds increased with testing sessions (**Figure 4**). However, we did not obtain a significant Age × Training interaction, $F(1, 41) = 2.615$, $p = 0.114$, which reveals that both groups obtained similar benefit from training. There is a similar progression for both groups. **Figure 4** shows that trained older observers obtained thresholds that were similar to those of untrained younger adults (week 1) [$t(1, 19) = 0.495$, $p = 0.626$].

Figure 5 represents normalized data relative to week-1 baseline scores and indicates that younger and older adults exhibit the same learning growth. However, at week 5, the improvement for older

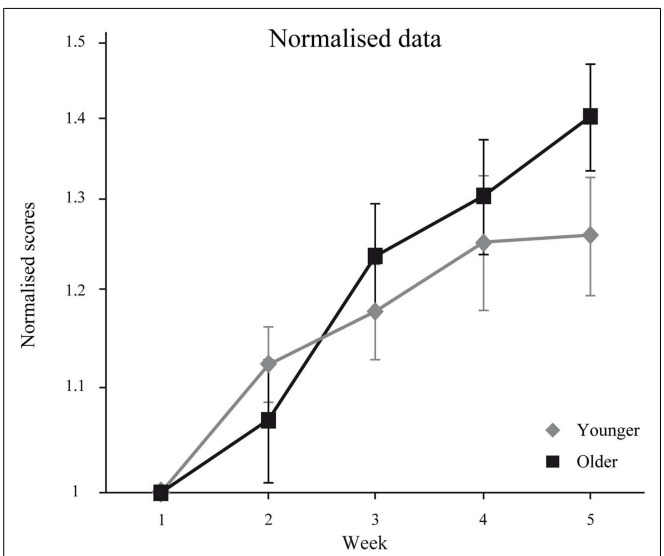

FIGURE 5 | Normalized speed thresholds (±SEM) for 20 younger and 20 older adults. (Ratio of speed threshold relative to week 1).

observers still appears on the rise, while younger observer group scores tend to level off. It is possible therefore, that improvement from training in the older group has not plateaued at 5 weeks. Interestingly, Richards et al. (2006) found that their older adults needed more practice to reach younger adult levels.

GENERAL DISCUSSION

In this paper, we assessed 3D-MOT for younger and older adults. In both experiments, we reported a significant age-related deficit, in which older adults obtained lower performance scores compared to younger adults. These results are generally consistent with previous MOT research showing reduced performance for older adults (Trick et al., 2005; Sekuler et al., 2008; Kennedy et al., 2009). Specifically, in Experiment 1, we showed that both younger and older adults obtained a significant reduction of their speed thresholds

when their performances are compared for the three-target condition with the four-target condition. Trick et al. (2005), found that older adults could only track around three moving objects under their stimuli conditions. However, our results cannot be explained by the fact that observers only tracked three balls + one by chance. If this were the case, the fourth ball would be identified correctly only one time out of six (17% chance), and the staircase would, on average, decrease ball speed. However, all thresholds obtained were higher than the initial starting staircase value of 3.75 cm/s. For the staircase to increase speed after the initial start value, the probability of identifying the correct four balls had to be higher than 50%, so observers must have followed all four balls. Older adults can track four items but they need a reduction of target movement speed to achieve this. Our results are generally consistent with previous studies showing that target quantity (Pylyshyn and Storm, 1988; Yantis, 1992; Alvarez and Franconeri, 2007) and object speed (Alvarez and Franconeri, 2007; Sekuler et al., 2008; Faubert and Sidebottom, 2012), are critical factors influencing performance. Trick et al. (2005) suggested that the difficulty for older participants to track four balls could be related to maintaining ball representation in working memory, until observers could report the targets. If an age-related effect on speed threshold was due to the ability of older observers to report four targets, then performance with slow speeds should have also been affected. However, at the slowest speed with four targets (i.e., staircase initial value of 3.75 cm/s) the percentage of correct trial was similar for older (89%) and young (90%) observers. Therefore, the difference between groups is unlikely related to working memory capacity alone. Furthermore, collisions cannot totally explain the differences observed between three and four targets. The proportion of collisions that occurs between a target and a non-target is, on average, 0.5357 ($2 \times 3 \times 5/8 \times 7$) and 0.5714 ($2 \times 4 \times 4/8 \times 7$) when tracking three and four balls out of eight, respectively. So everything else being equal, there will be only 1.0666 times more collisions between targets and non-targets when tracking four instead of three targets. So, if we measure observer's performance in relation with the number of collisions, we still have significant difference in both groups between three and four balls conditions [younger: $t(1, 9) = -1.099$, $p = 0.024$), older: $t(1, 8) = -7.275$, $p < 0.001$]. Consequently, the number of collisions cannot explain, by itself, the reduced speed thresholds when tracking four rather than three targets. This is consistent with Feria's (2013) conclusion that MOT performance cannot only be explained by the number of collisions. Nevertheless, 3D-MOT is a complex task that can be sensitive to many factors related to dividing attention, tracking, stereopsis, collisions, and occlusions. Thus, further experiments will be required to identify which functions may be affected by aging.

In Experiment 2, results show that both younger and older adults obtained similar training gains from 3D-MOT. Their performance after 5 weeks of training was significantly improved; participants processed the 3D-MOT task successfully at faster speeds. Overall, younger adults show better performance than older adults but the lack of significant interaction shows similar training gains between groups. **Figure 5**, clearly shows this trend. Our findings are consistent with previous work showing improvement of perceptual processing with training (Kramer et al., 1995; Richards et al., 2006; Andersen et al., 2010). Specifically, tasks become more automatic with training, reducing attentional costs (Ma et al., 2010).

As expected, our results show that younger adults obtained better performance than older adults. An element that can contribute to higher performance in younger adults is their previous exposure to certain stimuli as found in video games (Sekuler et al., 2008). Younger adults tend to be more exposed to video games, internet, television, etc. Some studies have shown that expertise can increase the ability to track multiple items (Green and Bavelier, 2006). However, we conducted a video game habit survey for each of our participants and video game experience cannot explain the difference between younger and older adults, because our participants did not play at any video games more than once a week except for one gamer (based on Green and Bavelier, 2006 criteria) and his MOT speed thresholds were not substantially different from the others. On the other hand, it could be assumed that older adults are less exposed to complex dynamic scenes in their everyday activities. It is possible that older observers engage less in certain activities because they have difficulty processing complex visual scenes.

In the present study, our 3D-MOT task was conducted in a virtual reality environment soliciting information integration across a large visual field. Consistent with previous research using UFOV (Richards et al., 2006), we observed that both younger and older adults can be trained and their performance improved, on an attention related task presented over a wide visual field. Richards et al. (2006), trained younger and older adults with an UFOV task, where central and peripheral vision and dual-tasking was required (see Figure 4 in Richards et al., 2006). After enough practice, older adults reduced the attentional cost to levels similar to those of younger adults, and both groups achieved performance without any divided-attention deficit, something we could not achieve with the 3D-MOT under our conditions. There are a number of differences between our MOT task and the Richards et al. (2006)'s UFOV task: our stimuli were dynamic, and the visual field size was twice that used by Richards et al. (2006). These differences may impact transferability to real-life situations. In previous studies, data show that older adults needed more training sessions to reach younger adult performance levels (Salthouse, 1990; Kramer and Willis, 2002; Richards et al., 2006). Our data (**Figure 5**) indicate that older adults' progression looks like it had not yet peaked, and there may still be room for improvement. More training sessions would be needed to determine if results obtained at week 5 reflect peak learning levels. To address this issue, we have conducted a pilot study in which we tested the same conditions as in Experiment 2, on eight young and eight older subjects for 10 instead of 5 sessions. The results did not conclusively show any closing of the gap between older and younger observers. From week 5 to week 10, younger adults maintained higher speed thresholds; however the learning progression was identical for both groups. The ANOVA shows a significant group effect [$F(1, 41) = 22.871$, $p < 0.001$] but no significant interaction [$F(4, 164) = 1.967$, $p = 0.102$)]. Furthermore, we have calculated the linear [$F(1, 41) = 3.342$, $p = 0.075$] and the quadratic [$F(1, 41) = 0.896$, $p = 0.349$] trends, and results showed similar learning rates in both groups (i.e., no learning × group interaction).

Given this lack of interaction one could propose that, in addition to learning, the older group is also gaining familiarity to the computer. We believe this is not the case for several reasons. First of all, we have previously shown that the same basic technique is quite sensitive to different levels of learning as demonstrated by a recent paper comparing pro-athletes, elite amateurs and university students (Faubert, 2013). Given the huge difference observed in the learning curves in these three categories for the same number of total thresholds reported here in the first phase (15 thresholds), if there was a significant difference between learning of the control group here and the older observers, we should have been quite sensitive to it early on. Secondly, it is important to note that the observers in this task are always passive, i.e., there is no interaction with the computer system and the subjects only identify the target spheres after the trial is over and therefore there is no motor control or dual-tasking in this regard. It is a passive viewing task and the only thing the subjects are learning is how to track the targets at increasing speeds. Thirdly, we have previously shown that older subjects (same age group as the present study) that trained in the same environment (CAVE) but on spatial discrimination task, showed very little learning and zero transfer to another dynamic task such as biological motion perception (Legault and Faubert, 2012). This was not the case for the group that trained on the 3D-MOT task that showed transfer to biological motion perception task at 4 m even if they had never seen the biological motion task before (see Legault and Faubert, 2012). Taking these points together, we feel it is highly unlikely that habituation to the computer set-up would explain our results with the older observers. Note that researchers have shown, using other research paradigms, transfer in everyday tasks (Tucker-Drob, 2011). There is further evidence that older adults with expertise can have high performing levels on real-world tasks (Nunes and Kramer, 2009). It would therefore be quite interesting to study the combined impact of expertise and training with the 3D-MOT task in future studies.

Our findings can be summed into two main points. We show that perceptual-cognitive training for a complex dynamic multifocal attention motion task, such as 3D-MOT, can be trained and, more importantly, that the training benefit for older observers is of the same magnitude as that for younger healthy adults. Consequently, it would certainly be worthwhile to conduct future studies on the transferability of this training to real-life tasks, such as driving or other socially relevant tasks.

ACKNOWLEDGMENTS

This work was supported by NSERC and the NSERC-Essilor Industrial Research Chair.

REFERENCES

Alvarez, G. A., and Franconeri, S. L. (2007). How many objects can you track? Evidence for a resource-limited attentive tracking mechanism. *J. Vis.* 7, 1–10. doi:10.1167/7.13.14

Andersen, G. J., Ni, R., Bower, J. D., and Watanabe, T. (2010). Perceptual learning, aging, and improved visual performance in early stages of visual processing. *J. Vis.* 10, 4. doi:10.1167/10.13.4

Ball, K., Berch, D. B., Helmers, K. F., Jobe, J. B., Leveck, M. D., Marsiske, M., et al. (2002). Effects of cognitive training interventions with older adults: a randomized controlled trial. *JAMA* 288, 2271–2281. doi:10.1001/jama.288.18.2271

Ball, K. K., Beard, B. L., Roenker, D. L., Miller, R. L., and Griggs, D. S. (1988). Age and visual-search – expanding the useful field of view. *J. Opt. Soc. Am. A* 5, 2210–2219. doi:10.1364/JOSAA.5.002210

Bennett, P. J., Sekuler, R., and Sekuler, A. B. (2007). The effects of aging on motion detection and direction identification. *Vision Res.* 47, 799–809. doi:10.1016/j.visres.2007.01.001

Cavanagh, P., and Alvarez, G. A. (2005). Tracking multiple targets with multifocal attention. *Trends Cogn. Sci. (Regul. Ed.)* 9, 349–354. doi:10.1016/j.tics.2005.05.009

Crum, R. M., Anthony, J. C., Bassett, S. S., and Folstein, M. F. (1993). Population-based norms for the Mini-Mental State Examination by age and educational level. *JAMA* 269, 2386–2391. doi:10.1001/jama.1993.03500180078038

Edwards, J. D., Myers, C., Ross, L. A., Roenker, D. L., Cissell, G. M., McLaughlin, A. M., et al. (2009). The longitudinal impact of cognitive speed of processing training on driving mobility. *Gerontologist* 49, 485–494. doi:10.1093/geront/gnp042

Faubert, J. (2002). Visual perception and aging. *Can. J. Exp. Psychol.* 56, 164–176. doi:10.1037/h0087394

Faubert, J. (2013). Professional athletes have extraordinary skills for rapidly learning complex and neutral dynamic visual scenes. *Sci. Rep.* 3, 1154. doi:10.1038/srep01154

Faubert, J., and Allard, R. (2004). "Effect of visual distortion on postural balance in a full immersion stereoscopic environment," in *Stereoscopic Displays and Virtual Reality Systems XI, Proceedings of SPIE-IS&T Electronic Imaging*, Vol. 5291, eds A. J. Woods, J. O. Merrit, S. A. Benton, and M. T. Bolas (San Jose: SPIE), 5491–5500.

Faubert, J., and Sidebottom, L. (2012). Perceptual-cognitive training of athletes. *J. Clin. Sports Psychol.* 6, 85–102.

Feria, C. S. (2013). Speed has an effect on multiple-object tracking independently of the number of close encounters between targets and distractors. *Atten. Percept. Psychophys.* 75, 53–67. doi:10.3758/s13414-012-0369-x

Frisby, J. P. (1980). The Frisby stereotest: amended instructions. *Br. Orthopt. J.* 37, 108–112.

Green, C. S., and Bavelier, D. (2006). Enumeration versus multiple object tracking: the case of action video game players. *Cognition* 101, 217–245. doi:10.1016/j.cognition.2005.10.004

Habak, C., and Faubert, J. (2000). Larger effect of aging on the perception of higher-order stimuli. *Vision Res.* 40, 943–950. doi:10.1016/S0042-6989(99)00235-7

Kennedy, G. J., Tripathy, S. P., and Barrett, B. T. (2009). Early age-related decline in the effective number of trajectories tracked in adult human vision. *J. Vis.* 9, 21.1–21.10. doi:10.1167/9.2.21

Kosnik, W., Winslow, L., Kline, D., Rasinski, K., and Sekuler, R. (1988). Visual changes in daily life throughout adulthood. *J. Gerontol.* 43, 63–70. doi:10.1093/geronj/43.3.P63

Kramer, A. F., Larish, J. F., and Strayer, D. L. (1995). Training for attentional control in dual-task settings – a comparison of young and old adults. *J. Exp. Psychol. Appl.* 1, 50–76. doi:10.1037/1076-898X.1.1.50

Kramer, A. F., and Willis, S. L. (2002). Enhancing the cognitive vitality of older adults. *Curr. Dir. Psychol. Sci.* 11, 173–177. doi:10.1111/1467-8721.00194

Legault, I., and Faubert, J. (2012). Perceptual-cognitive training improves biological motion perception: evidence for transferability of training in healthy aging. *Neuroreport* 23, 469–473. doi:10.1097/WNR.0b013e328353e48a

Legault, I., Troje, N. F., and Faubert, J. (2012). Healthy older observers cannot use biological-motion point-light information efficiently within 4 m of themselves. *Iperception* 3, 1–8. doi:10.1068/i0485

Levitt, H. (1971). Transformed up-down methods in psychoacoustics. *J. Acoust. Soc. Am.* 49(Suppl. 2), 467. doi:10.1121/1.1912375

Ma, L., Wang, B., Narayana, S., Hazeltine, E., Chen, X., Robin, D. A., et al. (2010). Changes in regional activity are accompanied with changes in inter-regional connectivity during 4 weeks motor learning. *Brain Res.* 1318, 64–76. doi:10.1016/j.brainres.2009.12.073

Nunes, A., and Kramer, A. F. (2009). Experience-based mitigation of age-related performance declines: evidence from air traffic control. *J. Exp. Psychol. Appl.* 15, 12–24. doi:10.1037/a0014947

Pylyshyn, Z. W. (1989). The role of location indexes in spatial perception: a sketch of the FINST spatial-index model. *Cognition* 32, 65–97. doi:10.1016/0010-0277(89)90014-0

Pylyshyn, Z. W. (1994). Some primitive mechanisms of spatial attention. *Cognition* 50, 363–384. doi:10.1016/0010-0277(94)90036-1

Pylyshyn, Z. W., and Storm, R. W. (1988). Tracking multiple independent targets: evidence for a parallel tracking mechanism. *Spat. Vis.* 3, 179–197. doi:10.1163/156856888X00122

Richards, E., Bennett, P. J., and Sekuler, A. B. (2006). Age related differences in learning with the useful field of view. *Vision Res.* 46, 4217–4231. doi:10.1016/j.visres.2006.08.011

Salthouse, T. A. (1990). Influence of experience on age differences in cognitive functioning. *Hum. Factors* 32, 551–569.

Sasieni, L. S. (1978). The Frisby stereotest. *Optician* 176, 7–10.

Sekuler, R., Mclaughlin, C., and Yotsumoto, Y. (2008). Age-related changes in attentional tracking of multiple moving objects. *Perception* 37, 867–876. doi:10.1068/p5923

Tang, Y., and Zhou, Y. (2009). Age-related decline of contrast sensitivity for second-order stimuli: earlier onset, but slower progression, than for first-order stimuli. *J. Vis.* 9, 18. doi:10.1167/9.7.18

Tinjust, D., Allard, R., and Faubert, J. (2008). Impact of stereoscopic vision and 3D representation of visual space on multiple object tracking performance. *J. Vis.* 8, 509. doi:10.1167/8.6.509

Trick, L. M., Perl, T., and Sethi, N. (2005). Age-related differences in multiple-object tracking. *J. Gerontol. B. Psychol. Sci. Soc. Sci.* 60, 102–105. doi:10.1093/geronb/60.2.P102

Tucker-Drob, E. M. (2011). Neurocognitive functions and everyday functions change together in old age. *Neuropsychology* 25, 368–377. doi:10.1037/a0022348

Viswanathan, L., and Mingolla, E. (2002). Dynamics of attention in depth: evidence from multi-element tracking. *Perception* 31, 1415–1437. doi:10.1068/p3432

Yantis, S. (1992). Multielement visual tracking: attention and perceptual organization. *Cogn. Psychol.* 24, 295–340. doi:10.1016/0010-0285(92)90010-Y

Conflict of Interest Statement: Isabelle Legault and Rémy Allard declare that the research was conducted in the absence of any commercial or financial relationships that could be construed as a potential conflict of interest. Jocelyn Faubert is the Chief Science Officer of CogniSens Inc., a company that has signed a licensing agreement for four technologies from the Université de Montréal and produces the NeuroTracker ™system, the commercial version of the 3D-MOT speed task.

Received: 27 November 2012; accepted: 17 May 2013; published online: 06 June 2013.

*Citation: Legault I, Allard R and Faubert J (2013) Healthy older observers show equivalent perceptual-cognitive training benefits to young adults for multiple object tracking. Front. Psychol. **4**:323. doi: 10.3389/fpsyg.2013.00323*

This article was submitted to Frontiers in Perception Science, a specialty of Frontiers in Psychology.

frontiers in
PSYCHOLOGY

ORIGINAL RESEARCH ARTICLE
published: 20 February 2013
doi: 10.3389/fpsyg.2013.00066

Perceptual learning and aging: improved performance for low-contrast motion discrimination

***Jeffrey D. Bower*[1], *Takeo Watanabe*[2] *and George J. Andersen*[1]*

[1] *Department of Psychology, University of California, Riverside, CA, USA*
[2] *Department of Cognitive, Linguistic and Psychological Sciences, Brown University, Providence, RI, USA*

Edited by:
Allison B. Sekuler, McMaster University and York University, Canada

Reviewed by:
Fang Fang, Peking University, China
Duje Tadin, University of Rochester, USA

***Correspondence:**
George J. Andersen, Department of Psychology, University of California, 900 University Avenue, Riverside, CA 92521, USA.
e-mail: andersen@ucr.edu

Previous research has shown age-related differences in discriminating motion at different levels of contrast (Betts et al., 2005, 2009, 2012). A surprising result of this research is that older as compared to younger observers showed improved performance in detecting motion of large high-contrast stimuli suggesting age-related differences in center-surround antagonism. In the present study we examined whether perceptual learning methods could be used to improve motion discrimination performance for older individuals under high- and low-contrast conditions. The stimuli were centrally presented Gaussian filtered sine-wave gratings (Gabors) that were either 5° or 0.7° diameter with contrast of 0.92, 0.22, or 0.028. Older and younger participants received 3 days of training. The task was to identify if the motion direction was leftward or rightward. Duration thresholds for motion discrimination were derived using two randomly interleaved staircases and compared between pre-/post-test sessions. Both older and younger subjects showed lower duration thresholds as a result of training. The improved performance, for older subjects, due to training was observed for all size and contrast conditions, with training with small low-contrast stimuli resulting in a 23% improvement in motion discrimination performance. Older observers, as compared to younger observers, did show evidence of decreased spatial suppression across all contrast levels. These results suggest that perceptual learning techniques are effective for improving motion discrimination performance, especially for conditions that are difficult for older individuals.

Keywords: perceptual learning, aging, motion perception, spatial suppression, contrast

INTRODUCTION

It is well documented that many aspects of visual processing decline with advanced age. Previous research has shown that age-related declines in processing orientation, luminance, contrast, and motion are not the result of changes in optics due to the aging eye (see Owsley, 2011; Andersen, 2012 for reviews). In addition, declines have been observed for mid- and high-level aspects of visual processing such as form, depth, slant, and 3D shape perception (see Andersen, 2012). Age-related declines in motion processing have been the focus of a considerable amount of research (see Hutchinson et al., 2012 for a review), and has been examined using several different types of motion stimuli – drifting sine-wave gratings, coherent motion random dot cinematograms (RDCs), and global motion RDCs. Early research on motion and aging found decreased sensitivity for older as compared to younger observers for drifting sinusoidal gratings, particularly low frequency gratings (Sekuler et al., 1980). More recent research (Snowden and Kavanagh, 2006) found age-related declines over a wide range of spatial frequencies. Studies examining coherent motion RDCs (the perception of the direction of motion of moving dots imbedded in noise) found significantly higher thresholds with increased age, with thresholds for individuals over age 70 twice that of younger college age individuals (Trick and Silverman, 1991). This finding has been replicated in several studies (Gilmore et al., 1992; Andersen and Atchley, 1995; Snowden and Kavanagh, 2006; Billino et al., 2008) including research on motion sensitivity and retinal eccentricity (Atchley and Andersen, 1998). Finally studies examining global motion RDCs (dots that move in an average motion direction with each dot motion path containing a random motion component) found clear evidence of age-related declines in the detection and identification of motion direction (Bennett et al., 2007) and proposed a model suggesting that age-related declines were due to the bandwidth of individual motion channels.

Previous neurophysiological studies (Schmolesky et al., 2000; Hua et al., 2006; Yang et al., 2008) have suggested that changes in visual processing due to aging are the result of declines in inhibition, possibly due to declines in levels of γ-aminobutyric acid or GABA. Psychophysical studies have also suggested that declines in visual processing with age, such as reduced motion perception, are the result of declines in inhibition. Evidence in support of age-related changes in inhibition and motion processing has been observed in a psychophysical study examining motion discrimination with high- and low-contrast stimuli (Betts et al., 2005, 2009, 2012). Subjects were presented with drifting Gabor patches that varied in size and contrast and asked to discriminate if the motion direction was leftward or rightward. Duration thresholds were derived and indicated the minimum amount of time needed to perform the task accurately. Younger observers had elevated

thresholds with high-contrast (92%) and large (5˚) stimuli – a result consistent with previous research (Tadin et al., 2003) suggesting that elevated thresholds for large-size high-contrast stimuli, as compared to small-size high-contrast stimuli, were due to center-surround antagonism. In Betts et al. (2005), both younger and older observers' thresholds also increased with increased contrast for large stimuli. However, older observers had lower duration thresholds than younger observers for high-contrast large stimuli. These results suggest that reduced center-surround suppression – possibly due to decreased neural inhibition – occurs with increased age (Betts et al., 2005).

Given the extensive evidence of age-related declines in motion processing an important question is whether any methods can be used to improve visual function. One approach would be to use training protocols found to be effective in studies on perceptual learning (PL; see Fahle and Poggio, 2002; Fine and Jacobs, 2002; Sagi, 2011). Recent research has found that perceptual learning protocols are effective for improving vision among older individuals. These studies have shown that PL can be used to improve texture discrimination (Andersen et al., 2010) and motion processing (Bower and Andersen, 2012). Bower and Andersen (2012) used the perceptual template model (Lu and Dosher, 1999, 2008; Lu et al., 2006) to assess age-related differences in motion processing by comparing perceptual efficiency between age groups both before and after perceptual training. The perceptual template model assumes that human perceptual performance is limited by inefficiencies in visual processing and that perceptual learning is a result of increased perceptual efficiency due to reduced internal noise and/or increased tolerance to external noise. Bower and Andersen (2012) used the model to examine age-related changes in additive internal noise and tolerance to external noise as a result of training. The results indicated elevated internal noise for older as compared to younger observers prior to training – a finding that is possibility related to the results suggesting reduced inhibition for older individuals in motion processing (Betts et al., 2005). In Bower and Andersen (2012), PL training resulted in decreased internal noise for older individuals. If changes in internal noise are related to changes in neural inhibition then reduced internal noise resulting from PL training might increase inhibition resulting in a change in center-surround inhibition and thus alter motion thresholds.

The purpose of the present study was to examine whether the use of PL protocols would result in changes in motion processing for older individuals due to changes in center-surround inhibition. To examine this issue we used stimuli that were matched to a subset of conditions examined by Betts et al. (2005), in which observers were presented with drifting Gabor patches that varied in contrast and size. Specifically, Betts et al. (2005) used Gabor patches at seven contrast levels (92, 46, 22, 11, 5.5, 4.2, and 2.8%) and four sizes (5.0˚, 2.7˚, 1.3˚, and 0.7˚) and found that older observers performed better than younger observers in the largest size tested (5.0˚) at contrasts above 22%. In the present study we used two sizes (5.0˚ and 0.7˚) and three contrasts levels (92, 22, and 2.8%) for a total of six unique conditions. These conditions represent the extreme size and contrast levels of the study by Betts et al. (2005) and include the conditions that resulted in age-related differences in center-surround inhibition.

The present study was run over a 5-day period, and included a pre- training and post-training assessment on separate days with three intervening training days. If the use of PL protocols results in increased inhibition for older observers then we should observe a reversal of the improved performance for older observers over younger observers with high-contrast large-size stimuli.

MATERIALS AND METHODS

PARTICIPANTS

The participants were nine younger (mean age 21.0) and nine older (mean age 66.8) observers (see **Table 1** for additional demographic information). The younger participants were recruited from the undergraduate population at the University of California, Riverside. The older participants were volunteers from continuing education courses at the University of California, Riverside's Extension center and volunteers obtained through a direct mailing for subject recruitment in the Riverside community. All participants were paid 10 dollars per hour of experimental time plus an additional bonus of 25 dollars after completing the last day of the experiment. All participants had normal or corrected to normal vision.

APPARATUS

Stimuli were presented on a Dell® t3500 workstation using an Nvidia Quatro FX video card. The monitor was a Viewsonic P225 perfect flat CRT monitor set at a resolution of 1025 × 768 and operating a 120 Hz. Viewing distance was set at 80 cm and was controlled using a chin rest. The display was modulated by a Cambridge Research Bitts++ system running in Mono++ mode. This system allows for 16,384 distinct grayscale levels (14 bit precision). The monitor's gamma was corrected to produce linear luminance output. The experiment was programmed in the Matlab (R2009a) environment using the Psychophysics Toolbox extension software (Brainard, 1997; Pelli, 1997). The experiment took place in a dark room. Participants responded using a standard keyboard.

STIMULI

The stimuli were moving Gaussian filtered sine-wave gratings (Gabor patches). The Gabor patches had a spatial frequency of

Table 1 | Means and standard deviations of participants' demographic information and results from perceptual and cognitive tests.

Variable	Younger		Older	
	M	SD	*M*	SD
Age (years)[a]	23.0	1.4	73.3	4.1
Years of education[a]	14.5	1.2	19.4	3.2
Snellen letter acuity	10/11.1	1.5	10/14.1	2.5
Log contrast sensitivity[a,b]	1.69	0.13	1.52	0.22
Digit span forward	11.3	2.1	9.9	1.9
Digit span backward	8.9	1.7	7.2	1.6
Perceptual encoding manual[a]	88.8	17.8	70.7	18.3
Kaufman brief intelligence test	25.5	4.1	28.7	5.8

[a]Differences between age groups were significant ($p \leq 0.05$). [b]Contrast sensitivity was measured using the Pelli Robson test (Pelli et al., 1988).

1 cycle/°. Weber contrast (luminance − mean/mean) of the Gabor patch was set at one of three levels – 2.8, 22, or 92%. Grating contrast decreased from the center of the patch outward by a Gaussian envelope with standard deviation of 2°. Two different sizes were examined 0.7 of 5.0°. The three contrast levels and two sizes resulted in six unique conditions. The background luminance of the display was 36.6 cd/m^2. On each trial the Gabor patch drifted to the right or left at a rate of 2°/s. The motion direction was determined randomly before each trial. On every trial the starting phase of the Gabor was randomized. The stimulus was presented within a square temporal window while the actual stimulus duration was manipulated on a trial-by-trial basis.

TASK AND PROCEDURE

The task was to indicate if the motion direction of the Gabor patch was leftward or rightward. Participants were informed that the motion direction was determined randomly before each trial. If the participant could not judge the motion direction they were told to make their best possible judgment.

The experiment took place over 5 days. Days 1 and 5 were treated as pre- and post-testing days with days 2, 3, and 4 treated as training days. On each day the participant was presented with a random order of six blocks that represented all possible combinations of the three contrast levels (2.8, 22, and 91%) and two sizes (0.7 or 5°). On day 1, prior to experimental data collection, each participant completed an introduction program that presented 10 trials at maximum duration for each of the six blocks to introduce the stimuli, task, and procedure. At the beginning of each trial during the experiment the message "Press a key to start next trial" was displayed on screen. The participant initiated each trial by pressing any key on the keyboard causing the screen to go blank (set to the mean background luminance). After a delay of 500 ms a fixation point appears that flickered between white and black every 400 ms for 1.6 s. After which the display went blank for an additional 500 ms before the stimuli appeared. After the stimulus was presented the screen went blank and the participant entered their judgment by pressing the left or right arrow keys on the keyboard. The program waited for the response and produced a high tone if the response was correct or a low tone if the response was incorrect.

Each block consisted of 150 trials. After the 75th trial the program prompted the participant to take a short break. During this time the participant could not resume the experimental trials for at least 10 s. The participants were instructed to take as long as needed to avoid fatigue. At the end of the block the participant was prompted to inform the experimenter that a block was completed and to take a brief break. Each block took between 7 and 12 min to complete based on the time taken during the rest period and how fast the participant responded to each trial.

Thresholds were derived by manipulating the duration of the stimulus using two randomly interleaved staircases. A 2/1 staircase tracked the 71% point and a 4/1 estimated the 84% correct point. The two thresholds were averaged to produce a final estimated threshold of 77.5%. The range of possible durations was 500 ms (60 frames) to 16.6 ms (two frames). For each block the staircases were initialized at 500 ms. The step sizes were adjusted for both staircases for each reversal in the following order – 250 ms (30 frames), 125 ms (15 frames), 125 ms (15 frames), 46.6 ms (5 frames), 46.6 ms (5 frames), 25 ms (3 frames), 25 ms (3 frames), and 8.3 ms (1 frame). After the sixth reversal the step size remained at 8.3 ms (1 frame). The final threshold for both staircases was the average of reversal points excluding the first reversal. Each observer completed 900 trials each day for a total of 4500 trials over the entire experiment.

RESULTS

BASELINE PERFORMANCE

To examine age-related differences in performance prior to training, we conducted a two (age) by two (size) by three (contrast) analysis of variance (ANOVA) on day 1 (pre-training) using the log transformed thresholds for each subject. The main effect of aging was significant, $F(1, 16) = 9.5$, partial $\eta^2 = 0.37$, $p < 0.05$. The mean duration threshold for older and younger observers was 161 and 81 ms, respectively. In addition, the main effects of size [$F(1, 16) = 10.2$, partial $\eta^2 = 0.38$] and contrast [$F(2, 32) = 48.5$, partial $\eta^2 = 0.75$] were significant, $p < 0.05$. The effects of these variables were mediated by age. Specifically, the age by size interaction [$F(1, 16) = 31.9$, partial $\eta^2 = 0.66$] and age by contrast interaction [$F(2, 32) = 4.3$, partial $\eta^2 = 0.21$] were significant, $p < 0.05$. Finally the age by size by contrast interaction was not significant, $F(2, 32) < 1$, $p > 0.05$ and for comparison purposes is shown in **Figure 1**. The general pattern of results is consistent with those reported by Tadin et al. (2003). For small size stimuli thresholds decreased with increased contrast whereas for large-size stimuli thresholds increased with increased contrast. This pattern of results occurred for both younger and older participants, with a much greater increase in thresholds for low-contrast/small stimuli for older as compared to younger participants. The present results, however, are not consistent with the results of Betts et al. (2005). According to their findings, older observers, as compared to younger observers had lower duration thresholds for large high-contrast stimuli. In the present study, we did not find any combination of size and contrast conditions that resulted in significantly lower duration thresholds for older as compared to younger observers.

TRAINING EFFECTS

To examine the effects of training we conducted a two (age) by two (size) by three (contrast) by two (pre- and post-training) ANOVA on the log transformed thresholds for each subject. The main effect of age [$F(1, 16) = 7.4$, partial $\eta^2 = 0.31$], training [$F(1, 16) = 44.7$, partial $\eta^2 = 0.73$], and the interaction of age and training [$F(1, 16) = 5.3$, partial $\eta^2 = 0.25$] were significant, $p < 0.05$. An analysis of the simple main effect of training indicated a significant effect for both older and younger observers, with a greater effect size of training occurring for older [$F(1, 8) = 67.8$, partial $\eta^2 = 0.89$] as compared to younger subjects [$F(1, 8) = 6.8$, partial $\eta^2 = 0.46$]. There were no other significant interactions with age and training (F values approximately 1). For comparison purposes the overall results are shown in **Figure 2**. As is shown in **Figure 2**, training resulted in improved performance for older subjects for all combinations of size and contrast examined, with

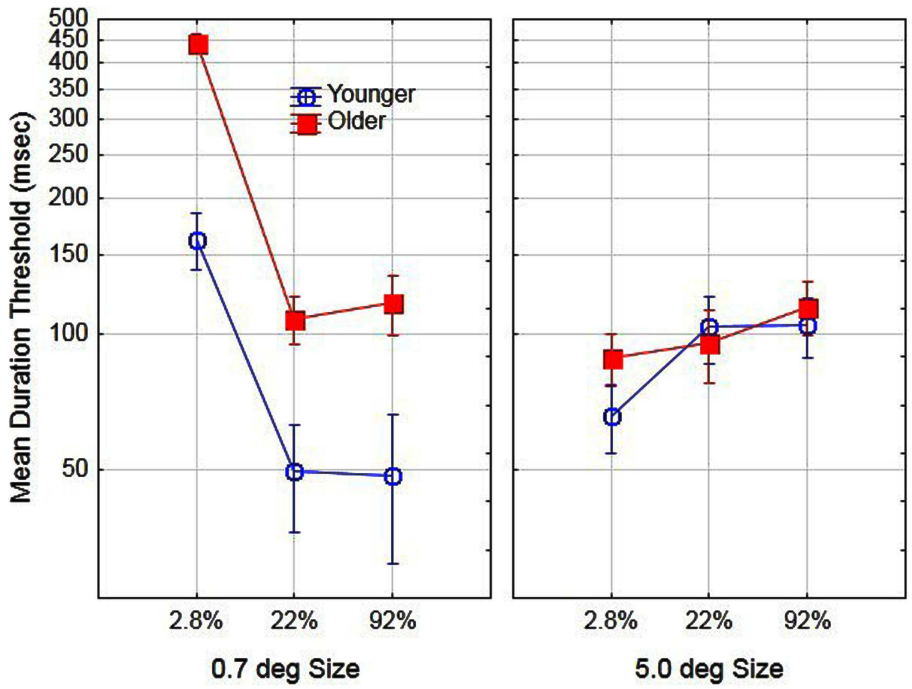

FIGURE 1 | Effects of stimulus size, contrast, and age on motion duration thresholds prior to training. Error bars represent ±1 SE.

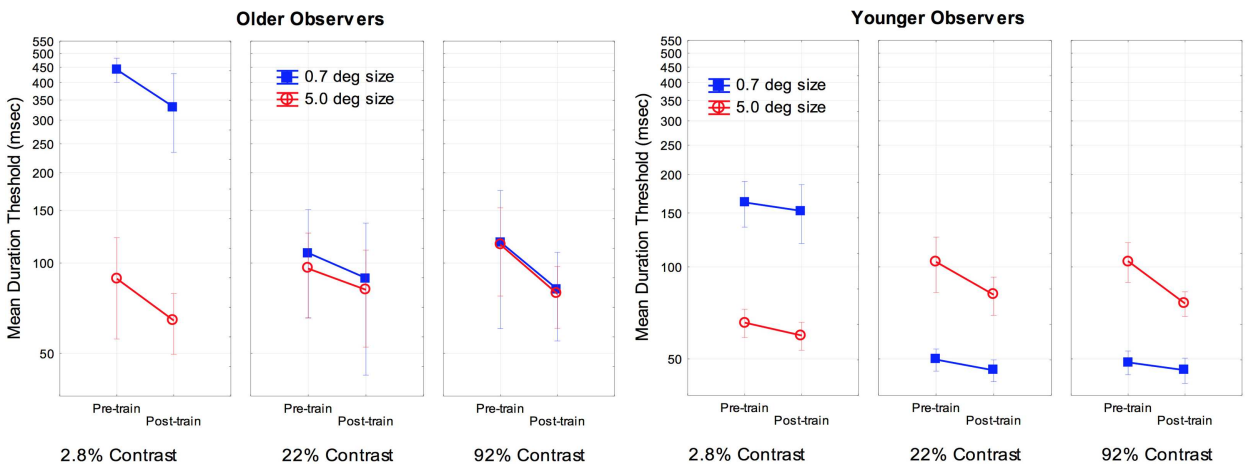

FIGURE 2 | Effects of training, size, contrast, and age on motion duration thresholds. Error bars represent ±1 SE.

a 23% improvement for the most difficult conditions (small-size and low-contrast).

SPATIAL SUPPRESSION

Previous research has suggested that better performance for older observers in detecting large high-contrast motion targets is due to age-related differences in spatial suppression (Betts et al., 2005). In their research, they estimated spatial suppression by calculating a spatial suppression index: the log thresholds for large targets minus the log threshold for the smallest target at each level of contrast. The sign of these scores provide evidence of spatial suppression (positive scores) or spatial summation (negative scores). In the present study we conducted a similar analysis by deriving the log threshold for large (5.0°) targets minus the log threshold for the small target (0.7°) for each level of contrast. To examine the effects of aging on spatial suppression we conducted a two (age) by three (contrast level) ANOVA on spatial suppression index scores. The main effects of age [$F(1, 16) = 31.1$, partial $\eta^2 = 0.66$] and contrast [$F(2, 32) = 91.6$, partial $\eta^2 = 0.85$] were significant ($p < 0.05$). These results (see **Figure 3**) do provide

evidence of reduced spatial suppression for older observers as compared to younger observers. However, the results indicate general age-related declines in spatial suppression (across all contrast levels) as opposed to declines exclusively for high-contrast targets. The interaction of age and contrast was not significant [$F(2, 32) = 1.19$]. These values were then calculated pre- and post-training to determine whether the use of PL training resulted in changes in spatial suppression and analyzed in a two (age) by two (training) by three (contrast) ANOVA. The overall results are shown in **Figure 4**. The main effect of age was significant, $F(1, 16) = 39.1$, partial $\eta^2 = 0.70$, $p < 0.05$ indicating lower overall spatial suppression scores for older (mean $= -0.24$) as compared to younger (mean $= 0.04$) subjects. In addition, the main effect of contrast was significant, $F(2, 32) = 121.7$, partial $\eta^2 = 0.88$, $p < 0.05$ indicating lower suppression index scores for low as compared to high-contrast stimuli. The main effect of training was not significant nor did training interact with age or contrast (F values less than 1.3). These results suggest that the effects of training did not result in changes in spatial suppression.

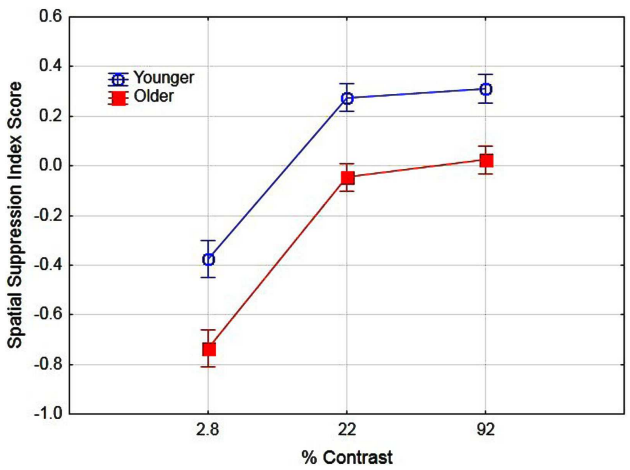

FIGURE 3 | Effects of contrast and age on spatial suppression index scores. Error bars represent ±1 SE.

DISCUSSION

The results of the present study indicate several important findings concerning motion processing and aging. First, consistent with previous research (Gilmore et al., 1992; Atchley and Andersen, 1998; Betts et al., 2005, 2009, 2012; Bennett et al., 2007) we found that older observers, as compared to younger observers, have increased motion discrimination thresholds. In addition, the ability to determine the direction of motion decreased with a decrease in contrast of the motion stimulus especially for small targets. Previous research (Betts et al., 2005) has reported improved motion thresholds for older as compared to younger observers for large high-contrast stimuli – a result interpreted to be associated declines in inhibition and changes in spatial suppression. In the present study we did not find this pattern of results. We did, however, find evidence of general age-related declines in spatial suppression across all contrast levels examined. So what might account for the failure to replicate this interesting finding regarding age, spatial suppression, and high-contrast stimuli? We currently do not have an explanation to account for these differences. There are some interesting differences between the two studies regarding

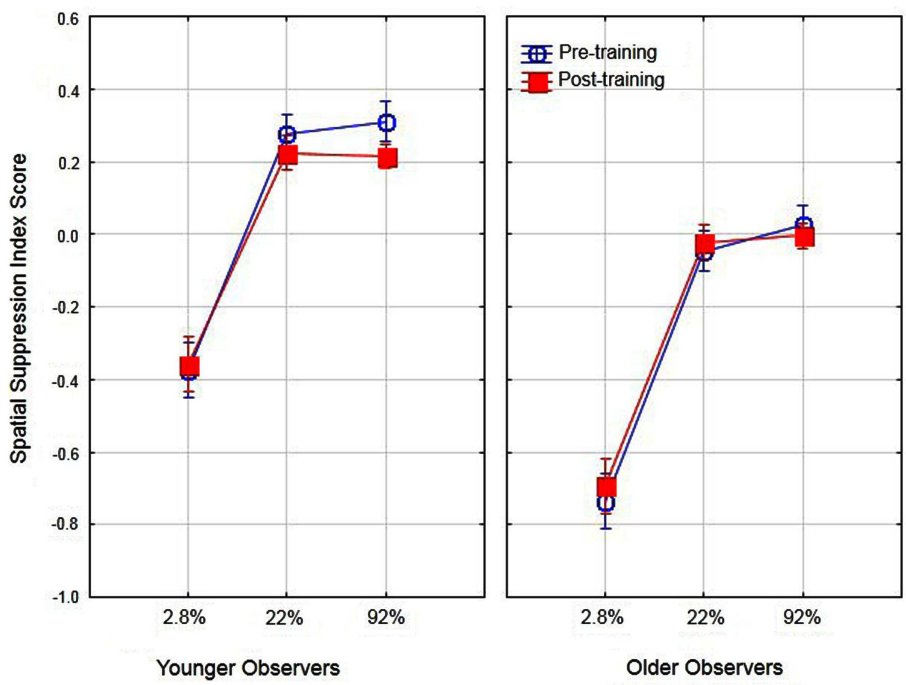

FIGURE 4 | Effects of training, contrast, and age on spatial suppression index scores. Error bars represent ±1 SE.

the older subjects (e.g., differences in baseline performance; the degree to which subjects might be considered high cognitive functioning) that might contribute to the differences obtained in spatial suppression. Clearly future research is needed to understand the different age effects obtained in the two studies.

The results of the present study also indicate an effect of training for older observers. We found an overall improvement in performance for older individuals as compared to younger individuals. In addition, training resulted in improvement for older observers for all combinations of contrast and size examined, with the greatest magnitude of improvement occurring for the small low-contrast target condition. Younger subjects also showed improvement due to training, but the effect size of training was lower than that observed with older subjects. These results provide further evidence that PL training is a useful procedure for improving vision among older individuals. Indeed, several of the older observers at the beginning of the study commented that they were unable to see the small low-contrast stimuli. However, following training these same individuals commented that they could easily see targets from these stimuli conditions. These results indicate a significant degree of improvement in motion thresholds for older observers as a result of 3 days of training.

The results regarding the spatial suppression index indicate that both older and younger observers have increased suppression with increased contrast, a finding consistent with previous research (Tadin et al., 2003) that showed greater suppression for large high-contrast stimuli. However, we did not find any evidence that training resulted in changes in suppression for either age group. These findings may be limited to the conditions (size and contrast) examined in the present study. In addition, it is possible that additional training beyond 3 days may be required to result in changes in spatial suppression. An important issue for future research will be to examine this possibility with a greater range of stimulus conditions.

In summary, the results of the present study provide further evidence of the utility of PL methods to improve vision among older individuals. The results suggest that training was effective for small low-contrast stimuli – conditions that were the most difficult for older observers prior to training. In addition, although we found evidence of general age-related differences in spatial suppression, we did not find evidence that training resulted in changes in suppression for either younger or older participants. Previous research (Bower and Andersen, 2012) has found evidence of changes in internal noise for older observers as a result of training with motion stimuli and has suggested that this finding might be due to changes in inhibition. Given that the present study did not find evidence of changes in inhibition, it suggests that other factors may be important in changing efficiency in motion processing.

ACKNOWLEDGMENTS

This research was supported by NIH AG031941 and EY18334.

REFERENCES

Andersen, G. J. (2012). Aging and vision: changes in function and performance from optics to perception. *Wiley Interdiscip. Rev. Cogn. Sci.* 3, 403–410.

Andersen, G. J., and Atchley, P. (1995). Age-related differences in the detection of three-dimensional surfaces from optic flow. *Psychol. Aging* 10, 650–658.

Andersen, G. J., Ni, R., Bower, J. D., and Watanabe, T. (2010). Perceptual learning, aging, and improved visual performance in early stages of visual processing. *J. Vis.* 10(13):4. doi:10.1167/10.13.4

Atchley, P., and Andersen, G. J. (1998). The effect of age, retinal eccentricity and speed on the detection of optic flow. *Psychol. Aging* 13, 650–658.

Bennett, P. J., Sekuler, R., and Sekuler, A. B. (2007). The effects of aging on motion detection and direction identification. *Vision Res.* 47, 799–809.

Betts, L. R., Sekuler, A. B., and Bennett, P. J. (2009). Spatial characteristics of center-surround antagonism in younger and older adults. *J. Vis.* 9(1):25. doi:10.1167/9.1.25

Betts, L. R., Sekuler, A. B., and Bennett, P. J. (2012). Spatial characteristics of motion-sensitive mechanisms change with age and stimulus frequency. *Vision Res.* 53, 1–14.

Betts, L. R., Taylor, C. P., Sekuler, A. B., and Bennett, P. J. (2005). Aging reduces center-surround antagonism in visual motion processing. *Neuron* 45, 361–366.

Billino, J., Bremmer, F., and Gegenfurtner, K. R. (2008). Differential aging of motion processing mechanisms: evidence against general perceptual decline. *Vision Res.* 48, 1254–1261.

Bower, J., and Andersen, G. J. (2012). Aging, perceptual learning and changes in efficiency of motion processing. *Vision Res.* 61, 144–156.

Brainard, D. H. (1997). The psychophysics toolbox. *Spat. Vis.* 10, 433–436.

Fahle, M., and Poggio, T. (eds). (2002). *Perceptual Learning*. MIT Press.

Fine, I., and Jacobs, A. J. (2002).Comparing perceptual learning across tasks: a review. *J. Vis.* 2, 190–203.

Gilmore, G. C., Wenk, H. E., Neylor, L. A., and Stuve, T. A. (1992). Motion perception and aging. *Psychol. Aging* 4, 654–660.

Hua, T., Li, X., He, L., Zhou, Y., Want, Y., and Leventhal, A. G. (2006). Functional degradation of visual cortical cells in old cats. *Neurobiol. Aging* 27, 155–162.

Hutchinson, C. V., Arena, A., Allen, H. A., and Ledgeway, T. (2012). Psychophysical correlates of global motion processing in the aging visual system: a critical review. *Neurosci. Biobehav. Rev.* 36, 1266–1272.

Lu, Z., Chu, W., and Dosher, B. A. (2006). Perceptual learning of motion direction discrimination in fovea: separable mechanisms. *Vision Res.* 46, 2315–2327.

Lu, Z., and Dosher, B. A. (1999). Characterizing human perceptual inefficiencies with equivalent internal noise. *J. Opt. Soc. Am.* 16, 764–778.

Lu, Z., and Dosher, B. A. (2008). Characterizing observers using external noise and observer models: assessing internal representations with external noise. *Psychol. Rev.* 115, 44–82.

Owsley, C. (2011). Aging and vision. *Vision Res.* 51, 1610–1622.

Pelli, D. G. (1997). The VideoToolbox software for visual psychophysics: Transforming numbers into movies. *Spat. Vis.* 10, 437–442.

Pelli, D. G., Robson, J. G., and Wilkins, A. J. (1988). Designing a new letter chart for measuring contrast sensitivity. *Clin. Vision Sci.* 2, 187–199.

Sagi, D. (2011). Perceptual learning in vision research. *Vision Res.* 51, 1552–1566.

Schmolesky, M. T., Wang, Y., Pu, M., and Leventhal, A. G. (2000). Degradation of stimulus selectivity of visual cortical cells in senescent rhesus monkeys. *Nat. Neurosci.* 3, 384–390.

Sekuler, R., Hutman, L. P., and Owsley, C. (1980).Human ageing and spatial vision. *Science* 209, 1255–1256.

Snowden, R. J., and Kavanagh, E. (2006). Motion Perception in the ageing visual system: minimum motion, motion coherence, and speed discrimination thresholds. *Perception* 35, 9–24.

Tadin, D., Lappin, J. S., Gilroy, L. A., and Blake, R. (2003). Perceptual consequences of center-surround antagonism in visual motion processing. *Nature* 424, 312–315.

Trick, G. L., and Silverman, S. E. (1991). Visual sensitivity to motion. *Neurology* 41, 1437–1440.

Yang, Y., Liang, Z., Li, G., Wang, Y., Zhou, Y., and Leventhal, A. G. (2008). Aging affects contrast response functions and adaptation of middle temporal visual area neurons in rhesus monkeys. *J. Neurosci.* 156, 748–757.

Conflict of Interest Statement: The authors declare that the research was conducted in the absence of any commercial or financial relationships that could be construed as a potential conflict of interest.

Received: 28 November 2012; accepted: 30 January 2013; published online: 20 February 2013.

Citation: Bower JD, Watanabe T and Andersen GJ (2013) Perceptual learning and aging: improved performance for low-contrast motion discrimination. Front. Psychology ***4****:66. doi: 10.3389/fpsyg.2013.00066*
This article was submitted to Frontiers in Perception Science, a specialty of Frontiers in Psychology.

frontiers in
PSYCHOLOGY

ORIGINAL RESEARCH ARTICLE
published: 07 March 2013
doi: 10.3389/fpsyg.2013.00107

An island of stability: art images and natural scenes – but not natural faces – show consistent esthetic response in Alzheimer's-related dementia

Daniel J. Graham[1]*, Simone Stockinger[2] and Helmut Leder[2]

[1] *Department of Psychology, Hobart and William Smith Colleges, Geneva, NY, USA*
[2] *Department of Psychological Basic Research and Research Methods, Faculty of Psychology, University of Vienna, Vienna, Austria*

Edited by:
Mark W. Greenlee, University of Regensburg, Germany

Reviewed by:
Yuka Sasaki, Brown University, USA
Camilo J. Cela-Conde, Universidad de las Islas Baleares, Spain

***Correspondence:**
Daniel J. Graham, Department of Psychology, Hobart and William Smith Colleges, Geneva, NY 14456, USA.
e-mail: graham@hws.edu

Alzheimer's disease (AD) causes severe impairments in cognitive function but there is evidence that aspects of esthetic perception are somewhat spared, at least in early stages of the disease. People with early Alzheimer's-related dementia have been found to show similar degrees of stability over time in esthetic judgment of paintings compared to controls, despite poor explicit memory for the images. Here we expand on this line of inquiry to investigate the types of perceptual judgments involved, and to test whether people in later stages of the disease also show evidence of preserved esthetic judgment. Our results confirm that, compared to healthy controls, there is similar esthetic stability in early stage AD in the absence of explicit memory, and we report here that people with later stages of the disease also show similar stability compared to controls. However, while we find that stability for portrait paintings, landscape paintings, and landscape photographs is not different compared to control group performance, stability for face photographs – which were matched for identity with the portrait paintings – was significantly impaired in the AD group. We suggest that partially spared face-processing systems interfere with esthetic processing of natural faces in ways that are not found for artistic images and landscape photographs. Thus, our work provides a novel form of evidence regarding face-processing in healthy and diseased aging. Our work also gives insights into general theories of esthetics, since people with AD are not encumbered by many of the semantic and emotional factors that otherwise color esthetic judgment. We conclude that, for people with AD, basic esthetic judgment of artistic images represents an "island of stability" in a condition that in most other respects causes profound cognitive disruption. As such, esthetic response could be a promising route to future therapies.

Keywords: Alzheimer's disease, dementia, face perception, esthetics, natural scenes, esthetic stability, art perception, memory

INTRODUCTION

Alzheimer's disease (AD) has devastating effects on many aspects of cognition including memory (e.g., Parasuraman and Haxby, 1993) and perception (e.g., Cronin-Golomb, 1995) systems. With 115 million people worldwide expected to develop dementia as a result of AD by 2050 due to demographic trends (Alzheimer's Disease International, 2009), there is an urgent need to understand the nature of these deficits and to explore possible routes to therapy, perhaps via partially spared cognitive systems.

Recent evidence suggests that one promising avenue for approaching Alzheimer's-related dementia is via esthetic perception. Halpern et al. (2008) reported that patients with early-stage AD show essentially the same degree of stability in esthetic judgment of paintings over a 2-week span compared to age-matched controls. Crucially, patients showed this performance despite performing at chance on an explicit memory test of the images, whereas controls performed well above chance on the explicit memory test.

This discovery coincides with a surge of research in esthetic perception from a variety of viewpoints and with diverse methodologies (for reviews, see: Leder et al., 2004; Graham and Redies, 2010; Bacci and Melcher, 2011; Chatterjee, 2011; Van de Cruys and Wagemans, 2011). Indeed, empirical and neuro-esthetic research is emerging as an important facet of visual perception and cognition. Coinciding with this basic research on esthetics, there are increasing attempts to show that interactions with art can lessen the severity of AD symptoms (e.g., Wald, 2003; Eekelaar et al., 2012). Programs such as the New York Museum of Modern Art's MeetMe program use art viewing as a route to reducing disease severity, which has shown some promising indications (Rosenberg et al., 2010). In addition, there are increasing efforts to integrate artistic and esthetic experiences into long-term care. For example, Hearthstone Alzheimer's Care in the United States has a number of long-term care facilities that are explicitly structured around interactions with art and music (http://thehearth.org).

However, beyond the pioneering work of Halpern et al. (2008) much remains unknown about esthetic perception in AD. Halpern

et al. (2008) demonstrated that the representationality of artwork does not seem to affect esthetic stability. In particular, paintings deemed by the investigators to be "representational," "quasi-representational," and "abstract" did not show significantly different interactions with stability (though both AD patients and controls showed the same small differences in stability for abstract versus quasi-representational images). Therefore, artistic style appears not to be a primary factor in generating stability.

We could look at this latter finding from a different perspective and ask whether it is an indication that artistic creation in the painted medium is itself a key element for esthetic perception. In other words, perhaps one component of the seemingly spared capacity to judge esthetic value consistently is the ability to recognize an art image as such. Given that the images used in Halpern et al. (2008) were presented outside of the traditional context of fine art (e.g., a museum), viewers were left only with visual cues to the images' handmade artistic visual quality (for research on context dependency in esthetics, see Kirk et al., 2009; Leder, 2013). Certainly, the lush fantasy of Alma-Tadema and the dramatic use of color in landscapes by Hopper (classified by Halpern et al., 2008, as representational), the surreal imagery of Kitaj (classified as quasi-representational), and the complete abstraction of Mondrian (classified as abstract), are powerful cues to the artificiality of the images. Therefore, one of our primary goals in the present study is to measure esthetic stability in AD for handmade artistic representations in comparison to photographs of the same content. We predicted that painted artwork would display greater stability compared to other classes of images for the AD group.

A second major goal of the present study is to test specific classes of image content, in both artistic and photographic representations. In particular, we are interested in the role of faces. From decades of research, it is now clear that the human brain devotes considerable resources to face perception (e.g., Haxby et al., 2000), and in many ways the human face is treated as a "special" type of stimulus vis à vis perception (e.g., Bruce and Young, 1998).

Importantly, faces appear to have particular relevance to the progression of AD. There is evidence that recognition of familiar scenes could be impaired more than the perception of familiar faces at the earliest stages of the disease (Cheng and Pai, 2010), implying that face deficits emerge more slowly over the progression of the disease. Also, Kurylo et al. (1996) found that AD patients performed well on a face-matching tasks (Benton Face Recognition Test) and were near the level of performance shown by controls.

However, there is active debate about how visual perception in general and face perception in particular are affected by AD. Indeed, there is great variability in the kinds of tests of visual perception that have been employed with AD patients, as well as conflicting findings on comparable tests (see Kirby et al., 2010). With regard to faces, the majority of research in AD patients concerns face memory (recognition) rather than face perception (e.g., gender judgment, after-effects, etc.).

If performance on an esthetic task for a group of faces primarily involves perceptual rather than memory systems, we are left with relatively little consistent evidence upon which to base a hypothesis for how specific content could affect the outcome of our experiments. On the other hand, our results using the innovative approach of Halpern et al. (2008) will potentially be of unique importance for understanding perception deficits in AD, especially given the conflicting findings regarding face perception in AD described above.

In addition to our goal of understanding how image content and art's handmade quality affect esthetic perception in AD, we also set out to test whether individuals with more severe stages of AD still show esthetic stability. Therefore, we test whether stable esthetic evaluations can be preserved even under conditions of severe memory impairment. We also ask if there are performance differences for varied image content that depend on the stage of AD. We predicted that esthetic stability would indeed be observed in later-stage AD patients, and that it would manifest itself in much the same way as it does in controls.

MATERIALS AND METHODS

OVERVIEW

In the present studies we employed methods similar to Halpern et al. (2008). Participants were asked to sort stimuli in rank-order according to how much they liked the stimuli esthetically, and they were also tested on their explicit memory for the images. The study compared a clinical population with a group of control participants. However, unlike Halpern et al. (2008) who used a small set of stimuli with no special consideration of content (aside from using unfamiliar material and not repeating main content) in our study we systematically compared different classes of paintings and content-matched photographs. We were especially interested to carefully test the possible effects of the presence of faces. Although the stimulus classes in Halpern et al. (2008) varied to some extent in terms of face content – e.g., representational images mostly contained faces, while abstract images did not – the delineation was not strict. For example the representational class also included an Audubon painting of a bird, and the quasi-representational class contained a mix of images with and without faces.

PARTICIPANTS

Participants were recruited from two institutions in Vienna, Austria: SeneCura Sozialzentrum Purkersdorf (3002 Purkersdorf, Bahnhofstraße 2) and Caritas (1190 Wien, Hameaustraße 45–47). All participants (via authorized caregivers) as well as both institutions gave consent to conduct the studies. All participants had been diagnosed according to ICD-10 in both intuitions by authorized persons, and were administered the Mini-Mental State Exam (MMSE; Folstein et al., 1975) prior to our experiments. Participants did not have a prior diagnosis of depression. Participants were not art experts, and they did not have perceptual problems that would have impaired the perception of the artworks (see Procedures).

From an initial set of 22, two participants were excluded because they could not finish the testing, and two others were excluded because they had missing values in the preference rank tasks. Data of 18 AD participants were therefore included in the analyses. Fifteen were female, and age varied between 74 and 97 years

($M = 89.5$, SD = 5.9). Art interest varied between 0 ("no interest at all") and 11 ("great interest"), with a mean of 5.83 (SD = 2.18). The mean score on the MMSE was 15.56 (SD = 5.79) with a range from 7 to 25. We split the variable AD into three levels, following the procedure by Wijk et al. (1999), with severe AD indicated when MMSE was below 12 (7 participants), moderate AD with a range of 13–19 (5 participants), and early stage, with values between 20 and 26 (6 participants).

The control consisted of a group healthy older adults who all achieved values of 27 and above on the MMSE (Max. possible value = 30). Control participants were recruited from the same two institutions and from the wider community. Controls were roughly matched with the experimental group according to age and self-indicated interest in art. Also, it was assured that no artists were included in the sample.

The 15 participants in the control group (10 female, 5 male) had an average age of 74.2 (SD = 13.2) with a range between 59 and 99 years. All control participants had MMSE values at least 27 ($M = 28.1$, SD = 0.96). The art interest varied between 0 and 10 ("very much interested in art"), with a mean very similar to that of the AD patients ($M = 5.4$, SD = 3.1).

STIMULI

Four sets of eight images were used as stimuli (see **Figure 1**). We used images of the following types: "painted portraits"; "photographic portraits"; "painted landscapes"; and "photographic landscapes." Images were printed in color on 185 cm × 135 cm high-quality photo paper. All artworks were of recognizable content. They were painted in representational style, mainly dating from late nineteenth and twentieth century (thus examples of various styles of modernism). The sets of photographs were chosen to correspond to the context of the artworks. For example, the paintings by Cézanne had photographic equivalents that were provided by Machotka (1996) and consisted of photographs taken from very similar contemporary perspectives as Cézanne's paintings. Likewise, the portraits depicted artists, politicians, etc., and their photographic counterparts consisted of photographs of the same individuals. A complete list of stimuli is shown in **Table 1**.

PROCEDURE

The study began with a pre-test in which the current cognitive state, as well as the stage of AD, were established with the MMSE. Also, participants were asked to indicate on an 11-point Likert-scale how much they are interested in art in general. In order to detect visual processing deficits, we employed a control task using colored drawings of everyday objects (Rossion and Pourtois, 2004). Participants were asked to rank-order eight objects according to their real-world size. This control task was tested in both sessions.

In the main experimental task, participants were asked to rank-order the stimuli for each of the four image sets. Each of the four sets of eight stimuli was put on a table in two rows in random order, and participants were asked to spatially sort them from left to right according to their esthetic preference. There was no time limit and positions could be changed until the person indicated that a solution was found. Participants were also told that no correct or wrong "answers" to any of the stimuli could be given. Afterward, the size-sorting control task was conducted.

Two weeks later, a second testing session was conducted. This session started with an explicit memory test. We performed a test of explicit recognition in which six pairs of images were shown, each comprising one old image (from the first session) plus a second distracter image, matched in terms of content. Distracter photographic images were chosen according to a definition by Konkle et al. (2010) to be conceptually similar, containing similar objects, regions, and color distributions. Distracter artworks were by the same artist,

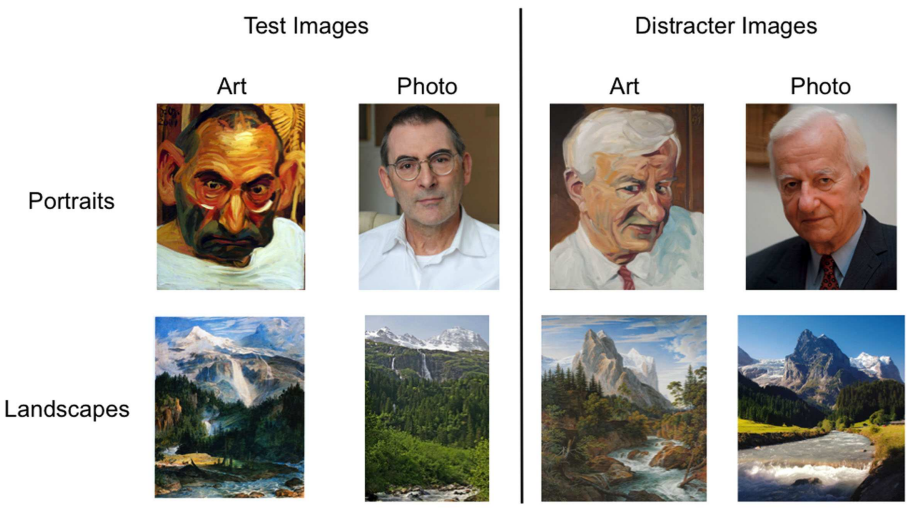

FIGURE 1 | Examples of stimuli used in the esthetic stability test (test images: P1, L5) and matched distracter images used in the explicit memory test (distracter images). Image metadata are provided in **Table 1**.

Table 1 | List of stimuli used in experimental task and explicit memory task.

I. EXPERIMENTAL STIMULI	
Four sets (8 matched pictures per set = 32 total images)	
Set 1: painted landscapes	**Set 2: photographic landscapes**
L1: Cézanne *"Maison en provence-le vallon"*	Photo Machotka
L2: Cézanne *"Bassin et lavoir du Jas de Bouffan"*	Photo Machotka
L3: Cézanne *"Rochers à l'estaque"*	Photo Machotka
L4: Cézanne *"Le Pont de maincy"*	Photo Machotka
L5: Anton Koch *"Der schmadribachfall"*	Photo *"Der Schmadribachfall"*
L6: Ralf Scherfose *"Düne mit strandkorb"*	Photo *"Amrum"*
L7: Van Gogh *"Olivenbäume"*	Photo *"Olivenbäume in St. Remy"*
L8: Van Gogh *"Die Brücke von Langlois"*	Photo *"Brücke von Langlois"*
Set 3: painted portraits portraits	**Set 4: photographic portraits**
P1: Johannes Gruetzke *"Selbstbildnis"*	Photo *"J. Gruetzke"*
P2: Norbert Weck *"portrait Heinrich Böll"*	Photo *"Heinrich Böll"*
P3: Ralf Scherfose *"portrait prof. Dr. Alfred Gutschelhofer"*	Photo *"Gutschelhofer"*
P4: Johannes Heisig *"portrait Willy Brandt"*	Photo *"Willy Brandt"*
P5: Julian Schnabel *"Potrait of Olatz"*	Photo *"Olatz Schnabel"*
P6: Alice steel "Faith Ringgold"	Photo *"Faith Ringgold"*
P7: Norbert Wagenbrett *"Matthias Goerne"*	Photo *"Matthias Goerne"*
P8: Oskar Kokoschka *"Adele Astaire"*	Photo *"Adele Astaire"*
II. EXPLICIT MEMORY TASK	
Four pairs of distracter images for each set (4 sets = 16 pictures)	
Painted and photographic landscapes	***Similar pictures* (painted & photographic l)**
L1: Cézanne/Machotka *"Maison en Provence"*	C./M. *"Le Pigeonnier de Bellevue"*
L5: Anton Koch/Photo *"Der Schmadribachfall"*	A. Koch *"Reichenbachtal Mit Wetterhorn"*
L7: Van Gogh/Photo *"Olivenbäume"*	Van Gogh *"Weizenfeld mit u. Sonne"*
L8: Van Gogh/Photo *"Die Brücke von Langlois"*	Van Gogh *"Brücke von Trinquetaille"*
Painted and photographic portraits	***Similar pictures* (painted & photographic p)**
P1: Johannes Gruetzke *"Selbstbildnis"*	J. Gruetzke *"Richard von Weizsäcker"*
P5: Julian Schnabel *"Potrait of Olatz"*	J. Schnabel *"Portrait Nina Chow"*
P7: Norbert Wagenbrett *"Matthias Goerne"*	N. Wagenbrett *"Musiker Wolfram Dix"*
P8: Otto Kokoschka *"Adele Astaire"*	O. Kokoschka *"Alma Mahler"*

and of similar content and palette. Participants were asked to indicate which of the images they had seen 2 weeks previously.

After the explicit memory task, participants were tested on the rank-order preference task with the same stimuli as in the first session with the same procedures.

RESULTS

CONTROL TASK

The purpose of the real-world size ranking control task was to detect deficits in visual perception. We found that on average, 76% of the healthy elderly participants ordered objects according to their real-world size correctly, and only 19% interchanged one position. In the group of people with AD, 11% ordered the objects correctly, 33% interchanged one object, and 25% interchanged more than three. Participants in the experimental group clearly had some difficulty in solving the task. Some were already exhausted after the sorting task; some did not understand that this was not a preference task but rather that "sorting by size" was required; and some had already lost concentration, or started conversations regarding other issues. However, although this task could not be meaningfully analyzed, participants in the experimental group were generally able to name the depicted objects.

EXPLICIT MEMORY TASK

Because the participants were more exhausted than initially expected, the recognition test comprised only four image pairs per set. In the experimental group the results of the forced choice task were at chance ($M = 2.04$, SD = 0.42), while in the control group the value was 3.03 (SD = 0.66). In other words, people in the control group recognized 76% of the images they had seen in the first testing session, the group with AD recognized 51% of them. A repeated measurement ANOVA with mean-correct recognition rates as dependent variable, and group (AD/control) as a between, and category (Portrait/landscape) and style (photography/art) factors, revealed a massive effect of group, with much higher performance for the control participants [$F(1,31) = 28.75$, $p < 0.001$, eta = 0.48] but only one trend for an interaction between group and style, with $F(1,31) = 3.76$, $p = 0.062$, eta = 0.11.

Table 2 | Esthetic stability for AD patients versus controls for each stimulus category.

	AD	Controls
Art portraits	1.86 (0.76)	1.53 (0.57)
Photo portraits	2.17 (0.66)*	1.55 (0.78)
Art landscape	1.53 (0.71)	1.75 (0.74)
Photo landscape	1.83 (0.84)	1.92 (0.79)

**Indicates that photo portraits showed significantly lower stability for AD patients compared to the control group (two-tailed t-test, $p = 0.019$).*

Table 3 | Esthetic stability as a function of disease severity for each stimulus type.

	Art portraits	Photo portraits	Art landscapes	Photo landscapes
Severe	1.79 (0.47)	2.11 (0.52)	1.50 (0.84)	2.25 (0.98)
Moderate	2.00 (0.64)	1.95 (0.97)	1.50 (0.59)	1.60 (0.76)
Early	1.83 (1.17)	2.25 (0.65)	1.58 (0.77)	1.52 (0.59)

PREFERENCE TASK

The stability of the ranks for preference was analyzed as in the Halpern et al. (2008) study, counting the change that each item had in the preference rankings between the two sessions. The added changes were computed to generate a change score. In particular, we first take the sum of the magnitude of the rank change for a given image set. For example, imagine if the rankings of the eight photo portrait images were in session 1 found to be (1,2,3,4,5,6,7,8), and in session 2 they were found to be (8,7,6,5,4,3,2,1). Let us consider the first four images in the session 1 ranking: they would change in rank by 7, 5, 3, and 1, respectively, giving a change score of 16. The last four images would have the same change scores (1, 3, 5, and 7, respectively), giving an overall summed change in ranking of 32 for this image set. Mean values of these scores were calculated for each category of images. Each of these change scores was then divided by the number of items (eight) in each set in order to make the scores comparable to the results of Halpern et al. (2008), who used this convention. Thus, the reported average rank change could vary in steps of 0.25, with a maximum value of 4 and a minimum value of 0. Higher values indicate lower consistency between first and second testing. **Table 2** shows the mean change score values (and SD) in all four stimulus categories for AD patients and control participants.

We found a significant difference between the AD and controls only for the photographic portraits ($p = 0.019$, two-tailed t-test), with AD patients showing less stability. Preference stability did not show significant differences for any of the other three categories. These results imply that in comparison to controls, AD patients' esthetic stability is impaired for images of natural faces but not for other types of painted images or photographs of landscapes.

All change-score means were in a range between 1.5 and 2.2, and the values seem to be more stable (smaller) in the control group for the portraits. We conducted an analysis of variance, with *art* (art-photograph) and *genre* (portrait-landscape) as within-factors and *group* (AD versus Controls) as between-factor, on the mean changes in preferences by participants as dependent variable. This analysis only revealed an interaction between *group* and *genre* [$F(1,31) = 8.127$, $p < 0.01$, eta $= 0.21$], but no other effect.

DISEASE SEVERITY

Our range of MMSE scores allowed us to test for possible influences of disease severity on esthetic stability in AD (in Halpern et al., 2008, no AD patient scored lower than 12 on the MMSE, while in our sample, 7 patients in the AD group scored lower than 12 on the MMSE). An ANOVA analysis found no significant differences among the AD participants grouped by disease severity, nor were there significant differences between control group and each of the three disease severity groups. Mean stability scores (with SD) are listed in **Table 3**.

VECTOR LENGTH ANALYSIS

We applied a second measure of esthetic stability based on vector length. Treating each subject's rankings in each session as a vector, we took the L_2-norm (Euclidean distance) of the difference in the vectors for the two sessions. This measure is in agreement with what was calculated above (average change score), which is effectively the L_1-norm (city-block distance). All significant and insignificant effects found with the L_1 metric were also found with the L_2 metric.

POSSIBLE CONFOUNDS

There are some possible confounds in our study. In the landscape category, there were four paintings by Cézanne, so perhaps if viewers had similar esthetic judgments of all Cézanne images, this would artificially bias their responses to be more stable (assuming all works by Cézanne are judged similarly). However, we found that there was no significant difference in the change scores for the Cézanne images versus the other images in the landscape painting set ($p = 0.91$). Moreover, we see no difference in stability for controls versus AD patients for landscape photographs, which presumably have less influence of authorship. We observe the same also for portrait paintings, which were all painted by different artists.

Werheid and Clare (2007) suggest that intra-class similarity could play a role in face perception deficits in AD, thus the fact that the face photographs were rather similar in content could have influenced our results. However, the same is true of the portraits, and in any case there is substantial variety in poses, lighting, hairstyles, facial hair, gaze, direction, and clothing in the face photographs. The criticism of Werheid and Clare (2007) is more germane to face stimuli from highly standardized databases that are used in many studies. Nevertheless, it remains possible that intra-class similarity could have had some effect on our results.

The AD group was significantly older than the control group (89.5 versus 74.2). But despite the more advanced age of the AD group, it still showed similar stability compared to controls as described above.

Given that the AD group was mostly female (15/18), and if one supposes that face attractiveness is more salient in face photographs, one might expect that the AD group would tend to be

biased to rate male faces as more attractive than female, which would tend to bias results in the face photograph task in the direction of greater stability. However, this does not appear to be the case because we find that the face photographs show significantly lower esthetic stability for the AD group. Moreover, only one face photograph showed greater stability in the AD group (P1, image of Johannes Gruetzke), and for this image the males showed greater stability than females. In addition, the control group was also biased toward females (10/15). However, gender effects deserve further study.

DISCUSSION

In general, our results replicate those of Halpern et al. (2008), though our results add substantial new understanding of esthetic perception in AD. We have provided evidence that people with both early- and later-stage Alzheimer's-related dementia show similar degrees of esthetic stability. And we report that esthetic stability in AD is not different from controls for paintings and photographs of landscapes and paintings of faces, but not for photographs of faces. And in agreement with Halpern et al. (2008), AD patients showed chance-level explicit memory for the image groups, while the control group showed far better explicit memory for the images.

We are left with a basic question: Why are face photographs different? We propose a route to explaining the observed effects. First, a fundamental separation of esthetic beauty from biological beauty – perhaps one rooted in basic visual dimensions of art (Graham and Meng, 2011) – could play a role. In particular, human judgment of esthetic quality for art objects may rely on different perceptual and cognitive mechanisms compared to judgment of face or body attractiveness. Our result showing that landscape photographs do show esthetic stability suggests that this explanation cannot fully explain our findings. However, landscape photographs may have elements of artful posing that could be less prominent in face photographs (McManus et al., 2011). Such differences could contribute to the observed effects.

Let us also consider natural faces as a special stimulus class. When humans see a face *as a face* (not as a scene to be esthetically evaluated), we may think, do I know this person? And a person with AD, especially in earlier stages of the disease, might think, am I *supposed* to know who this person is? Such may not be the case for artwork – we have freedom to evaluate it along other criteria, which may result in more amodal or less task-directed processing compared to faces.

In one of the very few previous studies that has bearing on the question of why stability for face photographs is different, Hönekopp (2006) showed that esthetic stability for face photographs in a sample of healthy young people (mean age ∼24 years) is very high over a 1-week span. Therefore, we would expect a high baseline even for older adults. And as noted above, some evidence indicates that recognition of familiar faces appears relatively intact compared to recognition of familiar scenes early in the progression of AD (Cheng and Pai, 2010). Face-matching ability is also somewhat spared in those with established AD (Kurylo et al., 1996). But without explicit memory for faces, as shown in our study, AD patients may experience cognitive interference, which impairs their esthetic stability. We therefore refer to this explanation of our results as the *cognitive interference hypothesis*. In this view, our results are consistent with the idea that partially spared memory for the familiarity of faces generates a cognitive conflict such that patients may suspect they should be able to name or recognize a face, but cannot.

Why, then, do portrait paintings yet show similar esthetic stability in AD and in controls? A partial answer can perhaps be found if we consider other previous results. Kurylo et al. (1996) found that AD patients' performance on the Mooney Face Test (a measure of face/non-face discrimination using binarized images) was poor compared to their performance on other visual perception tasks (e.g., a spatial position task). Thus, decreased ability to recognize stylized faces *as faces* (or as *specific faces*) could enable portrait paintings to be evaluated more easily on basic esthetic grounds, with less interference of face detection and recognition systems.

Our method does not elucidate the process by which AD patients evaluate esthetic qualities, nor does it prove that people with AD are truly judging esthetic quality in the same way as controls despite their comparable performance on the rank-order task. The situation is made all the more complex because if people with AD do possess esthetic perception much like that of healthy adults, we must explain how this is possible given that brain areas that seem to underlie normal esthetic perception appear to be damaged in AD. We speculate that apparent damage may not be so severe as to obliterate basic esthetic responses in AD, and that sub-cortical systems could help individuals compensate. Future studies – including those concerned with brain lesions – may help uncover what operations are necessary at a minimum to make esthetic judgments. This taps into an important debate on whether the multiple facets of the esthetic sense are essentially based on early sensory or later cognitive processes (Leder, 2013). In any case, we believe this is an important area for future research.

One might wonder why we would expect esthetic perception to be stable in the first place. However, our method probes preference of a set of stimuli *relative to themselves* over a 2-week span – which we (Halpern et al., 2008) presume to be stable. Images are also presented in the same context in both sessions. We certainly might expect instability in cases where new and old stimuli are mixed, as in Park et al. (2010). But even in the Park et al. (2010) study, preference shifts due to novelty/familiarity manipulations in one session were erased after a 1-week interval. Thus it would appear unlikely that judgments of preference should be affected by exposure (including repeated exposure) to other images during the interval. Nevertheless, other experiences in the interval could play a role, and this is an important but so far neglected question. It remains to be seen whether preference for a standard set of stimuli is malleable in healthy adults and other populations, and what could cause such shifts.

FUTURE STUDIES

We argue that the response of AD patients in the present experiments could be considered a "pure" form of visual esthetic

perception, one that relies solely on image content. Although we do not want to minimize the often tragic cognitive decline of those with AD, and we would not claim this is a kind of silver lining in this condition, we would advocate that the present study and future studies of AD be considered as novel and uniquely important form of evidence regarding human esthetics. If this interpretation is correct, one conclusion we can draw is that the current results support the idea that there is a fundamental dichotomy between biological and artistic esthetics for humans as a species.

However, as we have noted, an important question that will require further research in order to put the current study and Halpern et al. (2008) in context concerns the baseline esthetic stability in younger people and in other populations. While healthy older adults and AD patients mostly show similar esthetic stability, we currently do not have a well-established benchmark for humans as a whole. We are not aware of any studies that have examined this aspect of esthetics for artistic images, although a handful of papers have tested the stability of preference over time for other images (e.g., Hönekopp, 2006). We are currently undertaking a suite of experiments in a variety of populations to establish benchmarks for esthetic stability, taking account of contextual factors.

Finally, we propose that a main requirement for activating esthetic responses in AD could be for art images to be perceived as such. If true, this insight could help guide the development of novel therapies, particularly those involving art viewing. Future experiments examining the potential for art images to be used as avenues for lessening the severity of disease symptoms could therefore be fruitful. A deeper understanding of visual esthetics in AD could also assist in the development of more effective signage in care facilities by leveraging stimuli that promote esthetic stability.

CONCLUSION

Our results demonstrate that people with AD have esthetic stability for artistic images mostly like that of healthy older controls, and that this stability is roughly the same for early- and later-stage AD patients. This stability contrasts with the lack of explicit memory for the stimuli in the AD group. However, face photographs show decreased esthetic stability in AD patients compared to controls. Given these results, we conclude that, for people with Alzheimer's-related dementia, esthetic perception of artistic images represents an "island of stability" in a condition that in most other respects causes profound cognitive disruption. We have proposed interpretations of our results that give a novel perspective on face perception in AD, and also on perceptual esthetics. We hope that our findings will contribute to new approaches to therapy for AD patients.

ACKNOWLEDGMENTS

We are extremely grateful to Sylvia Merchiori, Wolfgang Neruda, Regina Sykora, Christine Wondrak-Dreitler, Regina Hermann, Maria Arbes, Konstanze Welley, Caritas Wien, and SeneCura Purkersdorf for their assistance in carrying out this study. We also thank Harriet Baldwin, Andrea Halpern, and Robert Santulli for helpful discussions in early stages of designing the study. This study was supported by grants from WWTF (CS11-023) and FWF (P23538) to Helmut Leder.

REFERENCES

Alzheimer's Disease International. (2009). *World Alzheimer Report 2009*. Available at: www.alz.co.uk.

Bacci, F., and Melcher, D. (eds). (2011). *Art and the Senses*. Oxford: Oxford University Press.

Bruce, V., and Young, A. (1998). *In the Eye of the Beholder: The Science of Face Perception*. Oxford: Oxford University Press.

Chatterjee, A. (2011). Neuroaesthetics: a coming of age story. *J. Cogn. Neurosci.* 23, 53–62.

Cheng, P.-J., and Pai, M.-C. (2010). Dissociation between recognition of familiar scenes and of faces in patients with very mild Alzheimer disease: an event-related potential study. *Clin. Neurophysiol.* 121, 1519–1525.

Cronin-Golomb, A. (1995). Vision in Alzheimer's disease. *Gerontologist* 35, 370–376.

Eekelaar, C., Camic, P. M., and Springham, N. (2012). Art galleries, episodic memory and verbal fluency in dementia: an exploratory study. *Psychol. Aesthet. Creat. Arts* 6, 262.

Folstein, M. F., Folstein, S. E., and McHugh, P. R. (1975). "Mini-mental state": a practical method for grading the cognitive state of patients for the clinician. *J. Psychiatr. Res.* 12, 189–198.

Graham, D. J., and Meng, M. (2011). Artistic representations: clues to efficient coding in human vision. *Vis. Neurosci.* 28, 371–379.

Graham, D. J., and Redies, C. (2010). Statistical regularities in art: relations with visual coding and perception. *Vision Res.* 50, 1503–1509.

Halpern, A. R., Ly, J., Elkin-Frankston, S., and O'Connor, M. G. (2008). "I know what I like": stability of aesthetic preference in Alzheimer's patients. *Brain Cogn.* 66, 65–72.

Haxby, J. V., Hoffman, E. A., and Gobbini, M. I. (2000). The distributed human neural system for face perception. *Trends Cogn. Sci. (Regul. Ed.)* 4, 223–233.

Hönekopp, J. (2006). Once more: is beauty in the eye of the beholder? Relative contributions of private and shared taste to judgments of facial attractiveness. *J. Exp. Psychol. Hum. Percept. Perform.* 32, 199.

Kirby, E., Bandelow, S., and Hogervorst, E. (2010). Visual impairment in Alzheimer's disease: a critical review. *J. Alzheimers Dis.* 21, 15–34.

Kirk, U., Skov, M., Christensen, M. S., and Nygaard, N. (2009). Brain correlates of aesthetic expertise: a parametric fMRI study. *Brain Cogn.* 69, 306–315.

Konkle, T., Brady, T. F., Alvarez, G. A., and Oliva, A. (2010). Conceptual distinctiveness supports detailed visual long-term memory for real-world objects. *J. Exp. Psychol. Gen.* 139, 558.

Kurylo, D. D., Corkin, S., Rizzo, J. F. III., and Growdon, J. H. (1996). Greater relative impairment of object recognition than of visuospatial abilities in Alzheimer's disease. *Neuropsychology* 10, 74.

Leder, H. (2013). Next steps in neuroaesthetics: which processes, and processing stages to study? *Psychol. Aesthet. Creat. Arts. Spec. Issue* 7, 27–37.

Leder, H., Belke, B., Oeberst, A., and Augustin, D. (2004). A model of aesthetic appreciation and aesthetic judgments. *Br. J. Psychol.* 95, 489–508.

Machotka, P. (1996). *Cézanne: Landscape into Art*. New Haven: Yale University Press.

McManus, I. C., Stöver, K., and Kim, D. (2011). Arnheim's Gestalt theory of visual balance: examining the compositional structure of art photographs and abstract images. *Iperception* 2, 615–647.

Parasuraman, R., and Haxby, J. V. (1993). Attention and brain function in Alzheimer's disease: a review. *Neuropsychology* 7, 242.

Park, J., Shimojo, E., and Shimojo, S. (2010). Roles of familiarity and novelty in visual preference judgments are segregated across object categories. *Proc. Natl. Acad. Sci. U.S.A.* 107, 14552–14555.

Rosenberg, F., Parsa, A., Humble, L., and McGee, C. (2010). *Meet Me: Making Art Accessible to People with Dementia*. New York: The Museum of Modern Art.

Rossion, B., and Pourtois, G. (2004). Revisiting snodgrass and Vanderwart's object pictorial set: the role of surface detail in basic-level object recognition. *Perception* 33, 217–236.

Van de Cruys, S., and Wagemans, J. (2011). Putting reward in art: a tentative prediction error account of visual art. *Iperception* 2, 1035–1062.

Wald, J. (2003). "Clinical art therapy with older adults," in *Handbook of Art Therapy*, ed. C. A. Malchiodi (New York: Guilford Press), 294–308.

Werheid, K., and Clare, L. (2007). Are faces special in Alzheimer's disease? Cognitive conceptualisation, neural correlates, and diagnostic relevance of impaired memory for faces and names. *Cortex* 43, 898–906.

Wijk, H., Berg, S., Sivik, L., and Steen, B. (1999). Colour discrimination, colour naming and colour preferences among individuals with Alzheimer's disease. *Int. J. Geriatr. Psychiatry* 14, 1000–1005.

Conflict of Interest Statement: The authors declare that the research was conducted in the absence of any commercial or financial relationships that could be construed as a potential conflict of interest.

Received: 30 November 2012; accepted: 15 February 2013; published online: 07 March 2013.

Citation: Graham DJ, Stockinger S and Leder H (2013) An island of stability: art images and natural scenes – but not natural faces – show consistent esthetic response in Alzheimer's-related dementia. Front. Psychol. ***4****:107. doi:10.3389/fpsyg.2013.00107*

This article was submitted to Frontiers in Perception Science, a specialty of Frontiers in Psychology.

frontiers in PSYCHOLOGY

ORIGINAL RESEARCH ARTICLE
published: 21 June 2013
doi: 10.3389/fpsyg.2013.00339

Age-related changes in visual exploratory behavior in a natural scene setting

Johanna Hamel[1]*†, Sophie De Beukelaer[2†], Antje Kraft[2], Sven Ohl[3], Heinrich J. Audebert[4,5] and Stephan A. Brandt[2]

[1] Department of Neurology, University of Rochester Medical Center, University of Rochester, Rochester, NY, USA
[2] Department of Neurology, Charité Campus Mitte, Universitätsmedizin Charité, Berlin, Germany
[3] Berlin School of Mind and Brain, Humboldt Universität zu Berlin, Berlin, Germany
[4] Department of Neurology, Charité Campus Benjamin Franklin, Universitätsmedizin Charité, Berlin, Germany
[5] Center for Stroke Research Berlin, Universitätsmedizin Charité, Berlin, Germany

Edited by:
Mark W. Greenlee, University of Regensburg, Germany

Reviewed by:
George L. Malcolm, The George Washington University, USA
Steven Paul Blurton, University of Regensburg, Germany

***Correspondence:**
Johanna Hamel, 21 Lilac Drive, 14620 Rochester, NY, USA
e-mail: johanna_hamel@urmc.rochester.edu
† *Johanna Hamel and Sophie De Beukelaer have contributed equally to this work.*

Diverse cognitive functions decline with increasing age, including the ability to process central and peripheral visual information in a laboratory testing situation (useful visual field of view). To investigate whether and how this influences activities of daily life, we studied age-related changes in visual exploratory behavior in a natural scene setting: a driving simulator paradigm of variable complexity was tested in subjects of varying ages with simultaneous eye- and head-movement recordings via a head-mounted camera. Detection and reaction times were also measured by visual fixation and manual reaction. We considered video computer game experience as a possible influence on performance. Data of 73 participants of varying ages were analyzed, driving two different courses. We analyzed the influence of route difficulty level, age, and eccentricity of test stimuli on oculomotor and driving behavior parameters. No significant age effects were found regarding saccadic parameters. In the older subjects head-movements increasingly contributed to gaze amplitude. More demanding courses and more peripheral stimuli locations induced longer reaction times in all age groups. Deterioration of the functionally useful visual field of view with increasing age was not suggested in our study group. However, video game-experienced subjects revealed larger saccade amplitudes and a broader distribution of fixations on the screen. They reacted faster to peripheral objects suggesting the notion of a general detection task rather than perceiving driving as a central task. As the video game-experienced population consisted of younger subjects, our study indicates that effects due to video game experience can easily be misinterpreted as age effects if not accounted for. We therefore view it as essential to consider video game experience in all testing methods using virtual media.

Keywords: oculomotor behavior, eye movements, visual attention, driving simulator, aging, video game experience

INTRODUCTION

It is widely accepted that as we age, cognitive function becomes increasingly impaired as part of the normal aging process (Park et al., 2003; Hedden and Gabrieli, 2004; Morrison and Baxter, 2012). Recent research efforts have focused their interest on the changes in higher cognitive functions such as memory systems (Podell et al., 2012) or on age-related changes in sensory functions, which represent an earlier step in cognitive processing (Cliff et al., 2012; Mozolic et al., 2012). In the visual domain, recent studies have addressed the hypothesis that visual perception deteriorates with increasing age: to test this, Owsley et al. (1998) developed a model of the "Useful Field of View" (UFOV), referring to the spatial area from which a person is able to simultaneously process central and peripheral visual information. The UFOV is measured by cognitive tests that are sensitive to declines in visual sensory function, slowed visual processing speed, and impaired visual attention skills.

It is of great interest how these laboratory test results correlate with relevant changes in daily life activities. While driving a vehicle for example the information processed is mainly visual (Robinson et al., 1972). Studies have ascribed a greater risk of causing road traffic accidents (Tefft, 2008) to older driving populations.

How does visual processing while driving change with age and how does this alter driving behavior? To address this question we set up a study to investigate age-related changes in visual exploratory behavior in a natural setting: we used a driving simulator with subjects driving routes of varying complexity while simultaneously wearing a head-mounted camera recording eye- and head-movements, as well as measuring reaction times (screenshot of driving course, Hamel et al., 2012).

It has been previously shown that UFOV parameters have a high sensitivity (89%) and specificity (81%) in predicting which older drivers have a history of car crashes (Ball et al., 1993). A

prospective study demonstrated that older drivers with a 40% or greater impairment in the UFOV were more than two times more likely to cause a crash during a 3-year follow-up period (Owsley et al., 1998).

Two different theories were developed of how the peripheral field deteriorates in a realistic setting, e.g., a driving situation, while central demand increases: either through an abrupt neglect of stimuli, referred to as general interference (Holmes et al., 1977; Crundall et al., 1999) or through gradual decline of attention with increasing eccentricity, referred to as tunnel vision (Williams, 1988; Miura, 1990). Recent studies demonstrated a combination of both in older drivers: while presenting stimuli not related to the driving task, tunnel vision was observed, whereas if stimuli were relevant to driving (e.g., because they were located on other vehicles), a general interference occurred (Rogé et al., 2004). In our study we used targets located at different eccentricities, but all relevant to the driving task.

Besides peripheral visual perception, gaze behavior also contributes to the acquisition of visual information in natural activities such as driving. To this end, an important approach was introduced by Mourant and Rockwell (1972). They demonstrated that fixations and saccadic eye movements provide important insights into the drivers' visual search behavior, information needs, and information-acquisition processes (Shinar, 2008). They showed that search and scan patterns of novice drivers differed from those of experienced drivers as they covered a smaller visual field, which was interpreted as unskilled and inadequate for the detection of potential hazards. However, not only eye movements give an insight into exploratory behavior, head-movements have become the focus of research interest in naturalistic tasks, and the role of age-dependent changes in head-movement-behavior remains unclear. Our study allows for and examines unrestrained movements of the head, as there is evidence supporting an increased number of head-movements among the elderly as a compensatory strategy in visual tasks (Proudlock et al., 2004). Also, in head-unrestrained conditions, eye movement characteristics change, depending on gaze amplitudes (Freedman, 2008).

A high variability in visual search behavior has been demonstrated among the elderly (Maltz and Shinar, 1999). During episodes in which the older participants had difficulty searching, their eye movements were characterized by shorter saccades and increased numbers of fixations. Other studies (Pradhan et al., 2005; Bao and Boyle, 2009) showed that older drivers scanned significantly less toward both sides when passing intersections compared to middle-aged and younger drivers and searched less often for possible hazards than younger drivers (Romoser and Fisher, 2009). This was interpreted as indicating visual inattention, e.g., in the form of (a) a poor visual search process with ineffective use of the peripheral field, or (b) a failure to extract maximum amounts of information from areas that were already fixated on (Maltz and Shinar, 1999).

In order to characterize possible visual inattention, one goal of the study is to describe visual information-acquisition skills in more detail: we differentiated between manual reaction times, which could be delayed by motor impairment, and the latency until an object or hazard is fixated by the driver and possibly seen. Manual (Crundall et al., 2002; Rogé et al., 2004; Jahn et al., 2005) or verbal (Cantin et al., 2009) reaction times have been chosen by previous studies as a response. If there was a difference between the two, it would not only be of diagnostic interest, but also training could be specified to improve manual reaction time either by raising more attention, or by training the pure motor responses. Observation of gaze fixations of risk relevant elements rather than manual reaction times was used to examine risk recognition in novice, young experienced, and older drivers (Pradhan et al., 2005). Overall, 25.82% of the younger, novice drivers, 40.14% of the younger, experienced drivers, and surprisingly 69.59% of the older drivers demonstrated visual exploratory behavior which indicated that they recognized the risks in a scenario. Nevertheless, the fatality rate of the older drivers was not smaller than that of the younger drivers, although the older drivers showed more awareness of the risks. The authors argued that the increasing risk awareness compensates for changes in the cognitive, perceptual, and motor status.

Interestingly, in a training session including a feedback mechanism displaying the participants point of gaze, older drivers could be successfully taught to perform more second looks for potential hazards (Pollatsek et al., 2012). Pollatsek argues that these findings may be explained by the following: older drivers develop an "unsafe habit," which can be reversed by training, rather than deteriorating physical or mental capabilities. Thus, training may be effective in reducing crashes. The unsafe habit could consist of the goal not to hit anything that is in front of their vehicle, similar to a central driving task. In this study, examining the gaze distribution and reaction times via fixation will investigate whether elderly drivers tend toward a central fixation bias.

Comparability of studies with each other and with actual driving situations is limited: Pollatsek offered stable pictures of traffic situations, which were explored and did not include a dynamic testing situation. In some studies head-movements were not measured (Pradhan et al., 2005) and eye movements were recorded via video recording instead using an eyetracker (Bao and Boyle, 2009). Another factor, which we accounted for in our study, is the experience of participants with video or computer games, which presents a potential confounder and major effect on study results. In previous studies testing spatial memory in a virtual driving task with pointing and navigating, virtual media experience was associated with greater pointing accuracy and greater navigational efficiency (Han et al., 2012). The authors argued that one reason for this pattern of results could be that the advantage conferred by video game experience in the task is due to better spatial encoding and recall of routes. It has been shown that video game-experienced subjects more successfully suppress distracting information and reveal enhanced attention to objects (Bavelier et al., 2011). They also reveal better performance in allocating spatial attention over the visual field at all eccentricities (Green and Bavelier, 2003). Action video game players tend to employ efficient executive strategies to reduce distraction during tasks (Chisholm and Kingstone, 2012). Video game interventions have offered some promise to help with cognitive decline in the elderly population. However, its mechanism and successful use remains unclear (Boot et al., 2013).

MATERIALS AND METHODS

PARTICIPANTS

Eighty-five participants were recruited (by newspaper advertisement, a local senior computer club, and among hospital employes)

of varying age (20–75 years of age, equally distributed). The study was conducted in conformity with the declaration of Helsinki and was approved by the local ethics committee. Written informed consent was obtained from all participants. All subjects were paid for their participation and were unaware of the purpose of the experiments. In the first session a medical history was taken and experiences with virtual media explored. All participants reported no cognitive deficits, neurological or psychiatric deficits or diseases, and visual acuity was higher than 0.5. Seven participants did not own a driver's license. One subject did not attend the second test day, 11 participants had to be excluded from analysis [due to strabismus (2), ptosis, multiple blinks, or difficulty in calibration (3), malposition of the head (2), or nausea (4)]. The remaining 73 participants fully completed all testing sessions and were included in the analysis.

EXPERIMENTAL SETUP

Participants were tested in a fixed base driving simulator (Hamel et al., 2012). The simulator consisted of a simulation car seat imitating a real car seat (including brake and accelerator pedals, steering wheel, and indicators). A special software (SILAB 3.0 by Wuerzburg Institute for Traffic Sciences GmbH (WIVW)] was used to program specific driving scenarios meeting the requirements of the study by providing courses with different amount of workload and recording the driver's performance.

The software was combined with a head-mounted binocular infrared video pupil tracker, recording head- and eye-movements at a sample rate of 100 Hz (EyeSeeCam by University of Munich Hospital, Clinical Neurosciences). The eye data were calibrated using a series of five fixation points.

A projector (Canon SX 80 Mark II, resolution: 1400 × 1050 pixels) displayed the visual information on a screen (1.52 m high × 2.03 m wide) located 2.0 m from the participant's head. The center of the screen was located at eye level through the midline of the subject, thus covering 58.15° of the visual angle on the horizontal axis and 43.61° on the vertical axis of the field of view.

DRIVING TASK

At the first session, instructions were given regarding the driving task and how to use the simulation vehicle. A practice run with less task density was conducted to allow familiarization to the simulation situation, the task and to prevent simulator sickness, a syndrome similar to motion sickness potentially confounding data and increasing the drop-out rate (Brooks et al., 2010). Prior to the start participants were informed that the simulator could cause experiencing nausea. They were specifically instructed to inform the experimenter if this happened and were told the experiment would stop immediately with no consequences. A rest of at least 1 day was assured between the practice and the experimental run. About 30% of the participants, when specifically asked after the completion of the experiment, reported retrospectively feeling slight malaise during the testing session.

The participants accomplished two experimental runs. Each consisted of a continuous scenario of 6500 m of rural roads (approximately 10 min duration) and different task difficulty due to level of distraction by surrounding environment (easy vs. difficult). Both drives were equal in setup and located in a rural scene. The easy course had lower stimulus density (referred to as "field"), with flat farmed fields allowing for clear visibility of all hazards. The difficult course was located in a wooded area with houses, trees, and bushes as distractions (referred to as "ancient").

The participants were instructed to drive and behave as they would in a real, non-simulated, driving situation. They were asked to be vigilant to street signs and break-down cars emerging on both sides of the road. In addition, they were instructed to react as soon as possible to these stimuli, as well as to potentially hazardous events such as wild boars or colored balls approaching the road, by either pressing the brake or using the indicator or both, as seemed appropriate to them in the respective driving situation. [A total of eight hazardous events occurred during each course, four (two wild boars and two colored balls) from both sides of the road at two different eccentricities.] This task was also practiced in the training session prior to the testing day. Speed was maintained by a cruise control. While depressing the pedal, the car sped up to a constant speed of 70 km/h unless the brake was used. This was implemented to assure comparability of reaction times between age groups, as it is known that older drivers reduce speed as a possible compensatory mechanism (Cantin et al., 2009).

After the examination participants were asked questions regarding their driving history and how they perceived the test and their performance. They were also asked about their experience with video computer games. We included a questionnaire to take into account video game experience as a possible effect on performance. As our group consisted of different ages engaged in different levels of video game experience, we categorized the participants in three groups according to their history. **Table 1** shows the grouping criteria for the video game experience. We differentiated virtual media history in PC or video games with animation, such as action games that require quick strategic assessment of situations, and one-dimensional strategic games, such as Tetris or card games. **Table 1** displays the division into groups by the time spent on game playing.

TEST PARAMETERS

SILAB Software recorded speed and reaction times (use of turn signal or brake). The MATLAB software (MathWorks Company, Natick, MA, USA) was used to analyze the recorded experimental

Table 1 | Grouping criteria for video game experience.

Groups	Experience with video games	Number of participants	Mean age
Group 1	Minimum experience (games without animation/motion perception, such as card games)	39	56.33
Group 2	Medium experience (one to two different kind of video games such as car-racing or flight simulation)	22	36.18
Group 3	Extensive experience (≥2 different kind of video games (see Group 2) regularly played)	12	27.5

data. Saccades were defined as sections of the gaze trajectory where gaze velocity exceeded 30° /s and gaze amplitude was larger than 1°. Sections between saccades were defined as fixations. Head-movements were defined as movements exceeding 6° /s and an amplitude of more than 3° (Einhäuser et al., 2007). Object fixations were defined as fixation on an object with gaze position maximally 1.24° apart from the object on the *X*-axis and 1.66° on the *Y*-axis. In addition to these measures, the average length of the participant's fixations (mean fixation durations) and the spread of search in the horizontal and vertical meridians (the variance of the fixation locations) were also calculated. The average number of successfully detected targets per participant was recorded.

Simultaneous head- and eye-movements with trajectory in the opposite direction were excluded, as they represent no gain in amplitude of gaze movement. They were subsumed as vestibulo-ocular reflexes (VOR) and excluded from head-movements.

Reaction time was measured in two ways: as a first mode (first detection) we measured reaction time as first detection by either fixation or manual detection: if the participant fixated the object first and responded manually afterward (represented the majority of cases), then we chose the fixation time as reaction time as first detection. If the subject used the turn signal or brake pedal first as an indicator fixating the object afterward, then manual reaction time represented reaction time as first detection. As a second mode (manual reaction), we measured reaction time by manual reaction (brake or turn signal) only.

ANALYSIS

For statistical analysis linear mixed models (LMM) were used to measure the fixed effects of age, eccentricity of target objects (close vs. distant), course difficulty (easy vs. difficult), and two dummy variables of our three video game experience groups (extensive video game experience and moderate video game experience) and their interactions on reaction times, parameters of saccades (mean fixation duration, mean gaze amplitude, number of saccades, distribution of fixations on the screen) and head-movements with subject as random factor. Effects with a *t*-value larger than ±2 were considered as significant (Kliegl et al., 2010; Ohl et al., 2011). Functions for LMMs were provided by the lme4 package (Bates and Maechler, 2010) in the R environment (R Development Core Team, 2010). Eccentricity of objects was coded as 0 for "close," 1 for "far" (appearing at 10 m or at 30 m distance to the road). The different types of courses were coded as 0 for the course with a lower level, "field," and 1 for the higher level of complexity, "ancient." The baseline group for the dummy variables was minimum video game experience and coded 0 for the variables extensive and moderate video game experience. The dummy variable "moderate video game experience" was coded as 1 for "yes" and 0 for "no," extensive video game experience and the baseline group. The dummy variable extensive video game experience was coded 1 for "yes," and 0 for "no" moderate video game experience and the baseline group. Gender was coded 0 for male, 1 for female. Incidence of malaise was coded as 0 for "no" and 1 for "yes." Age was uniformly distributed in range from 20 to 75 years and centered around the mean (mean = 0.000548, SEM = 0.964175), here referred to as age_c, for use as a covariate in the regression model. Logistic regression was used to calculate the effects of age, eccentricity of target stimuli, course type, and computer game experience on the incidence of simulator sickness. Correlation analyses were obtained by polycor package (Fox, 2007) between age and video game experience. Graphics were obtained by the ggplot2 package (Wickham, 2009) in the R environment (R Development Core Team, 2010).

RESULTS

DESCRIPTIVE STATISTICS

Head-restrained saccades have been characterized by a set of stereotyped relationships, referred to as "the main sequence" (Bahill et al., 1975): the duration and peak velocity of a saccade both increase with increasing magnitude of a saccade. These characteristics have been shown to alter with head-unrestrained movements with larger amplitudes above 20° (Freedman, 2008). **Figures 1–3** show saccade characteristics in our study. Some subjects performed saccades where the arc length exceeded the cord length by 15°. When examining these saccades in isolation and tracking their course, they represent curved saccades and hence are marked as such in **Figure 2** as they are lying out with the main sequence (see **Figure 2**). Overall these curved saccades presented 2.9% of all saccades. Curved saccades have been described in fixational eye movements (Guerrasio et al., 2010). In addition, these outliers occurred when subjects left the screen with their gaze and eye tracking signal was lost, e.g., to look at the equipment such as the foot pedals. These "off screen saccades" are marked separately in **Figure 2**. We did exclude vertical saccades with high speed peak velocity > 1000° /s as those likely represent blinks. We did not exclude curved vertical saccades with slower peak velocity directed toward the equipment or along the road as some were directly preceding object fixations, which then would have been missed.

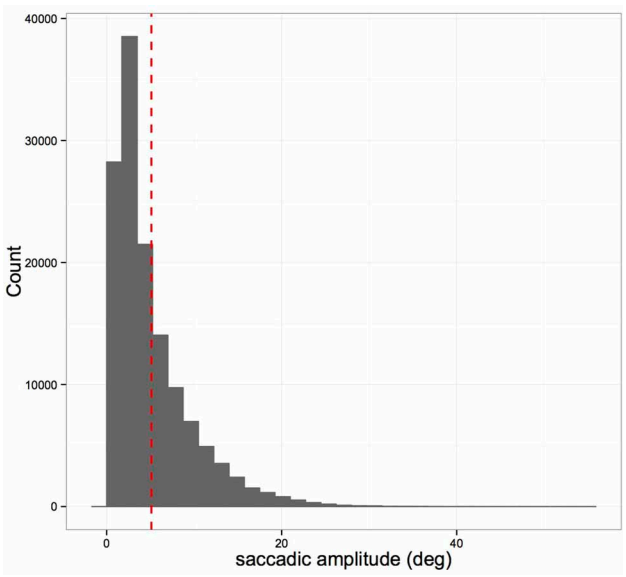

FIGURE 1 | Distribution of saccade amplitudes (in degree) of 73 subjects. The majority of saccade amplitudes ranged between 1 and 10°, and below 20°.

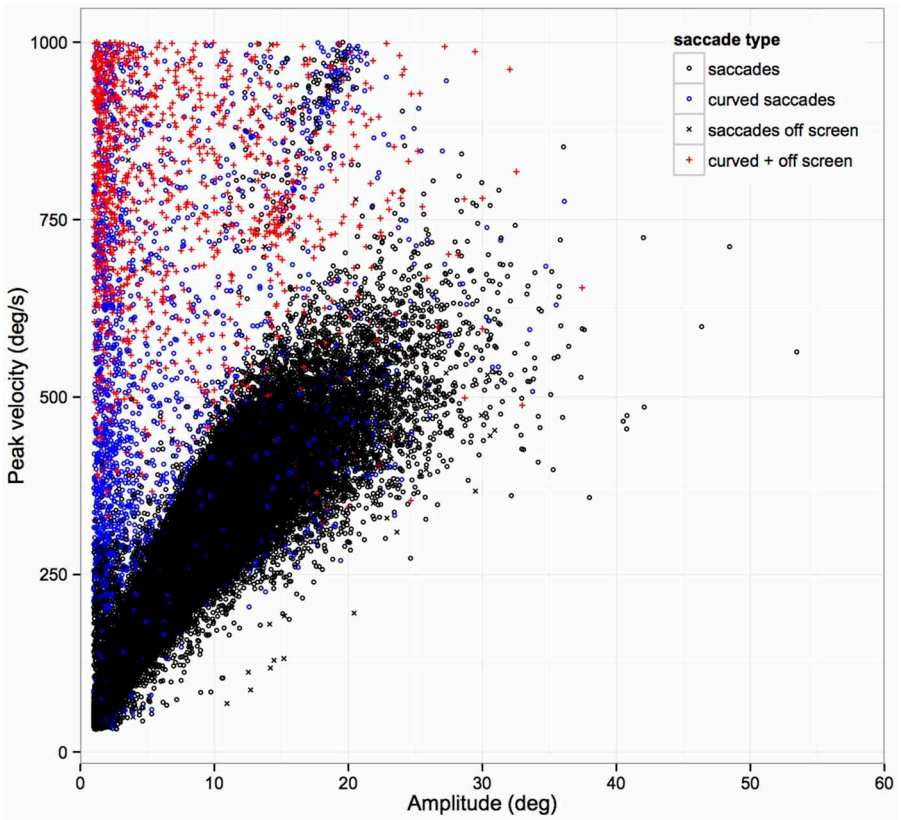

FIGURE 2 | Main sequence, peak velocity, and amplitudes of 73 subjects. Peak velocity increases with amplitude of saccades. There are subjects revealing saccades with high velocities and small amplitudes lying outside of the main sequence. These data points represent portions of the gaze trajectory where arc length exceeds cord length. These represent curved saccades or saccades directed downward toward the equipment or vertically along the road (see Descriptive Statistics). Overall these curved saccades presented 2.9% of all saccades. (Saccades are represented with black circles, curved saccades with blue circles, off screen saccades with black X and combined curved and off screen saccades with red crosses.)

Video game experience

To improve our knowledge about the constitution of the different video game level groups, we designed a binomial logistic regression model with video game experience as the dependent variable and age, gender, years of active driving as predictors. The model showed that video game experience was more likely in young and male participants. **Table 2** displays the logistic regression model with the video game experience as the dependent variable.

With increased age, video game experience reduced significantly, representing a major influence on the data, which needed to be controlled for (see **Figure 4**).

Furthermore we found a strong negative correlation ($r = -0.76$) between age and the different groups of video game experience, showing that participants with extensive video game experience were younger than people with less or no experience in video gaming.

REACTION TIMES

All objects were detected and none were missed by any participant. In order to disentangle a collinearity effect between the two main variables of interest, age and levels of video game experience, we calculated two different models for reaction time. In both models, the first with age as main predictor and the second with levels of video game experience as main predictor, regression estimates were not much changed. Therefore we chose to integrate both variables as fixed effects in the same model. We included median manual reaction time as the dependent variable and age, the dummy variables of videogame experience, type of course, target eccentricity as fixed effects as well as their two-way interactions. Subject was treated as random effect. **Table 3** displays the LMM statistics for median manual reaction time.

There was a significant main effect of eccentricity on manual reaction time showing that increasing eccentricity of objects is associated with an increase in manual reaction time. Type of course, age, and different levels of video game experience did not show significant main effects, but the interaction of type of course and eccentricity of objects significantly predicted an increase in manual reaction times (see **Figure 5**). We observed that the interaction of eccentricity of object and extensive video game experience predicted marginal significantly a decrease in manual reaction time. Therefore, manual reaction time to more peripherally located objects decreases with increased video game experience.

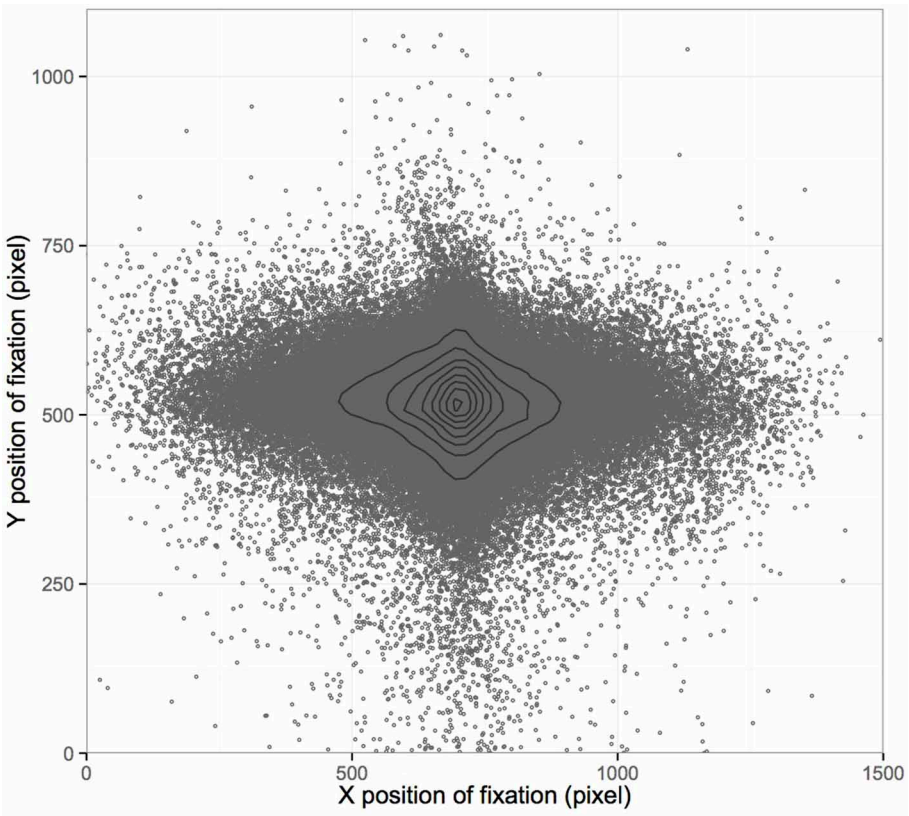

FIGURE 3 | Distribution of fixations on screen. Presented are all fixations of 73 subjects and their distribution on the screen, which depicted the driving scenario during the driving task. A density map estimation contours the areas fixated most on screen.

Table 2 | Logistic regression model for video game experience (significant effects in bold).

	Estimate	SE	*z*-Value	Pr(>|z|)
Intercept	−2.38666	1.75282	−1.362	0.17332
Gender	−2.74008	1.00837	−2.717	**0.00658**
Age (centered)	−0.18879	0.08548	−2.209	**0.02719**
Driving experience	0.01266	0.02297	0.551	0.58153

In a second step, we examined the reaction time as the first fixation or detection time of objects, and included the same fixed and random effects. **Table 4** presents the LMM statistics for the first detection or fixation of objects with both main predictors of interest.

And again, increasing eccentricity of objects as well as the interaction of course type and stimulus eccentricity significantly predicted an increase in reaction time. However, neither age nor level of video game experience did affect the first fixation of objects. Thus, our model revealed significant effects on reaction times: the further an object is located in the periphery, the longer the manual reaction time and reaction time by first detection; this effect is amplified by increased difficulty of test course. We found no significant effect of aging alone on reaction times. However, high level of video game experience seems to minimize this effect on manual reaction time, while reaction time by first detection is not influenced by levels of video game experience. We cannot provide a distinct prediction of age or video game experience on reaction times respectively due to their collinearity. Hence, in this study we consider both when examining the participant's performance.

EXPLORATORY BEHAVIOR

We included mean fixation duration, mean gaze amplitude, number of saccades, distribution of fixations on the screen and number of head movements as dependent variables in models. Although a strong correlation between age and videogame experience was found, we included the level of videogame experience as predictors in models, as practice of video games might influence the exploratory behavior in participants. Nevertheless, observed effects of video game experience and age alone as well as their interaction effect have to be interpreted carefully (see **Figure 4**). The video game experience variable was not uniformly distributed across age, because no elder participant had extensive videogame experience in our wide study population ($n = 73$). Therefore we have to consider an extrapolation and overfitting effect of our regression models. Fixed effects were age, type of course, eccentricity of targets, and levels of video game experience, as well as their two-way interactions. Subject was treated as a random effect. There were no significant effects of age alone regarding saccade parameters. However, there was a marginal effect of extensive

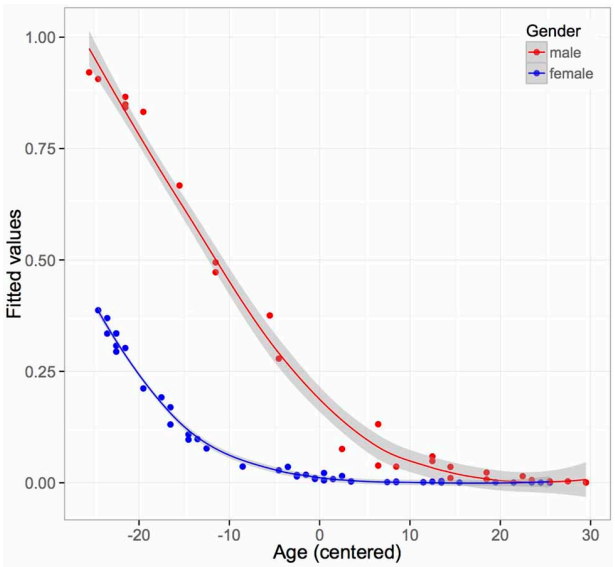

FIGURE 4 | Fitted values from binomial logistic regression on video game experience. Male and younger participants reveal more videogame experience than older and female participants ($n = 73$).

Table 3 | Linear mixed model for median manual reaction time (significant effects with *t*-value ±2 in bold).

	Estimate	SE	*t*-Value
Intercept	1168.8442	106.0349	11.023
Age	2.1077	5.9926	0.352
Eccentricity	1300.1934	102.1377	**12.730**
Type of course	−96.3001	102.1377	−0.943
Age × eccentricity	1.7190	4.6347	0.371
Age × type of course	0.2802	4.6347	0.060
Eccentricity × type of course	956.0274	105.0335	**9.102**
Moderate video game experience	−82.3265	170.3392	−0.483
Extensive video game experience	50.1128	402.1579	0.125
Eccentricity × extensive video game experience	−509.1063	199.4952	−2.552
Type of course × extensive video game experience	196.0442	199.4952	0.983
Eccentricity × moderate video game experience	−269.9960	151.7790	**−1.779**
Type of course × moderate video game experience	71.6985	151.7790	0.472
Age × extensive video game experience	7.1096	20.0873	0.354
Age × moderate video game experience	6.3935	8.4901	0.753
Variance components		S.D.	
Subject		311.22	
Residual		448.70	

video game experience on the mean of variance of horizontal fixations on the *X*-axis of the screen, displaying that participants with extensive video game experience covered a wider visual field during the task (see **Figure 6**). **Table 5** displays the LMM statistics for mean variance of horizontal eye movements (on the *X*-axis).

Likewise, the interaction of age and extensive video game experience significantly predicted an increase in the variance of fixations. Thus, the more the drivers have experience in video games and the younger they are, the broader is the field of view they covered with fixations (see **Figure 5**). In addition, increased video game experience had a significant main effect on mean saccadic amplitude. **Table 6** displays the LMM statistics for mean saccadic amplitude.

Participants with extensive video game experience performed larger mean saccadic amplitudes while driving.

Furthermore, we found a significant main effect of increased age on the number of head movements, demonstrating that with growing age the number of head movements during the task increases. **Table 7** displays the LMM statistics for the number of head movements performed.

Also, the interaction of moderate video game experience and age significantly predicted a decrease in head movements. Thus, older participants performed more head movements during the driving task, although if they had moderate video game experience, their frequency of head movements was less (see **Figure 7**).

SIMULATOR SICKNESS

In logistic regression analysis we included the incidence of malaise (such as headache, sweating, drowsiness, vertigo as symptoms of simulator sickness) as a dependent variable and age, course type, gender, number of saccades, and video game experience, as well as its two-way interactions, as predictors. We detected a marginally significant trend of an increased number of saccades on incidence of malaise [0.05 (Nagelkerkes), 0.032 (Cox and Snell), $\chi^2 = 9.75$, $p = 0.283$].

There were no significant effects of age, gender, type of course, and video game experience on the incidence of malaise.

DISCUSSION

We tested visual exploratory behavior in 73 participants of variable age and its effects on reaction times to hazardous objects relevant to driving safety. Our major interest focused on age-related effects on gaze behavior, information processing, and reaction times in the peripheral vs. central visual field with regard to deterioration of the peripheral visual field. We considered prior experience with video games as a possible influence on test results.

In summary, the results of the present study show that exploratory gaze behavior did not differ with increased age

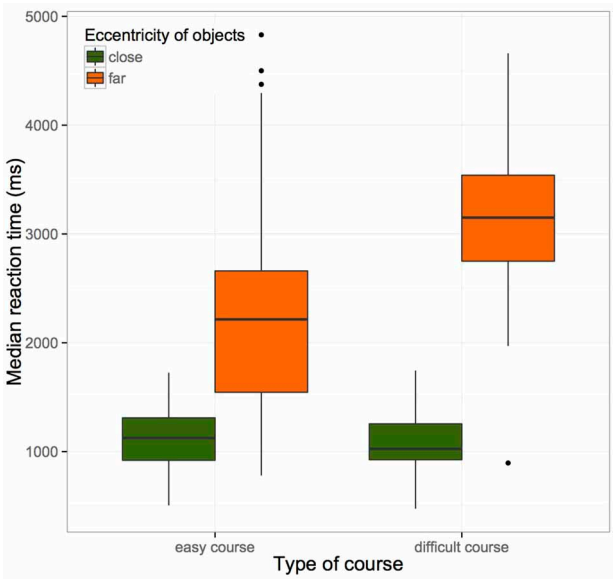

FIGURE 5 | Boxplots of median manual reaction time (in ms). Participants reacted faster to close than to peripheral objects. This effect was amplified by type of course and degree of complexity (easy vs. difficult).

Table 4 | Linear mixed model for first detection or fixation of objects (significant effects with *t*-value ±2 in bold).

	Estimate	SE	*t*-Value
Intercept	874.4402	117.1593	7.464
Age	8.5511	6.2387	1.371
Eccentricity	1243.5934	144.8606	**8.585**
Type of course	−187.0321	144.8606	−1.291
Age × eccentricity	−7.2829	6.5733	−1.108
Age × type of course	−2.4075	6.5733	−0.366
Eccentricity × type of course	852.9680	148.9677	**5.726**
Moderate video game experience	5.4606	187.6357	0.029
Extensive video game experience	230.5355	370.9499	0.621
Eccentricity × extensive video game experience	−514.5448	282.9414	−1.819
Type of course × extensive video game experience	−103.1475	282.9414	−0.365
Eccentricity × moderate video game experience	−280.6056	215.2662	−1.304
Type of course × moderate video game experience	51.5702	215.2662	0.240
Age × extensive video game experience	5.3405	16.6612	0.321
Age × moderate video game experience	0.4521	7.0420	0.064
Variance components		S.D.	
Subject		0.035566	
Residual		636.390273	

in many saccadic parameters: there were no significant effects of age on mean fixation duration, mean gaze amplitude, and mean number of saccades. However, with increasing age, participants performed more head-movements contributing to the gaze amplitude. While the latter does not change with age, the result suggests a possible compensatory role of head-movements allowing a gaze amplitude large enough to cover the field of view. The role of head-movements as a potential overt attention mechanism in the older populations merits further exploration. It is also unclear whether this could be a mechanism compensating for cognitive decline as suggested by Proudlock et al. (2004). In this respect it is very interesting, that elderly subjects with some video game experience seem to rely less on this potentially compensatory mechanism as they perform less head-movements, raising the question of whether simulation training can improve performance. We demonstrated that subjects with extensive video game experience, i.e., regular animated video game playing, covered a larger field of view with a wide distribution of fixations on screen, as well as slightly larger mean saccadic amplitude and reacted faster manually to peripheral objects, although they did not detect objects faster via fixation. These main findings will be discussed with respect to the deterioration of the UFOV in aging and the role of visual virtual media experience in visual exploratory behavior. We are aware of the fact, that older participants revealed less virtual media knowledge than younger participants, which advocates a careful interpretation of video and age effects on visual exploratory behavior respectively.

The position of the object had a significant effect on reaction times (both manually and via fixation): drivers reacted comparably promptly to close objects without differences in age or video gaming experience. The more distant the objects were located to the subject's gaze position, the longer were reaction times. In previous studies different courses with different visual layout complexity (higher "spatial density") showed an effect on driving performance (Rogé et al., 2004). Here we also report a significant interaction between object position and type of course. Participants reacted slower manually and fixated later on moving objects in the periphery in the more demanding driving course, including a higher spatial density of visual impressions including bushes, houses, and trees. To clarify whether reaction times to objects of diverse eccentricities change with age, implicating a deterioration of the functional field of view, we examined the reaction times to two different eccentricities with regards to age. Surprisingly, age did neither influence the manual reaction time nor the time it took the driver to fixate the peripheral object after its appearance on the screen. Nevertheless, video game-experienced participants, who were more common among the

Table 5 | Linear mixed model for mean variance of horizontal eye movements on the X-axis (significant effects with *t*-value ±2 in bold).

	Estimate	SE	*t*-Value
Intercept	23600	2063	11.438
Age (centered)	−110.3	123.9	−0.890
Eccentricity	−3.734e-10	2705	0.000
Type of course	−2898	2705	−1.071
Extensive videogame experience	25280	9090	**2.781**
Moderate videogame experience	−256.6	3326	−0.077
Course × eccentricity	8.256e-11	1030	0.000
Age × course	23.37	45.45	0.514
Age × eccentricity	5.251e-12	45.45	0.000
Age × moderate videogame experience	57.14	202.5	0.282
Eccentricity × moderate videogame experience	1.310e-10	1488	0.000
Course × moderate videogame experience	756.9	1488	0.509
Course × extensive videogame experience	−1219	1956	−0.623
Eccentricity × extensive videogame experience	2.155e-10	1956	0.000
Age × extensive videogame experience	1015	479.2	**2.119**
Variance components		SD	
Subject		8883.6	
Residual		4400.1	

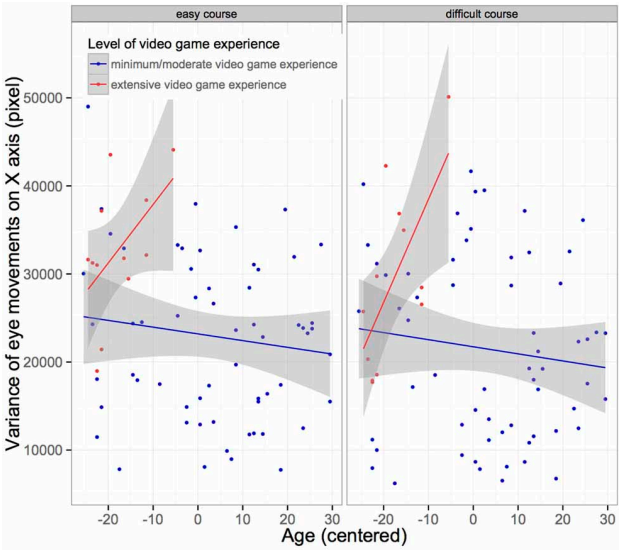

FIGURE 6 | Measure of mean variance of fixations on horizontal screen (in pixel) shown separately for both type of courses (easy vs. difficult). ($n = 73$) (see Materials and Methods). Subjects that had extensive video game experience, playing video action games regularly, showed a wider distribution of fixations on the *X*-axis of the screen. These subjects were of younger age. There were no elderly participants with extensive video game experience.

younger subjects, reacted faster manually to the targets, suggesting either an increase of selective spatial attention or faster manual responses due to better motor abilities (Green and Bavelier, 2003). In previous studies, deterioration of UFOV was supported by experiments relying exclusively on manual reaction (Crundall et al., 2002; Rogé et al., 2004; Jahn et al., 2005). Therefore our results raise the question, whether deterioration of peripheral vision with increased age exists at all when visual attention is measured non-manually, not as a motor-response, by including the measurement of eye movements and when the influence of video game experience is accounted for. Our study cannot address the question of how the peripheral visual field potentially deteriorates gradually providing the classification as general interference or tunnel vision, as we did not provide detailed testing of objects at various eccentricities. Another objection could be directed at the central task, which may be arguably too simple and not highly demanding enough (Williams, 1988) to provide a genuine central task. We did not present a leading car as a central task in our experiment since following a car does not resemble a common driving task in daily life. However we specified a certain speed to provide an equal amount of speed stress on all participants. Therefore we aimed at providing a more naturalistic driving environment which people in rural areas are exposed to.

Furthermore, the results can be interpreted by applying the hypothesis of Pollatsek et al. (2012): if drivers tend to adopt a "habit" perceiving and hence performing driving as a central task, then they react slower manually to peripheral objects because they do not judge them to be acutely relevant. Consequently, they see the objects but do not react immediately due to this habit. Increased video game experience generally seems to resolve this notion of a central task. Our data suggests that it is rather associated with a notion of a general detection task, reacting to all objects as soon as possible. This is of great interest considering a study, which described a general central bias in fixation behavior in subjects viewing a monitor (Tatler, 2007): this central bias was found to become weaker with an active search task, with which fixation distributions were shifted toward the distribution of image features rather than being focused on the center of the screen. Therefore it appears that video gaming experience in our subjects might have altered the understanding of the task, from a driving task to a search task, resulting in different oculomotor behavior with broader visual field and less central bias. Given the fact that the majority of our high level video game players were young drivers, the suspected acquired action video game skills had an effect on the overall performance of the young subjects. This is potentially masking an age effect itself, as in our study these two

Table 6 | Linear mixed model for mean saccadic amplitude (in bold significant effects with *t*-value ±2).

	Estimate	SE	*t*-Value
Intercept	4.918	0.2266	21.700
Age (centered)	−0.002116	0.01364	−0.155
Eccentricity	1.892e-13	0.2.822	0.000
Type of course	−0.2650	0.2822	−0.939
Extensive videogame experience	1.874	1.003	**1.869**
Moderate videogame experience	−0.001840	0.3654	−0.005
Course × eccentricity	9.735e-15	0.1075	0.000
Age × course	0.004080	0.004742	0.860
Age × eccentricity	−3.510e-15	0.004742	0.000
Age × moderate videogame experience	0.007429	0.02.237	0.332
Eccentricity × moderate videogame experience	−7.090e-14	0.1553	0.000
Course × moderate videogame experience	0.1134	0.1553	0.730
Course × extensive videogame experience	0.04.884	0.2041	0.239
Eccentricity × extensive videogame experience	−9.707e-14	0.2041	0.000
Age × extensive videogame experience	0.04777	0.05293	0.903
Variance components		SD	
Subject		0.98439	
Residual		0.45913	

Table 7 | Linear mixed model for the number of head movements (in bold significant effects with *t*-value ±2).

	Estimate	SE	*t*-Value
Intercept	5.644e + 00	2.264e + 00	2.493
Age (centered)	0.3459	0.1366	**2.532**
Eccentricity	1.916e-14	2.580	0.000
Type of course	−2.050	2.580	−0.794
Extensive videogame experience	12.18	10.08	1.208
Moderate videogame experience	−0.7415	3.651	−0.203
Course × eccentricity	−2.620e-15	0.9826	0.000
Age × course	0.06233	0.04336	1.438
Age × eccentricity	−2.851e-16	0.04336	0.000
Age × moderate videogame experience	−0.4682	0.2253	**−2.079**
Eccentricity × moderate videogame experience	−8.491e-15	1.420	0.000
Course × moderate videogame experience	−0.2510	1.420	−0.177
Course × extensive videogame experience	4.336	1.866	**2.323**
Eccentricity × extensive videogame experience	−3.405e-15	1.866	0.000
Age × extensive videogame experience	0.3286	0.5330	0.616
Variance components		SD	
Subject		9.9611	
Residual		4.1976	

factors need to be interpreted as linked. In order to further clarify the interaction between age and video game experience, older participants with action video game experience need to be examined, expecting faster manual reaction times to peripheral objects in this group. It will also elucidate the question whether and in what way attentional mechanisms and executive functions differ between video game players and non-video game players.

A critical objection could be raised regarding the recording of reaction times in this study: looking at something does not necessarily imply consciously perceiving it. Hence, reaction times assessed via first fixation (or seldom manual reaction before fixation) may represent an artifact. The error of "seen but not perceived" could jeopardize our interpretation and cannot be ruled out here. Nevertheless, it seems unlikely in the majority of cases that participants could focus via saccades accurately on an object while being unaware of it, especially when a manual reaction follows the fixation.

SUMMARY AND FUTURE PERSPECTIVES

The more demanding the course and the more peripheral the location of the object, the longer were the reaction times, independent of participant age. Deterioration of the useful visual field of view with increased age was not verified in the present study: peripheral objects were detected manually or via fixation at the same speed in all age groups. Interestingly, video game-experienced subjects reacted faster manually to peripheral objects, indicating faster manual responses vs. increased spatial attention and less tendency of perceiving driving "as a central task." This raised the question, first addressed by Pollatsek et al. (2012), of whether active training, e.g., with driving simulation or video games could improve driving performance, e.g., in the elderly, but also in patients with visual field deficits (Hamel et al., 2012). This exercise could shift attention and encourage faster actual manual response, e.g., with relevance at traffic intersections. It also remains questionable, whether tasks practiced in action video games could

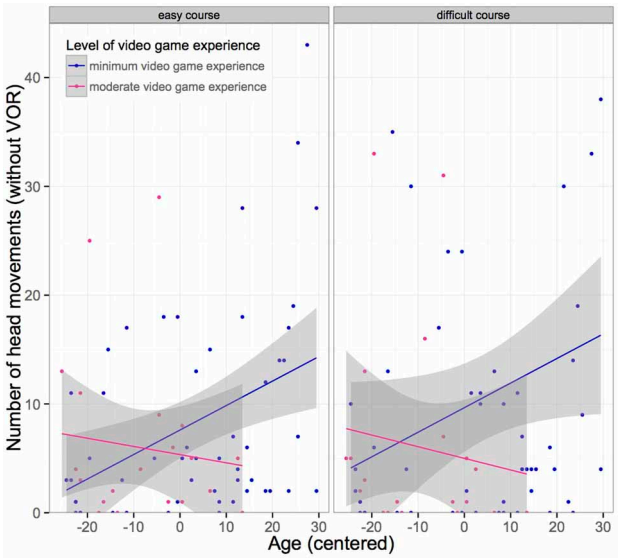

FIGURE 7 | Measure of the number of head movements without accounting for vestibulo-ocular reflexes (VOR) shown separately for both type of courses (easy vs. difficult). Older subjects performed significantly more head movements than younger subjects. However, elderly with moderate video game experience, performed less head movements ($n = 73$).

be transferred beyond the training task, allowing our subjects with extensive action game experience to better "learn to learn" (Green and Bavelier, 2012). One advantage of a driving simulator testing setting rather than other action gaming options [First person-shooters or Mario Kart DS® (Boot et al., 2013)] could be, that elderly will likely be more compliant, as driving presents autonomy and a daily useful activity. Whether positive effects could be transferred to real driving or even other cognitive functions, remains unclear.

In the older populations, head-movements increasingly contribute to gaze amplitude. As gaze amplitude does not change with increased age, head-movements seem to assure amplitude size in the elderly. Elderly subjects with some video game experience performed less head movements, again, raising the question of whether simulation training can improve performance.

Head-unrestrained testing in testing sessions with a larger visual field is necessary to uncover the role of head-movements as a compensatory mechanism in the elderly.

Here, we would like to emphasize that the effects of video game experience are more common among the younger subjects, and therefore if not accounted for, it can easily be misinterpreted as underlying age effect. We think it is essential to consider video game experience, specifically with respect to animation setup, in all testing methods using virtual media. Further testing sessions with participants with video game experience more equally distributed among all ages are needed. One hypothesis would be that older participants, experienced in video games, would demonstrate better performance in the driving simulation. The effect of video game experience on exploratory behavior with less central bias and faster reactions to peripheral objects raises the question of whether those subjects drive differently in a real life situation, and whether that would be associated with a lower crash risk in real life driving. This question needs to be addressed in real life driving studies.

ACKNOWLEDGMENTS

We thank Richard A. Dargie for correction of the English text.

REFERENCES

Bahill, A. T., Clark, M. R., and Stark, L. (1975). The main sequence, a tool for studying human eye movements. *Math. Biosci.* 24, 191–204. doi:10.1016/0025-5564(75)90075-9

Ball, K., Owsley, C., Sloane, M. E., Roenker, D. L., and Bruni, J. R. (1993). Visual attention problems as a predictor of vehicle crashes in older drivers. *Invest. Ophthalmol. Vis. Sci.* 34, 3110–3123.

Bao, S., and Boyle, L. N. (2009). Age-related differences in visual scanning at median-divided highway intersections in rural areas. *Accid. Anal. Prev.* 41, 146–152. doi:10.1016/j.aap.2008.10.007

Bates, D., and Maechler, M. (2010). lme4: Linear mixed-effects models using S4 classes, 2010. URL http://CRAN.R-project.org/package=lme4. R package version 0.999375-37.

Bavelier, D., Green, C. S., Han, D. H., Renshaw, P. F., Merzenich, M. M., and Gentile, D. A. (2011). Brains on video games. *Nat. Rev. Neurosci.* 12, 763–768. doi:10.1038/nrn3135

Boot, W. R., Champion, M., Blakely, D. P., Wright, T., Souders, D. J., and Charness, N. (2013). Video games as a means to reduce age-related cognitive decline: attitudes, compliance, and effectiveness. *Front. Psychol.* 4:31. doi:10.3389/fpsyg.2013.00031

Brooks, J. O., Goodenough, R. R., Crisler, M. C., Klein, N. D., Alley, R. L., Koon, B. L., et al. (2010). Simulator sickness during driving simulation studies. *Accid. Anal. Prev.* 42, 788–796. doi:10.1016/j.aap.2009.04.013

Cantin, V., Lavallière, M., Simoneau, M., and Teasdale, N. (2009). Mental workload when driving in a simulator: effects of age and driving complexity. *Accid. Anal. Prev.* 41, 763–771. doi:10.1016/j.aap.2009.03.019

Chisholm, J. D., and Kingstone, A. (2012). Improved top-down control reduces oculomotor capture: the case of action video game players. *Atten. Percept. Psychophys.* 74, 257–262. doi:10.3758/s13414-011-0253-0

Cliff, M., Joyce, D. W., Lamar, M., Dannhauser, T., Tracy, D. K., and Shergill, S. S. (2012). Aging effects on functional auditory and visual processing using fMRI with variable sensory loading. *Cortex* 4, 1–10. doi:10.1016/j.cortex.2012.04.003

Crundall, D., Underwood, G., and Chapman, P. (1999). Driving experience and the functional field of view. *Perception* 28, 1075–1087. doi:10.1068/p2894

Crundall, D., Underwood, G., and Chapman, P. (2002). Attending to the peripheral world while driving. *Appl. Cogn. Psychol.* 16, 459–475. doi:10.1002/acp.806

Einhäuser, W., Schumann, F., Bardins, S., Bartl, K., Böning, G., Schneider, E., et al., (2007). Human eyehead co-ordination in natural exploration. *Network (Bristol, England)* 18, 267–297. doi: 10.1080/09548980701671094

Fox, J. (2007). *Polycor: Polychoric and Polyserial Correlations.* R Package Version 0.7-5. Available at: http://CRAN.R-project.org/package$=$polycor

Freedman, E. G. (2008). Coordination of the eyes and head during visual orienting. *Exp. Brain Res.* 190, 369–387. doi:10.1007/s00221-008-1504-8

Green, C. S., and Bavelier, D. (2003). Action video game modifies visual selective attention. *Nature* 423, 534–537. doi:10.1038/nature01647

Green, C. S., and Bavelier, D. (2012). Learning, attentional control, and action video games. *Curr. Biol.* 22, R197–R206. doi:10.1016/j.cub.2012.02.012

Guerrasio, L., Quinet, J., Büttner, U., and Goffart, L. (2010). Fastigial oculomotor region and the control of foveation during fixation. *J. Neurophysiol.* 103, 1988–2001. doi:10.1152/jn.00771.2009

Hamel, J., Kraft, A., Ohl, S., De Beuke-laer, S., Audebert, H. J., and Brandt, S. A. (2012). Driving

simulation in the clinic: testing visual exploratory behavior in daily life activities in patients with visual field defects. *J. Vis. Exp.* 67:e4427. doi:10.3791/4427

Han, X., Byrne, P., Kahana, M., and Becker, S. (2012). When do objects become landmarks? A VR study of the effect of task relevance on spatial memory. *PLoS ONE* 7:e35940. doi:10.1371/journal.pone.0035940

Hedden, T., and Gabrieli, J. D. E. (2004). Insights into the ageing mind: a view from cognitive neuroscience. *Nat. Rev. Neurosci.* 5, 87–96. doi:10.1038/nrn1323

Holmes, D. L., Cohen, K. M., Haith, M. M., and Morrison, F. J. (1977). Peripheral visual processing. *Percept. Psychophys.* 22, 571–577. doi:10.3758/BF03198765

Jahn, G., Oehme, A., Krems, J. F., and Gelau, C., (2005). Peripheral detection as a workload measure in driving: effects of traffic complexity and route guidance system use in a driving study. *Transp. Res. Part F Traffic Psychol. Behav.* 8, 255–275. doi:10.1016/j.trf.2005.04.009

Kliegl, R., Masson, M., and Richter, E. (2010). A linear mixed model analysis of masked repetition priming. *Vis. Cogn.* 18, 655–681. doi:10.1080/13506280902986058

Maltz, M., and Shinar, D. (1999). Eye movements of younger and older drivers. *Hum. Factors* 41, 15–25. doi:10.1518/001872099779577282

Miura, T. (1990). "Active function of eye movement and useful field of view in a realistic setting," in *From Eye to Mind: Information Acquisition in Perception, Search and Reading*, eds R. Groner, G. d'Ydewalle, and R. Parham (Amsterdam: Elsevier), 119–127.

Morrison, J. H., and Baxter, M. G. (2012). The ageing cortical synapse: hallmarks and implications for cognitive decline. *Nat. Rev. Neurosci.* 13, 240–250. doi:10.1038/nrn3200

Mourant, R. R., and Rockwell, T. H. (1972). Strategies of visual search by novice and experienced drivers. *Hum. Factors* 14, 325–335.

Mozolic, J. L., Hugenschmidt, C. E., Peiffer, A. M., and Laurienti, P. J. (2012). "Multisensory integration and aging," in *The Neural Bases of Multisensory Processes*, eds M. M. Murray and M. T. Wallace (Boca Raton, FL: CRC Press). Chapter 20.

Ohl, S., Brandt, S. A., and Kliegl, R. (2011). Secondary (micro-) saccades: the influence of primary saccade end point and target eccentricity on the process of postsaccadic fixation. *Vision Res.* 51, 2340–2347. doi:10.1016/j.visres.2011.09.005

Owsley, C., Ball, K., McGwin, G.,Sloane, M. E., Roenker, D. L., White, M. F., et al. (1998). Visual processing impairment and risk of motor vehicle crash among older adults. *JAMA* 279, 1083–1088. doi:10.1001/jama.279.14.1083

Park, H. L., O'Connell, J. E., and Thomson, R. G. (2003). A systematic review of cognitive decline in the general elderly population. *Int. J. Geriatr. Psychiatry* 18, 1121–1134. doi:10.1002/gps.1023

Podell, J. E., Sambataro, F., Murty, V. P., Emery, M. R., Tong, Y., Das, S., et al. (2012). Neurophysiological correlates of age-related changes in working memory updating. *Neuroimage* 62, 2151–2160. doi:10.1016/j.neuroimage.2012.05.066

Pollatsek, A., Romoser, M. R. E., and Fisher, D. L. (2012). Identifying and remediating failures of selective attention in older drivers. *Curr. Dir. Psychol. Sci.* 21, 3–7. doi:10.1177/0963721411429459

Pradhan, A. K., Hammel, K. R., DeRamus, R., Pollatsek, A., Noyce, D. A., and Fisher, D. L. (2005). Using eye movements to evaluate effects of driver age on risk perception in a driving simulator. *Hum. Factors* 47, 840–852. doi:10.1518/001872005775570961

Proudlock, F. A., Shekhar, H., and Gottlob, I. (2004). Age-related changes in head and eye coordination. *Neurobiol. Aging* 25, 1377–1385. doi:10.1016/j.neurobiolaging.2004.02.024

R Development Core Team. (2010). *R: A Language and Environment for Statistical Computing. R Foundation for Statistical Computing*, (Vienna). ISBN:3-900051-07-0. http://www.R-project.org (software).

Robinson, G. H., Erickson, D. J., Thurston, G. L., and Clark, R. L. (1972). Visual search by automobile drivers. *Hum. Fact.* 14, 315–323.

Rogé, J., Pébayle, T., Lambilliotte, E., Spitzenstetter, F., Giselbrecht, D., and Muzet, A. (2004). Influence of age, speed and duration of monotonous driving task in traffic on the driver's useful visual field. *Vision Res.* 44, 2737–2744. doi:10.1016/j.visres.2004.05.026

Romoser, M. R. E., and Fisher, D. L. (2009). The effect of active versus passive training strategies on improving older drivers' scanning in intersections. *Hum. Factors* 51, 652–668. doi:10.1177/0018720809352654

Shinar, D. (2008). Looks are (almost) everything: where drivers look to get information. *Hum. Factors* 50, 380–384. doi:10.1518/001872008X250647

Tatler, B. (2007). The central fixation bias in scene viewing: selecting an optimal viewing position independently of motor biases and image feature distributions. *J. Vis.* 7, 1–17. doi:10.1167/7.14.4

Tefft, B. C. (2008). Risks older drivers pose to themselves and to other road users. *J. Safety Res.* 39, 577–582. doi:10.1016/j.jsr.2008.10.002

Wickham, H. (2009). *ggplot2. Elegant Graphics for Data Analysis.* Dordrecht: Springer.

Williams, L. J. (1988). Tunnel vision or general interference? Cognitive load and attentional bias are both important. *Am. J. Psychol.* 101, 171–191. doi:10.2307/1422833

Conflict of Interest Statement: The authors declare that the research was conducted in the absence of any commercial or financial relationships that could be construed as a potential conflict of interest.

Received: 30 December 2012; accepted: 24 May 2013; published online: 21 June 2013.

*Citation: Hamel J, De Beukelaer S, Kraft A, Ohl S, Audebert HJ and Brandt SA (2013) Age-related changes in visual exploratory behavior in a natural scene setting. Front. Psychol. **4**:339. doi: 10.3389/fpsyg.2013.00339*

This article was submitted to Frontiers in Perception Science, a specialty of Frontiers in Psychology.

frontiers in
PSYCHOLOGY

ORIGINAL RESEARCH ARTICLE
published: 03 May 2013
doi: 10.3389/fpsyg.2013.00244

A BOLD perspective on age-related neurometabolic-flow coupling and neural efficiency changes in human visual cortex

Joanna Lynn Hutchison[1,2]*, Ehsan Shokri-Kojori[1], Hanzhang Lu[3] and Bart Rypma[1,2]

[1] *School of Behavioral and Brain Sciences, University of Texas at Dallas, Richardson, TX, USA*
[2] *Department of Psychiatry, University of Texas Southwestern Medical Center, Dallas, TX, USA*
[3] *Advanced Imaging Research Center, University of Texas Southwestern Medical Center, Dallas, TX, USA*

Edited by:
Mark W. Greenleem, University of Regensburg, Germany

Reviewed by:
Fahmeed Hyder, Yale University, USA
Yuka Sasaki, Brown University, USA

***Correspondence:**
Joanna Lynn Hutchison, Center for Brain Health, 2200 West Mockingbird Lane, Dallas, TX 75235, USA.
e-mail: joanna.hutchison@utdallas.edu

Age-related performance declines in visual tasks have been attributed to reductions in processing efficiency. The neural basis of these declines has been explored by comparing the blood-oxygen-level-dependent (BOLD) index of neural activity in older and younger adults during visual task performance. However, neural activity is one of many factors that change with age and lead to BOLD signal differences. We investigated the origin of age-related BOLD changes by comparing blood flow and oxygen metabolic constituents of BOLD signal. Subjects periodically viewed flickering annuli and pressed a button when detecting luminance changes in a central fixation cross. Using magnetic resonance dual-echo arterial spin labeling and CO_2 ingestion, we observed age-equivalent (i.e., similar in older and younger groups) fractional cerebral blood flow (ΔCBF) in the presence of age-related increases in fractional cerebral metabolic rate of oxygen ($\Delta CMRO_2$). Reductions in ΔCBF responsiveness to increased $\Delta CMRO_2$ in elderly led to paradoxical age-related BOLD decreases. Age-related $\Delta CBF/\Delta CMRO_2$ ratio decreases were associated with reaction times, suggesting that age-related slowing resulted from less efficient neural activity. We hypothesized that reduced vascular responsiveness to neural metabolic demand would lead to a reduction in $\Delta CBF/\Delta CMRO_2$. A simulation of BOLD relative to $\Delta CMRO_2$ for lower and higher neurometabolic-flow coupling ratios (approximating those for old and young, respectively) indicated less BOLD signal change in old than young in relatively lower $CMRO_2$ ranges, as well as greater BOLD signal change in young compared to old in relatively higher $CMRO_2$ ranges. These results suggest that age-comparative studies relying on BOLD signal might be misinterpreted, as age-related BOLD changes do not merely reflect neural activity changes. Age-related declines in neurometabolic-flow coupling might lead to neural efficiency reductions that can adversely affect visual task performance.

Keywords: fMRI, BOLD, CBF, $CMRO_2$, hypercapnia, aging, neurometabolic-flow coupling, neural efficiency

INTRODUCTION

The human visual system exhibits age-related changes that lead to changes in the efficiency of information processing. Whereas structural changes are prominent in the periphery (i.e., the cornea, iris, lens, and vitreous and aqueous humors; e.g., Owsley and Sloane, 1987; Michaels, 1993), second- and third-order brain regions in the visual pathway appear to be less affected by aging. Specifically, structural studies of lateral geniculate nucleus (LGN) suggest age-equivalent (i.e., similar in older and younger groups) neuron density and minimal changes in size, and functional imaging studies suggest minimal age-related changes in LGN-cell response properties (Ahmad and Spear, 1993; Spear et al., 1994). Striate cortex similarly undergoes minimal age-related structural changes in neuron density and size (Haug et al., 1984; Vincent et al., 1989); functional changes in this region generally indicate sparing of LGN and V1 function. For example, mechanisms of chromatic contrast adaptation and color-coding have been determined to be largely unchanged with age (Elliott et al., 2012). Despite the apparent age-equivalence of these visual-pathway structures and at least some psychophysical functions, performance declines are often observed in visual tasks. Older adults' ability to switch between percepts in ambiguous figures is reduced compared to younger adults (e.g., Aydin et al., 2013), as is their ability to perceive shape from texture (e.g., Weymouth and McKendrick, 2012) and to detect objects in complex displays (e.g., Plude and Doussart-Roosevelt, 1989; Hommel et al., 2004; Bennett et al., 2012; Scialfa et al., 2012).

Age-related performance declines in visual tasks have been attributed to reductions in processing efficiency (e.g., Welford, 1981; Grady et al., 1994; Grady, 1996; Speranza et al., 2001). For instance, in a study investigating age-related pattern detection changes, Speranza et al. (2001) presented stereoscopic stimuli with varying degrees of background noise. They observed performance decrements for older adults when noise was introduced into the visual stimuli. Older adults' performance was not affected

differentially by binocular cues or internal noise, nor was their performance related to filter bandwidth changes. Instead, a decrement in processing efficiency, as measured by the signal energy necessary for a subject to detect a signal in a noisy background, was found to be responsible for age-related elevations in both binoptic and dichoptic processing thresholds.

The neural basis of such age-related performance declines has been explored by comparing the blood-oxygen-level-dependent (BOLD) index of neural activity in older and younger adults during visual task performance (e.g., Ross et al., 1997; Buckner et al., 2000; Huettel et al., 2001; Pasley et al., 2007; Ances et al., 2009; Hutchison et al., 2012). BOLD activity is measured by the hemodynamic response function (HRF, the time-response function that describes the relationship between neural and vascular activity; Gössl et al., 2001) using functional magnetic resonance imaging (fMRI). Age-related alterations in BOLD activity across cortex and tasks are often interpreted as age-related alterations in neural activity (e.g., Grady, 2002; Hedden and Gabrieli, 2004; Rajah and D'Esposito, 2005; Nyberg and Bäckman, 2011). Such a straightforward interpretation is complicated by the fact that neural activity is only one of several factors that can change with age and lead to BOLD signal differences (Moeller et al., 1996; Davis et al., 1998; Hoge et al., 1999a; Rypma and D'Esposito, 2000, 2001; D'Esposito et al., 2003; Iadecola, 2004; Rypma et al., 2005; Leontiev et al., 2007; Restom et al., 2007; Ances et al., 2009; Motes et al., 2010).

Hyder (2004) demonstrated that fractional changes in cerebral metabolic rate of oxygen ($\Delta CMRO_2$) closely approximate neural activity (measured by extracellular recording) during sensory stimulation. Thus, $\Delta CMRO_2$ would be preferable to the BOLD response as an index for neural activity. However, $\Delta CMRO_2$ is more expensive, time-intensive, and difficult to acquire, and thus many researchers must rely on the BOLD response as a proxy for neural activity. The BOLD signal is dependent upon structural brain integrity as well as physiological processes that change with age such as cerebral blood flow (CBF; D'Esposito et al., 2003; Buxton et al., 2004). Age-related changes in neurometabolic-flow coupling and vascular dynamics, triggered by a multiplicity of factors such as disease and developmental changes in astrocytic activity, have been observed that could bias estimations of neural activity with BOLD signal and its relationship to behavior (D'Esposito et al., 1999, 2003). For example, an age-related reduction in resting state CBF has been observed under circumstances of increased $CMRO_2$ when accounting for parenchyma volume, yielding a decrease in venous oxygenation (Y_v) with increased age (Lu et al., 2011). This finding suggests that if the supply of blood flow to cortical regions does not keep pace with age-associated increases in metabolic demand, then venous oxygenation is decreased. Additionally, cerebrovascular reactivity (CVR) decreases with age (Ances et al., 2009; Lu et al., 2011; Gauthier et al., 2012). That is, under conditions of activation, blood vessels respond less to changes in metabolic demand. Decreases in Y_v and decreases in CVR yield a relatively hypoxic cellular environment for older adults, which is a condition that has been shown to lead to increases in CBF and $CMRO_2$ (Xu et al., 2012; but, see Mintun et al., 2001) and could therefore alter the BOLD response.

The BOLD signal is strongly affected by vascular coupling to neural metabolic activity (see D'Esposito et al., 2003; Iadecola, 2004; Cauli and Hamel, 2010). Neural activity leads to fractional increases in cerebral perfusion of oxygenated blood (ΔCBF) that exceed fractional increases in oxygen metabolic rate ($\Delta CMRO_2$) for active neurons, leading to increases in the BOLD response (also known as the T2* MR signal; Ogawa and Lee, 1990; Ogawa et al., 1992). However, because ΔCBF and $\Delta CMRO_2$ are not always coupled across cortex and tasks, the $\Delta CBF/\Delta CMRO_2$ ratio and BOLD signal can be affected by the variability in these constituent components, leading to substantial regional differences (cf. Vafaee and Gjedde, 2000; Lu et al., 2004; Vafaee and Gjedde, 2004; Tuunanen and Kauppinen, 2006; Tuunanen et al., 2006; Chiarelli et al., 2007a,b; Ances et al., 2008; but, see Leenders et al., 1990). Mechanisms posited to mediate these differences include variation in oxygen metabolic requirements across cortex (Tuunanen et al., 2006), oxygen delivery, or blood flow alterations under certain conditions or in certain cortical areas (Vafaee and Gjedde, 2000; Lu et al., 2004), variable neurometabolic-flow coupling (Vafaee and Gjedde, 2004), and the accurate estimation of M (an index of maximal BOLD responding; Chiarelli et al., 2007a). Regardless of the precise mechanism behind this variability, the end result is that the BOLD response can be difficult to interpret across healthy, young cortex, and it can be even more complicated to interpret when making comparisons between younger and older groups (cf. D'Esposito et al., 2003).

We hypothesized that the relationship between activation-induced ΔCBF and $\Delta CMRO_2$ in primary visual cortex is fundamentally altered by the process of aging such that the BOLD response might differentially index neural activity in older compared to younger individuals. We further hypothesized that age-related changes in visual task performance – that is, in reaction times (RTs) – are related to changes in the $\Delta CBF/\Delta CMRO_2$ ratio. Few studies have extended concepts of neurometabolic-flow coupling differences to hypotheses of age-related variation in BOLD activity and behavior (Hutchison et al., 2012; Mohtasib et al., 2012). Our study focuses on these basic relationships within distinct sensory cortical areas, minimizing the complexities of functional activity related to higher cognition. To assess the extent to which differences can occur independently in ΔCBF and $\Delta CMRO_2$ across the cortex, we additionally assessed these relationships within motor cortex. Finally, we performed a simulation to assess effects of age-related neurometabolic-flow coupling changes on the BOLD response.

The use of dual-echo Arterial Spin Labeling (ASL; i.e., calibrated fMRI) technology allows for the separation of vascular and neural factors and permits the resolution of age-related BOLD signal ambiguities because the ASL signal (echo 1) is dependent on CBF while the BOLD signal (echo 2) is dependent on both CBF and $CMRO_2$ (cf. Davis et al., 1998; Hyder et al., 2000). In studies using calibrated fMRI, some results have suggested that the ASL and BOLD signals do not have the same signal-to-noise ratio (Wong et al., 2000), potentially affecting the calculation of $\Delta CMRO_2$. Collection of hypercapnic (Davis et al., 1998) or hyperoxic (Chiarelli et al., 2007b) data in tandem with calibrated fMRI ameliorates this concern to the extent that it allows for scaling of the BOLD response to account for differences in the signal-to-noise ratio. Previous work in both animals (e.g., Kida et al., 2000) and humans (e.g., Davis et al., 1998) has shown the components

of calibrated fMRI to be complementary to one another in elucidating the relationship between vasculature, neural activation, and the BOLD response (see Brown et al., 2007; Hoge, 2012).

In one study (Hutchison et al., 2012), we sought to observe age-related neurometabolic-flow coupling changes in visual cortex using calibrated fMRI and hypercapnia (cf. Hoge et al., 1999a,b; Pasley et al., 2007; Ances et al., 2009). The present paper extends this work by describing our investigation of neurometabolic-flow coupling changes within both visual and motor cortex. Additionally, we used simulation techniques to determine effects of reduced vascular responsivity on $\Delta CBF/\Delta CMRO_2$ and BOLD. Subjects periodically viewed flickering annuli and pressed a button as quickly as possible upon noticing changes in the luminance of a central fixation cross (cf. Pasley et al., 2007). Functional signal changes in visual cortex were assessed using both fixation and parafoveal stimulation as baseline conditions of interest. Functional signal changes in motor cortex were assessed in conjunction with button presses. Hypercapnic administration allowed for the calculation of M and thus allowed for the calculation of $\Delta CMRO_2$ and $\Delta CBF/\Delta CMRO_2$ (Leontiev and Buxton, 2007; Leontiev et al., 2007) within both visual and motor cortices.

Within visual cortex, we observed age-equivalent ΔCBF in the presence of age-related increases in $\Delta CMRO_2$. Reductions in ΔCBF responsiveness to increased $\Delta CMRO_2$ in the elderly led to paradoxical age-related decreases in BOLD – that is, increases in $\Delta CMRO_2$, a close index of neural activity, would be expected to result in increases in the BOLD response, but we found the opposite. Age-related $\Delta CBF/\Delta CMRO_2$ ratio decreases were related to RT, suggesting that age-related slowing observed in visual processing tasks results from less efficient neural cell assemblies. Within motor cortex, we found a different pattern of evidence. That is, we found age-related increases in both ΔCBF and $\Delta CMRO_2$ for older participants, but $\Delta CBF/\Delta CMRO_2$ ratios were not significantly different between younger and older groups. The relatively impoverished responsivity of ΔCBF for older adults still led to an age-related decrease in BOLD. We speculated that such reduced vascular responsiveness to neural metabolic demand would lead to variation in $\Delta CBF/\Delta CMRO_2$ with variation in task demand. A simulation of BOLD relative to $\Delta CMRO_2$ for lower and higher neurometabolic-flow coupling ratios (approximating those for old and young, respectively) indicated less BOLD signal change in old than young in relatively lower $CMRO_2$ ranges (i.e., reduced levels of $CMRO_2$ relative to baseline), as well as greater BOLD signal change in young compared to old in relatively higher $CMRO_2$ ranges (i.e., increased levels of $CMRO_2$ relative to baseline). This simulation illustrates the potential impact of age-related changes in neurometabolic-flow coupling on the responsiveness of the BOLD signal.

MATERIALS AND METHODS

PARTICIPANTS

Participants were 22 younger (ages 23–33, Mean age: 28.2 years; $n = 11$, six female) and older (ages 53–72, Mean age: 60.5 years; $n = 11$, six female) individuals recruited from throughout the greater Dallas–Fort Worth metropolitan area. Advertisements were posted in several locations, including the world-wide web, local community centers, and the University of Texas at Dallas (UTD) and the University of Texas Southwestern Medical Center (UTSWMC) campuses. All advertisements were approved by the UTSWMC and UTD Institutional Review Boards (IRBs).

Participants were physically and cognitively healthy. That is, they did not report any history of heart, lung, neurologic, or psychiatric difficulties and were not taking blood pressure medications, diuretics, or psychotropic/psychoactive medications. Participants were cognitively intact based on assessments during the telephone prescreening (de Jager et al., 2003) and in person on the day of the scans (Folstein et al., 1975), and they were screened and deemed safe within the 3-T MR scanning environment. Participants were compensated at the rate of $100 for their time, which was approximately $50/h, including time to consent using a form approved by both the UTSWMC and UTD IRBs.

VISUAL STIMULI

We considered that older participants might require differing amounts of activation compared to younger participants based upon the state of affairs prior to evoked stimulation. As noted in both Pasley et al. (2007) and Shulman et al. (2007), a condition within an experiment can be used as a baseline condition for purposes of comparison. We utilized fixation as one baseline condition and parafoveal stimulation (i.e., the use of parafoveal stimulation to artificially depress baseline activation within peripheral visual areas) as a second baseline condition. By utilizing both baselines, we were able to assess changes from two different levels of activation within parafoveal cortex.

Flashing sinusoidal grating annuli were presented to activate or depress activity within visual areas corresponding to the peripheral visual field (Pasley et al., 2007; Hutchison et al., 2012; cf. **Figure 1**). Three types of visual stimuli were presented: parafoveal stimuli (1.7–3.3° eccentricity, drift temporal frequency = 6 Hz, spatial frequency = 1 cycle/degree, 80% contrast), peripheral stimuli (6.8–9.9° eccentricity, drift temporal frequency = 6 Hz, spatial frequency = 1 cycle/degree, 25% contrast), and combined stimuli (parafoveal stimulus onset followed by peripheral stimulus onset after a 20-s delay; both images were maintained in view simultaneously after peripheral stimulus onset). Stimuli were presented in three runs, with two blocks of each stimulus type per run, and were randomized in order within each run. Thirty second fixation periods were spaced temporally between stimulus presentation blocks. Across runs, there were six instances of each type of stimulus block. Each run lasted a total of 600 s (i.e., 10 min).

A fixation cross was presented in the center of the screen throughout the visual task. It changed in luminance every 3–7 s (mean time between changes = 5 s; 118–120 luminance changes per run). Luminance changes were programed using red, green, blue (RGB) color formatting, which involves three integers representing the amounts of each of the three colors represented on the screen. By always maintaining all three components of the color equal to one another (i.e., R = G = B), the color of the fixation cross appeared as lighter and darker shades of gray. Luminance changes are henceforth discussed in terms of the change of single color values, given that all RGB values were equal for the fixation cross. These luminance changes were generally small (i.e., 20–30 U; across three runs, $n = 183$), but medium (50–90 U; $n = 111$) and large (120–240 U; $n = 63$) luminance changes were also included.

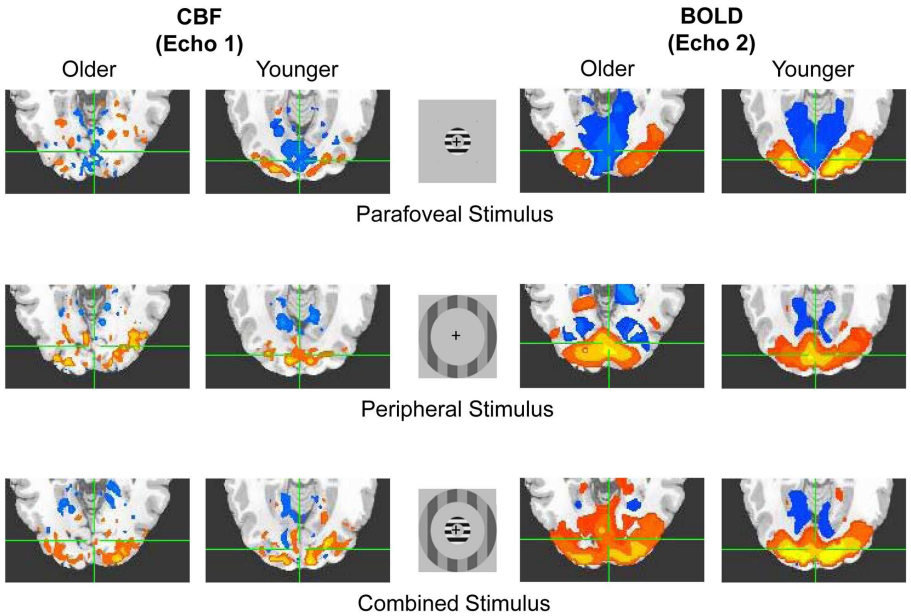

FIGURE 1 | Basic illustration of the Experiment. Representative older and younger positive (hot color) and negative (cool color) activations in response to flashing annuli (peripheral, parafoveal, and combined stimulus types) for both CBF (i.e., echo 1) and BOLD (i.e., echo 2) signals. Signal change is shown within the overlapping anatomical and functional ROIs within visual cortex. Similar ROIs were obtained within motor cortex in response to button presses (see Materials and Methods).

This variability served to keep the task challenging enough to maintain attention at the desired fixation point, but easy enough for participants to make many knowingly accurate judgments.

HYPERCAPNIA MATERIALS

$R2^*$ (i.e., transverse relaxation rate of tissue water) is affected by blood oxygenation and is the sum of R2 (i.e., intrinsic spin-spin relaxation), $R2'$ due to non-heme field inhomogeneity (e.g., imperfect shimming, iron content), and $R2'$ due to deoxyhemoglobin (i.e., M). It is well known (see Davis et al., 1998; Hoge et al., 1999a) that only this last term is associated with BOLD signal amplitude. M reflects both the amount of deoxyhemoglobin related to venous cerebral blood volume (i.e., how much venous blood a voxel contains) and the oxygenation level of the venous blood. It is therefore expected that M, which represents the maximum BOLD signal one can get from a particular voxel, is the most relevant parameter for BOLD modulation. Because CO_2 delivery induces vasodilation, washes out deoxyhemoglobin, and increases venous oxygenation, utilization of a hypercapnia task allowed us to infer M (Davis et al., 1998; Hoge et al., 1999a), which has been shown to vary across cortex (Gauthier and Hoge, 2013), and allowed for the calculation of $\Delta CBF/\Delta CMRO_2$.

Hypercapnia was induced by delivering a 5% CO_2 solution (balanced with 21% O_2 and 74% N_2; contained in a Douglas bag) via a two-way non-rebreathing valve/mouthpiece combination (Hans Rudolph, 2600 series, Shawnee, KS, USA). A capnograph device (Capnogard, Model 1265, Novametrix Medical Systems, CT, USA) was used to monitor end-tidal CO_2, and a pulse oximeter (MEDRAD, Pittsburgh, PA, USA) was used to monitor breathing rate, heart rate, and arterial oxygenation saturation. Data values collected from both devices were recorded on a tablet PC using the HyperTerminal program (Private Edition, Version 6.3, by Hilgraeve, Monroe, MI, USA).

APPARATUS AND SCANNING PARAMETERS

Scanning followed the same procedure as that of Hutchison et al. (2012). Imaging was conducted at the UTSWMC Advanced Imaging Research Center on a 3-T MRI system (Philips Medical Systems, Best, Netherlands). High resolution anatomical data were acquired using a T1-weighted magnetization-prepared rapid acquisition of gradient echo (MPRAGE) pulse sequence (Brant-Zawadzki et al., 1992). Calibrated fMRI using ASL allowed us to acquire both CBF (echo 1) and BOLD (echo 2) signals in a simultaneous, interleaved fashion.

A pseudo-continuous ASL sequence (Garcia et al., 2005) was used to acquire the calibrated fMRI data (visuomotor, hypercapnia) with echo times at TE1 = 11 ms and TE2 = 30 ms (Flip angle = 90°, 16 slices, 5 mm thick, orientation transverse, slice around calcarine sulcus linearly from bottom to top, TR = 4 s, 150 volumes). Global baseline CBF was measured in sagittal sinus (phase contrast voxel size 0.45 mm × 0.45 mm × 5 mm, maximum velocity 80 cm/s, duration 30 s; note that hypercapnia-induced CBF increases are comparable for sagittal sinus and feeding arteries, which perfuse the entire brain; Aslan et al., 2010) using phase contrast scans that were run immediately prior to and immediately following the hypercapnia sequence, representing normocapnic and hypercapnic conditions, respectively. Phase contrast MRI data were used to normalize ASL signals as described previously (Aslan et al., 2010). Scans were acquired in the following sequence: high resolution anatomical MPRAGE, three runs of the visuomotor

task, normocapnic phase contrast, hypercapnia, hypercapnic phase contrast.

PROCEDURE

As in Hutchison et al. (2012), the high resolution anatomical MPRAGE was acquired first, followed by three runs of the visuomotor task. Participants were asked to ignore the flashing annuli but to quickly press and release both buttons (incorporated into hand-held button boxes) every time they noticed the fixation cross changing in luminance – that is, appearing lighter or darker. The luminance judgment task served to maintain the participants' focus on the center of the screen so that positive response visual areas could be located functionally using calibrated fMRI responses to the flashing annuli. The button press portion of the task allowed us to assess functional changes in motor cortex.

At the conclusion of the visual stimulus runs, the patient table was withdrawn from the bore of the scanner and the mouthpiece for the hypercapnia portion of the experiment was placed into the participant's mouth. The participant wiped the exterior of his or her nose with a moist towelette, the nose clip was placed on the participant's nose, and it was verified that the participant could breathe comfortably and that the non-rebreathing valve was working properly. Button boxes were removed and a pulse oximeter finger monitor was clipped onto a finger of the participant's left hand. An emergency squeeze bulb was positioned near the right hand such that the participant could easily squeeze it without having to move or look for the bulb. The patient table was returned to the scanner bore and the hypercapnia experiment procedure was executed (4 min of room air followed by 6 min of CO_2), flanked by two, 30 s phase contrast scans (normocapnic and hypercapnic, respectively). A researcher stayed inside the magnet room throughout the phase contrast and hypercapnia portions of the experiment to manually switch the valve to control the breathing of air (either room air or CO_2 bag). At the termination of the final scan, the bag valve was returned to room air, the patient table was withdrawn from the bore of the scanner, and the hypercapnia equipment was removed from the participant.

DATA PRE-PROCESSING

Data were transformed from Philips PAR/REC format into SPM (Statistical Parametric Mapping, Wellcome Department of Imaging Neuroscience, University College London, London, UK) Analyze format using the GUI FOR R2A Rec-to-Analyze Converter (Hermans and Neggers, GUI for R2A, version 2.1 released March 2006, modified February 2008, Helmholtz Institute, Utrecht University, Department of Brain Research, University Medical Center, Utrecht, Netherlands). Files were then spatially pre-processed in SPM using the Realign-Estimate-Reslice algorithm for each echo and run. In-house MATLAB® (Version 7.4, Mathworks, Natick, MA, USA) code separated echo 1 and echo 2 into separate Rec files for each echo and run, and the new Rec files were then read into AFNI (Analysis of Functional NeuroImages; Cox, 1996) where the data were registered to the individual's MPRAGE space and aligned to the first brick of the first run of echo 2; dummy scans prevented the need to discard the first few volumes. Parameters were saved and applied to all runs for both echo 2 and echo 1. Labeled images were subtracted from control images in echo 1 to obtain CBF weighted images. Echo 2 data were subjected to a low pass temporal Fourier filter (cutoff frequency = 0.05 Hz) and were then spatially smoothed (FWHM = 8 mm). Noise was cleared from outside the head. A mask was then generated to restrict analyses to areas representing visual cortex – specifically, we utilized a morphometric approximation of Brodmann Areas (BAs; Brodmann, 1909/2006) 17, 18, and 19. BAs were defined by the demarcation of landmarks in each individual's native space using Caret (Van Essen et al., 2001) as detailed in Hutchison et al. (2012). Functional activation in response to the visual stimuli was used to narrow region of interest (ROI) selection as described below.

DATA ANALYSES, VISUAL DATA

Echo 1 and echo 2 data, reflecting CBF and BOLD respectively, were analyzed using the 3dDeconvolve command to conduct a regression analysis in AFNI (Cox, 1996). Beta values, along with their associated p values, were generated for each individual for each stimulus condition for each echo.

For further analysis, ROI selection was based on functional activation overlap between CBF and BOLD but was restricted to the morphometrically defined visual cortical areas BAs 17, 18, and 19 (see above). In light of evidence suggesting that the dependent measures of interest might be less prone to bias if blood flow is taken into account and ROIs are sufficiently large (Leontiev et al., 2007), we required overlap of CBF and BOLD activation but selected a generous thresholding measure (Poline et al., 2006) such that t values of 1.00 were adequate for positive and negative response conditions, and the combined condition had no statistical thresholding. (Positive responses were considered to be signal increases from the baseline condition of interest; negative responses were considered to be signal decreases from the baseline condition of interest.) Thus, in order for a voxel to be retained within the ROI, it had to: (1) react positively to the peripheral stimulus for both CBF and BOLD, (2) react negatively to the parafoveal stimulus for both CBF and BOLD, (3) react positively to the combined stimulus for both CBF and BOLD, and (4) be contained within the morphometrically defined BAs 17, 18, and 19 (cf. **Figure 1**). ROIs for individuals ranged from 6 to 269 voxels (older: 6–136 voxels, mean = 65.36, SEM = 12.45; younger: 18–269 voxels, mean = 128.70, SEM = 24.62). Concerns regarding biases introduced by ROI size differences between the groups are obviated by our results, which indicate a pattern opposite to previous observations that smaller functional ROIs tend to be associated with larger $\Delta CBF/\Delta CMRO_2$ ratios (Leontiev et al., 2007), and thus typically larger BOLD responses. Restated, although a negative association between ROI size and $\Delta CBF/\Delta CMRO_2$ would be expected, we observed no such association from fixation (Spearman $\rho = 0.37$, $p = 0.100$) nor from parafoveal stimulation, where we observed the opposite result – that is, a positive association between ROI size and $\Delta CBF/\Delta CMRO_2$ (Spearman $\rho = 0.47$, $p = 0.030$; FDR = 0.08). Age group was not a factor in these results (all $ps > 0.05$). This suggests that our results are not a simple reflection of ROI size differences. All results reported here were averaged over the ROI for the stimulus condition of interest unless specifically stated as being calculated over the whole brain.

Beta values from the regression analysis were adjusted to reflect percent signal change from fixation (for echoes 1 and 2,

respectively) and were then masked by the ROI selection that included the overlap area between CBF and BOLD activations to obtain mean values per stimulus condition for older and younger groups. Additional statistical analyses were conducted using SAS® software program (Version 9.1, SAS Institute, Cary, NC, USA) outside of brain space.

DATA ANALYSES, HYPERCAPNIA DATA

Data in echo 1 were used to obtain CBF weighted images and data in echo 2 represented the BOLD images, as described above. The ROI masks defined in the visual fMRI runs were applied to the hypercapnia data to obtain time courses of CBF and BOLD signals. The CBF and BOLD percent signal changes were calculated comparing the average hypercapnia signal (volumes 91–150) to the average normocapnia signal (volumes 1–60).

Continuing to use in-house Matlab code, we used the Davis et al. (1998) and Hoge et al. (1999a) model to estimate M (a calibration constant necessary for the calculation of $CMRO_2$; Davis et al., 1998) from calibrated fMRI hypercapnia data:

$$M = \frac{\frac{\Delta BOLD}{BOLD_0}}{\left(1 - \left(1 + \frac{CBF}{CBF_0}\right)^{\alpha-\beta}\right)}, \quad (1)$$

with the assumption that $CMRO_2$ and neural activity are not significantly affected by hypercapnic conditions (Hoge et al., 1999b). We assumed $\alpha = 0.38$ (Grubb et al., 1974) and $\beta = 1.33$ (Lu and van Zijl, 2005); Hoge et al. (1999a) demonstrated that although estimates of α and β affect asymptotic extrapolations of M, these values do not significantly impact results in the range of human imaging studies, and so the utilization of estimates for α and β was deemed adequate. M was calculated both over the ROI only and over the entire brain. There is some evidence that age-related differences in M can lead to differences in the BOLD response (Ances et al., 2009, but, see Hoge et al., 1999a). To be thorough, we investigated this possibility and did not find significant differences in M values between older and younger groups over the functionally derived ROI [older: mean $M = 0.12$, SEM $= 0.01$; younger: mean $M = 0.10$, SEM $= 0.02$; $t(20) = 0.92$, $p = 0.369$, *ns*]. Comparing M values averaged over the entire brain between the older and younger groups was similarly non-significant. Due to recent uncertainty in the literature regarding the appropriate value that should be used for α (e.g., Gauthier and Hoge, 2012), we also calculated M using $\alpha = 0.10$. This low α estimate likewise yielded non-significant age-related M differences [older: mean $M = 0.12$, SEM $= 0.01$; younger: mean $M = 0.15$, SEM $= 0.03$; $t(13.473) = -0.69$, $p = 0.502$, *ns*] and allowed us to feel confident that $\alpha = 0.38$ was sufficient for our visual analyses.

Finally, using M from the visually derived ROI, we calculated $\Delta CMRO_2$ and $\Delta CBF/\Delta CMRO_2$ from fixation and from parafoveal stimulation for each individual. (One younger participant had a $\Delta CBF/\Delta CMRO_2$ ratio more than 2.5 standard deviations greater than the remainder of the group. In order to present a clearer picture of the mean group values, this participant's $\Delta CBF/\Delta CMRO_2$ ratio data are not included in the analyses presented in the Section "Results," although the inclusion of this participant's data did not alter the significance of the results.) Similar ratios were calculated for BOLD and CBF data. The Davis et al. (1998) and Hoge et al. (1999a) model was also the basis for these calculations. Values reported in the paper use individual M values (cf. Chiarelli et al., 2007a) even though calculations including mean Ms across the experiment or across groups did not alter the results.

DATA ANALYSES, MOTOR CORTEX DATA

Data from motor cortex were analyzed similarly to the data from visual cortex, with a few minor adjustments based on the difference of the task. In order for a voxel to be retained in the analyses, it had to: (1) react positively to button presses for both CBF and BOLD using a cutoff t value of 1.00, and (2) be contained within the morphometrically defined BA 4, representing primary motor cortex. Because some of the luminance changes were subtle (as described above under Visual Stimuli) and were missed by several of the participants, we analyzed only the luminance change button presses that co-occurred with a change in the flashing annuli, as these changes were typically the most easily detected. A general linear model (GLM) was sufficient to model the data, as we collapsed across luminance change and annulus type. M values were calculated over the area of overlap between BA 4 and the hypercapnic data acquisition and did not differ significantly between older and younger groups [older: mean $M = 0.09$, SEM $= 0.03$; younger: mean $M = 0.07$, SEM $= 0.02$; $t(19) = 0.35$, $p = 0.733$, *ns*]; using $\alpha = 0.10$ did not affect this result [older: mean $M = 0.07$, SEM $= 0.02$; younger: mean $M = 0.06$, SEM $= 0.02$; $t(19) = 0.35$, $p = 0.733$, *ns*]. One older participant did not retain any significant voxels within BA 4. An additional older participant's functional values were determined to be outliers in the opposite direction (i.e., greatly exaggerated responses); however, the removal of the outlying data did not markedly affect the pattern of results. Data for the remaining 20 participants are therefore represented for the motor cortex analyses throughout the remainder of the paper. There was no significant association between ROI size and $\Delta CBF/\Delta CMRO_2$ (Spearman $\rho = -0.21$, $p = 0.361$).

NEUROMETABOLIC-FLOW COUPLING AND NEURAL EFFICIENCY SIMULATION

We speculated that reduced vascular responsiveness to neural metabolic demand would lead to variation in $\Delta CBF/\Delta CMRO_2$ with variation in task demand. We examined the effect of vascular responsiveness, indexed by age-differential $\Delta CBF/\Delta CMRO_2$ coupling ratios, on BOLD changes for different levels of $\Delta CMRO_2$. BOLD was plotted relative to $\Delta CMRO_2$ for lower and higher neurometabolic-flow coupling ratios (approximating those for old and young, respectively). We could thereby visualize the effect of age-related changes in $\Delta CBF/\Delta CMRO_2$ on the BOLD signal. Previous research has shown that, for a wide range of $\Delta CMRO_2$ and ΔCBF, these two metrics are tightly coupled in a linear fashion in younger adults (e.g., Stefanovic et al., 2004). This coupling appears to be adversely affected in aging, yielding age-related reductions in $\Delta CBF/\Delta CMRO_2$ for older compared to younger adults (Hutchison et al., 2012). Using the theoretical relationship between $\Delta CMRO_2$, ΔCBF, and $\Delta BOLD$, we investigated whether such changes in $\Delta CBF/\Delta CMRO_2$ would differentially affect the

rate of changes in the BOLD signal given (Davis et al., 1998; Hoge et al., 1999a):

$$\frac{\Delta BOLD}{BOLD_0} = M\left(1 - \left(\frac{CMRO_2}{CMRO_{2|0}}\right)^{\beta}\left(\frac{CBF}{CBF_0}\right)^{\alpha-\beta}\right) \quad (2)$$

Changes in the BOLD signal were considered across different levels of $\Delta CMRO_2$ relative to baseline conditions (fixation and parafoveal stimulation).

RESULTS

A priori hypotheses of age-related changes in $\Delta CBF/\Delta CMRO_2$ ratios and their relationships to behavior were tested using planned comparisons (cf. Keppel and Wickens, 2004). For additional tests we calculated, using False Discovery Rate (FDR) theory (Benjamini and Hochberg, 2000), that we would expect 0.85, or roughly between 0 and 1, of these tests to falsely reject the null hypothesis ($0.05 \times 17 = 0.85$). For these tests, we rejected the null hypothesis at $p < 0.05$, FDR < 0.05. Thus it is probable that our tests correctly rejected our null hypotheses, particularly given that the results portray a consistent picture. For the sake of clarity, the FDR is reported in addition to p when $p < 0.05$ and FDR < 0.10.

Blood-oxygen-level-dependent data and M values were normally distributed. All other variables deviated from normality (based on the Shapiro–Wilk W statistic, $ps < 0.05$). For example, $\Delta CBF/\Delta CMRO_2$ was not normally distributed when assessed from visual fixation ($W = 0.74$, $p < 0.0001$), parafoveal stimulation ($W = 0.81$, $p = 0.0008$), or within motor cortex ($W = 0.72$, $p < 0.0001$). Under such conditions of non-normality we used non-parametric (i.e., Kruskal–Wallis, Signed rank, or Spearman ρ) tests to assess group differences and associations between variables.

BEHAVIORAL RESULTS

Older participants were significantly slower than younger participants in responding to fixation cross luminance changes [older: mean RT = 687.66 ms, SEM = 34.88; younger: mean RT = 553.93 ms, SEM = 31.21; Kruskal–Wallis (K–W) $\chi^2(1) = 6.06$, $p = 0.014$]. Older participants were also less accurate than their younger counterparts [older: mean proportion correct = 0.69, SEM = 0.05; younger: mean proportion correct = 0.83, SEM = 0.02; K–W $\chi^2(1) = 4.55$, $p = 0.033$; FDR = 0.08]. RT was negatively associated with proportion correct (Spearman rho (ρ) = −0.67, $p = 0.0007$), yielding no support for a speed-accuracy trade-off.

VISUAL EXPERIMENT

Blood-oxygen-level-dependent

We first tested the *a priori* hypothesis of an age-related difference in the BOLD response within visual cortex, as the etiology of this difference was the topic under study. A mixed model incorporating group (older and younger), stimulus conditions of interest (from fixation: parafoveal, peripheral, and combined; from parafoveal stimulation: combined), and a group by stimulus condition interaction, was used to assess differences in the BOLD response in terms of proportion signal change. In addition to differences solely based on stimulus type [$F(3, 60) = 288.47$, $p < 0.0001$], there was a significant interaction between age group and stimulus type [$F(3, 60) = 5.21$, $p = 0.003$]. Most pronounced was the difference between older and younger groups when responding to the combined stimulus from parafoveal stimulation [older: least Squared Mean (LSM) = 0.0087, SEM = 0.0006; younger: LSM = 0.0114, SEM = 0.0006; difference estimate (de) = −0.0027; $t(48.8) = -3.00$, $p = 0.004$], but this group difference in responding to the combined stimulus was also significant from fixation [older: LSM = 0.0062, SEM = 0.0006; younger: LSM = 0.0081, SEM = 0.0006; $de = -0.0019$; $t(48.8) = -2.08$, $p = 0.043$; see **Table 1**]. Collapsing across all stimulus types, the younger group had a marginally greater BOLD response than the older group [$de = -0.0013$, $t(20) = -1.85$, $p = 0.079$].

Δ CBF/Δ CMRO$_2$ ratio

To test the *a priori* hypothesis that $\Delta CBF/\Delta CMRO_2$ differences could mediate age-related changes in the BOLD response, $\Delta CBF/\Delta CMRO_2$ was calculated for each individual from both resting and parafoveal stimulation conditions. $\Delta CBF/\Delta CMRO_2$ was significantly greater for the younger group than the older group, both from fixation [older: mean = 1.88, SEM = 0.06; younger: mean = 2.40, SEM = 0.24; K–W $\chi^2(1) = 4.17$, $p = 0.041$; see **Table 1**], and from parafoveal stimulation [older: mean = 1.69, SEM = 0.05; younger: mean = 2.00, SEM = 0.12; K–W $\chi^2(1) = 4.46$, $p = 0.035$]. These results support the hypothesis that age-related BOLD signal changes are the consequence of differences in the ratio of cerebral perfusion to oxygen metabolic rate (i.e., $\Delta CBF/\Delta CMRO_2$) between the older and younger groups, and these age-related differences occur regardless of baseline stimulation condition (i.e., fixation or parafoveal).

Components of the Δ CBF/Δ CMRO$_2$ ratio

Significant differences in the CBF response would indicate that age-related differences in the BOLD response are at least partially due to age-related changes in cerebral perfusion (i.e., blood flow). As with the BOLD data, we utilized a mixed model incorporating group, stimulus conditions of interest (from fixation: negative, positive, and combined; from parafoveal stimulation: combined), and a group by stimulus condition interaction to assess differences in proportion signal change (see Gupta et al., 2006, regarding the robustness of a balanced, mixed model to non-normality). As seen in **Table 1**, the ΔCBF difference between older and younger groups was not significant [$F(1, 20) = 0.20$, $p = 0.659$], indicating that age-related differences in $\Delta CBF/\Delta CMRO_2$ were not caused by differences in the ΔCBF response. Additionally, there were minimal differences in "absolute" (i.e., change from fixation) ΔCBF in the older compared to the younger group, both from fixation [K–W $\chi^2(1) = 0.24$, $p = 0.622$] and parafoveal stimulation [K–W $\chi^2(1) = 0.05$, $p = 0.818$].

We also sought to determine if there were age-related differences in the $\Delta CMRO_2$ component of $\Delta CBF/\Delta CMRO_2$. We observed age-related $\Delta CMRO_2$ differences in "absolute" measures (i.e., change from fixation) when measured from parafoveal stimulation [K–W $\chi^2(1) = 4.28$, $p = 0.039$; FDR = 0.08]. Additionally, we observed greater "incremental" (i.e., change from respective baseline stimulation condition – that is, either fixation or parafoveal stimulation) evoked $\Delta CMRO_2$ from

Table 1 | Mean proportion signal change (BOLD, $\Delta CBF/\Delta CMRO_2$, ΔCBF, $\Delta CMRO_2$) within visual cortex and motor cortex, from baseline (fixation and non-motor response periods, respectively).

Cortical area, task	BOLD*		$\Delta CBF/\Delta CMRO_2$*		ΔCBF		$\Delta CMRO_2$*	
	Older	Younger	Older	Younger	Older	Younger	Older	Younger
Visual cortex, response to flashing annuli (SEM)	0.0059 (0.0008)	0.0073 (0.0007)	1.8844 (0.0639)	2.3977 (0.2360)	0.3621 (0.0542)	0.3267 (0.0302)	0.1969 (0.0336)	0.1327 (0.0194)
	BOLD		$\Delta CBF/\Delta CMRO_2$		ΔCBF*		$\Delta CMRO_2$*	
	Older	Younger	Older	Younger	Older	Younger	Older	Younger
Motor cortex, response to flashing annuli (SEM)	0.0016 (0.0001)	0.0022 (0.0003)	1.6275 (0.0166)	1.6639 (0.0276)	0.8788 (0.1231)	0.5624 (0.0721)	0.5354 (0.0691)	0.3361 (0.0393)

**Difference between groups, $p < 0.05$.*

parafoveal stimulation than from fixation [from parafoveal stimulation: mean = 0.30, SEM = 0.02; from fixation: mean = 0.16, SEM = 0.02; Signed rank $S = 126.50$, $p < 0.0001$]; this effect was also found for BOLD and ΔCBF ($ps < 0.0001$). However, only the BOLD response showed smaller incremental evoked responses for the older group compared to the younger group [older: LSM = 0.0073, SEM = 0.0007; younger: LSM = 0.0094, SEM = 0.0007; assessed using a mixed model, $de = -0.0021$, $t(20) = -2.09$, $p = 0.050$; FDR = 0.09], indicating that age-related differences in $\Delta CMRO_2$ are not attributable to baseline stimulation condition differences. In sum, comparing differences between older and younger participants on the constituents of the BOLD response within visual cortex revealed minimal differences in ΔCBF but significant age-related differences in $\Delta CMRO_2$ (see **Table 1**). This change in $\Delta CMRO_2$ affected significant change in $\Delta CBF/\Delta CMRO_2$.

$\Delta CBF/\Delta CMRO_2$: relationships to behavior

The behavioral significance of age-related $\Delta CBF/\Delta CMRO_2$ differences could be demonstrated if we observed relationships between this physiologic factor and individual subject performance. A Spearman ρ test of association across older and younger groups confirmed our *a priori* hypothesis that RT was significantly negatively associated with $\Delta CBF/\Delta CMRO_2$ from fixation ($\rho = -0.49$, $p = 0.025$; and from parafoveal stimulation, $\rho = -0.43$, $p = 0.053$). **Figure 2** illustrates this relationship when broken out by group (older or younger) and RT (slower or faster, as determined by within-group median split). Likewise, a Spearman ρ test of association confirmed our *a priori* hypothesis that proportion correct was positively associated with $\Delta CBF/\Delta CMRO_2$ from fixation ($\rho = 0.46$, $p < 0.038$). Neither RT nor proportion correct was associated with the ΔCBF or $\Delta CMRO_2$ components separately. These results support the hypothesis that age-related behavioral indices – i.e., slowing of RTs and reduced proportion correct – are significantly associated with age-related reductions in $\Delta CBF/\Delta CMRO_2$.

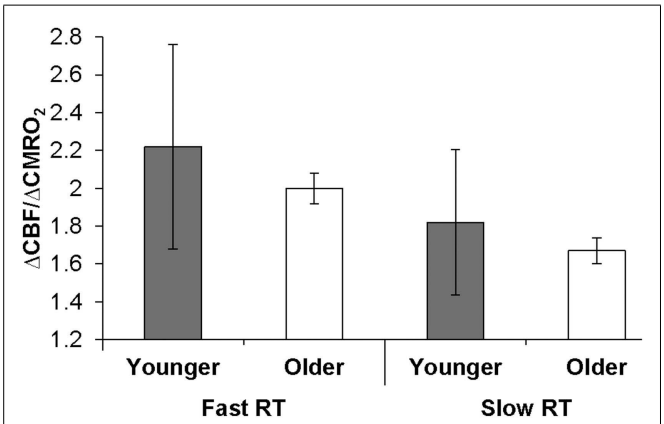

FIGURE 2 | Relationship of $\Delta CBF/\Delta CMRO_2$ to behavior within visual cortex. Older and younger participants were designated as fast or slow responders based on median reaction time (RT) within each group. Error bars represent the semi-interquartile range. The resulting median $\Delta CBF/\Delta CMRO_2$ ratios for each group from fixation illustrate the significant association between $\Delta CBF/\Delta CMRO_2$ and RT, which was calculated across groups.

MOTOR CORTEX ANALYSES

Because ΔCBF and $\Delta CMRO_2$ can vary independently across cortex, we additionally analyzed BOLD, $\Delta CBF/\Delta CMRO_2$, ΔCBF, and $\Delta CMRO_2$ data from the button press task within motor cortex (see **Table 1**). A GLM indicated that older participants had only a marginally smaller BOLD response within motor cortex than did younger participants [older: mean = 0.0016, SEM = 0.0001; younger: mean = 0.0022, SEM = 0.0003; $F(1, 18) = 3.33$, $p = 0.085$, *ns*] in response to button press stimulation. Also in contrast to the visual cortex results, $\Delta CBF/\Delta CMRO_2$ was statistically similar in older and younger groups [older: mean = 1.63, SEM = 0.02; younger: mean = 1.66, SEM = 0.03; K–W $\chi^2(1) = 1.39$, $p = 0.239$, *ns*]. Breaking the ratio down into its constituent components yielded increases in ΔCBF for the older group compared to the younger group [older: mean = 0.8788, SEM = 0.1231; younger: mean = 0.5624, SEM = 0.0721; K–W $\chi^2(1) = 6.10$, $p = 0.014$]. There were also increases in $\Delta CMRO_2$ for the older group compared to the younger group [older: mean = 0.5354, SEM = 0.0691; younger: mean = 0.3361, SEM = 0.0393; K–W $\chi^2(1) = 6.88$, $p = 0.009$].

In sum, comparing differences between older and younger participants on the constituents of the BOLD response within motor cortex revealed age-related differences in both ΔCBF and $\Delta CMRO_2$. Changes in both components of the ratio offset one another, leading to an absence of significant differences in $\Delta CBF/\Delta CMRO_2$. This difference was reflected in age-equivalent BOLD responding.

NEUROMETABOLIC-FLOW COUPLING AND NEURAL EFFICIENCY SIMULATION

Figure 3 shows BOLD signal variability as a function of $\Delta CMRO_2$. The simulation analysis revealed that the BOLD signal, in general, is less responsive to $\Delta CMRO_2$ changes in the older group than in the young group for both fixation and parafoveal stimulation conditions (**Figures 3A,B**). It can be seen that, for reduced levels of $CMRO_2$ (i.e., conditions demanding lower neuronal activity relative to a baseline condition), the older group showed less BOLD signal change than the younger group. However, for increased levels of $CMRO_2$ (i.e., conditions demanding higher neuronal activity relative to a baseline condition), the younger group showed greater BOLD signal change than the older group. In sum, decreased coupling ratios in the older group led to less responsiveness in BOLD signal in either direction (i.e., increased and decreased $CMRO_2$) compared to the younger group. These interaction patterns suggest that, for identical changes in $\Delta CMRO_2$ (which more directly reflect the level of neuronal activity), differing patterns of BOLD signal change are expected in older and younger groups, due to variations in the $\Delta CBF/\Delta CMRO_2$ coupling ratios. In relation to fMRI findings in the aging literature, it is worth noting that these BOLD changes are not exclusively a result of changes in levels of underlying neuronal activity. Instead, the BOLD changes are significantly affected by age-related changes in the relationship between ΔCBF and $\Delta CMRO_2$.

DISCUSSION

Using a visuomotor task, we observed age-related changes in neurometabolic-flow response patterns in both visual and motor cortices using calibrated fMRI. Specifically, within visual cortex, we found equivalent ΔCBF in the presence of age-related increases in $\Delta CMRO_2$. This reduction in the $\Delta CBF/\Delta CMRO_2$ ratio resulted in paradoxical age-related decreases in BOLD for older adults relative to younger adults, even in the face of increases in $\Delta CMRO_2$, a more direct index of neural activity (cf. Hyder, 2004). Additionally, these age-related $\Delta CBF/\Delta CMRO_2$ ratio decreases were related to RT, suggesting that age-related slowing observed in visual processing tasks might result from less efficient neural cell assemblies. Within motor cortex, we found age-related increases in both ΔCBF and $\Delta CMRO_2$. Changes in both aspects of the $\Delta CBF/\Delta CMRO_2$ ratio offset one another, yielding age-equivalence in $\Delta CBF/\Delta CMRO_2$ and in BOLD signal within motor cortex. A simulation illustrated how age-related changes in BOLD might reflect differential changes in $\Delta CBF/\Delta CMRO_2$ instead of simply reflecting changes in neural activity as indexed by $\Delta CMRO_2$. These results suggest that age-comparative studies relying solely on BOLD signal might be systematically misinterpreted depending on the cortical area, cognitive task, and the age group under investigation.

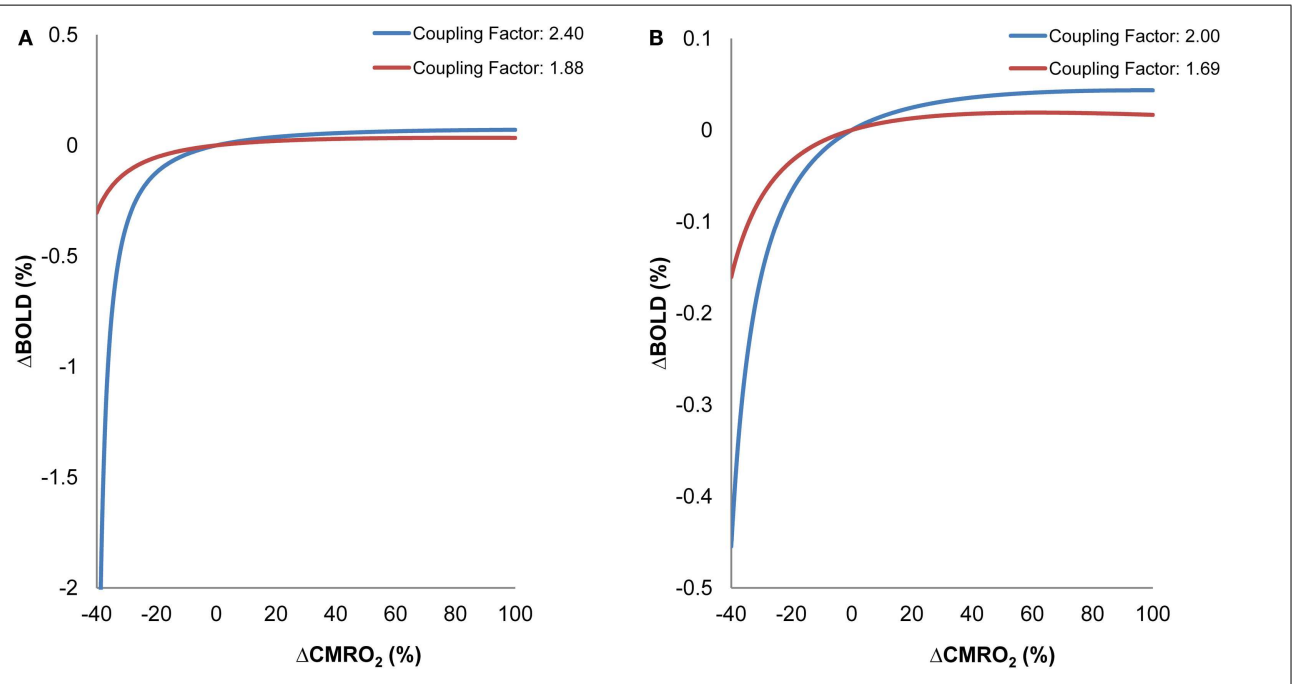

FIGURE 3 | Simulation Results: BOLD as a function of $\Delta CMRO_2$ for different $\Delta CBF/\Delta CMRO_2$ coupling ratios within visual cortex. (A) $\Delta CBF/\Delta CMRO_2$ coupling ratios derived from fixation for older (red) and younger (blue) participants. **(B)** $\Delta CBF/\Delta CMRO_2$ coupling ratios derived from parafoveal stimulation for older (red) and younger (blue) participants. Variations in BOLD and $CMRO_2$ were calculated relative to a baseline representing an intermediate activity level for each condition (fixation, parafoveal stimulation).

Age-differences in the BOLD response arise from the variable relationship between ΔCBF and $\Delta CMRO_2$; ΔCBF increases lead to BOLD amplitude increases, whereas $\Delta CMRO_2$ increases lead to BOLD amplitude decreases (Buxton et al., 2004). This complex relationship could explain much of the variability between studies comparing cerebrovascular characteristics of older and younger adults (Ross et al., 1997; Taoka et al., 1998; D'Esposito et al., 1999; Huettel et al., 2001; Restom et al., 2007; Ances et al., 2009; Lu et al., 2011). The present results, showing age-related $\Delta CBF/\Delta CMRO_2$ alterations in primary visual regions but no age-related $\Delta CBF/\Delta CMRO_2$ alterations in primary motor regions, suggest that between-study variance in previous results might be due to age-related regional differences in ΔCBF and $\Delta CMRO_2$ (Heo et al., 2010; Chen et al., 2011; Lu et al., 2011). The resulting $\Delta CBF/\Delta CMRO_2$ would lead to apparent age-equivalence – or age-differences – in the BOLD response.

There has been considerable investigation and debate regarding the ideal values for α and β parameters used to calculate M and $\Delta CMRO_2$, as an artificially large α value could significantly underestimate $\Delta CMRO_2$ (although biases of $\Delta CBF/\Delta CMRO_2$ are somewhat limited if the same α value is used to estimate both M and $\Delta CMRO_2$; Chen and Pike, 2009). In particular, several studies have found α values to be smaller than Grubb et al.'s (1974) value of 0.38 that is used widely throughout the literature (e.g., Chen and Pike, 2009, 2010). Recently, Gauthier and Hoge (2012) investigated ranges of α (0.1–0.38) and β (1–2) values in terms of their effect on M and oxygen extraction fraction (OEF) estimates. Using three different gas solutions, Gauthier and Hoge (2012) generated maps of M, OEF, CBF, and $CMRO_2$ across the brain and found convergent α and β values to result in only slightly different (i.e., statistically similar) M and oxygen extraction estimates compared to those generated using nominal α and β values. Likewise, using a paradigm similar to that of the current experiment, Pasley et al. (2007) conducted an error analysis using $\alpha = -1.0$ to 0.4; concluding that their results were not dependent on precise parameter values, they elected to utilize $\alpha = 0.38$ for their calculations. These two strong examples from the literature are consistent with our own observations and suggest that our results are robust.

Considering Gauthier and Hoge's (2012) maps of M, OEFs, and $CMRO_2$ across the brain, it is possible that α and β values vary across brain regions and/or tasks (but, see Chen and Pike, 2009, 2010, regarding statistical equivalence between brain regions). In a hypercapnia/hypocapnia experiment, Chen and Pike (2010) found α to be equivalent to 0.18 ($\pm$0.02); however, when implementing a high intensity, high-contrast visual stimulation condition much like that of the parafoveal stimulation condition in the current experiment, Chen and Pike (2009) found $\alpha = 0.31$ ($\pm$0.10), which subsumes the α value of 0.38 used in the current experiment. Further, Kida et al. (2007) found α to increase along with duration of forepaw stimulation. Because of our block design and thus long-duration stimulation conditions, larger as opposed to smaller α values would be warranted in the present study. But Kida et al. (2007) also found different values of α over different CBF phases within the stimulation timeframe, complicating the matter. Unfortunately, the determination of the correct value of α is not a settled science. Continued research on this topic is certainly needed to elucidate the influence of α and β estimates upon mixed results observed in the literature. In summary, given the range of estimates available in the literature, our choice of calculation parameters was informed in two ways. First, it was informed by those conditions in the above-cited studies most analogous to our own (i.e., long-duration, high-contrast stimuli). Second, it was informed by those studies upon which our methods were most directly based, and to which we hoped to most directly compare our results (i.e., Pasley et al., 2007; Restom et al., 2007; Ances et al., 2009; Mohtasib et al., 2012).

Cross-cortex variability (Rypma and D'Esposito, 2001; Rypma et al., 2006; Rypma and Prabhakaran, 2009) has important implications for neurocognitive aging hypotheses based on BOLD signal because it suggests that regional BOLD age-differences, or equivalences, cannot be unambiguously interpreted in terms of neural activity. Further, we found age-related performance reductions (greater RT and reduced proportion correct) to be significantly associated with reduced $\Delta CBF/\Delta CMRO_2$ within visual cortex, suggesting that alterations to $\Delta CBF/\Delta CMRO_2$ affected the processes by which the visual stimuli were perceived.

The present results have both practical and theoretical implications. From a practical standpoint, our results implicate a specific mechanism by which age-related changes in the BOLD response to neural activity arise. That is, age-related alterations in $\Delta CMRO_2$, reflecting alterations in neural activity, are not accompanied by an adequate CVR (cf. Ances et al., 2009; Lu et al., 2011; Gauthier et al., 2012). Both $\Delta CMRO_2$ and ΔCBF, and their ratio to one another, can be affected differentially across cortex and tasks. Thus BOLD responses might be indexing different underlying physiological changes in young and old across the cortex. Specifically, decreased $\Delta CBF/\Delta CMRO_2$ coupling ratios in the older population result in less responsiveness in BOLD signal in either direction (i.e., increased and decreased $CMRO_2$) compared to the younger population. This response leads to greater BOLD signal for the older group compared to the younger group in relatively lower $CMRO_2$ ranges but lower BOLD signal for old compared to young in relatively higher $CMRO_2$ ranges.

Neurocognitive aging research seeks to understand the neural basis of age-related performance changes using BOLD signal as a proxy for neural activity. The BOLD response, although relatively easy to acquire, and heavily reported in the aging literature, is not so easy to interpret. Our results showed age-related $\Delta CMRO_2$ increases in two different brain regions. In one region (primary visual cortex), BOLD signal was reduced in the older compared to the younger group. In the other region (motor cortex), BOLD signal was equivalent between the two groups. Together these results suggest that regional BOLD age-differences, or age-equivalence, cannot be unambiguously interpreted in terms of neural activity. Thus, our results suggest that techniques such as the dual-echo ASL method applied here, that allow for the calculation of $\Delta CMRO_2$, are necessary, as $\Delta CMRO_2$ is more readily interpretable as an index of neural activity compared to the BOLD response which appears to reflect a complex of neural, vascular, and probably glial factors.

From a theoretical standpoint, the associations we observed between age-related performance reductions and reductions in the $\Delta CBF/\Delta CMRO_2$ ratio support the hypothesis that increased oxygen demand in the aging neural apparatus, not accommodated by vascular activity, is the basis for reduced functional efficiency at

the neural level and reduced processing efficiency at the cognitive level. Our hypothesis receives support from observations of age-related variability increases in $\Delta CBF/\Delta CMRO_2$ (cf. **Figure 2**). Reduced BOLD signal variability in old compared to young has been documented in recent literature (e.g., Garrett et al., 2010, 2011). Consistent with our observations, Garrett et al. have suggested that this pattern might reflect inefficient processing due to reductions in the integrity of the aging neural system (Garrett et al., 2011; cf. MacDonald et al., 2009) or inflexibility in that system (Hong and Rebec, 2012).

Reductions in vascular responsiveness would have consequences for the oxygen available to neurons. Reduced oxygen availability has been associated with increased $\Delta CMRO_2$ such as that observed in the older adults in the present study. Infra-human positron-emission tomography (PET) studies show increased neural metabolism in limited oxygen conditions (e.g., Harik et al., 1995; Richards et al., 2007). Similar oxygen-metabolism relationships have been observed in humans (e.g., Rockswold et al., 2010; Smith et al., 2011; Xu et al., 2012). In one study, Xu et al. (2012) scanned young adults while they breathed room air (21% fraction of inspired O_2; FiO_2) or one of three gas mixtures that varied in O_2 content (14% O_2, hypoxic condition; 50 or 98% O_2, hyperoxic conditions). The results indicated that decreases in O_2 availability led to increases in $\Delta CMRO_2$, possibly owing to increased glycolytic and cytochrome oxidative activity in O_2-depleted cells (e.g., Hamberger and Hyden, 1963). Thus Xu et al.'s (2012) results support the hypothesis that increased $\Delta CMRO_2$ in older neurons results from the decreased O_2 availability afforded by reduced vascular responsiveness. The present experiment suggests that this mechanism forms the neural basis for the reduced processing efficiency that leads to slower and less accurate performance in older adults compared to younger adults, affecting among other things, their speed of response to changing hues in a central fixation cross. More research is certainly required to test the hypothesis that reduced oxygen availability to neurons in primary visual cortex leads to the broad-spread age-related declines that are observed in perceptual and visual-search tasks.

In summary, dual-echo ASL technology permitted acquisition of both ΔCBF and BOLD data in response to visuomotor stimulation. We observed that $\Delta CBF/\Delta CMRO_2$ and BOLD varied across visual and motor cortices, and that BOLD did not accurately index neural activity in either region. A simulation illustrated how $\Delta CBF/\Delta CMRO_2$ can alter relationships between neural activity and BOLD signal. These results suggest (1) that the calculation of $\Delta CMRO_2$ is necessary for accurate young-old comparisons of neural activity and (2) that the neural basis of processing efficiency declines observed in older adults' visual task performance might be related to reductions in the oxygen available to neurons via aging vasculature.

ACKNOWLEDGMENTS

This work was supported by the National Institutes of Health (1R01AG029523 to Bart Rypma and R01NS067015 to Hanzhang Lu). The authors wish to thank Andrew Hillis, Lee Jordan, Mary Jo Maciejewski, Traci Sandoval, Rani Varghese, Feng Xu, and Uma Yezhuvath for their assistance with various aspects of data collection and processing, and Nicholas Hubbard for offering suggestions on a previous manuscript draft.

REFERENCES

Ahmad, A., and Spear, P. D. (1993). Effects of aging on the size, density, and number of rhesus monkey lateral geniculate neurons. *J. Comp. Neurol.* 334, 631–643.

Ances, B. M., Leontiev, O., Perthen, J. E., Liang, C., Lansing, A. E., and Buxton, R. B. (2008). Regional differences in the coupling of cerebral blood flow and oxygen metabolism changes in response to activation: implications for BOLD-fMRI. *Neuroimage* 39, 5010–5021.

Ances, B. M., Liang, C. L., Leontiev, O., Perthen, J. E., Fleisher, A. S., Lansing, A. E., et al. (2009). Effects of aging on cerebral blood flow, oxygen metabolism, and blood oxygenation level dependent responses to visual stimulation. *Hum. Brain Mapp.* 30, 1120–1132.

Aslan, S., Xu, F., Wang, P. L., Uh, J., Yezhuvath, U. S., van Osch, M., et al. (2010). Estimation of labeling efficiency in pseudo continuous arterial spin labeling. *Magn. Reson. Med.* 63, 765–771.

Aydin, S., Strang, N. C., and Manahilov, V. (2013). Age-related deficits in attentional control of perceptual rivalry. *Vision Res.* 77, 32–40.

Benjamini, Y., and Hochberg, Y. (2000). On the adaptive control of the false discovery rate in multiple testing with independent statistics. *J. Educ. Behav. Stat.* 25, 60–83.

Bennett, I. J., Motes, M. A., Rao, N. K., and Rypma, B. (2012). White matter tract integrity predicts visual search performance in young and older adults. *Neurobiol. Aging* 33, 433.e21–433.e31.

Brant-Zawadzki, M., Gillan, G. D., and Nitz, W. R. (1992). MP RAGE: a three dimensional, T1-weighted, gradient-echo sequence – initial experience in the brain. *Radiology* 182, 769–775.

Brodmann, K. (1909/2006). *Brodmann's Localization in the Cerebral Cortex: The Principles of Comparative Localization in the Cerebral Cortex Based on Cytoarchitectonics*, trans. L. J. Garey. New York: Springer.

Brown, G. G., Perthen, J. E., Liu, T. T., and Buxton, R. B. (2007). A primer on functional magnetic resonance imaging. *Neuropsychol. Rev.* 17, 107–125.

Buckner, R. L., Snyder, A. Z., Sanders, A. L., Raichle, M. E., and Morris, J. C. (2000). Functional brain imaging of young, nondemented, and demented older adults. *J. Cogn. Neurosci.* 12, 24–34.

Buxton, R. B., Uludag, K., Dubowitz, D. J., and Liu, T. T. (2004). Modeling the hemodynamic response to brain activation. *Neuroimage* 23, S220–S233.

Cauli, B., and Hamel, E. (2010). Revisiting the role of neurons in neurovascular coupling. *Front. Neuroenergetics* 2:9. doi:10.3389/fnene.2010.00009

Chen, J. J., and Pike, G. B. (2009). BOLD-specific cerebral blood volume and blood flow changes during neuronal activation in humans. *NMR Biomed.* 22, 1054–1062.

Chen, J. J., and Pike, G. B. (2010). MRI measurement of the BOLD-specific flow-volume relationship during hypercapnia and hypocapnia in humans. *Neuroimage* 53, 383–391.

Chen, J. J., Rosas, H. D., and Salat, D. H. (2011). Age-associated reductions in cerebral blood flow are independent from regional atrophy. *Neuroimage* 55, 468–478.

Chiarelli, P. A., Bulte, D. P., Piechnik, S., and Jezzard, P. (2007a). Sources of systematic bias in hypercapnia-calibrated functional MRI estimation of oxygen metabolism. *Neuroimage* 34, 35–43.

Chiarelli, P. A., Bulte, D. P., Wise, R., Gallachan, D., and Jezzard, P. (2007b). A calibration method for quantitative BOLD fMRI based on hyperoxia. *Neuroimage* 37, 808–820.

Cox, R. W. (1996). AFNI: software for analysis and visualization of functional magnetic resonance neuroimages. *Comput. Biomed. Res.* 29, 162–173.

Davis, T. L., Kwong, K. K., Weisskoff, R. M., and Rosen, B. R. (1998). Calibrated functional MRI: mapping the dynamics of oxidative metabolism. *Proc. Natl. Acad. Sci. U.S.A.* 95, 1834–1839.

de Jager, C. A., Hogervorst, E., Combrinck, M., and Budge, M. M. (2003). Sensitivity and specificity of neuropsychological tests for mild cognitive impairment and Alzheimer's disease. *Psychol. Med.* 33, 1039–1050.

D'Esposito, M., Deouell, L. Y., and Gazzaley, A. (2003). Alterations in the BOLD fMRI signal with ageing and disease: a challenge for neuroimaging. *Nat. Rev. Neurosci.* 4, 863–872.

D'Esposito, M., Zarahn, E., Aguirre, G. K., and Rypma, B. (1999). The effect of normal aging on the coupling of neural activity to the BOLD hemodynamic response. *Neuroimage* 10, 6–14.

Elliott, S. L., Werner, J. S., and Webster, M. A. (2012). Individual and age-related variation in chromatic contrast adaptation. *J. Vis.* 12, 11.

Folstein, M. F., Folstein, S. E., and McHugh, P. R. (1975). "Mini-Mental State": a practical method for grading the cognitive state of patients for the clinician. *J. Psychiatr. Res.* 12, 189–198.

Garcia, D. M., de Bazelaire, C., and Alsop, D. (2005). Pseudo-continuous flow driven adiabatic inversion for arterial spin labeling. *Proc. Int. Soc. Magn. Reson. Med.* 13, 37.

Garrett, D. D., Kovacevic, N., McIntosh, A. R., and Grady, C. L. (2010). Blood oxygen level-dependent signal variability is more than just noise. *J. Neurosci.* 30, 4914–4921.

Garrett, D. D., Kovacevic, N., McIntosh, A. R., and Grady, C. L. (2011). The importance of being variable. *J. Neurosci.* 31, 4496–4503.

Gauthier, C. J., and Hoge, R. D. (2012). Magnetic resonance imaging of resting OEF and $CMRO_2$ using a generalized calibration model for hypercapnia and hyperoxia. *Neuroimage* 60, 1212–1225.

Gauthier, C. J., and Hoge, R. D. (2013). A generalized procedure for calibrated fMRI incorporating hyperoxia and hypercapnia. *Hum. Brain Mapp.* 34, 1053–1069.

Gauthier, C. J., Madjar, C., Desjardins-Crépeau, L., Bellec, P., Bherer, L., and Hoge, R. D. (2012). Age dependence of hemodynamic response characteristics in human fMRI. *Neurobiol. Aging* (in press).

Gössl, C., Fahrmeir, L., and Auer, D. P. (2001). Bayesian modeling of the hemodynamic response function in BOLD fMRI. *Neuroimage* 14, 140–148.

Grady, C. L. (1996). Age-related changes in cortical blood flow activation during perception and memory. *Ann. N. Y. Acad. Sci.* 777, 14–21.

Grady, C. L. (2002). Age-related differences in face processing: a meta-analysis of three functional neuroimaging experiments. *Can. J. Exp. Psychol.* 56, 208–220.

Grady, C. L., Maisog, J. M., Horowitz, B., Ungerleider, L. G., Mentis, M. J., Salerno, J. A., et al. (1994). Age-related changes in cortical blood flow activation during visual processing of faces and location. *J. Neurosci.* 14, 1450–1462.

Grubb, R. L., Raichle, M. E., Eichling, J. O., and Ter-Pogossian, M. M. (1974). The effects of changes in $PaCO_2$ on cerebral blood volume blood flow and vascular mean transit time. *Stroke* 5, 630–639.

Gupta, A. K., Harrar, S. W., and Fujikoshi, Y. (2006). Asymptotics for testing hypothesis in some multivariate components model under non-normality. *J. Multivar. Anal.* 97, 148–178.

Hamberger, A., and Hyden, H. (1963). Inverse enzymatic changes in neurons and glia during increased function and hypoxia. *J. Cell Biol.* 16, 521–525.

Harik, S. I., Lust, W. D., Jones, S. C., Lauro, K. L., Pundik, S., and LaManna, J. C. (1995). Brain glucose metabolism in hypobaric hypoxia. *J. Appl. Physiol.* 79, 136–140.

Haug, H., Kuhl, S., Mecke, E., Sass, N. L., and Wasner, K. (1984). The significance of morphometric procedures in the investigation of age changes in cytoarchitectonic structures of human brain. *J. Himforsch.* 25, 353–374.

Hedden, T., and Gabrieli, J. D. E. (2004). Insights into the ageing mind: a view from cognitive neuroscience. *Nat. Rev. Neurosci.* 5, 87–96.

Heo, S., Prakash, R. S., Voss, M. W., Erickson, K. I., Ouyang, C., Sutton, B. P., et al. (2010). Resting hippocampal blood flow, spatial memory and aging. *Brain Res.* 1315, 119–127.

Hoge, R. D. (2012). Calibrated fMRI. *Neuroimage* 62, 930–937.

Hoge, R. D., Atkinson, J., Gill, B., Crelier, G. R., Marrett, S., and Pike, G. B. (1999a). Investigation of BOLD signal dependence on cerebral blood flow and oxygen consumption: the deoxyhemoglobin dilution model. *Magn. Reson. Med.* 42, 849–863.

Hoge, R. D., Atkinson, J., Gill, B., Crelier, G. R., Marrett, S., and Pike, G. B. (1999b). Linear coupling between cerebral blood flow and oxygen consumption in activated human cortex. *Proc. Natl. Acad. Sci. U.S.A.* 96, 9403–9408.

Hommel, B., Li, K. Z., and Li, S. C. (2004). Visual search across the life span. *Dev. Psychol.* 40, 545–558.

Hong, S. L., and Rebec, G. V. (2012). Biological sources of inflexibility in brain and behavior with aging and neurodegenerative diseases. *Front. Syst. Neurosci.* 6:77. doi:10.3389/fnsys.2012.00077

Huettel, S. A., Singerman, J. D., and McCarthy, G. (2001). The effects of aging upon the hemodynamic response measured by functional MRI. *Neuroimage* 13, 161–175.

Hutchison, J. L., Lu, H., and Rypma, B. (2012). Neural mechanisms of age-related slowing: the $\Delta CBF/\Delta CMRO_2$ ratio mediates age differences in BOLD signal and human performance. *Cereb. Cortex*. doi:10.1093/cercor/bhs233

Hyder, F. (2004). Neuroimaging with calibrated fMRI. *Stroke* 35(Suppl. 1), 2635–2641.

Hyder, F., Renken, R., Kennan, R. P., and Rothman, D. L. (2000). Quantitative multi-modal functional MRI with blood oxygenation level dependent exponential decays adjusted for flow attenuated inversion recovery (BOLDED AFFAIR). *Magn. Reson. Imaging* 18, 227–235.

Iadecola, C. (2004). Neurovascular regulation in the normal brain and in Alzheimer's disease. *Nat. Rev. Neurosci.* 5, 347–360.

Keppel, G., and Wickens, T. D. (2004). *Design and Analysis: A Researcher's Handbook*, 4th Edn (Upper Saddle River, NJ: Pearson Prentice Hall), 111–130.

Kida, I., Kennan, R. P., Rothman, D. L., Behar, K. L., and Hyder, F. (2000). High resolution $CMRO_2$ mapping in rat cortex: a multiparametric approach to calibration of BOLD image contrast at 7 Tesla. *J. Cereb. Blood Flow Metab.* 20, 847–860.

Kida, I., Rothman, D. L., and Hyder, F. (2007). Dynamics of changes in blood flow, volume, and oxygenation: implications for dynamic functional magnetic resonance imaging calibration. *J. Cereb. Blood Flow Metab.* 27, 690–696.

Leenders, K. L., Perani, D., Lammertsma, A. A., Heather, J. D., Buckingham, P., Healy, M. J. R., et al. (1990). Cerebral blood flow, blood volume, and oxygen utilization: normal values and effect of age. *Brain* 113, 27–47.

Leontiev, O., and Buxton, R. B. (2007). Reproducibility of BOLD perfusion and $CMRO_2$ measurements with calibrated-BOLD fMRI. *Neuroimage* 35, 175–184.

Leontiev, O., Dubowitz, D. J., and Buxton, R. B. (2007). $CBF/CMRO_2$ coupling measured with calibrated-BOLD fMRI: sources of bias. *Neuroimage* 36, 1110–1122.

Lu, H., Golay, X., Pekar, J. J., and Van Zijl, P. C. (2004). Sustained poststimulus elevation in cerebral oxygen utilization after vascular recovery. *J. Cereb. Blood Flow Metab.* 24, 764–770.

Lu, H., and van Zijl, P. C. M. (2005). Experimental measurement of parenchymal BOLD effects and tissue oxygen extraction fractions using multiecho vassal fMRI at 1.5 and 3.0 T. *Magn. Reson. Med.* 53, 808–816.

Lu, H., Xu, F., Rodrigue, K. M., Kennedy, K. M., Cheng, Y., Flicker, B., et al. (2011). Alterations in cerebral metabolic rate and blood supply across the adult lifespan. *Cereb. Cortex* 21, 1426–1434.

MacDonald, S. W., Li, S. C., and Backman, L. (2009). Neural underpinnings of within-person variability in cognitive functioning. *Psychol. Aging* 24, 792–808.

Michaels, D. D. (1993). "Ocular disease in the elderly," in *Vision and Aging*, eds A. A. Rosenbloom and M. W. Morgan (Boston, MA: Butterworth-Heineman), 111–159.

Mintun, M. A., Lundstrom, B. N., Snyder, A. Z., Vlassenko, A. G., Shulman, G. L., and Raichle, M. E. (2001). Blood flow and oxygen delivery to human brain during functional activity: theoretical modeling and experimental data. *Proc. Natl. Acad. Sci. U.S.A.* 98, 6859–6864.

Moeller, J. R., Ishikawa, T., Dhawan, V., Spetsieris, P., Mandel, F., Alexander, G. E., et al. (1996). The metabolic topography of normal aging. *J. Cereb. Blood Flow Metab.* 16, 385–398.

Mohtasib, R. S., Lumley, G., Goodwin, J. A., Emsley, H. C. A., Slumig, V., and Parkes, L. M. (2012). Calibrated fMRI during a cognitive Stroop task reveals reduced metabolic response with increasing age. *Neuroimage* 59, 1143–1151.

Motes, M. A., Biswal, B. B., and Rypma, B. (2010). Age-dependent relationships between prefrontal cortex activation and processing efficiency. *Cogn. Neurosci.* 2, 1–10.

Nyberg, L., and Bäckman, L. (2011). "Memory changes and the aging brain: a multimodal imaging approach," in *Handbook of the Psychology of Aging*, eds K. W. Schaie and S. L. Willis (San Diego, CA: Academic Press), 121–132.

Ogawa, S., and Lee, T. M. (1990). Magnetic resonance imaging of blood vessels at high fields: in vivo and in vitro measurements and image simulation. *Magn. Reson. Med.* 16, 9–18.

Ogawa, S., Tank, D. W., Menon, R., Ellermann, J. M., Kim, S.-G., Merkle, H., et al. (1992). Intrinsic signal changes accompanying sensory stimulation: functional brain

mapping with magnetic resonance imaging. *Proc. Natl. Acad. Sci. U.S.A.* 89, 5951–5955.

Owsley, C., and Sloane, M. E. (1987). Contrast sensitivity, acuity, and the perception of 'real-world' targets. *Br. J. Ophthamol.* 71, 791–796.

Pasley, B. N., Inglis, B. A., and Freeman, R. D. (2007). Analysis of oxygen metabolism implies a neural origin for the negative BOLD response in human visual cortex. *Neuroimage* 36, 269–276.

Plude, D. J., and Doussart-Roosevelt, J. A. (1989). Aging, selective attention, and feature integration. *Psychol. Aging* 4, 98–105.

Poline, J.-B., Strother, S. C., Dehaene-Lamberta, G., Egan, G. F., and Lancaster, J. L. (2006). Motivation and synthesis of the FIAC experiment: reproducibility of fMRI results across expert analyses. *Hum. Brain Mapp.* 27, 351–359.

Rajah, M. N., and D'Esposito, M. (2005). Region-specific changes in prefrontal function with age: a review of PET and fMRI studies on working and episodic memory. *Brain* 128, 1964–1983.

Restom, K., Bangen, K. J., Bondi, M. W., Perthen, J. E., and Liu, T. T. (2007). Cerebral blood flow and BOLD responses to a memory encoding task: a comparison between healthy young and elderly adults. *Neuroimage* 37, 430–439.

Richards, E. M., Fiskum, G., Rosenthal, R. E., Hopkins, I., and McKenna, M. C. (2007). Hyperoxic reperfusion after global ischemia decreases hippocampal energy metabolism. *Stroke* 38, 1578–1584.

Rockswold, S. B., Rockswold, G. L., Zaun, D. A., Zhang, X., Cerra, C. E., Bergman, T. A., et al. (2010). A prospective, randomized clinical trial to compare the effect of hyperbaric to normobaric hyperoxia on cerebral metabolism, intracranial pressure, and oxygen toxicity in severe traumatic brain injury. *J. Neurosurg.* 112, 1080–1094.

Ross, M. H., Yurgelun-Todd, D. A., Renshaw, P. F., Maas, L. C., Mendelson, J. H., Mello, N. K., et al. (1997). Age-related reduction in functional MRI response to photic stimulation. *Neurology* 48, 173–176.

Rypma, B., Berger, J. S., Genova, H. M., Rebbechi, D., and D'Esposito, M. (2005). Dissociating age-related changes in cognitive strategy and neural efficiency using event-related fMRI. *Cortex* 41, 582–594.

Rypma, B., Berger, J. S., Prabhakaran, V., Bly, B. M., Kimberg, D. Y., Biswal, B. B., et al. (2006). Neural correlates of cognitive efficiency. *Neuroimage* 33, 969–979.

Rypma, B., and D'Esposito, M. (2000). Isolating the neural mechanisms of age-related changes in human working memory. *Nat. Neurosci.* 3, 509–515.

Rypma, B., and D'Esposito, M. (2001). Age-related changes in brain-behavior relationships: evidence from event-related functional MRI studies. *Eur. J. Cogn. Psychol.* 13, 235–256.

Rypma, B., and Prabhakaran, V. (2009). When less is more and when more is more: the mediating roles of capacity and speed in brain-behavior efficiency. *Intelligence* 37, 207–222.

Scialfa, C. T., Cordazzo, S., Bubric, K., and Lyon, J. (2012). Aging and visual crowding. *J. Gerontol. B Psychol. Sci. Soc. Sci.* doi:10.1093/geronb/gbs086

Shulman, R. G., Rothman, D. L., and Hyder, F. (2007). A BOLD search for baseline. *Neuroimage* 36, 277–281.

Smith, Z. M., Hunt, J. S., Li, E., Guo, J., Shin, D. D., Buxton, R. B., et al. (2011). "Elevated CO_2 mitigates the rise in $CMRO_2$ during acute hypoxia and improves cerebral tissue oxygenation," in *Proceeding of the International Society for Magnetic Resonance in Medicine*. Montreal.

Spear, P. D., Moore, R. J., Kim, C. B., Xue, J. T., and Tumosa, N. (1994). Effects of aging on the primate visual system: spatial and temporal processing by lateral geniculate neurons in young adult and old rhesus monkeys. *J. Neurophysiol.* 72, 402–420.

Speranza, F., Moraglia, G., and Schneider, B. A. (2001). Binocular detection of masked patterns in young and old observers. *Psychol. Aging* 16, 281–292.

Stefanovic, B., Warnking, J. M., and Pike, G. B. (2004). Hemodynamic and metabolic responses to neuronal inhibition. *Neuroimage* 22, 771–778.

Taoka, T., Iwasaki, S., Uchida, H., Fukusumi, A., Nakagawa, H., Kichikawa, K., et al. (1998). Age correlation of the time lag in signal change on EPI-fMRI. *J. Comput. Assist. Tomogr.* 22, 514–517.

Tuunanen, P. I., and Kauppinen, R. A. (2006). Effects of oxygen saturation on BOLD and arterial spin labelling perfusion fMRI signals studied in a motor activation task. *Neuroimage* 30, 102–109.

Tuunanen, P. I., Murray, I. J., Parry, N. R. A., and Kauppinen, R. A. (2006). Heterogeneous oxygen extraction in the visual cortex during activation in mild hypoxic hypoxia revealed by quantitative functional magnetic resonance imaging. *J. Cereb. Blood Flow Metab.* 26, 263–273.

Vafaee, M. S., and Gjedde, A. (2000). Model of blood-brain transfer of oxygen explains nonlinear flow-metabolism coupling during stimulation of visual cortex. *J. Cereb. Blood Flow Metab.* 20, 747–754.

Vafaee, M. S., and Gjedde, A. (2004). Spatially dissociated flow-metabolism coupling in brain activation. *Neuroimage* 21, 507–515.

Van Essen, D. C., Drury, H. A., Dickson, J., Harwell, J., Hanlon, D., and Anderson, C. H. (2001). An integrated software suite for surface-based analyses of cerebral cortex. *J. Am. Med. Inform. Assoc.* 8, 443–459.

Vincent, S. L., Peters, A., and Tigges, J. (1989). Effects of aging on the neurons within area 17 of rhesus monkey cerebral cortex. *Anat. Rec.* 223, 329–341.

Welford, A. T. (1981). Signal noise performance and age. *Hum. Factors* 23, 97–109.

Weymouth, A. E., and McKendrick, A. M. (2012). Shape perception is altered by normal aging. *Invest. Ophthamol. Vis. Sci.* 53, 3226–3233.

Wong, E. C., Luh, W.-M., and Liu, T. T. (2000). Turbo ASL: arterial spin labeling with higher SNR and temporal resolution. *Magn. Reson. Med.* 44, 511–515.

Xu, F., Liu, P., Pascual, J. M., Xiao, G., and Lu, H. (2012). Effect of hypoxia and hyperoxia on cerebral blood flow, blood oxygenation, and oxidative metabolism. *J. Cereb. Blood Flow Metab.* 32, 1909–1918.

Conflict of Interest Statement: The authors declare that the research was conducted in the absence of any commercial or financial relationships that could be construed as a potential conflict of interest.

Received: 01 January 2013; accepted: 14 April 2013; published online: 03 May 2013.

Citation: Hutchison JL, Shokri-Kojori E, Lu H and Rypma B (2013) A BOLD perspective on age-related neurometabolic-flow coupling and neural efficiency changes in human visual cortex. Front. Psychol. ***4****:244. doi: 10.3389/fpsyg.2013.00244*

This article was submitted to Frontiers in Perception Science, a specialty of Frontiers in Psychology.

frontiers in PSYCHOLOGY

ORIGINAL RESEARCH ARTICLE
published: 24 July 2013
doi: 10.3389/fpsyg.2013.00467

Neural correlates of saccadic inhibition in healthy elderly and patients with amnestic mild cognitive impairment

*K. K. Alichniewicz[1], F. Brunner[1], H. H. Klünemann[2] and M. W. Greenlee[1]**

[1] Institute of Experimental Psychology, University of Regensburg, Regensburg, Germany
[2] Departments of Psychiatry, Psychosomatics, and Psychotherapy, University of Regensburg, Regensburg, Germany

Edited by:
Allison B. Sekuler, McMaster University, Canada

Reviewed by:
Joseph F. X. DeSouza, York University, Canada
Frans W. Cornelissen, University Medical Center Groningen, Netherlands

****Correspondence:***
M. W. Greenlee, Institute of Experimental Psychology, University of Regensburg, Universitätsstraße 31, 93053 Regensburg, Germany
e-mail: mark.greenlee@psychologie.uni-regensburg.de

Performance on tasks that require saccadic inhibition declines with age and altered inhibitory functioning has also been reported in patients with Alzheimer's disease. Although mild cognitive impairment (MCI) is assumed to be a high-risk factor for conversion to AD, little is known about changes in saccadic inhibition and its neural correlates in this condition. Our study determined whether the neural activation associated with saccadic inhibition is altered in persons with amnestic mild cognitive impairment (aMCI). Functional magnetic resonance imaging (fMRI) revealed decreased activation in parietal lobe in healthy elderly persons compared to young persons and decreased activation in frontal eye fields in aMCI patients compared to healthy elderly persons during the execution of anti-saccades. These results illustrate that the decline in inhibitory functions is associated with impaired frontal activation in aMCI. This alteration in function might reflect early manifestations of AD and provide new insights in the neural activation changes that occur in pathological ageing.

Keywords: mild cognitive impairment, Alzheimer's disease (AD), ageing, inhibition functions, anti-saccades, fMRI

INTRODUCTION

Ageing is associated with a decline in cognitive functioning along with structural and functional changes in the brain. A large body of behavioral research on the effect of ageing on human cognition has found that age-related deteriorations are observed across a range of cognitive domains including processing speed, working memory and inhibition (Moscovitch and Winocur, 1992; Braver and Barch, 2002; Anderson et al., 2012; Heilbronner and Münte, 2013). The process of ageing, however, does not inevitably lead to cognitive decline and the extent of the cognitive decline varies in different individuals across various tasks (Rapp and Amaral, 1992; McDowd, 1997; Friedman et al., 2008; Park and Reuter-Lorenz, 2009). Thus, more research is required to understand neurocognitive changes related to human ageing. A major challenge for ageing researchers is to acquire a better distinction between normal and pathological changes with age.

A transitional state between normal and pathologic ageing that is associated with an increased risk of progression to AD is defined as mild cognitive impairment (MCI) (Petersen, 2004). Based on the results of numerous studies on pathological ageing, it is clear that there is no single framework that describes the neuropathology of MCI (Stephan et al., 2012a,b). The complexity and heterogeneity of this condition is reflected in the considerable variability in the definition, characterization and application of the MCI diagnosis in the clinical practice (for the review see: Stephan et al., 2012a). It is widely accepted, however, that there are many subtypes of MCI. According to Petersen (2004), amnestic (aMCI) or non-amnestic MCI (naMCI) should be differentiated from each other. This classification depends on whether memory decline is exhibited in MCI patients. Individuals with intact memory abilities are diagnosed with naMCI as opposed to the individuals with memory impairment diagnosed as aMCI (Petersen, 2003, 2007). It has been suggested that the various MCI subtypes have different etiologies and outcomes (Sachdev et al., 2012). Therefore, individuals diagnosed with aMCI are thought to be more likely to progress to AD (Hunderfund et al., 2006; Petersen and Jack, 2009). In addition to episodic and semantic memory deficits in aMCI patients (Fox et al., 1998; Petersen, 2004; Chertkow et al., 2008), several recent studies suggest that deterioration of executive functions is associated with the conversion to AD (Greenwood, 2000; Rozzini et al., 2007; Iachini et al., 2009; Alichniewicz et al., 2012). Furthermore, there is some evidence that individuals demonstrate deficits in executive functions 2–3 years before diagnosis of AD (Johnson et al., 2009).

Studies on changes in cognition with age showed that while excitatory aspects of attention (like directed visual attention) are preserved in elderly persons, inhibitory processes decline with age (Hasher and Zacks, 1988; Sweeney et al., 2001; Crawford et al., 2005; Peltsch et al., 2011). Age-related inhibitory impairment, however, is restricted to specific inhibitory functions associated with prepotent response inhibition (Butler et al., 1999; Friedman and Miyake, 2004; Mirsky et al., 2011). According to Friedman and Miyake (2004), inhibition of prepotent responses is an ability to deliberately suppress an automatic and dominant action or to ignore no longer relevant contents when necessary. The inhibition of prepotent responses reveals resistance to preseverate and to exhibit controlled and intended reaction (Miyake et al., 2000). As postulated by Miyake et al. (2000), the tasks used to assess this function are the Stroop task (Stroop, 1935), the antisaccade task (Hallett, 1978), and the stop-signal task (Logan, 1994) as

they all require the participants to intentionally stop an automatic response. Recent studies showed that performance on oculomotor tasks declines with age (Sweeney et al., 2001; Raemaekers et al., 2006; Peltsch et al., 2011). Elderly adults demonstrate reduced ability to voluntary inhibit saccadic response, as assessed by anti-saccade tasks, and exhibit significantly increased onset latencies of correct anti-saccades compared to young adults (Olincy et al., 1997; Butler et al., 1999; Nieuwenhuis et al., 2000; Crawford et al., 2005; Peltsch et al., 2011). In contrast, their performance on automatic saccadic initiation, as assessed by reflexive pro-saccadic tasks, does not deteriorate in healthy ageing. Older adults, however, need significantly more time to generate pro-saccades accurately (Sweeney et al., 2001; Peltsch et al., 2011).

Altered inhibitory functioning has also been reported in dementia of Alzheimer's type (Currie et al., 1991; Crawford et al., 2005; Mosimann et al., 2005). In a review, Amieva et al. (2004) suggests that the deterioration of inhibitory functions in Alzheimer's disease (AD) may not be a general deficit. In particular, patients with AD demonstrated impairments on tasks requiring controlled inhibitory processes, such as the Stroop task (Fisher et al., 1990; Amieva et al., 2002; Belleville et al., 2006) and the anti-saccade task (Fletcher and Sharpe, 1986; Kaufman et al., 2010, 2012), whilst there is no effect of AD on the performance on tasks requiring more automatic inhibition, such as inhibition of return (Langley and Madden, 2000). The inability of persons with AD to perform anti-saccades may be associated with substantial neural degeneration in the frontal cortex (Fletcher and Sharpe, 1986; Crawford et al., 2005; Kaufman et al., 2010). Furthermore, the literature shows that the anti-saccade task can also be used to distinguish between different types of dementia and other forms of degenerative disorders (Boxer et al., 2006; Garbutt et al., 2008; Lagun et al., 2011).

Despite the fact that there is clear evidence for inhibition deficits in AD, the extent of the deterioration of inhibition has rarely been studied in patients with MCI. Furthermore, there is some inconsistency in the literature with respect to the role of response inhibition in this disorder. While some authors point out that patients with aMCI demonstrate an impairment of inhibitory functions, as assessed by Stroop task (Kramer et al., 2006; Traykov et al., 2007; Bélanger et al., 2010), others argue that MCI has no effect on the performance on this task (Zhang et al., 2007). Moreover, patients with MCI show deterioration of the semantic inhibition of a prepotent response and impairment of inhibition functions may have predictive value with regard to a probable disease progression to AD (Bélanger and Belleville, 2009). On the neural level, increased activity in the dorsal anterior cingulate, bilateral middle and inferior frontal gyri, bilateral inferior parietal lobule, and the bilateral insula was evident in relation to the Stroop task reported in patients with MCI compared to young persons (Li et al., 2009). Crutcher et al. (2009) demonstrated that an oculomotor version of the visual paired-comparison task can be used for assessing normal and impaired recognition memory. Furthermore, Lagun et al. (2011) suggest that machine-learning techniques using the results of a visual paired-comparison task can be used to distinguish MCI from cognitive intact elderly persons. Therefore, there is some suggestions that eye movement functions are impaired in MCI.

To our knowledge, there is no study investigating the neural correlates of oculomotor functions in aMCI. The ability to voluntarily suppress an automatic response in favor of performing an alternative behavior is considered to be one of the crucial executive functions required in everyday life (Munoz and Everling, 2004). Since deterioration of this ability has been found in AD, we hypothesized that neural activation associated with oculomotor performance in anti-saccade tasks should be reduced in persons with aMCI, whereas neural activation for pro-saccades should be unaffected. Specifically, we hypothesize that patients with amnestic MCI will exhibit more errors on the anti-saccade task, while demonstrating reduced activation in saccade-controlling regions in prefrontal and parietal cortex.

METHODS

PARTICIPANTS

In order to investigate the effects of normal and pathological ageing on cognition and brain activation, three subject groups were assessed: aMCI patients [$n = 23$, mean age $= 60.3$ (9.3) years], healthy elderly controls [$n = 19$, mean age $= 58.8$ (7.4) years] and healthy young persons [$n = 13$, mean age $= 24.6$ (2.1) years]. Participants with MCI were recruited from the Memory Clinic of the Department of Psychiatry, Psychosomatics and Psychotherapy of the University of Regensburg or via advertising in print media seeking healthy adults over 50 years of age who would like to participate in an fMRI-study. In order to exclude possible presence of any other neurological, psychiatric, or systemic condition among both groups, which may lead to alterations in cognitive status, subjects underwent a two-stage screening process to identify those with probable MCI. The first stage consisted of a structured telephone interview assessing evidence of subjective and informant-corroborated reports of memory problems and the presence of any exclusion criteria, including: history of significant medical, neurological, or psychiatric condition, history of major risk factors for vascular disease, history of alcohol and nicotine abuse or sensory impairment (visual acuity), use of psychoactive medication and any aspect that would disqualify a person to enter the MRI scanner (e.g., cardiac pacemaker). The second stage of the screening procedure involved a standardized diagnostic assessment of the cognitive, neuropsychological, and psychological state of the participants. The healthy control group consisted of adults that were recruited from the community via the same ad in the local media. Healthy elderly adults underwent the same clinical and neuropsychological procedure as aMCI patients to ensure that they did not demonstrate any cognitive complaints and did not have any medical history of significance. Finally, young participants were recruited from the community and via word-of-mouth communication. They were examined in the same way as the other two groups of participants, with the exclusion of the test batteries for clinical diagnosis of MCI.

Persons with MCI met the revised criteria for amnestic MCI as proposed by Artero et al. (2006) that included: evidence of decline in memory and other cognitive functions that is, however, insufficient to meet the Diagnostic and Statistical Manual for Mental Disorders–Fourth Edition (DSM–IV) criteria for dementia of the Alzheimer type (American Psychiatric Association, 1994).

Neuropsychological assessment consisted of neuropsychological test battery contained in the Consortium to Establish a Registry for Alzheimer's Disease (CERAD+, German version; Memory Clinic Basel, 2005). The critical range of the CERAD was a z-score below −1.5 standard deviations (SD) but not less than −3 SD in at least one CERAD memory subtest for the MCI group and *z*-scores of at least above −1.5 SD in all CERAD subtests for the healthy control subjects. Memory subtests in CERAD+ critical for the diagnosis included: Wordlist Delayed Recall and Savings, TMT-A, Recall of Constructional Praxis, Constructional Praxis: Savings (see **Table 1**).

All participants were able to understand, and follow verbal instructions, and concentrate on the task for the duration of the experiment. They all were right-handed (according to the Handedness Inventory of Raczkowski et al., 1974), and had normal or corrected-to-normal vision using their own contact lenses or MR-safe refractive corrections provided by us.

STUDY DESIGN

Procedure

The procedures used in this study were approved by the Ethical Committee of the University of Regensburg. In accordance with the requirements of the Code of Ethical Principles for Medical Research Involving Human Subjects of the World Medical Association (Declaration of Helsinki), all participants provided written informed consent prior to the commencement of the study.

Pro-saccade and anti-saccade task

In order to investigate the effect of normal and pathological ageing on prepotent inhibition, the pro- and anti-saccades paradigm was employed. During each trial, a fixation cross (0°) appeared in the center of the computer display for a variable amount of time 5000, 5100, or 5200 ms (durations jittered with 100 ms increments). A target stimulus was presented on one of four different peripheral positions along the horizontal midline (±5 and 15°) for 200 ms. The location of the target was randomized and counterbalanced so that participants were unable to predict at which position the target would be presented next. The saccade target was presented at one of the possible locations for 200 ms. Then, a visual feedback appeared at the eccentric location of the pro-saccade target or anti-saccade location (a tiny green dot), visible only when the fovea was near the target location. The distractor locations were baited with a tiny red dot. On error trials, the red dot was visible to the participant, signaling that they executed a saccade to the wrong location. After this, the feedback dot was extinguished to be replaced immediately with the centrally located fixation dot, inducing a recentering saccade. Feedback was given on all trials in both training and fMRI sessions. After 1800 ms of central fixation, another trial began. Each task was performed 8 times during 5 blocks for pro- and

Table 1 | Description of demographic data and results of neuropsychological testing in amnestic mild cognitive impairment (aMCI) and healthy age-matched control groups.

Parameters	Healthy elderly	aMCI	*T* (*df* = 40)	*p*
DEMOGRAPHY				
N	19	23		
Age (years)	58.84 (7.41)	60.30 (9.31)	0.55	0.582
Gender (M/F)	8/11	5/18	2.02	0.192
Education (years)	14.74 (2.26)	13.09 (3.26)	−1.87	0.069
Mini-mental state exam	29.32 (0.82)	28.91 (1.13)	−1.30	0.201
CLINICAL CHARACTERISTICS[a]				
Verbal fluency	29.53 (6.15)	22.61 (5.70)	**−3.78**	**0.001**
Boston naming test	14.74 (0.45)	14.04 (1.11)	**−2.74**	**0.010**
Word list learning	22.58 (2.78)	18.70 (2.99)	**−4.33**	**0.000**
Word list recall	8.79 (1.08)	5.87 (1.71)	**−6.43**	**0.000**
Word list: savings	0.97 (0.09)	0.78 (0.22)	**−3.75**	**0.001**
Word list intrusions	0.16 (0.50)	0.65 (0.98)	**2.10**	**0.043**
Word list recognition	20.00 (0.00)	19.61 (0.66)	**−2.86**	**0.009**
Phonematic fluency	18.68 (3.43)	13.65 (5.01)	**−3.72**	**0.001**
TMT-A	30.67 (7.81)	45.39 (20.41)	**2.89**	**0.006**
TMT-B	69.33 (26.42)	84.83 (35.43)	1.55	0.130
Constructional praxis	10.95 (0.23)	10.74 (0.69)	−1.36	0.184
Recall of constructional praxis	10.58 (0.84)	8.48 (1.93)	**−4.72**	**0.000**
Constructional praxis: savings	0.96 (0.06)	0.79 (0.17)	**−4.50**	**0.000**

Statistical tests of possible group differences (T-values and p-values) are presented.

aMCI, amnestic mild cognitive impairment; denoted are mean values, standard deviations (in brackets), T-, degrees of freedom (df) and p-values.

[a] Clinical characteristics are mean raw-scores from subtests of the neuropsychological test battery contained in the Consortium to Establish a Registry for Alzheimer's Disease Plus (CERAD-Plus).

Significant values ($p < 0.05$) are marked in bold font.

anti-saccade tasks each, with a total number of 80 trials. On pro-saccade trials the central fixation dot turned green 500 ms prior to fixation offset, while on anti-saccade trials it turned red (see e.g., Connolly et al., 2002; Cornelissen et al., 2002). Also, a visual instruction ("look toward the target" vs. "look away from the target" ("Hinschauen" and "Wegschauen" in German, respectively) was presented for 5000 ms before each block of trials in each task. Participants were instructed to look toward the peripheral target as fast as they could during the "green" trials and to look as fast as possible to the mirror image location of the peripheral target during the "red" trials. During fixation epochs, participants were asked to keep their eyes on the central target. Approximately one week before the fMRI scan, all participants performed a pro-saccade and anti-saccade training experiment. We acquired 40 trials of pro-saccades and 40 trials of anti-saccades, in a similar blocked fashion as to be applied in the scanner, using the video eyetracker. Additionally, all participants were shown 8 trials of each task prior to the fMRI scan on the day of examination to refresh their memory on the task specifics. Feedback was also presented during these training trials.

Stimulus presentation and eye-tracking

For stimuli presentation we used Presentation 9.9 (Neurobehavioral Systems Inc., Albany, California, USA) on a standard PC, equipped with a standard graphics card and back projected via an LCD video projector (JVC, DLA-G20, Yokohama, Japan) onto a translucent circular screen (approximately 30 degrees visual angle in diameter), placed inside the scanner bore at 62 cm from the observer. The projector was running at 72 Hz with a resolution of 800×600 and a color resolution of 3×8 bit (RBG). During training outside the MR-scanner we used High Speed Video Eye-Tracker Toolbox™ (Cambridge, http://www.crsltd.com/catalog/eyetracker-250/index.html), where the participant was seated upright with their chin resting on a chinrest. During the fMRI scan, subjects viewed the stimuli through a mirror located above their eyes. Eye movements were recorded using the MR-Eyetracker (Cambridge Research Systems, Ltd), a fiberoptic limbus-tracking device positioned on the headcoil to monitor task performance. Owing to problems related to signal-to-noise in the eye-tracking data collected in the scanner, we were only able to verify task compliance "on-line" and could not conduct a off-line analysis of the eye-movement data. The results reported in **Table 3** (see below) were collected during the training period outside of the scanner using the video eyetracker.

Magnetic resonance imaging

Functional magnetic resonance imaging (fMRI) was conducted on a 3-Tesla head scanner (Siemens Allegra, Erlangen, Germany). A localizer scan for placing the volume of interest was first acquired. In order to obtain a 3D anatomical model of the brain scan, high-resolution, sagittal T1-weighted images were acquired by using a magnetization-prepared gradient echo (MP-RAGE) sequence. The anatomical data set consisted of 160 sagittal slices, FoV 256 mm, slice thickness 1.00 mm, TR 2250 ms, TE 2.6 ms, flip angle 90°. For functional analysis a total of 610 functional volumes were acquired. Each functional scan contained 34 3-mm slices, positioned oblique to the axial plane using a T2*-weighted EPI sequence ($TR = 2.0$ s, $TE = 30$ ms, $3 \times 3 \times 3$ mm^3 voxel size, flip angle 90°).

DATA ANALYSIS

The evaluation of the eye movements was conducted manually using Matlab. Owing to the limitations on the signal-to-noise of the in-scanner eyetracking data, we base our analysis of the behavioral data on the video eyetracking data acquired during the training session outside of the scanner. We analyzed the eye trajectories offline and evaluated the task performance of the subjects. For both tasks, hit rates of the correct eye movements and reaction times were calculated. Accuracy rates among the groups exceeded chance performance in every group. A saccadic response was considered correct when the eye-movement direction was correct and the saccade landing point was near ($\pm 2°$) the peripheral visual target location. Reflexive pro-saccades that were not executed toward the mirror image location of the peripheral target were classified as errors in the anti-saccade task. Saccadic reaction time was calculated as the time from stimulus onset to saccadic onset. In the anti-saccade task, only data from trials where the saccades directed gaze toward the mirror location of the visual stimulus were scored as correct. For both conditions, saccades with reaction time less than 100 ms were classified as anticipatory and thus excluded from further analysis (0.5% of all saccades). The groups did not differ with respect to frequency of anticipatory saccades. Group comparisons of the behavioral data were conducted using *T*-test for independent samples in SPSS 18.0 (SPSS Inc., Chicago, Illinois). All tests were two-tailed, with a value of $p < 0.05$ to determine statistical significance. During fMRI-scanning, the eye-position trace was observed to confirm in all participants that they performed the task as instructed. The experimenter noted any lapses on the part of the participant, as well as excessive eye blinks. We had no indication that any of the participants did not understand the tasks, nor did we have any evidence that any of the participants did not perform the task while in the scanner.

The functional MRI data were preprocessed and analysed using Statistical Parametric Mapping 5 (SPM, Wellcome Trust Centre for Neuroimaging, University College London, UK, http://www.fil.ion.ucl.ac.uk/spm). To correct for differences in image acquisition time between slices, *slice timing* correction was conducted. The movement artifacts in the time-series of images were removed using a least squares approach and a six-parameter (rigid body) spatial transformation. Maximum head movement never exceeded 3 mm and no scans had to be removed due to excessive head motion. The images were realigned to spatially match the first image. The structural image was realigned to a mean image computed from the functional series. All images were then normalized to the Montreal Neurological Institute (MNI-152) space. The realigned and normalized functional series were resampled to $2 \times 2 \times 2$ mm resolution and spatially smoothed with a Gaussian kernel of 8 mm *Full-Width at Half-Maximum* (FWHM).

For the statistical analysis, the convolution of a canonical hemodynamic response function (HRF) with square temporal

onset profiles (boxcars), representing the onsets of the relevant experimental conditions (the stimulus onset events for pro-saccades, anti-saccades, and fixation), were used to define the regressors, after removing the first three volumes. Except for anticipatory saccades, all trials (correct and incorrect) entered into the analysis. Motion parameters estimated during preprocessing of the functional images were included as additional regressors in the GLM model. Instructions and feedback were modeled as separate events of no interest. Single subject *T*-contrast maps were derived by *t*-statistics utilizing the canonical haemodynamic response function (HRF). In a second level random-effects analysis, between group differences in neural activation associated with the relevant contrasts were assessed using a one-way ANOVA. Within this ANOVA two-sample *t*-tests were computed to analyse effects between young healthy subjects and healthy elderly, as well as between healthy elderly and MCI patients. Clusters of $k \geq 10$ contiguous voxels large enough to pass a cluster-wise threshold of $p < 0.001$ were considered as significant. Active brain areas were labeled with anatomical loci and Brodmann areas by using the SPM5 extension Wake Forest University (WFU) pick-atlas (Maldjian et al., 2003). The WFU pick-atlas was also used to convert MNI- in Talairach-coordinates. To assess age related changes in brain activation, the regions of interest (ROI) based approach was employed. The analysis was done on subject-specific parameter estimates extracted from the peak voxel within each region of interest using the MarsBAR toolbox in SPM5 (*Mars*eille *B*oîte *À R*égion d'Intérêt; http://marsbar.sourceforge.net/). This strategy allows for an anatomically focused analysis of the role of specific brain areas in saccade and anti-saccade task performance (Connolly et al., 2002; Curtis et al., 2004). ROIs were chosen on the basis of the relevant literature and our *a priori* hypothesis that activation of these regions would be modulated by the age and cognitive status of the participants. The regions associated with pro-saccadic and anti-saccadic eye movements have been well-described in the literature (Connolly et al., 2002; Matsuda et al., 2004; Brown et al., 2006; Parton et al., 2007; Hutton, 2008). Previous studies showed that fronto-parietal network is crucial for the planning and execution of saccadic eye movements (Rivaud et al., 1994; Matsuda et al., 2004; Grosbras et al., 2005). There is some inconsistency; however, whether frontal eye fields (FEF) or intraparietal sulcus (IPS) is more active during anti-saccades compared with pro-saccades (Connolly et al., 2002; Cornelissen et al., 2002; Curtis et al., 2004; Brown et al., 2006; Ettinger et al., 2008). Thus, the sets of regions of interest were defined for prosaccades and anti-saccades that included frontal and parietal regions as well as supplementary eye fields. Therefore, we used a literature-derived anatomical approach to investigate the effect of normal and pathological ageing on saccade-rated activations within frontal, parietal and supplementary eye fields. The ROIs with 5 mm radius (10 mm diameter) are displayed in **Table 2** and labeled in **Figure 1**. First, we defined an anatomical mask (structural ROIs) for each subject based on his or her high-resolution structural scan. Then, the magnitude of activation within each ROI was calculated for each subject as the percent signal change for the relevant conditions over the voxels within the regions of interest (Poldrack, 2007).

Table 2 | Anatomical locations of regions of interest in the left and right hemispheres.

Cortical region (ROI)	Talairach coordinates (in mm)		
	x	*y*	*z*
Frontal eye fields	−32	16	48
	20	8	48
Parietal eye fields	38	−47	48
	−43	−50	52
Supplementary eye fields*	17	−17	56

**Activation in supplementary eye fields is pooled over left and right hemispheres.*

RESULTS

BEHAVIORAL DATA

The analysis of the behavioral performance measured outside of the scanner revealed that the groups did not differ in accuracy on the pro-saccade task (**Table 3**). In contrast, healthy elderly persons and aMCI-patients exhibited more direction errors while performing anti-saccades. However, the aMCI group did not differ significantly with respect to the proportion of omissions (i.e., proportion of trials where they executed no saccade) compared to the age-matched controls (**Table 3**). Compared to young persons, healthy elderly persons executed significantly fewer correct anti-saccades and needed significantly more time to perform the task correctly. Furthermore, healthy elderly persons were significantly slower in pro-saccade task in comparison with young persons. Patients with aMCI executed significantly fewer correct anti-saccades compared to elderly healthy persons. The reaction times, however, did not differ significantly in either of tasks between both groups.

FUNCTIONAL IMAGING DATA

Separate analyses for each group showed increased activation of distributed frontal and parietal regions in both pro-saccades and anti-saccades (**Table 4**). These areas are known to be involved in the execution of saccadic eye movements.

Region of interest analysis revealed that there are no significant differences in the neural activation between groups while performing pro-saccade task (pro-saccades > fixation of healthy elderly compared to pro-saccades > fixation of aMCI; **Table 4**). There are, however, significant changes in the activation associated with anti-saccade task with respect to age as well as with the aMCI diagnosis. While healthy elderly showed significantly less activation bilaterally in parietal regions compared to young persons, patients with aMCI exhibited significantly decreased activation bilateral in frontal regions (FEF) in comparison to healthy elderly participants.

DISCUSSION

The present study aimed to explore the effects of normal and pathological ageing on inhibitory processes underlying the control of reactive saccade execution. In particular, we investigated the behavioral and neural correlates of prepotent response

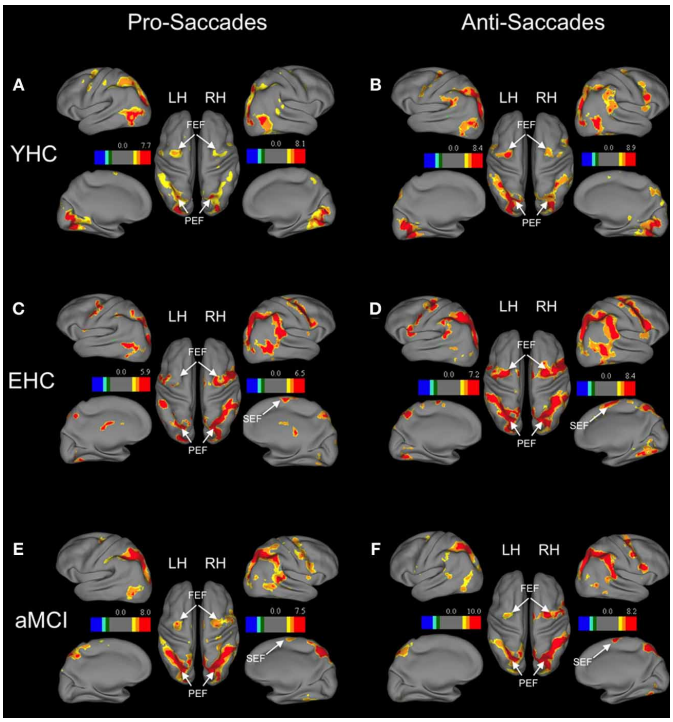

FIGURE 1 | Brain areas showing significant activation associated with pro-saccades and anti-saccades in all subject groups (contrasts: pro-saccades > baseline, anti-saccades > baseline). (Panels **A,C,E**) present the results for the pro-saccade condition, whereas (Panels **B,D,F**) display the results for the anti-saccade condition. Abbreviations: YHC, young healthy controls; EHC, elderly healthy controls; aMCI, patients with mild cognitive impairment; LH, left hemisphere; RH, right hemisphere; FEF, frontal eye fields; SEF, supplementary eye fields; PEF, parietal eye fields. Color insets present the *T*-values for the contrast saccade condition vs. baseline.

Table 3 | Performance measured outside of the scanner (proportion correct among executed saccades, proportion of omissions, reaction times in ms) of young persons, healthy elderly and aMCI patients in pro-saccade and anti-saccade task.

Parameters	Young persons vs. healthy elderly				Healthy elderly vs. aMCI		
	Young persons	Healthy elderly	*t*(df)	*p*	aMCI	*t*(df)	*p*
HIT RATES[a]							
Pro-saccades	0.99 (0.01)	0.99 (0.01)	0.462 (30)	0.648	0.98 (0.03)	1.100 (40)	0.278
Omissions	0.001 (0.0001)	0.043 (0.208)	−0.956	0.339	0.071 (0.262)	−0.416	0.676
Anti-saccades	0.96 (0.04)	0.74 (0.16)	**−4.865** (30)	**0.000***	0.57 (0.18)	**3.063** (40)	**0.04***
Omissions	0.0045 (0.0006)	0.023 (0.104)	−0.1.078	0.281	0.036 (0.089)	−1.496	0.135
REACTION TIMES (ms)							
Pro-saccades	249.2 (28.3)	285.6 (53.7)	**2.227** (30)	**0.034***	306.3 (241.4)	−0.908 (40)	0.370
Antisaccades	338.5 (21.8)	478.3 (119.6)	**4.146** (30)	**0.000****	509.0 (118.6)	−0.804 (40)	0.427

*aMCI, amnestic mild cognitive impairment; n.s., not significant; denoted are mean values, standard deviations (in brackets), Z- and p-values. Levels of significance indicated by askerisks: *p < 0.05; **p < 0.01.*

[a] *Note that there were 4 possible target positions. Thus, performance by chance would correspond to a hit rate of 25%.*

Significant values (p < 0.05) are marked in bold font.

inhibition, assessed by the anti-saccade task, as postulated by Miyake et al. (2000) and Friedman and Miyake (2004). Our findings point to a significant impairment in the ability of aMCI patients to perform the antisaccade task. Furthermore, our findings indicate that this impaired execution of antisaccades is associated with significantly reduced BOLD signal in the frontal eye fields in aMCI patients. Our results are consistent with earlier studies (e.g., Amieva et al., 2004) on the effects of ageing and dementia on saccadic execution.

SACCADIC AND ANTI-SACCADIC EYE MOVEMENTS IN NORMAL AGEING

In agreement with studies on the decline of inhibitory processes with age (e.g., Hasher and Zacks, 1988; Nieuwenhuis et al., 2000;

Table 4 | Results of regions of interest analysis in young persons, healthy elderly and aMCI patients (BOLD response as percent signal change within ROI across all trials).

Regions of interest	Young persons vs. healthy elderly				Healthy elderly vs. aMCI		
	Young persons	Healthy elderly	*t*(df)	*p*	aMCI	*t*(df)	*p*
PRO-SACCADES							
Frontal eye fields							
Right	0.20 (0.12)	0.21 (0.23)	0.155 (30)	0.878	0.14 (0.13)	1.238 (40)	0.223
Left	0.18 (0.15)	0.13 (0.16)	−0.827 (30)	0.415	0.11 (0.10)	0.308 (40)	0.759
Parietal oculomotor area							
Right	0.40 (0.24)	0.26 (0.20)	−1.670 (30)	0.106	0.23 (0.19)	0.535 (40)	0.596
Left	0.38 (0.24)	0.27 (0.18)	−1.363 (30)	0.183	0.22 (0.21)	0.750 (40)	0.458
Supplementary eye fields							
	0.17 (0.18)	0.11 (0.16)	0.827 (30)	0.422	0.19 (0.27)	−1.237 (40)	0.223
ANTI-SACCADES							
Frontal eye fields							
Right	0.32 (0.17)	0.32 (0.20)	−0.049 (30)	0.961	0.16 (0.12)	**3.030** (40)	**0.004****
Left	0.32 (0.19)	0.25 (0.14)	−1.003 (30)	0.329	0.15 (0.15)	**2.202** (40)	**0.033***
Parietal oculomotor area							
Right	0.57 (0.21)	0.39 (0.20)	**−2.319** (30)	**0.028**	0.29 (0.21)	1.645 (40)	0.108
Left	0.54 (0.17)	0.37 (0.18)	**−2.510** (30)	**0.018***	0.28 (0.22)	1.532 (40)	0.133
Supplementary eye fields							
	0.20 (0.23)	0.27 (0.28)	−0.633 (30)	0.534	0.23 (0.34)	0.406 (40)	0.687

*aMCI, amnestic mild cognitive impairment; denoted are mean values, standard deviations (in brackets), t- and p-values, df: degrees of freedom. Levels of significance indicated by askerisks: *$p < 0.05$; **$p < 0.01$.*

Significant values ($p < 0.05$) are marked in bold font.

Sweeney et al., 2001; Raemaekers et al., 2006; Peltsch et al., 2011), our study demonstrates a reduced ability of elderly adults to voluntarily inhibit saccadic responses compared to young adults. Moreover, the onset latencies of pro-saccades and anti-saccades were significantly longer in healthy elderly adults compared to young adults (**Table 3**). The performance of elderly adults on the automatic saccadic initiation, however, showed no decline compared to the performance of young adults on the pro-saccade task. Such findings have been documented by previous research on pro-saccadic and anti-saccadic eye movements (Olincy et al., 1997; Butler et al., 1999; Klein and Foerster, 2001; Sweeney et al., 2001; Crawford et al., 2005; Peltsch et al., 2011). Moreover, some researchers demonstrated that the poor performance in the anti-saccade task and longer saccadic latencies cannot only be found in elderly persons but also in children aged between 5 and 8 years (Munoz et al., 1998). Thus, these behavioral changes in performance may reflect different stages of normal development as well as degeneration in the nervous system (Munoz et al., 1998).

SACCADIC AND ANTI-SACCADIC EYE MOVEMENTS IN PATHOLOGICAL AGEING

The present study revealed impaired inhibitory functions in aMCI patients, as assessed by the anti-saccade task. Our results agree with those of previous studies that show altered inhibitory functions on Stroop task in aMCI patients (Traykov et al., 2007; Bélanger et al., 2010). Controversially, Zhang et al. (2007) failed to find significant differences in performance on Stroop task in MCI. These contrasting findings point to the heterogeneity underlying MCI (Nordlund, 2005). Furthermore, deterioration of controlled inhibition processes and preserved ability to execute pro-saccades has been widely reported in patients with AD (e.g., Currie et al., 1991; Amieva et al., 2002; Crawford et al., 2005; Mosimann et al., 2005; Collette et al., 2009). Moreover, there is evidence in the literature that persons diagnosed with AD demonstrate different performance patterns in oculomotor tasks compared to patients with Parkinson's disease with dementia, dementia with Lewy bodies (Mosimann et al., 2005), frontotemporal lobar degeneration, corticobasal syndrome and progressive supranuclear palsy (Garbutt et al., 2008). Thus, the anti-saccade task can also be used to distinguish between different types of dementia and other forms of degenerative disorders. Given the fact that persons with aMCI are likely to develop AD (Petersen and Jack, 2009), our findings illustrate that assessment of the prepotent inhibitory functions in aMCI might be sensitive to early manifestations of AD.

NEURAL CORRELATES OF INHIBITORY PROCESSES IN NORMAL AGEING

The analysis of neural activation associated with saccadic inhibition showed that all groups found significant activations in regions that are thought to underlie the execution of pro- and anti-saccades (Pierrot-Deseilligny et al., 1991; Matsuda et al., 2004; Ford et al., 2005; Parton et al., 2007). A ROI analysis of the anti-saccade task revealed that healthy elderly adults show significantly less activation bilaterally in the inferior parietal lobe compared to young adults. This change in neural activation was

accompanied by a significant reduction in performance accuracy and longer onset latencies. However, neither parietal nor frontal regions showed significant changes in activation during the pro-saccade task, even though elderly healthy adults needed significantly more time to perform as accurately as young adults. In contrast, Raemaekers et al. (2006) reported no significant effect of age on the neural activation with respect to saccadic inhibition but lower activation in older adults compared to young and middle-aged adults who executed pro-saccades. Nevertheless, no significant difference in performance on either task was found between groups (Raemaekers et al., 2006). Nelles et al. (2009) showed an age-dependent increase in activation in a pro-saccade task in bilateral parietal eye fields, the right frontal eye field, as well as in the right extrastriate cortex. However, the previous study did not report any findings on the task performance of the individuals. The discrepancy between studies of Raemaekers et al. (2006); Nelles et al. (2009) and our study may be explained with increased interindividual variability in performance in cognitive tasks, which has been widely reported in elderly adults (for a review: Hedden and Gabrieli, 2004; Bishop et al., 2010). Also, the number of participants in both studies is lower compared to our study: Raemaekers et al. (2006) investigated three groups with a total number of 36 persons whereas the subject population in the study of Nelles et al. (2009) contained in total 22 persons. Furthermore, the present findings are consistent with those of previous studies illustrating effects of normal ageing on performance in oculomotor tasks (e.g., Fletcher and Sharpe, 1986; Mulligan et al., 1996). Hence, our findings extend these results and show an association between decreased activation in the parietal lobe in elderly adults and a decline in response inhibition.

Previous fMRI studies stressed the role of parietal areas in the execution of anti-saccades (Kimmig et al., 2001; Curtis and D'Esposito, 2003; Brown et al., 2006). More recently, Sharpe et al. (2011) showed that impaired suppression of reflexive saccades and generation of anti-saccades could be attributed to a partial disconnection of the parietal lobe from frontal lobe ocular motor areas. Given that reduction in fractional anisotropy of frontal and parietal white matter increases with age (Abe et al., 2002; Grieve et al., 2007), a decrease in parietal activation in elderly adults may result as a change in functional connectivity between these regions as seen in our study. Moreover, decreased activation in parietal regions together with reduced performance was observed in elderly adults in a Stroop task (Milham et al., 2002). In another study, right prefrontal and parietal regions were more activated in elderly adults compared to young persons during "successful inhibition" assessed with the Stroop interference paradigm (Nielson et al., 2002). This activation patterns can be explained by theoretical models of ageing (Cabeza et al., 2004; Grady et al., 2008; Reuter-Lorenz and Park, 2010) postulating that increases (or decreases) in activation refer to neural resources that are engaged (or disengaged) in healthy elderly to cope with cognitive challenges. Consistent with those models, neuroimaging findings indicate that in cases of limited cognitive decline with age, an over-activation is observed in regions important for the cognitive tasks in question (Cabeza et al., 2004). However, when cognitive impairment is more advanced, both decreased neural activity and poor performance on behavioral tasks have been reported in elderly adults (Persson and Nyberg, 2006). Hence, the failure to differentially activate the parietal regions may indicate neural inefficiency in elderly adults as seen in our study, accompanied by a decline in the ability to perform the demanding anti-saccade task requiring saccadic inhibition. Owing to the limitations with respect to the signal-to-noise of the in-scanner eye-tracking data, we only used the eye-movement data online to confirm that the participants performed the task. The non-linear changes in the eye-tracking signal and the low signal-to noise level, however, made a detailed off-line analysis unfeasible. Thus, we were not able to conduct a detailed off-line analysis of the eye-movement data collected in the scanner.

NEURAL CORRELATES OF INHIBITORY PROCESSES IN PATHOLOGICAL AGEING

Another important focus of our study was directed to the effects of pathological ageing on saccadic inhibition. To our knowledge, this is the first study that investigated anti-saccades and their neural correlates in aMCI. We found that while there is no significant difference in activation related to the pro-saccade task between aMCI patients and elderly adults, aMCI patients show significantly reduced activation in FEF bilaterally during the execution of anti-saccades. Given the fact that aMCI patients demonstrate a significant decline in the ability to correctly execute anti-saccades as compared to healthy elderly, these findings provide new evidence for an association between neural and cognitive deficits in pathological ageing. The reduced activation we observed in the aMCI group compared to the age-matched controls cannot be explained by a larger proportion of omissions in the anti-saccade task. At least for the measurements made outside of the scanner the two groups did not differ with respect to the proportion of omissions during either anti- or pro-saccade tasks (**Table 3**).

Similar to the fMRI findings on the control of pro-saccades and anti-saccades in aMCI, there is only a limited number of studies that examine the effect of pathological ageing on neural activation associated with oculomotor tasks. Only one other study has investigated brain activation patterns during visually guided saccade paradigm in persons diagnosed with probable AD compared to healthy volunteers. Thulborn et al. (2000) observed left-dominant parietal and prefrontal cortical activation in most patients with probable AD while executing pro-saccades. An explanation for this contrasting result could be the difference between clinically diagnosed probable AD and MCI, which both are pathologically heterogeneous disorders that vary in presentation, onset, or clinical course (Schneider et al., 2009). Furthermore, the inability of persons with AD to perform anti-saccades has been attributed to frontal lobe degeneration (Fletcher and Sharpe, 1986). Also the level of the performance on the Stroop task in patients with AD depends on the functional integrity of the prefrontal cortices (Yun et al., 2011). In a study investigating white matter tracts in MCI, authors showed that tract degeneration in frontal and cingulate regions as well as cortical thinning in caudal middle frontal region are associated with impairment

in executive functions (Grambaite et al., 2011). Hence, the decrease in neural activation in FEF during anti-saccade task in patients with aMCI may be an analogous effect to the one seen in patients with AD. Furthermore, findings from our previous study demonstrated no significant differences in gray matter (VBM) between healthy elderly and persons with MCI (Alichniewicz et al., 2012). Moreover, the fact that the BOLD response is normal for pro-saccades in MCI speaks against an anatomical change in the gray matter in these patients and emphasizes the pathological functional disabilities. Therefore, our findings illustrate that the decline in functions for response inhibition accompanied by disrupted frontal activation in aMCI might be sensitive to early manifestations of AD.

SHORTCOMING OF CURRENT STUDY AND MOTIVATION FOR FUTURE RESEARCH

Our study characterizes the extent of oculomotor system impairment and altered neural activation in brain areas associated with response inhibition in normal and pathological ageing. The present study relies on eye-tracking performance outside the scanner for comparing the groups. Owing to problems related to signal-to-noise in the eye-tracking data collected in the scanner, we could only verify task compliance "on-line" and were unable to conduct any detailed off-line analysis of the eye-movement data that could have been used to determine error-related processing, perform a parametric analysis related to saccadic reaction times, or determine the role of correction saccades in the pattern of activation found in the aMCI group. Such interesting and relevant analyses are therefore left to future studies.

Moreover, randomized pro- and anti-saccade trial sequences would avoid habituation or adaptation effects associated with block presentation of the different saccade types. However, within each block saccade direction and amplitude were randomized to minimize such adaptation effects. The results of many previous studies suggest that a number of different processes underlie a cognitive decline in AD and MCI (for a review: Stephan et al., 2012a). Thus, we believe that determining the factors that account for behavioral and functional changes reported in this study requires further research.

Furthermore, studies investigating functional connectivity suggest that spontaneous fluctuations in the BOLD signal may contribute to the variability in evoked signals and performance levels (Fox et al., 2006; Fox and Raichle, 2007). Resting-state functional connectivity between the FEF and prefrontal as well as intraparietal cortex exhibits a remarkable similarity across macaque and humans (Hutchison et al., 2012). Also, the extent of task-related reduction in neural activity in default mode regions was shown to be less pronounced in older than in young adults (Lustig et al., 2003; Grady et al., 2006), especially with increasing cognitive task demands (Persson et al., 2007). Since we used a general linear model analysis that is not as sensitive to temporal change in activation and deactivation patterns in dementia as are exploratory data analysis techniques, such as independent component analysis (ICA) (Rombouts et al., 2009), we cannot eliminate the possibility that we may not have been able to detect additional unknown group differences in our neuroimaging data. Hence, important implications regarding the role of the age reductions in the ability to suppress default mode activity in elderly adults during demanding inhibition tasks such as anti-saccade task need to be investigated.

CONCLUSIONS

The aim of this study was to further our understanding of cognitive and neural changes in normal and pathological ageing with respect to inhibitory functions, in particular inhibition of prepotent responses measured in anti-saccade tasks. The present study confirms and extends existing results showing that healthy ageing leads to reduced response inhibition and decreased neural activation in the parietal lobe. Furthermore, our study provides new insights in the neural changes associated with the execution of anti-saccades that occur in pathological ageing. Our functional MRI data revealed that patients with aMCI show reduced activation in frontal eye fields together with reduced ability to execute anti-saccades. A reduced ability to voluntarily suppress an automatic response in favor of performing an alternative behavior is considered to be one of the crucial executive functions required in everyday life (Munoz and Everling, 2004). An analysis of the error-related activations on erroneous anti-saccade trials would have been informative. Thus, future work should address whether alteration of neural activation associated with oculomotor performance found in aMCI can help to detect persons at risk of developing Alzheimer's disease.

ACKNOWLEDGMENTS

This research was funded in part by Deutsche Forschun gsgemeinschaft (GR 988). Author K. K. Alichniewicz gratefully acknowledges The Bavarian Academic Center for Central, Eastern and Southeastern Europe (BAYHOST) for a PhD scholarship. We thank the participants for their enthusiastic support. The authors would like to thank the reviewers for their extensive and immensely helpful comments on this manuscript thoroughout the review process.

REFERENCES

Abe, O., Aoki, S., Hayashi, N., Yamada, H., Kunimatsu, A., Mori, H., et al. (2002). Normal aging in the central nervous system: quantitative MR diffusion-tensor analysis. *Neurobiol. Aging* 23, 433–441. doi: 10.1016/S0197-4580(01)00318-9

Alichniewicz, K. K., Brunner, F., Klünemann, H. H., and Greenlee, M. W. (2012). Structural and functional neural correlates of visuospatial information processing in normal aging and amnestic mild cognitive impairment. *Neurobiol. Aging* 33, 2782–2797. doi: 10.1016/j.neurobiolaging.2012.02.010

American Psychiatric Association. (1994). *Diagnostic and Statistical Manual of Mental Disorders (DSM). 4th Edn.* APA Publishing.

Amieva, H., Lafont, S., Auriacombe, S., Carret, N. L., Dartigues, J.-F., Orgogozo, J.-M., et al. (2002). Inhibitory breakdown and dementia of the Alzheimer type: a General Phenomenon? *J. Clin. Exp. Neuropsychol.* 24, 503–516. doi: 10.1076/jcen.24.4.503.1034

Amieva, H., Phillips, L. H., Della Sala, S., and Henry, J. D. (2004). Inhibitory functioning in Alzheimer's disease. *Brain* 127, 949–964. doi: 10.1093/brain/awh045

Anderson, S., Parbery-Clark, A., White-Schwoch, T., and Kraus, N. (2012). Aging affects neural precision of speech encoding. *J. Neurosci.* 32, 14156–14164. doi: 10.1523/JNEUROSCI.2176-12.2012

Artero, S., Petersen, R., Touchon, J., and Ritchie, K. (2006). Revised Criteria for mild cognitive impairment: validation within a longitudinal population study. *Dement. Geriatr. Cogn. Disord.* 22, 465–470. doi: 10.1159/000096287

Bélanger, S., and Belleville, S. (2009). Semantic inhibition impairment in mild cognitive impairment: a distinctive feature of upcoming cognitive decline? *Neuropsychology* 23, 592–606. doi: 10.1037/a0016152

Bélanger, S., Belleville, S., and Gauthier, S. (2010). Inhibition impairments in Alzheimer's disease, mild cognitive impairment and healthy aging: effect of congruency proportion in a Stroop task. *Neuropsychologia* 48, 581–590. doi: 10.1016/j.neuropsychologia.2009.10.021

Belleville, S., Rouleau, N., and Van der Linden, M. (2006). Use of the Hayling task to measure inhibition of prepotent responses in normal aging and Alzheimer's disease. *Brain Cogn.* 62, 113–119. doi: 10.1016/j.bandc.2006.04.006

Bishop, N. A., Lu, T., and Yankner, B. A. (2010). Neural mechanisms of ageing and cognitive decline. *Nature* 464, 529–535. doi: 10.1038/nature08983

Boxer, A. L., Garbutt, S., Rankin, K. P., Hellmuth, J., Neuhaus, J., Miller, B. L., et al. (2006). Medial versus lateral frontal lobe contributions to voluntary saccade control as revealed by the study of patients with frontal lobe degeneration. *J. Neurosci.* 26, 6354–6363. doi: 10.1523/JNEUROSCI.0549-06.2006

Braver, T. S., and Barch, D. M. (2002). A theory of cognitive control, aging cognition, and neuromodulation. *Neurosci. Biobehav. Rev.* 26, 809–817. doi: 10.1016/S0149-7634(02)00067-2

Brown, M. R. G., Goltz, H. C., Vilis, T., Ford, K. A., and Everling, S. (2006). Inhibition and generation of saccades: rapid event-related fMRI of prosaccades, antisaccades, and nogo trials. *Neuroimage* 33, 644–659. doi: 10.1016/j.neuroimage.2006.07.002

Butler, K., Zacks, R., and Henderson, J. (1999). Suppression of reflexive saccades in younger and older adults: age comparisons on an antisaccade task. *Mem. Cognit.* 27, 584–591. doi: 10.3758/BF03211552

Cabeza, R., Daselaar, S. M., Dolcos, F., Prince, S. E., Budde, M., and Nyberg, L. (2004). Task-independent and task-specific age effects on brain activity during working memory, visual attention and episodic retrieval. *Cereb. Cortex* 14, 364–375. doi: 10.1093/cercor/bhg133

Chertkow, H., Massoud, F., Nasreddine, Z., Belleville, S., Joanette, Y., Bocti, C., et al. (2008). Diagnosis and treatment of dementia: 3. Mild cognitive impairment and cognitive impairment without dementia. *CMAJ* 178, 1273–1285.

Connolly, J. D., Goodale, M. A., Menon, R. S., and Munoz, D. P. (2002). Human fMRI evidence for the neural correlates of preparatory set. *Nat. Neurosci.* 5, 1345–1352. doi: 10.1038/nn969

Collette, F., Schmidt, C., Scherrer, C., Adam, S., and Salmon, E. (2009). Specificity of inhibitory deficits in normal aging and Alzheimer's disease. *Neurobiol. Aging* 30, 875–889. doi: 10.1016/j.neurobiolaging.2007.09.007

Cornelissen, F. W., Kimmig, H., Schira, M., Rutschmann, R. M., Maguire, R. P., Broerse, A., et al. (2002). Event-related fMRI responses in the human frontal eye fields in a randomized pro- and antisaccade task. *Exp. Brain Res.* 145, 270–274. doi: 10.1007/s00221-002-1136-3

Crawford, T. J., Higham, S., Renvoize, T., Patel, J., Dale, M., Suriya, A., and Tetley, S. (2005). Inhibitory control of saccadic eye movements and cognitive impairment in Alzheimer's disease. *Biol. Psychiatry* 57, 1052–1060. doi: 10.1016/j.biopsych.2005.01.017

Crutcher, M. D., Calhoun-Haney, R., Manzanares, C. M., Lah, J. J., Levey, A. I., and Zola, S. M. (2009). Eye tracking during a visual paired comparison task as a predictor of early dementia. *Am. J. Alzheimers Dis. Other Demen.* 24, 258–266. doi: 10.1177/1533175093329093

Currie, J., Ramsden, B., McArthur, C., and Maruff, P. (1991). Validation of a clinical antisaccadic eye movement test in the assessment of dementia. *Arch. Neurol.* 48, 644–648. doi: 10.1001/archneur.1991.00530180102024

Curtis, C. E., and D'Esposito, M. (2003). Success and failure suppressing reflexive behavior. *J. Cogn. Neurosci.* 15, 409–418. doi: 10.1162/089892903321593126

Curtis, C. E., Rao, V. Y., and D'Esposito, M. (2004). Maintenance of spatial and motor codes during oculomotor delayed response tasks. *J. Neurosci.* 24, 3944–3952. doi: 10.1523/JNEUROSCI.5640-03.2004

Ettinger, U., ffytche, D. H., Kumari, V., Kathmann, N., Reuter, B., Zelaya, F., et al. (2008). Decomposing the neural correlates of antisaccade eye movements using event-related fMRI. *Cereb. Cortex* 18, 1148–1159. doi: 10.1093/cercor/bhm147

Fisher, L. M., Freed, D. M., and Corkin, S. (1990). Stroop Color-Word Test performance in patients with Alzheimer's disease. *J. Clin. Exp. Neuropsychol.* 12, 745–758. doi: 10.1080/01688639008401016

Fletcher, W. A., and Sharpe, J. A. (1986). Saccadic eye movement dysfunction in Alzheimer's disease. *Ann. Neurol.* 20, 464–471. doi: 10.1002/ana.410200405

Ford, K. A., Goltz, H. C., Brown, M. R. G., and Everling, S. (2005). Neural processes associated with antisaccade task performance investigated with event-related fMRI. *J. Neurophysiol.* 94, 429–440. doi: 10.1152/jn.00471.2004

Fox, M. D., and Raichle, M. E. (2007). Spontaneous fluctuations in brain activity observed with functional magnetic resonance imaging. *Nat. Rev. Neurosci.* 8, 700–711. doi: 10.1038/nrn2201

Fox, M. D., Snyder, A. Z., Zacks, J. M., and Raichle, M. E. (2006). Coherent spontaneous activity accounts for trial-to-trial variability in human evoked brain responses. *Nat. Neurosci.* 9, 23–25. doi: 10.1038/nn1616

Fox, N. C., Warrington, E. K., Seiffer, A. L., Agnew, S. K., and Rossor, M. N. (1998). Presymptomatic cognitive deficits in individuals at risk of familial Alzheimer's disease. A longitudinal prospective study. *Brain* 121, 1631–1639. doi: 10.1093/brain/121.9.1631

Friedman, N. P., Miyake, A., Young, S. E., DeFries, J. C., Corley, R. P., and Hewitt, J. K. (2008). Individual differences in executive functions are almost entirely genetic in origin. *J. Exp. Psychol. Gen.* 137, 201–225. doi: 10.1037/0096-3445.137.2.201

Friedman, N. P., and Miyake, A. (2004). The relations among inhibition and interference control functions: a latent-variable analysis. *J. Exp. Psychol. Gen.* 133, 101–135. doi: 10.1037/0096-3445.133.1.101

Garbutt, S., Matlin, A., Hellmuth, J., Schenk, A. K., Johnson, J. K., Rosen, H., et al.(2008). Oculomotor function in frontotemporal lobar degeneration, related disorders and Alzheimer's disease. *Brain* 131, 1268–1281. doi: 10.1093/brain/awn047

Grady, C. L., Springer, M. V., Hongwanishkul, D., McIntosh, A. R., and Winocur, G. (2006). Age-related changes in brain activity across the adult lifespan. *J. Cogn. Neurosci.* 18, 227–241. doi: 10.1162/089892906775783705

Grady, C. L., Yu, H., and Alain, C. (2008). Age-related differences in brain activity underlying working memory for spatial and nonspatial auditory information. *Cereb. Cortex* 18, 189–199. doi: 10.1093/cercor/bhm045

Grambaite, R., Selnes, P., Reinvang, I., Aarsland, D., Hessen, E., Gjerstad, L., et al. (2011). Executive dysfunction in mild cognitive impairment is associated with changes in frontal and cingulate white matter tracts. *J. Alzheimers Dis.* 27, 453–462.

Greenwood, P. M. (2000). The frontal aging hypothesis evaluated. *J. Int. Neuropsychol. Soc.* 6, 705–726. doi: 10.1017/S1355617700666092

Grieve, S. M., Williams, L. M., Paul, R. H., Clark, C. R., and Gordon, E. (2007). Cognitive aging, executive function, and fractional anisotropy: a diffusion tensor MR imaging study. *Am. J. Neuroradiol.* 28, 226–235.

Grosbras, M.-H., Laird, A. R., and Paus, T. (2005). Cortical regions involved in eye movements, shifts of attention, and gaze perception. *Hum. Brain Mapp.* 25, 140–154. doi: 10.1002/hbm.20145

Hallett, P. (1978). Primary and secondary saccades to goals defined by instructions. *Vision Res.* 18, 1279–1296. doi: 10.1016/0042-6989(78)90218-3

Hasher, L., and Zacks, R. T. (1988). "Working memory, comprehension, and aging: a review and a new view," in *The Psychology of Learning and Motivation*, Vol. 22, ed G. H. Bower (New York, NY: Academic Press), 193–225. doi: 10.1016/S0079-7421(08)60041-9

Hedden, T., and Gabrieli, J. D. E. (2004). Insights into the ageing mind: a view from cognitive neuroscience. *Nat. Rev. Neurosci.* 5, 87–96. doi: 10.1038/nrn1323

Heilbronner, U., and Münte, T. F. (2013). Rapid event-related near-infrared spectroscopy detects age-related qualitative changes in the neural correlates of response inhibition.

Neuroimage 65, 408–415. doi: 10.1016/j.neuroimage.2012.09.066

Hunderfund, A. L., Roberts, R. O., Slusser, T. C., Leibson, C. L., Geda, Y. E., Ivnik, R. J., et al. (2006). Mortality in amnestic mild cognitive impairment. *Neurology* 67, 1764–1768. doi: 10.1212/01.wnl.0000244430.39969.5f

Hutchison, R. M., Gallivan, J. P., Culham, J. C., Gati, J. S., Menon, R. S., and Everling, S. (2012). Functional connectivity of the frontal eye fields in humans and macaque monkeys investigated with resting-state fMRI. *J. Neurophysiol.* 107, 2463–2474. doi: 10.1152/jn.00891.2011

Hutton, S. B. (2008). Cognitive control of saccadic eye movements. *Brain Cogn.* 68, 327–340. doi: 10.1016/j.bandc.2008.08.021

Iachini, T., Iavarone, A., Senese, V. P., Ruotolo, F., and Ruggiero, G. (2009). Visuospatial memory in healthy elderly, AD and MCI: a review. *Curr. Aging Sci.* 2, 43–59.

Johnson, D. K., Storandt, M., Morris, J. C., and Galvin, J. E. (2009). Longitudinal study of the transition from healthy aging to Alzheimer Disease. *Arch. Neurol.* 66, 1254–1259. doi: 10.1001/archneurol.2009.158

Kaufman, L. D., Pratt, J., Levine, B., and Black, S. E. (2010). Antisaccades: a probe into the dorsolateral prefrontal cortex in Alzheimer's disease. A critical review. *J. Alzheimers Dis.* 19, 781–793. doi: 10.3233/JAD-2010-1275

Kaufman, L. D., Pratt, J., Levine, B., and Black, S. E. (2012). Executive deficits detected in mild Alzheimer's disease using the antisaccade task. *Brain Behav.* 2, 15–21. doi: 10.1002/brb3.28

Kimmig, H., Greenlee, M. W., Gondan, M., Schira, M., Kassubek, J., and Mergner, T. (2001). Relationship between saccadic eye movements and cortical activity as measured by fMRI: quantitative and qualitative aspects. *Exp. Brain Res.* 141, 184–194. doi: 10.1007/s002210100844

Klein, C., and Foerster, F. (2001). Development of prosaccade and antisaccade task performance in participants aged 6 to 26 years. *Psychophysiology* 38, 179–189. doi: 10.1111/1469-8986.3820179

Kramer, J. H., Nelson, A., Johnson, J. K., Yaffe, K., Glenn, S., Rosen, H. J., et al. (2006). Multiple cognitive deficits in amnestic mild cognitive impairment. *Dement. Geriatr. Cogn. Disord.* 22, 306–311. doi: 10.1159/000095303

Lagun, D., Manzanares, C., Zola, S. M., Buffalo, E. A., and Agichtein, E. (2011). Detecting cognitive impairment by eye movement analysis using automatic classification algorithms. *J. Neurosci. Methods* 201, 196–203. doi: 10.1016/j.jneumeth.2011.06.027

Langley, L. K., and Madden, D. J. (2000). Functional neuroimaging of memory: implications for cognitive aging. *Microsc. Res. Tech.* 51, 75–84.

Li, C., Zheng, J., Wang, J., Gui, L., and Li, C. (2009). An fMRI stroop task study of prefrontal cortical function in normal aging, mild cognitive impairment, and Alzheimers disease. *Curr. Alzheimer Res.* 6, 525–530. doi: 10.2174/156720509790147142

Logan, G. D., (ed.). (1994). *On the Bility to Inhibit Thought and Action: a User's Guide to the Stop Signal Paradigm. Inhibitory Processes in Attention, Memory and Language.* San Diego, CA: Academic Press.

Lustig, C., Snyder, A. Z., Bhakta, M., O'Brien, K. C., McAvoy, M., Raichle, M. E., et al. (2003). Functional deactivations: change with age and dementia of the Alzheimer type. *Proc. Natl. Acad. Sci. U.S.A.* 100, 14504–14509. doi: 10.1073/pnas.2235925100

Maldjian, J. A., Laurienti, P. J., Kraft, R. A., and Burdette, J. H. (2003). An automated method for neuroanatomic and cytoarchitectonic atlas-based interrogation of fMRI data sets. *Neuroimage* 19, 1233–1239. doi: 10.1016/S1053-8119(03)00169-1

Matsuda, T., Matsuura, M., Ohkubo, T., Ohkubo, H., Matsushima, E., Inoue, K., et al. (2004). Functional MRI mapping of brain activation during visually guided saccades and antisaccades: cortical and subcortical networks. *Psychiatry Res.* 131, 147–155. doi: 10.1016/j.pscychresns.2003.12.007

McDowd, J. M. (1997). Inhibition in attention and aging. *J. Gerontol. B Psychol. Sci. Soc. Sci.* 52, P265–P273. doi: 10.1093/geronb/52B.6.P265

Milham, M. P., Erickson, K. I., Banich, M. T., Kramer, A. F., Webb, A., Wszalek, T., et al. (2002). Attentional control in the aging brain: insights from an fMRI Study of the Stroop Task. *Brain Cogn.* 49, 277–296. doi: 10.1006/brcg.2001.1501

Mirsky, J. B., Heuer, H. W., Jafari, A., Kramer, J. H., Schenk, A. K., Viskontas, I. V., et al. (2011). Anti-saccade performance predicts executive function and brain structure in normal elders. *Cogn. Behav. Neurol.* 24, 50–58. doi: 10.1097/WNN.0b013e318223f6c6

Miyake, A., Friedman, N. P., Emerson, M. J., Witzki, A. H., Howerter, A., and Wager, T. D. (2000). The unity and diversity of executive functions and their contributions to complex "frontal lobe" tasks: a latent variable analysis. *Cogn. Psychol.* 41, 49–100. doi: 10.1006/cogp.1999.0734

Moscovitch, M., and Winocur, G. (1992). "The neuropsychology of memory and aging," in *The Handbook of Aging and Cognition*, eds F. I. M. Craik and T. A. Salthouse (Hillsdale, NJ: Lawrence Erlbaum Associates), 315–372.

Mosimann, U. P., Muri, R. M., Burn, D. J., Felblinger, J., O'Brien, J. T., and McKeith, I. G. (2005). Saccadic eye movement changes in Parkinson's disease dementia and dementia with Lewy bodies. *Brain* 128, 1267–1276. doi: 10.1093/brain/awh484

Mosimann, U. P., Müri, R. M., Burn, D. J., Felblinger, J., O'Brien, J. T., and McKeith, I. G. (2005). Saccadic eye movement changes in Parkinson's disease dementia and dementia with Lewy bodies. *Brain* 128, 1267–1276. doi: 10.1093/brain/awh484

Mulligan, R., Mackinnon, A., Jorm, A. F., Giannakopoulos, P., and Michel, J. P. (1996). A comparison of alternative methods of screening for dementia in clinical settings. *Arch. Neurol.* 53, 532–536. doi: 10.1001/archneur.1996.00550060074019

Munoz, D. P., Broughton, J. R., Goldring, J. E., and Armstrong, I. T. (1998). Age-related performance of human subjects on saccadic eye movement tasks. *Exp. Brain Res.* 121, 391–400. doi: 10.1007/s002210050473

Munoz, D. P., and Everling, S. (2004). Look away: the anti-saccade task and the voluntary control of eye movement. *Nat. Rev. Neurosci.* 5, 218–228. doi: 10.1038/nrn1345

Nelles, G., de Greiff, A., Pscherer, A., and Esser, J. (2009). Age-related differences of saccade induced cortical activation. *Neurosci. Lett.* 458, 15–18. doi: 10.1016/j.neulet.2009.04.026

Nielson, K. A., Langenecker, S. A., and Garavan, H. (2002). Differences in the functional neuroanatomy of inhibitory control across the adult life span. *Psychol. Aging* 17, 56–71. doi: 10.1037/0882-7974.17.1.56

Nieuwenhuis, S., Ridderinkhof, K. R., de Jong, R., Kok, A., and van der Molen, M. W. (2000). Inhibitory inefficiency and failures of intention activation: age-related decline in the control of saccadic eye movements. *Psychol. Aging* 15, 635–647. doi: 10.1037/0882-7974.15.4.635

Nordlund, A. (2005). The Goteborg MCI study: mild cognitive impairment is a heterogeneous condition. *J. Neurol. Neurosurg. Psychiatry* 76, 1485–1490. doi: 10.1136/jnnp.2004.050385

Olincy, A., Ross, R. G., Youngd, D. A., and Freedman, R. (1997). Age diminishes performance on an antisaccade eye movement task. *Neurobiol. Aging* 18, 483–489. doi: 10.1016/S0197-4580(97)00109-7

Park, D. C., and Reuter-Lorenz, P. (2009). The adaptive brain: aging and neurocognitive scaffolding. *Annu. Rev. Psychol.* 60, 173–196. doi: 10.1146/annurev.psych.59.103006.093656

Parton, A., Nachev, P., Hodgson, T. L., Mort, D., Thomas, D., Ordidge, R. et al. (2007). Role of the human supplementary eye field in the control of saccadic eye movements. *Neuropsychologia* 45, 997–1008. doi: 10.1016/j.neuropsychologia.2006.09.007

Peltsch, A., Hemraj, A., Garcia, A., and Munoz, D. P. (2011). Age-related trends in saccade characteristics among the elderly. *Neurobiol. Aging* 32, 669–679. doi: 10.1016/j.neurobiolaging.2009.04.001

Persson, J., Lustig, C., Nelson, J. K., and Reuter-Lorenz, P. A. (2007). Age differences in deactivation: a link to cognitive control? *J. Cogn. Neurosci.* 19, 1021–1032. doi: 10.1162/jocn.2007.19.6.1021

Persson, J., and Nyberg, L. (2006). Altered brain activity in healthy seniors: what does it mean? *Prog. Brain Res.* 157, 45–56. doi: 10.1016/S0079-6123(06)57004-9

Petersen, R. (2004). Mild cognitive impairment as a diagnostic entity. *J. Intern. Med.* 256, 183–194. doi: 10.1111/j.1365-2796.2004.01388.x

Petersen, R. C. (2003). Mild cognitive impairment clinical trials. *Nat. Rev. Drug Discov.* 2, 646–653. doi: 10.1038/nrd1155

Petersen, R. C. (2007). The current status of mild cognitive impairment[mdash]what do we tell our patients? *Nat. Clin. Pract. Neurol.* 3, 60–61. doi: 10.1038/ncpneuro0402

Petersen, R. C., and Jack, C. R. (2009). Imaging and biomarkers in early Alzheimer's disease and mild cognitive impairment. *Clin. Pharmacol. Ther.* 86, 438–441. doi: 10.1038/clpt.2009.166

Pierrot-Deseilligny, C., Rivaud, S., Gaymard, B., and Agid, Y. (1991). Cortical control of reflexive visually-guided saccades. *Brain* 114, 1472–1485. doi: 10.1093/brain/114.3.1473

Poldrack, R. A. (2007). Region of interest analysis for fMRI. *Soc. Cogn. Affect. Neurosci.* 2, 67–70. doi: 10.1093/scan/nsm006

Raczkowski, D., Kalat, J. W., and Nebes, R. (1974). Reliability and validity of some handedness questionnaire items. *Neuropsychologia* 12, 43–47. doi: 10.1016/0028-3932(74)90025-6

Raemaekers, M., Vink, M., Heuvel, M. P. V. D., Kahn, R. S., and Ramsey, N. F. (2006). Effects of aging on BOLD fMRI during prosaccades and antisaccades. *J. Cogn. Neurosci.* 18, 594–603. doi: 10.1162/jocn.2006.18.4.594

Rapp, P. R., and Amaral, D. G. (1992). Individual differences in the cognitive and neurobiological consequences of normal aging. *Trends Neurosci.* 15, 340–345. doi: 10.1016/0166-2236(92)90051-9

Reuter-Lorenz, P. A., and Park, D. C. (2010). Human neuroscience and the aging mind: a new look at old problems. *J. Gerontol. B Psychol. Sci. Soc. Sci.* 65, 405–415. doi: 10.1093/geronb/gbq035

Rivaud, S., Muri, R., Gaymard, B., Vermesch, A., and Pierrot-Deseilligny, C. (1994). Eye movement disorders after frontal eye field lesions in humans. *Exp. Brain Res.* 102, 110–120. doi: 10.1007/BF00232443

Rombouts, S. A. R. B., Damoiseaux, J. S., Goekoop, R., Barkhof, F., Scheltens, P., Smith, S. M., and Beckmann, C. F. (2009). Model-free group analysis shows altered BOLD FMRI networks in dementia. *Hum. Brain Mapp.* 30, 256–266. doi: 10.1002/hbm.20505

Rozzini, L., Chilovi, B. V., Conti, M., Bertoletti, E., Delrio, I., Trabucchi, M., and Padovani, A. (2007). Conversion of amnestic mild cognitive impairment to dementia of Alzheimer type is independent to memory deterioration. *Int. J. Geriatr. Psychiatry* 22, 1217–1222. doi: 10.1002/gps.1816

Sachdev, P. S., Lipnicki, D. M., Crawford, J., Reppermund, S., Kochan, N. A., Trollor, J. N., et al. (2012). Risk profiles of subtypes of mild cognitive impairment: the Sydney memory and ageing study. *J. Am. Geriatr. Soc.* 60, 24–33. doi: 10.1111/j.1532-5415.2011.03774.x

Schneider, J. A., Arvanitakis, Z., Leurgans, S. E., and Bennett, D. A. (2009). The neuropathology of probable Alzheimer disease and mild cognitive impairment. *Ann. Neurol.* 66, 200–208. doi: 10.1002/ana.21706

Sharpe, J. A., Cheng, P., and Eizenman, M. (2011). Antisaccade generation is impaired after parietal lobe lesions. *Ann. N.Y. Acad. Sci.* 1233, 194–199. doi: 10.1111/j.1749-6632.2011.06178.x

Stephan, B. C. M., Hunter, S., Harris, D., Llewellyn, D. J., Siervo, M., Matthews, F. E., et al. (2012a). The neuropathological profile of mild cognitive impairment (MCI): a systematic review. *Mol. Psychiatry* 17, 1056–1076. doi: 10.1038/mp.2011.147

Stephan, B. C. M., Matthews, F. E., Hunter, S., Savva, G. M., Bond, J., McKeith, I. G., et al. (2012b). Neuropathological profile of mild cognitive impairment from a population perspective. *Alzheimer Dis. Assoc. Disord.* 26, 205–212. doi: 10.1097/WAD.0b013e31822fc24d

Stroop, J. R. (1935). Studies of interference in serial verbal reactions. *J. Exp. Psychol.* 18, 643–662. doi: 10.1037/h0054651

Sweeney, J. A., Rosano, C., Berman, R. A., and Luna, B. (2001). Inhibitory control of attention declines more than working memory during normal aging. *Neurobiol. Aging* 22, 39–47. doi: 10.1016/S0197-4580(00)00175-5

Thulborn, K. R., Martin, C., and Voyvodic, J. T. (2000). Functional MR imaging using a visually guided saccade paradigm for comparing activation patterns in patients with probable Alzheimer's disease and in cognitively able elderly volunteers. *Am. J. Neuroradiol.* 21, 524–531.

Traykov, L., Raoux, N., Latour, F., Gallo, L., Hanon, O., Baudic, S., et al. (2007). Executive functions deficit in mild cognitive impairment. *Cogn. Behav. Neurol.* 20, 219–224. doi: 10.1097/WNN.0b013e31815e6254

Yun, J. Y., Lee, D. Y., Seo, E. H., Choo, I. H., Park, S. Y., Kim, S. G., et al. (2011). Neural correlates of stroop performance in Alzheimer's disease: a FDG-PET study. *Dement. Geriatr. Cogn. Disord. Extra* 1, 190–201. doi: 10.1159/000329517

Zhang, Y., Han, B., Verhaeghen, P., and Nilsson, L.-G. (2007). Executive functioning in older adults with mild cognitive impairment: MCI has effects on planning, but not on inhibition. *Aging Neuropsychol. Cogn.* 14, 557–570. doi: 10.1080/13825580600788118

Conflict of Interest Statement: The authors declare that the research was conducted in the absence of any commercial or financial relationships that could be construed as a potential conflict of interest.

Received: 03 January 2013; accepted: 04 July 2013; published online: 24 July 2013.
Citation: Alichniewicz KK, Brunner F, Klünemann HH and Greenlee MW (2013) Neural correlates of saccadic inhibition in healthy elderly and patients with amnestic mild cognitive impairment. Front. Psychol. ***4****:467. doi: 10.3389/fpsyg.2013.00467*
This article was submitted to Frontiers in Perception Science, a specialty of Frontiers in Psychology.

frontiers in PSYCHOLOGY

ORIGINAL RESEARCH ARTICLE
published: 17 July 2013
doi: 10.3389/fpsyg.2013.00428

Functional and structural brain modifications induced by oculomotor training in patients with age-related macular degeneration

Katharina Rosengarth[1], Ingo Keck[1], Sabine Brandl-Rühle[2], Jozef Frolo[1], Karsten Hufendiek[2], Mark W. Greenlee[1]* and Tina Plank[1]

[1] Institute for Experimental Psychology, University of Regensburg, Regensburg, Germany
[2] Department of Ophthalmology, University Medical Center Regensburg, Regensburg, Germany

Edited by:
Allison B. Sekuler, McMaster University, Canada

Reviewed by:
Frans W. Cornelissen, University Medical Center Groningen, Netherlands
Antony B. Morland, University of York, UK

***Correspondence:**
Mark W. Greenlee, Institute for Experimental Psychology, University of Regensburg, Universitaetsstrasse 31, 93053 Regensburg, Germany
e-mail: mark.greenlee@psychologie.uni-regensburg.de

Patients with age-related macular degeneration (AMD) are reliant on their peripheral visual field. Oculomotor training can help them to find the best area on intact peripheral retina and to efficiently stabilize eccentric fixation. In this study, nine patients with AMD were trained over a period of 6 months using oculomotor training protocols to improve fixation stability. They were followed over an additional period of 6 months, where they completed an auditory memory training as a sham training. In this cross-over design five patients started with the sham training and four with the oculomotor training. Seven healthy age-matched subjects, who did not take part in any training procedure, served as controls. During the 6 months of training the AMD subjects and the control group took part in three functional and structural magnetic resonance imaging (MRI) sessions to assess training-related changes in the brain function and structure. The sham-training phase was accompanied by two more fMRI measurements, resulting in five MRI sessions at intervals of 3 months for all participants. Despite substantial variability in the training effects, on average, AMD patients benefited from the training measurements as indexed by significant improvements in their fixation stability, visual acuity, and reading speed. The patients showed a significant positive correlation between brain activation changes and improvements in fixation stability in the visual cortex during training. These correlations were less pronounced on the long-term after training had ceased. We also found a significant increase in gray and white matter in the posterior cerebellum after training in the patient group. Our results show that functional and structural brain changes can be associated, at least on the short-term, with benefits of oculomotor and/or reading training in patients with central scotomata resulting from AMD.

Keywords: age-related macular degeneration, fMRI BOLD, voxel-based morphometry, cortical plasticity, aging

INTRODUCTION

Age-related macular degeneration (AMD) is among the most common causes for vision loss and blindness in developed countries (Liu et al., 2012). The visual deficit in AMD is characterized by atrophy of photoreceptor cells in the patients' macula resulting in a complete foveal scotoma. As a consequence these patients are forced to develop specific coping strategies concerning their visual loss. Many patients try to compensate for their impaired central vision by using strategies of eccentric viewing to manage daily visual tasks like reading. AMD patients often develop a pseudo fovea at a specific point in their eccentric retina, the so-called "preferred retinal locus" (PRL; Bäckman and Inde, 1979; Timberlake et al., 1987; Whittaker et al., 1988; Guez et al., 1993; Fletcher and Schuchard, 1997). The establishment of a PRL could be regarded as a consequence of an intense, though mostly implicit, form of perceptual learning. It is well-known that perceptual learning can lead to a permanent change in many aspects of visual performance in subjects with intact vision (e.g., Karni and Sagi, 1991; Schoups et al., 1995; Ahissar and Hochstein, 1997; Gilbert et al., 2001; Watanabe et al., 2001; Fahle and Poggio, 2002). Age might play a role here, since older persons might be less efficient in developing a PRL compared to younger persons. In a longitudinal study, Rovner et al. (2009) pointed out that AMD patients relinquish cognitive, physical and social activities due to their visual deficit, leading to an increased risk of cognitive decline. A review study by Mitchell and Bradley (2006) described specific training interventions for AMD patients to ensure a desirable quality of life. An oculomotor training program might be a suitable approach to train AMD patients to establish the best possible area in intact peripheral retina and to efficiently stabilize eccentric fixation (e.g., Bäckman and Inde, 1979; Nilsson et al., 2003; Coco-Martín et al., 2013). Seiple et al. (2005) showed that eccentric reading training in patients with AMD could improve their fixation quality and eye movement control. Such a training-induced improvement might be reflected in corresponding changes on a functional and structural level in the brain. Two recent voxel-based morphometry (VBM) studies in patients with juvenile macular dystrophy Plank et al. (2011)

and in patients with AMD (Hernowo et al., 2013) reported a significant decrease in gray matter volume in the lesion projection zone in the patients' primary visual cortex. Similar findings were demonstrated by Boucard et al. (2009) for patients with AMD or glaucoma.

In this study we investigated in 9 AMD patients with respect to the extent to which improvements in the efficient use of the PRL due to intensive oculomotor training are reflected in functional and structural neural changes. Participants completed an oculomotor training over a period of 6 months and a non-visual sham training (auditory memory training) for another 6 months in a cross-over design. Can oculomotor training improve fixation stability, reading speed and visual acuity in our patients with bilateral central scotoma resulting from AMD? If this is the case such training should also impact on the quality of these patients' everyday lives. In this study we examined how such behavioral changes correlate with functional and structural neural changes. In an fMRI study the patients' PRL and an untrained area in the opposite hemifield (OppPRL) were stimulated using either natural images of everyday objects or checkerboard stimuli. We expected to find an increase in the BOLD signal with oculomotor training effects in the PRL projection zone, but not in the projection zone of the untrained hemifield. In another fMRI study in our lab, where patients with hereditary retinal dystrophies performed a visual search task (Plank et al., 2012), we found that BOLD responses in early visual cortex were significantly up-regulated in patients with stable eccentric fixation in comparison to patients with unstable fixation. Since patients vary with respect to their success in the oculomotor training, we also expected to find a positive correlation between the change in fixation stability and the training-induced change in BOLD signal in visual cortex. Additionally anatomical scans were acquired in each MRI session to determine structural changes, where an increase in gray and white matter would reflect a positive consequence of successful fixation training.

METHODS

PATIENTS AND CONTROL SUBJECTS

Nine patients with diagnosed AMD and seven age-matched controls participated in the study. All participants signed an informed consent form prior to the participating in the study and they received modest monetary compensation for their participation. The study was approved by the Ethical Committee of the University of Regensburg and conducted in accordance to the ethical guidelines of the Declaration of Helsinki.

OPHTHALMOLOGIC METHODS AND EXAMINATIONS

The initial ophthalmologic examination included mydriatic fundus camera imaging as well as fundus autofluorescence (FAF) and infrared reflection (IR) imaging of the macular pathology (for examples see **Figure 1**). Before each fMRI visit, microperimetry and non-mydriatic fundus imaging were performed including either IR or, in selected cases, FAF.

Both IR and FAF imaging were conducted using the Spectralis Heidelberg Retina Angiograph 1 (Heidelberg Engineering, Heidelberg, Germany) confocal laser-scanning ophthalmoscope (cSLO).

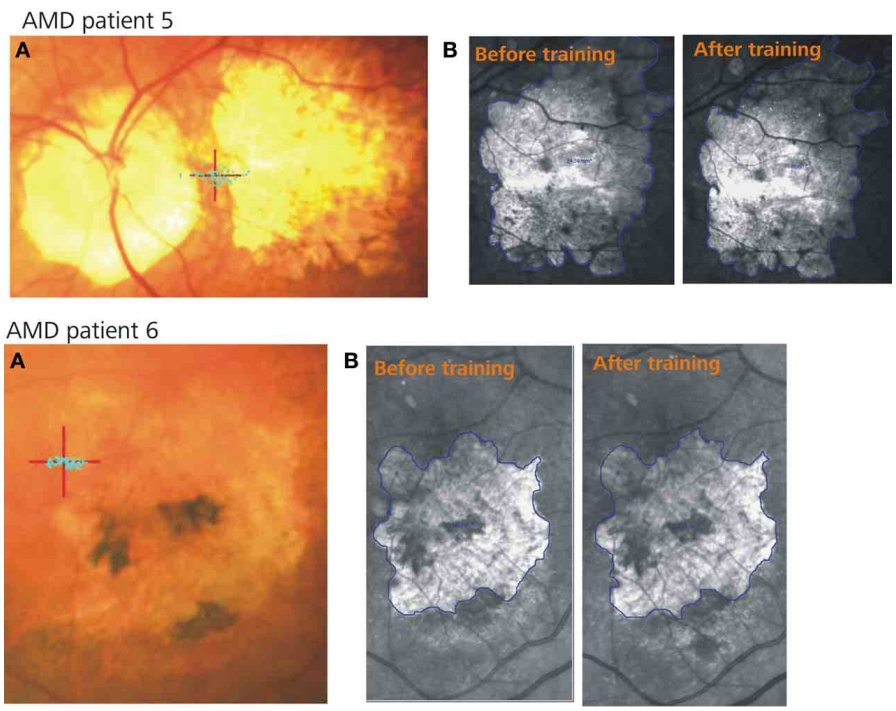

FIGURE 1 | Two example patients. (A) Shows the PRL (red cross) and the fixation stability (blue dots) after training, **(B)** represents the infrared images of the retina including the scotoma (blue lines) before (left) and after (right) training.

IR imaging is a variation of fundus photography using infrared light instead of white light or spectral colors for illumination. The infrared light penetrates unclear media better than white light, which is an advantage when imaging patients with cataracts. Since reflectance increases with wavelength, near infrared wavelengths have a better fundus reflectance than wavelengths from the visible spectrum and lead to deeper light penetration into the retina. IR imaging with SLO technology provides high contrast and allows for assessment of pathologies reaching into the extreme outer layers of the retina and the choroid. FAF is a well-established technique for the detection of alterations of the retinal pigment epithelium (RPE) based on changes of lipofuscin distribution in RPE cells. In geographic atrophy, the lost tissue is marked by hypofluorescence due to the loss of fluorophores, typically surrounded by a hyperfluorescent rim with accumulation of fluorophores. This aspect facilitates precise area measurement of the retinal lesions. The progression of geographic atrophy was measured by comparing a baseline IR or FAF image with one made at last visit. Mean follow-up was 14.7 months (range 7–20 months). On IR images, the area of atrophy was selected manually before calculating the size in mm^2 with graphical software. The size of the atrophic area on the FAF images was calculated with the Region Finder software tool.

CLINICAL CHARACTERISTICS AND VISUAL FIELD MEASUREMENTS

Table 1 presents details on demographic characteristics of patients and controls, including the gender, age, duration of disease at time of study, scotoma size, and position of PRL in the visual field.

Scotoma size was measured using kinetic Goldmann perimetry with the isopters III/4e, I/4e, I/3e, I/2e, and I/1e. Defined as edges of the scotomata, those points were marked, where isopter III/4e were no longer detected. Scotoma size is reported in **Table 1** as scotoma diameter in degrees of visual angle as an average of vertical and horizontal dimensions. Controls did not undergo Goldmann perimetry. Visual acuity, fixation stability, and reading speed were measured before, during and after training to indicate improvements induced by training.

Table 1 | Demographic characteristics of AMD patients (AMD 1-AMD 9) and matched controls (C 1–C 7) referring to their gender, age, duration of disease, scotoma size, study eye and location of the PRL in patients' visual field.

Subject	Gender	Age	Duration of disease (in years)	Scotoma size (diameter in degrees)	Position of PRL in visual field	Study eye
AMD 1	Male	55	3	15	Left	OD
AMD 2	Male	62	5	20	Left	OS
AMD 3	Female	70	2	15	Lower	OD
AMD 4	Female	80	15	10	Left	OS
AMD 5	Male	63	4	10	Left	OS
AMD 6	Male	79	8	15	Left	OD
AMD 7	Female	84	6	15	Lower	OS
AMD 8	Female	81	21	10	Lower	OS
AMD 9	Female	71	10	10	Right	OS
C1	Female	51				OD
C2	Female	62				OS
C3	Female	72				OD
C4	Male	83				OS
C5	Female	64				OS
C6	Female	78				OD
C7	Male	71				OS

Best-corrected visual acuity was determined by using a Vision Screener (Rodenstock Rodavist 524/S1) and Eye Charts for distant (Oculus Nr. 4616) and near visual acuity (Zeiss/Frohnhäuser). For the patient group the dominant eye was chosen as the study eye, for the controls the same eye as that used by their age-matched patient was chosen as the study eye.

We used a Nidek MP-1 microperimeter (Nidek Co, Japan) to measure fixation stability. Patients were requested to fixate (eccentrically) a red cross of 4 degrees visual angle in diameter for approx. 30 s, whereas controls fixated the target with their fovea. The technique measures 25 samples per second, resulting in 750 fixation samples over 30 s. During the measurement the camera sometimes lost track of the subject's eye. This can be due to eye blinks or fixation instability in the form of large saccades. The Nidek software records the time period that was measured and the proportion of the time span that was effectively tracked, as well as the percentages of fixation points that fell in a range of 2° or 4° diameter visual angle around the center of the fixation target, based on the time spans effectively tracked. Thus, fixation stability can be overestimated by long or frequent time spans where the camera had lost track of eye position due to large saccades. To compensate for this we corrected the given fixation stability in the following way (see Plank et al., 2011): first we calculated the mean time span for which the camera lost track of eye position in the normally sighted control group, who fixated with their fovea. The resulting mean value of 13 s ($SE = 10.3$ s) yielded an estimate of the time that could be attributed to eye blinks. In a second step we subtracted this amount from the measured time, in which the camera had lost track of the eye in the patient's group. The difference between the measured time remaining and the effectively tracked time we attribute to large saccades. This time span was added to the effectively tracked time. On this basis we recalculated the percentages of fixation points falling in a range of 2° visual angle around the target.

To measure reading speed patients read aloud a continuous text for 3 min, which was recorded. We then counted the number of words read and calculated the mean of words read per minute. All participants read the same text, taken from a book [German translation of Doris Lessing (2003): The Grandmothers], but different passages of the same book at each session, printed on a sheet of paper (font: Arial, font size: 10 pt, single spaced). Patients used magnification glasses customized to their needs. The same magnification was used for all reading test sessions, except for one session of patient AMD 9 (session "memory 1" conducted 3 months after the completion of the oculomotor training), who needed greater magnification in that session due to some minor disease progression.

To assess the patients' own perception of their visual function before and after eccentric viewing training

we used the National Eye Institute's Visual Function Questionnaire (VFQ-25; Mangione et al., 2001) in its German translation.

TRAINING PROCEDURE

The training procedure was implemented as a crossover design consisting of two parts, with an average duration of 6 months each. One part was a direct training of the PRL, the other part was a pseudo-training in the form of an auditory memory training. Participating patients completed both parts, half of the patients started with the direct training of the PRL, the other half with the pseudo-training. Patients were randomly assigned to one of the two groups.

DIRECT TRAINING OF PRL

To train the patients to establish, uphold and stabilize eccentric fixation we used techniques described by Bäckman and Inde (1979), Nilsson and Nilsson (1986), Nilsson et al. (2003), Gustafsson and Inde (2004), Seiple et al. (2005), Kasten et al. (2010). All training was conducted with one eye only, the chosen study eye (see **Table 1**), while the other eye was patched. In an initial phase we used the computer program Xcentric Viewing as described by Kasten et al. (2010), applying the program parts as recommended. At first we determined a prime viewing position in the peripheral visual field that was determined to be the best position for the patient's PRL. While the patient was asked to fixate the center of the screen, marked by crosshairs, at several positions in the peripheral visual field single letters and short words were presented in different sizes. The patient gave feedback about the readability of those stimuli and thus the best position was determined for training. Three patients (AMD 1, 6, and 9) did not have distinct regions on the peripheral retina that they used for viewing in daily life prior to training, so that a new "PRL" had to be determined. One patient (AMD 5) had some preference for directing his gaze to see eccentrically, but was retrained to a slightly different retinal location since the new "PRL" provided better reading performance. Five patients (AMD 2, 3, 4, 7, and 8) of our sample had already chosen a certain area as their PRL that also turned out to be the best peripheral region to train. During training the therapist (author Sabine Brandl-Rühle) presented letters, digits, words, and running text in different sizes at the chosen PRL. The font size was decreased and the word length increased in dependence of the individual improvements of the participants. Additionally the patients were asked to train their eccentric fixation in a similar manner at home (for a time spans of 10 min several times a day), using a simplified version of the software. Adequate optical magnification was provided. When the patients were able to read long words in small font size on the computer screen, the training passed on to reading printed text. As described by others, e.g., in Bäckman and Inde (1979), Nilsson et al. (2003), Gustafsson and Inde (2004), and Kasten et al. (2010), patients were trained to use the "moving text" technique with the aid of optical lenses and fixation lines. Subsequently, the patients were trained to exert oculomotor control using eye movement tasks as described in Seiple et al. (2005). Participants practiced executing visually-guided saccades with their PRL, starting with small horizontal saccades between simple stimuli like dots, passing on to larger saccades, horizontally as well as in a clockwise manner, while viewing more complex stimuli like single letters or two- to three-letter words. The training paradigms were implemented as described in Seiple et al. (2005), using the software Presentation (Neurobehavioral Systems) as well as a simplified version, implemented in C++ for use at home. Accordingly, patients were asked to practice the tasks at home for a recommended time span of 15–20 min daily. Eye movements and fixation stability were monitored using a video eyetracker (High Speed Video Eyetracker Toolbox, Cambridge Research Systems, UK) throughout the training whenever the computer-based training protocols were in use.

Twelve regular training sessions were scheduled over a 6-month period. Training sessions were more densely timed at the beginning of the training with weekly sessions to accompany the initial stabilization process of the more efficient eccentric viewing, while they were more spread out (at intervals of 2–3 weeks) at the end of the training schedule when patients already had established their PRL. Patient AMD6 had no computer at home, therefore he trained 1 h twice a week with the therapist instead of home training. Patient AMD7 had only 6 sessions with the therapist and practiced more at home due to the long distance between her home and the clinic.

SHAM-TRAINING

As sham-training for a further period of 6 months patients completed an auditory memory training (in German, *Gedächtnistraining für blinde Senioren, Memory training for the elderly blind*; Bernard, 2000), provided on audio-CDs. Participants were asked to complete two training units a week for about 10 min each. Participants were also asked to fill in questionnaires related to the memory exercises and to repeat training units as needed.

TRAINING SCHEDULE AND fMRI MEASUREMENTS

Direct training of the PRL and pseudo-training were accompanied by fMRI sessions as described above. Functional MRI measurements were repeated five times during the entire period of fixation and sham training. In a crossover design fixation training was either preceded by or followed by such sham training to control for placebo effects.

Due to vacation or critical life events, intervals between single sessions were sometimes longer, but they never exceeded 5 months. AMD1 suffered a minor stroke between session 4 and 5 (during auditory memory training phase), but recovered fully. For AMD5 only the PRL was stimulated in session 1, not the OppPRL, because it was not possible to determine the position of the PRL in relation to the fovea precisely. Therefore, an additional fMRI session was conducted 7 weeks after the first session and 7 weeks before the second session. For AMD8 the hourly fMRI sessions were split in pairs of 30-min sessions, completed on two different days, in each case not more than 2 days apart from each other, due to fatigue reported by the patient during hour-long sessions.

STIMULI AND PROCEDURE

The functional MRI measurements consisted of retinotopic mapping paradigms and a direct stimulation of patients' PRL. Here we primarily report the results of the direct stimulation of the patients' PRL and of a comparably peripheral area in the opposite hemifield (OppPRL) with flickering checkerboards and meaningful pictures of everyday objects. Additionally meridian mapping was employed to functionally determine the locations of visual areas V1, V2, and V3 for each participant. Visual stimuli were projected onto a circular screen (31° visual angle in diameter at a distance of 60 cm) placed behind the head of the participant at the end of the scanner bore and visible via a mirror placed within the MRI head coil. All visual sequences were presented with the software Presentation (Neurobehavioral Systems Inc.) and triggered by the scanner signal upon onset of volume acquisition. As in behavioral testing, the participants conducted all paradigms monocularly with their study eye, the other eye was patched during the measurement. All participants had to fixate at the center of the screen during all tasks. Controls fixated foveally a central fixation target (the letter "X"). For patients with central visual field scotomata we presented auxiliary stimuli to ensure fixation. These auxiliary stimuli were adapted to the individual needs of the patients depending on how well they could consciously perceive their scotoma and/or how well they were accustomed to fixate with their PRL. The auxiliary stimuli consisted of four red dots (one about 0.7° visual angle in diameter) positioned at the edges of the respective scotoma and/or the fixation target (letter "X") at the position of the PRL (see **Figure 2**). The fixation target was located at a position in the visual field that corresponded to the PRL and was adapted in size to the needs of the patients (between 0.95° and 2.1° visual angle). The positioning of the auxiliary stimuli on the screen and the direction of gaze was controlled prior to scanning by using a video eyetracker (MREyetracker, Cambridge Research Systems, UK) under comparable viewing conditions as during fMRI.

MERIDIAN MAPPING

In this paradigm we measured the cortical responses to the presentation of a pair of collinearly aligned wedges consisting of flickering checkerboards that were positioned at either the horizontal or vertical meridian with the goal to identify the borders of the retinotopic areas V1, V2, and V3 (DeYoe et al., 1996; Beer et al., 2009), as described in Plank et al. (2012). Black (1 cd/m^2) and white (330 cd/m^2) checkerboard stimuli with a flicker rate of 8 Hz were presented sequentially, covering the horizontal and vertical meridian, on a gray background of mean luminance in a block design together with a baseline condition of mean luminance. The blocks were presented over eight cycles, each cycle consisting of flickering checkerboards for 19 s and a blank baseline condition for 18 s. Auxiliary stimuli and fixation target were visible throughout the stimulation. The representations of the horizontal and vertical meridians on the visual cortex were then identified by computing the contrast between the horizontal and vertical meridian conditions. Vertical meridian representations marked the borders between V1 and V2, and horizontal meridian representations marked the borders between V2 and V3. The borders between dorsal and ventral regions within the same visual

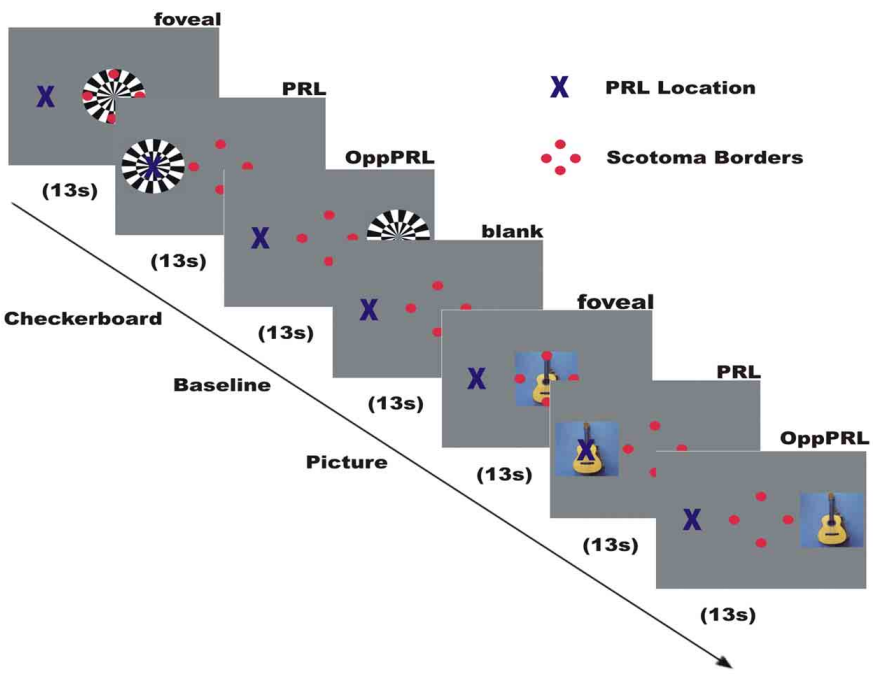

FIGURE 2 | Illustration of the time course of a typical run in an fMRI session. Direct stimulation was conducted in the fovea, the PRL, and the opposite PRL either with checkerboard or images of everyday objects. Blue cross marks the preferred retinal locus of fixation in the AMD patient. The 4 red dots were positioned at the scotoma rim and aided stable fixation.

area were set at the midline of the representation of the horizontal meridian coinciding with the calcarine sulcus.

DIRECT STIMULATION OF PRL

In this paradigm we stimulated the PRL of the patients directly, as well as a comparable peripheral area in the opposite hemifield (OppPRL) and the central area in the visual field with flickering checkerboards and pictures of everyday objects. By this means we wanted to identify possible differences in the projection zones for the PRL and OppPRL in the visual cortex in response to meaningful (pictures of everyday objects) and not meaningful, abstract (checkerboards) stimuli. The participants were instructed to view the stimuli and try to recognize the objects presented in the pictures. Stimuli in this paradigm were either a disk of black and white checkerboards (size: 9° × 9° visual angle) presented with a flicker rate of 8 Hz or chromatic images of natural objects (e.g., animals, tools, vehicles, musical instruments; 7.3° × 7.3° visual angle). Overall 72 different pictures were presented in each session in a random order. The photographs were collected from free Internet databases or taken by the authors. Stimuli were presented blockwise on a gray background, together with a baseline condition (gray background of medium luminance). The blocks were presented in four repetitions, the sequence of one repetition is depicted in **Figure 2**. Flickering checkerboards and meaningful pictures were presented in blocks of 13 s each, the baseline condition (blank screen) in blocks of 18 s. In a block with meaningful pictures the picture changed every 2.2 s without a gap, so that six different pictures were presented sequentially in each object block. In each block one of three positions in the visual field was stimulated: center, PRL or OppPRL. The exact location of PRL was determined individually. As OppPRL we used comparable coordinates in the opposite hemifield. Auxiliary stimuli and the fixation target were visible throughout the stimulation.

MAGNETIC RESONANCE IMAGING

Image acquisition was conducted on a 3T head scanner (Allegra Siemens, Erlangen, Germany).

Functional images were acquired using a T2*-weighted gradient echo-planar imaging (EPI) sequence ($TR = 2$ s, $TE = 30$ ms, 34 slices, FoV = 192 × 192 mm², flip angle = 90°, 3 × 3 × 3 mm³ voxel size). The axial slices were oriented parallel to the plane connecting the anterior and posterior commissure and covered the whole brain. Two dummy scans at the beginning of each measurement were removed automatically from the data set. Additionally a high-resolution T1-weighted image was acquired before training, during training and after training of fixation stability. We used a modified version of the MP-RAGE (3D magnetization prepared rapid gradient echo) sequence from "The Alzheimer's Disease Neuroimaging Initiative" (Jack et al., 2008). We obtained 160 slices with a resolution of $1 \times 1 \times 1\,mm^3$ using a FOV $= 256 \times 256\,mm^2$. The TR was 2250 ms, the TE 2.6 ms and the flip angle 9°. Functional T2* weighted images were also acquired before, during and after training. This resulted in five scanning sessions in total: the patient group that started with the oculomotor training had one session before any training, one session during training and one after training. Only one patient (AMD 5) was measured one additional time during training. Further two sessions were completed while the patients underwent sham training (auditory memory training). The group that started with the sham training had two sessions while conducting the sham training, subsequently one session before the start of the oculomotor training, one session during oculomotor training and one session after oculomotor training.

MRI DATA ANALYSIS

MRI data analysis was performed as described in Plank et al. (2012) and as is summarized below.

ANALYSIS OF FUNCTIONAL DATA

Cortical reconstruction

The T1-weighted structural image obtained from each subject was reconstructed by Freesurfer version 4.1 (Martinos Center for Biomedical Imaging, Charlestown, MA) as described in Beer et al. (2009, 2011). The cortical reconstruction procedure included the removal of non-brain tissue with a hybrid watershed/surface deformation procedure (Segonne et al., 2004), correction for intensity non-uniformities (Sled et al., 1998), and automatic transformation into Talairach space. After segmentation of the subcortical white matter and deep gray matter volumetric structures (Fischl et al., 2002, 2004), the gray-white matter boundary was tessellated and topologic inaccuracies automatically corrected (Fischl et al., 2001; Segonne et al., 2007). The surface was then deformed following intensity gradients to optimally place the gray/white and gray/cerebrospinal fluid borders at the location where the greatest shift in intensity defines the transition to the other tissue class (Dale et al., 1999; Fischl and Dale, 2000). Once the cortical models were complete, the cortical surface was inflated (Fischl et al., 1999a), registered to a spherical atlas which utilized individual cortical folding patterns to match cortical geometry across subjects (Fischl et al., 1999b), and automatically parcellated into units based on gyral and sulcal structures (Fischl et al., 2004; Desikan et al., 2006). Finally we created an occipital flat patch of the inflated surface posterior to the sylvian fissure (cut along the calcarine sulcus).

PREPROCESSING OF FUNCTIONAL DATA

Data analysis was performed with the FS-Fast tools of Freesurfer. Pre-processing steps included motion correction (Cox and Jesmanowicz, 1999), co-registration to the anatomical image acquired in the same session, smoothing with a Gaussian kernel of 5 mm FWHM and correction for intensity non-uniformities (Sled et al., 1998). Additionally, the first volume of each session was automatically co-registered to the structural volume and manually verified (and corrected) using visual ("blink") comparison.

STATISTICAL DATA ANALYSIS AND ROI LABELING

To obtain functional estimates of the anatomical borders between visual areas V1 and V2 as well as between V2 and V3 we contrasted conditions of horizontal meridian representations with vertical meridian stimulations (see also Beer et al., 2009). Statistical parametric maps were calculated based on the general linear model using the stimulation blocks convoluted with a cumulative gamma function (with parameters: delta = 2.25; tau = 1.25; alpha = 2) as predictors. Additionally, linear and

cubic predictors (modeling slow signal drifts) and motion correction parameters were added to the design matrix. Significance maps for each contrast were then overlaid on the flattened cortical surface of each individual hemisphere. On these flat maps, the borders between dorsal and ventral parts were set at the midline of the representation of the horizontal meridian coinciding with the calcarine sulcus, the borders between V1/V2 and V2/V3 were set at the midline of the representations of the vertical and horizontal meridian, respectively. The obtained ROIs V1d/v, V2d/v, V3d/v of each hemisphere were used for the subsequent ROI analysis. Visual areas V1, V2, and V3 could not be determined in one participant (control subject, C3) due to low levels of BOLD response. Anatomical ROIs for associated visual areas lateral occipital cortex (LOC), fusiform gyrus and inferior temporal gyrus, especially involved in object recognition and face perception (e.g., Grill-Spector et al., 1999; Grill-Spector, 2003; Nagy et al., 2012), were determined by using the automatic parcellation of the cortical surface provided by Freesurfer (aparc.annot; Desikan et al., 2006). A threshold of 0.5 was applied to determine the minimum fraction of a voxel's volume that must be filled with surface points of a ROI so that the voxel would be included in that ROI. A threshold of 0.5 assures that a voxel cannot belong to more than one ROI. **Table 2** shows the mean sizes of the ROIs for both hemispheres for the patient and control group over all sessions. The sizes of the ROIs V2d ($p = 0.03$) und V3v ($p = 0.007$) of the left hemisphere, as well as V1v ($p = 0.03$), V2d ($p = 0.04$) and V3v ($p = 0.02$) of the right hemisphere showed significant differences between patients and controls (see **Table 3**).

Table 2 | Sizes of ROIs, given in mean number of functional voxels ($3 \times 3 \times 3\,mm^3$) in the patient group and control group, together with their respective standard errors (SE) for the left and right hemisphere of dorsal (d) and ventral (v) parts of visual areas V1, V2, and V3, as well as for fusiform gyrus, inferotemporal gyrus (ITG) and lateral occipital cortex (LOC).

ROI	Left hemisphere		Right hemisphere	
	Size	SE	Size	SE
PATIENTS				
V1d	40.93	2.07	31.64	2.49
V1v	38.64	3.06	28.78	2.35
V2d	44.51	4.54	32.82	3.09
V2v	31.58	2.41	34.64	3.69
V3d	40.18	3.14	36.67	2.79
V3v	26.11	1.46	25.82	1.54
Fusiform gyrus	96.18	4.26	84.40	3.92
ITG	97.60	3.48	102.53	4.84
LOC	183.78	9.47	173.22	6.35
CONTROLS				
V1d	49.67	2.84	51.63	4.15
V1v	45.67	2.14	50.07	3.01
V2d	98.85	8.09	66.33	6.14
V2v	44.56	3.06	47.67	3.40
V3d	72.11	6.21	52.81	1.98
V3v	41.41	1.73	43.48	2.69
Fusiform gyrus	94.94	3.70	86.81	4.60
ITG	106.91	5.73	98.84	2.73
LOC	206.19	7.11	205.12	7.77

VOXEL-BASED-MORPHOMETRY

For data analysis the S(statistical) P(parametric) M(mapping)8 (Wellcome Department of Imaging Neuroscience Group, London, UK; http://www.fil.ion.ucl.ac.uk/spm) software package was used. To investigate longitudinal changes in gray and white matter density due to fixation training we applied the Dartel toolbox (Diffeomorphic Anatomical Registration Through Exponentiated Lie Algebra) implemented in SPM8 (Ashburner, 2007). Before any further analysis the origin of the structural images was set to the anterior-posterior commissure

Table 3 | Results of repeated-measures ANOVAs (significant main effects and interactions) with the three within-subject factors "sessions" (before, during, after training), "kind of stimulation" (flickering checkerboards vs. pictures of everyday objects) and "location of stimulation" (PRL vs. OppPRL) and the between subject factor "group" (patient vs. control) with respect to the dependent variable "percent signal change."

	Main effects	Interactions
ROI		
V1	None	Session × location of stimulation [$F_{(4, 44)} = 4.21$; $p = 0.006$]
V2	Session [$F_{(2, 22)} = 4.34$, $p = 0.026$] Group [$F_{(1, 11)} = 5.54$; $p = 0.038$]	Session × location of stimulation [$F_{(4, 44)} = 3.94$; $p = 0.008$] Kind of stimulation × location of stimulation [$F_{(2, 22)} = 4.98$; $p = 0.016$] Location of stimulation × group [$F_{(2, 22)} = 4.10$; $p = 0.031$]
V3	Session [$F_{(2, 22)} = 4.28$, $p = 0.027$] Group [$F_{(1, 11)} = 5.46$; $p = 0.039$]	Session × location of stimulation [$F_{(4, 44)} = 4.23$; $p = 0.006$] Location of stimulation × group [$F_{(2, 22)} = 4.90$; $p = 0.017$]
Fusiform gyrus	Kind of stimulation [$F_{(1, 12)} = 33.36$, $p < 0.001$] Group [$F_{(1, 12)} = 10.35$; $p = 0.007$]	Kind of stimulation × location of stimulation [$F_{(2, 24)} = 5.12$; $p = 0.014$] Location of stimulation × group [$F_{(2, 24)} = 3.92$; $p = 0.034$]
ITG	Kind of stimulation [$F_{(1, 12)} = 9.924$, $p = 0.008$]	None
LOC	Kind of stimulation [$F_{(1, 12)} = 10.59$, $p = 0.007$] Location of stimulation [$F_{(2, 24)} = 9.45$, $p = 0.001$]	Session × location of stimulation [$F_{(4, 48)} = 2.88$; $p = 0.032$] Location of stimulation × group [$F_{(2, 24)} = 10.01$; $p = 0.001$]

The ANOVAs were conducted separately for visual areas V1, V2 and V3 as well as for fusiform gyrus, inferotemporal gyrus (ITG) and lateral occipital cortex (LOC).

manually. Within every subject its T1-weighted structural scans from the three sessions were spatially realigned to the first image with SPM8 (realignment options were: Quality 0.9, Separation 4, Smoothing (FWHM) 5, Num Pass Register to first and Interpolation 2nd degree B-spline). Then the new segment toolbox in SPM8 was used to generate gray matter-, white matter- and cerebral spinal fluid CSF-images from each one of the realigned structural scans using a very light bias regularization (0.0001) and a bias FWHM cutoff of 60 mm. No cleanup of the resulting images was performed to avoid the accidental remove of important information. The warping regularization parameter was set to 4, the affine registration was made to the ICBM space template - European brains and the sampling distance was set to 4. With the help of the DARTEL-Toolbox from SPM8, in a first step a group-template (patient or control, respectively) and corresponding flow-fields for every subject were calculated from the segmented images within the group control and patient. We decided to generate different separate templates for each group to avoid that group-specific differences are diminished during this process. The parameters for this setting were as follows: Regularization form: linear elastic energy, six outer iterations with the following respective settings for inner iterations, registration parameters, time steps and smoothing parameter: (3, [4, 2, 1e-6], 1, 16), (3, [2, 1, 1e-6], 1, 8), (3, [1, 0.5, 1e-6], 2, 4), (3, [0.5, 0.25, 1e-6], 4, 2), (3, [0.25, 0.125, 1e-6],16, 1), (3, [0.25, 0.125, 1e-6], 64, 0.5). The optimization settings were: 0.01 for the LM regularization, 3 cycles, and 3 iterations. The segmented images of each subject were then normalized to the MNI space based on the flow-fields and the corresponding group template that were generated in the first DARTEL step. This was done with the "Normalize to NMI Space" module of the DARTEL toolbox. The spatially normalized images were then modulated with the Jacobi determinants of the deformations to preserve the signal amount in the images. Finally, the resulting images were smoothed with an 8-mm FWHM Gaussian kernel.

For statistical analysis two general linear models were constructed, for white and gray matter, respectively. Using the factorial design specification batch in SPM8, the "full factorial" design was selected in both cases, with the only factor being controls vs. patients. We assumed independence and unequal variance for both model specifications. Level one and level two in the design were the smoothed, normalized gray, and white matter likelihood maps for the controls and the patients, respectively, with each of the three sessions in ascending order. In an additional covariate we tried to capture the training effect by setting their values to "1", "2", and "3" for the first, second, and third sessions, while applying an overall mean centering for all subjects. Finally, for explicit masking we used the brainmask.nii image provided by SPM8. To assess group effects or differences one and two sample *t*-tests were conducted. Only clusters surviving a statistical threshold of less than 0.0001 (uncorrected for multiple comparisons) on voxel level and less than 0.05 [(F)false (D)discovery (R)rate corrected] on cluster level are supposed to be significant and are reported. Significant clusters are visualized on a volume-based standard brain from a single normal subject (ch2.nii.gz), using the software MRIcron (Rorden and Brett, 2000; http://www.nitrc.org/projects/mricron).

RESULTS

FIXATION STABILITY

Changes in fixation stability were assessed with the Nidek MP-1 microperimeter (Nidek Co, Japan) as described in the methods section. **Figure 3** shows an example of the development of fixation stability in one patient (AMD2) from before training, after 3 months training and after 6 months training. The left and middle columns show the distribution of fixation samples around the target, with the middle column additionally giving percentages of fixation samples falling in a range of 2° or 4° diameter visual angle around the target. We used the percentages of fixation points that fell in a range of 2° diameter visual angle around the center of the target as measure for fixation stability, in this patient (AMD2) increasing from 43% before training to 100% after training. The right column in **Figure 3** gives the respective time profile of the first 10 s of fixation, which also improved substantially for patient AMD2 over the training period of 6 months. **Figure 4** gives an overview of the mean development in fixation stability for all nine AMD patients. To assess immediate training effects of the eccentric viewing training, fixation stability data in **Figure 4** was pooled across the group that started with the auditory memory training and the group that started with the eccentric viewing training for the three sessions immediately "before training," "during training," and "after training" ($n = 9$), with the session "during training" and "after training" on average 3 months or 6 months after the start of the training, respectively. AMD5 had an additional measurement of fixation stability 7 weeks after the start of the oculomotor training (fixation stability of 82% within 2° degrees around target), not shown in **Figure 4**. The two remaining sessions, in which both groups completed the auditory memory training, were analysed separately for the group that started with the auditory memory training (sessions "memory before 1" and "memory before 2"; $n = 5$) and for the group who did the auditory memory training after the eccentric viewing training (sessions "memory after 1" and "memory after 2"; $n = 4$, patient AMD9 has, at the time of submission, not yet completed the last session "memory after 2").

Fixation stability of normally sighted controls was measured once yielding to values between 97 and 100%.

We conducted a repeated-measures ANOVA with the within-subject factor "session" (before, during, after) and the between-subject factor "training group" (oculomotor first, memory first). The analysis yielded a significant main effect "session" [$F_{(2,\ 14)} = 6.54$; $p = 0.01$]. Pair-wise comparisons showed a significant difference between the session "before" and "during" training ($p = 0.04$). The main effect "training group" and the interaction "session" × "training group" were not significant ($p > 0.05$).

Both training groups showed no significant differences in fixation stability between the two sessions conducted during auditory memory training (all $p > 0.05$).

READING SPEED

For measuring reading speed patients read aloud a continuous text for 3 min, which was recorded. We then counted the number of words read and calculated the mean number of words read per minute, as described in the methods section. Both patients (1.05/min) and controls (0.48/min) did not make more than one

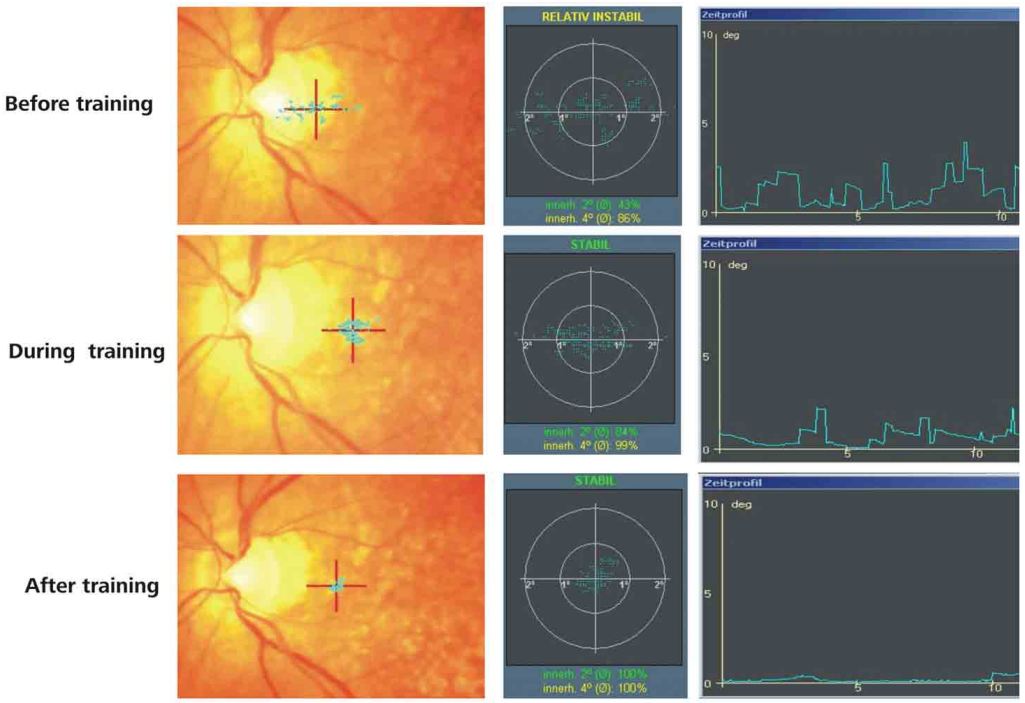

FIGURE 3 | Results of microperimetry and fixation stability measurements. An example is given for the development of fixation stability over training in a typical AMD Patient. The PRL is located at the red cross. The blue dots represent individual fixations and their spatial variability reflects fixation stability. An improvement in fixation stability can be observed over the training period in this patient.

reading error per minute on average, leading us to exclude reading error rates in further analyses. Controls completed only one reading test (mean reading speed 127 words per minute; $SE = 4.99$). Mean values of reading speed for the patients were calculated in the same way as described for fixation stability over five sessions (AMD9 has not yet completed session 5) and depicted in **Figure 4**. We conducted a repeated-measures ANOVA with the within-subject factor "session" (before, during, after) and the between-subject factor "training group" (oculomotor first, memory first). The analysis yielded a significant main effect "session" [$F_{(2,\ 14)} = 5.2$; $p = 0.020$]. The main effect "training group" and the interaction "session" × "training group" were not significant ($p > 0.05$).

Both training groups showed no significant differences in reading speed between the two sessions conducted during auditory memory training (all $p > 0.05$).

VISUAL ACUITY

Near and distant visual acuity were assessed at two time points—before the start and after completion of eccentric viewing training, as described in the methods section. **Figure 5** shows the mean development of visual acuity over those two time points for all nine AMD patients. A significant increase can be seen in near visual acuity [$t_{(8)} = 2.66$; $p = 0.029$].

VISUAL FUNCTION QUESTIONNAIRE

Figure 6 shows the obtained mean values of the subscales of the Visual Function Questionnaire (VFQ-25; Mangione et al., 2001), as collected from seven patients (for AMD1 and AMD2 did not complete the questionnaires). Three subscales (near activities, $p = 0.014$; vision specific: mental health, $p = 0.047$; vision specific: dependency, $p = 0.046$) showed significant improvements in one-sided t-tests.

fMRI ANALYSIS

BOLD signal in V1, V2, and V3 while directly stimulating PRL and OppPRL

In this analysis we were interested in the BOLD responses when the PRL and a comparably peripheral area in the opposite hemifield, the OppPRL, were directly stimulated. We compared activation in the respective projection zones of the PRL and the OppPRL in the visual cortex, namely visual areas V1, V2, and V3. We also compare these activations to those evoked by stimulation in the fovea (scotomatous region in patients). Accordingly, for the group of patients with the PRL in the lower visual field and their respective controls, we considered BOLD activation in the dorsal portions only, pooled over both hemispheres, as the PRL projection zone, and ventral portions only as the OppPRL projection zone, also pooled over hemispheres. For the patients with the PRL in the left visual field and their respective controls, we considered BOLD activation in the right hemisphere only as the PRL projection zone and BOLD activation in the left hemisphere only as the OppPRL projection zone, pooled over dorsal and ventral portions. For the patient with her PRL in the right visual field and her control, we considered BOLD activation in the left hemisphere only for the PRL projection zone and in the right hemisphere

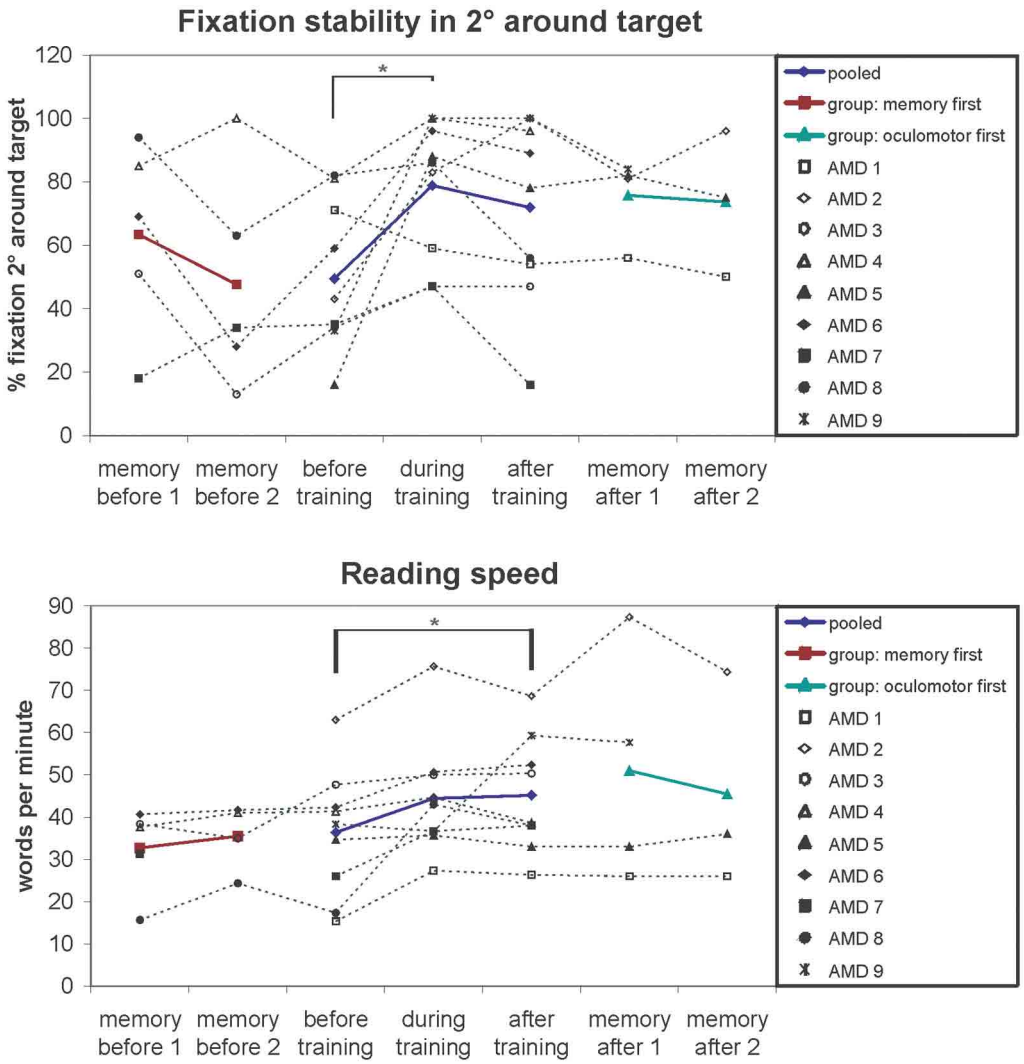

FIGURE 4 | Fixation stability (% fixation around 2 degrees of target) and reading speedfor the successive measurements periods depicted for individual patients (symbols, connected by dotted lines) and group means (colored lines). The results show improved fixation stability after training (significant main effect of session $p = 0.01$). Pairwise comparisons show a significant increase in fixation stability after on average 3 months of training ($p = 0.04$). The memory training has no effect on fixation stability regardless of whether memory training was performed before (memory first $p = 0.29$) or after fixation training (memory after $p = 0.93$), ruling out non-specific placebo effects. A similar pattern can be observed for the reading speed. Reading speed increases over the 6 months of training (significant main effect of session $p = 0.02$). Auditory memory training had no effect on reading speed regardless of whether memory training was performed before (memory first $p = 0.41$) or after fixation training (memory after $p = 0.57$).

only for the OppPRL projection zone, again pooled over dorsal and ventral portions. We computed % signal change of the BOLD signal for each condition (stimulation with flickering checkerboards or pictures of everyday objects at the PRL or OppPRL) and session, each as the difference to baseline. **Figure 7** shows the mean % signal change values as a difference to baseline for all conditions and the sessions "before," "during" and "after training," for the patient and control group, respectively. The data from one patient (AMD 7) was excluded from this analysis, because she showed strongly negative BOLD responses.

We computed repeated-measures ANOVA with the three within-subject factors "sessions" (before, during, after training), "kind of stimulation" (flickering checkerboards vs. pictures of everyday objects) and "location of stimulation" (Fovea, PRL, OppPRL) and the between subject factor "group" (patients vs. normal-sighted controls) with respect to the dependent variable "percent signal change", separately for visual areas V1, V2, and V3. The results are given in **Table 3**.

To test for possible changes in BOLD signal during sham training, we conducted a repeated-measures ANOVA with the within subjects factors visual area (V1, V2, V3), session (memory 1, memory 2), kind of stimulation (checkerboards, pictures) and location of stimulation (fovea, PRL, OppPRL), for both training groups (oculomotor first or memory first) separately. No main effects or interactions reached statistical significance (all $p > 0.05$).

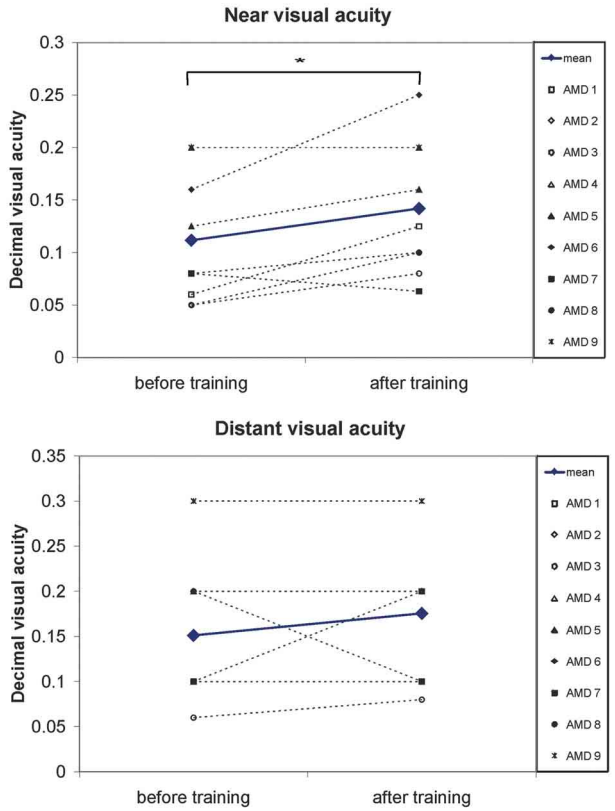

FIGURE 5 | A significant increase in visual acuity after the 6 months of training was observed. Pairwise comparisons show a significant increase in near visual acuity ($p = 0.03$) but not for distant visual acuity ($p = 0.3$). Symbols, connected with dotted lines, show the values of individual patients, blue lines show the mean values over all patients.

To examine the relation between BOLD signal and training effects, we correlated the increase in fixation stability between the sessions "before training" and "during training," as well as between the sessions "before training" and "after training," with the individual differences in % signal change in the BOLD signal between the same two sessions, respectively. The results for the correlations between sessions "before training" and "during training" can be seen in **Figure 8**. Improvements in fixation stability correlate significantly with increases in BOLD response, but only, when the PRL is stimulated with meaningful object pictures (see **Table 4**, upper left panel). The results for the correlations between sessions "before training" and "after training" can be seen in **Figure 9**. Significant correlations between improvements in fixation stability and increases in BOLD response are marked in bold font (see **Table 4**, lower left panel). A consistent significant positive correlation can be seen for the stimulation of the OppPRL area with flickering checkerboards, a trend that can already be observed for the comparison between the sessions "before" and "during training," but that does not reach statistical significance. The data from patient AMD 7 were also excluded from this analysis, because she showed strongly negative BOLD responses.

BOLD-responses in anatomical areas fusiform gyrus, inferior temporal gyrus and LOC

We examined activation in the respective projection zones of the fovea, the PRL, and the OppPRL in anatomical areas fusiform gyrus, inferior temporal gyrus (ITG) and LOC. Thus, for the patients with the PRL in the left visual field and their respective controls, we considered BOLD activation in the right hemisphere only as the PRL projection zone and BOLD activation in the left hemisphere only as the OppPRL projection zone. For the patient with her PRL in the right visual field and her control, we considered BOLD activation in the left hemisphere only for the PRL projection zone and in the right hemisphere only for the OppPRL projection zone. For the group of patients with the PRL in the lower visual field and their respective controls, we pooled over both hemispheres for both, the PRL projection zone and the OppPRL projection zone. We computed % signal change of the BOLD signal for each condition (stimulation with flickering checkerboards or pictures of everyday objects at the fovea, the PRL or OppPRL) and session, each with respect to baseline.

We computed repeated-measures ANOVA with the three within-subject factors "sessions" (before, during, after training), "kind of stimulation" (flickering checkerboards vs. meaningful pictures) and "location of stimulation" (Fovea, PRL, OppPRL) and the between-subject factor "group" (patients vs. normal-sighted controls) with respect to the dependent variable "percent signal change," separately for areas fusiform gyrus, ITG and LOC. The results are given in **Table 3**, lower panel. For all three areas fusiform gyrus, ITG and LOC pictures of everyday objects yielded, as expected, significantly more BOLD response than flickering checkerboards. **Figure 7** shows the mean % signal change values as a difference to baseline for the stimulation with everyday pictures and the sessions "before," "during" and "after training," for the patient and control group, respectively. The data from one patient (AMD 7) were again excluded due to strongly negative BOLD responses.

To test for possible changes in BOLD signal during sham training, we conducted a repeated-measures ANOVA with the within subjects factors anatomical area (fusiform gyrus, ITG, LOC), session (memory 1, memory 2), kind of stimulation (checkerboards, pictures) and location of stimulation (fovea, PRL, OppPRL), for both training groups (oculomotor first or memory first) separately. Both training groups showed a significant main effect "anatomical area" ($p = 0.014$ and $p = 0.001$, respectively). The main effect "session" was not significant ($p = 0.178$ and $p = 0.761$). Only the training group that conducted the oculomotor training first showed an additional significant main effect "kind of stimulation" ($p = 0.014$), and a significant interaction "anatomical area × kind of stimulation" ($p = 0.009$).

To investigate the relationship between BOLD signal and training effects we correlated the increase in fixation stability between the sessions "before training" and "during training," as well as between the sessions "before training" and "after training," with differences in % signal change between the two sessions, respectively. The results can be seen in correlation coefficients (**Figures 10**, **11**, and **Table 4**, upper and lower right panel). Also in areas fusiform gyrus and LOC improvements in fixation stability between the sessions "before" and "during training" correlate

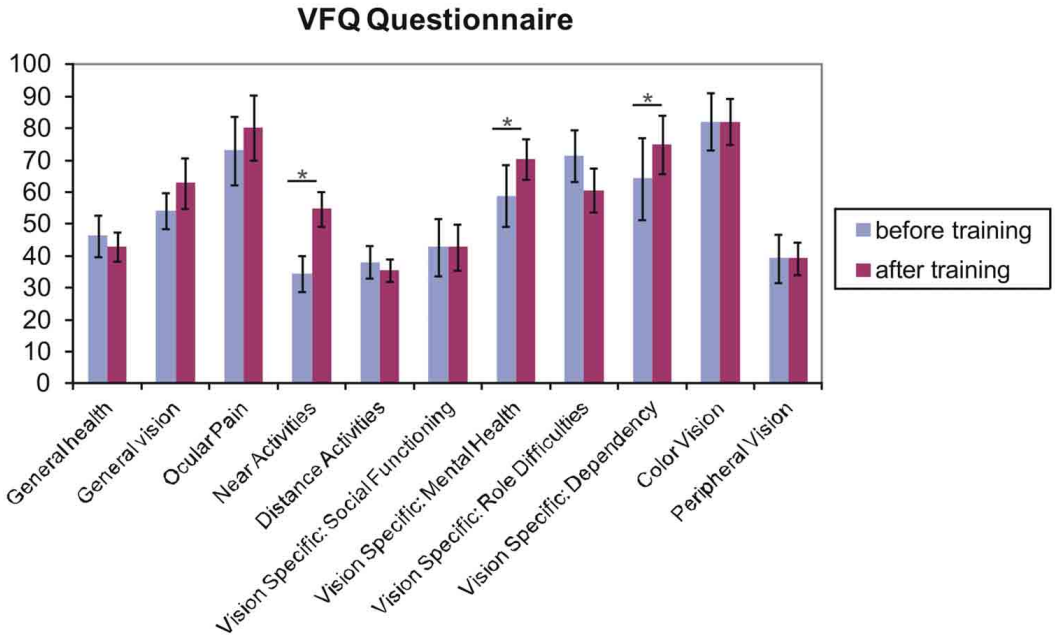

FIGURE 6 | Results from the Visual Functioning Questionnaire. One sided *t*-test revealed that fixation training significantly improved subjects' judgments of their near visual activities, their vision-specific mental health (depressive symptoms due to the vision deficit) and their vision specific dependency (e.g., rely on the help of others because of vision deficit) ($p < 0.05$). Other scales do not differ over training. Error bars reflect standard errors.

significantly with increases in BOLD response when the PRL is stimulated with pictures of everyday objects. For the correlations between the sessions "before" and "after training" there is no systematic trend observable. The data from patient AMD 7 were also excluded from this analysis, because she showed strongly negative BOLD responses.

VOXEL-BASED MORPHOMETRY RESULTS

A positive effect of training was reflected in brain increase in gray and white matter density in the left posterior cerebellum (semilunar lobule, Crus II) for the patient group (gray matter: peak MNI coordinate ($x = -20$, $y = -67$, $z = -56$), cluster size 520 voxel, $Z = 3.9$, $p_{corr(FDR)} = 0.034$; white matter: peak MNI coordinates ($x = -20$, $Y = -67$, $z = -53$), cluster size 580 voxel, $Z = 4.2$, $p_{corr(FDR)} = 0.02$) (**Figure 12**). The control group did not show any sequential effects from measurements 1, 2, and 3 during the same time period, neither for gray nor white matter. A direct group comparison did not yield any significant differences.

DISCUSSION

The aim of this study was to investigate how a specific training intervention that should lead to a more efficient use of eccentric viewing in patients suffering from AMD could be related to functional and structural brain changes. Behavioral data show a significant improvement in fixation stability, reading speed, and near visual acuity as a result of oculomotor training although there is substantial heterogeneity in the amount of benefit individual patients exhibited. Four patients (AMD 2, 5, 6, and 9) showed a clear improvement of fixation stability from before to after the training period. Patients AMD 4 and 8 started already with relatively high stability values and could not increase it much further through the training. Patients AMD 3 and 7 started with low stability values and had room for improvement, but critical life events in these two cases disrupted training, which might be the reason that the patients could not tap their full potential. Patient AMD 1, who did not show improvement in fixation stability over training, preferred to use devices with large magnification at home. He therefore might have lacked sufficient training in eccentric viewing in comparison to the other participants. In contrast reading speed increased in patient AMD 1 as well as in five other patients (AMD 2, 6, 7, 8, and 9) presumably due to training measures. For the three remaining patients (AMD 3, 4, and 5) changes in reading speed appear unsystematic and not directly related to training. Improvements in distant visual acuity were not statistically significant, while improvements in near visual acuity reached statistical significance. Six patients (AMD 1, 2, 3, 5, 6, and 8) showed an increase in near visual acuity, while only 1 patient (AMD 7) showed a slight decrease and two patients (AMD 4 and 9) maintained the same near visual acuity values before and after the training. The patients as a whole reported that they benefited from the training with respect to their near visual activities, as demonstrated by their responses in the VFQ-25 questionnaire (Mangione et al., 2001). But one must note that during training some of the patients started to use a hyperocular for the first time. They subsequently used it during the training, but also in their daily lives. So the significant improvement in the subscale "near visual activities" in the VFQ-25 questionnaire might not be related to the training alone. Our behavioral results are in line with other findings in the literature. In an earlier study (Nilsson et al., 2003) AMD

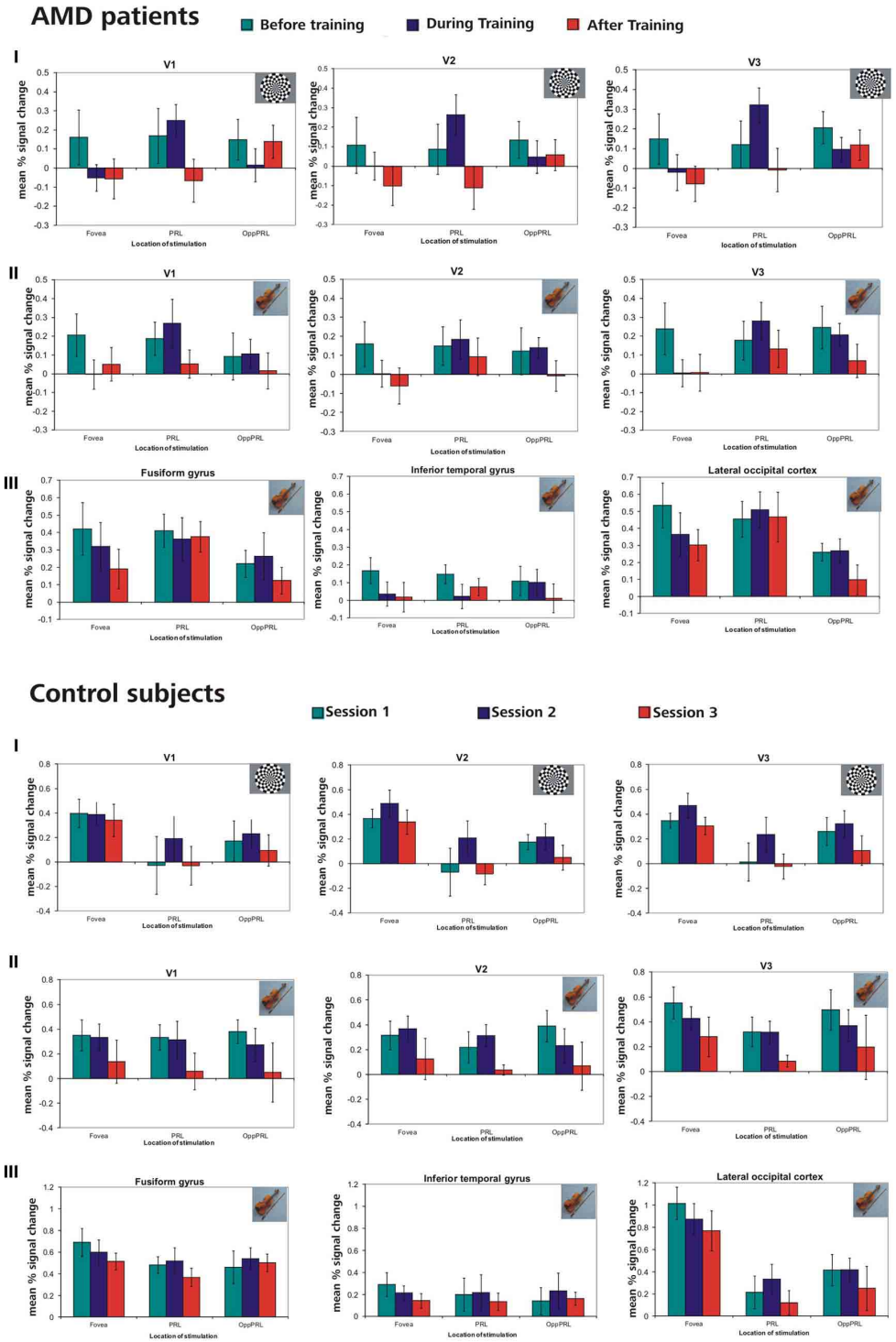

FIGURE 7 | Mean % signal changes (vs. baseline) in AMD patients and normally sighted controls before, during, and after fixation training in the individual primary (V1), secondary (V2), and tertiary (V3) visual cortex and in the anatomically predefined higher visual areas in the inferior temporal gyrus (ITG), the lateral occipital cortex (LOC), and the fusiform gyrus (as labeled in Freesurfer). The stimuli were either checkerboards (I) or meaningful pictures (II, III). For checkerboards % signal change is only reported for the individual primary cortices because no significant activation was found in higher visual areas for that kind of stimulus. The stimulus either appeared in the fovea, the PRL or the OppPRL. In the control subjects, sessions 1, 2, and 3 refer to the corresponding sessions of the individually matched AMD patients. Thus, if the corresponding AMD patient started with the oculomotor training, sessions 1, 2, and 3 refer to the first, second and third fMRI session for the matching control subject. If the corresponding AMD patient had the oculomotor training after the sham training, sessions 1, 2, and 3 in the figure refer to the third, fourth and fifth fMRI session for that control.

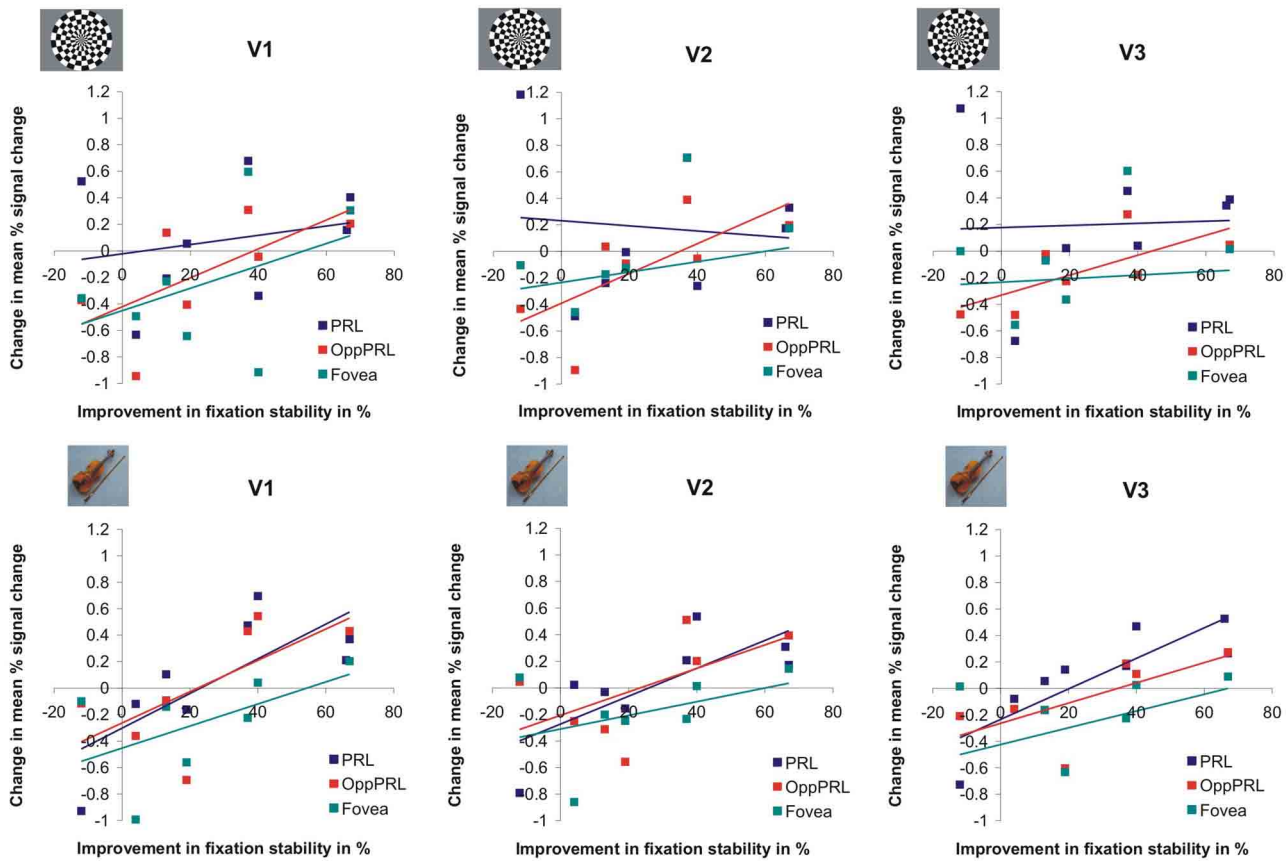

FIGURE 8 | Correlation between the change in % signal change and change in fixation stability, for the patient group only, before fixation training and during fixation training in individually mapped primary (V1), secondary (V2), and tertiary (V3) visual cortex. The upper row depicts the correlation between changes in % signal change and changes in fixation stability in case of checkerboard stimulation, the lower row depicts these correlations for everyday images. The differently colored symbols refer to the different retinal locations that were stimulated (green, fovea; red, OppPRL; blue, PRL).

patients with large absolute scotomata were trained in a reading task to establish a more favorable retinal locus on their eccentric retina for reading. As a consequence of training patients' reading speed increased. Nguyen et al. (2011) reported a study where the fixation behavior of patients with juvenile forms of macular degeneration was randomly trained with either a rapid serial visual presentation task or a low vision sensorimotor reading task. Both tasks led to an improvement in fixation behavior. Usually in studies on rehabilitation methods for patients with central vision loss it could be shown that an improvement in reading speed was accompanied by a stabilization of eccentric fixation (e.g., Sunness et al., 1996; Trauzettel-Klosinski and Tornow, 1996; Nilsson et al., 1998; Crossland et al., 2004; Rubin and Feely, 2009). Although in our study we also observed a significant increase in both—reading speed and fixation stability—across all patients due to training, surprisingly the amount of individual improvements in fixation stability was not directly correlated to individual improvements in reading speed ($r = -0.592$; $p = 0.12$). It is unclear at the moment what the reason for this could be. With regard to improvements in visual acuity, another study of Polat (2009) could also show that patients with amblyopia could benefit from a visual perceptual learning task with respect to their visual acuity and contrast sensitivity. Ishiko et al. (2010) showed an improvement in visual acuity for the worse eye in patients with age-related maculopathy over time, without having applied any training methods. While the better eye was deteriorating, this effect could in part be attributed to a more stable eccentric fixation with the worse eye. Overall, it could be shown that at least a subgroup of the AMD patients in our study showed substantial improvements in behavioral parameters over the training period. But the results also hint to the difficulty of the patients to hold on to their achieved standards without further active oculomotor training, as we observed some decline in measurements during the sham training after the oculomotor training phase.

Fixation stability also showed a significant positive correlation with brain activation changes in the individual primary, secondary, and tertiary visual cortex, the fusiform gyrus and the

Table 4 | Pearson correlation coefficients and respective *p*-values (in brackets) for the correlation between difference in % signal change and difference in fixation stability (A) between the sessions "before training" and "during training" and (B) between the sessions "before training" and "after training."

	Flickering checkerboards			Pictures				Flickering checkerboards			Pictures			
	Fovea (*N* = 7)	PRL (*N* = 8)	OppPRL (*N* = 7)	Fovea (*N* = 7)	PRL (*N* = 8)	OppPRL (*N* = 7)		Fovea (*N* = 7)	PRL (*N* = 8)	OppPRL (*N* = 7)	Fovea (*N* = 7)	PRL (*N* = 8)	OppPRL (*N* = 7)	
(A) Correlations for differences between sessions "before training" and "during training."														
V1	0.416 (0.353)	0.220 (0.601)	0.645 (0.118)	0.541 (0.210)	**0.745** (0.034)	0.666 (0.102)	***Fusiform gyrus***	0.234 (0.614)	−0.087 (0.837)	0.148 (0.751)	0.470 (0.288)	**0.766** (0.027)	0.414 (0.356)	
V2	0.194 (0.677)	−0.099 (0.815)	0.691 (0.085)	0.401 (0.373)	**0.753** (0.031)	0.588 (0.165)	***ITG***	−0.110 (0.815)	−0.433 (0.284)	−0.106 (0.821)	0.520 (0.231)	0.705 (0.051)	0.056 (0.905)	
V3	0.068 (0.886)	0.045 (0.916)	0.711 (0.073)	0.406 (0.366)	**0.840** (0.009)	0.66 (0.101)	***LOC***	0.292 (0.525)	−0.131 (0.758)	0.659 (0.108)	0.458 (.302)	**0.859** (0.006)	0.642 (0.120)	
(B) Correlations for differences between sessions "before training" and "after training."														
V1	0.376 (0.406)	0.54 (0.166)	**0.838** (0.019)	0.735 (0.060)	0.391 (0.339)	0.134 (0.775)	***Fusiform gyrus***	0.638 (0.123)	0.547 (0.161)	0.751 (0.052)	**0.859** (0.013)	0.536 (0.171)	**0.777** (0.040)	
V2	0.509 (0.244)	0.545 (0.163)	**0.885** (0.008)	**0.827** (0.022)	0.449 (0.265)	0.428 (0.338)	***ITG***	0.495 (0.258)	0.400 (0.326)	0.610 (0.146)	0.685 (0.089)	0.445 (0.269)	0.092 (0.844)	
V3	0.533 (.218)	**0.813** (0.014)	**0.825** (0.022)	**0.810** (0.027)	0.586 (0.127)	0.410 (0.360)	***LOC***	0.266 (0.564)	0.397 (.331)	**0.775** (0.041)	0.748 (0.053)	0.070 (0.869)	−0.031 (0.948)	

Left columns: correlation coefficients for visual areas V1, V2, and V3. Right columns: correlation coefficients for anatomical areas fusiform gyrus, inferior temporal gyrus (ITG) and lateral occipital cortex (LOC). Statistically significant correlations are marked in bold font.

lateral occipital lobe during the initial phase of the training, where the increases in fixation stability were most pronounced (comparison of sessions "before" and "during training"). Interestingly this PRL-specific positive correlation was only present when the PRL was stimulated with semantically meaningful pictures but not with checkerboard stimuli. Earlier findings suggest that active tasks lead to better stimulus-correlated activation in the PRL projection zone compared to the results for passive tasks (e.g., Masuda et al., 2008; Liu et al., 2010; Plank et al., 2012). Even if the task in this study only demanded passive viewing, the semantic quality of the stimuli seems to play an essential role with respect to the signal in the PRL projection zone. One reason could be that these stimuli have a more relevant character in patients' daily lives than abstract radial checkerboard stimuli and thus the former activate more top-down processing yielding greater BOLD responses. The effect could partially also be due to enhanced attention as oculomotor training may assist the patients to guide their attention to visual input at the PRL. Overall, our data show that the patients who showed the most pronounced increase in fixation stability were also the ones who showed an increase in BOLD signal for measurements made "before" and "during training," while the patients who showed no or only a slight improvement in fixation stability showed no increase or even a decrease in BOLD signal, as depicted in **Figures 8**, **10**. This positive correlation between change in BOLD signal and improvement in fixation stability is also evident in the comparison between the sessions "before training" and "after training" (see **Figures 9**, **11**), even though the correlations for several visual areas and conditions now lack statistical significance (see **Table 4**). It can be seen that especially the PRL-specific increase in BOLD signal that corresponded with the most pronounced increase in fixation stability between the two time points "before" and "during training" does not present itself as a sustainable effect up to the time point "after training." We assume that a general tendency of the BOLD response to decline over time, as discussed below with respect to the effects of sequential testing, might superimpose onto possible training effects to a certain extent. This could be attributed to habituation or attention effects related to doing the same task several times. Also the fact that we used the same set of pictures in our stimulation at each of the sessions could play a role here. Inspection of **Figure 7** reveals that repeated measurements in the controls also led to lower BOLD responses over time. These changes occurred in the controls, despite the fact that they did not undergo any training. Thus, the mere repetition of testing has an effect on the BOLD response in visual cortex. Such habituation effects should be taken into account when evaluating the effects of training on cortical responses. On the other hand, Yotsumoto et al. (2008) also found an initial increase in brain activation in the visual cortex of participants in a perceptual learning experiment that was followed by a decline while task performance levels remained high. Indeed, the patients in our study showed the most pronounced increase in fixation stability in the initial phase of the training period, where a PRL-specific correlation with BOLD response increases could be found. Later on most, but not all, patients were able to stabilize their fixation (see **Figure 4**).

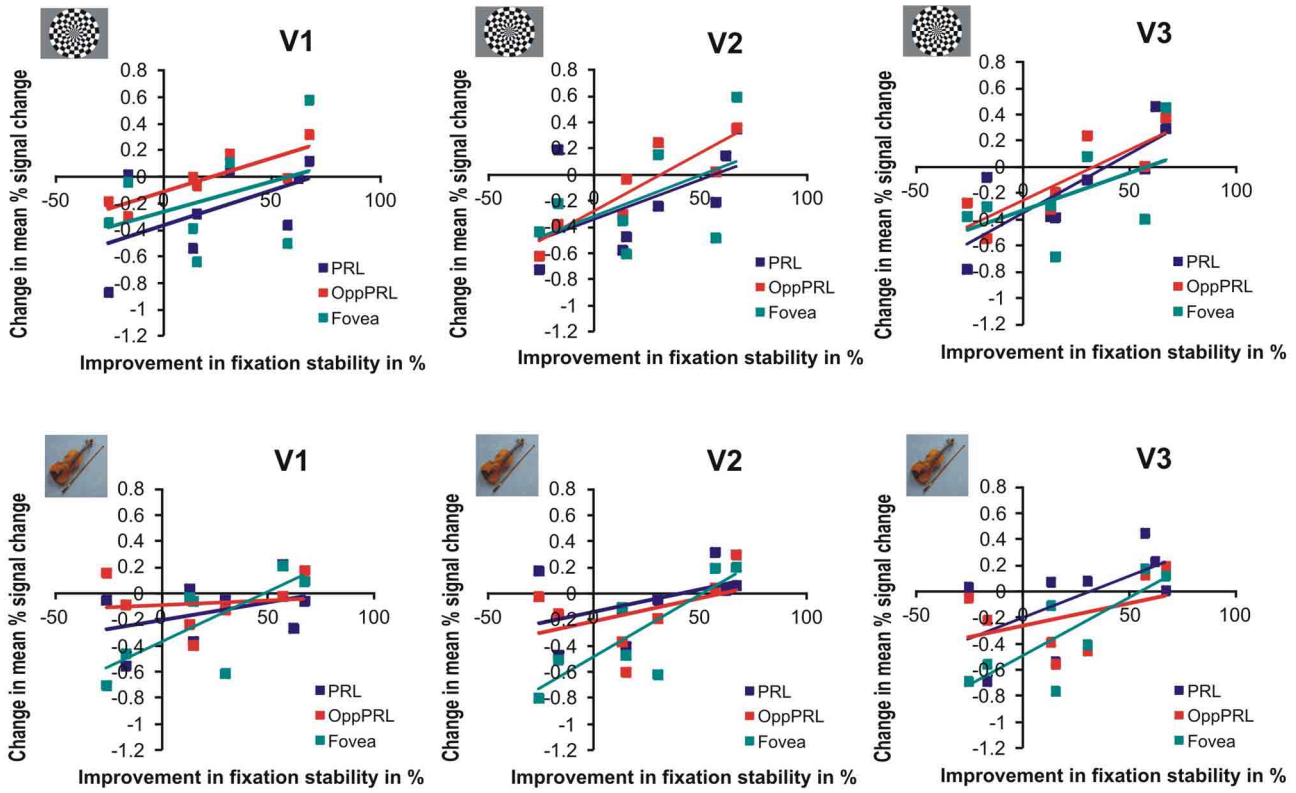

FIGURE 9 | Correlation between the change in % signal change and change in fixation stability for the patient group only before fixation training and after fixation training in individually mapped primary (V1), secondary (V2), and tertiary (V3) visual cortex. The upper row depicts the correlation between changes in % signal change and changes in fixation stability in case of checkerboard stimulation, the lower row depicts these correlations for everyday images. The differently colored symbols refer to the different retinal locations that were stimulated (green, fovea; red, OppPRL; blue, PRL).

Interestingly and surprisingly, correlation effects between changes in fixation stability and BOLD responses appear to get stronger for non-PRL areas over time (see **Table 4**). Thus, while we expected a more PRL-specific effect, a more stable eccentric fixation appears to improve the processing of visual information in the entire remaining visual field, not only in the PRL area. Stable fixation could thus help the patients to use their entire visual field more efficiently. In a previous study with patients with central vision loss (Plank et al., 2012) we also found that a group of patients with stable eccentric fixation performed better in a visual search task than another group with unstable eccentric fixation, even across those trials where the target stimuli did not appear in or near their PRL.

The analysis of the Visual Function Questionnaire showed a significant increase in scores with respect to the categories near vision abilities, vision specific mental health (depressive symptoms due to the vision deficit) and vision-specific dependency (e.g., reliance on the help of others because of visual deficit) due to training. Mitchell and Bradley (2006) reported that AMD causes severe decline in life quality. Furthermore, they speculated that the health status and the utility measures referring to the quality of live status in AMD patients are underestimated. Further the authors point out that medical interventions often only reach a small proportion of patients. Another study of Rovner et al. (2009) highlights the need for life quality improvements in AMD patients. In their study AMD patients tended to neglect cognitive, physical and social activities due to their visual deficit, which led to an increased risk of cognitive decline. Indeed in a multi-center study with a large number of JMD and AMD patients, Hernowo et al. (2013) found significant reductions in frontal lobe white matter in patients with AMD (but not patients with JMD), suggesting that AMD could also be associated with cognitive decline.

The results of the present study indicate that life quality could be improved by a suitable oculomotor training not only in terms of visual abilities in general (near vision abilities) but also in terms of general quality of life. Therefore, the training measurement showed a direct impact on at least some aspects of life quality as demanded by Mitchell and Bradley (2006). Such training could

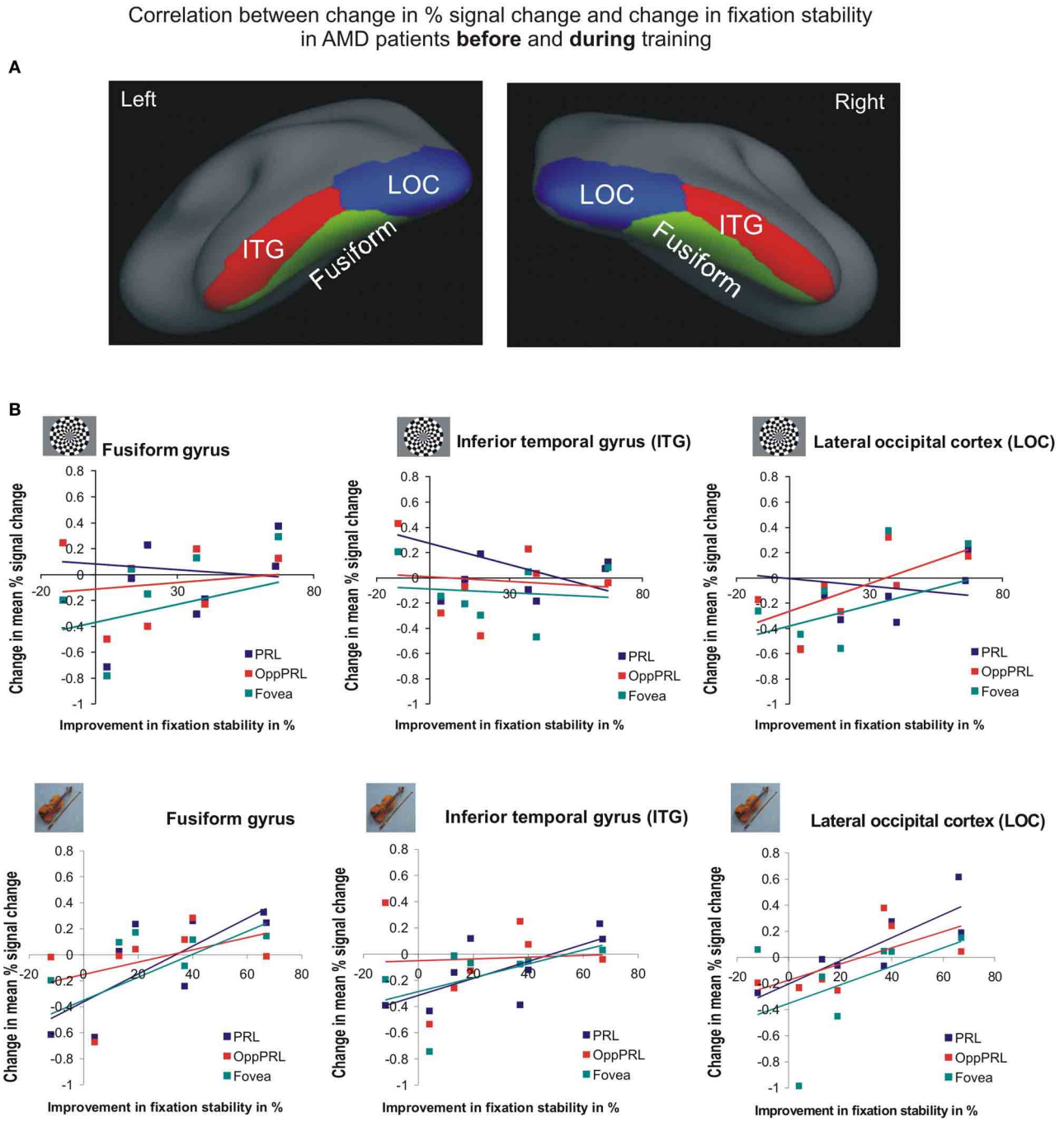

FIGURE 10 | Correlation between the change in% signal change and change in fixation stability for the patient group only before fixation training and during fixation training in the inferior temporal gyrus (ITG), the lateral occipital cortex (LOC), and the fusiform gyrus [(A) as labeled in Freesurfer]. (B) The upper row depicts the correlation between changes in % signal change and changes in fixation stability in case of checkerboard stimulation, the lower row depicts these correlations for everyday images. As in **Figures 8**, **9**, the differently colored symbols refer to the different retinal locations that were stimulated (green, fovea; red, OppPRL; blue, PRL).

lower the risk of cognitive deficits that can be often observed in elderly patients with chronic disease.

We observed increased gray and white matter density in patients with AMD as a consequence of oculomotor training in the left semi-lunar lobule of the cerebellum. This effect was absent in control subjects, which was expected since they did not participate in the oculomotor training. Such a gray matter increase might be related to the eccentric reading training. In a study by Fulbright et al. (1999) the semi-lunar lobule was associated with reading. They showed that the semi-lunar lobule showed

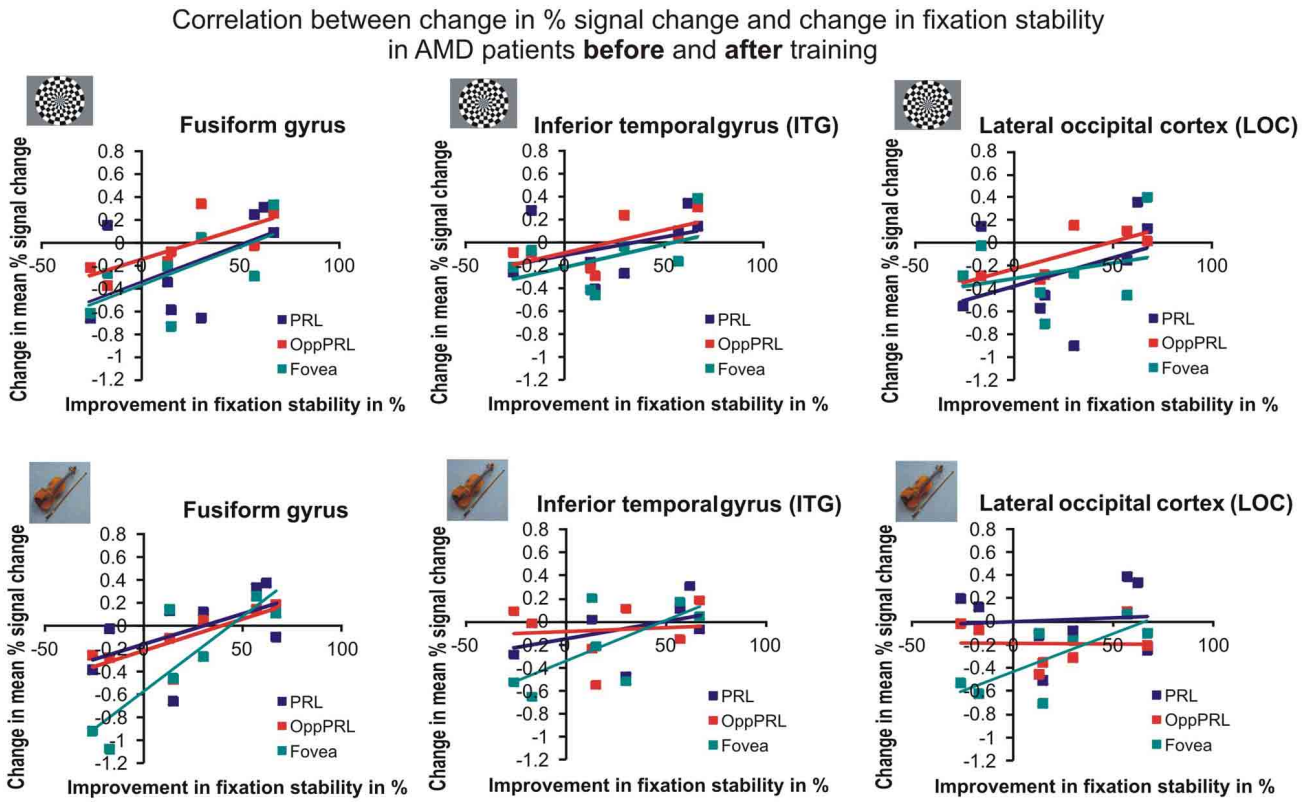

FIGURE 11 | Correlation between the change in % signal change and change in fixation stability for the patient group only before fixation training and after fixation training in the inferior temporal gyrus (ITG), the lateral occipital cortex (LOC), and the fusiform gyrus. The upper row depicts the correlation between changes in % signal change and changes in fixation stability in case of checkerboard stimulation, the lower row depicts these correlations for everyday images. As in **Figures 8**, **9**, the differently colored symbols refer to the different retinal locations that were stimulated (green, fovea; red, OppPRL; blue, PRL).

increased activation when non-meaningful phoneme assemblies should be read. The area was not active when real words were presented. An alternative explanation could be that the executive control of eye movement was enhanced due to training. Habas et al. (2009) showed in a model-free approach that the semi lunar lobule is part of the executive control network during resting state.

An fMRI study with AMD patients indicated that a reading task led to increased activation in the prefrontal and the parietal cortex (Szlyk and Little, 2009). Another study of Little et al. (2008) revealed that AMD patients exhibited decreased activation in the occipital cortex compared to healthy controls and increased activation in the prefrontal cortex and the intraparietal sulcus while they were executing saccades or pursuit eye movements. During pursuit eye movement there was also additional increased activation in the frontal and supplementary eye fields. In both studies executive tasks were performed but no cerebellar activations were reported. It is, however, well established that the cerebellum plays an essential role in eye movements and executive control. The increased gray matter density in the inferior cerebellum might reflect a general effect of learning rather than a specific one, since the semi-lunar lobule is not directly linked to eye movements *per se*.

EFFECTS OF SEQUENTIAL SCANNING OVER A 1-YEAR PERIOD

Overall 7 control subjects were recruited, who were matched on age and gender to the respective patients. Although they did not participate in the oculomotor or eccentric reading training they participated in the same fMRI measurements over the same period of time. We wanted to rule out any sequential effects that could take place by repeating the same measurements five times over a 12-month period. The results of the controls, together with the results of the patient group, are presented in **Figure 7** and indicate that indeed there are some sequential effects of repeated testing. As **Table 3** shows, there are significant main effects of the factor session for areas V2 and V3, as well as significant interactions between the factors session and location of stimulation, in regard to whether the fovea, the PRL or the OppPRL were stimulated, in areas V1, V2, V3, and LOC. The BOLD response exhibits a tendency to decline over time, suggesting a form of habituation, which is most pronounced when the fovea is stimulated. There is a slight tendency that the BOLD response due to stimulating the PRL is enhanced in the second session, which might be caused by attention effects or perceptual learning in the periphery (Yotsumoto et al., 2008). With the exception of the LOC no ROI shows a significant main effect of location of stimulation. Areas V2, V3 and fusiform gyrus show a significant main effect

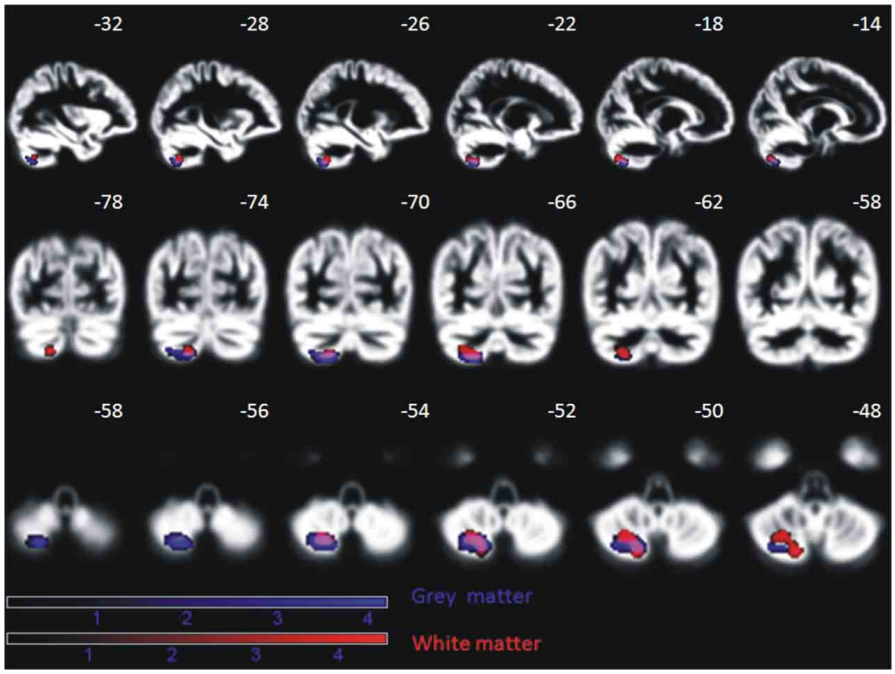

FIGURE 12 | Significant increase of gray and white matter in the posterior cerebellum of nine AMD patients over the period of oculomotor training for, on average, 6 months ($p < 0.05$, FDR corrected on cluster level). This effect is absent in age-matched controls. Effects are depicted on a mean normalized gray matter image of all subjects (patients and controls). The MNI coordinates in terms of millimeter deviation from the anterior commissure are presented.

for group and areas V2, V3, fusiform gyrus and LOC show a significant interaction of location of stimulation and group, which points to an overall reduced neural response in the patients in these areas when the fovea is stimulated. Nevertheless, the patients showed some positive signal even when the stimuli fell in an area covered by their scotoma. An explanation could be that the scotomata are not symmetrical in all cases and some residual vision could be spared at the rim of the scotomata, leading to some residual perception in the patients when this area is stimulated with high-contrast stimuli as were used here. Part of the significant interaction between location of stimulation and group can also be attributed to the difference between PRL and OppPRL stimulation that only the patient group shows, since the significant interaction also holds when the fovea is excluded from the analysis in the fusiform gyrus ($p = 0.049$) and in the LOC ($p = 0.028$). The difference between groups (patients vs. controls) is also no longer significant, when the BOLD responses of the foveal stimulation are excluded (all $p > 0.05$). Together with the clear correlation effects between individual improvements in fixation stability and increase in BOLD signal over the same period of time, especially during the initial phase of the training, we therefore conclude that the training effects reported in the patient group cannot be accounted for by mere repetition effects.

SUMMARY

In this study we trained AMD patients to improve their fixation stability using specific oculomotor training protocols. Patients benefited from training with respect to their fixation stability, reading speed and near visual acuity. Training also led to an improvement in some aspects of the patients' quality of daily life. After training, patients reported that they needed less help from others and were more autonomous than before training. Training led to significant albeit modest changes in brain functions and structure. We found a positive correlation between fixation stability and an increase in neural response in the PRL projection zones in AMD patients during the initial phase of the training. Interestingly structural changes were also found in the cerebellum of these patients following oculomotor training. Increases of gray and white matter density in the cerebellum were found that might be due to learning to perform visual tasks with eccentric viewing. Overall the study showed that patients with AMD can benefit from specific oculomotor training procedures. Such training is associated with measureable changes in brain functions and structure.

ACKNOWLEDGMENTS

This work was supported by the Deutsche Forschungsgemeinschaft within the framework of Research Group FOR 1075: Regulation and Pathology of Homeostatic Processes in Visual Function. The authors thank the Pro Retina Foundation and the City of Regensburg (Senior Citizens' Office) for their assistance in participant recruitment as well as all participants of our study. Additional thanks goes to Stefan Ringbauer for programming the simplified version of the eye-movement training, to Susanne Hammer for helping with data analysis and to Anton L. Beer for helpful comments on data analysis.

REFERENCES

Ahissar, M., and Hochstein, S. (1997). Task difficulty and the specificity of perceptual learning. *Nature* 387, 401–406. doi: 10.1038/387401a0

Ashburner, J. (2007). A fast diffeomorphic image registration algorithm. *Neuroimage* 38, 95–113. doi: 10.1016/j.neuroimage.2007.07.007

Bäckman, Ö., and Inde, K. (1979). *Low Vision Training*. Malmö: Hermods.

Beer, A. L., Plank, T., and Greenlee, M. W. (2011). Diffusion tensor imaging shows white matter tracts between human auditory and visual cortex. *Exp. Brain Res.* 213, 299–308. doi: 10.1007/s00221-011-2715-y

Beer, A. L., Watanabe, T., Ni, R., Sasaki, Y., and Andersen, G. J. (2009). 3D surface perception from motion involves a temporal-parietal network. *Eur. J. Neurosci.* 30, 703–713. doi: 10.1111/j.1460-9568.2009.06857.x

Bernard, S. (2000). *Entwicklung Und Evaluation eines Gedächtnistrainings Für Blinde Senioren Auf Tonbandkassetten*. Unpublished dissertation, University of Erlangen-Nürnberg, Germany.

Boucard, C. C., Hernowo, A. T., Maguire, R. P., Jansonius, N. M., Roerdink, J. B. T. M., Hooymans, J. M. M., et al. (2009). Changes in cortical gray matter density associated with long-standing retinal visual field defects. *Brain* 132, 1898–1906. doi: 10.1093/brain/awp119

Coco-Martín, M. B., Cuadrado-Asensio, R., López-Miguel, A., Mayo-Iscar, A., Maldonado, M. J., and Pastor, J. C. (2013). Design and evaluation of a customized reading rehabilitation program for patients with age-related macular degeneration. *Ophthalmology* 120, 151–159. doi: 10.1016/j.ophtha.2012.07.035

Cox, R. W., and Jesmanowicz, A. (1999). Real-time 3D image registration for functional MRI. *Magn. Reson. Med.* 42, 1014–1018.

Crossland, M. D., Culham, L. E., and Rubin, G. S. (2004). Fixation stability and reading speed in patients with newly developed macular disease. *Ophthalmic Physiol. Opt.* 24, 327–333. doi: 10.1111/j.1475-1313.2004.00213.x

Dale, A. M., Fischl, B., and Sereno, M. I. (1999). Cortical surface-based analysis. I. Segmentation and surface reconstruction. *Neuroimage* 9, 179–194. doi: 10.1006/nimg.1998.0395

Desikan, R. S., Segonne, F., Fischl, B., Quinn, B. T., Dickerson, B. C., Blacker, D., et al. (2006). An automated labelling system for subdividing the human cerebral cortex on MRI scans into gyral based regions of interest. *Neuroimage* 31, 968–980. doi: 10.1016/j.neuroimage.2006.01.021

DeYoe, E. A., Carman, G. J., Bandettini, P., Glickman, S., Wieser, J., Cox, R., et al. (1996). Mapping striate and extrastriate visual areas in human cerebral cortex. *Proc. Natl. Acad. Sci. U.S.A.* 93, 2382–2386. doi: 10.1073/pnas.93.6.2382

Fahle, M., and Poggio, T. (2002). *Perceptual Learning*. Cambridge, MA: The MIT Press.

Fischl, B., and Dale, A. M. (2000). Measuring the thickness of the human cerebral cortex from magnetic resonance images. *Proc. Natl. Acad. Sci. U.S.A.* 97, 11050–11055. doi: 10.1073/pnas.200033797

Fischl, B., Liu, A., and Dale, A. M. (2001). Automated manifold surgery: constructing geometrically accurate and topologically correct models of the human cerebral cortex. *IEEE Trans. Med. Imaging* 20, 70–80. doi: 10.1109/42.906426

Fischl, B., Salat, D. H., Busa, E., Albert, M., Dieterich, M., Haselgrove, C., et al. (2002). Whole brain segmentation: automated labeling of neuroanatomical structures in the human brain. *Neuron* 33, 341–355. doi: 10.1016/S0896-6273(02)00569-X

Fischl, B., Sereno, M. I., and Dale, A. M. (1999a). Cortical surface-based analysis. II. Inflation, flattening, and a surface-based coordinate system. *Neuroimage* 9, 195–207. doi: 10.1006/nimg.1998.0396

Fischl, B., Sereno, M. I., Tootell, R. B., and Dale, A. M. (1999b). High-resolution intersubject averaging and a coordinate system for the cortical surface. *Hum. Brain Mapp.* 8, 272–284.

Fischl, B., van der Kouwe, A., Destrieux, C., Halgren, E., Segonne, F.,Salat, D. H., et al. (2004). Automatically parcellating the human cerebral cortex. *Cereb. Cortex* 14, 11–22. doi: 10.1093/cercor/bhg087

Fletcher, D. C., and Schuchard, R. A. (1997). Preferred retinal loci relationship to macular scotomas in a low vision population. *Ophthalmology* 104, 632–638. doi: 10.1016/S0161-6420(97)30260-7

Fulbright, R. K., Jenner, A. R., Mencl, W. E., Pugh, K. R., Shaywitz, B. A., Shaywitz, S. E., et al. (1999). The cerebellum's role in reading: a functional MR imaging study. *Am. J. Neuroradiol.* 20, 1925–1930.

Gilbert, C. D., Sigman, M., and Crist, R. E. (2001). The neural basis of perceptual learning. *Neuron* 31, 681–697. doi: 10.1016/S0896-6273(01)00424-X

Grill-Spector, K. (2003). The neural basis of object perception. *Curr. Opin. Neurobiol.* 13, 159–166. doi: 10.1016/S0959-4388(03)00040-0

Grill-Spector, K., Kushnir, T., Edelman, S., Avidan,G., Itzchak,Y., and Malach, R. (1999). Differential, processing of objects under various viewing conditions in the humanlat- eraloccipitalcomplex. *Neuron* 24, 187–203. doi: 10.1016/S0896-6273(00)80832-6

Guez, J. E., Le Gargasson, J. F., Rigaudiere, F., and O'Regan, J. K. (1993). Is there a systematic location for the pseudo-fovea in patients with central scotoma? *Vision Res.* 33, 1271–1279. doi: 10.1016/0042-6989(93)90213-G

Gustafsson, J., and Inde, K. (2004). The MoviText method: efficient preoptical reading training in persons with central visual field loss. *Technol. Disabil.* 6, 211–221.

Habas, C., Kamdar, N., Nguyen, D., Prater, K., Beckmann, C. F., Menon, V., et al., (2009). Distinct cerebellar contributions to intrinsic connectivity networks. *J. Neurosci.* 29, 8586–8594. doi: 10.1523/JNEUROSCI.1868-09.2009

Hernowo, A. T., Prins, D., Baseler, H. A., Plank, T., Gouws, A., Hooymans, J. M. M., et al. (2013). Morphometric analyses of the visual pathway in macular degeneration. *Cortex*. doi: 10.1016/j.cortex.2013.01.003. [Epub ahead of print].

Ishiko, S., van de Velde, F., and Yoshida, A. (2010). Paradoxical improvement of visual acuity in macular disease. *Curr. Eye Res.* 35, 6451–6656. doi: 10.3109/02713681003707235

Jack, C. R. Jr., Bernstein, M. A., Fox, N. C., Thompson, P., Alexander, G., Harvey, D., et al. (2008). The Alzheimer's Disease Neuroimaging Initiative (ADNI): MRI methods. *J. Magn. Reson. Imaging* 27, 685–691.

Karni, A., and Sagi, D. (1991). Where practice makes perfect in texture discrimination: evidence for primary visual cortex plasticity. *Proc. Natl. Acad. Sci. U.S.A.* 88, 4966–4970. doi: 10.1073/pnas.88.11.4966

Kasten, E., Haschke, P., Meinhold, U., and Oertel-Verweyen, P. (2010). A computer program for training eccentric reading in persons with central scotomata. *J. Vis. Imp. Blind.* 104, 303–311.

Little, D. M., Thulborn, K. R., and Szlyk, J. P. (2008). An FMRI study of saccadic and smooth-pursuit eye movement control in patients with age-related macular degeneration. *Invest. Ophthalmol. Vis. Sci.* 49, 1728–1735.

Liu, M. M., Chan, C.-C., and Tuo, J. (2012). Genetic mechanisms and age-related macular degeneration: common variants, rare variants, copy number variations, epigenetics, and mitochondrial genetics. *Hum. Genomics* 6:13. doi: 10.1186/1479-7364-6-13

Liu, T., Cheung, S.-H., Schuchard, R. A., Glielmi, C. B., Hu, X., He, S., et al. (2010). Incomplete cortical reorganization in macular degeneration. *Invest. Ophthalmol. Vis. Sci.* 51, 6826–6834. doi: 10.1167/iovs.09-4926

Mangione, C. M., Lee, P. P., Gutierrez, P. R., Spritzer, K., Berry, S., and Hays, R. D. (2001). Development of the 25-item National Eye Institute Visual Function Questionnaire. *Arch. Ophthalmol.* 119, 1050–1058. doi: 10.1001/archopht.119.7.1050

Masuda, Y., Dumoulin, S. O., Nakadomari, S., and Wandell, B. A. (2008). V1 projection zone signals in human macular degeneration depend on task, not stimulus. *Cereb. Cortex* 18, 2483–2493. doi: 10.1093/cercor/bhm256

Mitchell, J., and Bradley, C. (2006). Quality of life in age-related macular degeneration: a review of the literature. *Health Qual. Life Outcomes* 21, 4.

Nagy, K., Greenlee, M. W., and Kovács, G. (2012). The lateral occipital cortex in the face perception network: an effective connectivity study. *Front. Psychol.* 3:141. doi: 10.3389/fpsyg.2012.00141

Nguyen, N. X., Stockum, A., and Hahn, G. A., and Trauzettel-Klosinski, S. (2011). Training to improve reading speed in patients with juvenile macular dystrophy: a randomized study comparing two training methods. *Acta Ophthalmol.* 89, e82–e89. doi: 10.1111/j.1755-3768.2010.02081.x

Nilsson, U. L., Frennesson, C., and Nilsson, S. E. G. (1998). Location and stability of a newly established eccentric retinal locus suitable for reading, achieved through training of patients with a dense central scotoma. *Optom. Vis. Sci.* 75, 873–878.

Nilsson, U. L., Frennesson, C., and Nilsson, S. E. G. (2003). Patients with AMD and a large absolute central scotoma can be trained successfully to use eccentric viewing, as demonstrated in a scanning laser ophthalmoscope. *Vision Res.* 43, 1777–1787. doi: 10.1016/S0042-6989(03)00219-0

Nilsson, U. L., and Nilsson, S. E. (1986). Rehabilitation of the visually handicapped with advanced macular degeneration: a follow-up study at the Low Vision Clinic, Department of Ophthalmology, University of Linköping. *Doc. Ophthalmol.* 62, 345–367. doi: 10.1007/BF00168266

Plank, T., Frolo, J., Brandl-Rühle, S., Renner, A. B., Hufendiek, K., Helbig, H., et al. (2011). Gray matter alterations in visual cortex of patients with loss of central vision due to hereditary retinal dystrophies. *Neuroimage* 56, 1556–1565. doi: 10.1016/j.neuroimage.2011.02.055

Plank, T., Frolo, J., Farzana, F., Brandl-Rühle, S., Renner, A. B., and Greenlee, M. W. (2012). Neural correlates of visual search in patients with hereditary retinal dystrophies. *Hum. Brain Mapp*. doi: 10.1002/hbm.22088. [Epub ahead of print].

Polat, U. (2009). Perceptual learning induces neuroplasticity, enabling improvement of visual functions. *Expert Rev. Ophthalmol.* 4, 573–576. doi: 10.1586/eop.09.54

Rorden, C., and Brett, M. (2000). Stereotaxic display of brain lesions. *Behav. Neurol.* 12, 191–200.

Rovner, B. W., Casten, R. J., Leiby, B. E., and Tasman, W. S. (2009). Activity loss is associated with cognitive decline in age-related macular degeneration. *Alzheimers Dement.* 5, 12–17. doi: 10.1016/j.jalz.2008.06.001

Rubin, G. S., and Feely, M. (2009). The role of eye movements during reading in patients with Age-related Macular Degeneration (AMD). *Neuroophthalmology* 33, 120–126. doi: 10.1080/01658100902998732

Schoups, A. A., Vogels, R., and Orban, G. A. (1995). Human perceptual learning in identifying the oblique orientation: retinotopy, orientation specificity and monocularity. *J. Physiol.* 483, 797–810.

Segonne, F., Dale, A. M., Busa, E., Glessner, M., Salat, D., Hahn, H. K., et al. (2004). A hybrid approach to the skull stripping problem in MRI. *Neuroimage* 22, 1060–1075. doi: 10.1016/j.neuroimage.2004.03.032

Segonne, F., Pacheco, J., and Fischl, B. (2007). Geometrically accurate topology correction of cortical surfaces using nonseparating loops. *IEEE Trans. Med. Imaging* 26, 518–529. doi: 10.1109/TMI.2006.887364

Seiple, W., Szlyk, J. P., McMahon, T., Pulido, J., and Fishman, G. A. (2005). Eye-movement training for reading in patients with age-related macular degeneration. *Invest. Ophthalmol. Vis. Sci.* 46, 2886–2896. doi: 10.1167/iovs.04-1296

Sled, J. G., Zijdenbos, A. P., and Evans, A. C. (1998). A nonparametric method for automatic correction of intensity nonuniformity in MRI data. *IEEE Trans. Med. Imaging* 17, 87–97. doi: 10.1109/42.668698

Sunness, J. S., Applegate, C. A., Haselwood, D., and Rubin, G. S. (1996). Fixation patterns and reading rates in eyes with central scotomas from advanced atrophic age-related macular degeneration and Stargardt disease. *Ophthalmology* 103, 1458–1466.

Szlyk, J. P., and Little, D. M. (2009). An FMRI study of word-level recognition and processing in patients with age-related macular degeneration. *Invest. Ophthalmol. Vis. Sci.* 50, 4487–4495. doi: 10.1167/iovs.08-2258

Timberlake, G. T., Peli, E., Essock, E. A., and Augliere, R. A. (1987). Reading with a macular scotoma. II. Retinal locus for scanning text. *Invest. Ophthalmol. Vis. Sci.* 28, 1268–1274.

Trauzettel-Klosinski, S., and Tornow, R. P. (1996). Fixation behaviour and reading ability in macular scotoma. *Neuroophthalmology* 16, 241–253. doi: 10.3109/01658109609044632

Watanabe, T., Nanez, J. E., and Sasaki, Y. (2001). Perceptual learning without perception. *Nature* 413, 844–848. doi: 10.1038/35101601

Whittaker, S. G., Budd, J., and Cummings, R. W. (1988). Eccentric fixation with macular scotoma. *Invest. Ophthalmol. Vis. Sci.* 29, 268–278.

Yotsumoto, Y., Watanabe, T., and Sasaki, Y. (2008). Different dynamics of performance and brain activation in the time course of perceptual learning. *Neuron* 57, 827–833. doi: 10.1016/j.neuron.2008.02.034

Conflict of Interest Statement: The authors declare that the research was conducted in the absence of any commercial or financial relationships that could be construed as a potential conflict of interest.

Received: 05 January 2013; accepted: 22 June 2013; published online: 17 July 2013.

*Citation: Rosengarth K, Keck I, Brandl-Rühle S, Frolo J, Hufendiek K, Greenlee MW and Plank T (2013) Functional and structural brain modifications induced by oculomotor training in patients with age-related macular degeneration. Front. Psychol. **4**:428. doi: **10.3389/fpsyg.2013.00428***

This article was submitted to Frontiers in Perception Science, a specialty of Frontiers in Psychology.

frontiers in PSYCHOLOGY

ORIGINAL RESEARCH ARTICLE
published: 07 February 2014
doi: 10.3389/fpsyg.2014.00074

Visual cortex in aging and Alzheimer's disease: changes in visual field maps and population receptive fields

Alyssa A. Brewer* and Brian Barton

Laboratory of Visual Neuroscience, Department of Cognitive Sciences, Center for Cognitive Neuroscience, University of California, Irvine, CA, USA

Edited by:
Mark W. Greenlee, University of Regensburg, Germany

Reviewed by:
Alex R. Wade, University of York, UK
Serge O. Dumoulin, Utrecht University, Netherlands

****Correspondence:***
Alyssa A. Brewer, Laboratory of Visual Neuroscience, Department of Cognitive Sciences, Center for Cognitive Neuroscience, University of California, 3151 Social Sciences Plaza, Irvine, CA 92697, USA
e-mail: aabrewer@uci.edu

Although several studies have suggested that cortical alterations underlie such age-related visual deficits as decreased acuity, little is known about what changes actually occur in visual cortex during healthy aging. Two recent studies showed changes in primary visual cortex (V1) during normal aging; however, no studies have characterized the effects of aging on visual cortex beyond V1, important measurements both for understanding the aging process and for comparison to changes in age-related diseases. Similarly, there is almost no information about changes in visual cortex in Alzheimer's disease (AD), the most common form of dementia. Because visual deficits are often reported as one of the first symptoms of AD, measurements of such changes in the visual cortex of AD patients might improve our understanding of how the visual system is affected by neurodegeneration as well as aid early detection, accurate diagnosis and timely treatment of AD. Here we use fMRI to first compare the visual field map (VFM) organization and population receptive fields (pRFs) between young adults and healthy aging subjects for occipital VFMs V1, V2, V3, and hV4. Healthy aging subjects do not show major VFM organizational deficits, but do have reduced surface area and increased pRF sizes in the foveal representations of V1, V2, and hV4 relative to healthy young control subjects. These measurements are consistent with behavioral deficits seen in healthy aging. We then demonstrate the feasibility and first characterization of these measurements in two patients with mild AD, which reveal potential changes in visual cortex as part of the pathophysiology of AD. Our data aid in our understanding of the changes in the visual processing pathways in normal aging and provide the foundation for future research into earlier and more definitive detection of AD.

Keywords: aging, Alzheimer's disease, vision, visual field mapping, population receptive field modeling

INTRODUCTION

In order to carefully evaluate alterations of visual cortex in age-related neurodegenerative diseases such as Alzheimer's disease (AD), we must first have a clear understanding of what changes occur across visual cortex during healthy aging (Jackson and Owsley, 2003; Yankner et al., 2008). Studies of the aging visual cortex are limited, however. Although the organization and function of early visual cortex (i.e., V1, V2, V3, hV4) have been well characterized in human, these measurements have almost exclusively been in healthy young adults or specific patient populations (Sereno et al., 1995; Deyoe et al., 1996; Dougherty et al., 2003; Crossland et al., 2008; Baseler et al., 2011; Brewer and Barton, 2012b).

Two recent neuroimaging studies have examined V1 in healthy aging subjects. Using functional magnetic resonance imaging (fMRI) with traveling wave visual field mapping (VFM) methods, Crossland et al. (2008) showed that primary visual cortex (V1) of healthy aging subjects has lower blood-oxygen-level-dependent (BOLD) activity in the fovea compared to healthy young adults. This study also demonstrated that aging has no effect on fixation stability, which is important to demonstrate the feasibility of VFM measurements in this subject population. Building on these results, we (Brewer and Barton, 2012a) used fMRI population receptive field (pRF) modeling methods (Dumoulin and Wandell, 2008) to demonstrate several changes in the V1 of aging subjects compared to young subjects, including (1) a decrease in surface area of foveal V1 from 0 to 3°, and (2) an increase in the pRF sizes within this same foveal region. These alterations may account for behavioral changes associated with vision in aging such as reduced visual acuity and decreased contrast sensitivity at medium and high spatial frequencies (Elliott, 1987; Whitaker and Elliott, 1992). In addition, these previous neuroimaging findings may also reflect anatomical changes in the aging visual pathways, such as a decline in the retinal nerve fiber layer thickness (Balazsi et al., 1984; Parikh et al., 2007) and a loss of retinal photoreceptors (Gao and Hollyfield, 1992; Curcio et al., 1993; Jackson et al., 2002).

These measurements have demonstrated several changes in healthy aging just within primary visual cortex, but very little is known about the effects of aging on the structural and functional characteristics of VFMs beyond V1. The present measurements are the first to expand our fledgling understanding of the effects of normal aging beyond primary visual cortex.

Once we can distinguish the cortical changes related to healthy aging from those resulting from the pathophysiology of the disease, we can begin to investigate changes in visual cortex in age-related disorders like AD. AD, the most common form of dementia, is characterized by progressive cognitive deficits

including disturbances in memory, language, executive function, and vision (Black, 1996; Yankner et al., 2008). Early detection and accurate diagnosis are key in the hope for a cure for dementias such as AD, as early, accurate diagnosis would allow for more timely initiation of treatments. As visual symptoms can occur early in AD, it is possible that measurements of changes in visual cortex in these patients could aid early detection of neurodegeneration. Cortical representations of visual space (e.g., VFMs) in particular provide a highly-structured functional measurement that might be used to detect subtle effects of neurodegeneration early in the disease process. A better understanding of the progression of the pathology within visual cortex could also help to target drug research for therapeutic interventions (Rosen, 2004).

AD can present with a variable range of visual symptoms across subjects, from lower level deficits such as changes in visual field coverage, contrast sensitivity, color discrimination, visuospatial perception, and visual processing speed (Cronin-Golomb et al., 1993; Chan et al., 2001; Jackson and Owsley, 2003; Mapstone et al., 2003; Sauer et al., 2006; Thiyagesh et al., 2009) to higher level deficits such as problems in visual attention and in feature recognition of complex objects such as faces (Parasuraman et al., 1992; Giannakopoulos et al., 1999, 2000; Holroyd and Shepherd, 2001; Pache et al., 2003; Tang-Wai et al., 2004; van Rhijn et al., 2004; Bokde et al., 2006; Thiyagesh et al., 2009). These deficits could be attributed perhaps to a random pattern of neurodegeneration across regions of visual cortex (Jackson and Owsley, 2003). However, there is also emerging evidence for a more precise distribution of neurodegeneration in the AD visual pathways, with some studies showing neurofibrillary tangles and neuritic senile plaques increasing steadily from primary to associative visual cortex (Lewis et al., 1987; Black, 1996; Giannakopoulos et al., 1999; Yankner et al., 2008). In addition, several studies have found that AD patients have widespread axonal degeneration of the optic nerves and a reduction of retinal ganglion cells (Hinton et al., 1986; Danesh-Meyer et al., 2006; Iseri et al., 2006; Berisha et al., 2007; Paquet et al., 2007). These cortical and retinal lesions both result in the disruption of normal inputs to the visual processing streams, which we expect to be reflected in changes in the organization, functionality and connectivity of visual cortex. However, despite many descriptions of visual symptoms in AD, little is known about the extent of changes in visual cortex that underlie these visual deficits.

Here we use pRF modeling (Dumoulin and Wandell, 2008) to compare detailed structural and functional measurements of occipital VFMs V1, V2, V3, and hV4 between healthy young adults and normally aging subjects. We also demonstrate the feasibility of these measurements in patients with early, mild AD and present the first characterization of VFMs V1, V2, V3, and hV4 in these patients.

METHODS

SUBJECT RECRUITMENT AND CHARACTERIZATION

Eleven subjects were recruited for this study: five healthy young adult subjects aged 24–36 years (two female; mean age = 28 years, $SD = 4.8$ years), four healthy, normally aging subjects aged 57–70 years (three female; mean age = 63.5 years, $SD = 5.4$ years), and two patients diagnosed with early, mild probable AD aged 70 (AD-S11; female) and 72 (AD-S10; male) years (mean age = 71 years, $SD = 1.4$ years). There was no significant difference between the ages of the healthy aging and AD subject groups, as determined by a two-tailed, independent samples t-test [$t_{(4)} = 1.816$; $p = 0.14$]. The young adult subjects were recruited from the students and faculty at the University of California, Irvine (UCI). The aging and AD subjects were recruited from the normally aging and AD cohorts enrolled at the Alzheimer's Disease Research Center (ADRC) at UCI. Subjects are included in each cohort based upon neuropsychiatric testing and clinical diagnosis through the ADRC, with a normal Mini-Mental State Exam (MMSE) (Folstein et al., 1975) score between 29 and 30 for healthy aging subjects and between 21 and 26 for subjects with a diagnosis of mild probable AD. AD subjects were included in the study with a diagnosis of mild probable AD within the last year. ADRC cohorts undergo a battery of tests and longitudinal data collection including: demographics, medical history, medications, family history, physical exam, neurological exam, cognitive testing and diagnosis, APOE genotypes, and comprehensive neuropsychological testing. Neuropsychological tests are scored by ADRC expert raters and clinicians. Clinical diagnosis is confirmed by consensus among two or more ADRC physicians. All subjects recruited for this study had no history of previous head injury, alcoholic brain damage, a pre-existing visual disorder, or any additional significant physical or psychiatric conditions. All subjects had normal or corrected-to-normal visual acuity (at least 20/25) with no underlying visual disease. The Institutional Review Board at UCI approved all aspects of the experimental protocol. Informed consent was obtained from all subjects prior to the initiation of any experiments.

EXPERIMENTAL DESIGN

Each subject underwent 1–2 fMRI scan sessions, in which one high-resolution, T1-weighted anatomical volume, one T1-weighted in-plane anatomical scan, and 8 functional VFM scans were collected. Visual stimuli were generated using the Psychophysics Toolbox (Brainard, 1997; Pelli, 1997) in the Matlab programming environment on a Dell Optiplex desktop. Stimuli were back-projected via a Christie DLV1400-DX DLP projector onto a screen at the head end of the bore of the magnet (spatial resolution: 1024 × 768 pixels, refresh rate: 60 Hz).

All subjects were shown the stimulus display and experiment room setup prior to starting the experiment. Particular time was spent with the AD subjects in order to ensure their abilities to comply with the experimental task throughout each scan. Subjects performed several trials of the stimulus on a display in the scanner control room. During this practice, they were shown the stimulus characteristics, practiced fixating on the center cross, and practiced attending to the movements of the checkerboard pattern. All subjects were able to perform these tasks well prior to starting data collection within the scanner.

For the scans, subjects lay supine in the bore of the magnet and viewed the display on an angled front surface mirror mounted on the head coil (viewing distance = ∼70 cm). Head movements were minimized with padding and tape. Subjects were required to maintain fixation on a central cross for the duration of a single scan; regular blinking was encouraged. Each scan

was ∼3 min in length, with short breaks between each scan. Subjects were reminded to fixate and to perform the attentional task between each 3 min scan. Eye position at fixation was verified using an MR-compatible long range remote eye tracking system (*Applied Science Laboratories*, Bedford, MA). All subjects were able to maintain fixation throughout all scans. No effects of problems with eye position (e.g., consistent offset, nystagmus) could explain the results presented below (for models of poor fixation, see Baseler et al., 2002; Crossland et al., 2008; Levin et al., 2010).

MOVING BAR STIMULUS FOR VISUAL FIELD MAPPING

During all functional scans, the subject viewed a moving bar stimulus comprised of high-contrast, flickering, black, and white checkerboard patterns similar to the pattern used in typical wedge and ring traveling wave stimuli. The checkerboard pattern reversed contrast at a temporal frequency of 2 Hz, producing checkerboard rows that appeared to be moving in the opposite direction to adjacent rows (Brewer and Barton, 2012b). The stimulus subtended a maximum radius of 11° of visual angle. The moving bar was displaced in discrete steps every 2 s in synchrony with the fMRI volume acquisition and moved across the visible screen in eight different configurations (four orientations: 0, 45, 90, and 135° from vertical with two orthogonal motion directions) for a total presentation time of 192 s at one cycle/scan. Four mean-luminance ("blank") periods for use in the pRF analysis (Dumoulin and Wandell, 2008) were inserted in the last 12 s of each 48 s period, at a frequency of four cycles/scan (a non-stimulus frequency).

Subjects maintained fixation on one of two large fixation crosses, spanning either the diagonals from the corners of the field of view ("**X**") or the midpoints of each of the sides of the field of view ("**+**"). The lines of each fixation cross were roughly 0.5° wide, and they randomly switched between the two screen positions every 2–4 s during the progression of the bar stimulus across the visual field. Subjects were instructed to attend to the moving bar stimulus and were required to respond with a button press (not in sync with the visual stimulus position changes or mean-luminance periods) to an intermittent, subtle change in the motion direction of the checkerboard pattern.

ANATOMICAL DATA ACQUISITION AND PROCESSING

Scanning was conducted on the 3T Philips Achieva MR scanner at UCI with an eight channel SENSE imaging head coil. One high-resolution, whole-brain anatomical data set was acquired for each subject (T1-weighted 3D MPRAGE, 1 mm^3 voxels, TR = 8.4 ms, TE = 3.7 ms, flip = 8°, SENSE factor = 2.4). There were no problems with T1 acquisition (e.g., due to subject motion) for any scans. Custom Matlab-based software (*mrGray* in the *mrVista* package, freely available online at http://white.stanford.edu/software) was used to define the white matter in the structural anatomical image for each individual subject (Teo et al., 1997). This software uses an automated algorithm to initially select the white matter, followed by hand-editing to minimize segmentation errors (Dougherty et al., 2003). Hand-editing allows for careful, accurate segmentation of cortex not only in individual subjects with normal anatomy, but also in individuals with unusual and/or abnormal anatomy, such as is expected in aging and AD subjects (**Figure 1**). Gray matter was grown from the segmented white matter to form a layer covering the white matter surface. The cortical surface was then represented as a mesh at the white/gray-matter border, which was used to render a smooth 3D cortical surface or to flatten the cortical representation, with light gray regions indicating gyri and dark gray regions representing sulci (Wandell et al., 2000).

In addition, one anatomical in-plane image was acquired before each set of functional scans, with the same slice prescription as the functional scans, but with a higher spatial resolution (1 × 1 × 3 mm voxels). These T1-weighted slices were physically in register with the functional slices and were used to align the functional data with the high-resolution anatomical data, first by a manual co-registration and then by a semi-automated 3D co-registration algorithm, a mutual information method (Maes et al., 1997; Nestares and Heeger, 2000).

FUNCTIONAL DATA ACQUISITION AND PROCESSING

Functional MR data for VFM measurements were acquired on the same scanner as the anatomical data, with ∼35 oblique slices oriented close to parallel to the calcarine sulcus (T2-weighted, gradient echo imaging, TR = 2 s, TE = 30 ms, flip = 90°, SENSE factor = 1.7, reconstructed voxel size of 1.875 × 1.875 × 3 mm,

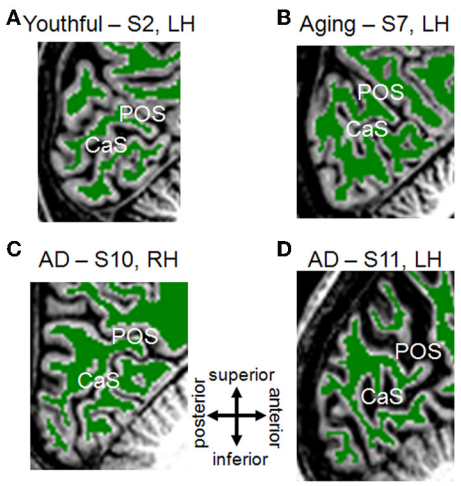

FIGURE 1 | White/Gray matter segmentation for young, healthy aging, and mild Alzheimer's disease subjects. Each panel is a T1-weighted 3D MPRAGE image showing a sagittal slice near the midline of the brain, cropped to the occipital lobe with the calcarine sulcus (CaS; home to V1) and the parietal-occipital sulcus (POS) visible. Green-colored overlay represents white matter identified by an automated algorithm (Teo et al., 1997) and adjusted by hand-editing to minimize segmentation errors (Dougherty et al., 2003). Gray regions are gray matter, and white regions are white matter not segmented in the cerebellum. Gray matter is grown from the boundary of the white matter and bounded by the cerebral spinal fluid (CSF; black adjacent to gray matter). Portions of skull and dura mater are also visible. **(A)** Youthful Subject 2, left hemisphere. **(B)** Aging Subject 7, left hemisphere. **(C)** Mild Alzheimer's disease Subject 10, right hemisphere. **(D)** Mild Alzheimer's disease Subject 11, left hemisphere. Compare AD-S10's intact anatomy to the visibly altered visual field maps from this subject in **Figure 2**. Note also the reverse pattern for AD-S11, who has grossly intact map sizes, but more strikingly increased CSF-filled space.

no gap). For each subject, data in each fMRI session were analyzed voxel-by-voxel with no spatial smoothing, using the same custom Matlab-based software package (*mrVista*; http://white.stanford.edu/software). Head movements across scans were examined by comparing the mean value maps of the BOLD signals. Because all scans had less than one voxel of head motion, no motion correction algorithm was applied here. The BOLD time series from each scan was high-pass filtered to remove low-frequency sources of physiological noise and averaged together to form one mean time series for each subject, which was then used in the pRF model analysis (Dumoulin and Wandell, 2008).

POPULATION RECEPTIVE FIELD MODELING ANALYSIS

pRF modeling is an emerging method for detailed VFM experiments (Dumoulin and Wandell, 2008; Amano et al., 2009; Baseler et al., 2011; Harvey and Dumoulin, 2011; Haak et al., 2012a,b; Zuiderbaan et al., 2012; Harvey et al., 2013) that can estimate cortical visual field responses to any stimulus that periodically covers visual space, such as the moving bars used here. Briefly, in retinotopically-organized regions of visual cortex, each voxel in a VFM contains a population of neurons with similar receptive fields (RFs). We call the average RF measured across a voxel a "population receptive field" (pRF). Thus, pRF modeling treats each voxel in a VFM as a pRF with a preferred center (x, y) and spread (σ). To determine this, the model creates a bank of 2D Gaussian pRFs of numerous possible sizes and visual field locations spanning the field of view, convolves each predicted response to the presented stimulus with the hemodynamic response function (HRF) (Boynton et al., 1996; Friston et al., 1998), and tests the result against the data. The pRF which best matches the data is then used to determine that voxel's variance explained, visual field representation, and pRF size. This method not only replicates results of VFM measurements from the traveling wave method in a model-based way, but allows for additional measures such as pRF sizes. Complete details of the pRF model analysis are described in Dumoulin and Wandell (2008).

Here we used the pRF method to estimate VFMs and pRFs for posterior occipital VFMs V1, V2, V3, and hV4. Eccentricity [$\sqrt{(x^2+y^2)}$] and angle [$\tan^{-1}(y/x)$] were derived from the 2D Gaussian models and plotted on the unfolded cortical surface for each hemisphere in each subject. pRF modeling uses percent variance explained as a primary measurement of the goodness-of-fit of the model to the BOLD time series data; here we independently assign each voxel a value for variance explained. Only voxels with variance explained $\geq$0.04 (corresponding to the standardly-used coherence threshold in traveling wave studies of 0.20) were assigned a phase corresponding to that voxel's peak response to the stimuli presented and considered for further analysis. We have measured the noise in visual cortex of all our subject groups using baseline measurements in early visual cortex with a combination of approaches, including photopic and scotopic visual stimuli (bars, wedges, rings) with traveling wave and pRF modeling methods. Our measurements show a maximum baseline noise level for coherence (from traveling wave measurements) of 0.15 and for variance explained (from pRF modeling measurements) of 0.03. The majority of our measurements presented here are well above these values (**Figures 2**, **6**, **7**).

Finally, it is important to note that the pRF modeling method allows for the use of the single moving bar stimulus to determine both the polar angle and eccentricity dimensions of the cortical representations of visual space within a single scan. This means that alterations seen in one dimension (e.g., eccentricity) that are not observed in the second dimension (e.g., polar angle) cannot be simply attributed to a problem with that particular scan.

VISUAL FIELD MAP DEFINITION

We define VFMs by the following criteria: (1) both a polar angle and an eccentricity gradient must be present, (2) the polar angle and eccentricity gradients must be orthogonal to one another,

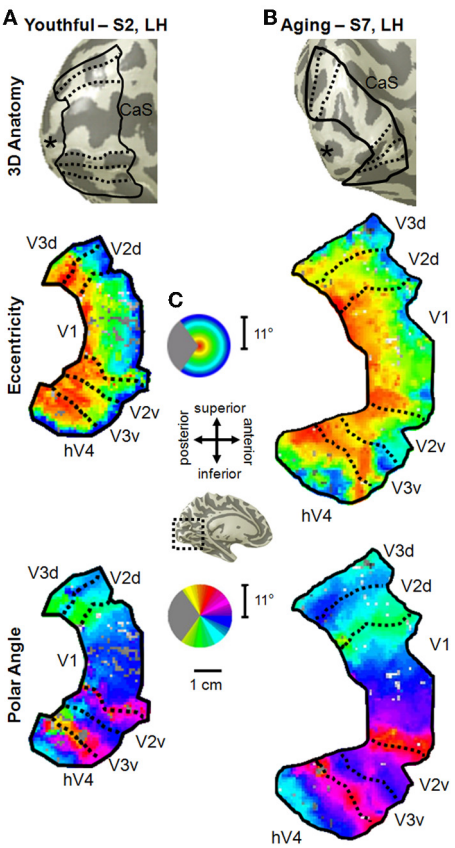

FIGURE 2 | Visual field map measurements in healthy young and aging subjects. (A) Example of VFMs V1, V2, V3, and hV4 from a healthy young adult (S2, left hemisphere). VFM boundaries are overlaid on a 3D representation of S2's left hemisphere (top panel). The "*" denotes the occipital pole. A cropped, close-up view of the flattened cortical surface surrounding the calcarine sulcus is shown for measurements of eccentricity and polar angle in the middle and bottom panels, respectively. The pseudo-color overlay on each flattened cortical rendering represents the position in visual space that produces the strongest response at each cortical location [see colored legend insets in **(C)**]. The stimuli covered the central 11° radius of visual space. For clarity, the visual responses are only shown for the VFMs of interest, V1, V2, V3, hV4. **(B)** Example of VFMs V1, V2, V3, and hV4 from a healthy aging subject (S7, left hemisphere). Note regular, organized, orthogonal VFMs as seen in **(A)**. **(C)** Legends and scale bar for flattened cortical maps are shown. Approximate cortical location is depicted on an example left hemisphere 3D rendering (black dotted lines, central inset).

and (3) each VFM must represent a complete contralateral hemifield of visual space (e.g., Wandell et al., 2007; Brewer and Barton, 2012b). Here, as usual, the boundaries between V1, V2, V3, and hV4 were determined by manually tracing the polar angle reversals along the medial occipital wall and along the periphery of the eccentricity gradient representing the 11° radius stimulus. Because hemodynamic changes have been shown to occur with normal aging, we identified the phases at which boundary reversals occurred in order to compare the correct stimulus location in visual space with the corresponding cortical responses (D'Esposito et al., 1999, 2003; Crossland et al., 2008).

STATISTICAL ANALYSIS

For the following comparisons between young adult and healthy aging subjects of the measurements of VFM surface areas, variance explained, and pRF sizes, we divided up the eccentricity representation in each map in each hemisphere of each subject into specific bands. For each VFM, we created 10 regions of interest (ROIs) spanning 1° of visual angle along the eccentricity gradient from 0 to 10°, centered on every half degree (**Figures 4–9**). Each measurement was drawn from these 10 eccentricity-band ROIs for each subject, averaged between hemispheres for each subject, and then analyzed across subjects within each group. Two previous fMRI VFM studies comparing youthful and normal aging subjects indicated that the central 3° of visual angle about fixation is the most likely area to be affected by aging in V1. Aging subjects' V1 maps have significantly less surface area and larger pRF sizes in the central 3° relative to youthful subjects (Crossland et al., 2008; Brewer and Barton, 2012a). These neuroimaging results may reflect cortical changes related to behavioral measures of decreased visual acuity in normal aging (Elliott, 1987; Whitaker and Elliott, 1992). The same subjects are analyzed here as in the previous Brewer and Barton (Brewer and Barton, 2012a) study; however, we use a different statistical approach, and we present novel measurements of V2, V3, and hV4. Here, we perform one multivariate analysis of variance (MANOVA) for the central 3° and peripheral 3–10° of V1, V2, V3, and hV4 for each of the three measurements (surface area, variance explained, and pRF size).

RESULTS

COMPARISONS BETWEEN HEALTHY AGING AND YOUTHFUL SUBJECTS

Aging vs. youth: overall visual field map organization

For the youthful and healthy aging subjects, we were able to easily define the boundaries of V1, V2, V3, and hV4 in all subjects (**Figure 2**). All four VFMs in all hemispheres contained a complete representation of the contralateral hemifield, in line with previous measurements of these VFMs in young subjects (e.g., Engel et al., 1994, 1997; Sereno et al., 1995; Black, 1996; Brewer et al., 2005; Wandell et al., 2007; Brewer and Barton, 2012b) and in V1 in healthy aging subjects (Crossland et al., 2008; Brewer and Barton, 2012a). Note that human V2 and V3 are standardly considered in each hemisphere to be VFMs that represent complete hemifields of visual space with non-contiguous quarterfields (e.g., Brewer et al., 2002; Wandell et al., 2007).

In all hemispheres of these two subject groups, the confluent eccentricity gradient of the posterior VFMs corresponding to the 11° radius of our stimulus spanned from the foveal representation (**Figure 2**, *middle panel*, eccentricity—red/orange) on the occipital pole along calcarine to the more anterior peripheral representation (**Figure 2**, *middle panel*, eccentricity—green/blue/purple). The second dimension of visual space necessary to separate the confluent eccentricity representation of the occipital pole into specific VFMs is the polar angle. The polar angle gradient of V1 spanned the medial surface of the occipital pole from the dorsal edge of the calcarine sulcus on the cuneus (**Figure 2**, *bottom panel*, polar angle—cyan) to the ventral edge of the calcarine sulcus on the lingual gyrus (**Figure 2**, *bottom panel*, polar angle—magenta), with the lower vertical meridian of visual space represented dorsally and vice versa, as expected from our previous V1 measurements in these young and aging subjects (Brewer and Barton, 2012a). The dorsal lower vertical meridian representation of V1 reversed into V2d along the dorsal edge of the calcarine, which then reversed from the horizontal meridian of V2d into V3d. Similarly, the ventral upper vertical meridian representation of V1 reversed into the polar angle gradient of the upper quarterfield of V2v and onto V3v. In addition, a full hemifield of visual space for hV4 adjacent to V3v was measured in all subjects along the posterior fusiform gyrus.

The total surface area of each VFM is shown for individual young (blue symbols), healthy aging (red symbols) and AD (green symbols) subjects in **Figure 3A** and for the group averages for individual young (blue bars) and healthy aging (red bars) in **Figure 3B**. To determine whether there were total surface area differences between youth and aging subjects, we performed a One-Way analysis of variance (ANOVA) for each map, V1, V2, V3, and hV4. These ANOVAs revealed no difference for V1, $F_{(7,\ 1)} = 1.371$, $p = 0.280$ or V2, $F_{(7,\ 1)} = 2.177$, $p = 0.184$. There was a marginally significant difference for V3, $F_{(7,\ 1)} = 4.082$, $p = 0.083$. Finally, the total surface area of hV4 was significantly different between the groups $F_{(7,\ 1)} = 5.903$, $p = 0.045$.

Aging vs. youth: surface area percent distributions across eccentricity

Cortical magnification is a general property of sensory systems that reflects sensitivity to important regions of sensory space; measuring a change in the extent of a particular part of the eccentricity gradient along cortex between subject groups would suggest differences in the functional properties of that region of cortex. While historically more common, existing estimates of the cortical magnification factor from human fMRI measurements typically only take one dimension of cortical space into account (position along eccentricity axis) and ignore the other (position along polar angle axis) (e.g., Dougherty et al., 2003). Thus, the cortical magnification factor as a function of position along the eccentricity axis does not reflect the magnification of representation along an iso-eccentricity line (i.e., across polar angles). Here we measured surface area percent distribution across the eccentricity-band ROIs to provide a measure that takes this "width" across polar angles into account.

In order to examine differences in VFM surface area percent distribution between the healthy aging and young subjects, we compared the average surface area percent distribution for the eccentricity-band ROIs in each VFM (**Figures 4**, **5**, blue (young)

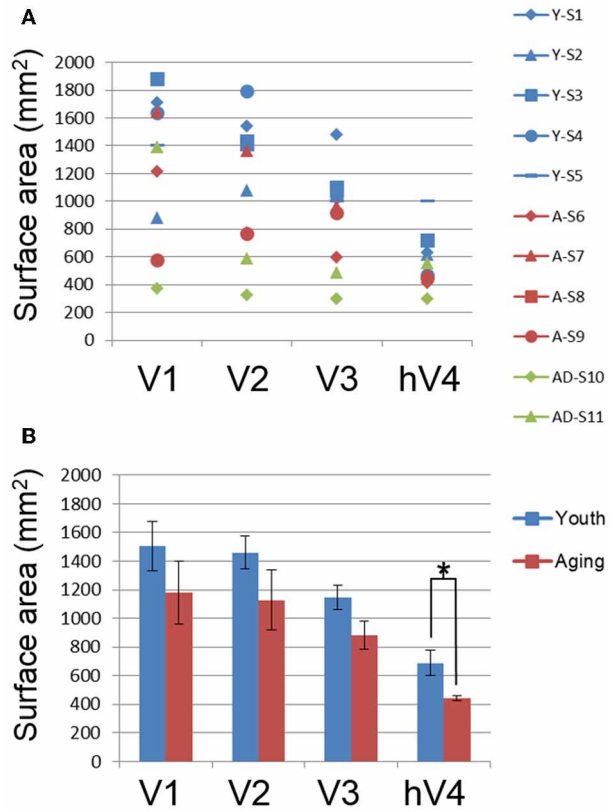

FIGURE 3 | Total surface area measurements for visual field maps. (A) Total surface area for each map for individual young (blue), healthy aging (red), and mild Alzheimer's disease (green) subjects. **(B)** Total surface area for each map averaged from ∼0.5 to 10° across youthful subjects (blue bars) and normal aging subjects (red bars). Error bars indicate s.e.m. "*" marks statistically significant differences ($p < 0.05$) between youthful and healthy aging subjects in hV4.

and red (aging) lines). With the parameters (e.g., width, spatial frequency) of the moving bar stimulus, we cannot obtain clear measurements of surface area to the full center (0°) of the visual field representation nor at the very peripheral edge of the stimulus range (11°), as is typical for these stimuli (Dumoulin and Wandell, 2008). Thus, for the percent surface area measurements, we restrict the data presented in **Figures 4**, **5** to the 1–10° eccentricity range (i.e., the bins centered on 1.5–9.5°), allowing better comparison of these measurements to previous measures of cortical magnification with human fMRI. Although we standardly define the boundaries of VFMs on a flattened representation of cortex for optimal visualization of the polar angle and eccentricity gradients and boundaries, all ROIs are always transformed back into the 3D cortical representation to make the measurements of surface area along the 3D, folded cortical manifold to avoid the distortions induced by flattening cortex (Wandell et al., 2007; Brewer and Barton, 2012b). Overall, we observed a significant decrease ($p < 0.05$; see comparisons below) of surface area percent distribution in the central 3° for V1, V2, and hV4 between young and aging subjects, consistent with both previous measures in V1 (Crossland et al., 2008; Brewer and Barton, 2012a) and expectations from behavioral measures of decreased acuity (Elliott, 1987; Whitaker and Elliott, 1992).

Statistical analyses.

- V1 Comparisons: We previously reported a comparison of V1 measurements of *absolute* surface area for specific eccentricity ranges between young and healthy aging subjects in Brewer and Barton (2012a). Here we have normalized this absolute surface area by total VFM surface area and present the surface area percent distribution. A MANOVA revealed a significant decrease in surface area representing the central 3° for aging relative to youthful subjects [$F_{(3, 5)} = 6.618$, $p = 0.034$], but not the peripheral 3–10° of V1 [$F_{(7, 1)} = 1.737$, $p = 0.527$].
- V2 Comparisons: A MANOVA revealed a significant decrease in surface area representing the central 3° for aging relative to youthful subjects [$F_{(3, 5)} = 13.224$, $p = 0.008$], but not the peripheral 3–10° of V2 [$F_{(7, 1)} = 11.038$, $p = 0.224$].
- V3 Comparisons: A MANOVA revealed a marginally significant decrease in surface area representing the central 3° for aging relative to youthful subjects [$F_{(3, 5)} = 3.665$, $p = 0.098$]), but not the peripheral 3–10° of V3 [$F_{(7, 1)} = 3.297$, $p = 0.401$].
- hV4 Comparisons: A MANOVA revealed a significant decrease in surface area representing the central 3° for aging relative to youthful subjects [$F_{(3, 5)} = 11.685$, $p = 0.011$], and a marginally significant decrease in the peripheral 3–10° of hV4 [$F_{(7, 1)} = 81.063$, $p = 0.085$].

Aging vs. youth: visual field map response variance explained

Another useful characterization of the functional differences between two groups is to evaluate the responsivity of particular regions of cortex. To compare the levels of BOLD activity of each VFM between healthy aging and young subjects, we measured the average variance explained of all voxels (no threshold) within each of the 10 eccentricity-band ROIs in each VFM for each subject (**Figure 6**, blue (young) and red (aging) lines). This average variance explained per ROIs was then averaged by ROI across each VFM within each subject group (**Figure 7**, blue (young) and red (aging) lines). Statistical results are again shown for each VFM in the sections below. Overall, we observed a significant increase ($p = 0.032$; see comparisons below) in the variance explained of the central 3° of V1 in aging relative to youthful subjects.

Statistical analyses.

- V1 Comparisons: A MANOVA revealed a significant increase in the variance explained representing the central 3° for aging relative to youthful subjects [$F_{(3, 5)} = 6.817$, $p = 0.032$], but not the peripheral 3–10° of V1 [$F_{(7, 1)} = 0.559$, $p = 0.777$].
- V2 Comparisons: A MANOVA revealed no significant change in the variance explained representing the central 3° for aging relative to youthful subjects [$F_{(3, 5)} = 2.346$, $p = 0.190$], or the peripheral 3–10° of V2 [$F_{(7, 1)} = 0.601$, $p = 0.762$].
- V3 Comparisons: A MANOVA revealed no significant change in the variance explained representing the central 3° for aging relative to youthful subjects [$F_{(3, 5)} = 0.458$, $p = 0.723$], or the peripheral 3–10° of V3 [$F_{(7, 1)} = 0.223$, $p = 0.801$].

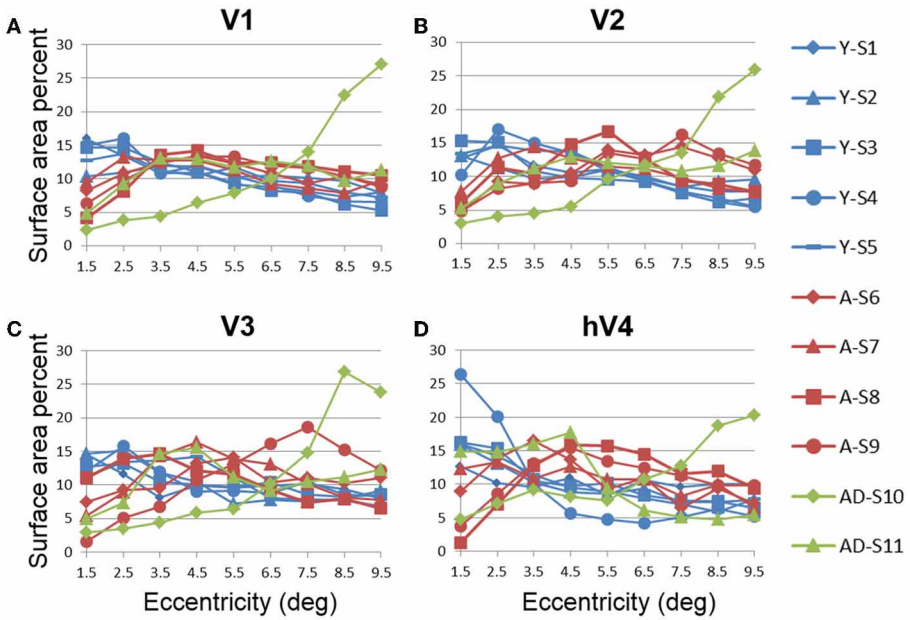

FIGURE 4 | Surface area percent distribution measurements for visual field maps in individual young, healthy aging, and mild Alzheimer's disease subjects. (A) V1. **(B)** V2. **(C)** V3. **(D)** hV4. Blue lines represent data from healthy young subjects, red lines represent data from healthy aging subjects, and green lines represent data from mild AD subjects. Each line represents data measured in individual subjects and averaged across both of each subject's hemispheres. Surface area percent is plotted as a function of degrees of eccentricity from 1 to 10° eccentricity (bins centered on 1.5–9.5°). Note the consistency for both the youthful and healthy aging subjects. Note also the different distribution for AD-S10 relative to the other subjects.

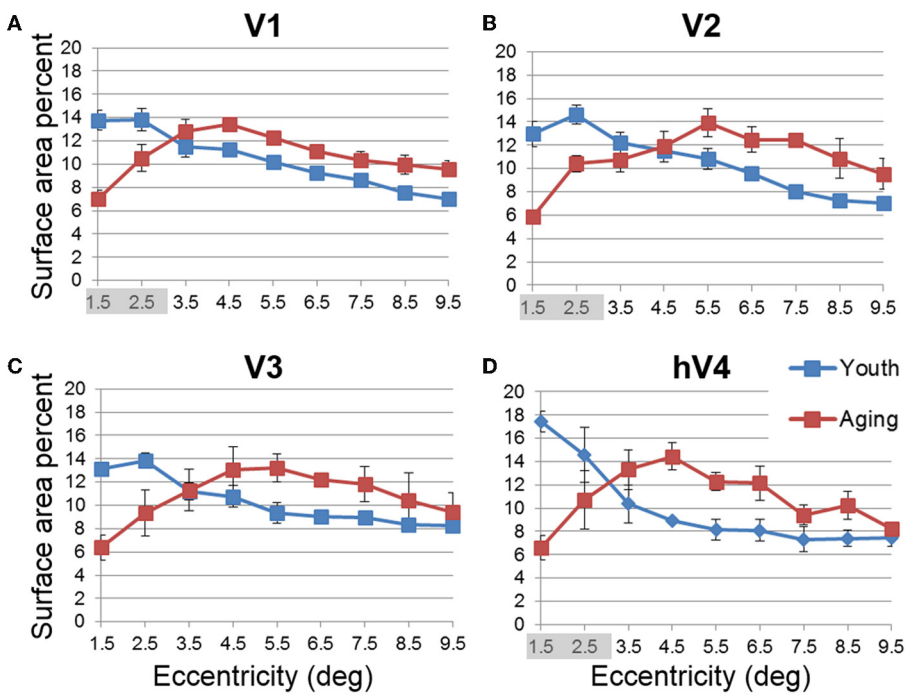

FIGURE 5 | Average surface area percent distribution measurements for visual field maps in young and healthy aging subjects. (A) V1. **(B)** V2. **(C)** V3. **(D)** hV4. Blue lines represent data from healthy young subjects, and red lines represent data from healthy aging subjects. Each bar represents data measured in individual subjects and then averaged by eccentricity band across hemispheres. Surface area percent is plotted as a function of degrees of eccentricity from 1 to 10° eccentricity (bins centered on 1.5–9.5°). Shaded gray regions indicate significant differences ($p < 0.05$) between regions (0.5–3°) in each map. Note the relatively increased fovea distribution in the youthful subjects. Error bars indicate s.e.m.

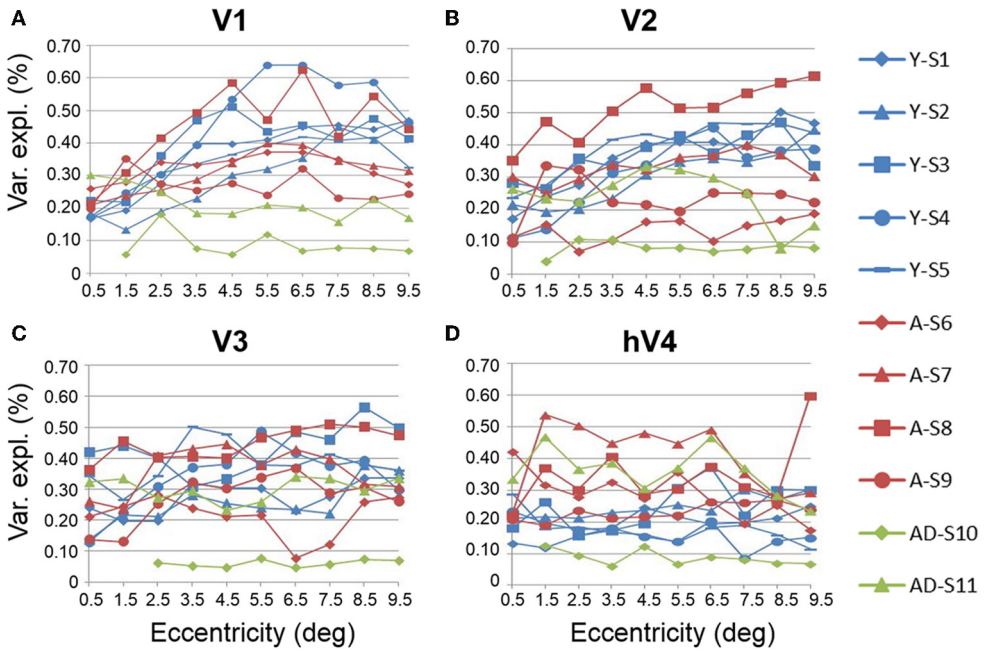

FIGURE 6 | Measurements of variance explained for visual field maps in individual young, healthy aging, and mild Alzheimer's disease subjects. (A) V1. **(B)** V2. **(C)** V3. **(D)** hV4. Blue lines represent data from healthy young subjects, red lines represent data from healthy aging subjects, and green lines represent data from mild AD subjects. Each line represents data measured in individual subjects and averaged across both of each subject's hemispheres. Variance explained is plotted as a function of degrees of eccentricity from 0 to 10° eccentricity (bins centered on 0.5–9.5°g). Note the consistency for the youthful subjects and the somewhat greater variability for the healthy aging subjects. Note also the different distribution for AD-S10 relative to the other subjects.

- hV4 Comparisons: A MANOVA revealed no significant change in the variance explained representing the central 3° for aging relative to youthful subjects [$F_{(3,\ 5)} = 0.350$, $p = 0.128$], or the peripheral 3–10° in hV4 [$F_{(7,\ 1)} = 1.832$, $p = 0.516$].

Aging vs. youth: pRF sizes across visual field maps

Like cortical magnification, the receptive field spread (or size) of sensory systems reflects sensitivity to important regions of sensory space, with smaller receptive fields giving a higher resolution of processing. In the healthy young human, the foveal representation is not only magnified in terms of cortical surface area, but also has the smallest receptive fields as measured with fMRI using pRF modeling (Dougherty et al., 2003; Dumoulin and Wandell, 2008). Here we also measured the sizes of pRFs (σ) as a function of eccentricity, averaged across subjects for each of the 10 eccentricity-band ROIs in each VFM (**Figures 8**, **9**, blue (young) and red (aging) lines) and compared these measurements between healthy aging and young subjects. Statistical results are again shown for each VFM in the sections below. Generally, we observed a statistically significant ($p < 0.05$; see comparisons below) increase in pRF sizes for the central 3° in V1, V2, and hV4. These changes are also consistent with previous measures in V1 (Crossland et al., 2008; Brewer and Barton, 2012a) and expectations from behavioral measures of decreased visual acuity (Elliott, 1987; Whitaker and Elliott, 1992).

Statistical analyses.

- V1 Comparisons: A MANOVA revealed a significant increase in pRF size in the central 3° for aging relative to youthful subjects [$F_{(3,\ 5)} = 6.285$, $p = 0.038$], but not the peripheral 3–10° of V1 [$F_{(7,\ 1)} = 0.932$, $p = 0.665$].
- V2 Comparisons: A MANOVA revealed a significant increase in pRF size in the central 3° for aging relative to youthful subjects [$F_{(3,\ 5)} = 5.869$, $p = 0.043$], but not the peripheral 3–10° of V2 [$F_{(7,\ 1)} = 28.343$, $p = 0.144$].
- V3 Comparisons: A MANOVA revealed a marginally significant increase in pRF size in the central 3° for aging relative to youthful subjects [$F_{(3,\ 5)} = 4.294$, $p = 0.075$] and the peripheral 3–10° of V3 [$F_{(7,\ 1)} = 89.348$, $p = 0.081$].
- hV4 Comparisons: A MANOVA revealed a significant increase in pRF size in the central 3° for aging relative to youthful subjects [$F_{(3,\ 5)} = 6.205$, $p = 0.039$], but not the peripheral 3–10° of hV4 [$F_{(7,\ 1)} = 25.680$, $p = 0.151$].

VISUAL FIELD MAP MEASUREMENTS IN SUBJECTS WITH MILD ALZHEIMER'S DISEASE

In contrast to the healthy aging and young subject groups, the AD subjects had more irregularities in the organization of the posterior VFMs and also differed substantially from each other (**Figure 10**). We describe these two AD subjects here as individual cases. In AD subject S10, all four VFMs measured here in both hemispheres (**Figures 10A,B**) were visibly reduced in size. Despite the smaller sizes, the polar angle representations were still

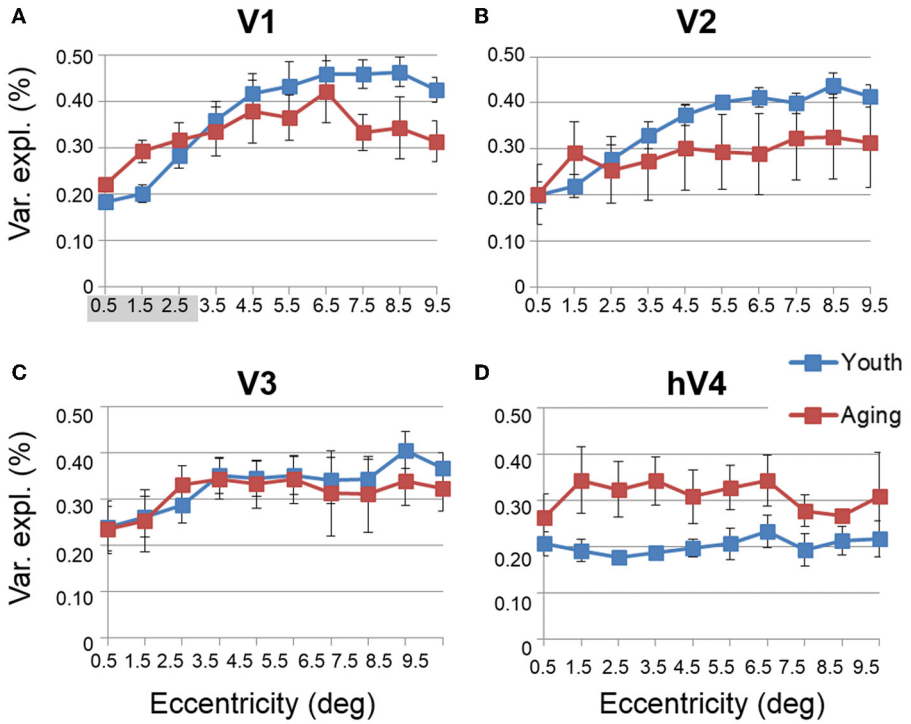

FIGURE 7 | Average measurements of percent variance explained for visual field maps in young and healthy aging subjects. (A) V1. **(B)** V2. **(C)** V3. **(D)** hV4. Blue lines represent data from healthy young subjects, and red lines represent data from healthy aging subjects. Each bar represents data measured in individual subjects and then averaged by eccentricity band across hemispheres. Variance explained percent is plotted as a function of degrees of eccentricity from 0 to 10° eccentricity (bins centered on 0.5–9.5°). Shaded gray regions indicate significant differences ($p < 0.05$) between regions (0–3°) in each map. Error bars indicate s.e.m.

regularly ordered across the region, with clearly definable boundaries of the vertical and horizontal vertical meridia between each VFM (**Figures 10A,B**, *lower panel*). In contrast, the eccentricity representations within these maps were extremely disordered in this subject. **Figures 1A,B**, *middle panel*, displays the patchy peripheral (cyan-blue) and parafoveal (yellow-orange) representations throughout each of the four VFMs. Across all four VFMs in this subject, the variance explained of the pRF model fit for these measurements was decreased compared to the measurements acquired for the other subjects (**Figure 6**, green diamonds). This lower variance explained may reflect noisy data arising from sources other than the neurodegenerative effects of AD. However, note that the measurements of both the eccentricity and polar angle representations were drawn from the same scan, using the moving bar stimulus with the pRF modeling method as described in **METHODS** above. Thus, changes in one representation (e.g., eccentricity) that are not seen in the other (e.g., polar angle) are unlikely to arise from general problems in that particular scan. In addition, the total surface area of each VFM is shown for individual AD subjects in **Figure 3A** (green diamonds). The percent surface area measurements across the eccentricity-band ROIs in this subject showed a shift in representation from the foveal regions to the relatively peripheral measurements (**Figure 4**, green diamonds). Finally, we observed decreases in the pRF sizes within relatively more peripheral regions of V2, V3, and hV4 of this subject (**Figure 8**, green diamonds).

The second AD subject, S11, had a total surface area of V1 and hV4 within the ranges of aging and young subjects, but the total surface area of V2 and V3 in this subject were similarly reduced in size to those of AD subject 10 (**Figure 3A**, green triangles, and **Figures 10C,D**). The polar angle representations in this subject were also regularly ordered across the four measured VFMs (**Figures 10C,D**, *lower panel*). The eccentricity representations in these VFMs in this subject contained more normal foveal representations than those seen in S-10, but were now lacking the full extent of the expected peripheral representations (**Figures 10C,D**, *middle panel*). The percent surface area measurements across the eccentricity-band ROIs fall within the healthy aging ranges (**Figure 4**, green triangles). Similarly, the measurements of variance explained in this subject were within the ranges of the healthy aging subjects for four VFMS, though slightly lower in V1 (**Figure 6**, green triangles). As in AD subject S-10, we also observed in S-11 decreases in the pRF sizes within relatively more peripheral regions of V2, V3, and hV4 (**Figure 8**, green triangles).

DISCUSSION

Here we have shown differences in specific structural and functional characteristics of early occipital VFMs among young, healthy aging, and AD subjects. These VFM changes may underlie many of the behavioral deficits that develop in healthy aging and AD. Measurements of disordered VFMs in some AD subjects may

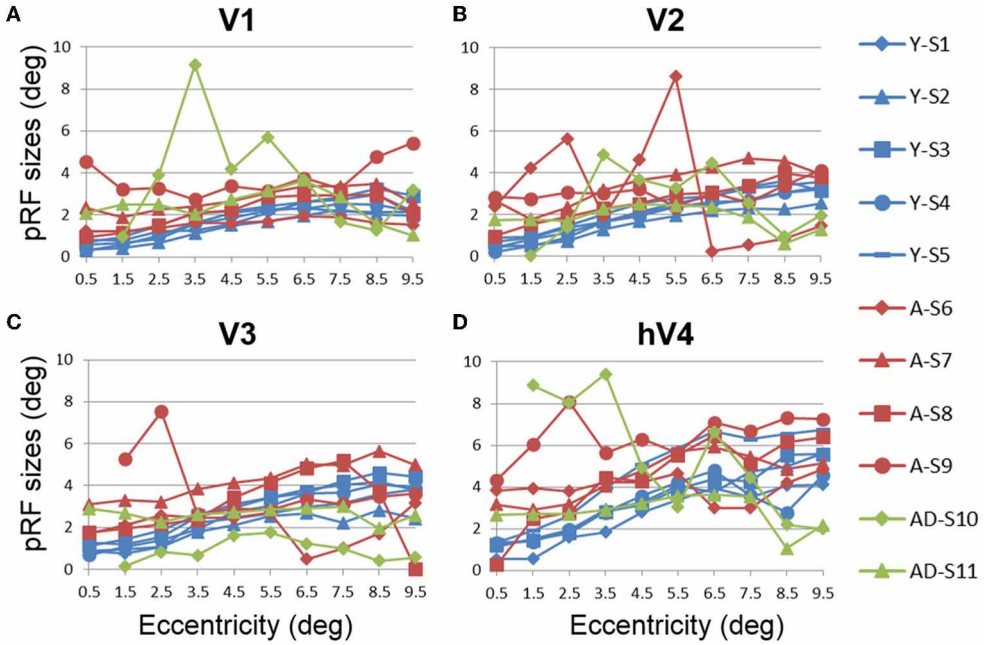

FIGURE 8 | Population receptive field size measurements for visual field maps in individual young, healthy aging, and mild Alzheimer's disease subjects. (A) V1. **(B)** V2. **(C)** V3. **(D)** hV4. Blue lines represent data from healthy young subjects, red lines represent data from healthy aging subjects, and green lines represent data from mild AD subjects. Each line represents data measured in individual subjects and averaged across both of each subject's hemispheres. pRF size is plotted as a function of degrees of eccentricity from 0 to 10° eccentricity (bins centered on 0.5–9.5°). Note the strong consistency for the youthful subjects, whereas healthy aging subjects are generally consistent, with one subject showing large deviations for each map. Also note the differences between the two AD subjects.

also be useful for improving early diagnosis of this devastating neurodegenerative disease.

VISUAL FIELD MAP CHANGES IN HEALTHY AGING

Previous studies in healthy aging showed no change in V1 volume (Raz et al., 2004) and no change in V1 surface area spanning the tested field of view (Crossland et al., 2008; Brewer and Barton, 2012a). Our results across the entire 10 eccentricity-band ROIs in VFMs V1, V2, and V3 are consistent with these findings, with no significant differences for total VFM surface area measured between the subject groups for any of these three VFMs (**Figures 2**, **3**). Interestingly, the total surface area of hV4 was significantly smaller in the healthy aging subjects. These are the first measurements to our knowledge of cortical surface areas for VFMs V2, V3, and hV4 in healthy aging subjects.

How do our results relate to previously reported visual deficits in healthy aging?

Decline in visual acuity. Our measurements of the differences between subject groups demonstrated a significant decrease in the foveal surface area percent distributions of VFMs V1, V2, and hV4 for healthy aging subjects relative to young subjects, with marginally significant differences in V3 (**Figures 4**, **5**). These aging foveal decreases are consistent with the decline in visual acuity seen normally in aging (Weale, 1975; Pitts, 1982; Gao and Hollyfield, 1992; Kline et al., 2001). Our measurements of foveal changes here are unlikely to have arisen from unstable eye position, as Crossland et al. (2008) demonstrated that aging has no effect on fixation stability, and models of improper fixation do not predict our results (Baseler et al., 2002; Levin et al., 2010). Crossland et al. (2008) further measured a similar decrease in the proportion of V1 representing the fovea. Their study first defined the surface area of V1 using the wedge stimulus (polar angle response) and then measured the proportion of voxels activated by their ring stimulus (eccentricity response) within the polar-angle defined span of V1. This produces a measure of the *extent* of activity within a VFM similar to our surface area percent distribution measurements (**Figures 4**, **5**; Brewer and Barton, 2012a). Such a decrease in the size of the aging foveal representations seen here across multiple early VMFs and in V1 in these previous studies could lead to a loss in the resolution of cortical processing of visual information within the fovea, thus diminishing visual acuity.

Further cortical changes that may contribute to the decreased visual acuity in normal aging include the differences in pRF sizes measured across the VFMs (**Figures 8**, **9**). We measured a significant increase in pRF sizes in the foveal representations across V1, V2, and hV4 from 0 to 3° of eccentricity, with marginally significant differences in V3. The ∼2° *foveal* pRF size in the aging subjects in V1 is near that of the more *peripheral* pRF sizes (e.g., 5–7° of eccentricity) in young adults seen in this study and previously (Dumoulin and Wandell, 2008; Brewer and Barton, 2012a). The increased foveal pRF sizes in aging V2, V3, and hV4 similarly are also closer to the more peripheral pRF sizes of each of

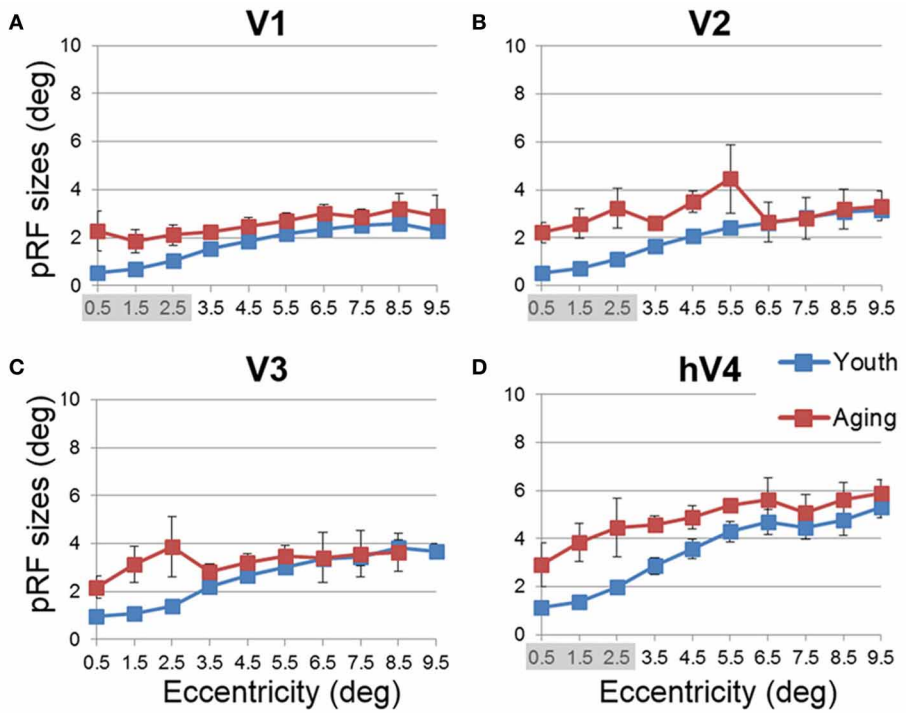

FIGURE 9 | Average population receptive field size measurements for visual field maps in young and healthy aging subjects. (A) V1. **(B)** V2. **(C)** V3. **(D)** hV4. Blue lines represent data from healthy young subjects, and red lines represent data from healthy aging subjects. Each bar represents data measured in individual subjects and then averaged by eccentricity band across hemispheres. Average pRF size is plotted as a function of degrees of eccentricity from 0 to 10° eccentricity (bins centered on 0.5–9.5°). Shaded gray regions indicate significant differences ($p < 0.05$) between regions (0–3°) in each map. Error bars indicate s.e.m.

these VFMs in healthy young subjects. These increases in pRF sizes could account for the previously reported decrease in visual acuity in healthy aging (Elliott, 1987; Gao and Hollyfield, 1992; Whitaker and Elliott, 1992; Kline et al., 2001). It is possible that these increases in pRF sizes are a compensatory mechanism for the decreases in the aging foveal surface area percent distributions in these VFMs. It remains to be seen whether these changes in the pRF sizes in aging early VMFs are intrinsic to these maps or are the result of changes in other regions, such as retinal thinning or changes in feedback from higher order visual areas.

Deficits in spatial and temporal contrast sensitivity. Elliot et al. (Elliott, 1987; Whitaker and Elliott, 1992) demonstrated a decrease in spatial contrast sensitivity at medium and high spatial frequencies with increasing age and showed that these changes are likely due to retinal and cortical changes rather than optical changes in the eye. The broadening of pRF sizes in the aging foveae of these early occipital VFMs is consistent with these reports of decreased contrast sensitivity (**Figures 8**, **9**). The decreases in foveal surface area percent distribution in these VFMs could also play a role in these spatial contrast sensitivity impairments (**Figures 4**, **5**; Sloane et al., 1988; Burton et al., 1993).

In addition to changes in spatial contrast sensitivity, aging subjects have decreased temporal contrast sensitivity at intermediate and high temporal frequencies (Wright and Drasdo, 1985; Mayer et al., 1988), as well as problems with motion discrimination (Gilmore et al., 1992; Wojciechowski et al., 1995). As human V1 and V3 have been implicated in motion processing (McKeefry et al., 1997; Smith et al., 1998), the significant and marginally significant decreases in foveal surface area percent distributions and increased pRF sizes of aging V1 and V3, respectively, may similarly play a role in these temporal contrast sensitivity and motion discrimination deficits (**Figures 5A,C, 9A,C**).

Changes in spatial attention. Deficits in spatial attention have been proposed to contribute to the shrinkage of the useful field of view in aging (Haas et al., 1986; Johnson et al., 1989; Haegerstrom-Portnoy et al., 1999). Measurements in macaque and human visual areas V1, V2, and V4 have demonstrated neural mechanisms possibly subserving selective spatial attention (Luck et al., 1997; Gallant et al., 2000; Reynolds et al., 2000; Serences and Yantis, 2006). Here we observe response patterns across the V1, V2, and hV4 VFMs that could similarly contribute to deficits in spatial attention, including the significantly smaller surface area percent distributions in the fovea of these VFMs (**Figures 5A,B,D**). In addition, the total surface area of hV4 was decreased in the aging subjects, and V2 and hV4 both showed increases in pRF sizes across larger foveal and parafoveal regions (**Figures 9B,D**), all of which could reflect deficits in the proper tuning of spatial attention.

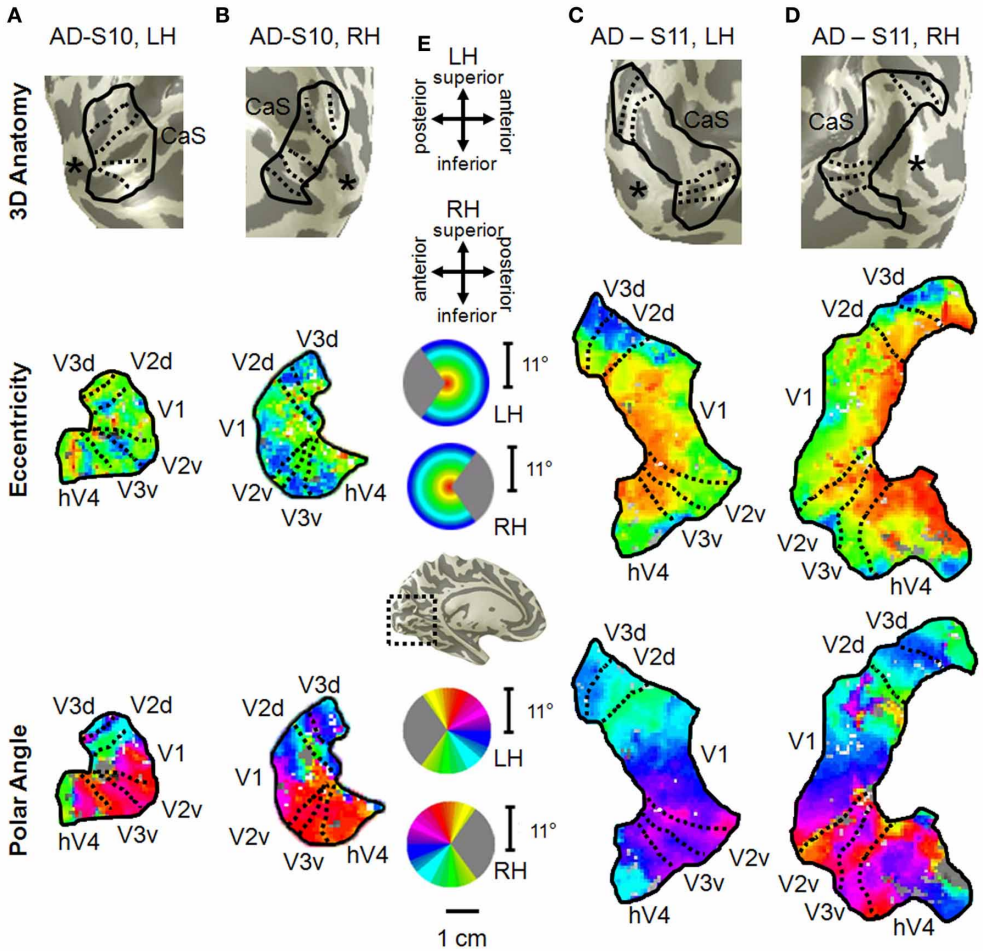

FIGURE 10 | Visual field map measurements in mild Alzheimer's disease subjects. Occipital VFMs V1, V2, V3, and hV4 are shown for the left **(A)** and right **(B)** hemispheres of a single subject with mild AD (S10). While the polar angle gradients (bottom panel) still contained the expected representations of contralateral visual space with orderly reversals between VFMs, the eccentricity measurements (middle panel), drawn from the same fMRI scans, were more disorganized. Also note the visibly smaller size of these VFMs in this subject compared to those shown for young and healthy aging subjects in **Figure 2**. A second set of VFMs is also shown for the left **(C)** and right **(D)** hemispheres from a second subject (S11) with mild Alzheimer's disease. This AD subject displayed more normal VFM sizes and foveal eccentricity representations, but also has visible changes in the peripheral eccentricity representations. **(E)** Legends and scale bar. Other details are as described in **Figure 2**. The "*" denotes the occipital pole.

Color vision deficiencies. Finally, aging subjects frequently demonstrate losses in color discrimination, especially along the blue-yellow axis, much of which can be attributed to changes in the aging lens (Haegerstrom-Portnoy et al., 1988; Johnson et al., 1988; Haegerstrom-Portnoy et al., 1999; Bron et al., 2000). However, concurrent or consequential neural changes have not been ruled out. Here we note significant differences in pRF sizes for 0 to 3° in V1, V2, and hV4 (**Figures 9A,B,D**). In addition, our measurements showed both a decrease in total surface area in hV4 and an *increase* in the BOLD variance explained over the central 0 to 3° of eccentricity in V1 in healthy aging relative to youthful subjects (**Figures 1B, 7A**). It is possible that these expanded pRFs in aging subjects are associated with aging changes specific to a ventral visual color and form pathway involving V1, V2, and hV4. Also, similar increases in occipital activity in healthy aging subjects in studies of visual working memory have been suggested to be a sign of some form of compensatory cognitive activity (Alichniewicz et al., 2012), which could be playing a role here.

VISUAL FIELD MAP CHANGES IN MILD ALZHEIMER'S DISEASE

Our measurements in mild AD subjects here both demonstrate the feasibility of making these VFM measurements in patients with dementia and highlight the need for such detailed analyses in individual subjects for these types of investigations. Each subject differed in the changes in the overall organization of these VFMs, with one subject (S10) having visibly small, disordered VFMs with low variance explained across the medial occipital surface and one (S11) having grossly normal VFM organization (**Figure 2**). These differences are likely due to variations in the pattern and progression of neurodegeneration in each subject. Even so, there are patterns of changes across these four hemispheres that may reflect more uniform effects of AD on the visual

pathways. Such changes may underlie the visual symptoms seen early in the disease (Katz and Rimmer, 1989) and may prove to be a useful tool for early and accurate diagnosis of AD.

Potential for improvement of dementia diagnosis

One of the goals in optimizing the diagnosis of dementia is to detect cortical changes very early with the hope that early intervention can lead to more effective treatments that stop the progression of dementia before much irreversible cortical damage ensues (Rosen, 2004). Recent research in early diagnosis spans cognitive testing to biochemical markers to neuroimaging methods such as positron emission tomography (PET), structural MRI, and functional MRI (Graham et al., 2004; Naggara et al., 2006; Ringman et al., 2008). Our neuroimaging results here in subjects soon after a diagnosis of mild AD open up the possibility of the use of detailed VFM measurements for early diagnosis as well. Individual subject VFM analysis allows both for these detailed measurements and for the ability to track these changes in specific individuals over time. Because VFMs are highly-structured functional responses in cortex that can be measured non-invasively with fMRI, they may prove useful for demonstrating very subtle changes early in AD. Future studies should expand upon our findings in AD with a broader range of AD subjects as well as measurements of the development of visual symptoms in patients with mild cognitive impairment (MCI; Mapstone et al., 2003; Tabert et al., 2006; Alichniewicz et al., 2012).

Disagreement also persists in the categorization of neurodegenerative symptoms into specific types of dementia. Criteria have been outlined to differentiate AD from other dementias (e.g., Dementia with Lewy Bodies, Posterior Cortical Atrophy), but there still remains significant overlap across the symptoms associated with each dementia (e.g., Harding et al., 2002; Tang-Wai et al., 2004; Armstrong et al., 2005; Sauer et al., 2006). The differences in the initiation of the neuropathology of the various types of dementia are not well understood, but these differences may be important to the types of treatment required for each specific dementia. Highly detailed measurements of specific changes within VFMs such as those we present here may be able to provide distinctive differences between types of dementia, which likely have different patterns in the onset and severity of visual symptoms.

Patterns of neurodegeneration in the visual cortex of AD subjects

Our measurements here in 2 mild AD subjects provide the initial steps toward reaching this goal of improved diagnosis. Our results in these first subjects show that such measurements are possible in this patient population and suggest a combination of patterns of neurodegeneration, with specific changes in cortical representations (**Figures 3**, **4**, **6**, **8**) in addition to differences in gross VFM organization (**Figure 10**). Measurements of both aspects of distributed neurodegeneration in the visual pathways may be useful in the diagnosis of AD in a specific individual and for understanding the progression this disease across cortex.

Visual deficits often reported as one of the first symptoms of AD include problems with visual attention, visual processing speed, visual field defects, contrast sensitivity, color discrimination, visuospatial processing, and feature recognition of complex objects such as faces (Parasuraman et al., 1992; Cronin-Golomb et al., 1993; Giannakopoulos et al., 1999; Chan et al., 2001; Holroyd and Shepherd, 2001; Jackson and Owsley, 2003; Mapstone et al., 2003; Tang-Wai et al., 2004; Thiyagesh et al., 2009). Interestingly, Subject S10 had very disorganized eccentricity maps with little foveal representation, possibly due to an idiosyncratic pattern of neurodegeneration around the occipital pole, although these eccentricity measurements may be complicated by the low variance explained of the pRF fit for these measurements (**Figures 10A,B**). Patients with such foveal loss might present with the deficiencies in color and form processing frequently described in AD (Cronin-Golomb et al., 1993; Chan et al., 2001; Sauer et al., 2006). These changes in VFMs could arise either from bottom-up effects from degenerative disease in the retina and optic nerves or from top-down changes in feedback from higher order visual areas, which have been shown in some studies to have a greater lesion load in AD than primary visual cortex (Lewis et al., 1987; Jackson and Owsley, 2003). Overall, our first characterization of these VFMs in AD subjects shows intriguing individual differences in the neurodegenerative patterns affecting visual cortex and emphasizes the need for additional studies of the timing and extent of VFM alterations in a large population of AD patients.

CONCLUSIONS

Our measurements first investigate whether there is a systematic change in visual cortex as part of the normal aging process Such knowledge of how visual representations change with healthy aging will allow us to explore both the effects of normal aging on the perceptual system and improve our ability to use age-matched controls in studies of age-related diseases (Jackson and Owsley, 2003; Yankner et al., 2008). We then demonstrate the feasibility and first characterization of these measurements in patients with mild AD. Our hope is that such data will contribute to earlier and more definitive detection of these forms of dementia and a better understanding of the differences between AD and other dementias.

ACKNOWLEDGMENTS

This work was supported by a grant to Alyssa A. Brewer from the MIND Institute and Alzheimer's Disease Research Center at the University of California, Irvine, supported by the National Institutes of Health grant no. AG16573. Alyssa A. Brewer and Brian Barton conceived of and designed the experiment and collected the data. Brian Barton processed and analyzed the data. The manuscript was written by Alyssa A. Brewer and then revised by Brian Barton.

REFERENCES

Alichniewicz, K. K., Brunner, F., Klunemann, H. H., and Greenlee, M. W. (2012). Structural and functional neural correlates of visuospatial information processing in normal aging and amnestic mild cognitive impairment. *Neurobiol. Aging.* 33, 2781–2797. doi: 10.1016/j.neurobiolaging.2012.02.010

Amano, K., Wandell, B. A., and Dumoulin, S. O. (2009). Visual field maps, population receptive field sizes, and visual field coverage in the human MT+ complex. *J. Neurophysiol.* 102, 2704–2718. doi: 10.1152/jn.00102.2009

Armstrong, R. A., Lantos, P. L., and Cairns, N. J. (2005). Overlap between neurodegenerative disorders. *Neuropathology* 25, 111–124. doi: 10.1111/j.1440-1789.2005.00605.x

Balazsi, A. G., Rootman, J., Drance, S. M., Schulzer, M., and Douglas, G. R. (1984). The effect of age on the nerve fiber population of the human optic nerve. *Am. J. Ophthalmol.* 97, 760–766.

Baseler, H. A., Brewer, A. A., Sharpe, L. T., Morland, A. B., Jagle, H., and Wandell, B. A. (2002). Reorganization of human cortical maps caused by inherited photoreceptor abnormalities. *Nat. Neurosci.* 5, 364–370. doi: 10.1038/nn817

Baseler, H. A., Gouws, A., Haak, K. V., Racey, C., Crossland, M. D., Tufail, A., et al. (2011). Large-scale remapping of visual cortex is absent in adult humans with macular degeneration. *Nat. Neurosci.* 14, 649–655. doi: 10.1038/nn.2793

Berisha, F., Feke, G. T., Trempe, C. L., McMeel, J. W., and Schepens, C. L. (2007). Retinal abnormalities in early Alzheimer's disease. *Invest. Ophthalmol. Vis. Sci.* 48, 2285–2289. doi: 10.1167/iovs.06-1029

Black, S. E. (1996). Focal cortical atrophy syndromes. *Brain Cogn.* 31, 188–229. doi: 10.1006/brcg.1996.0042

Bokde, A. L., Lopez-Bayo, P., Meindl, T., Pechler, S., Born, C., Faltraco, F., et al. (2006). Functional connectivity of the fusiform gyrus during a face-matching task in subjects with mild cognitive impairment. *Brain* 129, 1113–1124. doi: 10.1093/brain/awl051

Boynton, G. M., Engel, S. A., Glover, G. H., and Heeger, D. J. (1996). Linear systems analysis of functional magnetic resonance imaging in human V1. *J. Neurosci.* 16, 4207–4221.

Brainard, D. H. (1997). The Psychophysics Toolbox. *Spat. Vis.* 10, 433–436. doi: 10.1163/156856897X00357

Brewer, A. A., and Barton, B. (2012a). Effects of healthy aging on human primary visual cortex. *Health* 4, 695–702. doi: 10.4236/health.2012.429109

Brewer, A. A., and Barton, B. (2012b). "Visual field map organization in human visual cortex," in *Visual Cortex—Current Status and Perspectives*, eds S. Molotchnikoff and J. Rouat (New York, NY: InTech), 29–60.

Brewer, A. A., Liu, J., Wade, A. R., and Wandell, B. A. (2005). Visual field maps and stimulus selectivity in human ventral occipital cortex. *Nat. Neurosci.* 8, 1102–1109. doi: 10.1038/nn1507

Brewer, A. A., Press, W. A., Logothetis, N. K., and Wandell, B. A. (2002). Visual areas in macaque cortex measured using functional magnetic resonance imaging. *J. Neurosci.* 22, 10416–10426.

Bron, A. J., Vrensen, G. F., Koretz, J., Maraini, G., and Harding, J. J. (2000). The ageing lens. *Ophthalmologica* 214, 86–104. doi: 10.1159/000027475

Burton, K. B., Owsley, C., and Sloane, M. E. (1993). Aging and neural spatial contrast sensitivity: photopic vision. *Vision Res.* 33, 939–946. doi: 10.1016/0042-6989(93)90077-A

Chan, D., Crutch, S. J., and Warrington, E. K. (2001). A disorder of colour perception associated with abnormal colour after-images: a defect of the primary visual cortex. *J. Neurol. Neurosurg. Psychiatry* 71, 515–517. doi: 10.1136/jnnp.71.4.515

Cronin-Golomb, A., Sugiura, R., Corkin, S., and Growdon, J. H. (1993). Incomplete achromatopsia in Alzheimer's disease. *Neurobiol. Aging* 14, 471–477. doi: 10.1016/0197-4580(93)90105-K

Crossland, M. D., Morland, A. B., Feely, M. P., Von Dem Hagen, E., and Rubin, G. S. (2008). The effect of age and fixation instability on retinotopic mapping of primary visual cortex. *Invest. Ophthalmol. Vis. Sci.* 49, 3734–3739. doi: 10.1167/iovs.07-1621

Curcio, C. A., Millican, C. L., Allen, K. A., and Kalina, R. E. (1993). Aging of the human photoreceptor mosaic: evidence for selective vulnerability of rods in central retina. *Invest. Ophthalmol. Vis. Sci.* 34, 3278–3296.

Danesh-Meyer, H. V., Birch, H., Ku, J. Y., Carroll, S., and Gamble, G. (2006). Reduction of optic nerve fibers in patients with Alzheimer disease identified by laser imaging. *Neurology* 67, 1852–1854. doi: 10.1212/01.wnl.0000244490.07925.8b

D'Esposito, M., Deouell, L. Y., and Gazzaley, A. (2003). Alterations in the BOLD fMRI signal with ageing and disease: a challenge for neuroimaging. *Nat. Rev. Neurosci.* 4, 863–872. doi: 10.1038/nrn1246

D'Esposito, M., Zarahn, E., Aguirre, G. K., and Rypma, B. (1999). The effect of normal aging on the coupling of neural activity to the bold hemodynamic response. *Neuroimage* 10, 6–14. doi: 10.1006/nimg.1999.0444

Deyoe, E. A., Carman, G. J., Bandettini, P., Glickman, S., Wieser, J., Cox, R., et al. (1996). Mapping striate and extrastriate visual areas in human cerebral cortex. *Proc. Natl. Acad. Sci. U.S.A.* 93, 2382–2386. doi: 10.1073/pnas.93.6.2382

Dougherty, R. F., Koch, V. M., Brewer, A. A., Fischer, B., Modersitzki, J., and Wandell, B. A. (2003). Visual field representations and locations of visual areas V1/2/3 in human visual cortex. *J. Vis.* 3, 586–598. doi: 10.1167/3.10.1

Dumoulin, S. O., and Wandell, B. A. (2008). Population receptive field estimates in human visual cortex. *Neuroimage* 39, 647–660. doi: 10.1016/j.neuroimage.2007.09.034

Elliott, D. B. (1987). Contrast sensitivity decline with ageing: a neural or optical phenomenon? *Ophthalmic Physiol. Opt.* 7, 415–419. doi: 10.1111/j.1475-1313.1987.tb00771.x

Engel, S. A., Glover, G. H., and Wandell, B. A. (1997). Retinotopic organization in human visual cortex and the spatial precision of functional MRI. *Cereb. Cortex* 7, 181–192. doi: 10.1093/cercor/7.2.181

Engel, S. A., Rumelhart, D. E., Wandell, B. A., Lee, A. T., Glover, G. H., Chichilnisky, E. J., et al. (1994). fMRI of human visual cortex. *Nature* 369, 525. doi: 10.1038/369525a0

Folstein, M. F., Folstein, S. E., and McHugh, P. R. (1975). "Mini-mental state." A practical method for grading the cognitive state of patients for the clinician. *J. Psychiatr. Res.* 12, 189–198. doi: 10.1016/0022-3956(75)90026-6

Friston, K. J., Fletcher, P., Josephs, O., Holmes, A., Rugg, M. D., and Turner, R. (1998). Event-related fMRI: characterizing differential responses. *Neuroimage* 7, 30–40. doi: 10.1006/nimg.1997.0306

Gallant, J. L., Shoup, R. E., and Mazer, J. A. (2000). A human extrastriate area functionally homologous to macaque V4. *Neuron* 27, 227–235. doi: 10.1016/S0896-6273(00)00032-5

Gao, H., and Hollyfield, J. G. (1992). Aging of the human retina. Differential loss of neurons and retinal pigment epithelial cells. *Invest. Ophthalmol. Vis. Sci.* 33, 1–17.

Giannakopoulos, P., Gold, G., Duc, M., Michel, J. P., Hof, P. R., and Bouras, C. (1999). Neuroanatomic correlates of visual agnosia in Alzheimer's disease: a clinicopathologic study. *Neurology* 52, 71–77. doi: 10.1212/WNL.52.1.71

Giannakopoulos, P., Gold, G., Duc, M., Michel, J. P., Hof, P. R., and Bouras, C. (2000). Impaired processing of famous faces in Alzheimer's disease is related to neurofibrillary tangle densities in the prefrontal and anterior cingulate cortex. *Dement. Geriatr. Cogn. Disord.* 11, 336–341. doi: 10.1159/000017263

Gilmore, G. C., Wenk, H. E., Naylor, L. A., and Stuve, T. A. (1992). Motion perception and aging. *Psychol. Aging* 7, 654–660. doi: 10.1037/0882-7974.7.4.654

Graham, D. P., Cully, J. A., Snow, A. L., Massman, P., and Doody, R. (2004). The Alzheimer's Disease Assessment Scale-Cognitive subscale: normative data for older adult controls. *Alzheimer Dis. Assoc. Disord.* 18, 236–240.

Haak, K. V., Cornelissen, F. W., and Morland, A. B. (2012a). Population receptive field dynamics in human visual cortex. *PLoS ONE* 7:e37686. doi: 10.1371/journal.pone.0037686

Haak, K. V., Winawer, J., Harvey, B. M., Renken, R., Dumoulin, S. O., Wandell, B. A., et al. (2012b). Connective field modeling. *Neuroimage* 66C, 376–384. doi: 10.1016/j.neuroimage.2012.10.037

Haas, A., Flammer, J., and Schneider, U. (1986). Influence of age on the visual fields of normal subjects. *Am. J. Ophthalmol.* 101, 199–203.

Haegerstrom-Portnoy, G., Hewlett, S. E., and Barr, S. A. N. (1988). "S-cone loss with aging," in *Colour Vision Deficiencies IX*, ed G. Verriest (The Hague: Junk Publisher), 349–356.

Haegerstrom-Portnoy, G., Schneck, M. E., and Brabyn, J. A. (1999). Seeing into old age: vision function beyond acuity. *Optom. Vis. Sci.* 76, 141–158. doi: 10.1097/00006324-199903000-00014

Harding, A. J., Broe, G. A., and Halliday, G. M. (2002). Visual hallucinations in Lewy body disease relate to Lewy bodies in the temporal lobe. *Brain* 125, 391–403. doi: 10.1093/brain/awf033

Harvey, B. M., and Dumoulin, S. O. (2011). The relationship between cortical magnification factor and population receptive field size in human visual cortex: constancies in cortical architecture. *J. Neurosci.* 31, 13604–13612. doi: 10.1523/JNEUROSCI.2572-11.2011

Harvey, B. M., Vansteensel, M. J., Ferrier, C. H., Petridou, N., Zuiderbaan, W., Aarnoutse, E. J., et al. (2013). Frequency specific spatial interactions in human electrocorticography: V1 alpha oscillations reflect surround suppression. *Neuroimage* 65, 424–432. doi: 10.1016/j.neuroimage.2012.10.020

Hinton, D. R., Sadun, A. A., Blanks, J. C., and Miller, C. A. (1986). Optic-nerve degeneration in Alzheimer's disease. *N. Engl. J. Med.* 315, 485–487. doi: 10.1056/NEJM198608213150804

Holroyd, S., and Shepherd, M. L. (2001). Alzheimer's disease: a review for the ophthalmologist. *Surv. Ophthalmol.* 45, 516–524. doi: 10.1016/S0039-6257(01)00193-X

Iseri, P. K., Altinas, O., Tokay, T., and Yuksel, N. (2006). Relationship between cognitive impairment and retinal morphological and visual functional abnormalities in Alzheimer disease. *J. Neuroophthalmol.* 26, 18–24. doi: 10.1097/01.wno.0000204645.56873.26

Jackson, G. R., and Owsley, C. (2003). Visual dysfunction, neurodegenerative diseases, and aging. *Neurol. Clin.* 21, 709–728. doi: 10.1016/S0733-8619(02)00107-X

Jackson, G. R., Owsley, C., and Curcio, C. A. (2002). Photoreceptor degeneration and dysfunction in aging and age-related maculopathy. *Ageing Res. Rev.* 1, 381–396. doi: 10.1016/S1568-1637(02)00007-7

Johnson, C. A., Adams, A. J., and Lewis, R. A. (1989). Evidence for a neural basis of age-related visual field loss in normal observers. *Invest. Ophthalmol. Vis. Sci.* 30, 2056–2064.

Johnson, C. A., Adams, A. J., Twelker, J. D., and Quigg, J. M. (1988). Age-related changes in the central visual field for short-wavelength-sensitive pathways. *J. Opt. Soc. Am. A* 5, 2131–2139. doi: 10.1364/JOSAA.5.002131

Katz, B., and Rimmer, S. (1989). Ophthalmologic manifestations of Alzheimer's disease. *Surv. Ophthalmol.* 34, 31–43. doi: 10.1016/0039-6257(89)90127-6

Kline, D. W., Culham, J. C., Bartel, P., and Lynk, L. (2001). Aging effects on vernier hyperacuity: a function of oscillation rate but not target contrast. *Optom. Vis. Sci.* 78, 676–682. doi: 10.1097/00006324-200109000-00013

Levin, N., Dumoulin, S. O., Winawer, J., Dougherty, R. F., and Wandell, B. A. (2010). Cortical maps and white matter tracts following long period of visual deprivation and retinal image restoration. *Neuron* 65, 21–31. doi: 10.1016/j.neuron.2009.12.006

Lewis, D. A., Campbell, M. J., Terry, R. D., and Morrison, J. H. (1987). Laminar and regional distributions of neurofibrillary tangles and neuritic plaques in Alzheimer's disease: a quantitative study of visual and auditory cortices. *J. Neurosci.* 7, 1799–1808.

Luck, S. J., Chelazzi, L., Hillyard, S. A., and Desimone, R. (1997). Neural mechanisms of spatial selective attention in areas V1, V2, and V4 of macaque visual cortex. *J. Neurophysiol.* 77, 24–42.

Maes, F., Collignon, A., Vandermeulen, D., Marchal, G., and Suetens, P. (1997). Multimodality image registration by maximization of mutual information. *IEEE Trans. Med. Imaging* 16, 187–198. doi: 10.1109/42.563664

Mapstone, M., Steffenella, T. M., and Duffy, C. J. (2003). A visuospatial variant of mild cognitive impairment: getting lost between aging and AD. *Neurology* 60, 802–808. doi: 10.1212/01.WNL.0000049471.76799.DE

Mayer, M. J., Kim, C. B., Svingos, A., and Glucs, A. (1988). Foveal flicker sensitivity in healthy aging eyes. I. Compensating for pupil variation. *J. Opt. Soc. Am. A* 5, 2201–2209. doi: 10.1364/JOSAA.5.002201

McKeefry, D. J., Watson, J. D., Frackowiak, R. S., Fong, K., and Zeki, S. (1997). The activity in human areas V1/V2, V3, and V5 during the perception of coherent and incoherent motion. *Neuroimage* 5, 1–12. doi: 10.1006/nimg.1996.0246

Naggara, O., Oppenheim, C., Rieu, D., Raoux, N., Rodrigo, S., Dalla Barba, G., et al. (2006). Diffusion tensor imaging in early Alzheimer's disease. *Psychiatry Res.* 146, 243–249. doi: 10.1016/j.pscychresns.2006.01.005

Nestares, O., and Heeger, D. J. (2000). Robust multiresolution alignment of MRI brain volumes. *Magn. Reson. Med.* 43, 705–715. doi: 10.1002/(SICI)1522-2594(200005)43:5%3C705::AID-MRM13%3E3.0.CO;2-R

Pache, M., Smeets, C. H., Gasio, P. F., Savaskan, E., Flammer, J., Wirz-Justice, A., et al. (2003). Colour vision deficiencies in Alzheimer's disease. *Age Ageing* 32, 422–426. doi: 10.1093/ageing/32.4.422

Paquet, C., Boissonnot, M., Roger, F., Dighiero, P., Gil, R., and Hugon, J. (2007). Abnormal retinal thickness in patients with mild cognitive impairment and Alzheimer's disease. *Neurosci. Lett.* 420, 97–99. doi: 10.1016/j.neulet.2007.02.090

Parasuraman, R., Greenwood, P. M., Haxby, J. V., and Grady, C. L. (1992). Visuospatial attention in dementia of the Alzheimer type. *Brain* 115(Pt 3), 711–733. doi: 10.1093/brain/115.3.711

Parikh, R. S., Parikh, S. R., Sekhar, G. C., Prabakaran, S., Babu, J. G., and Thomas, R. (2007). Normal age-related decay of retinal nerve fiber layer thickness. *Ophthalmology* 114, 921–926. doi: 10.1016/j.ophtha.2007.01.023

Pelli, D. G. (1997). The VideoToolbox software for visual psychophysics: transforming numbers into movies. *Spat. Vis.* 10, 437–442. doi: 10.1163/156856897X00366

Pitts, D. G. (1982). "The effects of aging on selected visual functions: dark adaptation, visual acuity, stereopsis, and brightness contrast," in *Aging and Human Visual Function*, eds R. Sekuler, D. Kline, and K. Dismukes (New York, NY: Alan R. Liss), 131–159.

Raz, N., Gunning-Dixon, F., Head, D., Rodrigue, K. M., Williamson, A., and Acker, J. D. (2004). Aging, sexual dimorphism, and hemispheric asymmetry of the cerebral cortex: replicability of regional differences in volume. *Neurobiol. Aging* 25, 377–396. doi: 10.1016/S0197-4580(03)00118-0

Reynolds, J. H., Pasternak, T., and Desimone, R. (2000). Attention increases sensitivity of V4 neurons. *Neuron* 26, 703–714. doi: 10.1016/S0896-6273(00)81206-4

Ringman, J. M., Younkin, S. G., Pratico, D., Seltzer, W., Cole, G. M., Geschwind, D. H., et al. (2008). Biochemical markers in persons with preclinical familial Alzheimer disease. *Neurology* 71, 85–92. doi: 10.1212/01.wnl.0000303973.71803.81

Rosen, P. N. (2004). Vision screening for Alzheimer's disease: prevention from an ophthalmologist's perspective (There is More to Vision than Meets the Eye). *Perm. J.* 8, 15–21.

Sauer, J., Ffytche, D. H., Ballard, C., Brown, R. G., and Howard, R. (2006). Differences between Alzheimer's disease and dementia with Lewy bodies: an fMRI study of task-related brain activity. *Brain* 129, 1780–1788. doi: 10.1093/brain/awl102

Serences, J. T., and Yantis, S. (2006). Selective visual attention and perceptual coherence. *Trends Cogn. Sci.* 10, 38–45. doi: 10.1016/j.tics.2005.11.008

Sereno, M. I., Dale, A. M., Reppas, J. B., Kwong, K. K., Belliveau, J. W., Brady, T. J., et al. (1995). Borders of multiple visual areas in humans revealed by functional magnetic resonance imaging. *Science* 268, 889–893. doi: 10.1126/science.7754376

Sloane, M. E., Owsley, C., and Jackson, C. A. (1988). Aging and luminance-adaptation effects on spatial contrast sensitivity. *J. Opt. Soc. Am. A* 5, 2181–2190. doi: 10.1364/JOSAA.5.002181

Smith, A. T., Greenlee, M. W., Singh, K. D., Kraemer, F. M., and Hennig, J. (1998). The processing of first- and second-order motion in human visual cortex assessed by functional magnetic resonance imaging (fMRI). *J. Neurosci.* 18, 3816–3830.

Tabert, M. H., Manly, J. J., Liu, X., Pelton, G. H., Rosenblum, S., Jacobs, M., et al. (2006). Neuropsychological prediction of conversion to Alzheimer disease in patients with mild cognitive impairment. *Arch. Gen. Psychiatry* 63, 916–924. doi: 10.1001/archpsyc.63.8.916

Tang-Wai, D. F., Graff-Radford, N. R., Boeve, B. F., Dickson, D. W., Parisi, J.E., Crook, R., et al. (2004). Clinical, genetic, and neuropathologic characteristics of posterior cortical atrophy. *Neurology* 63, 1168–1174. doi: 10.1212/01.WNL.0000140289.18472.15

Teo, P. C., Sapiro, G., and Wandell, B. A. (1997). Creating connected representations of cortical gray matter for functional MRI visualization. *IEEE Trans. Med. Imaging* 16, 852–863. doi: 10.1109/42.650881

Thiyagesh, S. N., Farrow, T. F., Parks, R. W., Accosta-Mesa, H., Young, C., Wilkinson, I. D., et al. (2009). The neural basis of visuospatial perception in Alzheimer's disease and healthy elderly comparison subjects: an fMRI study. *Psychiatry Res.* 172, 109–116. doi: 10.1016/j.pscychresns.2008.11.002

van Rhijn, S. J., Glosser, G., De Vries, J. J., Clark, C. M., Newberg, A. B., and Alavi, A. (2004). Visual processing impairments and decrements in regional brain activity in Alzheimer's disease. *J. Clin. Exp. Neuropsychol.* 26, 11–23. doi: 10.1076/jcen.26.1.11.23931

Wandell, B. A., Chial, S., and Backus, B. T. (2000). Visualization and measurement of the cortical surface. *J. Cogn. Neurosci.* 12, 739–752. doi: 10.1162/089892900562561

Wandell, B. A., Dumoulin, S. O., and Brewer, A. A. (2007). Visual field maps in human cortex. *Neuron* 56, 366–383. doi: 10.1016/j.neuron.2007.10.012

Weale, R. A. (1975). Senile changes in visual acuity. *Trans. Ophthalmol. Soc. U.K.* 95, 36–38.

Whitaker, D., and Elliott, D. B. (1992). Simulating age-related optical changes in the human eye. *Doc. Ophthalmol.* 82, 307–316. doi: 10.1007/BF00161018

Wojciechowski, R., Trick, G. L., and Steinman, S. B. (1995). Topography of the age-related decline in motion sensitivity. *Optom. Vis. Sci.* 72, 67–74. doi: 10.1097/00006324-199502000-00005

Wright, C. E., and Drasdo, N. (1985). The influence of age on the spatial and temporal contrast sensitivity function. *Doc. Ophthalmol.* 59, 385–395. doi: 10.1007/BF00159172

Yankner, B. A., Lu, T., and Loerch, P. (2008). The aging brain. *Annu. Rev. Pathol.* 3, 41–66. doi: 10.1146/annurev.pathmechdis.2.010506.092044

Zuiderbaan, W., Harvey, B. M., and Dumoulin, S. O. (2012). Modeling center-surround configurations in population receptive fields using fMRI. *J. Vis.* 12, 10. doi: 10.1167/12.3.10

Conflict of Interest Statement: The authors declare that the research was conducted in the absence of any commercial or financial relationships that could be construed as a potential conflict of interest.

Received: 19 September 2012; paper pending published: 29 October 2012; accepted: 20 January 2014; published online: 07 February 2014.

Citation: Brewer AA and Barton B (2014) Visual cortex in aging and Alzheimer's disease: changes in visual field maps and population receptive fields. Front. Psychol. ***5****:74. doi: 10.3389/fpsyg.2014.00074*

This article was submitted to Perception Science, a section of the journal Frontiers in Psychology.

frontiers in PSYCHOLOGY

ORIGINAL RESEARCH ARTICLE
published: 14 May 2013
doi: 10.3389/fpsyg.2013.00268

Early ERPs to faces: aging, luminance, and individual differences

Magdalena M. Bieniek[1]*, Luisa S. Frei[1,2] and Guillaume A. Rousselet[1]

[1] Institute of Neuroscience and Psychology, College of Medical, Veterinary and Life Sciences, University of Glasgow, Glasgow, UK
[2] Institute of Health and Wellbeing, College of Medical, Veterinary and Life Sciences, University of Glasgow, Glasgow, UK

Edited by:
Mark W. Greenlee, University of Regensburg, Germany

Reviewed by:
Roberto Caldara, University of Fribourg, Switzerland
Jocelyn Faubert, Université de Montréal, Canada
Ela I. Olivares, Universidad Autónoma de Madrid, Spain

***Correspondence:**
Magdalena M. Bieniek, Institute of Neuroscience and Psychology, 58 Hillhead Street, G12 8QB, Glasgow, UK.
e-mail: magdalena.bieniek@glasgow.ac.uk

Recently, Rousselet et al. reported a 1 ms/year delay in visual processing speed in a sample of healthy aged 62 subjects (Frontiers in Psychology 2010, 1:19). Here, we replicate this finding in an independent sample of 59 subjects and investigate the contribution of optical factors (pupil size and luminance) to the age-related slowdown and to individual differences in visual processing speed. We conducted two experiments. In experiment 1 we recorded EEG from subjects aged 18–79. Subjects viewed images of faces and phase scrambled noise textures under nine luminance conditions, ranging from 0.59 to 60.8 cd/m^2. We manipulated luminance using neutral density filters. In experiment 2, 10 young subjects (age < 35) viewed similar stimuli through pinholes ranging from 1 to 5 mm. In both experiments, subjects were tested twice. We found a 1 ms/year slowdown in visual processing that was independent of luminance. Aging effects became visible around 125 ms post-stimulus and did not affect the onsets of the face-texture ERP differences. Furthermore, luminance modulated the entire ERP time-course from 60 to 500 ms. Luminance effects peaked in the N170 time window and were independent of age. Importantly, senile miosis and individual differences in pupil size did not account for aging differences and inter-subject variability in processing speed. The pinhole manipulation also failed to match the ERPs of old subjects to those of young subjects. Overall, our results strongly suggest that early ERPs to faces (<200 ms) are delayed by aging and that these delays are of cortical, rather than optical origin. Our results also demonstrate that even late ERPs to faces are modulated by low-level factors.

Keywords: event related potentials, aging, luminance, pupil size, senile miosis, retinal illuminance, individual differences, N170

INTRODUCTION

One of the most prominent phenomena associated with aging is a progressive cognitive slowing. Age-related slowing is visible across a variety of cognitive tasks (Salthouse and Ferrer-Caja, 2003), and seems to be linked to a number of neurodegenerative changes, including total brain volume shrinkage (Resnick et al., 2003), and alterations in gray matter (Brickman et al., 2008; Chee et al., 2009) and white matter integrity (Davis et al., 2009; Peters, 2009; Piguet et al., 2009; Salat et al., 2009). Whereas some brain regions, in particular pre-frontal areas, seem to suffer substantial age-related structural and functional deterioration, no significant shrinkage of primary visual cortex has been observed (Resnick et al., 2003; Raz et al., 2005, 2010). However, important neural changes in visual areas have been documented in animal models, including delayed latencies (Wang et al., 2005, 2006) and degradation in response selectivity of neurons in striate and extrastriate cortical areas (Schmolesky et al., 2000; Hua et al., 2006; Yu et al., 2006; Peters, 2009). In keeping with findings in animals, fMRI studies in humans have described weaker differentiation between categorical responses in old subjects (Park et al., 2004; Voss et al., 2008). Such changes in tuning may lead to longer processing times, following a model of perceptual decision by accumulation of evidence in neuronal populations (Perrett and Ashbridge, 1998). There is also more direct evidence from human ERP studies, showing delayed evoked responses to checkerboards (Sokol et al., 1981; Tobimatsu et al., 1993). These neural changes suggest an overall slowdown of perception with age (Rousselet et al., 2009, 2010), which in turn could affect higher cognitive functions, such as working memory (Gazzaley et al., 2008).

We can identify at least five main questions about age-related slowing of perception:

1. When and where in the brain does it start to manifest itself?
2. By how much do we slow down?
3. From what age do we slow down?
4. Why do we slow down?
5. What are the consequences?

In this study, we tried to address, to some extent, the first four questions by measuring event-related potentials (ERPs) to pictures of faces and noise textures. Previously, using a similar approach, Rousselet et al. (2009, 2010) reported age-related visual processing slowing of about 1 ms/year from age 20 onward. Aging effects started at about 120 ms post-stimulus onset, suggesting a cortical origin, and the potential involvement of face and object

processing cortical areas. However, these results remain controversial. Several other studies did not find aging effects on the latencies of early ERPs to complex objects, such as faces (Chaby et al., 2001, 2003; Pfutze et al., 2002; Gao et al., 2009; Daniel and Bentin, 2010; Wiese et al., 2012). These studies observed age-related delays only at later stages of visual processing (>200 ms). Contrary to these negative results, several studies reported age-related latency increases of early ERPs to faces (Nakamura et al., 2001; Gazzaley et al., 2008; Wiese et al., 2008), letters (Falkenstein et al., 2006; Kolev et al., 2006), letter-number pairs (De Sanctis et al., 2008) and diffuse light flashes (Diaz and Amenedo, 1998).

Given the discrepancies in the literature, the first goal of our study was to replicate the age-related delays described in Rousselet et al. (2009, 2010) using an independent sample of subjects. The second goal of our study was to determine the origin of the aging effects, as well as the origin of the very large inter-individual differences we observed within age groups. There are many potential and non-mutually exclusive contributors to these effects, from bottom-up optical and neural factors, to various high-level explanations—see discussions in Rousselet et al. (2009, 2010). One particularly important factor is senile miosis, the age-related reduction in pupil size (Winn et al., 1994). Pupil size also varies considerably within the same age group (Winn et al., 1994). Hence, because senile miosis reduces retinal illuminance, it could contribute to the delays and the considerable within age-group individual differences in cortical processing speed found in previous studies. Several elements support this idea. First, delayed latencies of the early evoked potentials (<200 ms) have been observed in subjects with smaller pupils (Hawkes and Stow, 1981) and when subjects viewed stimuli through a pinhole aperture of 1.5 mm size (Vanmaele et al., 2003). Second, a link between luminance and the latencies of neuronal responses have been documented in animals using multi-focal ERG (Raz et al., 2002) and in humans using pattern ERG and ERP recordings (Froelich and Kaufman, 1991). Previous research has shown that decreasing luminance increases the latencies of neuronal responses in various cortical areas including V1 (Geisler et al., 2007), the superior colliculus (Marino et al., 2012) and the LIP—lateral intraparietal area (Tanaka et al., 2013). Importantly, it seems that age-related delays in retinal and cortical activity can be abolished after equating retinal illuminance between groups by using neutral density filters (Trick et al., 1986). In the same vein, Shaw and Cant (1980) reported that the age-related P100 delays observed at lower (5 cd/m^2) luminance levels were considerably reduced at higher luminance (90 cd/m^2). However, this finding was challenged by a report of similar aging effects at 11 and 180 cd/m^2 luminance levels (Tobimatsu et al., 1993).

Thus, to assess the relationship between observers' retinal illuminance and their ERPs we conducted two experiments in which we recorded EEG from subjects whose retinal illuminance was manipulated using neutral density filters (Experiment 1) and pinholes (Experiment 2). Both of these methods were used previously to manipulate the amount of light that reaches observers' retinas (Eagan et al., 1999).While neutral density filters allow to control stimulus luminance, pinholes placed in front of observers' eyes act as artificial pupils altering retinal illuminance without changing stimulus luminance. Thus, the two methods complement each other and serve as a control to one another.

We tested our subjects twice to assess the reliability of our results. Our first goal was to replicate the previous finding of Rousselet et al. (2010) that aging slows down visual processing at the rate of 1 ms/year, which we successfully achieved. Further, we aimed to determine whether retinal illuminance modulates age-related delays in ERP measures of processing speed. We hypothesized that if ERP aging delays depend on senile miosis and retinal illuminance, there should be no difference in processing speed if differences in retinal illuminance are abolished. However, we found that age-related changes in processing speed are not due to senile miosis, as they were independent of luminance. Additionally, we aimed to answer whether individual differences in visual processing speed can be accounted for by variability in retinal illuminance, which they could not. Finally, by manipulating retinal illuminance in young observers, we intended, and failed, to match their ERPs to those of old observers tested at higher luminance levels. Overall, our results strongly suggest that age-related face ERP delays are not due to optical factors.

MATERIALS AND METHODS

SUBJECTS

The study involved 59 subjects (31 females, 28 males, age range of 18–79, **Table 1**). To assess the test-retest reliability of the results and to control for luminance manipulation order, all but eight subjects took part in a second experimental session. Prior to

Table 1 | Subjects' information.

Age bracket	Age (median [min, max])	Number of subjects (females, males)	Visual acuity		MOCA scores (median, [min, max])	Years of education (median, [min, max])
			High contrast 63 cm (median [min, max])	Low contrast 63 cm (median [min, max])		
18–19	19 [18, 19]	5 (4, 1)	105 [100, 110]	95 [90, 100]	n/a	15 [15, 16]
20–29	22 [21, 29]	12 (6, 6)	105 [95, 108]	94.5 [90, 102]	n/a	18 [17, 25]
30–39	32 [30, 38]	9 (2, 7)	107 [99, 109]	97 [90, 102]	n/a	18 [14, 23]
40–49	43.5 [41, 49]	8 (4, 4)	106 [95, 112]	98.5 [88, 103]	n/a	18 [12, 23]
50–59	54 [50, 59]	6 (2, 4)	105 [95, 105]	94 [90, 95]	n/a	17 [13, 19]
60–69	64.5 [60, 67]	10 (7, 3)	94 [80, 106]	85.5 [75, 95]	29 [27, 30]	15.5 [5, 21.5]
70–79	72 [70, 79]	9 (6, 3)	98 [78, 105]	88 [63, 94]	28 [26, 30]	14 [11, 21]

the experiment, all subjects read a study information sheet and signed an informed consent form. The experiment was approved by the School of Psychology Ethics Committee (approval no. FIMS00740). We excluded persons who reported any eye condition (i.e., lazy eye, glaucoma, macular degeneration, cataract), had a history of mental illness, were taking psychotropic medications (e.g., antidepressants, beta-blockers) at the moment of testing or use to take them, suffered from any neurological condition (i.e., Parkinson's, Alzheimer's, dementia), had diabetes, had suffered a stroke or a serious head or eye injury and who had their vision tested more than 2 years ago (for people under 60 year old) or more than 1 year ago (for people aged 60 and above). Subjects' visual acuity and contrast sensitivity were assessed in the lab on the day of the first session using a Colenbrander mixed contrast card set and a Pelli–Robson chart. All subjects had normal or corrected-to-normal vision (**Table 1**) and contrast sensitivity in the range of 1.95 and above (normal score). One older subject reported the start of a monocular cataract that did not require medical treatment at the moment of testing. All subjects filled in a general health and life style questionnaire. All reported very good or excellent hearing and most reported at least weekly exercise. All subjects in the older group (>60) were in good cognitive health as indicated by their scores (>26 out of 30) at the MOCA test during the first experimental session. Subjects were compensated £6/h for their participation.

STIMULI

The stimuli were pictures of faces and textures (**Figure 1A**). There were 10 identities of faces (Rousselet et al., 2008). Faces were gray-scaled front view photographs oval-cropped to remove hair and pasted on a uniform gray background. A unique image was presented on each trial by introducing noise into the face images. Faces had 70% phase coherence [see details in Rousselet et al. (2008)]. Textures had random phase (0% phase coherence). All stimuli had an amplitude spectrum set to the mean amplitude of all faces. All stimuli also had the same mean pixel intensity, RMS contrast = 0.1, and occupied 9 × 9° of visual angle.

EXPERIMENTAL PROCEDURE AND DESIGN

Most subjects participated in two experimental sessions. The screen luminance progressively decreased in bright to dark (b2d) sessions, and increased in dark to bright (d2b) sessions. The order of the sessions was randomly assigned on the first day of testing. We altered screen luminance by placing neutral density filters in front of the computer screen. The filters were attached to thin wooden frames, which were pierced at the top, so that they could hang from pegs attached to the wall above the screen. The filters covered the screen completely. Each filter had 0.3 optical density (f-stop reduction = 2). This is equivalent to a 50% reduction in optical power transmitted through the filter. In other words, adding one filter in front of the screen reduced the screen's luminance by 50%, adding another filter reduced it by another 50% and so on.

The luminance levels from the brightest to the darkest were: 60.8, 31, 16, 8.16, 4.19, 2.17, 1.12, and 0.59 cd/m^2. Both sessions commenced with the highest luminance block (60.8 cd/m^2). In the b2d session, starting from block 2, the luminance was progressively reduced by adding one filter in each block to reach seven filters in block 8 (0.59 cd/m^2). In the d2b session, in block 2 we used the maximum number of filters, seven. Then in each block we removed one filter, to reach one filter in block 8. Block 9 in each session was again conducted without any filters, as in block one (60.8 cd/m^2). The luminance of the screen with and without filters was measured using a Minolta CS-100 colorimeter. The measurements were done at the center of the monitor about 1 h after switching it on and before running each participant.

During the experiment, subjects sat in a sound attenuated booth and rested their head on a chin rest. Stimuli were displayed

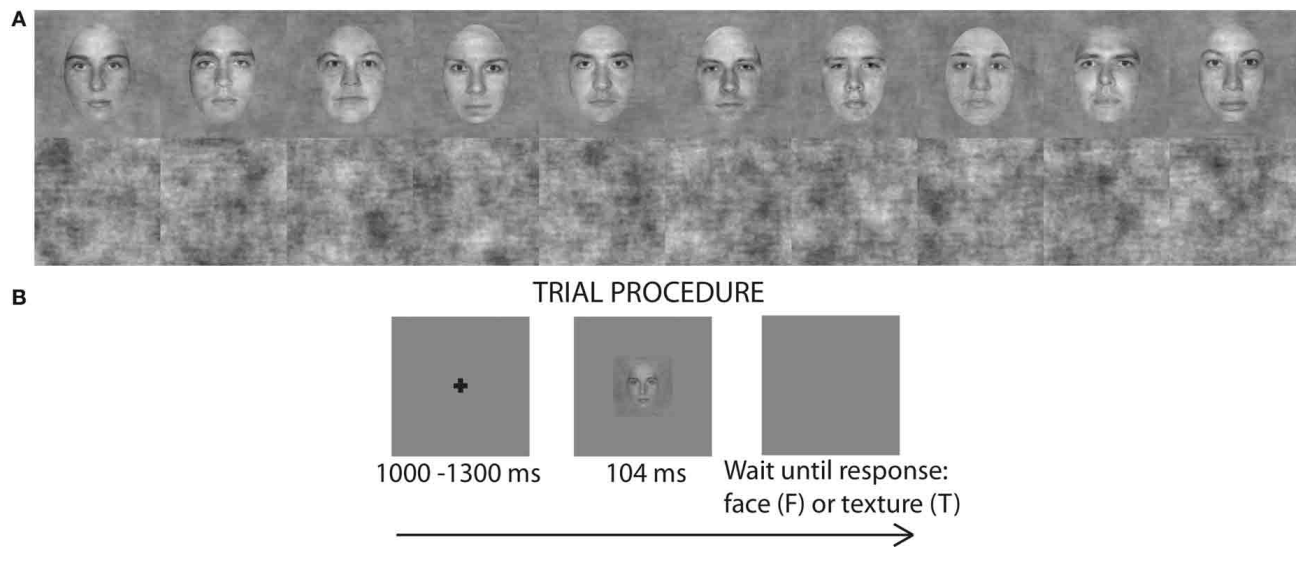

FIGURE 1 | (A) 10 face identities at 70% phase coherence and 10 examples noise textures (0% phase coherence) used in the luminance experiment. **(B)** Single trial procedure. For presentation purposes the fixation cross and the face image are not to scale.

on a Samsung SyncMaster 1100Mb monitor (600 × 800 pixels, height and width: 30 × 40 cm, 21 × 27° of visual angle; refresh rate—85 Hz, bits per pixel—32). Viewing distance measured from the chin rest to the monitor screen was 80 cm. Subjects were given experimental instructions including a request to minimize blinking and movement. Subjects were asked to categorise images of faces and textures by pressing "1" for face and "2" for texture, on the numerical pad of a keyboard, using the index and middle fingers of their dominant hand. Before the main experiment, subjects performed a 40 trial practice block containing 20 trials with auditory feedback, followed by another 20 trials without feedback. After the practice block, the dim lights in the booth were switched off and an adaptation screen with gray uniform background (RGB 128,128,128) was turned on. A 60 s light adaptation was performed at the beginning of all blocks, except in block 2 of d2b sessions, in which the adaptation lasted for 5 min. This longer duration was necessary due to the large luminance difference between zero and seven filters. After the adaptation and before each experimental block, pupil size in participant's right eye was measured three consecutive times (the mean of these three measurements was later used for the analyses). For the first 22 subjects we used a Colvard (Oasis Mediacla Inc.) pupillometer; for the remaining subjects we used a NeurOptics VIP™-200 pupillometer. When pupil measurement was completed, subjects were ready to proceed with the experiment.

We used a mixed design with image category and luminance as within-subject factors and age as between-subject factor. There were 9 experimental blocks, each consisting of 150 trials: 70 faces (10 face identities, each repeated 7 times, each time with a unique noise field) and 70 unique noise textures. Additionally, there were 10 practice trials (5 faces and 5 textures) at the beginning of each block with auditory feedback signaling to subjects whether their response was correct or not. The whole experiment consisted of 1350 trials, including 90 practice trials. Each trial began with a small fixation cross (size: 12 × 12 pixels; 0.4 × 0.4° of visual angle) displayed at the center of the monitor screen for a random time interval of about 1000–1300 ms, followed by an image of a face or a texture presented for about nine frames (∼104 ms) (**Figure 1B**). These durations are multiples of refresh screen durations and do not necessarily reflect the actual duration during which image pixels were active (Elze, 2010). After the stimulus, a blank screen was displayed until subject's response. The fixation cross, the stimulus and the blank response screen were all displayed on a gray uniform background (RGB 128, 128, 128). The importance of accuracy over speed was stressed to subjects. Subjects performed the task very well: in all the luminance levels, most subjects had accuracy above 95% and all exceeded 90%. One experimental block lasted for ∼4 min and the whole experiment (with breaks but excluding electrode application) lasted for about 1 h 30 min.

EEG RECORDING

EEG data were recorded at 512 Hz using an Active Electrode Amplifier System (BIOSEMI) with 128 electrodes mounted on an elastic cap. Four additional electrodes were placed at the outer canthi and below the eyes.

EEG DATA PRE-PROCESSING

EEG data were pre-processed using Matlab 2011a and the open-source toolbox EEGLAB 11.0.2.1b (Delorme and Makeig, 2004). Data were first re-referenced off-line to an average reference and an individual channel mean was removed from each channel. Data were then band-pass filtered between 0.3 and 40 Hz using a non-causal two-way least square FIR filter (pop_eegfilt function in EEGLAB). Non-causal filtering can potentially distort onsets (Vanrullen, 2011; Acunzo et al., 2012; Rousselet, 2012; Widman and Schroeger, 2012). Therefore, we analysed onsets of ERP differences by creating a second dataset in which data were pre-processed with 4th order Butterworth filters: high-pass causal filter at 2 Hz and low-pass non-causal filter at 40 Hz. Data from the two datasets were then epoched between −300 and 1200 ms around stimulus onset. Noisy electrodes were detected by visual inspection of the non-causal dataset and rejected on a subject-by-subject basis (the same electrodes were rejected in the two datasets). Baseline correction was performed using the average activity between time 0 and −300 ms. The reduction of artifacts, such as eye-movements or blinks was performed using Independent Component Analysis (ICA), as implemented in the infomax algorithm from EEGLAB. If ICA yielded components representing noisy electrodes (e.g., IC with a very focal, non-dipole activity restricted to one electrode whereas the rest of the map was flat), the noisy channels were removed and the ICA was repeated. ICA was performed on the non-causal FIR-filtered datasets and the ICA weights were then applied to the causal Butterworth-filtered datasets (on a subject by subject basis) in order to ensure removal of the same components from both datasets. After rejection of artifactual components, data were re-epoched between −300 and 500 ms and baseline correction was performed again. Finally, artifactual data epochs were removed based on an absolute threshold value larger than 100 μV and the presence of a linear trend with an absolute slope larger than 75 μV per epoch and R^2 larger than 0.3. The median number of trials accepted for analysis was 1313 out of 1350 [min: 1163, max: 1345] in bright to dark sessions and 1318 [min: 1166, max: 1344] in dark to bright sessions.

ERP STATISTICAL ANALYSES

Statistical analyses were conducted in single subjects and at the group level using Matlab 2011a and the LIMO EEG toolbox (Pernet et al., 2011). To model EEG data we used a general linear model (GLM) across trials, at all-time points and all electrodes. We controlled for multiple comparisons using a bootstrap spatial-temporal clustering technique (Pernet et al., 2011; Rousselet et al., 2011; Bieniek et al., 2012).

Aging effects on visual processing speed

Single subject data analyses. We extracted several measures of visual processing speed based on the timing and the amplitude of the difference between face and texture ERPs. To that end, we used a GLM with faces and textures at each luminance level as categorical predictors. Then we computed linear contrasts (*t*-tests) between beta coefficients for faces and textures for each luminance level. This model was applied separately to the causal-filtered and non-causal filtered datasets of each subject. Thus, for

each subject we obtained for every electrode the time course of model fit and of t statistics associated with each linear contrast. Then, for each subject, we determined the electrode with the highest squared t statistics in the block with the brightest luminance (60.8 cd/m^2). It is a data-driven approach that does not make assumptions about the localization of the effects, and allows us to identify the electrode with the maximum sensitivity to our experimental manipulation, independently in each subject. We refer to this electrode as the max t^2 electrode and report it according to the electrode numbering in Biosemi format (see **Figure S4** for the Biosemi electrode map with corresponding electrodes from the 10/10 system).

From the outputs of our single-subject GLMs, we derived three estimates of processing speed. The first measure was the onset of the earliest significant differences between face and texture ERPs at each luminance level. The onsets were obtained from the GLM applied to all the electrodes of the causal-filtered dataset of each subject. The second measure was the time it takes to integrate 50% of the cumulative t^2 function, which we refer to as the 50% integration time (50IT) (Rousselet et al., 2010). This measure incorporates potential changes in the shape of the ERP difference waveform that may occur with age. The integration was done over time, from 0 to 500 ms, and across all electrodes. The last measure was the latency of the maximum ERP difference (peak latency) between faces and textures recorded at the max t^2 electrode for each subject. Although ERP latency is not a direct index of processing speed, it could reflect the accumulation of information in neuronal population that ceases when an ERP peaks (Schyns et al., 2009). In that sense, it can potentially carry an indication of timing of neuronal processes. Both, 50IT and peak latency were obtained from the non-causal filtered data, for each luminance level and for each subject.

Group data analyses. To visualize age-related changes in the shape of the t^2 functions (that reflects changes in the ERP difference waveform) we calculated the quantiles of the age distribution of our sample using the Harrell–Davis estimator, which is based on a weighted sum of sorted values (Wilcox, 2005). We then applied the same weights to our t^2 functions for each luminance level individually (Rousselet et al., 2010).

To calculate descriptive statistics [median 50ITs with 95% confidence intervals (CI, reported in square brackets)] we used a percentile bootstrap procedure with 1000 samples and with the Harrell–Davis estimator of the median. Comparisons between 50IT for the 60.8 cd/m^2 luminance condition and all the other luminance conditions were done using a two-tailed percentile bootstrap test for dependent groups; comparisons between young 50ITs in each pinhole condition and the 50ITs of old adults obtained in the luminance experiment (in 60.8 cd/m^2 condition) were done using a two-tailed percentile bootstrap test for independent groups.

To determine if pupil size, retinal illuminance, our measures of processing speed (50IT, onsets, peak latencies) and peak amplitudes of ERP differences varied with age, we computed group level regressions for each luminance level using Matlab's *robustfit* function, with the default parameters. Then, we calculated percentile bootstrap confidence intervals around the slopes and intercepts in the following way. First, we sampled subjects with replacement, keeping their corresponding age, 50ITs, onsets, peak latencies and amplitudes of ERP differences. Second, we performed regressions between each measure of processing speed and age, at each luminance level. We performed these two steps 1000 times, and each time saved all the slopes and intercepts. Then, we sorted the bootstrapped slopes and intercepts, and used the 2.5 and 97.5 percentiles to form the boundaries of 95% bootstrap confidence intervals. To calculate whether the regression slopes and intercepts for the brightest condition differed from the other luminance conditions, we subtracted the bootstrapped slopes and intercepts of pairs of conditions to derive 95% bootstrap confidence intervals of the differences.

Next, we aimed to find out if, after accounting for age, we could explain individual variability in 50ITs and peak latencies of ERP differences by the variability in subjects' pupil sizes. To address that question we regressed the 50IT/age residuals and the peak latencies/age residuals against the pupil/age residuals. Again, we used a percentile bootstrap procedure to build confidence intervals of the slopes and intercepts.

Finally, we determined the onset and maximum latency of the aging effects by calculating how much of the cumulative t^2 function of each subject has been integrated up to each time point between 0 and 500 ms. Then, at each time point, and for each luminance level separately, we calculated regressions across subjects between the integrated t^2 and age. We determined when the regression slopes became significantly different from zero using a bootstrap procedure (see Rousselet et al., 2010 for description).

Luminance effect on face-texture ERP differences

Single subject data analyses. In the second part of the analyses, we quantified the time course of luminance effects on face and texture ERPs using a single-trial ANCOVA model. The model had two categorical predictors—faces and textures, one continuous predictor—luminance, and an interaction term between luminance and category. Luminance was entered into the model as the z-score of the log luminance levels. This model was applied to causal and non-causal filtered datasets of individual subjects. From the analyses of the causal-filtered datasets we obtained onsets of luminance and luminance × category interactions. From the analyses of the non-causal filtered data we obtained the latency of the strongest luminance and interaction F values.

Group data analyses. To determine if the ERP onsets and the latencies of maximum sensitivity to luminance and luminance × category change with age, we regressed the onsets and maximum latencies of each effect against age. Then, we calculated 95% bootstrap confidence intervals around the slopes and intercepts as well as around the difference between the slopes and intercepts of the two effects. We used a similar procedure as described in section Group data analyses.

Overlap between the ERPs of young and old observers

In the third part of our analyses, we determined if we could match the ERPs of old observers in the brightest condition, to that of young observers at lower luminance levels. To this end, we quantified the overlap between the t^2 functions of older

(>60, $n = 18$) observers in the brightest luminance condition and young observers (<30, $n = 15$) at each luminance level. First, we normalized the t^2 functions within participant by dividing their t^2 functions by the maximum t^2 across all luminance levels and time points. Then, we averaged the t^2 functions across subjects, separately for young and old subjects. To calculate the percentage of t^2 overlap between young and old, we computed the area under the mean t^2 functions for young and old observers using trapezoidal numerical integration (*trapz* function in Matlab) and expressed it as a proportion of the overall area under the two functions. The overlaps where calculated between the mean t^2 function of young subjects at each luminance level and the mean t^2 function of old subjects in the two conditions with the highest luminance (60.8 cd/m^2—conditions 1 (c1) and 9 (c9)).

The 95% confidence intervals around the overlaps as well as around mean t^2 functions of young and old adults were computed using a bootstrap procedure. First, separately for the young and old group, we sampled subjects with replacement. We then computed mean t^2 functions for young and old samples and calculated the overlap between the two functions for each luminance level. We performed this procedure 1000 times, each time saving the mean t^2 functions for young and old groups in each condition, the overlaps and the difference in overlaps between the two brightest conditions (the first and the last block). We then sorted each of the bootstrap estimates and used the 2.5 and 97.5 percentiles to form the boundaries of 95% bootstrap confidence intervals. We also computed within-old-group overlaps by sampling with replacement two samples of old subjects, and calculating the overlap between their means following the same procedure we used for between-group overlaps. Within-young-group overlaps were obtained using the same approach.

RESULTS

The first goal of this study was to replicate the ERP aging effects reported in Rousselet et al. (2010). Second, we aimed to determine if age-related delays in ERP measures of visual processing speed are luminance dependent. Third, we set to answer whether individual differences in processing speed can be explained by the variability in observers' retinal illuminance. Finally, we wanted to determine if the ERPs of old observers can be matched to the ERPs of young observers tested at lower retinal illuminance levels.

First, we replicated previous findings of Rousselet et al. (2010): aging slows down visual processing, expressed in the 50IT, at the rate of 1 ms/year. We observed this delay at all luminance levels, which suggests that age effects are not luminance dependent. We also found that aging prolongs peak latencies of the face-texture ERP differences at the average rate of 1.5 ms/year. However, we found no effects of age on the onset of ERP differences. We also found that early ERPs to faces and textures were delayed with decreasing luminance, an effect visible in individual subjects in both sessions (**Figure 2**). Finally, we were unable to explain individual differences in visual processing speed by inter-subject variability in retinal illuminance. We also did not manage to match the ERPs of old observers to those of young adults at lower luminances. These findings suggest that the age-related visual slowdown is not due to optical factors.

AGE EFFECTS ON 50% INTEGRATION TIMES, PEAK LATENCIES, ONSETS AND AMPLITUDES OF FACE-TEXTURE ERP DIFFERENCES

First, we observed a qualitative age-related change in the overall shape of the t^2 functions for all luminance levels (**Figure S1**). This qualitative change was captured by our measure of processing speed (50IT), showing a significant age-related delay of ∼1 ms/year (**Figure 3A**, **Tables S1, S2**). This effect was present at all luminance levels, and in both experimental sessions. There was no significant difference between the 50IT/age regression slope at the brightest luminance level (60.8 cd/m^2) and at all the other luminance conditions, suggesting that the 1 ms/year slope is similar across luminance levels (**Tables S1–S4**). The peak latencies of face-texture ERP differences were also delayed by age at all luminance levels and in both sessions, with an average slope of 1.5 ms/year (**Figure 3B**, **Tables S1, S2**).

Our analyses revealed no age effect on the onsets of face-texture ERP differences, except for some small effects that were inconsistent across sessions, present at 0.59 cd/m^2 in the bright to dark session only, and at the 60.8, 1.12, and 2.17 cd/m^2 in the dark to bright session only (**Figure 4**, **Tables S1, S2**). We also found no aging effect on the amplitude of face-texture ERP differences at all luminance levels and in the two experimental sessions (**Figure 6**, **Tables S1, S2**).

Finally, aging started to affect processing speed at 131 ms (b2d) and at 125 ms (d2b) post-stimulus at 60.8 cd/m^2, except in blocks 7 (8.16 cd/m^2) and 9 (60.8 cd/m^2) of the d2b session, where aging effects commenced already at 94 and 106 ms, respectively. Aging effects were the strongest around 201 ms (b2d) and 203 ms (d2b) at the highest luminance and were delayed up to ∼260 ms at 0.59 cd/m^2. Reduced luminance also prolonged the onset of aging effects from ∼125 ms at 60.8 cd/m^2 up to 162 ms at 0.59 cd/m^2 (**Figures 5A** and **5B**).

AGE EFFECTS ON PUPIL SIZE AND RETINAL ILLUMINANCE

The regressions between pupil size and age revealed senile miosis—a significant reduction of pupil size with age that was present at all luminance levels in both sessions (**Figure 6**). The slope of the pupil/age regression was in the range of −0.03 mm (60.8 cd/m^2) to −0.05 mm (0.59 cd/m^2) per year (**Tables S1, S2**). This is equivalent to about 0.6–1 mm decrease in pupil size every 20 years—from ∼5 mm at 20 years old to ∼3.5 mm at 80 years old at 60.8 cd/m^2 and from ∼7 mm at 20 years old to ∼4.5 mm at 80 years old at 0.59 cd/m^2. The pupil/age regression slope at the brightest luminance did not differ from the slopes at the lower luminance levels (**Tables S1, S2**). The intercepts of the pupil/age regressions differed between the brightest luminance and all the other conditions and increased from 5 mm at 60.8 cd/m^2 to 7 mm at 0.59 cd/m^2.

As expected, retinal illuminance decreased with increasing age (**Figure 6**) and both the slope and the intercept of the retinal illuminance/age regression differed significantly between 60.8 cd/m^2 and all the other luminance conditions (**Tables S1, S2**). The slope ranged from about −12 at 60.8 cd/m^2 to −0.2 at 0.59 cd/m^2 in both sessions. The intercept was 1400 Td at 60.8 cd/m^2 and dropped to 24 Td at 0.59 cd/m^2.

After partialling out the effect of age from 50IT, from peak latencies of face-texture ERP differences and from pupil size,

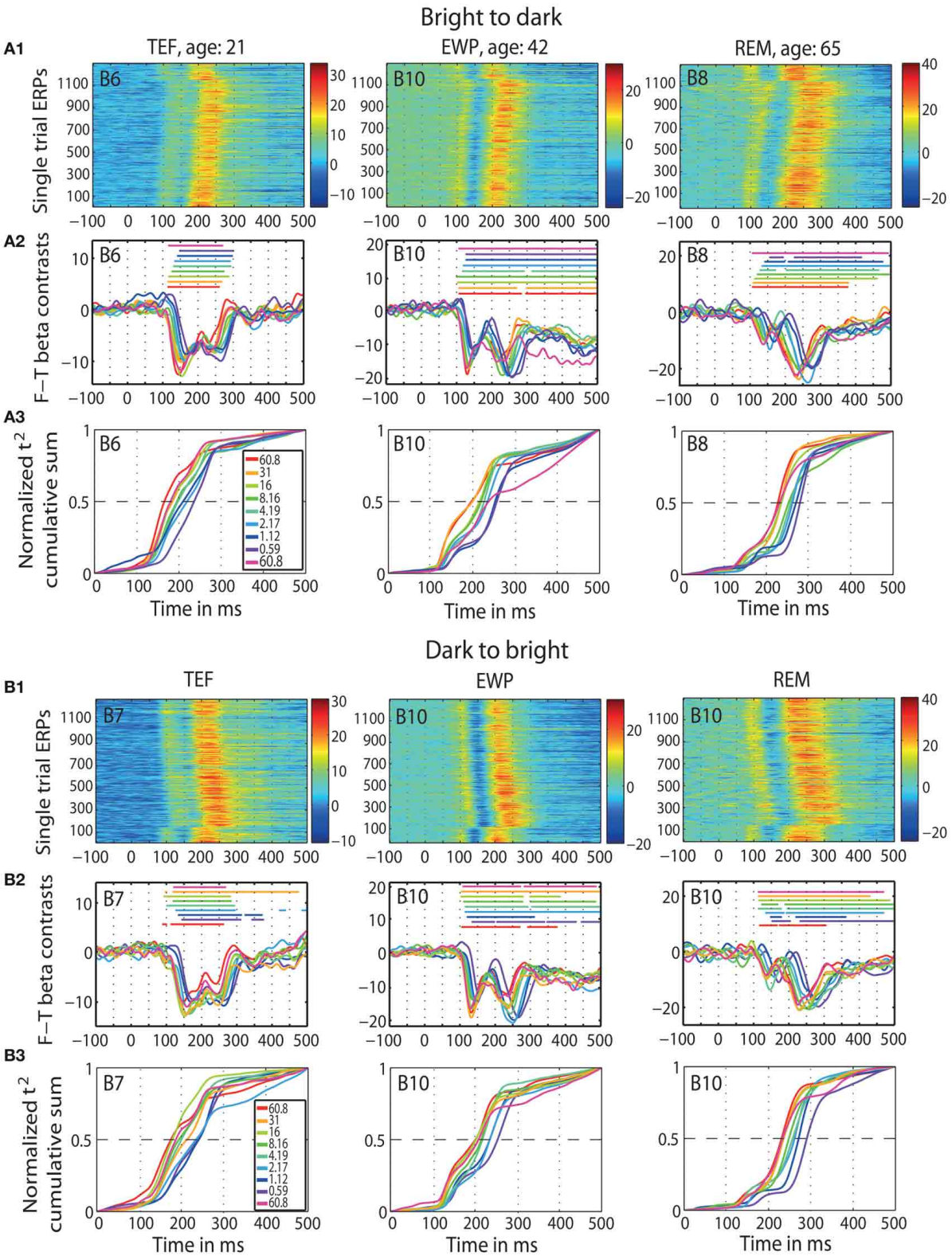

FIGURE 2 | ERP results in individual subjects. Data of three representative subjects: one young (TEF, age 21), one middle-age (EWP, age 42) and one old (REM, age 65) for b2d session (panel **A**) and d2b session (panel **B**) at the max t^2 electrode (indicated in the top left corner of each subplot). An electrode map is provided in **Figure S4**. (**A1** and **B1**) Single trial ERPs, in μV. (**A2** and **B2**) Time-courses of contrasts between face and texture beta-coefficients for each luminance level; horizontal lines indicate significant contrasts. (**A3** and **B3**) Normalized t^2 cumulative sums at each luminance level.

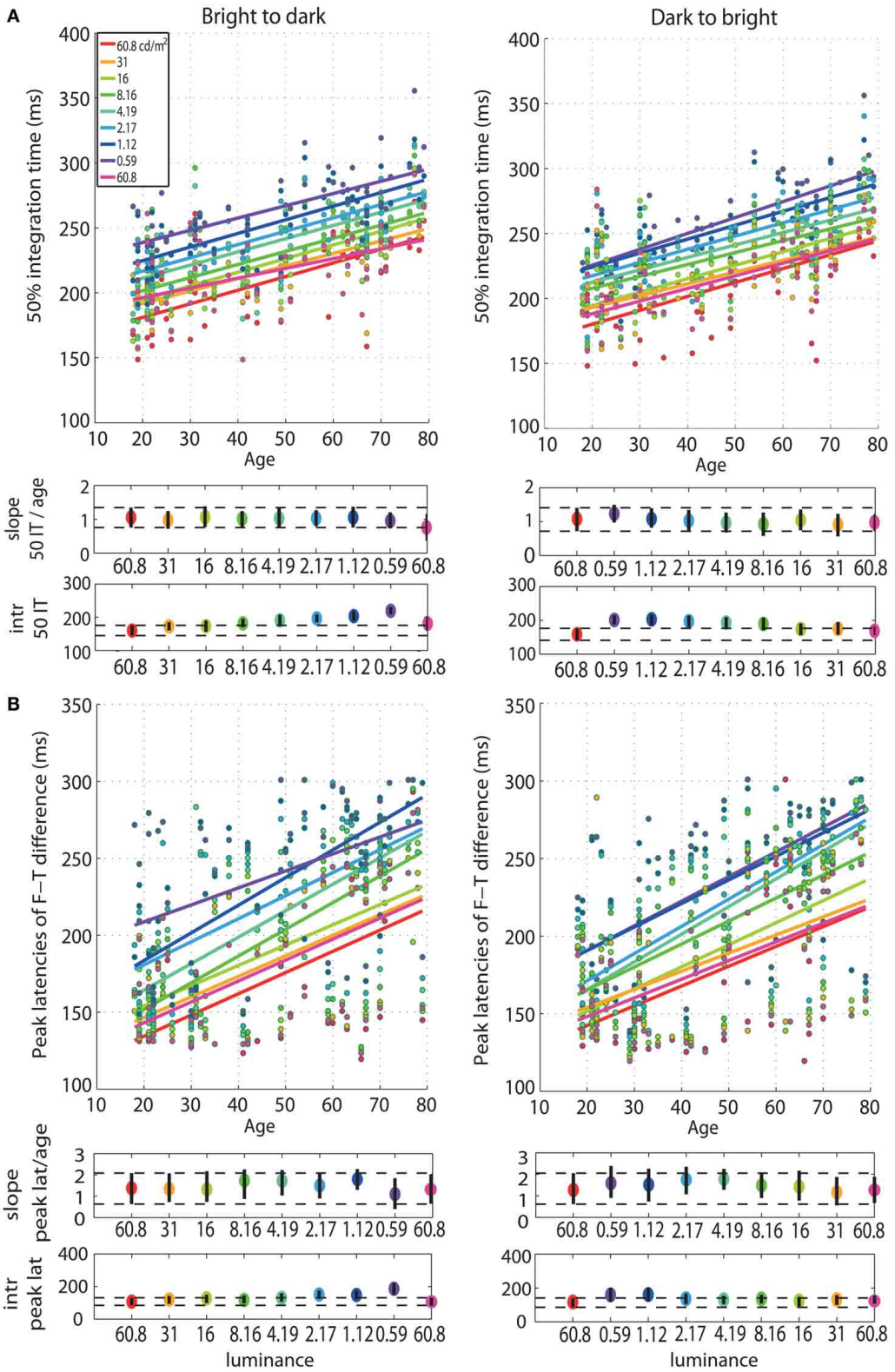

FIGURE 3 | Regressions of 50IT and peak latencies of face-texture ERP differences against age. (A) Regression fits between 50IT and age and **(B)** latencies of maximum face-texture ERP differences, for all luminance levels. B2d sessions are shown in column 1, d2b sessions in column 2. The two horizontal plots below each regression plot contain slopes and intercepts (intr) as colored dots, with confidence intervals as vertical black lines. Horizontal dashed black lines show the boundaries of the confidence intervals of the slopes and intercepts in the first brightest condition (60.8 cd/m^2).

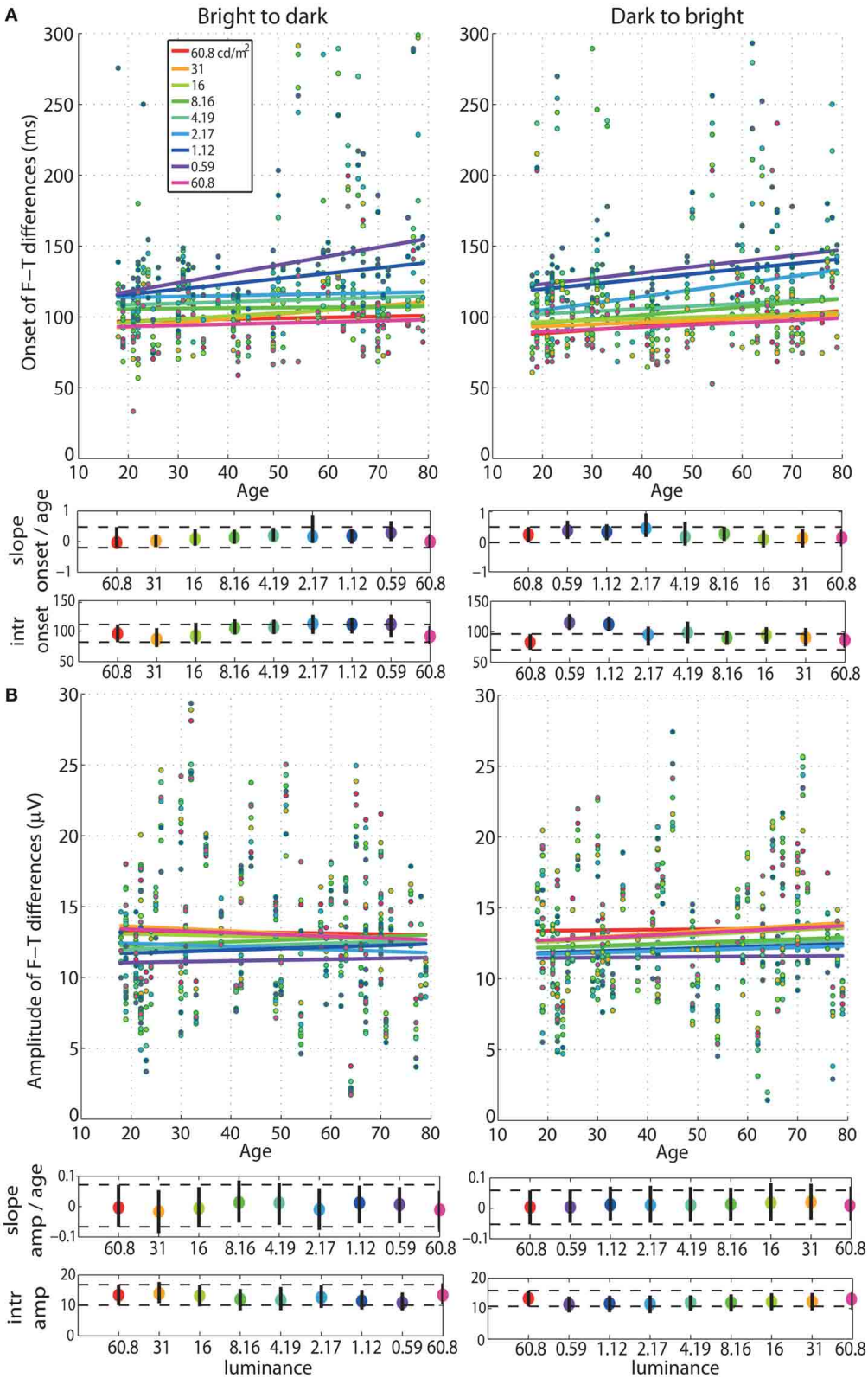

FIGURE 4 | Regressions of onset and amplitude ERP differences against age. (A) Regression fits between the onset of significant face-texture ERP differences and age and **(B)** between maximum amplitude of face-texture ERP differences and age, for all luminance levels.

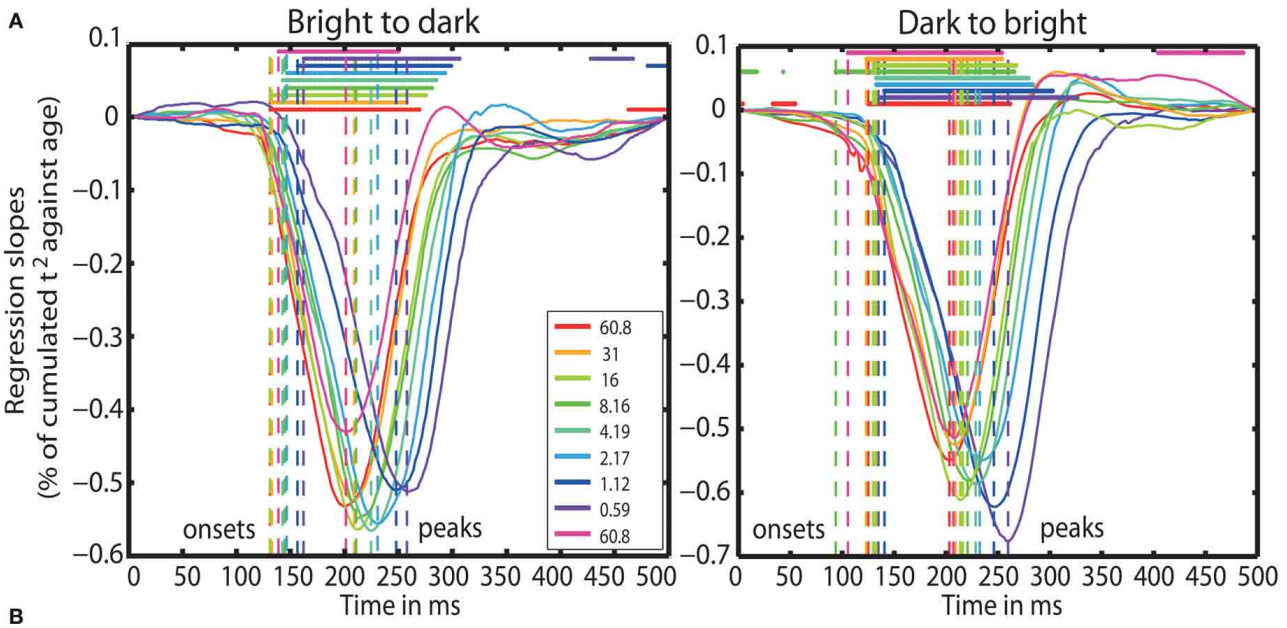

B

b2d	Luminance	60.8	31	16	8.16	4.19	2.17	1.12	0.59	60.8
	Onset	131	133	131	145	143	147	156	162	139
	Peak latency	201	209	211	211	225	231	248	259	201
d2b	**Luminance**	**60.8**	**0.59**	**1.12**	**2.17**	**4.19**	**8.16**	**16**	**31**	**60.8**
	Onset	125	135	141	133	133	94	131	123	106
	Peak latency	203	260	246	232	229	221	215	209	207

FIGURE 5 | (A) Time-courses of % of cumulated t^2/age regression slopes. Each curve shows the time-course at one luminance level. Horizontal lines indicate significant regression slopes. Vertical dashed lines mark the onsets and the peak latencies of significant aging effects. **(B)** Table of onsets (ms) and peak latencies (ms) of the aging effects on processing speed for all luminance levels (cd/m^2) for b2d and d2b experimental sessions.

individual differences in 50IT (**Figure 7A**) and in peak latencies (**Figure 7B**) could not be accounted for by variability in pupil size across subjects (**Table S5**). Regression slopes between 50IT/age residuals and pupil size/age residuals were not significant at any luminance level.

AGE EFFECTS ON ERP SENSITIVITY TO LUMINANCE AND CATEGORY × LUMINANCE INTERACTION

The onsets of ERP sensitivity to luminance and to category × luminance interaction did not change with age (**Figure 8A**) and the age regression slopes for the two effects did not differ (b2d: diff = −0.19 [−0.51, 0.10]; d2b: diff = −0.13 [−0.42, 0.15]). Luminance started to affect the ERPs at about 66 ms [60, 72] in the b2d session and 60 ms [52, 71] in d2b session (**Figure 8A**). This is about 20 ms before (b2d: diff = −20 ms [−36 −3]; d2b: diff = −19 ms [−34, −4]) luminance began to interact with stimulus category at 86 ms [68, 103] (b2d) or 80 ms [66, 97] (d2b) (**Figures 8A,B**). The ERP sensitivity to luminance was the strongest around 152 ms in b2d session and 129 ms in d2b session, whereas the category × luminance interactions peaked at about 118 ms (b2d) and 104 ms (d2b) post-stimulus (**Figures 8B,C**). However, the latencies of the two effects did not differ significantly (differences between regression intercepts, b2d: diff = 34 [−9, 84]; d2b: diff = 25 [−32, 91]). There was also no age effect on the timing of maximum sensitivity to luminance in any of the sessions (**Figure 8C**). However, aging delayed the latency of maximum interaction between stimulus category and luminance at the rate of 1.03 ms [0.05, 1.93] per year in b2d and 1.69 ms [0.79, 2.59] per year in d2b. The difference between the regression slopes of luminance and category × luminance effects was not significant (b2d: diff = −0.64 [−1.83, 0.69]; d2b: diff = −0.89 [−2.17, 0.26]).

OVERLAP BETWEEN YOUNG AND OLD SUBJECTS

The median 50IT of young adults (<30) at the highest luminance (60.8 cd/m^2) was 181 ms (95% bootstrap CI = [169, 196] in b2d) and 183 ms [168, 199] in d2b (**Figure 9A** tables). At the same luminance, the median 50IT of older subjects (>60) was 232 ms [225, 238] (b2d) and 237 ms [222, 247] (d2b), which is ∼50 ms slower than the processing speed of young subjects in both experimental sessions (b2d: diff = −50 ms [−64, −34]; d2b: diff = −53 ms [−72, −33]). Indeed, visual processing of young adults was significantly faster than that of old adults in all but

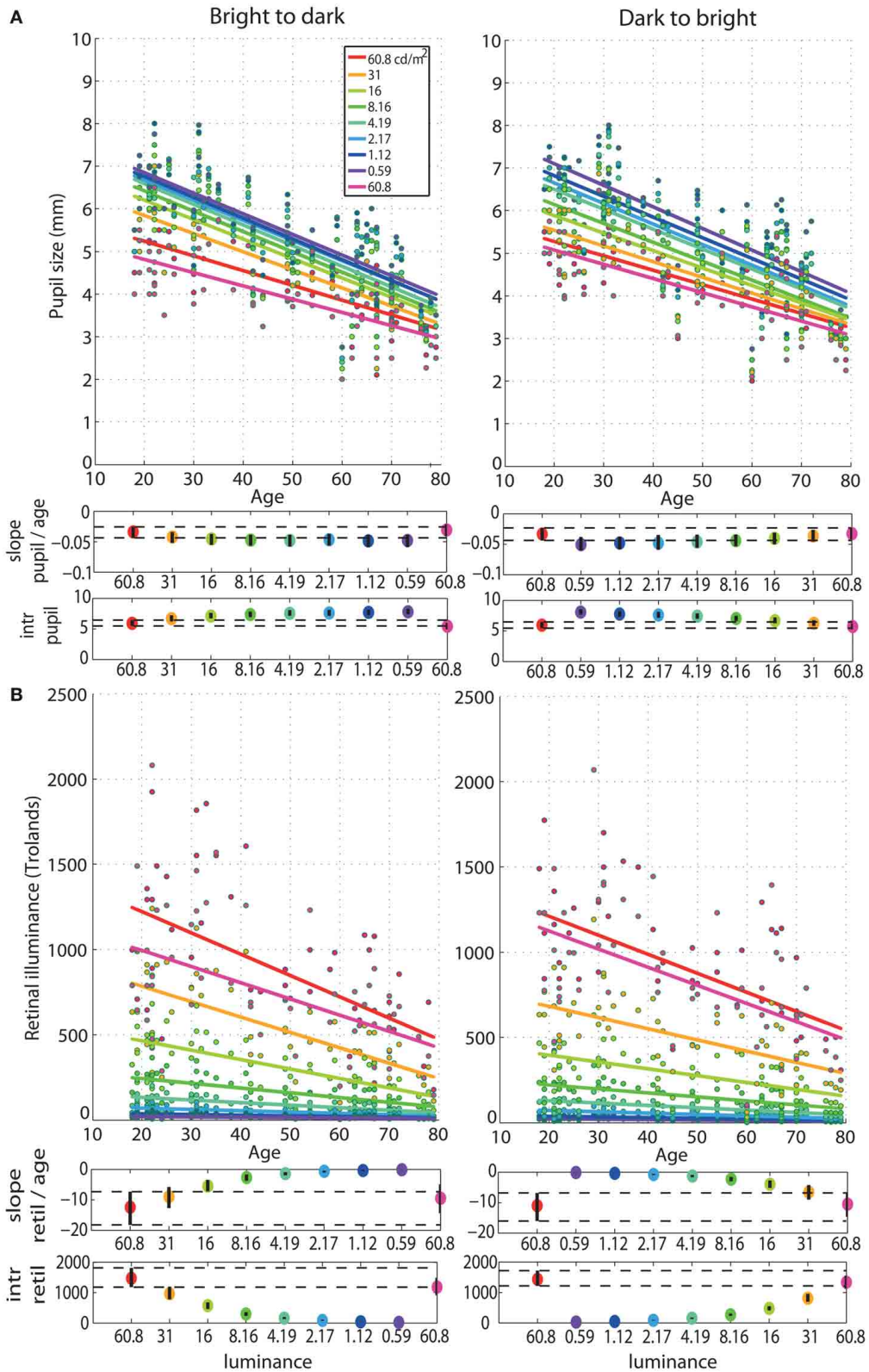

FIGURE 6 | Regressions of pupil size and retinal illuminance against age. (A) Regression fits between pupil size and age and **(B)** between retinal illuminance (retil) and age, for all luminance levels. See **Figure 4** caption for details.

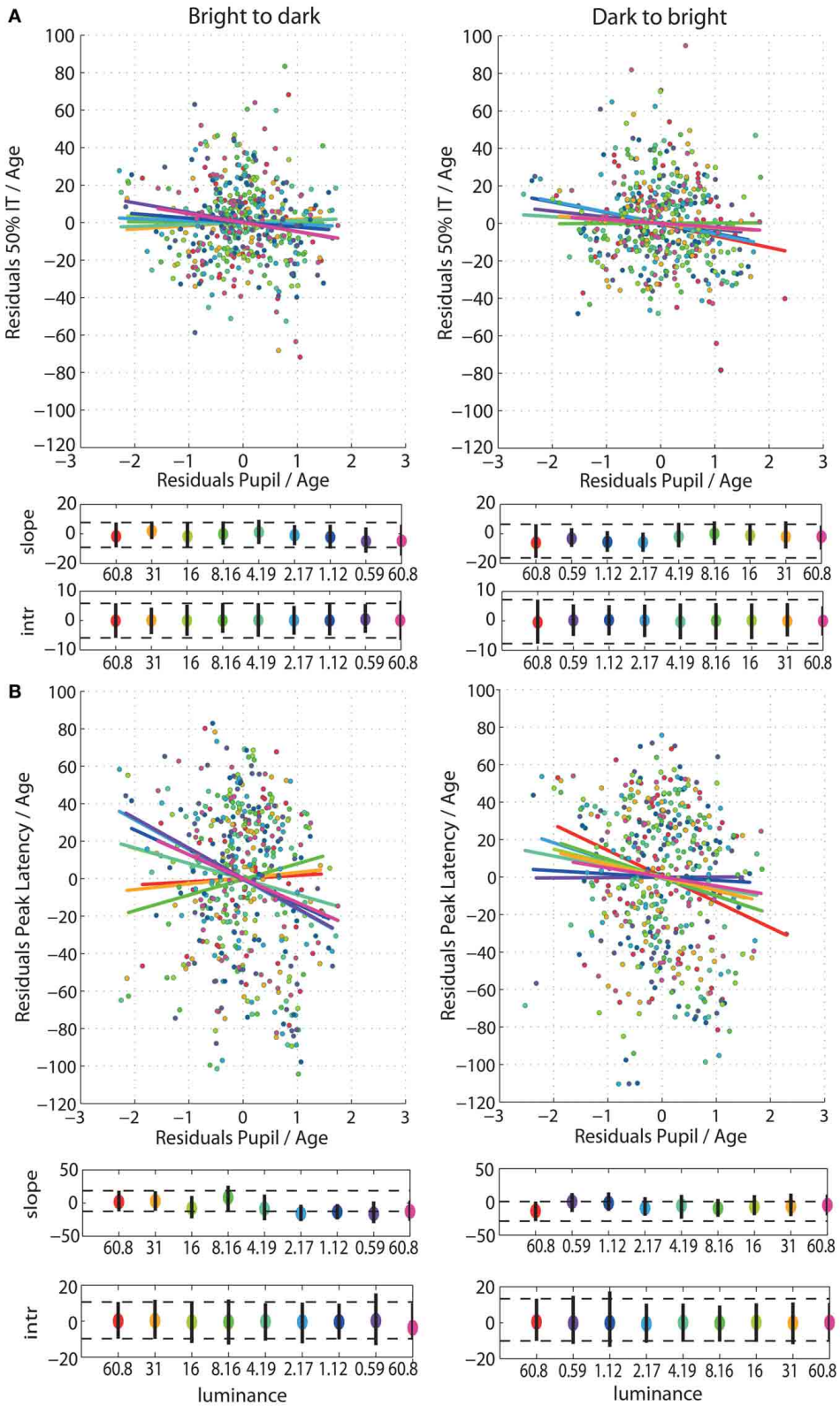

FIGURE 7 | (A) Regressions of residuals of 50IT/age against residuals of pupil size/age for all luminance levels. **(B)** Regressions of residuals of peak latency of face-texture ERP differences/age against residuals of pupil size/age for all luminance levels. See **Figure 4** caption for details.

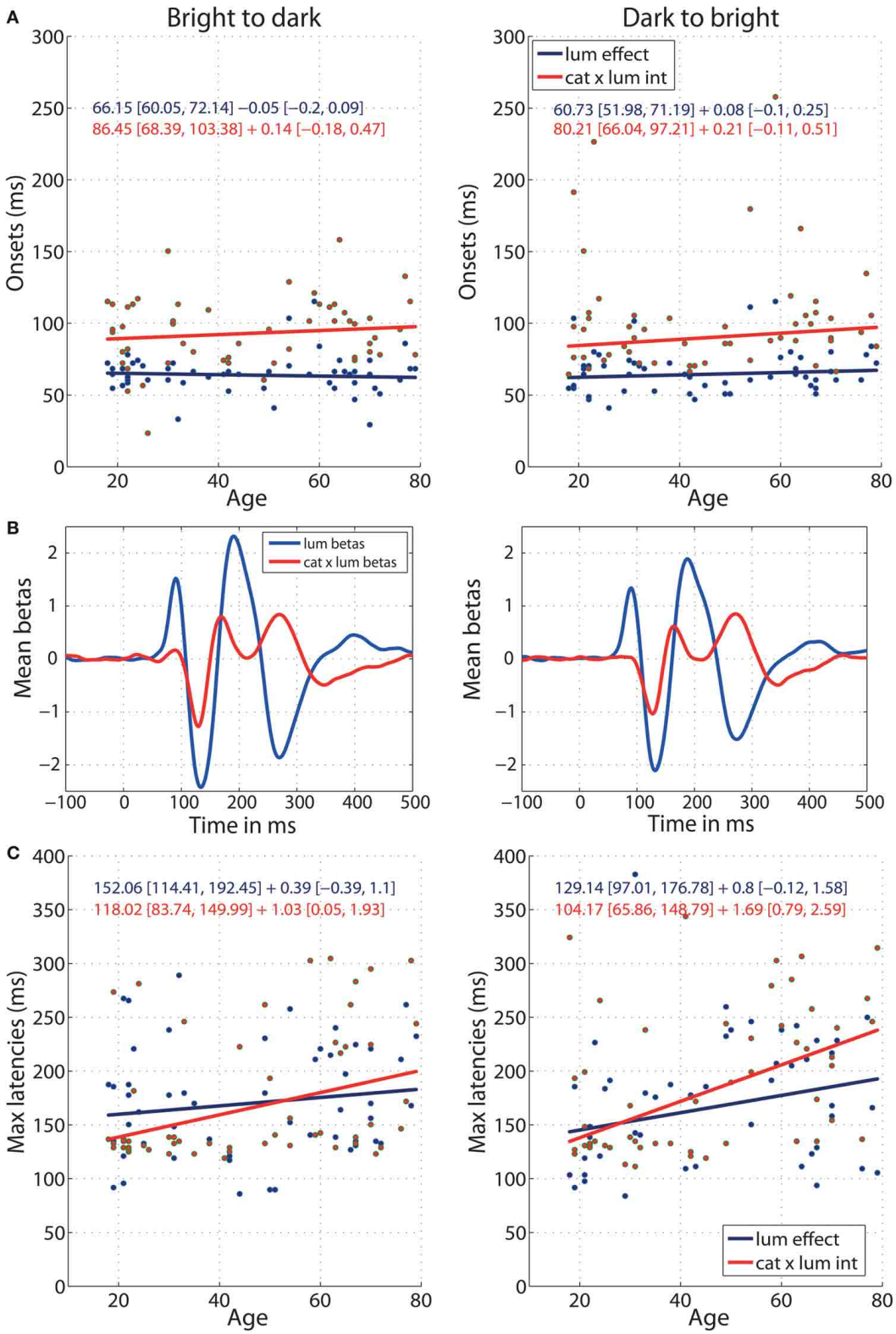

FIGURE 8 | Regressions of luminance effect and category × luminance interaction against age. (A) Onsets of the two effects against age for b2d (left column) and d2b sessions (right column). **(B)** Mean (across all subjects) beta coefficients associated with two predictors: luminance and category × luminance interaction. **(C)** Latencies of the maximum effects against age. Each subplot contains regression equations in the format intercept + slope with their confidence intervals in square brackets. The color of each equation corresponds to the regression line for each effect.

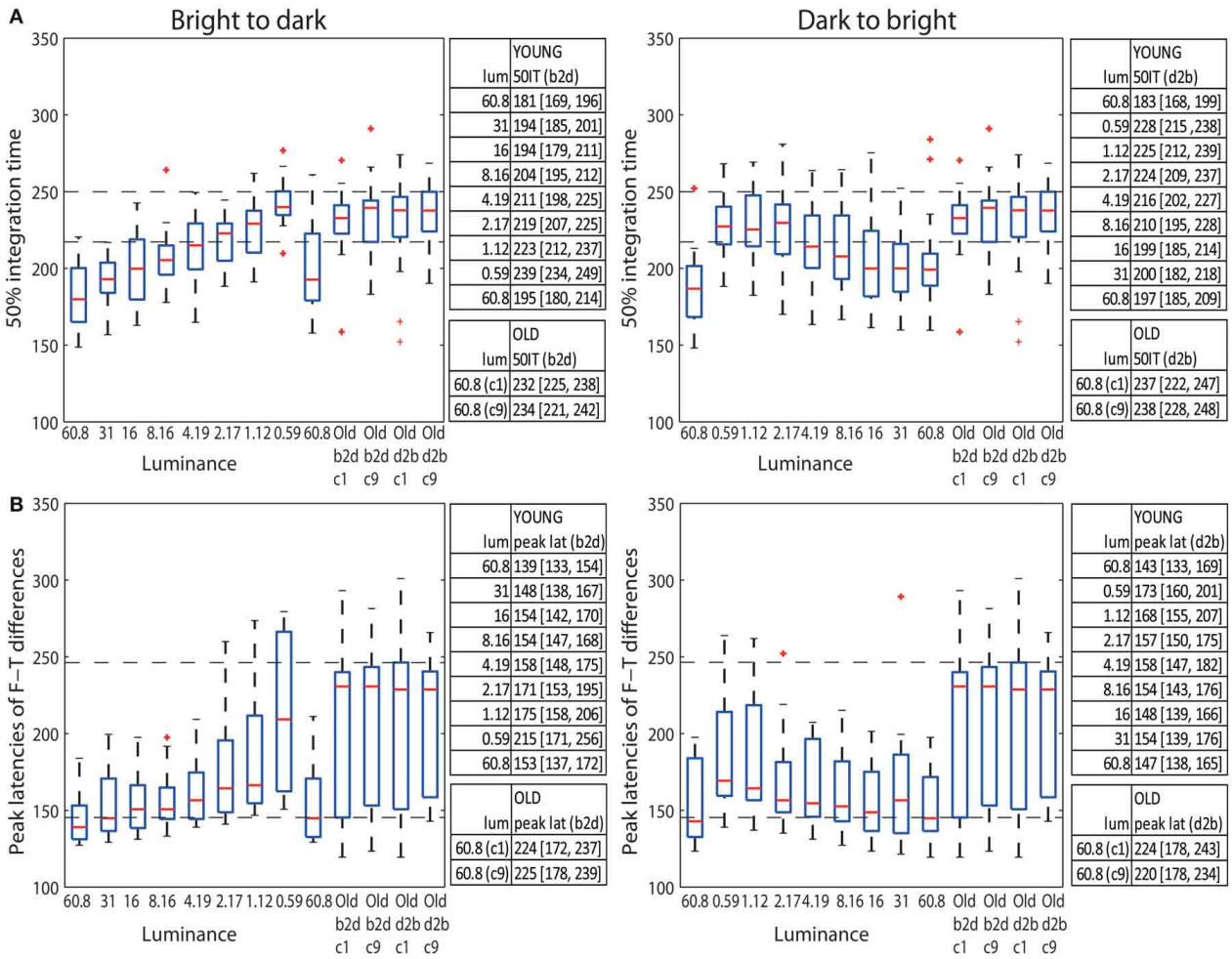

FIGURE 9 | (A) Boxplots of 50% integration times (ms) and **(B)** peak latencies (ms) of face-texture ERP differences for young (<30 years old) and old (>60 years old) adults. The median (across subjects) 50ITs and peak latencies along with confidence intervals are provided in the tables to the right of the subplots. For young subjects median 50IT and peak latencies for all conditions are given; for old subject, they are given for the two brightest conditions [condition 1 (c1) and 9 (c9)].

the two darkest conditions (1.12 and 0.59 cd/m^2) in both sessions, and the 2.17 cd/m^2 condition in d2b session (**Table S6**).

The latencies of maximum face-texture ERP differences were also delayed by age in both sessions. ERP differences in young adults at the luminance of 60.8 cd/m^2 peaked at the median latency of 139 ms [133, 154] (b2d) and at 143 ms [133, 169] (d2b), whereas for old adults the differences peaked at 224 ms [162, 238] (b2d) and at 224 ms [175, 242] (d2b) (**Figure 9B** tables). This is an ∼80 ms difference between peak ERP latencies of young and old subjects at the highest luminance (b2d: diff = −84 ms [−100, −33]; d2b: diff = −80 ms [−100, −27]). The latencies of the peak ERP differences of old adults (at 60.8 cd/m^2) were significantly longer than those of young adults for all luminance levels, apart from 1.12 and 0.59 cd/m^2 conditions in both sessions and 2.17 cd/m^2 in b2d session only (**Table S6**).

A qualitative age-related change in the shape of t^2 functions was shown in **Figure 2**; **Figure 10A** shows the mean t^2 functions for young (<30 years old) and old (>60 years old) adults. We computed the percentage of overlap between normalized t^2 functions of these two age groups to determine if the brain responses of old adults could be matched to that of young adults experiencing reduced retinal illuminance. The overlap increased with decreasing luminance, starting from about 69–74% at 60.8 cd/m^2 to about 83–86% at 0.59 cd/m^2 in both sessions (**Figures 10B,C**, **11A**). The overlap within the old group exceeded 90% indicating that old subjects are more similar to each other than to young subjects at any luminance level (**Figure 11A**). In addition, even in the two conditions where the overlap was the highest—86% at 0.59 cd/m^2 and 85% at 1.12 cd/m^2, the retinal illuminance of young subjects was only about 5% of that of old subjects (**Figure 11B**), thus suggesting that retinal illuminance cannot account for young vs. old differences in processing speed.

PINHOLE EXPERIMENT

To investigate if there is a causal relationship between pupil size and processing speed, we conducted a second

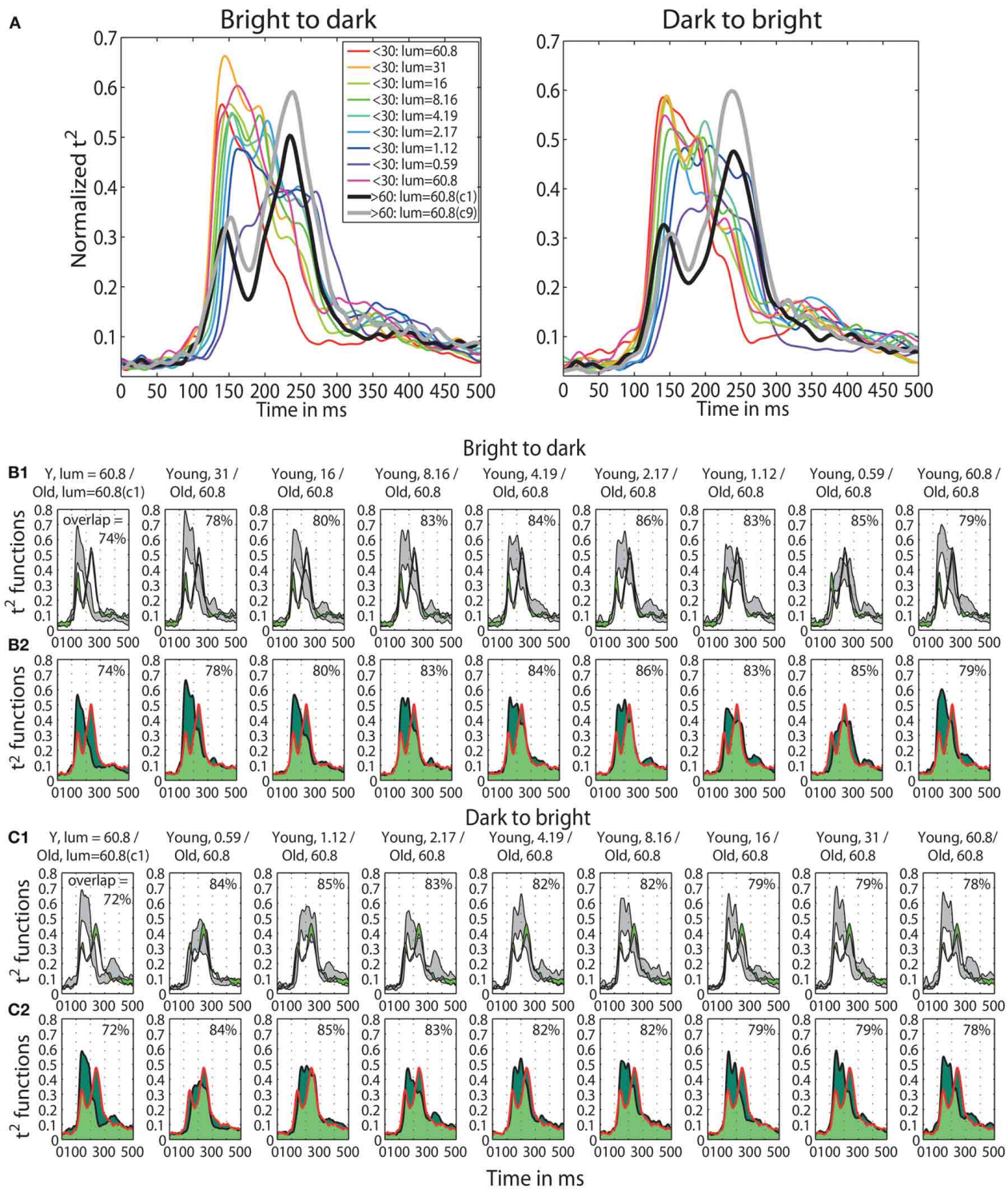

FIGURE 10 | (A) Time-course of normalized t^2 functions for young and old subjects. Each subplot shows mean time-courses, across young subjects (<30 years old), at each luminance level, and across old subjects (>60 years old) in the two conditions with the highest luminance: condition 1 (c1) plotted in black and condition 9 (c9) plotted in gray. **(B1,C1)** Confidence intervals of young and old t^2 functions. Each subplot shows the time-course of 95% confidence intervals of the mean t^2 functions of young subjects (in gray) at each luminance level and of old subjects (in green) in the first brightest condition (luminance = 60.8 cd/m^2). **(B2,C2)** Overlaps between young and old t^2 functions. Each subplot depicts the area under the t^2 function of young (<30) and old (>60) subjects shaded in dark green. The edges of the young t^2 functions are black, those of old t^2 functions are red. The overlap between t^2 functions for young and old subjects is shaded in light green. The proportion of overlap is given inside each subplot and the luminances are given in the title of each subplot.

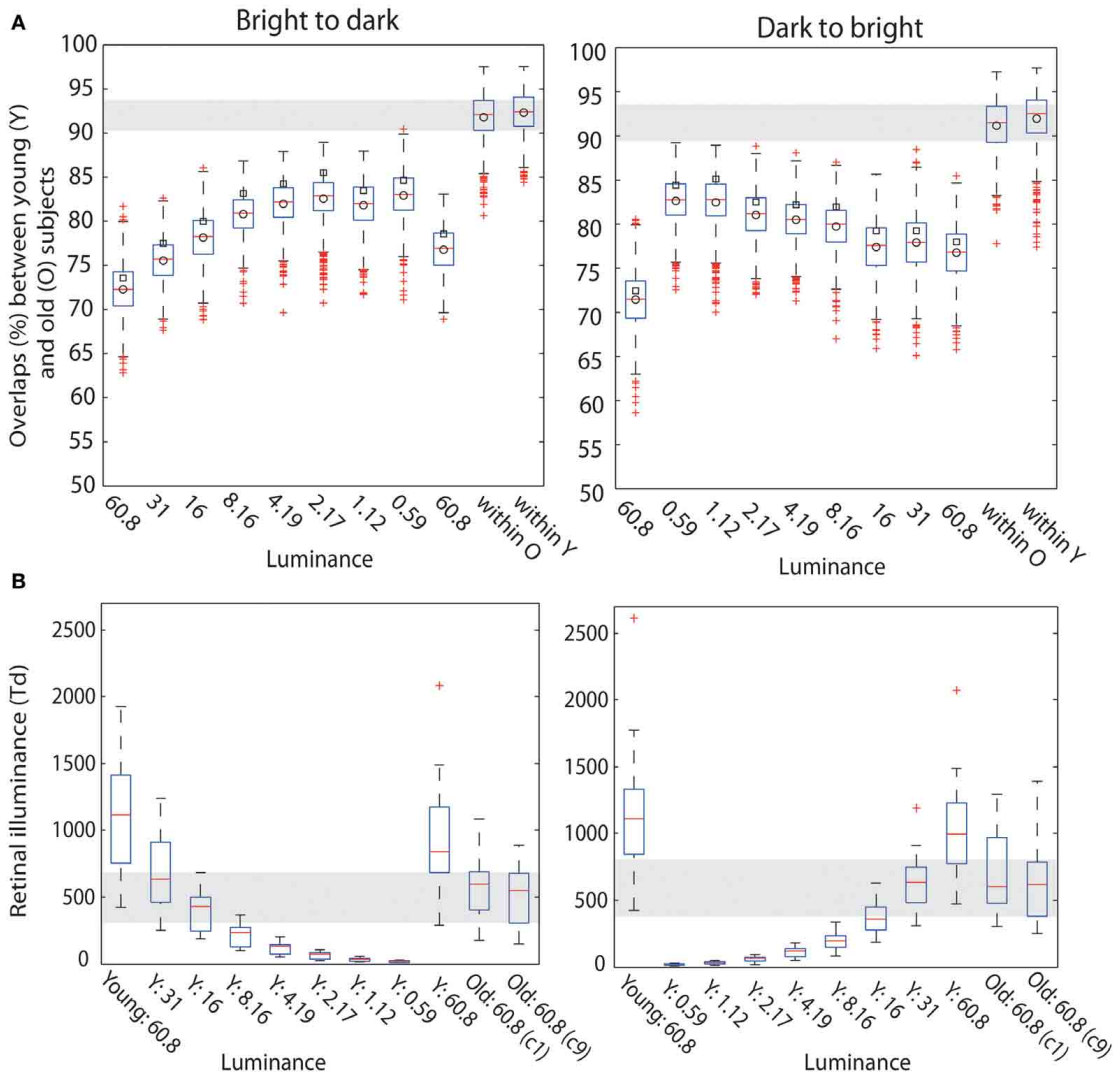

FIGURE 11 | (A) Boxplots of overlaps. Boxplots of bootstrapped t^2 function overlaps between young and old adults. In each subplot, the first nine boxplots show overlaps (%) between young subjects in each luminance level and old subjects in the first brightest luminance condition (c1, lum = 60.8 cd/m^2). The last two boxplots show the within group overlaps for old and young subjects, in the first brightest condition (60.8 cd/m^2) for b2d and d2b session. In each boxplot the square indicates the percentage of overlap between young and old yielded by our calculation; the circle is the mean of the bootstrapped overlaps—thus, the difference between the values for circle and square suggests that our estimation of the overlap is positively biased. **(B)** Retinal illuminance of young and old subjects. The first nine boxplots in each subplot depict the distributions of retinal illuminances in young subjects, at nine luminances; the two last boxplots in each subplot show results in old subjects in the two brightest conditions (luminance = 60.8 cd/m^2).

experiment in which young subjects were wearing pinholes ranging from 1 to 5 mm. We aimed to establish if we could match old subjects' processing speed at high luminance (60.8 cd/m^2) to that of young subjects wearing pinholes.

METHODS

SUBJECTS

10 subjects (median age = 28.5, min. = 22, max. = 34, six males, 10 right handed) took part in two experimental sessions conducted 1 week apart. Seven of them also participated in the luminance experiment 5–6 months earlier. Each subject's visual acuity and contrast sensitivity were measured for both eyes separately (monocular testing), on the day of the first session, using the same materials as in the luminance experiment. All subjects had normal or corrected-to-normal vision and contrast sensitivity (**Table 2**), and all reported very good hearing, at least weekly exercise and none reported smoking. None of the subjects reported suffering from an eye disease, or a mental condition and none was taking psychotropic medications. All subjects gave written informed consent and were compensated for their participation at the rate of £6/h.

STIMULI

The stimuli were faces and textures generated as in the luminance experiment.

Table 2 | Pinhole experiment subjects' information.

Visual acuity						
High contrast 63 cm (median [min, max])		Low contrast 63 cm (median [min, max])		Contrast sensitivity (median [min max])		Years of education (median [min max])
Right eye	Left eye	Right eye	Left eye	Right eye	Left eye	
107 [89, 109]	105.5 [98, 112]	95 [88, 99]	93 [89, 99]	1.95 [1.95, 2.10]	1.95 [1.95, 2.10]	19 [15, 25]

EXPERIMENTAL DESIGN

The experiment consisted of seven blocks in each session. Pinhole order differed in the two experimental sessions: in the "small to big" (s2b) session, a 1 mm pinhole was applied in block 2. Pinhole size then increased by 1 mm in each subsequent block to reach 5 mm in block 6. In the "big to small" (b2s) session, a 5 mm pinhole was used in the 2nd block and then pinhole size decreased by 1 mm in each block, up to 1 mm in block 6. The first and the last blocks in both sessions were conducted without any pinholes. All subjects participated in one s2b and one b2s session that were randomly assigned.

Each block contained 210 trials: 100 faces (10 face identities repeated 10 times, each time with unique noise field), 100 unique noise textures, and 10 practice trials at the beginning of every block (five faces and five textures). The whole experiment had a total of 1470 trials. The task and trial procedure were the same as in the luminance experiment.

PROCEDURE

The experiment was conducted in the same lab booth as the luminance experiment. The stimuli were displayed on the same monitor with a luminance of 60.8 cd/m^2, which was constant across blocks. The viewing distance was also 80 cm. Subjects performed the experiment monocularly using the eye with best visual acuity—four subjects used their left eye and six subjects used their right eye. The other eye was occluded with an optician eye patch. For the purpose of light adaptation, before each experimental block, subjects were instructed to look at the monitor screen with uniform gray background (128 128 128) and luminance of 60.8 cd/m^2 for 60 s. After adaptation, subjects' pupil size in the non-occluded eye was measured using a NeurOptics pupillometer, following the same procedure as in the luminance experiment. After pupil measurement, an optical trial lens frame (model TF-1002, Danyang Huasu Optical Co., Ltd.) was put on subjects' head. The pinholes were black circular plates 4 cm in diameter with a circular aperture of 1, 2, 3, 4, or 5 mm located in the middle of the plate. To determine the optimal position of the pinhole in front of the non-occluded eye, the smallest (1 mm) pinhole plate was inserted into the trial frame. Subsequently, the experimenter adjusted the pinhole position until a rectangular frame displaying the message "Press any key to start . . . (Block 1 of 7)" (size: 256 × 256 pixels, 9° × 9° of visual angle, displayed in the center of the screen) was centered in the subjects' visual field (the message was not displayed during light adaptation). Each subject's visual field extent, while looking through the pinhole, was computed by taking into consideration the distance between the eye and the pinhole plate and the pinhole size. The median visual angle across subjects for pinholes of 1, 2, 3, 4, or 5 mm was 15, 17, 18, 20, and 22°, respectively, in the s2b and 14, 16, 18, 20, and 22° in the b2s procedure. Thus, the 9 × 9° stimuli were visible even through the smallest pinhole. Once the trial frame with 1 mm pinhole was optimally installed, subjects conducted a 40 trial practice block, which was similar to the practice block in the luminance experiment. After the practice block and a small break, subjects proceeded with the experiment.

EEG DATA ACQUISITION AND PRE-PROCESSING

Data were acquired and pre-processed as in the luminance experiment, except that we did not create causal-filtered datasets. All analyses were done on the non-causal filtered data (band-pass filtered between 0.3–40 Hz using a two-way least square FIR filter (pop_eegfilt function in EEGLAB).

EEG DATA ANALYSIS

EEG data were analysed using Matlab 2011a and the LIMO EEG toolbox (Pernet et al., 2011). We used general linear modeling of single-trial EEG data and the procedure was similar to the one used in the luminance experiment, except there were seven face-texture contrasts, instead of nine—one for each of the seven pinhole conditions. As in the luminance experiment, the results were corrected for multiple comparisons using a spatial-temporal clustering approach.

For descriptive statistics and all comparisons, we used percentile bootstrap procedures as in the luminance experiment.

RESULTS

The goal of the second experiment was to determine if, by decreasing young subjects' pupil size, we could slow their processing speed and match their ERPs to those of old subjects. We found that the ERPs of young subjects were delayed for all pinhole sizes compared to the no pinhole condition. This effect was the strongest with the 1 mm pinhole and was visible at the level of single trial ERPs (**Figure 12A**), face-texture ERP differences (**Figure 12B**), and cumulative sums of t^2 functions (**Figure 12C**). Also, contrary to our hypothesis that the smaller the pinhole, the bigger the overlap between young and old subjects' ERPs, the overlap was higher for 4 and 5 mm pinholes compared to 1 and 2 mm pinholes (**Figure 15**). However, even at 4 or 5 mm, we were unable to match the ERPs of young observers to those of old observers.

EFFECT OF PINHOLES ON ERP PROCESSING SPEED

Young subjects' 50ITs increased from 189 ms in the first no pinhole condition to 265 ms (b2s) and 251 ms (s2b) with a 1 mm

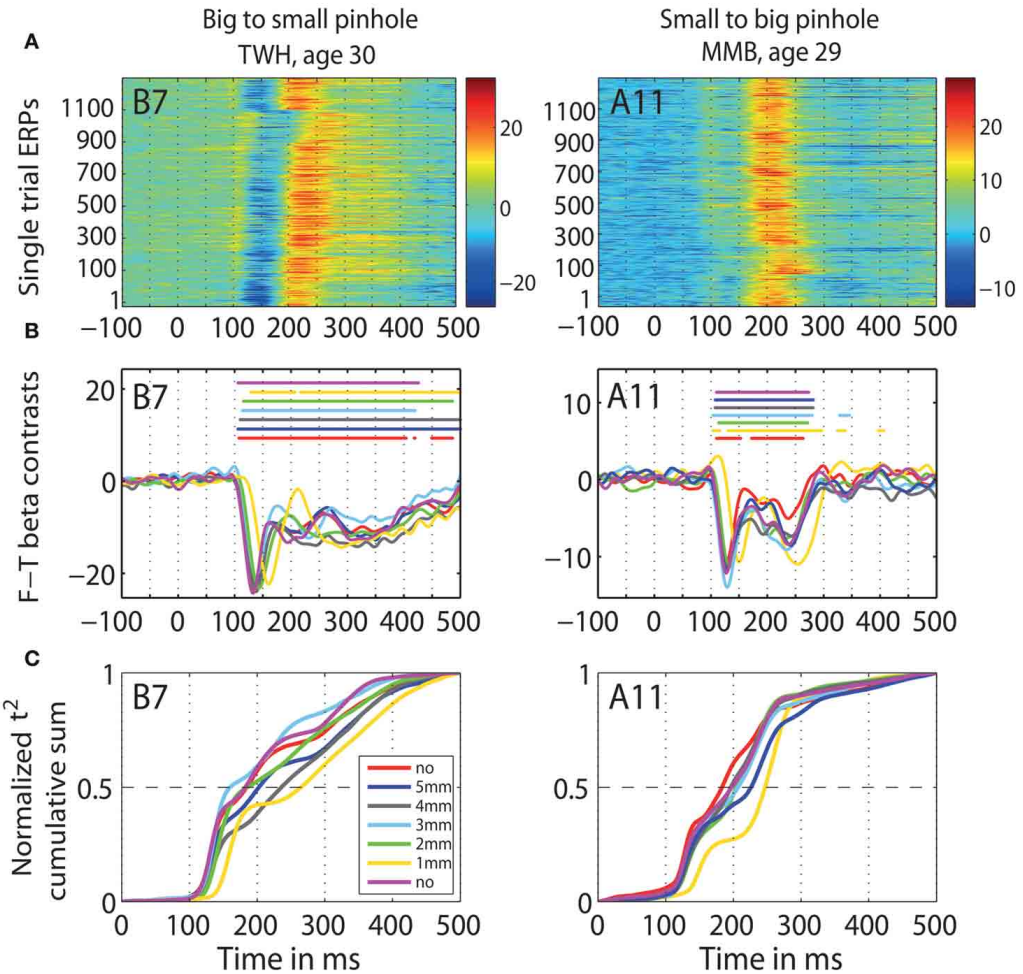

FIGURE 12 | Individual subjects data. Data of two representative subjects: TWH (age 30), and MMB (age 29) in b2s (column 1) and s2b (column 2) sessions at the max t^2 electrode for that subject, indicated in the top left corner of each plot. **(A)** Single-trial ERPs. **(B)** Time-courses of contrasts between face and texture beta-coefficients for each pinhole condition. Horizontal lines indicate significant differences. **(C)** Cumulative sums of t^2 functions for each pinhole condition.

pinhole (**Figure 13**, **Table 3**). We found significant differences in 50ITs between the no pinhole condition and 1, 2, and 3 mm pinhole sizes in both sessions; for 4 mm the difference was significant only in the b2s session, and for 5 mm pinhole in the s2b session. There was no significant difference between the two no pinhole conditions within the same session.

MATCHING OF PROCESSING SPEED BETWEEN YOUNG AND OLD SUBJECTS

Young subjects' 50ITs for 2 and 3 mm pinholes in the b2s session matched those of old subjects from both b2d and d2b luminance sessions (b2d: 2 mm—diff = −14 [−39, 16]; 3 mm—diff = −14 [−41, 11]). However, in the s2b session, 50IT matched between young and old subjects (from both luminance sessions) for 1 and 5 mm pinhole sizes (b2d: 1 mm—diff = 19 [−15, 36]; 5 mm—diff = −16 [−38, 5]; d2b: 1 mm—diff = 14 [−16, 37]; 5 mm—diff = −20 [−43, 1]). 50ITs for all the remaining pinhole sizes differed significantly from those of old subjects (**Figure 13**, **Table S7**).

Furthermore, we observed a qualitative difference in the shape of the t^2 functions of young adults with no pinhole (and luminance level = 60.8 cd/m^2) and old subjects tested at 60.8 cd/m^2 (**Figure 14**). This shape difference was visible for all pinhole conditions. Additionally, in the 1 mm pinhole condition, the onsets of the face-texture ERP differences in young subjects were delayed compared to the onsets of the old adults in the luminance experiment (**Figure 14**). Our calculation of the overlap between t^2 functions of young and old adults revealed that in both pinhole sessions, the overlap was 5–14% higher when young subjects wore pinholes compared to the no pinhole condition (**Figure 15**). For the b2s session the overlap was the highest for 2 and 3 mm pinholes ∼81–82% (**Figures 15A**, **S2**), whereas for the s2b session it was the highest for the 5 mm pinhole ∼73–74% (**Figures 15B**, **S3**). This result converges with our previous finding that 50ITs of young and old adults matched for 2 and 3 mm pinholes in b2s session and for the 5 mm pinhole in s2b session. Finally, the overlaps were 3–8% higher for the 5 mm pinhole

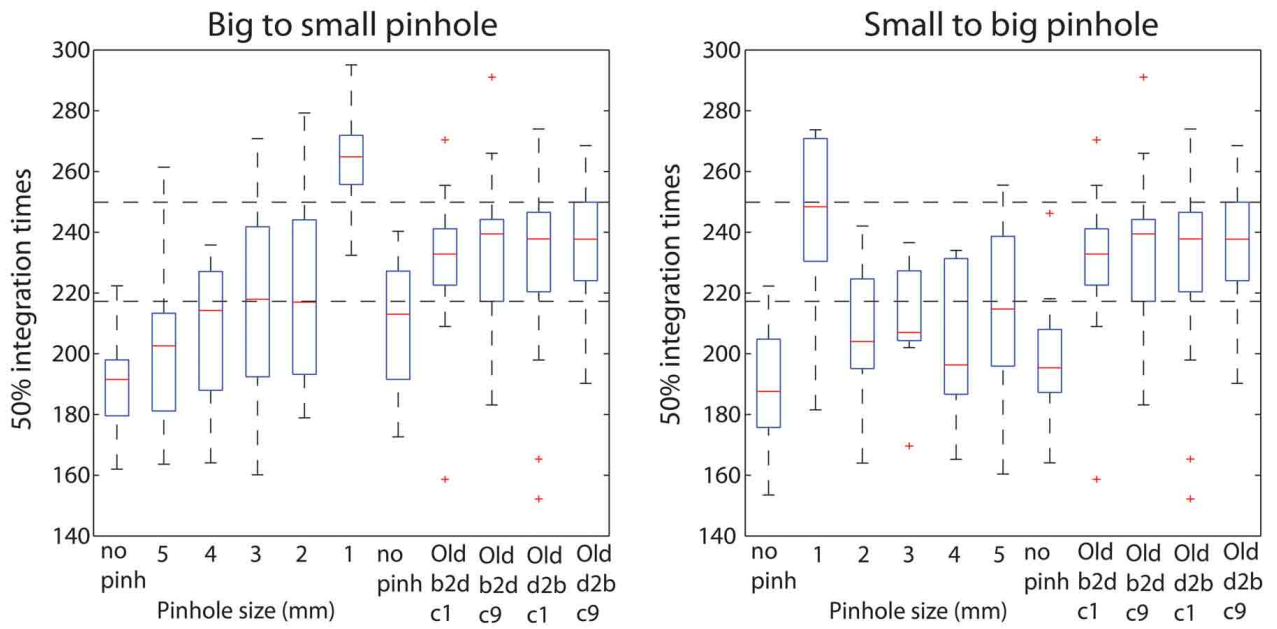

FIGURE 13 | Boxplots of 50% integration times. Boxplots 1–7 show 50ITs across all pinhole subjects, in each pinhole condition. Boxplots 8–11 show old subjects' 50ITs from the two brightest conditions of the luminance experiment (60.8 cd/m^2—c1 and c9), for the b2d and d2b sessions. Horizontal dashed lines indicate the lowest 25th and the highest 75th quantile across the old subjects' four conditions.

Table 3 | 50% integration times (50IT) for all pinhole conditions.

	No pinhole (first)	1 mm pinhole	2 mm pinhole	3 mm pinhole	4 mm Pinhole	5 mm pinhole	No pinhole (last)
b2s session	189 [177, 204]	265 [251, 277]	219 [194, 248]	219 [191, 243]	211 [187, 227]	198 [180, 216]	211 [190, 226]
	Difference	−75 [−88, −62]	−29 [−57, −10]	−29 [−54, −4]	−22 [−38, −3]	−9 [−24, 5]	−22 [−40, 2]
s2b session	189 [174, 205]	251 [216, 267]	205 [193, 228]	210 [200, 225]	204 [186, 226]	217 [195, 237]	196 [180, 212]
	Difference	−62 [−73, −42]	−16 [−28, −5]	−20 [−30, −13]	15 [−35, 1]	−27 [−47, −5]	−7 [−27, 15]

The median 50IT (ms) and its 95% CI (in square brackets) is given for each pinhole condition and each session. Differences between the first "no pinhole" condition and each of the remaining pinhole conditions (1–5 mm and the last condition with "no pinhole") are also provided along with the 95% CIs.

size compared to 1 mm, which goes against our hypothesis that the smaller the pinhole in young subjects the bigger the overlap between young and old ERPs. Thus, although pinholes delay visual processing, they are not sufficient to make young subjects' ERPs look old.

DISCUSSION

Our study addressed several enduring questions about aging effects on visual processing speed, as reflected in ERPs. We measured by how much the visual processing of faces slows down throughout adulthood; the onset of the slowdown; and the contribution of luminance and pupil size to the age-related delay.

AGE-RELATED ERP DELAYS

First, our data confirms previous findings of Rousselet et al. (2010), suggesting that aging slows down visual processing speed by 1 ms/year. We extended this result by showing that this rate of slow-down is constant across luminance levels, from 60.8 to 0.59 cd/m^2. At the highest luminance (60.8 cd/m^2), the processing speed of older (>60) subjects was ∼230 ms, about 50 ms slower than that of younger (<30) subjects (∼180 ms). Aging also prolonged the latencies of maximum face-texture ERP differences, but at a sharper rate: on average by ∼1.5 ms/year; the strongest face-texture ERP differences were observed ∼140 ms post-stimulus in young adults, but only after 220 ms in older adults – about 80 ms later. Aging effects started around ∼125 ms post-stimulus at 60.8 cd/m^2 and, because of a main effect of luminance, were delayed up to 162 ms at 0.59 cd/m^2; maximum aging effects appeared at ∼200 ms at 60.8 cd/m^2 and were delayed to ∼260 ms at 0.59 cd/m^2.

Previous research yielded inconclusive results regarding the dependency of aging effects on luminance: some research showed similar ERP aging delays regardless of the luminance level (Tobimatsu et al., 1993), whereas others suggested that ERP aging effects were stronger at low luminances (e.g., Shaw and Cant, 1980). The findings of Shaw and Cant (1980) do not contradict our observations—the luminance level beyond which their aging effect became weaker (∼72 cd/ m^2) is higher than our

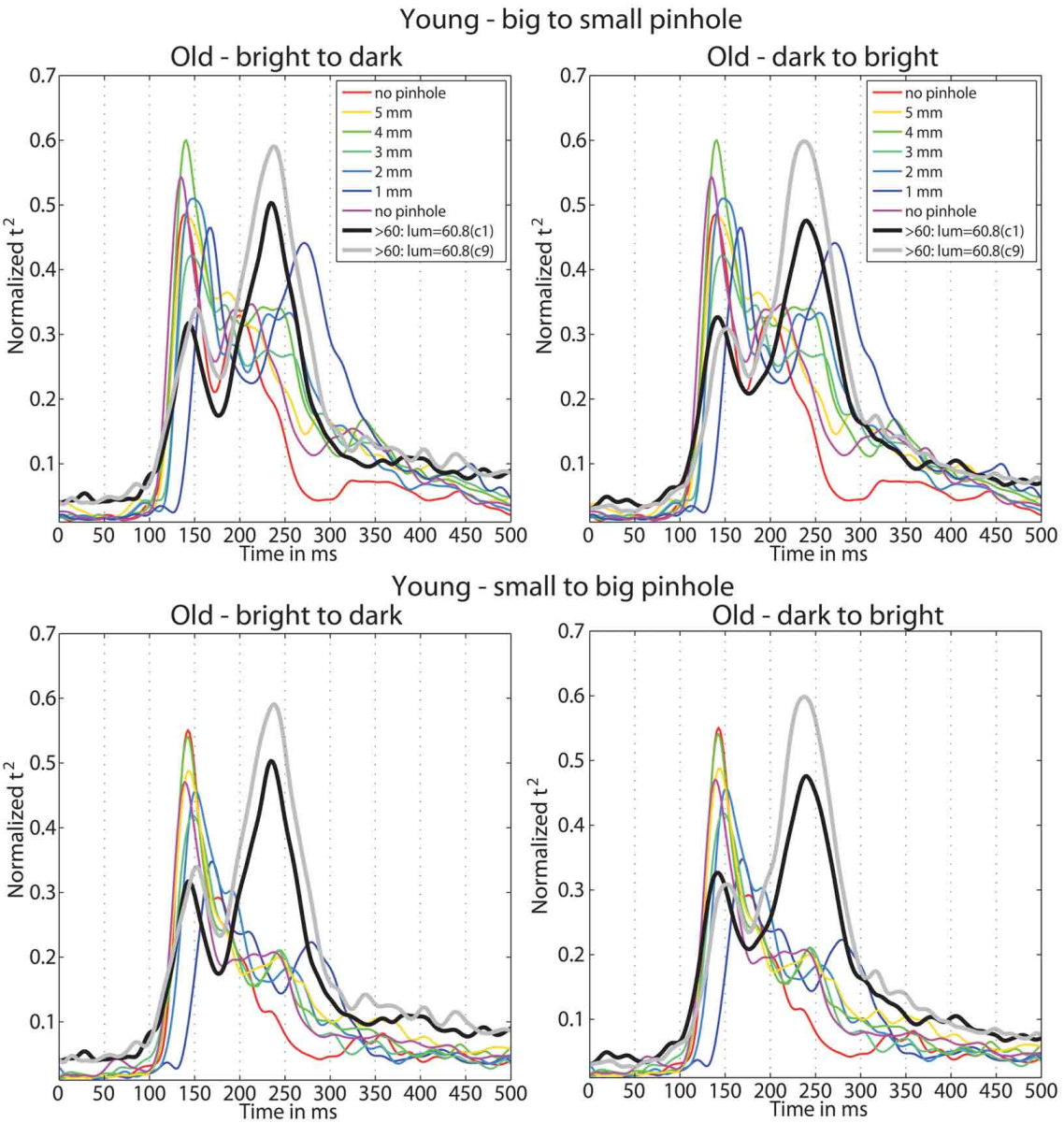

FIGURE 14 | Time-course of normalized t^2 functions for young and old subjects. Each subplot shows the time-courses of mean normalized t^2 functions of young subjects, in all conditions of the pinhole experiment, and of old subjects from the luminance experiment, in the two conditions with the highest luminance 60.8 cd/m^2: condition 1 (c1) plotted in black, and condition 9 (c9) plotted in gray.

maximum luminance (60.8 cd/m^2). Unfortunately, we are unable to relate the dependency between luminance and aging effects found in our study to other face ERP aging studies, because only one of them reported the mean luminance of their stimuli: 64 cd/m^2 (Pfutze et al., 2002). In this study, Pfutze et al. (2002) reported no changes in P1 and N170 peak latencies with age. However, their results cannot be directly compared to our results because they did not consider the entire time-course of the effects, as is done in our approach. Nevertheless, it is possible that at luminances higher than the ones used in our study, ERP aging effects may decrease and future studies should address this question. Including information about luminance and contrast of the stimuli into method sections would also facilitate the comparison of age-related effects across studies.

In the current study, and the previous ones (Rousselet et al., 2009, 2010), our lab found ERP aging effects starting at about ∼125 ms post-stimulus, and lasting for about 200 ms, with the strongest effects in the N170 time window. Aging effects in the N170 time window have been reported in several studies (Nakamura et al., 2001; Gazzaley et al., 2008; Wiese et al., 2008). However, we confirm that aging effects start earlier than the N170 peak, in keeping with the idea that peak analyses should be abandoned in favor of systematic time-point by time-point

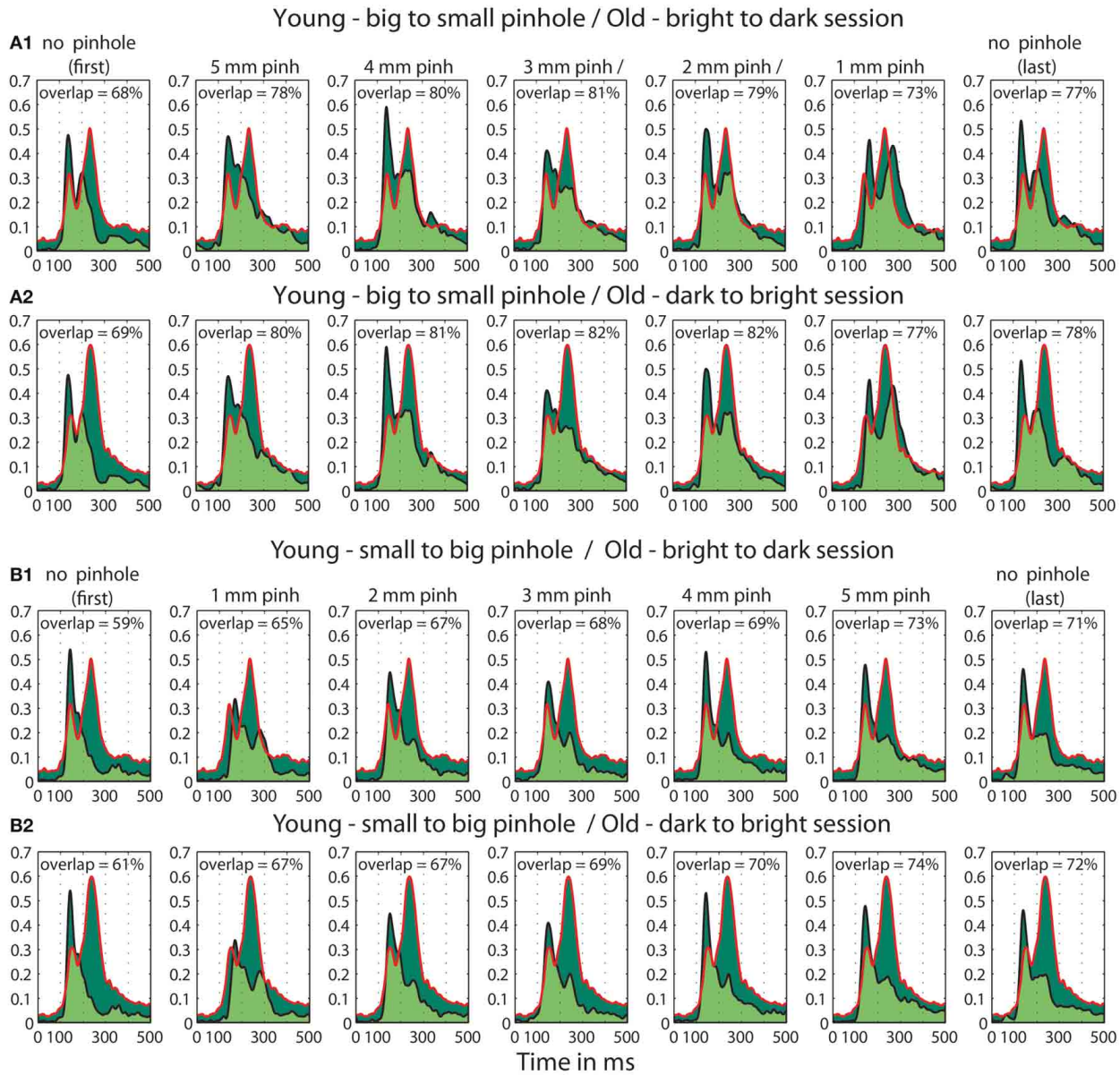

FIGURE 15 | Overlaps between t^2 functions of young subjects tested in the pinhole experiment and old subjects tested in the luminance experiment. (A) Overlap between old (>60) adults in the first brightest (60.8 cd/m^2) condition from the b2d **(A1)** and d2b **(A2)** session of the luminance experiment and young subjects in all the pinhole conditions of the pinhole experiment's b2s session. **(B)** Overlap between old subjects in the brightest (60.8 cd/m^2) condition from the b2d **(B1)** and d2b **(B2)** session of the luminance experiment and young subjects in all the pinhole conditions of the pinhole experiment's s2b session. Each subplot depicts the area under the t^2 functions of young and old subjects, shaded in dark green. The edges of the t^2 functions for young and old subjects are highlighted in black and in red, respectively. The overlap between t^2 functions for young and old subjects is shaded in light green. The proportion of overlap is given inside each subplot.

analyses (Rousselet and Pernet, 2011). Noteworthy, ERP studies using checkerboards have reported age-related latency increases already around 100–110 ms post-stimulus (Shaw and Cant, 1980; Sokol et al., 1981; Tobimatsu, 1995). However, checkerboards and faces differ in spatial frequency content, and it is thus difficult to compare the absolute latencies of the ERPs elicited by these two types of stimuli.

Among studies using faces (Chaby et al., 2001, 2003; Nakamura et al., 2001; Pfutze et al., 2002; Gazzaley et al., 2008; Wiese et al., 2008, 2012; Gao et al., 2009; Daniel and Bentin, 2010) discrepancies in N170 aging effects could be due to variability in stimulus parameters (e.g., whether or not external features were preserved, size, color, contrast, luminance), or ERP analysis approach (focused on peak amplitude and latency or peak-independent analyses), or both. It seems unlikely that particular stimuli could explain the presence of early aging effects because very different stimuli were used also among studies that did find delays in early ERPs, as well as among those that did not.

Nevertheless, future work should determine how our aging effects are linked to potential differences in ERP information content, for instance using reverse correlation techniques (Schyns et al., 2009; Smith et al., 2012). This would allow us to determine if age-related changes in ERP shape are due to changes in diagnostic information, which might reflect, for instance, differences in task related strategies.

At present, it seems more plausible that the differences in ERP aging effects between our study and the existing literature stem from the application of different measures of age-related delays. Most studies focus on component peak latencies in predefined time windows, whereas our analyses take into consideration changes in the overall shape of the ERP, and is independent of ERP peaks and regions of interests. Thus, it is entirely possible that similar aging effects would be obtained by applying our approach to data from other studies. Moreover, the 1 ms/year age-related delay in processing speed, obtained with our analysis approach, has been replicated both within studies (testing our subjects twice), and across studies in independent samples of subjects from two countries (Rousselet et al., 2009, 2010).

LUMINANCE EFFECT ON THE ERPs

We found that, independently of age, luminance strongly modulated ERPs. Previous research has shown that decreasing luminance increases the latencies of neuronal responses in cortical areas including V1 (Geisler et al., 2007), the superior colliculus (Marino et al., 2012) and the LIP - lateral intraparietal area (Tanaka et al., 2013). Early ERPs (∼100 ms) are also delayed by changes in luminance (Wicke et al., 1964; Cant et al., 1978; Tobimatsu et al., 1993; Johannes et al., 1995). Our study extends this finding by showing that luminance affects most of the ERP time-course, within 500 ms post-stimulus, starting about 60 ms post-stimulus, with maximum modulations occurring between 130 and 150 ms. These strongest luminance effects occurred after the P100 time-window, a period of activity commonly thought to be most sensitive to changes in low-level visual factors, such as luminance (Shaw and Cant, 1980), contrast (MacKay and Jeffreys, 1973), size (Yiannikas and Walsh, 1983) or color (Anllo-Vento and Hillyard, 1996). Our results suggest that it is not the P100 but the 130–150 ms period that is most strongly modulated by luminance—the period usually associated with higher-order cognitive processes, such as object and face categorization (Itier and Taylor, 2004), expertise (Tanaka and Curran, 2001), or task-related processes (Rousselet et al., 2011). Stronger sensitivity to changes in luminance around 130–200 ms, rather than around 100 ms, has also been observed in a study using short flashes of vertical bars (Johannes et al., 1995). Thus, visual ERP studies should not underestimate the effects of low-level factors beyond the P1 time window. Reporting the screen luminance is also essential to be able to compare ERP latencies across studies.

CONTRIBUTION OF PUPIL SIZE AND SENILE MIOSIS TO AGE-RELATED ERP DELAYS

Our data show that pupil size decreases with aging at the rate of ∼0.03 mm/year at 60.8 cd/m^2, ∼0.04 mm/year at intermediate luminances, and ∼0.05 mm/year at 0.59 cd/m^2. This is equivalent to about 0.6–1 mm reduction every 20 years. These estimates match quite well those obtained in previous studies—for instance Winn et al. (1994) found a decrease in pupil size of about 0.03 mm/year at 220 cd/m^2 and ∼0.04 mm/year at 44 and 9 cd/m^2. Birren et al. (1950) reported a 2.5 mm difference in pupil size between subjects in their twenties and subjects in their eighties (∼0.04 mm/year) at 3.18 cd/m^2. Between the same age groups, Sokol et al. (1981) observed a slightly smaller reduction in pupil size of 1.5 mm (0.025 mm/year) at 1.9 cd/m^2. Finally, our senile miosis measurements fit well with a recent model that estimates pupil size based on age, luminance, size of adaptive field and whether one or two eyes have been adapted (Watson and Yellott, 2012).

Contrary to our expectations, senile miosis is unlikely to be a factor explaining age-related delays in visual ERPs. Moreover, individual variability in pupil size within age groups cannot account for individual differences in visual processing speed. First, after partialling out the effect of age from our processing speed measurements and from pupil size, we failed to find a relationship between processing speed and pupil size. Second, at 31 and 16 cd/m^2, the luminance conditions providing the best retinal illuminance match between young and old subjects, the overlap between their ERPs was the second smallest (after 60.8 cd/m^2). Additionally, in the conditions where young-old ERP overlap was the highest (0.59, 1.14, 2.17 cd/m^2), the retinal illuminance of young subjects was only about 5–10% of that of old adults. Furthermore, in experiment 2, we failed to match the ERPs of old subjects tested at high luminance to those of young subjects wearing pinholes. In fact, we found a counterintuitive result: the young-old ERP overlap was 3–8% higher in the 5 mm pinhole size condition compared to the 1 mm condition. Overall, our results demonstrate that ERPs to faces are delayed by aging at the early stages of visual processing (< 200 ms) and strongly suggest that these delays are of cortical, rather than optical origin.

CONTRIBUTION OF OTHER OPTICAL FACTORS AND CONTRAST SENSITIVITY TO ERP AGING DELAYS

Ruling out senile miosis as possible contributor to age-related visual processing delays does not necessarily mean that no other optical factors are involved. With age, there is a reduction in lens light transmittance (Boettner and Wolter, 1960), as well as in the eye's ability to accommodate, which decreases from the fifth decade of life onwards and seems to disappear altogether in the sixth decade (Birren and Schaie, 2001). Additionally, after the age of 40, the amount of intraocular light scatter increases, leading to a reduction in retinal image contrast (Fujisawa and Sasaki, 1995). Under these circumstances, senile miosis is actually beneficial because it diminishes optical aberrations (Applegate et al., 2007); it also boosts depth of focus, improving contrast and the overall quality of the retinal image (Weale, 1992). Despite the positive effects of senile miosis, overall, reduction in pupil diameter, increase scatter and a decrease in ocular transmittance lead to ∼60% of light loss at the retina, at lower light levels, between the ages of 20 and 60 years. However, this reduced retinal illuminance in old subjects is unlikely to account for the ERP aging delays found in our study because even when retinal illuminances of young and old subjects matched, their ERPs did not.

Another factor that could potentially contribute to our ERP aging delays is a decline in spatial contrast sensitivity with age.

The effects of diminished contrast sensitivity in the elderly have been primarily studied at the early stages of visual processing, especially around the P100 (Morrison and Reilly, 1989; Tobimatsu et al., 1993; Tobimatsu, 1995). Morrison and Reilly (1989) showed that incrementing stimulus contrast makes ERPs of older observers resemble those of young observers. Tobimatsu et al. (1993) found that a reduction in contrast of checkerboard patterns leads to significant differences in P100 latency between young and middle age groups, contrary to high contrast checks for which no difference was observed. In the older group, P100 latencies were delayed compared to the middle age group for both low and high contrast checks. Our stimuli had RMS contrast of 0.1, which is similar to the low contrast stimuli used by Tobimatsu et al. (1993). It is therefore possible that for higher contrast stimuli, our aging effects would be less pronounced; to our knowledge no face ERP study has yet addressed the link between stimulus contrast and aging delays.

However, it is unlikely that reduction in contrast sensitivity could fully explain our ERP aging delays. Contrast sensitivity loss under photopic light conditions has been observed in particular for intermediate and high spatial frequencies—above 2 cycles/degree of visual angle (Owsley et al., 1983). In our stimuli, 90% of the total power was contained within the low to intermediate spatial frequency range (Bieniek et al., 2012, Figure 1)—below 20 cycles/image, which for our image size of 9° of visual angle is equivalent to ∼2.2 cycles/degree. This suggests that most of the spatial frequency content of our images is below the range that is typically affected by aging. Also, age-related differences in contrast sensitivity are larger under mesopic and scotopic light conditions than in photopic conditions (Sloane et al., 1988; Owsley, 2011). In our study, only the 0.59 cd/m^2 luminance condition falls within the mesopic range. However, the aging effect for that luminance level did not differ from the one observed at the highest luminance level. Thus, a link between our aging effects and contrast sensitivity loss is unlikely.

POSSIBLE ACCOUNTS OF THE ERP AGING EFFECTS

Finally, in this last section, we speculate about the main factors that could account for age-related processing speed slow-down, including: alteration in axons' myelination, reduced synaptic and network efficiency, decrease in neuronal response selectivity, inhibitory deficits, and neuronal network reorganization.

First, slow-down of visual processing speed with age may be due to myelin alteration: aging is associated with degeneration of myelin sheaths of cortical neurons that subsequently get remyelinated, but with shorter internodes, leading to slower conduction along nerve fibers (Peters, 2002, 2009). Changes in myelin sheaths are distributed across gray matter and white matter, suggesting that communication both within and between cortical regions might be disturbed (Peters, 2002). In keeping with these anatomical observations, there is direct evidence for age-related slowing in the visual system: Wang et al. (2005) reported delays in the latency of inter-cortical spiking activity, between V1 and V2, as well as intra-cortical activity, within V1 and V2, and this effect was more pronounced in V2 compared to V1.

In humans, post-mortem analysis reveals stronger changes in white-matter density than in gray-matter density with healthy aging (Piguet et al., 2009). Using *in vivo* techniques, several studies have suggested a relationship between age-related decline in white matter and cognitive function including speed of processing (Bucur et al., 2008; Eckert et al., 2010; Eckert, 2011; Salami et al., 2012). However, some of these studies potentially suffer from a statistical problem arising from the artificial correlation between time-dependent variables (Hofer and Sliwinski, 2001; Lazic, 2010). These studies also use composite behavioral measures of processing speed that do not have the specificity and the temporal resolution potentially afforded by EEG and MEG.

Additionally, animal studies suggest that aging is associated with a decrease in spine numbers and spine density (Duan et al., 2003), as well as with alterations in the strength and efficiency of synaptic connections (Mostany et al., 2013). Although at a different scale, reduced efficiency of cortical networks in older individuals has also been suggested in humans (Achard and Bullmore, 2007). This loss in efficiency may be linked to the degradation of neuronal response selectivity, which in turn could translates into slower processing times. Indeed, animal research shows that aging is associated with an increase in spontaneous activity of neurons, a reduction in signal to noise ratio, and a deterioration of orientation and direction selectivity in V1 and V2 (Schmolesky et al., 2000; Hua et al., 2006; Yu et al., 2006). This increase in noise and decrease in selectivity of neuronal responses may lead to broader tuning of neuronal populations and impair face-specialized processing. This notion is supported by fMRI findings of reduced differentiation of BOLD signal between faces and pink noise textures (Park et al., 2004) accompanied by an increase in BOLD response to all categories in regions normally preferentially active for certain categories only (Park et al., 2004; Payer et al., 2006; Voss et al., 2008). If populations of cells become less tuned to a specific stimulus, the rate of accumulation of evidence supporting its recognition would slow down, leading to longer processing times (Perrett and Ashbridge, 1998).

The deterioration of visually driven neuronal responses has also been linked to an age-related reduction in GABA concentration. The administration of GABA to V1 cells of senescent monkeys' improved selectivity of visual responses, demonstrating a direct link between inhibitory processes and healthy visual function (Leventhal et al., 2003). In humans, inhibitory deficits in elderly subjects have been captured at the level of populations of neurons using EEG. For instance, Gazzaley et al. (2008) found that older adults have more difficulties with suppressing task-irrelevant information, which manifests itself in longer N170 latencies (but unaffected P1 latencies). It is unclear whether our results of most prominent aging effects occurring in the N170 time window can be linked to inhibitory deficits or decreased specialization of face-selective processes: further research should address this question.

Although they cannot yet be linked to particular processes, it seems plausible that our earliest aging effects (∼125) involve activity from higher-order visual areas. Intracranial recordings showed face-sensitive responses in extrastriate areas (Halgren et al., 1994), occipital and temporal structures (Liu et al., 2009), and in the fusiform gyrus (Barbeau et al., 2008) as early as ∼100 ms. Strikingly, one small cortical patch can generate the

whole P1-N170-P2 complex (Allison et al., 1999; Sehatpour et al., 2008; Rosburg et al., 2010). Studies using scalp recordings have also reported responses differentiating between faces and other objects already ∼100 ms post stimulus (Linkenkaer-Hansen et al., 1998; Pizzagalli et al., 1999; Yamamoto and Kashikura, 1999; Halit et al., 2000; Itier and Taylor, 2002; Liu et al., 2002; Herrmann et al., 2005). However, some of these studies used non-causal filters with relatively large high-pass cut-offs between 0.8 and 1.5 Hz, which could have shortened onsets by smearing effects back in time (Acunzo et al., 2012; Rousselet, 2012; Widman and Schroeger, 2012). In our study we used a causal Butterworth high-pass filter, which does not distort onsets, and found face-texture ERP differences starting around 90 ms post-stimulus. This suggests that the visual system detects faces very rapidly, and that aging starts to affect visual processes within 35–40 ms after face detection.

However, if degeneration of myelin and increased noise of neuronal responses are visible already in V1 (Schmolesky et al., 2000; Peters et al., 2001), we would expect to see ERP aging differences earlier than ∼125 ms post-stimulus. This is assuming serial processing from V1 onward, and our capacity to measure evoked responses from all successive stages, which is a rather unrealistic model (Foxe and Simpson, 2002). Additionally, face stimuli are not optimal to capture very early brain activity, and different strategies have been suggested to measure the earliest cortical onsets, as reflected in the C1 component, starting around 60 ms post-stimulus (Kelly et al., 2008). Whether age-related differences in activity from striate and early extra-striate areas might occur in the absence of differences in the onset of face related areas remain to be investigated.

Reduced selectivity of neuronal responses and deficits in inhibition of irrelevant information may lead to slower accumulation of evidence useful for decision making. It has been suggested that subjects' behavioral choices can be predicted from the activity in two EEG time windows associated with the accumulation of evidence useful for decision making: one early (∼N170) and one late (>300 ms) (Philiastides and Sajda, 2006; Philiastides et al., 2006). In our study, aging effects started 35–40 ms after the onsets of face/texture differences. Moreover, subjects' behavioral performance did not change with age and was close to 100%. Thus, it seems plausible that, for all age groups, stimulus processing starts at the same time, but when the aging effects appear, the whole cascade of information accumulation necessary for a behavioral decision is disturbed, leading to longer processing times, without necessarily hampering subjects' performance—at least in an easy task such as ours. The task used in our study was designed to be very easy in order to measure age-related ERP differences in processing speed in the absence of behavioral differences.

Age-related neuronal changes might also lead to the involvement of additional or different neuronal circuits—reorganizations that could potentially explain our aging results. Indeed, age-related reorganization of neuronal networks during face processing has been observed by Grady et al. (2000). They discovered that in young adults better recognition of degraded face images was positively correlated with the activity in the fusiform gyrus, in contrast to old adults for whom behavioral performance correlated with activity in the posterior occipital cortex. Other studies found that when task difficulty increases (for instance because faces are degraded), older observers rely more on prefrontal areas, suggesting that, with age, there is an over recruitment of frontal activity to compensate for poorer performance of the sensory systems (Grady, 2008). In our study, the behavioral task was very simple, most likely not requiring the involvement of compensatory brain circuits. However, the exact task conditions that promote frontal compensation in old adults are still poorly understood. Also, evidence for over-recruitment and compensation have been obtained from cross-sectional designs, and have been challenged by a recent longitudinal study (Nyberg et al., 2010, 2012).

Finally, our aging effects could be related to a decline in perceptual grouping abilities (Kurylo, 2006) and contour integration (Roudaia et al., 2008, 2011). Because face and object recognition rely to a large extent on contours and edges carried by image phase information (Gaspar and Rousselet, 2009; Bieniek et al., 2012), any deficit in a mechanism responsible for contour integration is likely to affect face and object processing. An important research question would thus be to determine the relationship between ERP aging delays and age-related contour integration deficits, which might themselves be due to inhibitory deficits and other neuronal changes.

ACKNOWLEDGMENTS

This research was supported by the Leverhulme Trust grant F/00 179/BD. We would like to thank Jennifer Fairweather, Terri-Louise Fountain, Eilidh Pattison, Lesley Mackay and Christina Xanthi Moustaka for their help with data collection. Lesley Mackay and Christina Xanthi Moustaka were supported by a summer scholarship from the University of Glasgow Settlement charity. Very special thanks to all the subjects for their time and dedication. We also thank Robin Gilmore from Glasgow Caledonian University for preparing the pinholes.

SUPPLEMENTARY MATERIAL

The Supplementary Material for this article can be found online at: http://www.frontiersin.org/Perception_Science/10.3389/fpsyg.2013.00268/abstract

REFERENCES

Achard, S., and Bullmore, E. (2007). Efficiency and cost of economical brain functional networks. *PLoS Comput. Biol.* 3:e17. doi: 10.1371/journal.pcbi.0030017

Acunzo, D. J., MacKenzie, G., and van Rossum, M. C. (2012). Systematic biases in early ERP and ERF components as a result of high-pass filtering. *J. Neurosci. Methods* 209, 212–218.

Allison, T., Puce, A., Spencer, D. D., and McCarthy, G. (1999). Electrophysiological studies of human face perception, I: potentials generated in occipitotemporal cortex by face and non-face stimuli. *Cereb. Cortex* 9, 415–430.

Anllo-Vento, L., and Hillyard, S. A. (1996). Selective attention to the color and direction of moving stimuli: electrophysiological correlates of hierarchical feature selection. *Percept. Psychophys.* 58, 191–206.

Applegate, R. A., Donnelly, I., Marsack, J., Koenig, D. E., and Pesudovs, K. (2007). Three-dimensional relationship between high-order root-mean-square wavefront error, pupil diameter and aging. *J. Opt. Soc. Am. A Opt. Image Sci. Vis.* 24, 578–587.

Barbeau, E. J., Taylor, M. J., Regis, J., Marquis, P., Chauvel, P., and

Liegeois-Chauvel, C. (2008). Spatio temporal dynamics of face recognition. *Cereb. Cortex* 18, 997–1009.

Bieniek, M. M., Pernet, C. R., and Rousselet, G. A. (2012). Early ERPs to faces and objects are driven by phase, not amplitude spectrum information: evidence from parametric, test-retest, single-subject analyses. *J. Vis.* 12, 1–24.

Birren, J. E., Casperson, R. C., and Botwinick, J. (1950). Age changes in pupil size. *J. Gerontol.* 5, 216–221.

Birren, J. E., and Schaie, K. W. (2001). *Handbook of Psychology of Aging.* London: Elsevier.

Boettner, E. A., and Wolter, J. R. (1960). Transmission of the ocular media. *Invest. Ophthalmol.* 1, 776–783.

Brickman, A. M., Schupf, N., Manly, J. J., Luchsinger, J. A., Andrews, H., Tang, M. X., et al. (2008). Brain morphology in older African Americans, Caribbean Hispanics, and whites from northern Manhattan. *Arch. Neurol.* 65, 1053–1061.

Bucur, B., Madden, D. J., Spaniol, J., and Provenzale, J. M. (2008). Age-related slowing of memory retrieval: contributions of perceptual speed and cerebral white matter integrity. *Neurobiol. Aging* 29, 1070–1079.

Cant, B., Hume, A., and Shaw, N. (1978). Effects of luminance on the pattern visual evoked potential in multiple sclerosis. *Electroencephalogr. Clin. Neurophysiol.* 45, 496–504.

Chaby, L., George, N., Renault, B., and Fiori, N. (2003). Age realted changes in brain responses to personally known faces: an event-related potential (ERP) study in humans. *Neurosci. Lett.* 349, 125–129.

Chaby, L., Jemel, B., George, N., Renault, B., and Fiori, N. (2001). An ERP study of famous face incongruity detection in middle age. *Brain Cogn.* 45, 357–377.

Chee, M. W., Chen, K. H., Zheng, H., Chan, K. P., Isaac, V., Sim, S. K., et al. (2009). Cognitive function and brain structure correlations in healthy elderly East Asians. *Neuroimage* 46, 257–269.

Daniel, S., and Bentin, S. (2010). Age-related changes in processing faces from detection to identification: ERP evidence. *Neurobiol. Aging* 33, 206.e1–206.e28.

Davis, S., Dennis, N., Buchler, N., White, L., Madden, D., and Cabeza, R. (2009). Assessing the effects of age on long white matter tracts using diffusion tensor tractography. *Neuroimage* 46, 530–541.

Delorme, A., and Makeig, S. (2004). EEGLAB: an open source toolbox for analysis of single-trial EEG dynamics including independent component analysis. *J. Neurosci. Methods* 134, 9–21.

De Sanctis, P., Katz, R., Wylie, G. R., Sehatpour, P., Alexopoulos, G. S., and Foxe, J. J. (2008). Enhanced and bilateralized visual sensory processing in the ventral stream may be a feature of normal aging. *Neurobiol. Aging* 29, 1576–1586.

Diaz, F., and Amenedo, E. (1998). Ageing effects on flash visual evoked potentials (FVEP) recorded from parietal and occipital electrodes. *Neurophysiol. Clin.* 28, 399–412.

Duan, H., Wearne, S. L., Rocher, A. B., Macedo, A., Morrison, J. H., and Hof, P. R. (2003). Age-related dendritic and spine changes in corticocortically projecting neurons in macaque monkeys. *Cereb. Cortex* 13, 950–961.

Eagan, S. M., Jacobs, R. J., and Demers-Turco, P. L. (1999). Study of luminance effects on pinhole test results in visually impaired patients. *Optom. Vis. Sci.* 76, 50–58.

Eckert, M. A. (2011). Slowing down: age-related neurobiological predictors of processing speed. *Front. Neurosci.* 5:25. doi: 10.3389/fnins.2011.00025

Eckert, M. A., Keren, N. I., Roberts, D. R., Calhoun, V. D., and Harris, K. C. (2010). Age-related changes in processing speed: unique contributions of cerebellar and prefrontal cortex. *Front. Hum. Neurosci.* 4:10. doi: 10.3389/neuro.09.010.2010

Elze, T. (2010). Misspecifications of stimulus presentation durations in experimental psychology: a systematic review of the psychophysics literature. *PLoS ONE* 5:e12792. doi: 10.1371/journal.pone.0012792

Falkenstein, M., Yordanova, J., and Kolev, V. (2006). Effects of aging on slowing of motor-response generation. *Int. J. Psychophysiol.* 59, 22–29.

Foxe, J. J., and Simpson, G. V. (2002). Flow of activation from V1 to frontal cortex in humans. A framework for defining "early" visual processing. *Exp. Brain Res.* 142, 139–150.

Froelich, J., and Kaufman, D. I. (1991). Effect of decreased retinal illumination on simultaneously recorded pattern electroretinograms and visual-evoked potentials. *Invest. Ophthalmol. Vis. Sci.* 32, 310–318.

Fujisawa, K., and Sasaki, K. (1995). Changes in light scattering intensity of the transparent lenses of subjects selected from population-based surveys depending on age: analysis through Scheimpflug images. *Ophthalmic Res.* 27, 89–101.

Gao, L., Xu, J., Zhang, B., Zhao, L., Harel, A., and Bentin, S. (2009). Aging effects on early-stage face perception: an ERP study. *Psychophysiology* 46, 1–14.

Gaspar, C. M., and Rousselet, G. A. (2009). How do amplitude spectra influence rapid animal detection? *Vision Res.* 49, 3001–3012.

Gazzaley, A., Clapp, W., Kelley, J., McEvoy, K., Knight, R., and D'Esposito, M. (2008). Age-related top-down suppression deficit in the early stages of cortical visual memory processing. *Proc. Natl. Acad. Sci. U.S.A.* 105, 13122–13126.

Geisler, W. S., Albrecht, D. G., and Crane, A. M. (2007). Responses of neurons in primary visual cortex to transient changes in local contrast and luminance. *J. Neurosci.* 27, 5063–5067.

Grady, C. L. (2008). Cognitive neuroscience of aging. *Ann. N.Y. Acad. Sci.* 1124, 127–144. doi: 10.1196/annals.1440.009

Grady, C. L., McIntosh, A. R., Horwitz, B., and Rapoport, S. I. (2000). Age-related changes in the neural correlates of degraded and nondegraded face processing. *Cogn. Neuropsychol.* 17, 165–186.

Halgren, E., Baudena, P., Heit, G., Clarke, M., Marinkovic, K., and Chauvel, P. (1994). Spatio-temporal stages in face and word processing. 2. Depth-recorded potentials in the human frontal and Rolandic cortices. *J. Physiol. Paris* 88, 51–80.

Halit, H., de Haan, M., and Johnson, M. J. (2000). Modulation of event-related potentials by prototypical and atypical faces. *Neuroreport* 11, 1871–1875.

Hawkes, C. H., and Stow, B. (1981). Pupil size and the pattern evoked visual response. *J. Neurol. Neurosurg. Psychiatry* 44, 90–91.

Herrmann, M. J., Ehlis, A.-C., Ellgring, H., and Fallgatter, A. J. (2005). Early stages (P100) of face perception in hmans as measured with event-related potentials (ERPs). *J. Neural Transm.* 112, 1073–1081.

Hofer, S., and Sliwinski, M. (2001). Understanding ageing. An evaluation of research designs for assessing the interdependence of ageing-related changes. *Gerontology* 47, 341–352.

Hua, T., Li, X., He, L., Zhou, Y., Wang, Y., and Leventhal, A. (2006). Functional degradation of visual cortical cells in old cats. *Neurobiol. Aging* 27, 155–162.

Itier, R. J., and Taylor, M. J. (2002). Inversion and contrast polarity reversal affect both encoding and recognition processes of unfamiliar faces: a repetition study using ERPs. *Neuroimage* 15, 353–372.

Itier, R. J., and Taylor, M. J. (2004). N170 or N1? Spatiotemporal differences between object and face processing using ERPs. *Cereb. Cortex* 14, 132–142.

Johannes, S., Munte, T. F., Heinze, H. J., and Mangun, G. R. (1995). Luminance and spatial attention effects on early visual processing. *Cogn. Brain Res.* 2, 189–205.

Kelly, S. P., Gomez-Ramirez, M., and Foxe, J. J. (2008). Spatial attention modulates initial afferent activity in human primary visual cortex. *Cereb. Cortex* 18, 2629–2636.

Kolev, V., Falkenstein, M., and Yordanova, J. (2006). Motor-response generation as a source of aging-related behavioural slowing in choice-reaction tasks. *Neurobiol. Aging* 27, 1719–1730.

Kurylo, D. D. (2006). Effects of aging on perceptual organization: efficacy of stimulus features. *Exp. Aging Res.* 32, 137–152.

Lazic, S. E. (2010). Relating hippocampal neurogenesis to behavior: the dangers of ignoring confounding variables. *Neurobiol. Aging* 31, 2169–2171.

Leventhal, A. G., Wang, Y., Pu, M., Zhou, Y., and Ma, Y. (2003). GABA and its agonists improved visual cortical function in senescent monkeys. *Science* 300, 812–815.

Linkenkaer-Hansen, K., Palva, J. M., Sams, M., Hietanen, J. K., Aronen, H. J., and Ilmoniemi, R. J. (1998). Face-selective processing in human extrastriate cortex around 120 ms after stimulus onset revealed by magneto- and electroencephalography. *Neurosci. Lett.* 253, 147–150.

Liu, H., Agam, Y., Madsen, J. R., and Kreiman, G. (2009). Timing, timing, timing: fast decoding of object information from intracranial field potentials in human visual cortex. *Neuron* 62, 281–290.

Liu, J., Harris, A., and Kanwisher, N. (2002). Stages of processing in face perception: an MEG study. *Nat. Neurosci.* 5, 910–916.

MacKay, D. M., and Jeffreys, D. A. (1973). "Visually evoked potentials and visual perception in man," in *Handbook of Sensory Physiology,* ed R. Jung (Berlin: Springer-Verlag), 674–678.

Marino, R. A., Levy, R., Boehnke, S., White, B. J., Itti, L., and Munoz, D. P. (2012). Linking visual response properties in the superior colliculus to saccade behavior. *Eur. J. Neurosci.* 35, 1738–1752.

Morrison, J. D., and Reilly, J. (1989). The pattern visual evoked cortical

responses in human ageing. *Q. J. Exp. Physiol.* 74, 311–328.

Mostany, R., Anstey, J. E., Crump, C. L., Maco, B., Knott, G., and Portera-Cailliau, C. (2013). Altered synaptic dynamics during normal brain aging. *J. Neurosci.* 33, 4094–4104.

Nakamura, A., Yamada, T., Abe, Y., Nakamura, K., Sato, N., Horibe, K., et al. (2001). Age-related changes in brain neuromagnetic responses to face perception in humans. *Neurosci. Lett.* 312, 13–16.

Nyberg, L., Lovden, M., rilund, K., Lindenberger, U., and Backman, L. (2012). Memory aging and brain maintance. *Trends Cogn. Sci.* 16, 292–305.

Nyberg, L., Salami, A., Andersson, M., Eriksson, J., Kalpouzos, G., Kauppi, K., et al. (2010). Longitudinal evidence for diminished frontal cortex function in aging. *Proc. Natl. Acad. Sci. U.S.A.* 107, 22682–22686.

Owsley, C. (2011). Aging and vision. *Vision Res.* 51, 1610–1622.

Owsley, C., Sekuler, R., and Siemsen, D. (1983). Contrast sensitivity throughout adulthood. *Vision Res.* 23, 689–699.

Park, D. C., Polk, T. A., Park, R., Minear, M., Savage, A., and Smith, M. R. (2004). Aging reduces neural specialization in ventral visual cortex. *Proc. Natl. Acad. Sci. U.S.A.* 101, 13091–13095.

Payer, D., Marshuetz, C., Sutton, B., Hebrank, A., Welsh, R., and Park, D. (2006). Decreased neural specialization in old adults on a working memory task. *Neuroreport* 17, 487–491.

Pernet, C. R., Chauveau, N., Gaspar, C. M., and Rousselet, G. A. (2011). LIMO EEG: a toolbox for hierarchical linearmodeling of electroencephalographic data. *Comput. Intell. Neurosci.* 2011:831409. doi: 10.1155/2011/831409

Perrett, D. M., and Ashbridge, E. (1998). Evidence accumulation in cell populations responsive to faces: an account of generalisation of recognition without mental transformations. *Cognition* 67, 111–145.

Peters, A. (2002). The effects of normal aging on myelin and nerve fibers: a review. *J. Neurocytol.* 31, 581–593.

Peters, A. (2009). The effects of normal aging on myelinated nerve fibers in monkey central nervous system. *Front. Neuroanat.* 3:11. doi: 10.3389/neuro.05.011.2009

Peters, A., Sethares, C., and Killiany, R. J. (2001). Effects of age on the thickness of myelin sheaths in monkey primary visual cortex. *J. Comp. Neurol.* 435, 241–248.

Pfutze, E., Sommer, W., and Schweinberger, S. (2002). Age related slowing in face and name recognition: evidence from event-related brain potentials. *Psychol. Aging* 17, 140–160.

Philiastides, M. G., Ratcliff, R., and Sajda, P. (2006). Neural representation of task difficulty and decision making during perceptual categorization: a timing diagram. *J. Neurosci.* 26, 8965–8975.

Philiastides, M. G., and Sajda, P. (2006). Temporal characterization of the neural correlates of perceptual decision making in the human brain. *Cereb. Cortex* 16, 509–518.

Piguet, O., Double, K. L., Kril, J. J., Harasty, J., MacDonald, V., McRitchie, D. A., et al. (2009). White matter loss in healthy ageing: a postmortem analysis. *Neurobiol. Aging* 30, 1288–1295.

Pizzagalli, D., Regard, M., and Lehmann, D. (1999). Rapid emotional face processing in the human right and left brain hemispheres: an ERP study. *Neuroreport* 10, 2691–2698.

Raz, D., Seeliger, M. W., Geva, A. B., Percicot, C. L., Lambrou, G. N., and Ofri, R. (2002). The effect of contrast and luminance on mfERG responses in a monkey model of glaucoma. *Invest. Ophthalmol. Vis. Sci.* 43, 2027–2035.

Raz, N., Ghisletta, P., Rodrigue, K. M., Kennedy, K. M., and Lindenberger, U. (2010). Trajectories of brain aging in middle-aged and older adults: regional and individual differences. *Neuroimage* 51, 501–511.

Raz, N., Lindenberger, U., Rodrigue, K. M., Kennedy, K. M., Head, D., Williamson, A., et al. (2005). Regional brain changes in aging healthy adults: general trends, individual differences and modifiers. *Cereb. Cortex* 15, 1676–1689.

Resnick, S. M., Pham, D. L., Kraut, M. A., Zonderman, A. B., and Davatzikos, C. (2003). Longitudinal magnetic resonance imaging studies of older adults: a shrinking brain. *J. Neurosci.* 23, 3295–3301.

Rosburg, T., Ludowig, E., Dumpelmann, M., Alba-Ferrara, L., Urbach, H., and Elger, C. E. (2010). The effect of face inversion on intracranial and scalp recordings of event-related potentials. *Psychophysiology* 47, 147–157.

Roudaia, E., Bennett, P. J., and Sekuler, A. B. (2008). The effect of aging on contour integration. *Vision Res.* 48, 2767–2774.

Roudaia, E., Farber, L. E., Bennett, P. J., and Sekuler, A. B. (2011). The effects of aging on contour discrimination in clutter. *Vision Res.* 51, 1022–1032.

Rousselet, G. A. (2012). Does filtering preclude us from studying ERP time-courses? *Front. Psychol.* 3:131. doi: 10.3389/fpsyg.2012.00131

Rousselet, G. A., Gaspar, C. M., Wieczorek, K. P., and Pernet, C. R. (2011). Modeling single-trial ERP reveals modulation of bottom-up face visual processing by top-down task contraints (in some subjects). *Front. Psychol.* 2:137. doi: 10.3389/fpsyg.2011.00137

Rousselet, G. A., Gaspar, C. M., Pernet, C. R., Husk, J. S., Bennett, P., and Sekuler, A. (2010). Healthy aging delays scalp EEG sensitivity to noise in a face discrimination task. *Front. Psychol.* 1:19. doi: 10.3389/fpsyg.2010.00019

Rousselet, G. A., Husk, J. S., Pernet, C. R., Gaspar, C. M., Bennett, P. J., and Sekuler, A. B. (2009). Age-related delay in information accrual for faces: evidence from a parametric, single-trial EEG approach. *BMC Neurosci.* 10:114. doi: 10.1186/1471-2202-10-114

Rousselet, G. A., and Pernet, C. R. (2011). Quantifying the time course of visual object processing using ERPs: it's time to up the game. *Front. Psychol.* 2:107. doi: 10.3389/fpsyg.2011.00107

Rousselet, G. A., Pernet, C. R., Bennett, P. J., and Sekuler, A. B. (2008). Parametric study of EEG sensitivity to phase noise during face processing. *BMC Neurosci.* 9:98. doi: 10.1186/1471-2202-9-98

Salami, A., Eriksson, J., Nilsson, L.-G., and Nyberg, L. (2012). Age-related white matter microstructural differences partly mediate age-related decline in processing speed but not cognition. *Biochim. Biophys. Acta* 1822, 408–415.

Salat, D., Grevea, D., Pacheco, J., Quinna, B., Helmera, K., Bucknera, R., et al. (2009). Regional white matter volume differences in nondemented aging and Alzheimer's disease. *Neuroimage* 44, 1247–1258.

Salthouse, T. A., and Ferrer-Caja, E. (2003). What needs to be explained to account for age-related effects on multiple cognitive variables? *Psychol. Aging* 18, 91–110.

Schmolesky, M., Wang, Y., Pu, M., and Leventhal, A. (2000). Degradation of stimulus selectivity of visual cortical cells in senescent rhesus monkeys. *Nat. Neurosci.* 3, 384–390.

Schyns, P., Gosselin, F., and Smith, M. L. (2009). Information processing algorithms in the brain. *Trends Cogn. Sci.* 13, 21–26.

Sehatpour, P., Molholm, S., Schwartz, T. H., Mahoney, J. R., Mehta, A. D., Javitt, D. C., et al. (2008). A human intracranial study of long-range oscillatory coherence across a frontal– occipital–hippocampal brain network during visual object processing. *Proc. Natl. Acad. Sci. U.S.A.* 105, 4399–4404.

Shaw, N. A., and Cant, B. R. (1980). Age-dependent changes in the latency of the pattern visual evoked potential. *Electroencephalogr. Clin. Neurophysiol.* 48, 237–241.

Sloane, M. E., Owsley, C., and Alvarez, S. L. (1988). Aging, senile miosis and spatial contrast sensitivity at low luminance. *Vision Res.* 28, 1235–1246.

Smith, M. L., Gosselin, F., and Schyns, P. G. (2012). Measuring internal representations from behavioral and brain data. *Curr. Biol.* 22, 191–196.

Sokol, S., Moskowitz, A., and Towle, V. L. (1981). Age-related changes in the latency of the visual evoked potential: influence of check size. *Electroencephalogr. Clin. Neurophysiol.* 51, 559–562.

Tanaka, J. W., and Curran, T. (2001). A neural basis for expert object recogntion. *Psychol. Sci.* 12, 43–47.

Tanaka, T., Nishida, S., Aso, T., and Ogawa, T. (2013). Visual response of neurons in the lateral intraparietal area and saccadic reaction time during a visual detection task. *Eur. J. Neurosci.* 37, 942–956.

Tobimatsu, S. (1995). Aging and pattern visual evoked potentials. *Optom. Vis. Sci.* 72, 192–197.

Tobimatsu, S., Kurita-Tashima, S., Nakayama-Hiromatsu, M., Akazawa, K., and Kato, M. (1993). Age-related changes in pattern visual evoked potentials: differential effects of luminance, contrast and check size. *Electroencephalogr. Clin. Neurophysiol.* 88, 12–19.

Trick, G. L., Trickl, L., and Haywood, K. M. (1986). Altered pattern evoked retinal and cortical potentials associated with human. *Curr. Eye Res.* 5, 717–724.

Vanmaele, C., Van Malderen, L., and Spileers, W. (2003). The use of a pinhole aperture during teh recordings of pattern reversal visual evoked potentials. *Bull. Soc. Belge Ophtalmol.* 290, 21–27.

Vanrullen, R. (2011). Four common conceptual fallacies in mapping the time course of recognition. *Front. Psychol.* 2:365. doi: 10.3389/fpsyg.2011.00365

Voss, M. W., Erickson, K. I., Chaddock, L., Prakash, R. S., Colcombe, S. J., Morris, K. S., et al. (2008). Dedifferentiation in the visual cortex: an fMRI investigation of individual differences in older adults. *Brain Res.* 1244, 121–131.

Wang, H., Xie, X., Li, X., Chen, B., and Zhou, Y. (2006). Functional degradation of visual cortical cells in aged rats. *Brain Res.* 1122, 93–98.

Wang, Y., Zhou, Y., Ma, Y., and Leventhal, A. G. (2005). Degradation of signal timing in cortical areas V1 and V2 of senescent monkeys. *Cereb. Cortex* 15, 403–408.

Watson, A. B., and Yellott, J. I. (2012). A unified formula for light-adapted pupil size. *J. Vis.* 12, 1–16.

Weale, R. A. (1992). *The Senescence of Human vision.* Oxford: Oxford University Press.

Wicke, J. D., Donchin, E., and Lindlsey, D. B. (1964). Visual evoked potentials as a function of flash luminance and duration. *Science* 146, 83–85.

Widman, A., and Schroeger, E. (2012). Filter effects and filter artifacts in the analysis of electrophysiological data. *Front. Psychol*. 3:233. doi: 10.3389/fpsyg.2012.00233

Wiese, H., Komes, J., and Schweinberger, S. R. (2012). Daily-life contact affects the own-age bias and neural correlates of face memory in elderly participants. *Neuropsychologia* 50, 3496–3508.

Wiese, H., Schweinberger, S., and Hansen, K. (2008). The age of the beholder: ERP evidence of an own-age bias in face memory. *Neuropsychologia* 46, 2973–2985.

Wilcox, R. R. (2005). *Introduction to Robust Estimation and Hypothesis Testing.* San Diego, CA: Elsevier Academic Press.

Winn, B., Whitaker, D., Elliott, D. B., and Phillips, N. J. (1994). Factors affecting light-adapted pupil size in normal human subjects. *Invest. Ophthalmol. Vis. Sci.* 35, 1132–1137.

Yamamoto, S., and Kashikura, K. (1999). Speed of face recognition in humans: an event-related potentials study. *Neuroreport* 10, 3531–3534.

Yiannikas, C., and Walsh, J. C. (1983). The variation of the pattern shift visual evoked response with the size of the stimulus field. *Electroencephalogr. Clin. Neurophysiol.* 55, 427–435.

Yu, S., Wang, Y., Li, X., Zhou, Y., and Leventhal, A. G. (2006). Functinal degradation of extrastriate visual cortex in senescent rhesus monkeys. *Neuroscience* 140, 1023–1029.

Conflict of Interest Statement: The authors declare that the research was conducted in the absence of any commercial or financial relationships that could be construed as a potential conflict of interest.

Received: 07 January 2013; accepted: 25 April 2013; published online: 14 May 2013.

*Citation: Bieniek MM, Frei LS and Rousselet GA (2013) Early ERPs to faces: aging, luminance, and individual differences. Front. Psychol. **4**:268. doi: 10.3389/fpsyg.2013.00268*

This article was submitted to Frontiers in Perception Science, a specialty of Frontiers in Psychology.

frontiers in PSYCHOLOGY

ORIGINAL RESEARCH ARTICLE
published: 20 June 2013
doi: 10.3389/fpsyg.2013.00356

Contour integration and aging: the effects of element spacing, orientation alignment and stimulus duration

Eugenie Roudaia[1,2]*, Patrick J. Bennett[1] and Allison B. Sekuler[1]

[1] Vision and Cognitive Neuroscience Lab, Department of Psychology, Neuroscience and Behaviour, McMaster University, Hamilton, ON, Canada
[2] Institute of Neuroscience, Multisensory Cognition Research Group, Trinity College Dublin, Dublin, Ireland

Edited by:
Mark W. Greenlee, University of Regensburg, Germany

Reviewed by:
Jocelyn Faubert, Université de Montréal, Canada
Gregor Volberg, Universität Regensburg, Germany

***Correspondence:**
Eugenie Roudaia, Vision and Cognitive Neuroscience Lab, Department of Psychology, Neuroscience and Behaviour, McMaster University, PC 428, 1280 Main Street West, Hamilton, ON L8S 4K1, Canada
e-mail: eugenie.roudaia@gmail.com

The ability to extract contours in cluttered visual scenes, which is a crucial step in visual processing, declines with healthy aging, but the reasons for this decline are not well understood. In three experiments, we examined how the effect of aging on contour discrimination varies as a function of contour and distracter inter-element spacing, collinearity, and stimulus duration. Spiral-shaped contours composed of Gabors were embedded within a field of distracter Gabors of uniform density. In a four alternative forced-choice task, younger and older subjects were required to report the global orientation of the contour. In Experiment 1, the absolute contour element spacing varied from two to eight times the Gabor wavelength and contour element collinearity was disrupted with five levels of orientation jitter. Contour discrimination accuracy was lower in older subjects, but the effect of aging did not vary with contour spacing or orientation jitter. Experiment 2 found that decreasing stimulus durations from 0.8 to 0.04 s had a greater effect on older subjects' performance, but only for less salient contours. Experiment 3 examined the effect of the background on contour discrimination by varying the spacing and orientation of the distracter elements for contours with small and large absolute spacing. As in Experiment, the effect of aging did not vary with absolute contour spacing. Decreasing the distracter spacing, however, had a greater detrimental effect on accuracy in older subjects compared to younger subjects. Finally, both groups showed equally high accuracy when all distracters were iso-oriented. In sum, these findings suggest that aging does not affect the sensitivity of contour integration to proximity or collinearity. However, contour integration in older adults is slower and is especially vulnerable when distracters are denser than contour elements.

Keywords: aging, contour integration, orientation, collinearity, perceptual grouping, distracters, suppression

INTRODUCTION

Extracting contours is an important step in the process of translating incoming visual information into a meaningful percept. Because visual scenes often contain multiple objects that overlap and partially occlude each other, grouping different features into contours is not a trivial task, as features belonging to a single contour need to be grouped with one another and not grouped with other objects, or with elements of the background. Contours in natural scenes contain important statistical regularities (Geisler et al., 2001; Sigman et al., 2001; Elder and Goldberg, 2002) and human observers appear to use the statistical properties of contours in natural images to detect contours (Field et al., 1993; Hess et al., 2003; Geisler and Perry, 2009).

The rules governing contour grouping have been studied successfully using variations on the path paradigm (Field et al., 1993), in which subjects detect a contour whose path is defined by a group of discrete, oriented elements (e.g., Gabors) that are embedded within a field of similar distracters. Several studies have shown that contour saliency strongly depends on the alignment of local element orientations along the contour path and, to a lesser extent, on the separation of contour elements (Field et al., 1993; Kovács and Julesz, 1993; Saarinen and Levi, 2001). Other factors known to influence contour detection are contour curvature, length, eccentricity, spatial scale and phase alignment of contour elements (Hess and Dakin, 1997; Dakin and Hess, 1998; Beaudot and Mullen, 2001, 2003; Hess et al., 2003; Ledgeway et al., 2005; Kuai and Yu, 2006), as well as characteristics of the surrounding context, closure, and contour object identity (Kovács and Julesz, 1993; Braun, 1999; Mathes and Fahle, 2007; Dakin and Baruch, 2009; Nygård et al., 2011).

Neuroimaging studies in humans and primates have revealed contour-specific activity both in the primary visual cortex and extrastriate visual areas (Altmann et al., 2003; Kourtzi et al., 2003; Kourtzi and Huberle, 2005; Tanskanen et al., 2008). Neurophysiological studies using single-cell recordings have demonstrated response facilitation of V1 neurons to oriented lines presented in the context of a contour (Kapadia et al., 1995; Li et al., 2006). More recently, Gilad et al. (2013) used voltage-sensitive dye imaging to examine the population responses of primary visual neurons of monkeys engaged in a contour detection task. Their findings revealed that, whereas the initial rise in activity in response to the stimulus is not affected by the presence of a contour, the later part of the neural response follows the perceptually-grouped percept: activation to the contour region

increased, while activation throughout the background region was suppressed. Moreover, this difference in activity across the stimulated region was correlated with behavioral performance in a contour detection task, providing strong evidence that activity in primary visual cortex underlies perceptual grouping of contours. Finally, the contour-related modulation of V1 responses has been shown to be affected by learning, spatial attention, and task demands (Gilbert et al., 2000; Li et al., 2008; Gilad et al., 2013), indicating that top-down feedback from higher-order areas plays an important role in perceptual grouping (Angelucci and Bullier, 2003; Ciaramelli et al., 2007; Verghese, 2009; Volberg et al., 2013).

Healthy aging is accompanied by changes in many aspects of visual function, but the changes are not uniform: some functions remain completely unimpaired, while others decline rapidly (for reviews see Spear, 1993; Sekuler and Sekuler, 2000; Faubert, 2002). The intriguing variation in the effects of aging in vision may be due to differences in the level of processing complexity required in different stimuli and tasks (Habak and Faubert, 2000; Faubert, 2002), and the availability of compensatory mechanisms to mask the sensory and perceptual deficits (McIntosh et al., 1999; Della-Maggiore et al., 2000; Bennett et al., 2001). Thus, age-related changes in visual function may be more pronounced in situations where multiple stages of processing contribute to successful performance, as is the case in contour integration.

Growing evidence suggests that contour integration declines with healthy aging (Del Viva and Agostini, 2007; Roudaia et al., 2008; McKendrick et al., 2010; Roudaia et al., 2011; Casco et al., 2011). Del Viva and Agostini (2007) first showed that older subjects were able to tolerate fewer distracters than younger subjects when detecting closed circular contours embedded among distracters. Roudaia et al. (2011) found that older subjects required longer stimulus durations than younger subjects to successfully discriminate the location of the gap in a "C"-shaped contour embedded among distracters. McKendrick et al. (2010) used closed circular contours to examine the effect of aging on shape discrimination; Contrary to what was found in previous studies, McKendrick et al. found that the ability to discriminate closed contour shapes was only slightly (and not significantly) worse in older subjects. Moreover, the addition of background elements or the addition of orientation jitter to contour elements did not have a differential effect on the two age groups. However, McKendrick et al. did find that older subjects required more contour elements (or smaller contour spacing) than younger subjects to make the contour shape discrimination, suggesting that older subjects had greater difficulty extracting the shape of contours containing large inter-element spacings. Casco et al. (2011) measured thresholds in a task that required subjects to detect the radial displacement of a single Gabor belonging to a circular contour. Consistent with McKendrick et al. (2010), thresholds for older and younger subjects were not different when the contour was composed of aligned Gabors and presented without distracters. However, older subjects required a larger displacement than younger subjects when the contour was composed of Gabors alternating between aligned and orthogonal orientations, or when the contour was embedded among randomly-oriented distracter Gabors.

The reasons for the observed age-related changes in contour integration are not well understood. Previous research has demonstrated that performance in contour integration tasks requires the integration of contour elements, as well as the suppression of the distracters in the background (Dakin and Baruch, 2009; Sassi et al., 2010; Machilsen et al., 2011; Schumacher et al., 2011). Casco et al. (2011) argued that the ability to integrate contour elements together did not change with aging, and that the age-related deficit in contour detection and discrimination resulted primarily from a decreased ability to suppress distracters with irrelevant orientations. Although this hypothesis is consistent with the pattern of results obtained in their task, and with evidence of reductions in inhibitory mechanisms in the visual cortex (e.g., Leventhal et al., 2003; Fu et al., 2010), there is also evidence that contour grouping abilities decline with aging even in the absence of visual clutter (Roudaia et al., 2008), a finding that is difficult to explain by deficits in suppressive mechanisms alone.

In the following studies, we further characterized the effects of aging on contour integration by examining contour discrimination performance for a range of stimuli varying in contour and distracter inter-element spacing and local orientation alignment. Contour element spacing is known to affect contour detection (Kovács and Julesz, 1993; Li and Gilbert, 2002; Beaudot and Mullen, 2003; Watt et al., 2008) and it has been suggested that contour integration mechanisms operate over a limited spatial range that scales with the spatial frequency of the contour elements (Beaudot and Mullen, 2003). In Experiment 1, we examined whether the spatial range of contour integration changes with aging by measuring contour discrimination performance for contours with varying inter-element spacing. Moreover, we examined the sensitivity to contour element collinearity as a function of contour spacing by disrupting the alignment of contour element orientations with orientation jitter. Knowing that older subjects require longer stimulus durations than younger subjects to integrate contours (Roudaia et al., 2011), any effects of aging on performance in Experiment 1 were expected to depend on stimulus duration. To examine this relationship, a subset of representative conditions from Experiment 1 were repeated in Experiment 2 with a range of stimulus durations. In addition to contour element spacing, the relative spacing of contour and distracter elements is also known to affect contour detection (Kovács et al., 1999; Li and Gilbert, 2002). Therefore in Experiment 3 we examined the effect of relative contour and distracter spacing on contour discrimination in older and younger subjects. Considering previous evidence that older subjects experience greater impairments in performance in the presence of visual noise or clutter (e.g., Sekuler and Ball, 1986; Betts et al., 2005; Del Viva and Agostini, 2007; Rousselet et al., 2009), changes in relative spacing may have a greater effect on older subjects. Finally, we also measured contour discrimination against a background of iso-oriented Gabors to examine whether aging also affects the ability to segregate contours from a relatively uniform background.

In all three experiments, the stimuli consisted of spiral shaped contours sampled with Gabor elements and embedded in a uniform field of distracter Gabors. Subjects were required to report

the global orientation of the spiral contour on every trial in a four alternative forced-choice task. Spiral contours were chosen because (1) we wanted to avoid closed or circular contours, due to possible additional detection benefits for closure and circularity (Regan and Hamstra, 1992; Kovács and Julesz, 1993; Dumoulin and Hess, 2007); (2) we wanted to use smooth contours that would be comparable to previous studies that have used open "C"-shaped contours (Roudaia et al., 2008, 2011) and closed circular and ellipsoid shapes (Del Viva and Agostini, 2007; Casco et al., 2011; Hadad, 2012); (3) using a familiar spiral shape allowed us to devise an easily-understood task that assessed global contour discrimination, as opposed to contour detection; and (4) drawing spiral contours, as opposed to straight contours, allowed for a greater range of contour spacings.

EXPERIMENT 1: EFFECTS OF CONTOUR ELEMENT SPACING AND LOCAL ORIENTATION ALIGNMENT

This experiment examined the effects of contour element separation and local orientation alignment on contour integration in younger and older subjects. The separation between adjacent elements comprising the contour was varied across blocks, while the relative contour and distracter separation was kept constant. Within blocks, alignment of contour element orientations was manipulated by the addition of varying amounts of orientation jitter.

METHODS

Subjects

Seventeen younger ($M = 25$ years; range: 22–33) and 16 older ($M = 66$ years; range: 60–82) subjects participated in this study and were compensated at a rate of $10/h. Near and far visual acuities were measured in all subjects using the SLOAN Two Sided ETDRS Near Point Test and the 4 Meter 2000 Series Revised ETDRS charts (Precision Vision, LaSalle, Illinois, USA). Contrast sensitivity was estimated using the Pelli-Robson Contrast Sensitivity Test (Pelli et al., 1988). Subjects wore their habitual optical correction during the vision testing and during the experiment. All subjects had normal or corrected-to-normal near and far Snellen visual acuity (range: −0.29 to 0.16 logMAR), although, on average, older subjects showed poorer acuity than younger subjects. All subjects showed normal contrast sensitivity for their age group (Elliott et al., 1990; Mäntyjärvi and Laitinen, 2001). The mini-mental state examination assessment (Folstein et al., 1975) was used to screen for cognitive impairment among older subjects and all scored above the normal cut-off score of 25/30. All subjects were free of visual pathology such as cataracts, glaucoma, and retinopathy, as assessed by a self-report questionnaire. One subject underwent successful bilateral cataract surgery 4 years prior to the experiment. **Table 1** summarizes the relevant demographic information for the two groups.

Apparatus

The experiment was programmed using the Psychophysics and Video Toolboxes (v. 3; Brainard, 1997; Pelli, 1997) in the Matlab environment (v. 7.5) driven by a Macintosh G5 computer. The stimuli were presented on a 20-inch (51 cm) Sony Trinitron monitor with a 1280 × 1024 resolution (pixel size: 0.014°) and a refresh rate of 75 Hz. The display was the only light source in the room and had an average luminance of 52 cd/m^2. Subjects viewed the display binocularly through natural pupils from a viewing distance of 114 cm. Viewing position was stabilized with a chin/forehead rest.

Stimuli

The stimulus consisted of a spiral-shaped contour sampled with Gabor micropatterns and embedded in a square region (9.5 × 9.5°) of randomly oriented distracter Gabors (**Figure 1**). Gabor micropatterns were created by multiplying a 3.33 cycles/deg sine wave grating ($\lambda = 0.30°$, 20 pixels/cycle) of 90% contrast by a circular Gaussian envelope with a standard deviation (σ) of 0.11° (≈1.4 visible cycles). All Gabors were in positive sine phase with respect to the center of the Gaussian window. The shape of the contour was defined by the formula for a logarithmic spiral,

$$r = ae^{b(t+t_j)} \quad (1)$$

where $a = 1.18°$, $b = 0.20$, and $1.25 < t < 3$. The position of the first Gabor on the contour relative to the beginning of the spiral path was jittered by parameter t_j, a uniform random variable ranging from −0.1 to 0.1. Subsequent Gabors were placed at the appropriate locations along the spiral path such that the inter-element distance between all elements remained constant. The long axis of the spiral spanned ≈6.9°.

The center of the spiral was placed in the center of the 9.5° square and then displaced horizontally and vertically by random amounts selected from a Normal distribution with $\sigma = 1.5°$. An iterative procedure was used to fill the remaining portion of the square region with distracter Gabors. Gabors were placed in random locations subject to the contstraint that all neighboring Gabors were not closer than a pre-determined minimum inter-element distance and the procedure continued until no more elements could be placed (Dakin and Baruch, 2009). On half the trials, the pattern was reflected along the vertical axis to create clockwise and counterclockwise spirals. Finally, the pattern was rotated by 90°, 180°, or 270° to create spirals of four different global orientations (see **Figure 1**).

The inter-element distance between neighboring Gabor elements was varied across blocks. Inter-element distance were set

Table 1 | Mean ± 1 SD age, near and far logMAR acuity, Pelli-Robson contrast sensitivity, and mini-mental state examination (MMSE).

N (M:F)	Age	Near acuity	Far acuity	Pelli-Robson	MMSE
17 (11:6)	24.9 ± 3.20	−0.15 ± 0.08	−0.11 ± 0.09	1.95 ± 0.05	
16 (9:7)	65.9 ± 6.37	0.03 ± 0.11	−0.05 ± 0.08	1.92 ± 0.06	28.9 ± 1.06

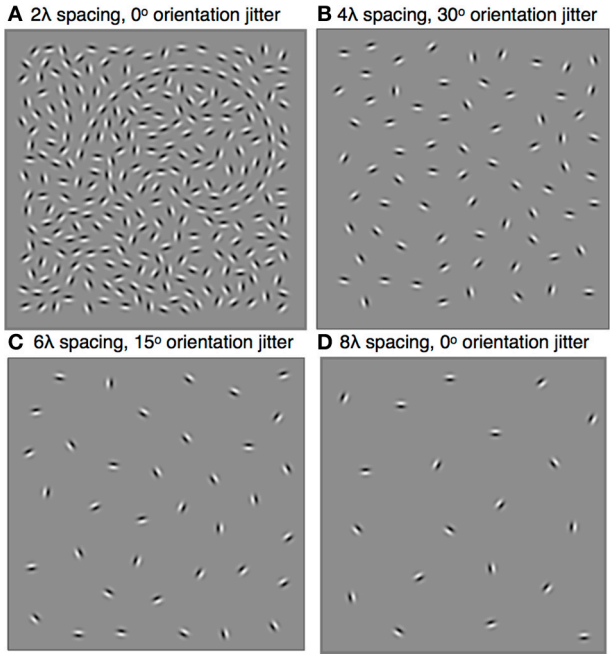

FIGURE 1 | Stimuli were spiral-shaped contours sampled with Gabors ($\lambda = 0.30°$, $\sigma = 0.11°$) and embedded in a field of randomly oriented distracter Gabors. The shape and size of the spiral, which could be clockwise or counter-clockwise, remained constant throughout the experiment, but its global orientation and position varied randomly across trials. Subjects reported the global orientation of the spiral by indicating the location of its tail. The minimum inter-element distance varied across blocks and ranged from 0.6° to 2.4°, or 2λ to 8λ. Within each block, contour element orientations were jittered by the addition of local orientation jitter ranging from 0° to 60°. Four stimulus examples are shown: **(A)** 2λ distance, 0° jitter, tail is on the left; **(B)** 4λ distance, 30° jitter, tail is on the right; **(C)** 6λ spacing, 15° jitter, tail is at the top; **(D)** 8λ spacing, 0° jitter, tail is at the bottom.

to be 2, 4, 6, or 8 times the Gabor wavelength (λ), corresponding to 0.6, 1.2, 1.8, or 2.4°. Setting the minimum distance between distracter elements equal to the contour inter-element spacing created, by definition, a background with the smallest number of distracters needed to avoid any density or spacing cues to the location of the contour. The approximate ratios of the number of contour and distractor Gabors for the 2λ, 4λ, 6λ, and 8λ inter-element spacings were 26:240, 13:60, 9:25, and 7:14 Gabors, respectively. Due to the random nature of the iterative process, the number of background elements varied slightly from trial to trial.

For each inter-element spacing condition, contour discrimination performance was measured for different levels of contour element collinearity. Collinearity was manipulated by adding varying amounts of orientation jitter to the contour element orientations. Collinear (or aligned) contours were created by setting the orientation of each element to equal the tangent to the contour path at that position. An independent orientation jitter angle was then added to each element by picking random numbers from a uniform distribution spanning ranges of ±15°, ±30°, ±45°, or ±60°.

Procedure

The McMaster University Research Ethics Board approved the experimental protocol. Written informed consent was obtained from all subjects prior to their participation in the experiment.

A four-alternative forced-choice (4-AFC) procedure was used to measure contour discrimination accuracy. A stimulus containing a spiral contour was presented on every trial and subjects were asked to report whether the tail of the spiral was located in the top-center, bottom-center, right-middle, left-middle locations in the display. At the beginning of the experiment, each subject was shown examples of stimuli where the spiral contour was made clearly visible by reducing the contrast of background elements. After adapting to the luminance of the display for 60 s, subjects completed five practice trials. The experimenter ensured that all subjects understood the task before proceeding to the experimental trials.

Each trial began with a black fixation point (diameter = 0.12°) presented in the center of the blank screen of mean luminance. Subjects were instructed to fixate the fixation point, which remained in the center throughout the trial. The fixation point flickered a rate of 10 Hz for 0.3 s at the beginning of each trial, after which the stimulus array was presented for 1 s, followed by a blank screen for 0.5 s. The fixation point was then displayed until the subject's response. The global orientation of the spiral was randomized across trials and the subjects reported the location of the end of the spiral by pressing either the up, down, left, or right arrow key. Auditory feedback was given on every trial with a high pitch tone indicating a correct response and a low pitch tone indicating an error. The subsequent trial began after a 1.5 s inter-trial interval. The four inter-element distance conditions were tested in separate blocks in randomized order. Each block consisted of 25 trials at orientation jitter levels of 0°, ±15°, ±30°, ±45°, and ±60°.

Preliminary control experiment

The stimuli and task used in the main experiments assessed subjects' ability to perceive the spiral's global shape/orientation by requiring them to report the location of the spiral's tail. To examine whether this task could be performed on the basis of local contour information, a preliminary control experiment measured the minimum number of contour elements required to locate the tail of the spiral contour.

The stimuli and methods used in that control experiment were created using the same procedure described above, except that the distracter elements were removed and, on every trial, a staircase procedure determined the number of adjacent contour elements that would be displayed. The location of the adjacent elements on the spiral path was chosen randomly on every trial to be either the head, tail, or middle of the spiral. The two young subjects who participated in this experiment were shown the full shape of the spiral prior to the experiment and were told that only portions of the spiral contour would be visible on any given trial. Their task was to report whether the tail of the complete spiral would be at the top-center, bottom-center, right-middle, and left-middle locations of the square pattern.

RESULTS

For all of the current experiments, statistical analyses were performed using the statistical computing environment R (R Development Core Team, 2008; Lawrence, 2011). Mean accuracy and sensitivity (i.e., d') were obtained for each level of orientation jitter and inter-element distance. Since the pattern of results was similar for accuracy and d', only accuracy data are presented here. When conducting ANOVA, an arcsine transformation was applied to accuracy values to ensure the data satisfied the assumption of normality. For all within-subjects tests, the Geisser-Greenhouse correction was used to adjust the degrees-of-freedom to correct for violations of the sphericity assumption (Maxwell and Delaney, 2004). In such cases, the adjusted p-values are reported. Generalized eta-squared, η_g^2, is reported as a measure of association strength for all significant effects (Olejnik and Algina, 2003; Bakeman, 2005).

Our preliminary experiment found that 11 Gabors were required to locate the tail for contours with 2λ spacing, and 4.5 Gabors were required for contours with 6λ spacing. Thus, reporting the location of the tail of the spiral (without distracters) with 75% accuracy in our stimuli requires grouping approximately half of the contour elements composing the contour.

Figure 2 shows mean accuracy for contour discrimination as a function of orientation jitter for all contour spacing conditions separately. As expected, accuracy in both groups declined with increasing orientation jitter at each level of element spacing.

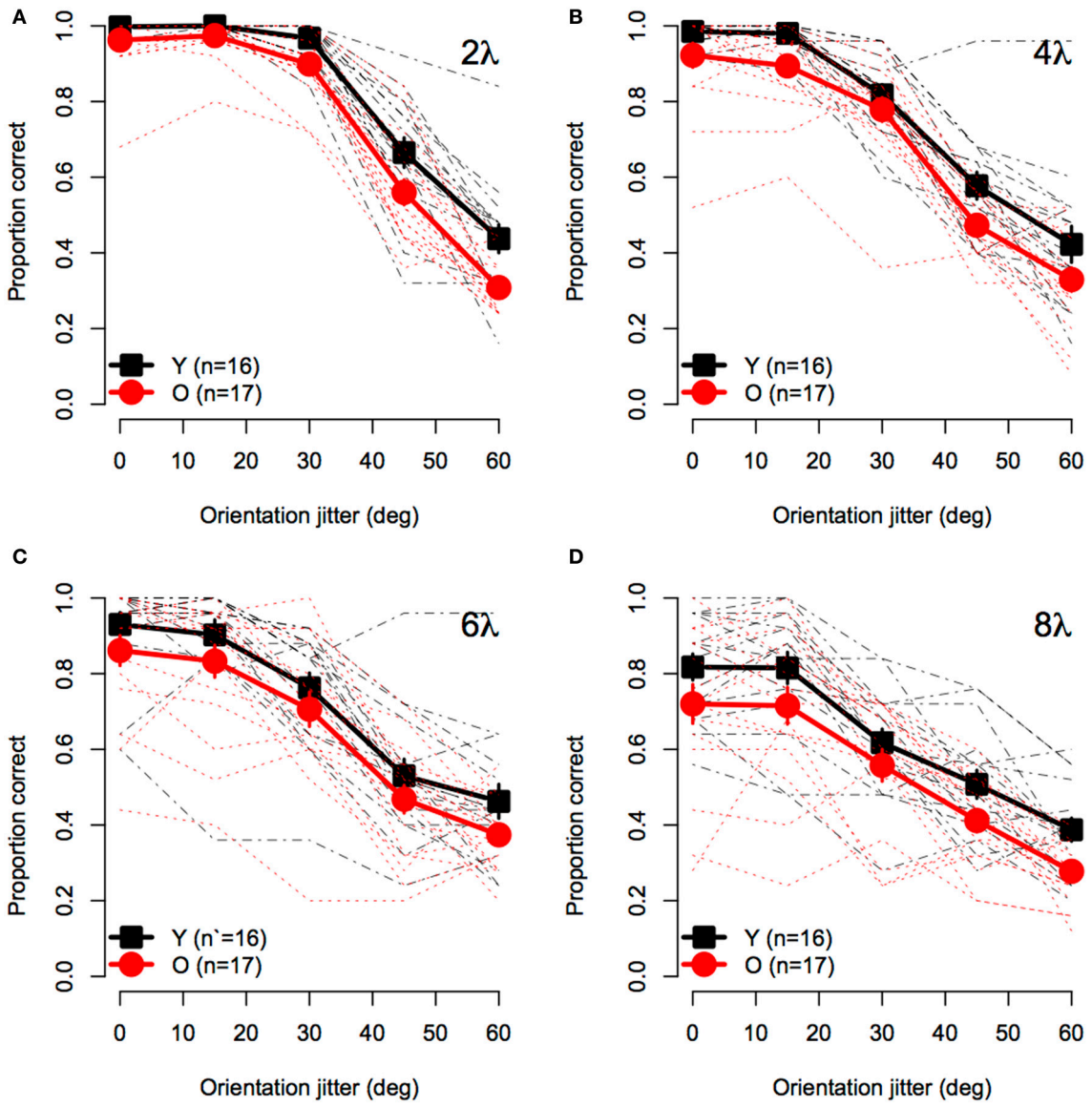

FIGURE 2 | Experiment 1 results: Contour discrimination accuracy is shown as a function of contour element orientation jitter for four inter-element spacing conditions (A–D). Black squares show mean accuracy of younger subjects and red circles show mean accuracy of older subjects. Error bars represent ±1 SEM. Individual subjects' data are shown in black dashed line for younger subjects and dotted red lines for older subjects.

Furthermore, at any fixed level of orientation jitter, response accuracy in both groups decreased with increasing separation between elements. Accuracy in both groups was at ceiling when discriminating aligned (0° jitter) contours with 2λ spacing. However, accuracy was lower in older subjects than younger subjects in all other conditions. A mixed-model 2 (Age) × 4 (Spacing) × 5 (Orientation Jitter) ANOVA revealed significant main effects of age [$F_{(1,\ 31)} = 10.5, p = 0.0028, \eta_g^2 = 0.10$], spacing [$F_{(3,\ 93)} = 54.4, \hat{\epsilon} = 0.92, p < 0.0001, \eta_g^2 = 0.29$], and orientation jitter [$F_{(4,\ 124)} = 480.3, \hat{\epsilon} = 0.49, p < 0.0001, \eta_g^2 = 0.72$]. The Spacing × Orientation Jitter interaction also was significant [$F_{(12,\ 372)} = 17.0, \hat{\epsilon} = 0.63, p < 0.0001, \eta_g^2 = 0.14$], indicating that the effect of orientation jitter varied with inter-element spacing. Importantly, none of the interactions with age were significant [Age × Spacing: $F_{(3,\ 93)} = 0.08, \hat{\epsilon} = 0.92, p = 0.96$; Age × Orientation Jitter: $F_{(4,\ 124)} = 0.53, \hat{\epsilon} = 0.49, p = 0.57$; Age × Spacing × Orientation Jitter: $F_{(12,\ 372)} = 0.74, \hat{\epsilon} = 0.63, p = 0.65$]. These results indicate that the effect of age on contour integration did not vary significantly with inter-element spacing or orientation jitter.

To visualize the Spacing × Orientation Jitter interaction, the data were redrawn in **Figure 3** to compare the effect of orientation jitter on contours with different inter-element spacings. The data show that accuracy achieved with low levels of jitter decreased with increasing inter-element spacing, but that the effect of spacing declined as jitter increased beyond ≈30°. In other words, contour discrimination showed greater resistance to small amounts of orientation jitter when inter-element separations were small.

Figure 4 shows the effect of element spacing for collinear contours (i.e., 0° orientation jitter) for younger and older subjects separately. The average accuracy in the two groups declined monotonically with increasing spacing and the rate of decline was similar for both groups. However, not all subjects showed the same rate of decline with spacing. As can be seen in **Figure 4**, several subjects in each group showed consistently high accuracy at all spacings. On the other hand, other subjects showed sharp declines in accuracy, even with spacing as small as 4 λ. Moreover, the number of subjects who showed poor performance (≤75%) at larger spacings was greater in the older group than in the younger group.

DISCUSSION

This experiment examined the effects of contour-element separation and collinearity on contour discrimination in younger and older subjects. Overall, contour discrimination was poorer in older subjects, but the age difference did not vary significantly with element separation or collinearity.

Field et al. (1993) found that contour detection accuracy declined to chance level with orientation jitter of only 30°, whereas subjects in the current experiment were able to tolerate much greater levels of orientation jitter. The reason for this discrepancy lies in the definitions of orientation jitter used in the two studies: A 30° orientation jitter in Field et al. signifies that each contour element's orientation either increased or decreased by 30°, whereas 30° orientation jitter in our experiment means that the jitter angle applied to any individual contour element can take on any value between −30° and 30°. Hence, the effects of orientation jitter in the two studies are not comparable.

Beaudot and Mullen (2003) estimated the spatial limit of contour integration by determining the maximum inter-element distance at which observers could reliably detect contours embedded in a field of randomly oriented Gabors. They found that the critical separation was proportional to spatial frequency and was unaffected by contour curvature. The average spatial limit for the achromatic mechanism of their four younger subjects was ≈6.8λ. Kuai and Yu (2006) reported a similar estimate

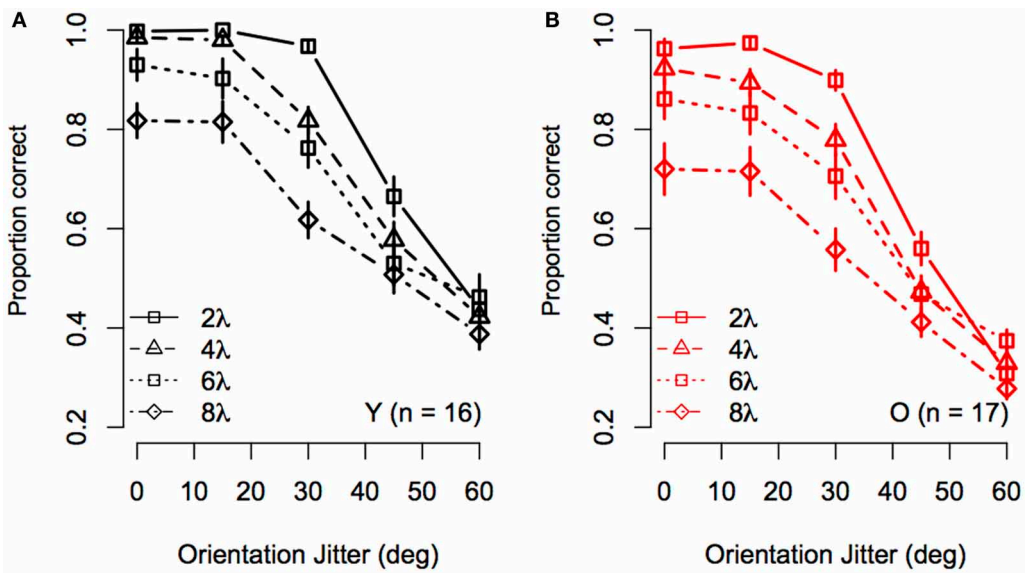

FIGURE 3 | Experiment 1 results: Effect of inter-element spacing on contour discrimination accuracy is shown as a function of orientation jitter for younger subjects (A) and older subjects (B). Different symbols show accuracy for 2λ *to* 8λ conditions separately (see legend). Error bars represent ±1 SEM.

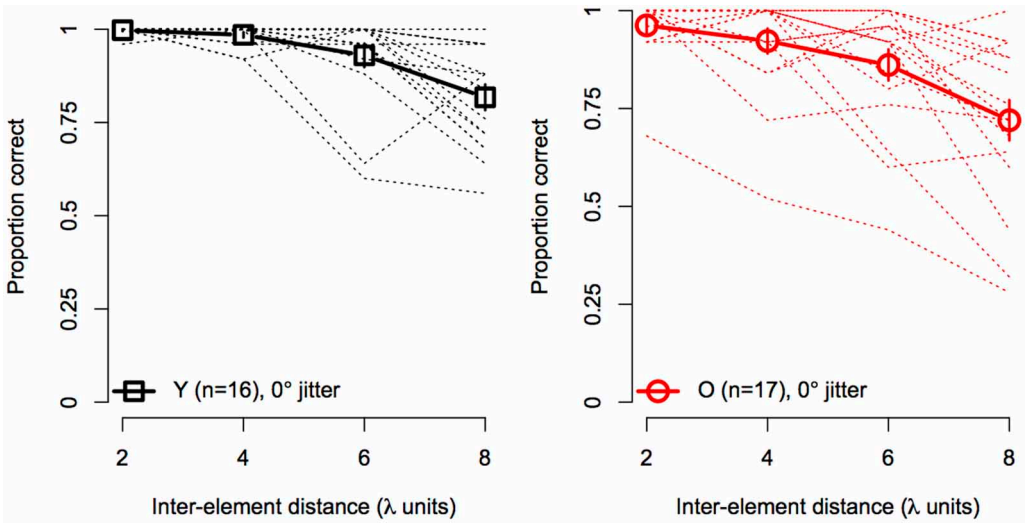

FIGURE 4 | Experiment 1 results: contour discrimination accuracy is shown a function of inter-element distance for contours with 0° orientation jitter (collinear). Dashed lines show individual subjects' data, solid lines show mean accuracy, and error bars represent ±1 SEM.

(6.9λ) in a contour detection task and a smaller (4.4λ) limit in a contour shape discrimination task. Although the maximum element separation in the current experiment was 8λ, we did not observe a sharp decline in performance at the largest contour spacing in either group. Instead, average contour discrimination performance decreased gradually with element spacing, with some subjects showing a steeper decline and others maintaining high discrimination accuracy even at 8λ. Interestingly, Beaudot and Mullen (2003) also reported that some subjects showed constant performance as a function of contour-element separation. Thus, the spatial range for contour integration may not have a sharp boundary and may vary across individuals. However, if the spatial range of contour integration was reduced with aging, the age-difference in contour discrimination accuracy would be greater for contours with larger spacings, compared to smaller spacings. This pattern was not observed as the effect of age was approximately constant across all contour spacing conditions. Hence, the spatial range of contour integration does not appear change with age.

Consistent with the idea that proximity increases overall contour salience (Li and Gilbert, 2002), the asymptotic level of performance decreased with increasing contour spacing for younger and older subjects. Contours with small spacing were also more resistant to orientation jitter than contours with large spacing.

These results are consistent with previous studies showing that co-alignment of local orientation is required to group elements spaced far apart, but is less important for grouping elements that are placed close together (Nikolaev and van Leeuwen, 2007; Hadad et al., 2010). In the current study, the effect of orientation jitter was the same for younger and older subjects across all contour spacing conditions. This finding is consistent with McKendrick et al. (2010), who found that orientation jitter increased closed-contour shape discrimination thresholds by similar amounts in younger and older subjects. Similarly, Hadad (2012) found that disruption of collinearity had a similar effect on closed contour shape discrimination in younger and older subjects for stimuli with high and low proximity levels. In sum, converging evidence from several studies shows that aging does not affect the ability to use collinearity for grouping contours and extracting the contour shape.

EXPERIMENT 2: EFFECT OF STIMULUS DURATION AS A FUNCTION OF CONTOUR SPACING AND LOCAL ORIENTATION ALIGNMENT

Previous research has shown that older subjects require longer stimulus durations than younger subjects to discriminate contours (Roudaia et al., 2011). A 1 s stimulus duration was used in Experiment 1 to ensure that older subjects had sufficient time to group the contours, so that the effects of contour spacing and collinearity could be observed independently of differences in processing time. Processing time for detecting contours in clutter increases with curvature (Beaudot and Mullen, 2001; Hess et al., 2001) and appears to increase with contour element spacing (Beaudot and Mullen, 2003). Similarly, the stimulus duration required for collinear facilitation—i.e., the reduction of contrast threshold for a target Gabor when flanked by high contrast, collinear flanker Gabors (Polat and Sagi, 1993)—has been shown to increase proportionally to the distance between target and flankers (Cass and Spehar, 2005). Thus, the dynamics of contour discrimination in Experiment 1 may also vary with inter-element separation and collinearity, and these dynamics may change with age in a non-linear way. In the current experiment, we tested contour discrimination for a range of stimulus durations to examine how the effect of aging for contours with different spacing and collinearity levels may be affected by the stimulus duration.

METHODS

Subjects

Fourteen younger and fourteen older subjects who participated in Experiment 1 were tested. Subjects were compensated ($10/h) for participating. One older subject completed only three out of four conditions in the experiment. For this reason, data from this subject were excluded from statistical analyses, however, they are included in the data plots. Demographic information is presented in **Table 1**.

Apparatus

The apparatus was the same as in Experiment 1.

Stimuli

The stimuli were generated using the same procedure as described in Experiment 1. Only two levels of inter-element spacing (2λ and 6λ) and two levels of orientation jitter (0° and 30°) were used in this experiment.

Procedure

The task and trial sequence was the same as in Experiment 1, except that the stimulus duration was randomized on every trial. The stimulus durations were 0.04, 0.093, 0.20, 0.40, or 0.80 s (i.e., 3, 7, 15, 30, or 60 frames). The trials were blocked by inter-element spacing and orientation jitter and the order of the blocks was randomized across subjects. Each block contained 150 trials, with 30 trials at each stimulus duration. As in Experiment 1, accuracy and d' were calculated for each subject. The pattern of results was similar for accuracy and d' and only accuracy data are shown here.

RESULTS

Statistical analyses were performed with the same software and procedures used in Experiment 1. **Figure 5** shows the contour discrimination accuracy of younger and older subjects as a function of stimulus duration for stimuli with small (**Figure 5A**) and large (**Figure 5B**) inter-element separations. As can be seen, accuracy generally increased with stimulus duration, but the rate of increase and the asymptotic level of performance varied as a function of age, inter-element separation, and orientation jitter. A mixed-model 2 (Age) × 4 (Spacing) × 5 (Orientation Jitter) × 5 (duration) ANOVA on arcsine-transformed accuracy values revealed significant main effects of age [$F_{(1,\ 25)} = 5.78$, $p = 0.02$, $\eta_g^2 = 0.09$], spacing [$F_{(1,\ 25)} = 219.9, p < 0.0001$, $\eta_g^2 = 0.45$], orientation jitter [$F_{(1,\ 25)} = 232.1$, $p < 0.001$, $\eta_g^2 = 0.43$], and duration [$F_{(4,\ 100)} = 26.4$, $\hat{\epsilon} = 0.80$, $p < 0.0001$, $\eta_g^2 = 0.10$]. The effects of stimulus duration, contour spacing, and orientation jitter also interacted with each other, as revealed by significant Spacing × Orientation jJitter [$F_{(1,\ 25)} = 9.79$, $p = 0.004$, $\eta_g^2 = 0.03$], Spacing × Duration [$F_{(4,\ 100)} = 4.10$, $\hat{\epsilon} = 0.76$, $p = 0.009$, $\eta_g^2 = 0.01$], and Spacing × Orientation Jitter × Duration [$F_{(4,\ 100)} = 3.33$, $\hat{\epsilon} = 0.84$, $p = 0.02$, $\eta_g^2 = 0.009$] interactions. The Orientation Jitter × Duration interaction was not significant [$F_{(4,\ 100)} = 1.68, \hat{\epsilon} = 0.87, p = 0.16, \eta_g^2 = 0.004$]. The significant three-way Spacing × Orientation Jitter × Duration interaction reflects the fact that the effect of spacing was greater for non-collinear contours, especially at short stimulus durations.

Consistent with Experiment 1, the effect of age did not vary with spacing or orientation jitter, as the Age × Spacing [$F_{(1,\ 25)} = 0.06$ $p = 0.81$, $\eta_g^2 \approx 0$], and Age × Orientation Jitter [$F_{(1,\ 25)} = 0.64$, $p = 0.43$, $\eta_g^2 = 0.002$] interactions were not significant. Unlike what was found in Experiment 1, the Age × Spacing × Orientation Jitter interaction was significant [$F_{(1,\ 25)} = 12.3$, $p = 0.002$, $\eta_g^2 = 0.04$]. This result reflects the fact that disruption of collinearity had a greater effect in younger subjects in the 6λ compared to the 2λ condition. On the other hand, adding orientation jitter affected older subjects' accuracy approximately

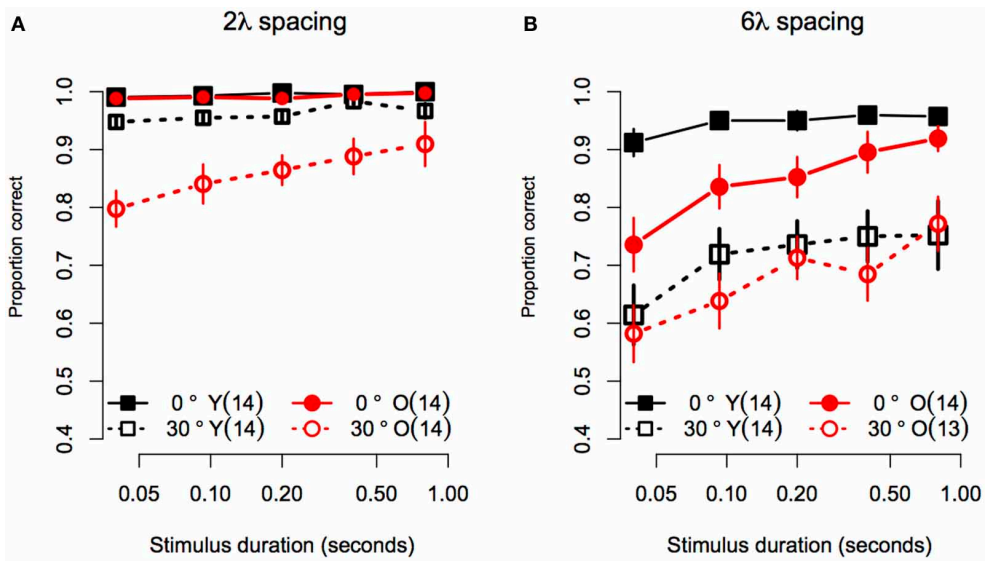

FIGURE 5 | Experiment 2 results: Contour discrimination accuracy is shown as a function of stimulus duration for (A) contours with small contour element spacing and (B) contour with large contour element spacing. Younger subjects' mean accuracy is plotted in black squares and older subjects' mean accuracy is plotted in red circles. Error bars represent ±1 SEM.

to the same extent in the small and large spacing conditions (compare the difference in the vertical separation of the two black curves in **Figures 5A,B** versus the same comparison in the red curves). However, it is likely that this interaction is due, at least in part, to ceiling effects in the no-jitter, 2λ conditions.

Importantly, the effect of age also varied with stimulus duration, as revealed by a significant Age × Duration interaction [$F_{(4,\ 100)} = 2.97$, $\hat{\epsilon} = 0.80$, $p = 0.02$, $\eta_g^2 = 0.01$]. None of the three- and four-way interactions that included Age and Duration factors were significant [Age × Spacing × Duration: $F_{(4,\ 100)} = 0.29, \hat{\epsilon} = 0.76, p = 0.88$; Age × Orientation Jitter×Duration: $F_{(4,\ 100)} = 1.94$, $\hat{\epsilon} = 0.87$, $p = 0.11$; Age × Spacing × Orientation Jitter × Duration: ($F_{(4,\ 100)} = 1.90$, $\hat{\epsilon} = 0.84, p = 0.12, \eta_g^2 = 0.005$)].

Given that the effect of age interacted with spacing and orientation jitter, we conducted separate 2 (Age) × 5 (Duration) ANOVAs for each contour type. In addition, the effect of stimulus duration was analysed by computing linear trend scores of accuracy across log stimulus duration, and comparing these trend scores across age groups with One-Way ANOVAs. **Figure 5A** shows the data for stimuli with a small (2λ) inter-element spacing. For collinear contours, both groups showed ceiling performance for all durations: average response accuracy in the two groups did not differ [Age: $F_{(1,\ 25)} = 1.50$, $p = 0.23$, $\eta_g^2 = 0.03$], the linear trend of accuracy across duration did not reach significance [$F_{(1,\ 25)} = 4.01$, $p = 0.06$], and the linear trend did not differ between age groups [$F_{(1,\ 25)} = 0.03$, $p = 0.59$]. When collinearity was disrupted by 30° orientation jitter, response accuracy in the two age groups differed at all stimulus durations except the longest (i.e., 0.8 s): average response accuracy was lower in older subjects [$F_{(1,\ 25)} = 11.25$, $p = 0.003$, $\eta_g^2 = 0.23$], the linear trend of accuracy across duration was significant [$F_{(1,\ 25)} = 44.8$, $p < 0.0001$]. Importantly, the linear trend differed between age groups [$F_{(1,\ 25)} = 5.60$, $p = 0.03$], reflecting the fact that response accuracy in older subjects declined more than that of younger subjects as duration decreased. In summary, for contours with short inter-element spacings, the effect of aging on contour discrimination accuracy increased at shorter stimulus durations, but only for non-collinear contours.

Figure 5B shows the data for stimuli with a large (6λ) inter-element spacing. For collinear contours, younger subjects' accuracy improved from 91 to 95% between 0.04 and 0.093 s, after which it remained constant as stimulus duration increased. On the other hand, older subjects' accuracy was ≈73% when the stimulus duration was 0.04 s, and showed an approximately linear increase until reaching younger subjects' accuracy at 0.8 s. Consistent with these observations, the main effect of age was significant [$F_{(1,\ 25)} = 7.11, p = 0.01, \eta_g^2 = 0.16$], the linear trend across log duration was significant [$F_{(1,\ 25)} = 39.35, p < 0.0001$] and the linear trend was greater in older compared to younger subjects [$F_{(1,\ 25)} = 7.72, p = 0.01$]. For non-collinear (30° jitter) contours, both groups showed similar levels of accuracy at all durations. The main effect of age was not significant [$F_{(1,\ 25)} = 0.48$, $p = 0.49$, $\eta_g^2 = 0.01$]. The linear trend across log duration was significant [$F_{(1,\ 25)} = 20.60$, $p = 0.0001$], but it did not differ across the two age groups [$F_{(1,\ 25)} = 0.32$, $p = 0.57$]. In summary, for contours with 6λ spacing, the effect of aging increased with decreasing stimulus duration when contour elements were collinear, but the effect of aging remained constant for non-collinear contours.

DISCUSSION

When spiral contours were composed of closely spaced collinear elements, younger and older subjects showed nearly perfect contour discrimination performance, even when stimulus duration was decreased to 0.04 s. However, contour discrimination accuracy declined with decreasing stimulus duration when contour element spacing was large and when contour element collinearity was disrupted by local orientation jitter. When both proximity and collinearity were disrupted (6λ and 30° jitter condition), both groups showed similar, poor performance at all durations. However, when only proximity *or* collinearity was disrupted, performance was more severely impaired in older subjects than younger subjects at short stimulus durations.

These findings are consistent with a previous study showing an age-related increase in duration thresholds for discriminating contours in clutter (Roudaia et al., 2011). Roudaia et al. demonstrated that this age difference in processing time could not be ascribed to age-related reductions in retinal illuminance (Weale, 1963), nor to delays in the processing of individual Gabor elements, and therefore argued that the age difference in contour discrimination reflected delays in the contour integration process *per se*. Similar to the current results, Roudaia et al. found that older subjects were disproportionately slower at processing less salient contours composed of elements oriented orthogonally to the contour path.

Roudaia et al. (2011) reported that older subjects required longer durations to process collinear contours than younger subjects, and that younger and older subjects in that study required 0.05 and 0.150 s, respectively to discriminate contours with 75% accuracy. It may be surprising, therefore, that the current study found that response accuracy in both age groups was quite high at short stimulus durations. However, the difference between experiments is likely due to the fact that stimuli used by Roudaia et al. were followed by a mask, whereas those used in the current study were not. This hypothesis is supported by Hess et al. (2001), who found that successful contour detection required a stimulus duration ≥ 0.83 s when stimuli were preceded and followed by a mask, but only 0.013 s when stimuli were not masked.

The current data suggest that processing time for contour integration increases with increasing inter-element spacing. Subjects in both groups showed a steeper decrease in accuracy with decreasing stimulus duration for contours with large, compared to small, inter-element spacings. The only other study that measured contour detection as a function of stimulus duration and inter-element separation was conducted in macaque monkeys and also reported increased processing time for integrating across larger separations (Mandon and Kreiter, 2005).

Finally, consistent with Experiment 1, the effect of aging on discrimination of contours did not systematically differ as a function of contour spacing in this experiment. This result corroborates the conclusion made in Experiment 1, namely that aging does not differentially affect the ability to group contours across large distances.

EXPERIMENT 3: THE EFFECT OF RELATIVE CONTOUR AND DISTRACTER SPACING IN ISO- AND RANDOMLY-ORIENTED BACKGROUNDS

In Experiments 1 and 2, the average spacing between adjacent distracters and between adjacent contour elements were equal in order to minimize the number of distracters while simultaneously ensuring that the contour could not be detected on the basis of density cues. Previous studies have shown that contour detection becomes more difficult when the minimum distracter element spacing is less than the minimum contour element spacing, resulting in displays where any given contour element is closer to a distracter than to their neighboring contour element (Braun, 1999; Kovács et al., 1999; Li and Gilbert, 2002). Del Viva and Agostini (2007) found that younger subjects are able to tolerate a greater number of distracter Gabors than older subjects when detecting circular contours, which suggests that older subjects are less efficient than younger subjects at extracting contours from dense backgrounds. However, the stimuli in that study did not equate the average spacing between elements across the display, resulting in differences in local density that may have been used to locate the contour. In this experiment, we investigated the effect of relative spacing of contour and distracter elements on contour discrimination in younger and older subjects by decreasing distracter spacing while keeping the spacing between contour elements constant. In addition, we examined whether contour integration in older subjects is differentially affected by the variability of the orientations of the background elements.

METHODS

Subjects

Twelve younger and twelve older subjects, none of whom had participated in Experiments 1 or 2, were recruited to participate in this experiment. Subjects were compensated for their time at a rate of $10/h. **Table 2** summarizes the demographic factors, visual acuity, contrast sensitivity, and cognitive measures for these two groups.

Apparatus

The apparatus was the same as in Experiment 1.

Stimuli

Spiral contours were sampled with Gabors ($\lambda = 0.30°$, $\sigma = 0.11°$) and positioned at equally spaced intervals of 3λ (0.9°) or 6λ (1.8°) along the path of a logarithmic spiral, as described in Experiment 1. The global spiral orientation was either clockwise or counterclockwise and was oriented in one of four directions. The spiral was centered in a 9.5° square region and then displaced horizontally and vertically by random amounts selected from a Normal distribution with $\sigma = 1.5°$. The orientations of the Gabors composing the spiral were tangential to the contour path.

Distracter elements were positioned randomly within the square stimulus area using an iterative procedure that maintained a pre-determined minimum separation between distracter elements. The iterative procedure continued until no more distracters could be placed. The 3λ contours were embedded in backgrounds with minimum distracter spacing of 2.9, 2.4, 2.0, 1.7, and 1.5λ. The 6λ contours were embedded in backgrounds with minimum distracter spacing of 6.1, 5.0, 4.0, 3.4, and 2.9λ. Thus, the relative spacing between contour and distracter elements were equal to 1.0, 1.2, 1.5, 1.8, or 2.1, where numbers greater than 1 indicate that contour spacing was larger than distracter spacing. The orientation of distracter elements varied in two conditions: random and iso-oriented. In the random condition, distacter orientations were sampled from a uniform distribution of angles from 0° to 360°. In the iso-oriented condition, each distracter orientation was sampled from a Gaussian normal distribution with $\sigma = 5°$ and a mean that was equal to a randomly chosen angle between 0° and 360°. The iso-oriented background was tested only for relative spacing levels of 1.0 and 2.1, and the randomly-oriented background was tested with all five levels of relative spacing. Examples of stimuli are shown in **Figure 6**.

Procedure

The task and trial sequence were similar to Experiments 1 and 2. Subjects were asked to maintain fixation on a black fixation point displayed in the middle of the screen of mean luminance throughout the trials. The fixation point flickered to indicate the start of each trial. The stimulus contained a spiral contour oriented in one of four directions, was displayed for 0.4 s and followed by a blank screen of mean luminance for 0.5 s. In a four alternative forced-choice procedure, subjects reported the location of the tail of the spiral by pressing one of the four arrow keys on the keyboard. Auditory feedback was provided after every trial with a high pitch tone following a correct response and a low pitch tone following an error. The subsequent trial began after a 1.5 s inter-trial interval.

Trials were blocked by contour spacing: half the subjects in each group completed all the 3λ contour trials first and the other half of the subjects completed all the 6λ contour trials first. Within each block, all relative spacing levels and background context conditions (iso- or randomly-oriented) were intermixed. There were 50 trials per condition, resulting in a total of 600 trials. Subjects were allowed to take a short break after every 125 trials and the experiment lasted approximately 50 min.

Table 2 | Experiment 3: Mean ± 1 SD age, near and far logMAR acuity, Pelli-Robson contrast sensitivity, and mini-mental state examination (MMSE).

N (M:F)	Age	Near acuity	Far acuity	Pelli-Robson	MMSE
12 (4:8)	20.0 ± 3.5	−0.12 ± 0.07	−0.12 ± 0.11	1.90 ± 0.07	
12 (6:6)	67.6 ± 6.5	0.03 ± 0.08	0.01 ± 0.09	1.95 ± 0	28.8 ± 1.03

RESULTS

Statistical analyses were performed with the same software and procedures used in Experiments 1 and 2. **Figure 7** shows contour discrimination accuracy as a function of background element spacing and **Figure 8** shows the same data as a function of the relative spacing of contour and background elements.

To compare performance in the iso-oriented (upright and inverted triangles) and random background conditions (circles

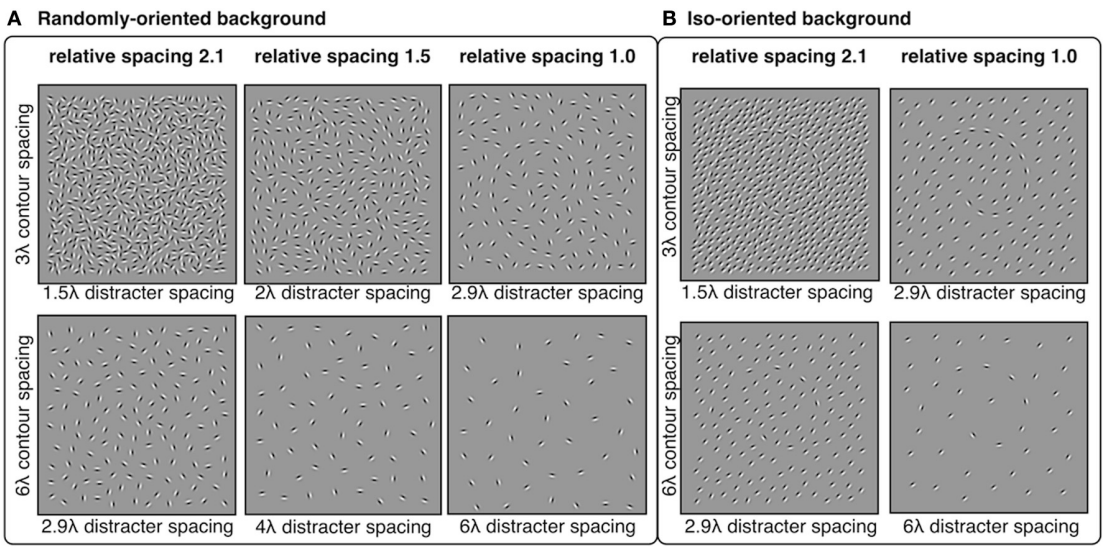

FIGURE 6 | Experiment 3 stimuli: spiral contours embedded in a background of randomly-oriented (A) or iso-oriented (B) Gabors with varying inter-element spacing. Contour elements had either 3λ (top row) or 6λ (bottom row) spacing. Distracter spacing varied from 1.5λ to 6.1λ, resulting in contour-distracter relative spacing ranging from 1.0 to 2.1. Three levels of relative spacing—1, 1.5, and 2.1—are shown here.

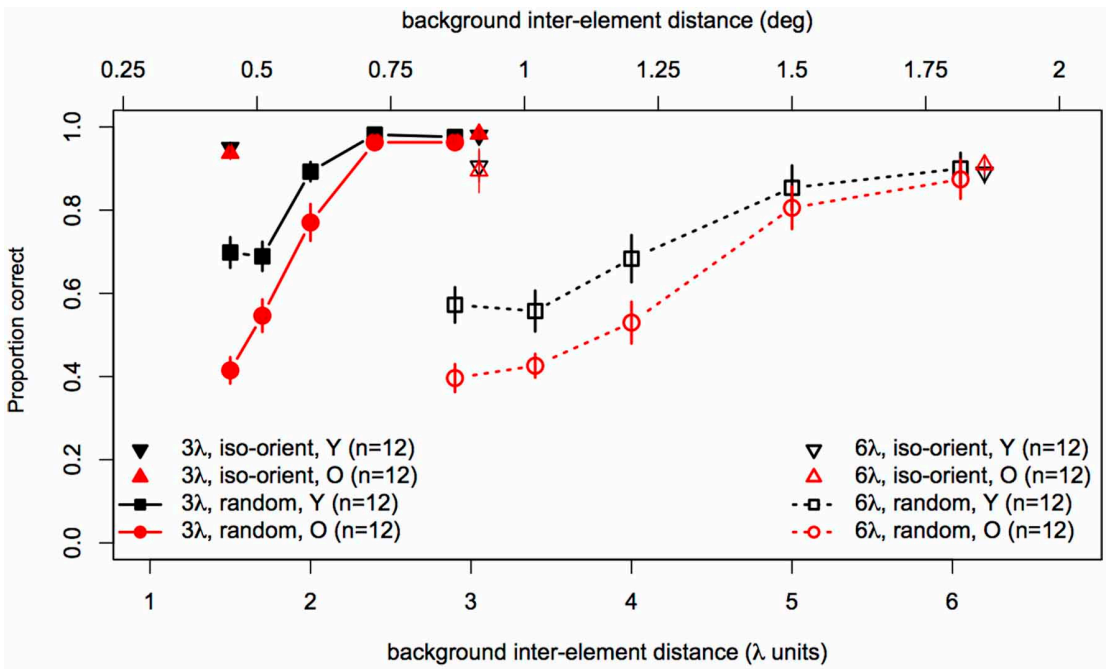

FIGURE 7 | Experiment 3 results: contour discrimination accuracy is shown as a function of background inter-element spacing for all conditions tested. Data for the iso-oriented background conditions are shown by the triangle symbols (up, black for younger subjects and down, red for older subjects). Black squares and red circles show younger and older subjects' performance in the random background condition. Solid lines and filled symbols show data for contours with 3λ spacing and dotted lines with open symbols show data for contours with 6λ spacing. Error bars represent ±1 SEM.

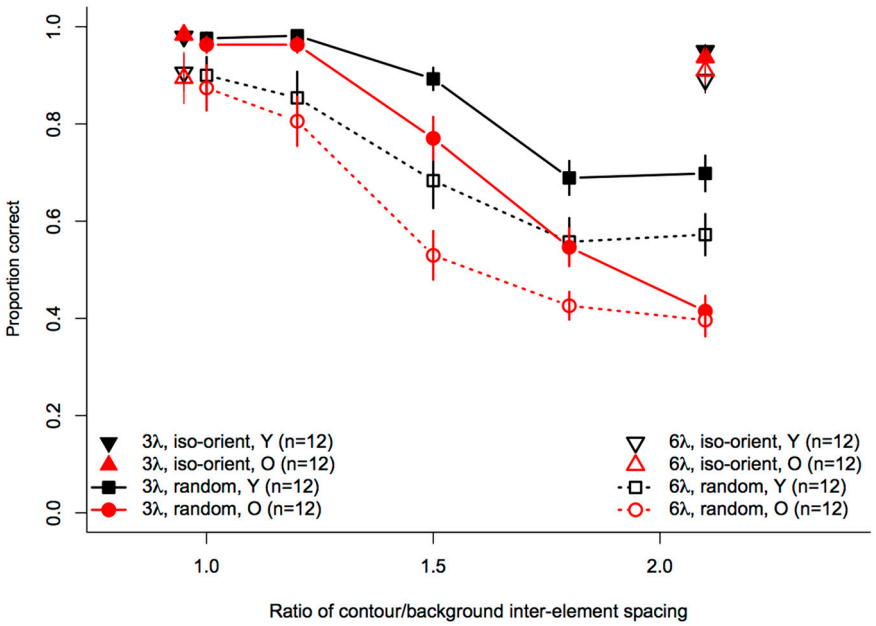

FIGURE 8 | Experiment 3 results: contour discrimination accuracy is shown as a function of relative contour and background spacing. Data for the iso-oriented background conditions are shown by the triangle symbols (up, black for younger subjects and down, red for older subjects) that are displaced horizontally to avoid overlap. Data for the random orientation condition background condition are shown with filled symbols and solid lines for the 3λ contours and with open symbols and dashed lines for the 6λ contours. Error bars represent ±1 SEM.

and squares), we conducted a 2 (Age) × 2 (Context: random or iso-oriented) × 2 (Contour Spacing: 3λ and 6λ) × 2 (Relative Spacing: 1.1 and 2.2) mixed-model ANOVA on arcsine-transformed accuracy values. The ANOVA revealed significant main effects of background context [$F_{(1,\ 22)} = 230$, $p < 0.001$], contour spacing [$F_{(1,\ 22)} = 19.3$, $p = 0.0002$], and relative spacing [$F_{(1,\ 22)} = 201.6$, $p < 0.0001$], but no main effect of age [$F_{(1,\ 22)} = 2.3$, $p = 0.14$]. The Contour Spacing × Relative Spacing interaction [$F_{(1,\ 22)} = 9.9$, $p = 0.005$] was significant, as were all of the two-way and three-way interactions between age, context, and relative spacing [Age × Context : $F_{(1,\ 22)} = 16.5$, $p = 0.0005$; Age × Relative Spacing: $F_{(1,\ 22)} = 4.1$, $p = 0.05$; Context × Relative Spacing: $F_{(1,\ 22)} = 393.1$, $p < 0.0001$, Age × Context × Relative Spacing: $F_{(1,\ 22)} = 19, 7$, $p = 0.0002$]. The significant three-way interaction implies that the effects of relative spacing and age on contour discrimination accuracy differed significantly for contours embedded among iso-oriented or randomly oriented background elements.

Next, arcsine-transformed accuracy values from the iso-oriented and random background conditions were analysed separately with 2 (Age) × 2 (Contour Spacing) × 2 (Relative Spacing) mixed-model ANOVAs. For the iso-oriented background (i.e., the upright and inverted triangles in **Figure 8**), the ANOVA revealed significant main effects of contour spacing [$F_{(1,\ 22)} = 14.6$, $p = 0.001$, $\eta_g^2 = 0.13$] and relative pacing [$F_{(1,\ 22)} = 16.7$, $p = 0.004$, $\eta_g^2 = 0.07$], as well as a significant Contour Spacing × Relative Spacing interaction [$F_{(1,\ 22)} = 9.58$, $p = 0.005$, $\eta_g^2 = 0.04$]. Accuracy was higher for contours with 3λ spacing than 6λ spacing in both groups, but this difference was slightly diminished when relative spacing was high, as accuracy for 3λ contours decreased but that for 6λ contours remained constant. The main effect of age was not significant [$F_{(1,\ 22)} = 0$, $p = 0.92$], nor were any of the two-way and three-way interactions with age ($F \leq 1.29$ and $p \geq 0.26$ in each case). Thus, contour discrimination accuracy in the iso-oriented background condition did not differ significantly between age groups.

For the random background condition (indicated by the circles and squares in **Figure 8**), the ANOVA revealed significant main effects of contour spacing [$F_{(1,\ 22)} = 54.7$, $p < 0.001$, $\eta_g^2 = 0.25$], relative spacing [$F_{(4,\ 88)} = 225.5$, $\hat{\epsilon} = 0.67$, $p < 0.001$, $\eta_g^2 = 0.67$], and age [$F_{(1,\ 22)} = 7.39$, $p = 0.01$, $\eta_g^2 = 0.15$]. Accuracy was higher overall for 3λ compared to 6λ contours and decreased with increasing relative spacing. The Contour Spacing × Relative Spacing interaction also was significant [$F_{(4,\ 88)} = 8.68$, $\hat{\epsilon} = 0.61$, $p = 0.0001$, $\eta_g^2 = 0.05$], indicating that the difference in accuracy for 3λ and 6λ spacing contours depended on the relative spacing. The significant main effect of age confirmed that older subjects showed poorer accuracy than younger subjects. As in Experiments 1 and 2, the Age × Contour Spacing interaction was not significant [$F_{(1,\ 22)} = 0.13$, $p = 0.72$], indicating that the effect of contour spacing did not differ for the two age groups. On the other hand, the Age × Relative Spacing interaction was significant [$F_{(4,\ 88)} = 5.11$, $\hat{\epsilon} = 0.67$, $p = 0.004$, $\eta_g^2 = 0.04$]. As can be seen in **Figure 8**, younger and older subjects showed equally good performance at a relative spacing of 1.0. However, as distracter spacing decreased, accuracy decreased more in older subjects than younger subjects. Finally, the Age × Contour Spacing × Relative Spacing interaction was not significant [$F_{(4,\ 88)} = 1.07$,

$\hat{\epsilon} = 0.61$, $p = 0.36$], indicating that the increased sensitivity to relative spacing in older subjects was not significantly different for contours with 3λ and 6λ spacing.

The effect of relative spacing was analysed further by computing the linear trend scores of accuracy across relative spacing and submitting them to a 2 (Age) × 2 (Contour Spacing) mixed-model ANOVA. The grand mean differed significantly from zero [$F_{(1, 22)} = 476.9, p < 0.0001$], confirming the presence of a significant linear trend. The main effect of contour spacing [$F_{(1, 22)} = 8.14, p = 0.009$] was significant, with higher linear trend scores for 3λ spacing than 6λ spacing. The main effect of Age also was significant [$F_{(1, 22)} = 9.92, p = 0.005$], reflecting the increased effect of relative spacing (i.e., a greater linear trend) in older subjects. The Age × Contour Spacing interaction was not significant [$F_{(1, 22)} = 1.74, p = 0.20$], indicating that the age difference in the linear trend across relative spacing was similar for contours with small and large spacings.

DISCUSSION

This experiment examined the effect of distracter inter-element spacing on contour discrimination for contours composed of elements with small and large spacing. We found that the effect of aging depended critically on the variability of the orientations of the distractor elements. When the orientation of each distracter was selected randomly and independently, contour discrimination accuracy declined monotonically with increasing relative spacing (i.e., the ratio of contour- and distractor-element spacing), consistent with previous reports (Kovács et al., 1999; Li and Gilbert, 2002), but the effect of relative spacing differed between age groups. Specifically, reducing distracter spacing decreased older subjects' accuracy much more than that of younger subjects. For example, response accuracy was equal in both groups when contour and distracter elements had equal spacing, but accuracy was as much as 28% lower in older subjects when distractor spacing was reduced by half. On the other hand, when all of the distractor elements had the same, randomly selected orientation, older and younger subjects were equally accurate at discriminating the spiral contours, even when contour elements were spaced far apart and were interspersed with distracter elements.

As in Experiment 1, the effect of aging did not vary with contour element separation, and the increase in the effect of aging with relative spacing also did not differ as a function of contour element separation. Thus, older subjects are not disproportionately impaired at integrating contours across larger distances, even when relative spacing of contour and distracter elements is high.

Overall, our results are consistent with findings of Del Viva and Agostini (2007) who showed that younger subjects could tolerate more distracters than older subjects when detecting circular closed contours composed of a varying number of Gabors (i.e., with varying inter-element separations). They also reported a greater effect of age for contours with small spacing (3.2λ), suggesting that aging may have a greater effect on contour integration over short-range separations (Del Viva and Agostini, 2007). Similarly, if we examine performance at the largest relative spacing condition in our data—i.e., conditions with the maximum number of distracters for each contour spacing (see **Figure 8**, relative spacing = 2.1)—the difference in average accuracy of younger and older subjects was in fact greater for contours with 3λ spacing compared to 6λ spacing. However, this differential effect was apparent only at the largest relative spacing and was not significant when examined over the full range of relative spacings.

GENERAL DISCUSSION

Previous research has shown that older subjects are less accurate at detecting and discriminating contours embedded in noisy or cluttered backgrounds (Del Viva and Agostini, 2007; McKendrick et al., 2010; Casco et al., 2011; Roudaia et al., 2011; Hadad, 2012). The current experiments examined how the age difference in contour discrimination accuracy varies with absolute and relative spacing between contour and distracter elements, contour element collinearity, stimulus duration, and background context. In all experiments, subjects were required to report the global orientation of a spiral contour composed of Gabor elements embedded within a homogeneous field of distracter Gabors having the same contrast, spatial frequency, and phase as the contour elements. The spiral contour was either clockwise or counter-clockwise, but its overall shape and size remained constant. The position and global orientation of the spiral varied across trials. The subjects' task in all three experiments was to report the location of the tail of the spiral. Care was taken to ensure that the alignment of the orientations of the contour elements was the only cue available for grouping the contour. A preliminary experiment indicated that young subjects required half of the contour elements to be visible in order to perform this task accurately in a condition that did not include distractor elements, which suggests that the task is a reasonable measure of how well subjects perceive the shape of an extended contour.

The current experiments revealed several novel findings. First, Experiment 1 showed that the effect of aging on contour discrimination does not vary with contour element spacing, at least over the range of spacings tested here (i.e., 2–8 times the Gabor wavelength). Second, Experiment 1 also showed that younger and older subjects are equally sensitive to disruptions in contour element collinearity at all contour element spacings tested. Third, Experiment 2 revealed that younger and older subjects can discriminate salient contours (collinear contours with small spacing) at very short stimulus durations (0.04 s). For less salient contours, older subjects showed a greater decline in performance with decreasing stimulus duration than younger subjects, consistent with previous research (Roudaia et al., 2011). Fourth, Experiment 3, revealed that the age difference in contour integration depended on the relative spacing between contour and distracter elements, rather than the absolute separation between contour elements. Lastly, both groups performed equally well when discriminating contours embedded in a dense field of iso-oriented distracters, showing that the presence of distracters *per se* is not sufficient to impair older subjects' performance.

The current study was the first to systematically examine contour discrimination for a range of contour spacings and collinearity levels in older subjects; however, the current results are consistent with several previous findings. For example, Del Viva

and Agostini (2007) found that the age-related reduction in sensitivity for detecting aligned contours among distracters did not vary with contour element spacing. In addition, a recent study found that the effect of aging on contour discrimination accuracy remained constant for contours with small and large inter-element spacings (Hadad, 2012). One seemingly contradictory study found that older subjects required a greater number of contour elements to correctly discriminate the shape of a sampled contour than younger subjects, leading its authors to conclude that older adults are especially impaired at integrating contours across large separations (McKendrick et al., 2010). However, their results may also be explained by a general decline in contour discrimination with aging as observed in our study. Indeed, if older subjects' accuracy is overall lower at all contour spacings, the minimum number of contour elements required to support a criterion level of performance will also be higher than that of younger subjects. Nonetheless, examining contour integration across a range of contour spacings in Experiment 1 revealed that aging affects performance equally for a range of contour spacings, not only at larger spacings. Finally, the current results also complement findings by McKendrick et al. by showing that increasing orientation jitter impairs contour shape discrimination to the same extent in younger and older subjects.

The sensitivity to collinearity in contour integration is thought to rely on orientation-tuned neurons in primary visual cortex and long-range horizontal connections between columns of similar orientation preference (Polat, 1999; Hess et al., 2003). Neurophysiological studies in older primates have revealed significant functional changes in V1 neurons, such as increased spontaneous activity, broader orientation tuning bandwidths, and decreased signal-to-noise ratios (Schmolesky et al., 2000; Zhang et al., 2008). Such changes in human visual cortex would be expected to lead to age-related changes in tolerance to orientation jitter in contour integration tasks. However, psychophysical and electrophysiological studies in humans have found no evidence for changes in orientation tuning (Delahunt et al., 2008; Govenlock et al., 2009, 2010) or orientation discrimination ability with age (Betts et al., 2007; Delahunt et al., 2008), even for very brief stimulus durations (Roudaia et al., 2011). Thus, the finding that sensitivity to collinearity in contour integration does not change with aging is consistent with human psychophysics and electrophysiology showing preserved mechanisms for orientation encoding.

Although contour element spacing and local orientation alignment had no influence on the effect of aging on contour discrimination, older subjects were more affected by decreasing stimulus duration than younger subjects when discriminating less salient contours in Experiment 2. This change in the time needed to discriminate contours is consistent with the results of (Roudaia et al., 2011), who found that older subjects needed longer stimulus durations to discriminate contours embedded in clutter. Roudaia et al. argued that the increase in duration thresholds could not be explained by age-related reductions in retinal illuminance (Weale, 1963, 1982), because reducing stimulus luminance by 90% did not increase duration thresholds in younger subjects. Moreover, Roudaia et al. found no age difference in the amount of time needed to detect individual Gabors or discriminate their orientation. Together with the current findings, these results suggest that the longer time needed to perceive extended contours with aging results from changes in processes involved in grouping the contours and/or segregating them from the background, as opposed to processing of individual elements.

The stimulus duration required to detect or discriminate a contour among distracters varies with the characteristics of the contour and background elements, the nature of the task (detection or discrimination), the presentation of a mask, as well as subjects' previous experience with the task (Braun, 1999; Hess et al., 2001; Mandon and Kreiter, 2005; Mathes et al., 2006; May and Hess, 2007; Dakin and Baruch, 2009). On the one hand, contour detection can be very rapid, especially when stimuli are not masked (Hess et al., 2001). Mandon and Kreiter (2005) reported that monkeys can detect and discriminate contours after a masked presentation of only 0.03 s. Fast contour integration in some cases could result from the involvement of linear filters in the detection of contours comprising collinear elements with constant contrast phase (Hess et al., 2003). In the current experiments, such linear detectors may have been involved in the discrimination of collinear contours in the 2λ spacing condition, which might explain the exceptionally good performance at short durations in that condition. The absence of an age effect in that condition is consistent with our previous results showing that the contribution of linear filters for contour discrimination does not change with aging (Roudaia et al., 2011). On the other hand, when contours comprise phase-alternating elements and linear filters cannot be employed, contour detection requires stimulus durations of ≈0.1 s for straight contours and up to ≈0.5 s for curved contours (Hess et al., 2001). The earliest contour-specific neural correlate appears ≈0.15 s after stimulus onset for collinear contours and its latency is significantly delayed for less detectable contours (Mathes et al., 2006; Tanskanen et al., 2008). The current results confirmed previous findings that the processing time for contour discrimination increases with aging, especially for less detectable contours (Roudaia et al., 2011). In contrast, previous studies have found no evidence of slower processing with aging for shape discrimination (Habak et al., 2009) or detection of motion (Bennett et al., 2007). What's more, younger subjects required longer stimulus durations than older subjects to discriminate the direction of large, high-contrast drifting gratings (Betts et al., 2005, 2009). Thus, contrary to the general slowing hypothesis (Salthouse, 2000), increases in processing time are not ubiquitous in aging and the nature of age-related slowing of the dynamics of contour integration poses an interesting question for future research.

In addition to requiring longer stimulus durations to discriminate contours, older subjects showed lower accuracy when the relative spacing of contour and distracter elements was high (i.e., when contour elements were sparser than distracter elements). By varying relative spacing for contours with small and large spacing in Experiment 3, we found that the effect of aging does not depend on the absolute number or density of distracters, but rather on the relative spacing of contour

and distracter elements. Previous studies have shown that contour detection is limited by the relative spacing of contour and background elements (Kovács, 1996; Braun, 1999; Kovács et al., 1999). When contour elements are spaced closer together than distracters, proximity and density cues may be used to locate and group the contour elements; when distracters are spaced closer together than contour elements, it is no longer possible to group contours based on density or proximity cues, so contour grouping must be based on the relative positions and orientations of the local elements (e.g., collinearity). Thus, contour integration becomes more difficult with increasing relative spacing because (a) greater proximity of distracters to contour elements increases the likelihood of grouping contour elements with adjacent distracters, instead of the neighboring contour elements; and (b) greater proximity of distracters to each other increases the likelihood of a chain of distractors grouping together to form false-positive contours that will compete with the target contour. Thus, differences in contour detection accuracy may be due to differences in grouping contour elements together and/or differences in the ability to select the appropriate contour among competing alternatives. Given that changes in the proximity and collinearity of contour elements had the same effect on younger and older subjects' contour discrimination performance in Experiment 1, the greater effect of relative spacing on contour integration in older subjects is likely to be caused by a reduced ability to segregate the contour from a cluttered background containing many distracters and false-positive contours.

What are the potential causes of the reduced ability to tolerate dense visual clutter in contour integration? Contour processing requires both the facilitation between responses to contour elements and suppression of responses to the background distracters (Polat, 1999; Hess et al., 2003; Dakin and Baruch, 2009; Gilad et al., 2013). The contour-related facilitation of V1 neurons is thought to be mediated by the intrinsic excitatory horizontal connections that link neurons with similar orientation preference and spatially non-overlapping receptive fields (Rockland and Lund, 1983; Gilbert and Wiesel, 1989; Amir et al., 1993; Malach et al., 1993; Stettler et al., 2002). The source of the suppression of distracters is not well known; however, Gilad et al. (2013) suggested that it may be mediated by top–down feedback on to the local inhibitory interneurons in V1, or through decreased excitatory feedback. Several investigators have suggested that age-related reductions in the efficacy of inhibitory interactions in the visual cortex (e.g., Leventhal et al., 2003) may contribute to age differences in contour integration (e.g., Roudaia et al., 2008, 2011; Casco et al., 2011). Furthermore, there is also evidence that aging may be associated with a delay in deploying top–down suppression (Gazzaley et al., 2008). To the extent that top–down suppression may be involved in contour integration, this delay may contribute to the increase in processing time needed to extract the target contour. A recent EEG study on contour detection revealed that prior knowledge that a stimulus was likely to contain a contour resulted in a decrease in posterior alpha power and fronto-posterior theta phase couplings, both of which have been proposed to reduce local inhibitory activity and increase excitability of the cortex (Volberg et al., 2013), leading to the suggestion that top–down control increases perceptual grouping by modulating the level of inhibition in early visual areas. Future studies are needed to clarify the relationship between age-related changes in levels of inhibition in visual areas, top–down control, and contour integration deficits.

Lastly, it is important to consider whether differences in cognitive strategy or perceptual decision-making may have contributed to age-related differences in performance in the current experiments. For example, in the current task, subjects may have accurately reported the location of the tail of the spiral on trials where they perceived only a part of the spiral by correctly extrapolating the rest of the spiral's shape. It can be argued that the small main effect of age observed in Experiment 1 may be due to differences in the use of such a cognitive strategy. However, such differences can not easily account for the increase in the effect of aging at short durations in Experiment 2, or the greater effect of relative spacing in older subjects in Experiment 3. Perceptual decision-making refers to the process of acquiring information from sensory neurons to make an appropriate response (Gold and Shadlen, 2007). Previous studies analysing response times in several perceptual tasks have found that older subjects were as efficient as younger subjects at accumulating sensory evidence in the decisional process, and that their slower performance was mainly due to more conservative response criteria and non-decisional processes (Ratcliff et al., 2006; Kühn et al., 2011). If the quality of contour-related sensory evidence was the same in both groups, but the efficiency of gathering the evidence was poorer in older subjects, decreases in stimulus duration should have had an equal detrimental effect on older subjects across all contour types, which was not the case. Moreover, given that subjects were not encouraged to respond quickly in the current experiments, age-differences in response criteria should not have affected performance in the current experiments. In sum, although differences in the use of cognitive strategies or perceptual decision making may contribute to age-differences in contour discrimination, they are not sufficient to explain the full pattern of results. Instead, the current findings are more consistent with age-related changes at the level where local elements are grouped into perceptual wholes.

CONCLUSION

The current study replicated previous findings of impaired contour integration with aging and revealed that the effect of aging does not vary with contour element spacing or with the local orientation alignment of contour elements. Instead, the effect of aging on contour integration increased with increasing contour-distracter relative spacing. Thus, perceptual grouping of contours is especially vulnerable to distracters with aging.

ACKNOWLEDGMENTS

This research was supported by grants from the Canadian Institute of Health Research and the Canada Research Chair Programme to Allison B. Sekuler and Patrick J. Bennett. We thank Donna Waxman for collecting data and all the participants for their contribution to research.

REFERENCES

Altmann, C. F., Bülthoff, H. H., and Kourtzi, Z. (2003). Perceptual organization of local elements into global shapes in the human visual cortex. *Curr. Biol.* 13, 342–349. doi: 10.1016/S0960-9822(03)00052-6

Amir, Y., Harel, M., and Malach, R. (1993). Cortical hierarchy reflected in the organization of intrinsic connections in macaque monkey visual cortex. *J. Comp. Neurol.* 334, 19–46. doi: 10.1002/cne.903340103

Angelucci, A., and Bullier, J. (2003). Reaching beyond the classical receptive field of V1 neurons: horizontal or feedback axons? *J. Physiol. (Paris)* 97, 141–154. doi: 10.1016/j.jphysparis.2003.09.001

Bakeman, R. (2005). Recommended effect size statistics for repeated measures designs. *Behav. Res. Meth.* 37, 379–384. doi: 10.3758/BF03192707

Beaudot, W. H., and Mullen, K. T. (2001). Processing time of contour integration: the role of colour, contrast, and curvature. *Perception* 30, 833–853. doi: 10.1068/p3164

Beaudot, W. H., and Mullen, K. T. (2003). How long range is contour integration in human color vision? *Vis. Neurosci.* 20, 51–64. doi: 10.1017/S0952523803201061

Bennett, P. J., Sekuler, A. B., McIntosh, A. R., and Della-Maggiore, V. (2001). The effects of aging on visual memory: evidence for functional reorganization of cortical networks. *Acta Psychol. (Amst.)* 107, 249–273. doi: 10.1016/S0001-6918(01)00037-3

Bennett, P. J., Sekuler, R., and Sekuler, A. B. (2007). The effects of aging on motion detection and direction identification. *Vis. Res.* 47, 799–809. doi: 10.1016/j.visres.2007.01.001

Betts, L. R., Sekuler, A. B., and Bennett, P. J. (2007). The effects of aging on orientation discrimination. *Vis. Res.* 47, 1769–1780. doi: 10.1016/j.visres.2007.02.016

Betts, L. R., Sekuler, A. B., and Bennett, P. J. (2009). Spatial characteristics of center-surround antagonism in younger and older adults. *J. Vis.* 9, 25.1–25.15. doi: 10.1167/9.1.25

Betts, L. R., Taylor, C. P., Sekuler, A. B., and Bennett, P. J. (2005). Aging reduces center-surround antagonism in visual motion processing. *Neuron* 45, 361–366. doi: 10.1016/j.neuron.2004.12.041

Brainard, D. H. (1997). The psychophysics toolbox. *Spat. Vis.* 10, 433–436. doi: 10.1163/156856897X00357

Braun, J. (1999). On the detection of salient contours. *Spat. Vis.* 12, 211–225. doi: 10.1163/156856899X00120

Casco, C., Robol, V., Barollo, M., and Cansino, S. (2011). Effects of aging on visual contour integration and segmentation. *Invest. Ophthalmol. Vis. Sci.* 52, 3955–3961. doi: 10.1167/iovs.10-5439

Cass, J. R., and Spehar, B. (2005). Dynamics of collinear contrast facilitation are consistent with long-range horizontal striate transmission. *Vis. Res.* 45, 2728–2739. doi: 10.1016/j.visres.2005.03.010

Ciaramelli, E., Leo, F., Del Viva M. M., Burr, D. C., and Ladavas, E. (2007). The contribution of prefrontal cortex to global perception. *Exp. Brain Res.* 181, 427–434. doi: 10.1007/s00221-007-0939-7

Dakin, S. C., and Baruch, N. J. (2009). Context influences contour integration. *J. Vis.* 9, 13.1–13.13. doi: 10.1167/9.2.13

Dakin, S. C., and Hess, R. F. (1998). Spatial-frequency tuning of visual contour integration. *J. Opt. Soc. Am., Opt. Image Sci. Vis.* 15, 1486–1499. doi: 10.1364/JOSAA.15.001486

Delahunt, P. B., Hardy, J. L., and Werner, J. S. (2008). The effect of senescence on orientation discrimination and mechanism tuning. *J. Vis.* 8, 1–9. doi: 10.1167/8.3.5

Della-Maggiore, V., Sekuler, A. B., Grady, C. L., Bennett, P. J., Sekuler, R., and McIntosh, A. R. (2000). Corticolimbic interactions associated with performance on a short-term memory task are modified by age. *J. Neurosci.* 20, 8410–8416.

Del Viva M. M., and Agostini, R. (2007). Visual spatial integration in the elderly. *Invest. Ophth. Vis. Sci.* 48, 2940–2946. doi: 10.1167/iovs.06-0729

Dumoulin, S. O., and Hess, R. F. (2007). Cortical specialization for concentric shape processing. *Vis. Res.* 47, 1608–1613. doi: 10.1016/j.visres.2007.01.031

Elder, J. H., and Goldberg, R. M. (2002). Ecological statistics of Gestalt laws for the perceptual organization of contours. *J. Vis.* 2, 324–353. doi: 10.1167/2.4.5

Elliott, D. B., Sanderson, K., and Conkey, A. (1990). The reliability of the pelli-robson contrast sensitivity chart. *Opht. Physiol. Opt.* 10, 21–24. doi: 10.1111/j.1475-1313.1990.tb01100.x

Faubert, J. (2002). Visual perception and aging. *Can. J. Exp. Psychol.* 56, 164–176. doi: 10.1037/h0087394

Field, D. J., Hayes, A., and Hess, R. F. (1993). Contour integration by the human visual system: Evidence for a local "association field." *Vis. Res.* 33, 173–193. doi: 10.1016/0042-6989(93)90156-Q

Folstein, M. F., Folstein, S. E., and McHugh, P. R. (1975). "Mini-mental state." A practical method for grading the cognitive state of patients for the clinician. *J. Psychiatr. Res.* 12, 189–198. doi: 10.1016/0022-3956(75)90026-6

Fu, Y., Wang, X. S., Wang, Y. C., Zhang, J., Liang, Z., Zhou, Y. F., et al. (2010). The effects of aging on the strength of surround suppression of receptive field of v1 cells in monkeys. *Neuroscience* 169, 874–881. doi: 10.1016/j.neuroscience.2010.05.015

Gazzaley, A., Clapp, W., Kelley, J., McEvoy, K., Knight, R. T., and D'Esposito, M. (2008). Age-related top-down suppression deficit in the early stages of cortical visual memory processing. *Proc. Natl. Acad. Sci. U.S.A.* 105, 13122–13126. doi: 10.1073/pnas.0806074105

Geisler, W. S., and Perry, J. S. (2009). Contour statistics in natural images: grouping across occlusions. *Vis. Neurosci.* 26, 109–121. doi: 10.1017/S0952523808080875

Geisler, W. S., Perry, J. S., Super, B. J., and Gallogly, D. P. (2001). Edge co-occurrence in natural images predicts contour grouping performance. *Vis. Res.* 41, 711–724. doi: 10.1016/S0042-6989(00)00277-7

Gilad, A., Meirovithz, E., and Slovin, H. (2013). Population responses to contour integration: early encoding of discrete elements and late perceptual grouping. *Neuron* 78, 389–402. doi: 10.1016/j.neuron.2013.02.013

Gilbert, C., Ito, M., Kapadia, M., and Westheimer, G. (2000). Interactions between attention, context and learning in primary visual cortex. *Vis. Res.* 40, 1217–1226. doi: 10.1016/S0042-6989(99)00234-5

Gilbert, C. D., and Wiesel, T. N. (1989). Columnar specificity of intrinsic horizontal and corticocortical connections in cat visual cortex. *J. Neurosci.* 9, 2432–2442.

Gold, J. I., and Shadlen, M. N. (2007). The neural basis of decision making. *Annu. Rev. Neurosci.* 30, 535–574. doi: 10.1146/annurev.neuro.29.051605.113038

Govenlock, S. W., Taylor, C. P., Sekuler, A. B., and Bennett, P. J. (2009). The effect of aging on the orientational selectivity of the human visual system. *Vis. Res.* 49, 164–172. doi: 10.1016/j.visres.2008.10.004

Govenlock, S. W., Taylor, C. P., Sekuler, A. B., and Bennett, P. J. (2010). The effect of aging on the spatial frequency selectivity of the human visual system. *Vis. Res.* 50, 1712–1719. doi: 10.1016/j.visres.2010.05.025

Habak, C., and Faubert, J. (2000). Larger effect of aging on the perception of higher-order stimuli. *Vis. Res.* 40, 943–950. doi: 10.1016/S0042-6989(99)00235-7

Habak, C., Wilkinson, F., and Wilson, H. R. (2009). Preservation of shape discrimination in aging. *J. Vis.* 9, 18.1–18.8. doi: 10.1167/9.12.18

Hadad, B.-S. (2012). Sensitivity of spatial integration to perceptual cues is preserved in healthy aging. *Vis. Res.* 60, 1–6. doi: 10.1016/j.visres.2012.03.002

Hadad, B.-S., Maurer, D., and Lewis, T. L. (2010). The effects of spatial proximity and collinearity on contour integration in adults and children. *Vis. Res.* 50, 772–778. doi: 10.1016/j.visres.2010.01.021

Hess, R. F., Beaudot, W. H., and Mullen, K. T. (2001). Dynamics of contour integration. *Vis. Res.* 41, 1023–1037. doi: 10.1016/S0042-6989(01)00020-7

Hess, R. F., and Dakin, S. C. (1997). Absence of contour linking in peripheral vision. *Nature* 390, 602–604. doi: 10.1038/37593

Hess, R. F., Hayes, A., and Field, D. J. (2003). Contour integration and cortical processing. *J. Physiol. (Paris)* 97, 105–119. doi: 10.1016/j.jphysparis.2003.09.013

Kapadia, M. K., Ito, M., Gilbert, C. D., and Westheimer, G. (1995). Improvement in visual sensitivity by changes in local context: parallel studies in human observers and in v1 of alert monkeys. *Neuron* 15, 843–856. doi: 10.1016/0896-6273(95)90175-2

Kourtzi, Z., and Huberle, E. (2005). Spatiotemporal characteristics of form analysis in the human visual cortex revealed by rapid event-related fMRI adaptation. *Neuroimage* 28, 440–452. doi: 10.1016/j.neuroimage.2005.06.017

Kourtzi, Z., Tolias, A. S., Altmann, C. F., Augath, M., and Logothetis, N. K. (2003). Integration of local features into global shapes: monkey and human fmri studies. *Neuron*

37, 333–346. doi: 10.1016/S0896-6273(02)01174-1

Kovács, I. (1996). Gestalten of today: early processing of visual contours and surfaces. *Behav. Brain Res.* 82, 1–11. doi: 10.1016/S0166-4328(97)81103-5

Kovács, I., and Julesz, B. (1993). A closed curve is much more than an incomplete one: effect of closure in figure-ground segmentation. *Proc. Natl. Acad. Sci. U.S.A.* 90, 7495–7497. doi: 10.1073/pnas.90.16.7495

Kovács, I., Kozma, P., Fehér, A., and Benedek, G. (1999). Late maturation of visual spatial integration in humans. *Proc. Natl. Acad. Sci. U.S.A.* 96, 12204–12209. doi: 10.1073/pnas.96.21.12204

Kuai, S.-G., and Yu, C. (2006). Constant contour integration in peripheral vision for stimuli with good Gestalt properties. *J. Vis.* 6, 1412–1420. doi: 10.1167/6.12.7

Kühn, S., Schmiedek, F., Schott, B., Ratcliff, R., Heinze, H.-J., Düzel, E., et al. (2011). Brain areas consistently linked to individual differences in perceptual decision-making in younger as well as older adults before and after training. *J. Cogn. Neurosci.* 23, 2147–2158. doi: 10.1162/jocn.2010.21564

Lawrence, M. A. (2011). *ez: Easy Analysis and Visualization of Factorial Experiments*. [Computer software manual] (R package version 3.0-0).

Ledgeway, T., Hess, R. F., and Geisler, W. S. (2005). Grouping local orientation and direction signals to extract spatial contours: empirical tests of "association field" models of contour integration. *Vis. Res.* 45, 2511–2522. doi: 10.1016/j.visres.2005.04.002

Leventhal, A. G., Wang, Y. C., Pu, M. L., Zhou, Y. F., and Ma, Y. Y. (2003). Gaba and its agonists improved visual cortical function in senescent monkeys. *Science* 300, 812–815. doi: 10.1126/science.1082874

Li, W., and Gilbert, C. D. (2002). Global contour saliency and local colinear interactions. *J. Neurophysiol.* 88, 2846–2856. doi: 10.1152/jn.00289.2002

Li, W., Piëch, V., and Gilbert, C. D. (2006). Contour saliency in primary visual cortex. *Neuron* 50, 951–962. doi: 10.1016/j.neuron.2006.04.035

Li, W., Piëch, V., and Gilbert, C. D. (2008). Learning to link visual contours. *Neuron* 57, 442–451. doi: 10.1016/j.neuron.2007.12.011

Machilsen, B., Novitskiy, N., Vancleef, K., and Wagemans, J. (2011). Context modulates the erp signature of contour integration. *PLoS ONE* 6:e25151. doi: 10.1371/journal.pone.0025151

Malach, R., Amir, Y., Harel, M., and Grinvald, A. (1993). Relationship between intrinsic connections and functional architecture revealed by optical imaging and *in vivo* targeted biocytin injections in primate striate cortex. *Proc. Natl. Acad. Sci. U.S.A.* 90, 10469–10473. doi: 10.1073/pnas.90.22.10469

Mandon, S., and Kreiter, A. K. (2005). Rapid contour integration in macaque monkeys. *Vis. Res.* 45, 291–300. doi: 10.1016/j.visres.2004.08.010

Mäntyjärvi, M., and Laitinen, T. (2001). Normal values for the Pelli-Robson contrast sensitivity test. *J. Cataract. Ref. Surg.* 27, 261–266. doi: 10.1016/S0886-3350(00)00562-9

Mathes, B., and Fahle, M. (2007). Closure facilitates contour integration. *Vis. Res.* 47, 818–827. doi: 10.1016/j.visres.2006.11.014

Mathes, B., Trenner, D., and Fahle, M. (2006). The electrophysiological correlate of contour integration is modulated by task demands. *Brain Res.* 1114, 98–112. doi: 10.1016/j.brainres.2006.07.068

Maxwell, S., and Delaney, H. (2004). *Designing Experiments and Analyzing Data: A Model Comparison Approach*. 2nd Edn. Mahwah, NJ: Lawrence Erlbaum Associates.

May, K. A., and Hess, R. F. (2007). Dynamics of snakes and ladders. *J. Vis.* 7, 13.1–13.9. doi: 10.1167/7.12.13

McIntosh, A. R., Sekuler, A. B., Penpeci, C., Rajah, M. N., Grady, C. L., Sekuler, R., et al. (1999). Recruitment of unique neural systems to support visual memory in normal aging. *Curr. Biol.* 9, 1275–1278. doi: 10.1016/S0960-9822(99)80512-0

McKendrick, A. M., Weymouth, A. E., and Battista, J. (2010). The effect of normal aging on closed contour shape discrimination. *J. Vis.* 10, 1.1–1.9. doi: 10.1167/10.2.1

Nikolaev, A. R., and van Leeuwen, C. (2007). Collinearity, curvature interpolation, and the power of perceptual integration. *Psychol. Res.* 71, 427–437. doi: 10.1007/s00426-005-0026-2

Nygård, G. E., Sassi, M., and Wagemans, J. (2011). The influence of orientation and contrast flicker on contour saliency of outlines of everyday objects. *Vis. Res.* 51, 65–73. doi: 10.1016/j.visres.2010.09.032

Olejnik, S., and Algina, J. (2003). Generalized eta and omega squared statistics: measures of effect size for some common research designs. *Psychol. Meth.* 8, 434–447. doi: 10.1037/1082-989X.8.4.434

Pelli, D., Robson, J., and Wilkins, A. (1988). The design of a new chart for measuring contrast sensitivity. *Clin. Vis. Sci.* 2, 187–199.

Pelli, D. G. (1997). The videotoolbox software for visual psychophysics: transforming numbers into movies. *Spat. Vis.* 10, 437–442. doi: 10.1163/156856897X00366

Polat, U. (1999). Functional architecture of long-range perceptual interactions. *Spat. Vis.* 12, 143–162. doi: 10.1163/156856899X00094

Polat, U., and Sagi, D. (1993). Lateral interactions between spatial channels: suppression and facilitation revealed by lateral masking experiments. *Vis. Res.* 33, 993–999. doi: 10.1016/0042-6989(93)90081-7

R Development Core Team (2008). *R: A Language and Environment for Statistical Computing*. R Foundation for Statistical Computing, Vienna, Austria (http://www.R-project.org).

Ratcliff, R., Thapar, A., and McKoon, G. (2006). Aging and individual differences in rapid two-choice decisions. *Psychon. Bull. Rev.* 13, 626–635. doi: 10.3758/BF03193973

Regan, D., and Hamstra, S. J. (1992). Shape discrimination and the judgement of perfect symmetry: dissociation of shape from size. *Vis. Res.* 32, 1845–1864. doi: 10.1016/0042-6989(92)90046-L

Rockland, K. S., and Lund, J. S. (1983). Intrinsic laminar lattice connections in primate visual cortex. *J. Comp. Neurol.* 216, 303–318. doi: 10.1002/cne.902160307

Roudaia, E., Bennett, P. J., and Sekuler, A. B. (2008). The effect of aging on contour integration. *Vis. Res.* 48, 2767–2774. doi: 10.1016/j.visres.2008.07.026

Roudaia, E., Farber, L. E., Bennett, P. J., and Sekuler, A. B. (2011). The effects of aging on contour discrimination in clutter. *Vis. Res.* 51, 1022–1032. doi: 10.1016/j.visres.2011.02.015

Rousselet, G. A., Husk, J. S., Pernet, C. R., Gaspar, C. M., Bennett, P. J., and Sekuler, A. B. (2009). Age-related delay in information accrual for faces: evidence from a parametric, single-trial eeg approach. *BMC Neurosci.* 10:114. doi: 10.1186/1471-2202-10-114

Saarinen, J., and Levi, D. M. (2001). Integration of local features into a global shape. *Vis. Res.* 41, 1785–1790. doi: 10.1016/S0042-6989(01)00058-X

Salthouse, T. A. (2000). Aging and measures of processing speed. *Biol. Psychol.* 54, 35–54. doi: 10.1016/S0301-0511(00)00052-1

Sassi, M., Vancleef, K., Machilsen, B., Panis, S., and Wagemans, J. (2010). Identification of everyday objects on the basis of gaborized outline versions. *i-Perception* 1, 121–142. doi: 10.1068/i0384

Schmolesky, M. T., Wang, Y., Pu, M., and Leventhal, A. G. (2000). Degradation of stimulus selectivity of visual cortical cells in senescent rhesus monkeys. *Nat. Neurosci.* 3, 384–390. doi: 10.1038/73957

Schumacher, J. F., Quinn, C. F., and Olman, C. A. (2011). An exploration of the spatial scale over which orientation-dependent surround effects affect contour detection. *J. Vis.* 11:12. doi: 10.1167/11.8.12

Sekuler, R., and Ball, K. (1986). Visual localization: age and practice. *J. Opt. Soc. Am. A* 3, 864–867. doi: 10.1364/JOSAA.3.000864

Sekuler, R., and Sekuler, A. B. (2000). "Visual perception and cognition," in *Oxford Textbook of Geriatric Medicine*. 2nd Edn., eds J. Evans, T. Williams, B. Beattie, J.-P. Michel and G. Wilcock (New York, NY: Oxford University Press), 753–756.

Sigman, M., Cecchi, G. A., Gilbert, C. D., and Magnasco, M. O. (2001). On a common circle: natural scenes and gestalt rules. *Proc. Natl. Acad. Sci. U.S.A.* 98, 1935–1940. doi: 10.1073/pnas.98.4.1935

Spear, P. D. (1993). Neural bases of visual deficits during aging. *Vis. Res.* 33, 2589–2609. doi: 10.1016/0042-6989(93)90218-L

Stettler, D. D., Das, A., Bennett, J., and Gilbert, C. D. (2002). Lateral connectivity and contextual interactions in macaque primary visual cortex. *Neuron* 36, 739–750. doi: 10.1016/S0896-6273(02)01029-2

Tanskanen, T., Saarinen, J., Parkkonen, L., and Hari, R. (2008). From local to global: cortical dynamics of contour integration. *J. Vis.* 8, 15.1–15.12. doi: 10.1167/8.7.15

Verghese, P. (2009). Contours in noise: a role for self-cuing? *J. Vis.* 9, 2.1–2.16. doi: 10.1167/9.13.2

Volberg, G., Wutz, A., and Greenlee, M. W. (2013). Top-down control in contour grouping. *PLoS ONE* 8:e54085. doi: 10.1371/journal.pone.0054085

Watt, R., Ledgeway, T., and Dakin, S. C. (2008). Families of models for gabor paths demonstrate the importance of spatial adjacency. *J. Vis.* 8, 23. 1–23.19. doi: 10.1167/8.7.23

Weale, R. A. (1963). *The Aging Eye*. London: Lewis.

Weale, R. A. (1982). "Senile ocular changes, cell death, and vision," in *Aging and Visual Function*, eds R. Sekuler, D. Kline, and K. Dismukes (New York, NY: Liss), 161–171.

Zhang, J., Wang, X., Wang, Y., Fu, Y., Liang, Z., Ma, Y., et al. (2008). Spatial and temporal sensitivity degradation of primary visual cortical cells in senescent rhesus monkeys. *Eur. J. Neurosci.* 28, 201–207. doi: 10.1111/j.1460-9568.2008.06300.x

Conflict of Interest Statement: The authors declare that the research was conducted in the absence of any commercial or financial relationships that could be construed as a potential conflict of interest.

Received: 08 January 2013; accepted: 31 May 2013; published online: 20 June 2013.

Citation: Roudaia E, Bennett PJ and Sekuler AB (2013) Contour integration and aging: the effects of element spacing, orientation alignment and stimulus duration. Front. Psychol. ***4****:356. doi: 10.3389/fpsyg.2013.00356*

This article was submitted to Frontiers in Perception Science, a specialty of Frontiers in Psychology.

frontiers in PSYCHOLOGY

ORIGINAL RESEARCH ARTICLE
published: 23 May 2013
doi: 10.3389/fpsyg.2013.00267

Aging and audio-visual and multi-cue integration in motion

Eugenie Roudaia[1,2], Allison B. Sekuler[1]*, Patrick J. Bennett[1] and Robert Sekuler[3]

[1] Department of Psychology, Neuroscience, and Behaviour, McMaster University, Hamilton, ON, Canada
[2] Institute of Neuroscience, Trinity College Dublin, Dublin, Ireland
[3] Volen Center for Complex Systems, Brandeis University, Waltham, MA, USA

Edited by:
Mark W. Greenlee, University of Regensburg, Germany

Reviewed by:
Gyula Kovács, Budapest University of Technology, Hungary
John Andersen, University of California, USA
Clara Casco, University of Padova, Italy

***Correspondence:**
Allison B. Sekuler, Vision and Cognitive Neuroscience Laboratory, PC 428, Department of Psychology, Neuroscience, and Behaviour, McMaster University 1280 Main Street West Hamilton, ON L8S 4K1, Canada.
e-mail: sekuler@mcmaster.ca

The perception of naturalistic events relies on the ability to integrate information from multiple sensory systems, an ability that may change with healthy aging. When two objects move toward and then past one another, their trajectories are perceptually ambiguous: the objects may seem to stream past one another or bounce off one another. Previous research showed that auditory or visual events that occur at the time of disks' coincidence could bias the percept toward bouncing or streaming. We exploited this malleable percept to assay age-related changes in the integration of multiple inter- and intra-modal cues. The disks' relative luminances were manipulated to produce stimuli strongly favoring either bouncing or streaming, or to produce ambiguous motion (equal luminances). A sharp sound coincident with the disks' overlap increased both groups' perception of bouncing, but did so significantly less for older subjects. An occluder's impact on motion perception varied with its duration: a long duration occluder promoted streaming in both groups; a brief occluder promoted bouncing in younger subjects, but not older ones. Control experiments demonstrated that the observed differences between younger and older subjects resulted from neither age-related changes in retinal illuminance nor age-related changes in hearing, pointing to weakened inter- and intra-modal integration with aging. These changes could contribute to previously demonstrated age-related perceptual and memory deficits.

Keywords: ageing, aging, multisensory integration, motion perception, audio-visual integration, multiple cues combination, bounce-stream

INTRODUCTION

How the brain manages to coordinate and integrate information received from multiple sources is one of cognitive neuroscience's central questions. After all, integration of information from multiple sources is crucial for perception and for other cognitive functions. Many studies have focused on one particular form of integration that holds especial importance: the integration of information from multiple senses (e.g., Soto-Faraco et al., 2003; Yuval-Greenberg and Deouell, 2007; Bruns and Getzmann, 2008; Schutz and Kubovy, 2009; Bizley et al., 2012; Naci et al., 2012). Given the fact that we inhabit a world in which events tend to be multisensory, researchers' emphasis on multisensory integration is well placed. As is the case with many other cognitive functions, multisensory integration seems to change with age (for review, see Mozolic et al., 2012). In particular, older subjects show greater multisensory enhancement than younger subjects when processing complex audio-visual stimuli, such as speech (Cienkowski and Carney, 2002; Maguinness et al., 2011; Winneke and Phillips, 2011), or when detecting or discriminating simple multisensory stimuli (Laurienti et al., 2006; Peiffer et al., 2007; Mahoney et al., 2011, c.f., Stephen et al., 2010). However, the reasons for enhanced multisensory integration in aging are not well understood. Because various aspects of motion perception are also affected by age (Habak and Faubert, 2000; Norman et al., 2003; Bennett et al., 2007; Andersen and Ni, 2008; Billino et al., 2008; Pilz et al., 2010; Roudaia et al., 2010), we decided to use motion perception as an arena within which to examine age-related changes in multisensory integration. For this purpose, we focused on a visual stimulus whose alternative, competing percepts are strongly influenced by accompanying sound.

This bistable, but malleable, percept arises when an observer observes two identical objects that move steadily toward one another, coincide, and then move apart. The appearance of the objects' trajectory fluctuates: the two moving objects sometimes appear to stream directly through one another, but sometimes they seem to bounce off one another (Metzger, 1934). The ambiguity of the stimulus is curtailed when a sharp sound is presented as the objects coincide (Sekuler et al., 1997; Shimojo et al., 2001; Watanabe and Shimojo, 2001; Remijn et al., 2004; Sanabria et al., 2004; Zhou et al., 2007). The sound strongly biases the percept, causing the objects to seem to bounce off one another.

The perceptual outcome of the ambiguous visual stimulus also can be biased by changes in the visual display itself. For example, when an opaque occluder obscures the region of the display in which the objects will coincide, the presence of the occluder promotes the appearance that the moving objects streamed through one another (Sekuler and Sekuler, 1999). This result may be related to other conditions in which an object's perceptual continuity is preserved in the face of a temporary occlusion (Feldman and Tremoulet, 2006). The ability to track an occluded object has obvious potential evolutionary value. In the laboratory, this ability has been studied most intensively with multiple object tracking (Scholl and Pylyshyn, 1999; Alvarez et al., 2005; Horowitz et al., 2006), which has been shown to decline with aging (Trick et al.,

2005; Sekuler et al., 2008; Kennedy et al., 2009). Assad and Maunsell (1995) described a class of neurons that may contribute to this preservation of identity by signaling the presence of a briefly occluded moving object.

To preview, we exploited the ambiguous bouncing-streaming percept as a vehicle for assaying possible age-related changes in the integration of both inter- and intra-modal cues for visual motion. Because an occluder's perceptual impact seems to vary with its temporal properties (Sekuler and Palmer, 1992; Murray et al., 2001; Guttman et al., 2003; Remijn et al., 2004), we simultaneously examined how age affected occlusion's impact on the bistable, bouncing-streaming percept.

EXPERIMENT ONE

METHODS

Apparatus

The experiment was programed in the Matlab environment (version 7.2) using the Psychophysics and Video Toolboxes, v. 3.0.8) (Brainard, 1997; Pelli, 1997) on a Macintosh G5 computer running OS X (10.4.11). Visual stimuli were presented in a dark room on a 21-inch Sony Trinitron monitor with 1280 × 1024 resolution (pixel size = 0.03°) and a refresh rate of 60 Hz. The display area subtended 38.4 × 30.7° visual angle, at a viewing distance of 57 cm. The mean luminance of the display was 37.5 cd/m^2, and provided the only light source in the testing room. Head position and viewing distance were stabilized using a forehead/chin support. Auditory stimuli were presented through Harman/Kardan SoundSticks III speakers located at display height, 33° to the left and right of the subject's mid-sagittal plane. The speakers' frequency response was 44–20 kHz, ±10 dB. As the speakers' subwoofer emits a distinct glow when the speakers are powered up, we covered them with black fabric to render them invisible during testing. Sound measurements were made with a Brüel & Kjaer 2239 sound level meter located where a subject's head would be during the experiment. Subjects' responses were collected with a standard English language keyboard.

Stimuli and design

Two disks (radius = 1.5°) appeared at ±9° horizontal eccentricity and 3° above fixation, and moved horizontally toward each other, overlapped in the middle of the display, and continued on, finally reaching the opposite sides of the display. The disks maintained a constant speed of 12°/s for 1.5 s, after which time they disappeared.

The relative luminances of the two disks were manipulated in order to promote ambiguity of motion, or to strongly favor a particular percept, either bouncing or streaming. In all *Ambiguous* conditions, the two disks had the same luminance with −0.7 contrast with the background. To generate stimuli for two *Unambiguous* conditions, we exploited a previous demonstration that two objects' perceived trajectories depend upon the way that the objects' features vary or do not vary over time (Feldman and Tremoulet, 2006). Specifically, in *Unambiguous* conditions, the two disks had −0.85 and −0.55 contrast with the background respectively, and their motion was either unambiguously *Streaming*, so that each disk crossed from one side to the other, or unambiguously *Bouncing*, so that each disk traveled to the point of coincidence and returned to its starting point (see **Figure 2**).

In some conditions, a synthesized click (90 dBC; 0.070 s duration) sounded as the disks were coinciding. The click was produced by modifying the Karplus-Strong algorithm (Karplus and Strong, 1983) to generate a broadband stimulus with sharp onset and flat frequency spectrum. **Figure 1A** shows this click's spectrogram[1]. In some conditions, an opaque rectangular occluder (3.14° × 5.4°; contrast = −0.4) was presented above the fixation point and obscured the disks' coincidence. The duration of the occluder was either *Short* (0.117 s in duration), *Medium* (0.233 s in duration) or *Long* (extending over the entire trial, that is, 1.5 s), centered around the time of coincidence (i.e., 0.75 s).

There were 12 stimulus conditions. In six conditions, the disks had unbalanced luminances, with three conditions consistent with a bouncing percept and three conditions consistent with a streaming percept. The unambiguous disk motions were presented alone (*Bounce*, *Stream*), together with a sound at coincidence (*Bounce* + *Sound*, *Stream* + *Sound*), or along with a medium duration occluder (*Bounce* + *Medium*, *Stream* + *Medium*). In the remaining six conditions, the disks had equal luminance, rendering their movement trajectory ambiguous. In these conditions, the disks were presented alone (*Ambiguous*), with a sound at coincidence (*Ambiguous* + *Sound*), with occluders of different duration (*Ambiguous* + *Short*, *Ambiguous* + *Medium*, *Ambiguous* + *Long*), or with a sound and an medium duration occluder (*Ambiguous* + *Sound* + *Medium*). This combination of conditions promoted a relatively equal proportion of "Bouncing" and "Streaming" responses, and balanced the distribution of cues (sound and occluders) across conditions of unambiguous and ambiguous motion. **Figure 2** illustrates the sequence of events comprising all 12 conditions.

Subjects

Thirteen younger and 16 older subjects, who were naïve as to the purposes of the study, participated in this experiment and were compensated for their time at a rate of $10/h. Near and far Snellen acuities and Pelli-Robson contrast sensitivity were measured while subjects wore their customary prescription. All subjects had Snellen acuity of 20/30 or better, as well as good contrast sensitivity. Older subjects averaged 29.1/30 on the Mini-Mental State Exam (Folstein et al., 1975). To be included in the analyses, subjects had to report "streaming" 70% of the time in the *Stream* condition and report "bouncing" 70% of the time in the *Bounce* condition. This criterion resulted in the exclusion of one younger and three older subjects. The demographic information for the remaining 12 younger subjects and 13 older subjects included in the analyses is presented in **Table 1**.

Procedure

The McMaster University Research Ethics Board approved the experimental protocol. Written informed consent was obtained from all subjects prior to their participation in the experiment.

Prior to beginning the experiments, subjects were told that they would be asked to judge whether two disks that traveled toward

[1]The sound is more properly categorized as a *pluck*, but for consistency with previous reports we opt to use the term *click*.

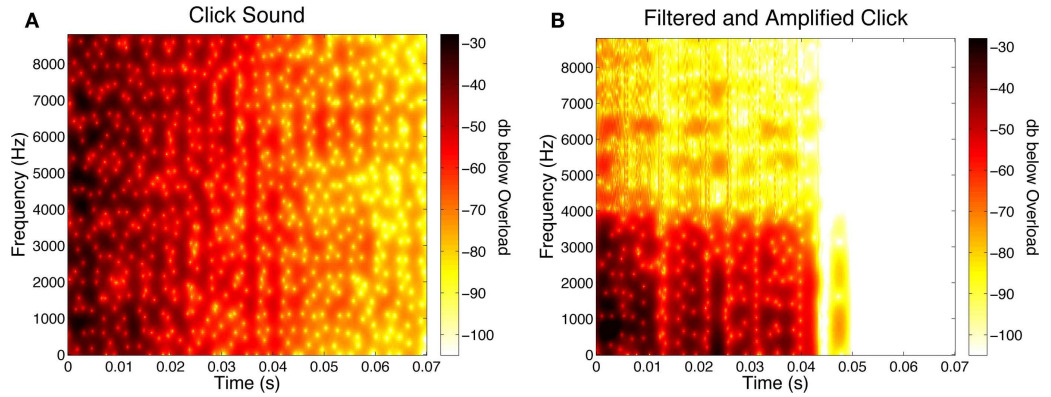

FIGURE 1 | (A) Spectrogram of the click sound used in Experiment One. This plot shows the amplitude of different frequencies of the sound over time. The color bar represent values of dBov (decibels below overload, which is the maximum amplitude before signal clipping would occur). In the bar in the spectrogram, darker colors represent higher amplitudes. Note that in the spectrogram stimulus amplitude initially is high at frequencies over the entire spectrum, but gradually diminishes over time. **(B)** Spectrogram of a click used in Experiment Three. The spectrogram shown is for the age-sensitive, filtered click that has been amplified to match the loudness of the unfiltered click. Note that early on, high amplitude is seen only at the lowest frequencies. Notice also, that above ∼3 kHz, amplitudes are less than at the corresponding frequencies in the unfiltered click.

each other streamed past each other, or bounced off of each other. To demonstrate these two situations, subjects were shown four examples of a red and blue disk that seemed to stream past each other and four examples of a red and blue disk that seemed to bounce off each other. Subjects were then informed that sometimes the two disks will have different luminance, or have the same luminance. Subjects were also informed that a brief sound, an occluder, or both a sound and an occluder will sometimes be presented during the disks' motion. Subjects were told to ignore these events and to concentrate on reporting the disks' pattern of motion.

Each trial began with the presentation of a black fixation point (diameter = 0.25˚) at the center of the screen. Subjects were instructed to fixate this location throughout each trial. The fixation point flickered at 10 Hz for 0.3 s to attract the subject's attention. After a delay of 0.1 s, the disks appeared and moved steadily across the screen for 1.5 s. After the disks disappeared, the letters "B" and "S" appeared on either side of fixation and remained on the screen until the subject's response. The mapping of "B" and "S" to right and left sides was counterbalanced in each group, so that half the subjects in each group responded by pressing "B" with their dominant hand and "S" with their non-dominant hand. No response feedback was given. The following trial began 1.5 s after the response.

Each subject completed nine blocks of trials, each containing four repetitions of each of 12 stimulus conditions presented in randomly intermixed order, resulting in a total of 36 trials per condition. The experimental blocks were preceded by a practice block of 24 trials consisting of two trials per condition in randomly intermixed order.

After the experiment, older subjects also completed a short hearing test to determine whether they could successfully hear our sound stimulus. In the test, 10 sounds were played at random intervals ranging from 3 to 10 s. Subjects were asked to press the space-bar on a computer keyboard as soon as they heard the sound. Every subject successfully detected all 10 sounds. Two subjects each gave one false alarm, that is, they pressed the space-bar when no sound had been presented. One other subject committed eight false alarms. That subject had also shown low accuracy in conditions of unambiguous motion, and was excluded from further data analyses.

RESULTS

All statistical analyses were performed using the statistical computing environment R (The R Project for Statistical Computing, 2012). The proportion of "Bouncing" and "Streaming" responses was calculated for each condition. As mentioned earlier, for four subjects (one younger), the unambiguous conditions failed to produce their intended effect: one younger subject showed 0.47 "Streaming" judgments in the *Stream* condition, one older subjects produced 0.67 "Bouncing" judgments the *Bounce* condition and only 0.56 "Streaming" judgments in the *Stream* condition, and two other older subjects produced just 0.56 and 0.44 "Bouncing" judgments in the *Bounce* condition. All data from these subjects were excluded.

UNAMBIGUOUS CONDITIONS RESULTS

The proportion of "Bouncing" responses in the six unambiguous conditions whose unbalanced disk luminances were meant to promote perceptual consistency are shown in **Figure 3**. With the exception of the subjects whose data were excluded, the stimuli in these conditions were equally effective for younger and older subjects. Moreover, for either group, the addition of a sound or of an occluder to these stimuli had no effect on perceptual judgments. The proportion of "Bouncing" responses in both age groups in the unambiguous *Bounce* and unambiguous *Stream* conditions were analysed in two separate 2 (age) × 3 (condition: *alone*, with *Sound*, with *Occluder*) split-plot ANOVAs. The main effects of age, condition, and the Age × Condition interaction were not significant for either the *Bounce* condition (age: $F(1, 23) = 0.42$, $p = 0.53$; condition: $F(2, 46) = 1.58$, $\hat{\epsilon} = 0.91$, $p = 0.22$; Age × Condition: $F(2, 46) = 2.04$, $\hat{\epsilon} = 0.98$, $p = 0.14$)

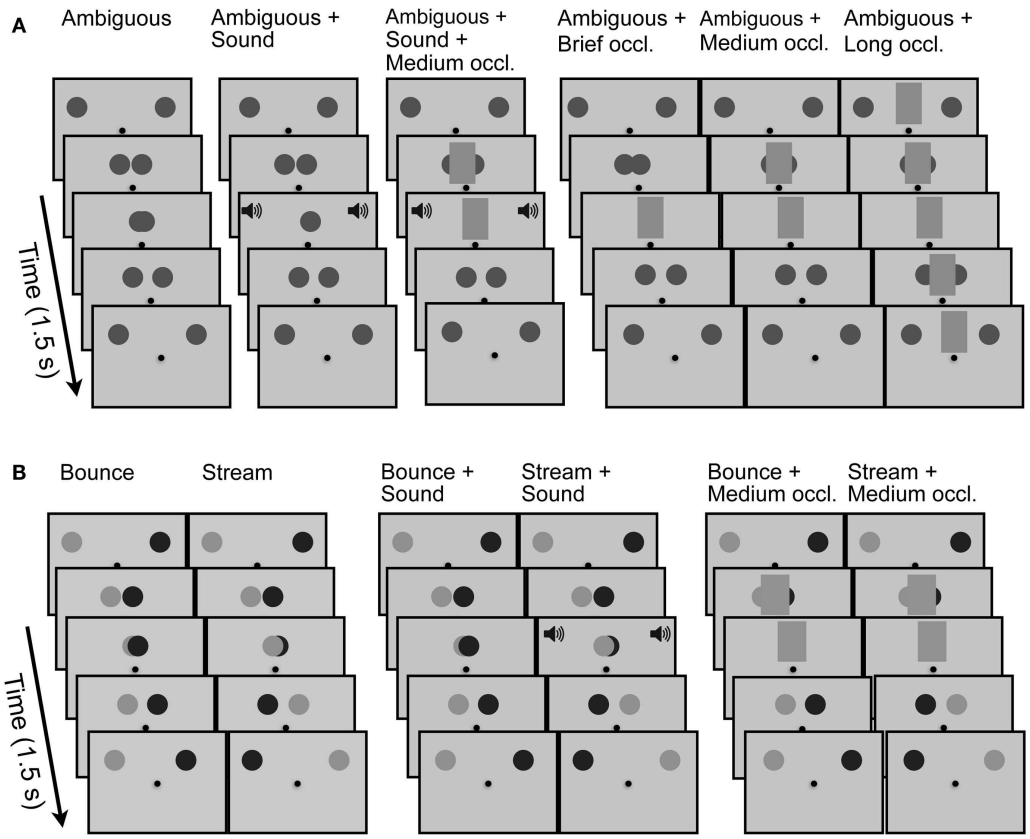

FIGURE 2 | Schematic representations of the five key events comprising conditions in Experiment One. (A) Key events in the six conditions that are meant to generate perceptually ambiguous motion, that is, motion in which the two equal contrasts disks could be seen either as streaming through one another or bouncing off one another. *Ambiguous*: key events in the basic, control condition; *Ambiguous + Sound*: a click sound is presented as the two disks coincide; *Ambiguous + Sound + Medium occluder*: in addition to the click sound, the disks' coincidence is obscured by opaque occluder presented for 0.233 s. In the next three conditions, no sound is presented. *Ambiguous + Short occluder*: the disks' coincidence is obscured by opaque occluder presented for 0.117 s; *Ambiguous + Medium occluder* the disks' coincidence is obscured by opaque occluder presented for 0.233 s; *Ambiguous + Long occluder*: the location at which the disks would coincide is obscured by opaque occluder presented for 1.5 s, that is, the entire duration of the moving stimulus. **(B)** Key events in the six conditions that promoted unambiguous motion. Two disks of unequal luminances moved toward each other, coincided, and then either returned to their respective starting locations (promoting a percept of bouncing; shown in sequence 1) or continued to the opposite side of the display (promoting a percept of streaming; shown in sequence 2). In sequences 3 and 4, at the moment of the disks' coincidence, a click sound was inserted into a stimulus that promoted bouncing (sequence 3) or one that promoted streaming (sequence 4). In the final two sequences, a 0.233-s occluder was inserted into a sequence that promoted bouncing (sequence 5) or one that promoted streaming (sequence 6).

Table 1 | Mean ± 1 SD age, near and far logMAR acuity, Pelli-Robson contrast sensitivity, and Mini-Mental State Examination (MMSE).

Expt	*N* (M:F)	Age (years)	Near acuity (logMAR)	Far acuity (logMAR)	Pelli-Robson (log contrast)	MMSE (max = 30)
1	13 (7:6)	67.7 ± 6.25	0.03 ± 0.11	−0.04 ± 0.09	1.95 ± 0	29.1 ± 0.76
	12 (2:10)	20.0 ± 1.8	−0.13 ± 0.05	−0.09 ± 0.08	1.95 ± 0	
2	8 (4:4)	24.8 ± 2.4	−0.14 ± 0.05	−0.09 ± 0.14	1.95 ± 0	
3	13 (4:9)	20.1 ± 2.8	−0.14 ± 0.05	−0.11 ± 0.13	1.93 ± 0.04	

or the *Stream* condition (age: $F(1, 23) = 0.11$, $p = 0.74$; condition: $F(2, 46) = 3.56$, $\hat{\epsilon} = 0.58$, $p = 0.06$; Age × Condition: $F(2, 46) = 0.45$, $\hat{\epsilon} = 0.59$, $p = 0.54$).

AMBIGUOUS CONDITION RESULTS

Figure 4 shows results for the six conditions where the disks had equal luminance and, therefore, where motion was perceptually ambiguous. When the disks were presented alone (*Ambiguous* condition), younger subjects showed a bias toward "Streaming" responses ($M = 31\%$, $t(11) = -3.30$, $p = 0.007$), whereas older subjects showed no significant bias toward either "Bouncing" or "Streaming" ($M = 52\%$, $t(12) = 0.38$, $p = 0.71$). The proportion "Bouncing" responses was significantly lower in younger subjects compared to older subjects ($t(23) = -2.61$, $p = 0.02$).

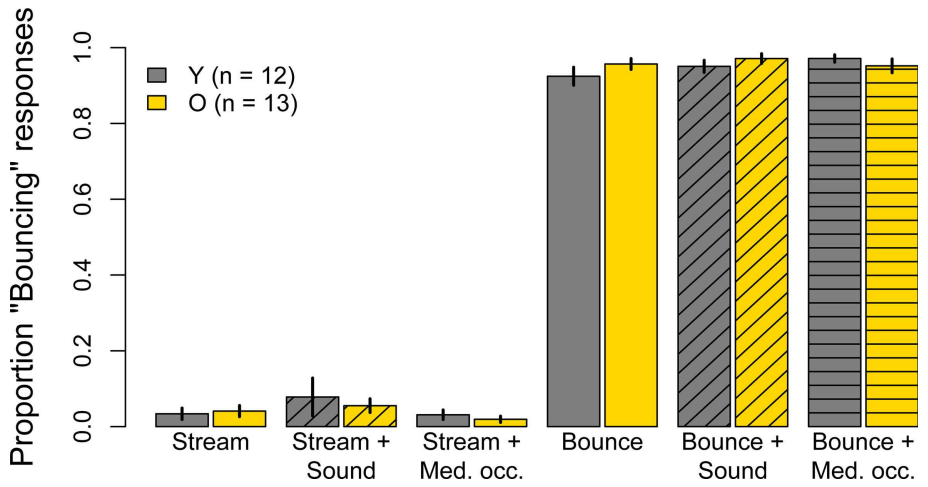

FIGURE 3 | Experiment One results: mean Pr("Bouncing") responses for younger subjects (gray) and older subjects (yellow) for six conditions in which disk luminances had been unbalanced in order to maximize "Streaming" and "Bouncing" judgments. Data are for 12 younger and 13 older subjects. Error bars are ±1 standard error of the mean.

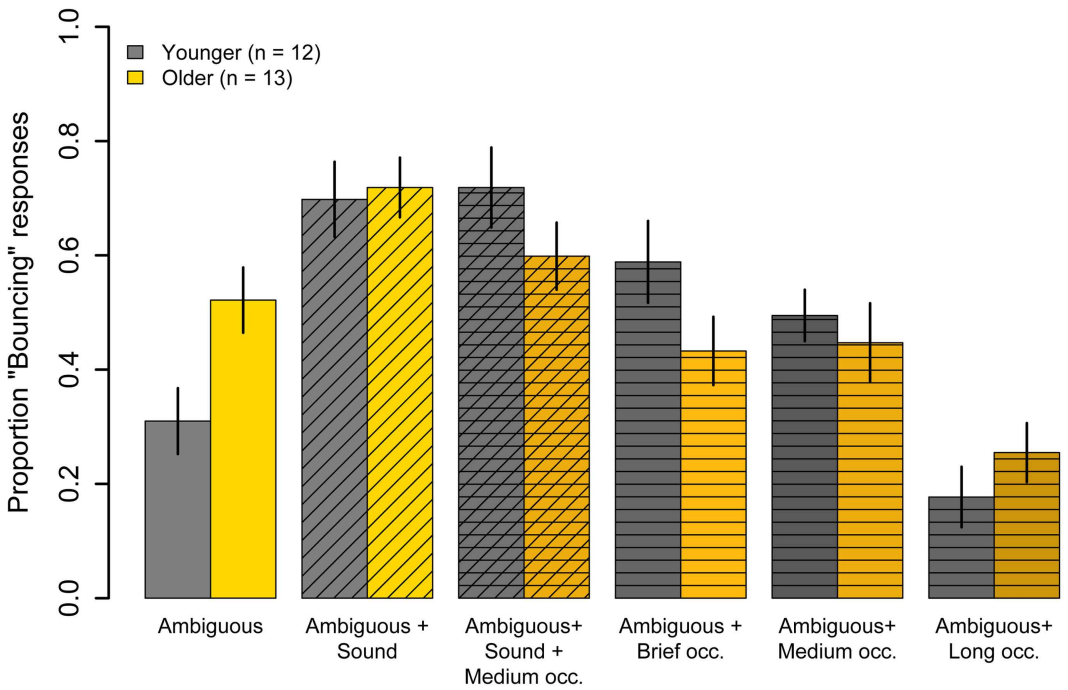

FIGURE 4 | Experiment One results: mean Pr("Bouncing") responses for younger subjects (gray) and older subjects (yellow) in six conditions where the motion of the disks was ambiguous. The disks were accompanied by a sharp sound at the point of coincidence (diagonal hatching), or an opaque occluder of different durations that obscured the point of coincidence (horizontal hatching), or both a sound and an occluder (horizontal and diagonal hatching). Data are for 12 younger and 13 older subjects. Error bars are ±1 standard error of the mean.

Effect of sound

Presenting a sound at the point of coincidence in the *Ambiguous* condition significantly increased the proportion of "Bouncing" responses given by younger subjects (31 vs 70%, $t(11) = 6.94$, $p < 0.001$) and by older subjects (52 vs 72%, $t(12) = 5.05$, $p < 0.001$). However, the increase for younger subjects was significantly greater than that for older subjects ($F(1, 23) = 8.05$, $p = 0.009$). For both age groups, the *Ambiguous + Sound* condition evoked significantly fewer "Bouncing" responses than did the unambiguous *Bounce* condition (younger: $t(11) = -3.32$,

$p = 0.007$; older: $t(11) = -3.83$, $p = 0.002$), suggesting that the significant interaction was probably not the result of some ceiling effect for older subjects.

Effect of occluder

The presentation of an opaque occluder during the disks' motion influenced the percept of the disks' ambiguous motion. However, the magnitude and sign of the effect varied with the duration of the occluder and with age (see bars with horizontal hatching in **Figure 4**). This observation was confirmed by a 2 (age) × 4 (condition: no occluder, *Short*, *Medium*, and *Long* occluder durations) split-plot ANOVA that revealed a significant main effect of condition ($F(3, 69) = 112.6$, $p < 0.001$, $\hat{\epsilon} = 0.85$) and a significant Age × Condition interaction ($F(3, 69) = 4.75$, $p = 0.007$, $\hat{\epsilon} = 0.85$). The main effect of age was not significant ($F(1, 23) = 0.16$, $p = 0.69$).

To decompose the interaction, we examined the effects for different occluder durations separately for each age group. For younger subjects, both the *Brief* ($M = 59\%$) and *Medium* ($M = 49\%$) duration occluders significantly increased the proportion "Bouncing" responses relative to the *Ambiguous* condition (*Brief:* $t(11) = -4.17$, $p = 0.001$; *Medium*: $t(11) = -2.84$, $p = 0.02$). For older subjects, however, the *Brief* ($M = 43\%$) and *Medium* ($M = 45\%$) duration occluders had no significant effect on proportion "Bouncing" responses relative to the *Ambiguous* condition (*Brief:* $t(12) = 1.24$, $p = 0.23$; *Medium*: $t(12) = 1.10$, $p = 0.29$). Finally, the sustained occluder promoted "Streaming" responses in younger subjects ($M = 18\%$) and in older subjects ($M = 25\%$), consistent with previous reports in young adults (Sekuler and Sekuler, 1999). Proportion "Bouncing" with the *Long* duration occluder did not differ significantly from the *Ambiguous* condition in younger subjects ($t(11) = 1.6$, $p = 0.14$), but was significantly lower in older subjects ($t(12) = 3.18$, $p = 0.008$).

Effect of combined sound and occluder

Proportion "Bouncing" evoked by the combination of an opaque occluder and a sound click at the point of coincidence of the disks is shown in **Figure 4** (cross-hatched bars). This condition promoted "Bouncing" responses in younger ($M = 72\%$) and older ($M = 60\%$) subjects. In younger subjects, the combination of both transient events significantly increased Pr("Bouncing") compared to the *Ambiguous* condition ($t(11) = 5.47$, $p = 0.0002$), but the bouncing bias was not significantly different from that evoked in the *Ambiguous* + *Sound* condition ($M = 72$ vs $M = 70\%$, $t(11) = 0.31$, $p = 0.76$), indicating that the effects of the sound and the medium occluder were sub-additive. In older subjects, on the other hand, Pr("Bouncing") evoked in the *Ambiguous* + *Sound* + *Medium Occluder* did not differ significantly from Pr("Bouncing") seen in the *Ambiguous* condition ($t(12) = -1.10$, $p = 0.29$). Moreover, the addition of a medium occluder significantly reduced the older group's proportion "Bouncing" responses compared to the *Ambiguous* + *Sound* condition (60 vs 72%, $t(12) = -2.13$, $p = 0.05$).

EXPERIMENT TWO: RETINAL ILLUMINANCE CONTROL

This experiment examined the possibility that differences between younger and older results seen in Experiment One might have resulted from the reduction in retinal illuminance that accompanies aging. As a result of senile miosis, while viewing the background luminance of our display, an average 68-year-old's pupil diameter would be 4.70 mm, while an average 20-year-old's pupil diameter would be 6.60 mm (Winn et al., 1994). The accompanying age-related difference in pupil area would reduce the average older subject's retinal illuminance by ∼2×. Previous research found that changes in display luminance affect the perceived speed of moving objects (Hammett et al., 2007), allowing for the possibility that age-related reductions in retinal illuminance affected the disks' perceived speed, thereby promoting group differences in the bouncing/streaming percept (Hammett et al., 2007). To check this, we tested a group of younger subjects who viewed the stimulus display through neutral density filters chosen to reduce retinal illuminance considerably in excess of what would have been expected in Experiment One from senile miosis alone.

METHODS

Subjects

Twelve younger subjects participated in this experiment and were compensated for their time at a rate of $10/h. None had participated in Experiment One. Four subjects' data were excluded because their accuracy in the unambiguous *Bounce* condition was <70% (accuracy range: 12–68%, mean: 43%). Demographic information for the eight remaining subjects is presented in **Table 1**.

In addition, to assess the stability of older subjects' performance in Experiment One, all older subjects who participated in Experiment One were re-tested in this experiment.

Apparatus

The apparatus was the same as in Experiment One. For younger subjects, display luminance was varied by interposing neutral density filters between a subject and the display, reducing display luminance by ≈90%, from 39.5 to 4.24 cd/m^2. Note that this reduction far exceeds the reduction in retinal illumination that would have resulted from normal age-related reduction in pupil size (senile miosis).

Stimuli and procedure

Half of the conditions used in Experiment One were used in this experiment: *Bounce*, *Stream*, *Ambiguous* presented with no accompanying sound, and *Bounce*, *Stream*, and *Ambiguous* each accompanied by the click sound at the moment of the disks' coincidence. As in Experiment One, there were nine blocks of trials comprising four trials of each condition in random order, which were preceded by a practice block comprising two trials of each condition. Half the younger subjects completed the six conditions first without neutral density filters and then again with neutral density filters, whereas the other half of the subjects followed the opposite order. Older subjects completed the six conditions once, always without neutral density filters.

RESULTS

Effect of neutral density filters

Figure 5 shows results for the *Bounce* and *Stream* conditions, with and without sound, for younger subjects viewing the stimuli without neutral density filters (light gray bars) and with neutral

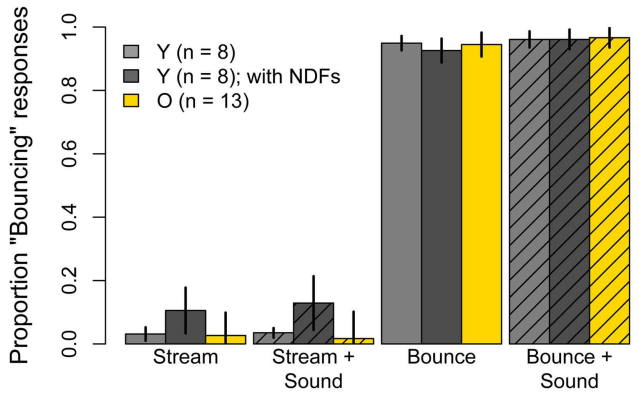

FIGURE 5 | Mean Pr("Bouncing") responses produced in the unambiguous conditions of Experiment One: Bouncing and Streaming motion and Bouncing and Streaming motion accompanied by the sound used in Experiment One. Light gray bars represent data for eight younger subjects when they viewed the stimuli normally, without neutral density filters, and the dark gray bars represent results obtained when subjects viewed the stimuli through three neutral density filters. Yellow bars represent data of 13 older subjects who participated in Experiment One and were tested again in these conditions without neutral density filters. Error bars are ±1 standard error of the mean.

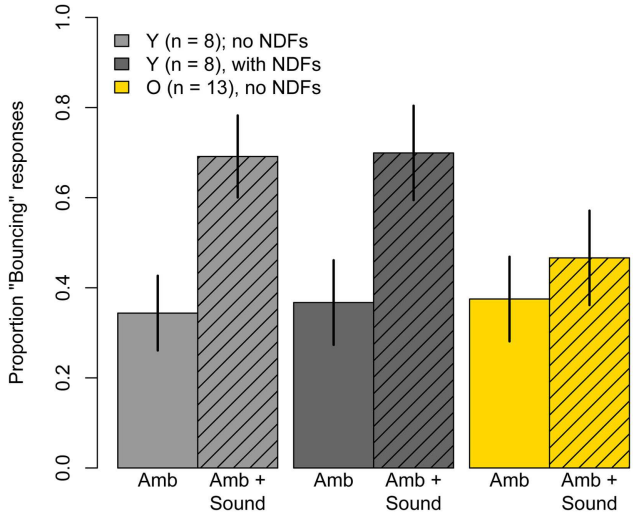

FIGURE 6 | Mean Pr("Bouncing") responses produced in the ambiguous conditions of Experiment Two: *Ambiguous* motion and *Ambiguous* motion accompanied by the sound used in Experiment One. Light gray bars represent data for eight younger subjects when they viewed the stimuli normally, without neutral density filters, and the dark gray bars represent results obtained when subjects viewed the stimuli through three neutral density filters. Yellow bars represent data of 13 older subjects who participated in Experiment One and were retested in these conditions without neutral density filters. Error bars are ±1 standard error of the mean.

density filters (dark gray bars). The effect of luminance on proportion of bouncing responses in the unambiguous conditions was analyzed with two separate 2 (sound) × 2 (luminance) repeated-measures ANOVAs. For bouncing conditions, the main effects of sound, luminance, and the Sound × Luminance interaction were not significant (sound: $F(1, 7) = 1.13$, $p = 0.32$; luminance: $F(1, 7) = 0.14$, $p = 0.71$; Luminance × Sound: $F(1, 7) = 0.51$, $p = 0.50$). For streaming conditions, the main effect of sound was significant ($F(1, 7) = 8.79$, $p = 0.02$), as the presentation of the sound increased proportion "Bouncing." The main effect of luminance was not significant ($F(1, 7) = 1.46$, $p = 0.27$) and the Luminance × Sound interaction was not significant ($F(1, 7) = 0.69$, $p = 0.43$).

Figure 6 shows results for the *Ambiguous* and *Ambiguous + Sound* conditions viewed with and without neutral density filters. A 2 (sound) × (luminance) repeated-measures ANOVA revealed a significant main effect of sound ($F(1, 7) = 13.9$, $p = 0.007$), no significant main effect of luminance ($F(1, 7) = 0.04$, $p = 0.85$), and no significant Sound × Luminance interaction ($F(1, 7) = 0.04$, $p = 0.86$). Thus, the ≈9.5× reduction in luminance had no discernible effect on the proportion of "Bouncing" responses evoked in the *Ambiguous* condition, or on the increase in proportion "Bouncing" by the brief sound click.

Replication of older subjects' performance?

Figures 5 and **6** also show results for 13 older subjects who participated in Experiment One and were re-tested with six conditions in this experiment. To examine the test-retest reliability of older subjects' performance, proportion "Bouncing" for the six conditions used in this experiment were compared with performance in Experiment One using a 6 (condition) × 2 (time) repeated-measured ANOVA. The main effects of time, condition, and the Condition × Time interaction were all significant (time: $F(1,12) = 10.3$, $p = 0.007$; condition: $F(5,60) = 217.7$, $\hat{\epsilon} = 0.37$, $p < 0.001$; Condition × Time: $F(5,60) = 6.47$, $\hat{\epsilon} = 0.28$, $p = 0.01$). To decompose the interaction, we evaluated the simple main effect of time for each condition separately. The simple main effect of time was significant in the *Ambiguous + Sound* condition ($F(1, 12) = 12.7$, $p = 0.004$) and in the *Stream + Sound* condition ($F(1, 12) = 8.98$, $p = 0.01$), with lower Pr("Bouncing") in Experiment Two in both cases. Proportion of "Bouncing" responses for the *Ambiguous* condition was also lower in Experiment Two, but this difference was not statistically significant ($F(1, 12) = 4.02$, $p = 0.07$) and, as in Experiment One, average proportion "Bouncing" was not significantly different from 50% ($t(12) = -1.87$, $p = 0.09$). Proportion "Bouncing" in all other conditions did not differ between experiments ($F(1, 12) < 1.06$, $p < 0.32$).

Unlike in Experiment One, Pr("Bouncing") in the *Ambiguous* condition did not differ significantly different between age groups ($t(19) = -0.29$, $p = 0.77$). However, similar to Experiment One, the increase in Pr("Bouncing") associated with the presentation of the sound click was smaller in older subjects compared to younger subjects ($F(1, 19) = 6.14$, $p = 0.02$). Indeed, the effect of sound on proportion "Bouncing" responses in older subjects was significantly smaller than the effect obtained in Experiment One (9 versus 19% increase, $F(1, 12) = 6.84$, $p = 0.02$). Hence, Experiment Two, like Experiment One, found evidence for an age-related reduction in the influence of sound on the bouncing-streaming percept.

EXPERIMENT THREE: SOUND QUALITY CONTROL

Experiments One and Two showed that inserting a sound into the *Ambiguous* stimulus increased Pr("Bouncing") responses for both younger and older subjects, but had significantly reduced impact for the older subjects. We speculated that this reduced impact might have resulted from presbycusis, age-related hearing loss. Presbycusis diminishes overall sensitivity to sound, and is characterized by a particular loss in sensitivity to high frequencies (Morrell et al., 1996). As a result, presbycusis would effectively filter out higher frequency components in the spectrum of the sharp-onset, "click" sound used in Experiments One and Two. As the perceptually sharp onset of the click depends upon the higher frequencies in its spectrum, loss of higher frequencies would make the click qualitatively less sharp. Previously, with young subjects, Grassi and Casco (2009) found that the onset attack of a sound can modify the sound's impact on the ambiguous bouncing-streaming display. Because Grassi and Casco's (2009) sound differed substantially from our synthesized click, we thought a test of presbycusis' effect on our synthesized click's ability to increase Pr("Bouncing") was in order. To do this test, we modified our click sound by passing it through a filter that mimicked the audiogram of an older person, and then tested a new group of younger subjects with this filtered sound.

METHODS

Stimuli

To modify the spectrum of the preceding experiments' click sound, we used Matlab's Signal Processing Toolbox (Mathworks, 2012) to construct a linear-phase, finite impulse response filter, using least squares to fit the target audiogram. We generated a filter whose pass characteristics mimicked the audiogram of the average otologically normal[2] 70-year-old male. This average audiogram was calculated from values specified in International Organization for Standardization (ISO) 7029:2000E (prepared by Technical Committee ISO/TC 43, Acoustics). To take one example, relative to an otologically normal 18-year-old male, at 4 KHz, the audiogram of the average otologically normal 70-year-old male is −43.3 dB.

Zhou et al. (2007) showed that once the amplitude of a click was sufficient to be audible, further increases in amplitude had little or no effect on the sound's ability to bias the percept produced by *Ambiguous* motion. But, to be safe, our test conditions included one in which the filtered sound's amplitude had been increased to match the loudness produced by the original, unfiltered sound. To determine by how much the filtered sound had to be amplified so that its loudness matched the loudness of the original, unfiltered sound, eight additional young subjects (mean age: 18.5 years) took part in a loudness matching experiment. None of these had participated in any bouncing-streaming experiments. On each trial, subjects were presented with the original click sound (at 90 dBC) and the filtered sound with varying loudness in random order. In a two-interval forced-choice procedure, subjects identified the interval, first or second, that contained the louder sound. On every trial, the amplitude of the filtered sound was controlled by three interleaved staircases: a 1-down/1-up staircase, a 2-down/1-up staircase, and a 2-up/1-down staircase. Each staircase terminated after 20 trials, or upon reaching 12 reversals, whichever came first. The proportion of "Louder" responses was plotted as a function of dB adjustment of the filtered sound, and a Weibull function was fit to each subjects' data to estimate the point of subjective equality (PSE), or the dB adjustment necessary to yield "Louder" responses 50% of the time. The obtained PSEs for the eight subjects ranged from 11.7 to 12.6, with a mean of 12.13 dB. That mean amplification value was used for one of the conditions in the experiment proper. **Figure 1B** shows the spectrogram for this amplified, filtered click.

Subjects

Twenty-two younger subjects were recruited for this experiment, and were compensated for their time at a rate of $10/h. None had taken part in either of the preceding experiments. As we did in those earlier experiments, we excluded subjects whose responses showed less than the expected accuracy with the unambiguous stimulus. Data from nine subjects were excluded from analyses because their accuracy in the unambiguous *Bounce* condition was <70% (accuracy range: 3–68%, average: 38%). **Table 1** presents demographic information for the 13 remaining subjects.

Apparatus

The apparatus was the same as in Experiment One.

Design and procedure

There were six conditions in this Experiment: two unambiguous motion conditions (*Bounce*, *Stream*), the *Ambiguous* condition presented with no sound, and the *Ambiguous* condition accompanied by three different sounds – the original click sound from Experiment One (*Ambiguous + original click*), that click sound filtered to attenuate primarily high frequencies (*Ambiguous + filtered click*), and the filtered sound amplified by 12.13 dB to match the loudness of the unfiltered sound (*Ambiguous + filtered, amplified click*).

The procedure was the same as in Experiment One. Subjects were tested in nine blocks of trials comprising four trials of each condition in random order. Experimental trials were preceded by a practice block comprising two trials of each condition presented in random order.

RESULTS

Figure 7 shows the mean proportion "Bouncing" obtained in the six conditions used in this Experiment. The two unambiguous motion conditions were successful in promoting perceptual consistency, as subjects gave 92% "Bouncing" responses in the *Bounce* condition and 98% "Streaming" responses in the *Stream* condition. Mean accuracy was significantly higher in the *Stream* condition than in the *Bounce* condition ($t(12) = -3.03$, $p = 0.01$), indicating that subjects showed a bias for "Streaming" responses. As in Experiments One and Two, the *Ambiguous* condition promoted the streaming percept ($M = 30\%$) and the presentation of the original sound click biased the percept toward bouncing ($M = 74\%$). A 3 (Experiment) × 2 (sound) mixed-model ANOVA comparing performance in the *Ambiguous* and *Ambiguous + original Sound*

[2]ISO 7029-2000 defines otologically normal as "a person in a normal state of health who is free from all signs or symptoms of ear disease and from obstructing wax in the ear canals, and who has no history of undue exposure to noise."

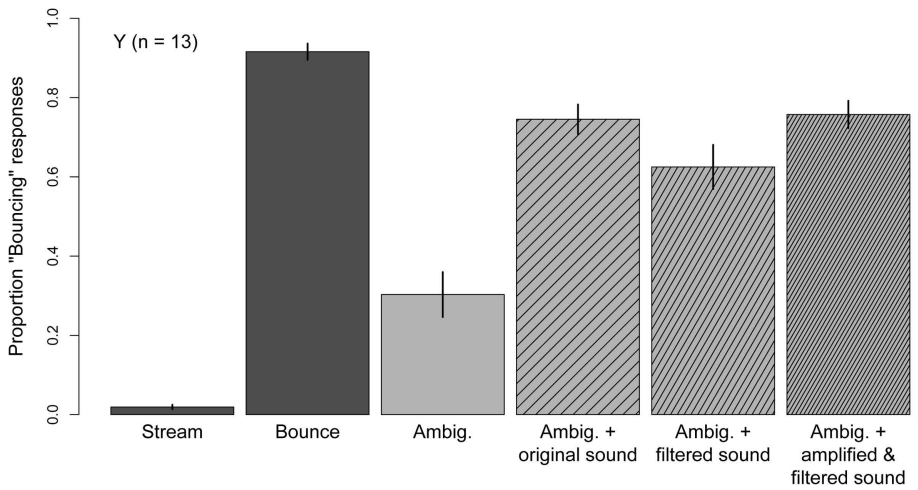

FIGURE 7 | Mean Pr("Bouncing") responses produced in each condition of Experiment Three: *stream* and *Bounce*; *Ambiguous*; *Ambiguous* accompanied by the sound used in Experiments One and Two; *Ambiguous* accompanied by a filtered version of the sound used in Experiments One and Two; *Ambiguous* accompanied by a filtered-and-amplified version of the sound used in Experiments One and Two. Data are for 13 younger subjects. Error bars are ±1 standard error of the mean.

conditions in Experiments One, Two, and Three revealed a significant main effect of sound ($F(1, 30) = 96.9$, $p < 0.001$), no main effect of Experiment ($F(2, 30) = 0.04$, $p = 0.96$) and no significant Experiment × Sound interaction ($F(2, 30) = 0.47$, $p = 0.63$). Thus, the proportion "Bouncing" associated with the Ambiguous condition, and the bouncing bias associated with the original sound click, show very good replicability across three separate groups of younger subjects.

Both the filtered sound ($M = 63\%$) and the filtered-and-amplified sound ($M = 76\%$) significantly biased the disks' motion percept toward bouncing (*Ambiguous + filtered sound* versus *Ambiguous*, $t(12) = -5.95$, $p < 0.001$; *Ambiguous + amplified, filtered sound* versus *Ambiguous*: $t(12) = -8.06$, $p < 0.001$). The bouncing bias associated with the filtered sound was lower than that induced by the original sound ($t(12) = 2.39$, $p = 0.03$); however, the effect of the filtered-and-amplified sound was not different from the effect of the original sound ($t(12) = -0.34$, $p = 0.74$). Thus, the original click and an equivalently loud filtered click were equally effective at biasing younger subjects' percept of the ambiguous motion stimulus toward bouncing, suggesting that age-differences in audition cannot explain the attenuated effect of the sound click observed in Experiments One and Two.

DISCUSSION AND CONCLUSION

The current experiments examined age-related changes in inter- and intra-modal integration by measuring the effects of visual and auditory events on the bistable bouncing/streaming percept of a visual motion stimulus.

INTER-MODAL INTEGRATION

Consistent with previous studies (Sekuler et al., 1997; Shimojo et al., 2001; Watanabe and Shimojo, 2001; Remijn et al., 2004; Sanabria et al., 2004; Zhou et al., 2007), presenting a brief sound at the time of disks' coincidence strongly biased the motion percept toward bouncing in both groups. Importantly, as can be seen in **Figure 8**, the sound-induced bias was significantly weaker in older subjects, both in Experiments One and Two. The age-related reduction in the effect of sound on the bouncing/streaming percept is surprising given previous findings that multisensory integration is preserved, or even enhanced, in older age (Peiffer et al., 2007; Diederich et al., 2008; Mahoney et al., 2011; Winneke and Phillips, 2011, for review, see Mozolic et al., 2012), as well as the reduced ability of older subjects to inhibit task-irrelevant information (Andrés et al., 2006; Gazzaley et al., 2008).

Results in Experiments Two and Three showed that the observed age-differences cannot be explained by age-related reductions in retinal illuminance, nor by age-related hearing loss. As can be seen in **Figure 8**, the effect of the sound in younger subjects was highly replicable and robust to reductions in display luminance (Experiment Two boxplot) and to changes in the amplitude and frequency spectrum of the sound (Experiment Three boxplots), that were designed to mimic the effect of presbycusis in older adults.

Previous studies also have shown that the perceived timing of the sound relative to the time of disks' coincidence is important: the sound biases the percept toward bouncing only if it occurs between 150 ms before and up to 50 ms after the disks' coincidence (Sekuler et al., 1997; Shimojo et al., 2001). However, it is not likely that age-differences in the strength of the sound-induced bouncing bias resulted from group differences in the perceived timing of the click and visual events, as aging does not appear to affect the point of subjective simultaneity for visual and auditory stimuli (Fiacconi et al., 2013). Moreover, some studies suggest that older subjects have a wider, not narrower, time window of audio-visual integration than younger subjects (Laurienti et al., 2006; Diederich et al., 2008; Setti et al., 2011), implying that strict simultaneity of sound and visual collision would be less critical for older subjects.

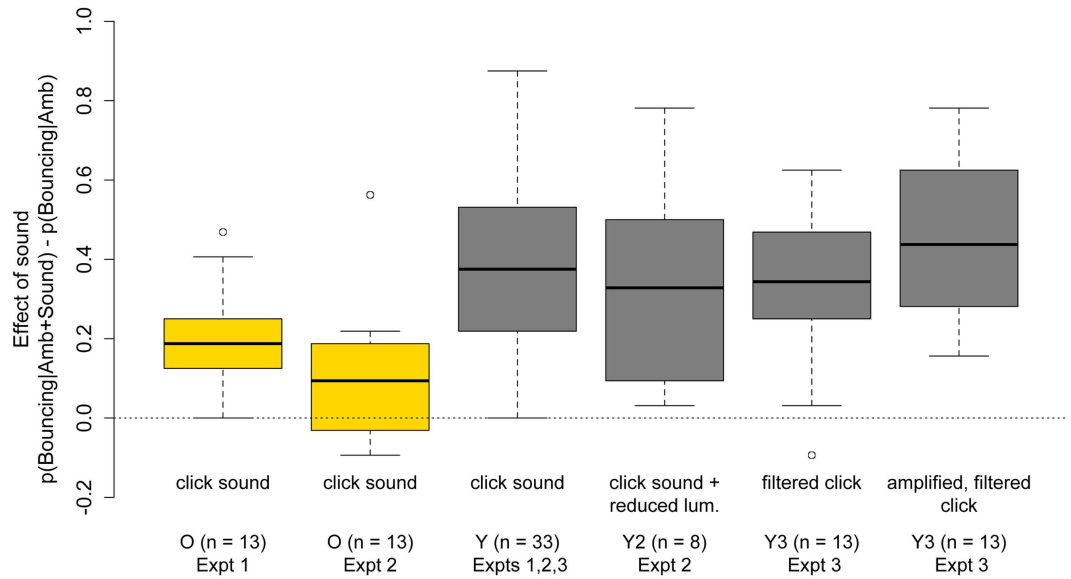

FIGURE 8 | Boxplots of the increase in Pr("Bouncing") responses induced by the presentation of a sound at the point of disks' coincidence. First and second boxplots show the bouncing bias induced by the click sound for 13 older subjects tested in Experiments One and Two. The third boxplot shows the bouncing bias induced by the click sound for 33 younger subjects across Experiments One, Two, and Three. The fourth boxplot shows the bouncing bias induced by the click sound in Experiment Two when display luminance was reduced with neutral density filters. The fifth and sixth boxplots show the bouncing bias induced by the filtered and filtered-and-amplified clicks for 13 younger subjects in Experiment Three.

Thus, age-differences in perceived timing of events, if such exist, are likely to have been inconsequential for our results.

INTRA-MODAL INTEGRATION

Experiment One also examined age-related changes in intra-modal integration in the microgenesis of the perceptual influence of a visual occluder on the bouncing/streaming percept. The sustained occluder promoted streaming in both groups, consistent with previous results (Sekuler and Sekuler, 1999; Grove and Sakurai, 2009) and with the fact that occlusion can promote perceptual continuity (Assad and Maunsell, 1995; Feldman and Tremoulet, 2006). In contrast, the brief and medium duration occluders promoted bouncing in younger subjects, with the briefest occluder inducing a stronger bouncing bias than the medium duration occluder. Interestingly, the brief and medium duration occluders did not promote bouncing in older subjects. Thus, the weakened inter-modal effect in aging was also paralleled by a reduced intra-modal effect of the transient visual occluders.

The bias toward bouncing induced by the transient visual occluder in younger subjects is consistent with several previous studies that found that transient *visual* events occurring in close spatiotemporal proximity to the point of coincidence promote bouncing (Sekuler et al., 1997; Watanabe and Shimojo, 1998; Zhou et al., 2007). Remijn and Ito (2007) showed that an increased in bouncing percepts can also be induced by occluders that do not obscure the disks' coincidence, but that are situated in close proximity to the point of coincidence and suggested that processing the moving objects behind occluders interferes with processing of the continuity of the disks' motion, thereby reducing the probability of a streaming percept. Kawachi et al. (2011) showed that determining whether two colored disks that intersected behind an occluder bounced off each other or streamed past each other required ≈0.2 s of post-coincidence object motion, independently of the disks' speed, suggesting that some amount of time is necessary to match the disks' motion across the point of coincidence. Thus, the transient occluders in Experiment One may have interfered with processing of the objects' motion at their coincidence, resulting in an increase in bouncing percepts.

MULTIPLE CUE COMBINATION

Finally, Experiment One also briefly examined the influence of combined auditory and visual cues on the resulting percept by concurrently presenting the medium occluder and sound click. For younger subjects, the bouncing bias induced by the combination of medium occluder and sound was equal to the bias induced by the sound alone, indicating a sub-additive effect of sound and occluder. On the other hand, the bouncing bias induced by the sound in older subjects was significantly attenuated by the presentation of the occluder, consistent with the slight reduction in proportion bouncing by the occluder alone. Thus, for both groups, performance in the combined occluder and sound condition was approximately consistent with an additive effect of the two separate cues. Zhou et al. (2007) showed that when several visual and/or auditory cues are presented with the bouncing/streaming display, the resulting percept was well predicted by a weighted sum of the effects of the cues presented in isolation. Although cue weighting varied across subjects, visual cues generally dominated auditory cues. Kawachi and Gyoba (2006) showed that intra-modal perceptual grouping of the moving disks also can override the effect of sound on the motion percept. Current results show that older

subjects do combine the effects of visual and auditory cues in motion perception; however, our experiments were not designed to determine the relative weighting of these cues. Future studies should investigate whether aging affects the relative weighting of auditory and visual cues in multisensory cue combination.

COMMON CAUSES FOR REDUCED INTRA- AND INTER-MODAL INTEGRATION

In both the intra- and inter-modal effects, integration of cues is critical, so it is possible that age-related differences in integration time might play a role. Working with younger observers, Bodelón et al. (2007) analyzed the time taken to integrate simple visual features such as color and orientation into a perceptual whole and showed that the time required to process a combination of features is longer than any individual component. If similar time constants hold for multisensory features, older subjects' weaker integration may be explained by prolonged time required to process a combination of features. For example, older subjects require longer stimulus durations to perceive contours composed of discrete oriented elements that are embedded among distractors, suggesting that older adults require more time to integrate basic features spatially (Roudaia et al., 2011, submitted). Moreover, several studies have found changes in integration of motion signals with aging (Andersen and Ni, 2008; Roudaia et al., 2010; Arena et al., 2012). Perception of continuous object motion behind an occluder is thought to rely on the temporal integration of signals from local motion detectors tuned to the direction of motion (Bertenthal et al., 1993). Age-related changes in integration of motion signals may contribute to the reduced effect of transient occlusion on the bouncing/streaming percept in older subjects. It is interesting to note that older adults also show weaker representational momentum for motion (Piotrowski and Jakobson, 2011), a phenomenon that may be related to the effects observed here. More broadly, age-related differences in internal noise and calculation efficiency of motion detectors may affect both intra- and inter-modal effects (Bennett et al., 1999, 2007; Betts et al., 2007; Casco et al., 2012).

Some authors have suggested that transient events presented in close spatiotemporal proximity of the point of coincidence promote bouncing by disrupting the sustained attention to the disks' motion that is necessary for the streaming percept (Watanabe and Shimojo, 1998; Shimojo et al., 2001; Kawabe and Miura, 2006). However, other studies found that removal of attention alone can not account for the effect, as some concurrent events presented at disks' coincidence did not increase the proportion of bouncing percepts, while still distracting attention from the moving disks (Sekuler et al., 1997; Watanabe and Shimojo, 2001; Grassi and Casco, 2009). In addition, Dufour et al. (2008) showed that the presentation of a subliminal sound, an event that was unlikely to have disrupted sustained attention, also promoted the bouncing percept. Therefore, it is unlikely that differences in sustained attention can fully explain the weakened effects of the visual and auditory events.

REDUCED MULTISENSORY INTEGRATION?

The most likely cause of the increase in bouncing percepts induced by the click is the integration of the sound with the visual motion stimulus into a single multisensory event (e.g., Ecker and Heller, 2005). Bushara et al. (2003) examined the neural correlates underlying the effect of sound using fMRI by comparing cortical activation for trials on which subjects reported a bouncing percept versus trials where subjects reported a streaming percept. Trials on which bouncing was perceived were accompanied by increased activation in several subcortical structures, as well as frontal and prefrontal areas, and in left posterior parietal cortex, all of which are known to be involved in multisensory processing. Conversely, trials on which streaming was perceived showed greater activation in the superior temporal gyri and occipital cortices, known to primarily process unisensory auditory and visual information, respectively. The authors suggested that the bistability of the percept arises from a competitive interaction between multisensory and unisensory areas. Consistent with these findings, Maniglia et al. (2012) showed that disrupting activity in the right posterior parietal cortex with transcranial magnetic stimulation reduced the strength of the bouncing bias that was induced by the sound, but did not affect the proportion of bouncing percepts in the silent, control condition. The authors interpreted these results as evidence for the key role of the posterior parietal cortex in the inter-modal binding of the coincidence event.

Although attentional effects alone cannot explain the effects of auditory and visual cues on the perception of the bouncing/streaming display, top-down attention has been shown to play an important role in resolving the competitive interactions between alternative percepts produced by perceptually malleable stimuli (Senkowski et al., 2005; Talsma et al., 2007, for review, see Talsma et al., 2010). Evidence for the interplay of attention and multisensory integration in the bouncing/streaming percept comes from an MEG study by Zvyagintsev et al. (2011). Similar to the study by Bushara et al. (2003), the authors presented the bouncing/streaming stimulus with a sound at the objects' coincidence and compared activation for trials yielding each of the alternative percepts. Trials that generated a bouncing percept showed greater activity in frontal areas within 80 ms after the disks' coincidence, followed by greater activity in the cuneus and the superior parietal lobule. Trials that generated a streaming percept showed greater activity in the auditory cortex starting 80 ms after the disks' coincidence, closely followed by increased activity in the visual cortices and later followed by activation in the frontal areas. The authors interpreted these results as indicating that early supramodal attention mediates multisensory binding of the sound and visual stimulus to generate the bouncing percept. Thus, on trials where attention is low, multisensory binding does not occur, and the visual and auditory stimuli are processed as separate items, which yields a streaming percept.

Thus, the age-related changes in inter-modal integration shown in **Figure 4** may reflect age-related declines in multisensory integration, or changes in the interaction between attentional and multisensory integration processes. Contrary to this suggestion, most studies of multisensory integration and aging show greater, not lesser multisensory enhancement in older subjects (for review, see Mozolic et al., 2012). For example, a recent MEG study (Diaconescu et al., 2013) found increased activity to audio-visual stimuli in the posterior parietal and medial prefrontal areas in older

subjects, which was also correlated with the behavioral response time enhancement to audio-visual stimuli. This study highlighted the role of posterior parietal and prefrontal regions in mediating multisensory integration in older age. It is noteworthy that these same regions have been shown to be involved in the bouncing percept (Bushara et al., 2003; Zvyagintsev et al., 2011; Maniglia et al., 2012). What can account for these differential findings? Differences among measures of age-related variation in multisensory integration may be related to differences in the studies' stimuli and tasks. Previous studies showing multisensory enhancement in older subjects primarily compared response times for detecting or discriminating brief, static unimodal or inter-modal stimuli (e.g., Laurienti et al., 2006; Peiffer et al., 2007; Mahoney et al., 2011), or examined the integration of audio-visual speech signals (e.g., Cienkowski and Carney, 2002; Maguinness et al., 2011; Winneke and Phillips, 2011). In one notable exception, Stephen et al. (2010) found evidence of reduced multisensory integration in older subjects. Interestingly, similar to our study, Stephen et al. (2010) examined the integration of sound with a visual motion stimulus. Future research should examine the possibility that aging affects multisensory interaction for static and dynamic stimuli differently.

CONCLUSION

In sum, the present experiments revealed an age-related reduction in the influence of auditory and visual cues on the way that a bistable visual motion stimulus was perceived. Control experiments ruled out the possibility that this reduced influence resulted from normal, age-related sensory changes. Instead, our findings point to age-related changes in the integration of multiple cues. Because we inhabit a world in which events are defined by relationships among multiple stimuli, including stimuli from multiple senses, inter- and intra-modal integration is crucial for effective cognitive function and for successful navigation of the environment. As a result, age-related weakening of multisensory and intrasensory integration could significantly impact older adults' performance in various aspects of everyday perception, cognition, and mobility. This suggests the importance of an expanded examination of age-related changes in cue integration more generally, both within a single sensory modality and between multiple senses. Finally, normal age-related change in vision or audition affords a potentially valuable arena within which to test theoretical accounts of the way in which multisensory integration tracks changes in the reliability of information provided by one sense or another (Ernst and Banks, 2002; Gori et al., 2012).

ACKNOWLEDGMENTS

Research supported by grants MH068404, AFOSR 4-01748, CIHR, the Canada Research Chairs Program, and CELEST, a National Science Foundation Science of Learning Center. We are indebted to Donna Waxman for her excellent help with this study, to Neel Kishan for the code that generates our synthetic click sound, and to Hari Bharadwaj for counsel on age-related filtering of the click sound.

REFERENCES

Alvarez, G. A., Horowitz, T. S., Arsenio, H. C., Dimase, J. S., and Wolfe, J. M. (2005). Do multielement visual tracking and visual search draw continuously on the same visual attention resources? *J. Exp. Psychol. Hum. Percept. Perform.* 31, 643–667.

Andersen, G. J., and Ni, R. (2008). Aging and visual processing: declines in spatial not temporal integration. *Vision Res.* 48, 109–118.

Andrés, P., Parmentier, F. B. R., and Escera, C. (2006). The effect of age on involuntary capture of attention by irrelevant sounds: a test of the frontal hypothesis of aging. *Neuropsychologia* 44, 2564–2568.

Arena, A., Hutchinson, C. V., and Shimozaki, S. S. (2012). The effects of age on the spatial and temporal integration of global motion. *Vision Res.* 58C, 27–32.

Assad, J. A., and Maunsell, J. H. (1995). Neuronal correlates of inferred motion in primate posterior parietal cortex. *Nature* 373, 518–521.

Bennett, P. J., Sekuler, A. B., and Ozin, L. (1999). Effects of aging on calculation efficiency and equivalent noise. *J. Opt. Soc. Am. A. Opt. Image Sci. Vis.* 16, 654–668.

Bennett, P. J., Sekuler, R., and Sekuler, A. B. (2007). The effects of aging on motion detection and direction identification. *Vision Res.* 47, 799–809.

Bertenthal, B. I., Banton, T., and Bradbury, A. (1993). Directional bias in the perception of translating patterns. *Perception* 22, 193–207.

Betts, L. R., Sekuler, A. B., and Bennett, P. J. (2007). The effects of aging on orientation discrimination. *Vision Res.* 47, 1769–1780.

Billino, J., Bremmer, F., and Gegenfurtner, K. R. (2008). Differential aging of motion processing mechanisms: evidence against general perceptual decline. *Vision Res.* 48, 1254–1261.

Bizley, J. K., Shinn-Cunningham, B. G., and Lee, A. K. C. (2012). Nothing is irrelevant in a noisy world: sensory illusions reveal obligatory within-and across-modality integration. *J. Neurosci.* 32, 13402–13410.

Bodelón, C., Fallah, M., and Reynolds, J. H. (2007). Temporal resolution for the perception of features and conjunctions. *J. Neurosci.* 27, 725–730.

Brainard, D. H. (1997). The psychophysics toolbox. *Spat. Vis.* 10, 433–436.

Bruns, P., and Getzmann, S. (2008). Audiovisual influences on the perception of visual apparent motion: exploring the effect of a single sound. *Acta Psychol. (Amst)* 129, 273–283.

Bushara, K. O., Hanakawa, T., Immisch, I., Toma, K., Kansaku, K., and Hallett, M. (2003). Neural correlates of cross-modal binding. *Nat. Neurosci.* 6, 190–195.

Casco, C., Robol, V., Grassi, M., and Venturini, C. (2012). Positional noise in landolt-c stimuli reduces spatial resolution: a study with younger and older observers. *Vision Res.* 67, 37–43.

Cienkowski, K. M., and Carney, A. E. (2002). Auditory-visual speech perception and aging. *Ear Hear.* 23, 439–449.

Diaconescu, A. O., Hasher, L., and McIntosh, A. R. (2013). Visual dominance and multisensory integration changes with age. *Neuroimage* 65, 152–166.

Diederich, A., Colonius, H., and Schomburg, A. (2008). Assessing age-related multisensory enhancement with the time-window-of-integration model. *Neuropsychologia* 46, 2556–2562.

Dufour, A., Touzalin, P., Moessinger, M., Brochard, R., and Després, O. (2008). Visual motion disambiguation by a subliminal sound. *Conscious. Cogn.* 17, 790–797.

Ecker, A. J., and Heller, L. M. (2005). Auditory-visual interactions in the perception of a ball's path. *Perception* 34, 59–75.

Ernst, M. O., and Banks, M. S. (2002). Humans integrate visual and haptic information in a statistically optimal fashion. *Nature* 415, 429–433.

Feldman, J., and Tremoulet, P. D. (2006). Individuation of visual objects over time. *Cognition* 99, 131–165.

Fiacconi, C. M., Harvey, E. C., Sekuler, A. B., and Bennett, P. J. (2013). The influence of aging on audiovisual temporal order judgments. *Exp. Aging Res.* 39, 179–193.

Folstein, M. F., Folstein, S. E., and McHugh, P. R. (1975). "Mini-mental state". A practical method for grading the cognitive state of patients for the clinician. *J. Psychiatr. Res.* 12, 189–198.

Gazzaley, A., Clapp, W., Kelley, J., McEvoy, K., Knight, R. T., and D'Esposito, M. (2008). Age-related top-down suppression deficit in the early stages of cortical visual memory processing. *Proc. Natl. Acad. Sci. U.S.A.* 105, 13122–13126.

Gori, M., Sandini, G., and Burr, D. (2012). Development of visuo-auditory integration in space and time. *Front. Integr. Neurosci.* 6:77. doi:10.3389/fnint.2012.00077

Grassi, M., and Casco, C. (2009). Audio-visual bounce-inducing effect: attention alone does not explain why the discs are bouncing. *J. Exp. Psychol. Hum. Percept. Perform.* 35, 235–243.

Grove, P. M., and Sakurai, K. (2009). Auditory induced bounce perception persists as the probability of a motion reversal is reduced. *Perception* 38, 951–965.

Guttman, S. E., Sekuler, A. B., and Kellman, P. J. (2003). Temporal variations in visual completion: a reflection of spatial limits? *J. Exp. Psychol. Hum. Percept. Perform.* 29, 1211–1227.

Habak, C., and Faubert, J. (2000). Larger effect of aging on the perception of higher-order stimuli. *Vision Res.* 40, 943–950.

Hammett, S. T., Champion, R. A., Thompson, P. G., and Morland, A. B. (2007). Perceptual distortions of speed at low luminance: evidence inconsistent with a bayesian account of speed encoding. *Vision Res.* 47, 564–568.

Horowitz, T. S., Birnkrant, R. S., Fencsik, D. E., Tran, L., and Wolfe, J. M. (2006). How do we track invisible objects? *Psychon. Bull. Rev.* 13, 516–523.

Karplus, K., and Strong, A. (1983). Digital synthesis of plucked-string and drum timbres. *Comp. Music J.* 7, 43–55.

Kawabe, T., and Miura, K. (2006). Effects of the orientation of moving objects on the perception of streaming/bouncing motion displays. *Percept. Psychophys.* 68, 750–758.

Kawachi, Y., and Gyoba, J. (2006). Presentation of a visual nearby moving object alters stream/bounce event perception. *Perception* 35, 1289–1294.

Kawachi, Y., Kawabe, T., and Gyoba, J. (2011). Stream/bounce event perception reveals a temporal limit of motion correspondence based on surface feature over space and time. *Iperception* 2, 428–439.

Kennedy, G. J., Tripathy, S. P., and Barrett, B. T. (2009). Early age-related decline in the effective number of trajectories tracked in adult human vision. *J. Vis.* 9, 21.1–21.10.

Laurienti, P. J., Burdette, J. H., Maldjian, J. A., and Wallace, M. T. (2006). Enhanced multisensory integration in older adults. *Neurobiol. Aging* 27, 1155–1163.

Maguinness, C., Setti, A., Burke, K. E., Kenny, R. A., and Newell, F. N. (2011). The effect of combined sensory and semantic components on audio-visual speech perception in older adults. *Front. Aging Neurosci.* 3:19. doi:10.3389/fnagi.2011.00019

Mahoney, J. R., Li, P. C. C., Oh-Park, M., Verghese, J., and Holtzer, R. (2011). Multisensory integration across the senses in young and old adults. *Brain Res.* 1426, 43–53.

Maniglia, M., Grassi, M., Casco, C., and Campana, G. (2012). The origin of the audiovisual bounce inducing effect: a TMS study. *Neuropsychologia* 50, 1478–1482.

Mathworks. (2012). *MATLAB Signal Processing Toolbox*. Available at: http://www.mathworks.com/products/signal/

Metzger, W. (1934). Beobachtungen über phaenomenale identität (observations on phenomenal identity). *Psychol. Forsch.* 19, 1–60.

Morrell, C. H., Gordon-Salant, S., Pearson, J. D., Brant, L. J., and Fozard, J. L. (1996). Age- and gender-specific reference ranges for hearing level and longitudinal changes in hearing level. *J. Acoust. Soc. Am.* 100, 1949–1967.

Mozolic, J. L., Hugenschmidt, C. E., Peiffer, A. M., and Laurienti, P. J. (2012). "Multisensory integration and aging," in *The Neural Bases of Multisensory Processes*, eds M. Murray, and M. T. Wallace (Boca Raton: CRC Press), 381–395.

Murray, R. F., Sekuler, A. B., and Bennett, P. J. (2001). Time course of amodal completion revealed by a shape discrimination task. *Psychon. Bull. Rev.* 8, 713–720.

Naci, L., Taylor, K. I., Cusack, R., and Tyler, L. K. (2012). Are the senses enough for sense? Early high-level feedback shapes our comprehension of multisensory objects. *Front. Integr. Neurosci.* 6:82. doi:10.3389/fnint.2012.00082

Norman, J. F., Ross, H. E., Hawkes, L. M., and Long, J. R. (2003). Aging and the perception of speed. *Perception* 32, 85–96.

Peiffer, A. M., Mozolic, J. L., Hugenschmidt, C. E., and Laurienti, P. J. (2007). Age-related multisensory enhancement in a simple audiovisual detection task. *Neuroreport* 18, 1077–1081.

Pelli, D. G. (1997). The videotoolbox software for visual psychophysics: transforming numbers into movies. *Spat. Vis.* 10, 437–442.

Pilz, K. S., Bennett, P. J., and Sekuler, A. B. (2010). Effects of aging on biological motion discrimination. *Vision Res.* 50, 211–219.

Piotrowski, A. S., and Jakobson, L. S. (2011). Representational momentum in older adults. *Brain Cogn.* 77, 106–112.

Remijn, G. B., and Ito, H. (2007). Perceptual completion in a dynamic scene: an investigation with an ambiguous motion paradigm. *Vision Res.* 47, 1869–1879.

Remijn, G. B., Ito, H., and Nakajima, Y. (2004). Audiovisual integration: an investigation of the "streaming-bouncing" phenomenon. *J. Physiol. Anthropol. Appl. Human Sci.* 23, 243–247.

Roudaia, E., Bennett, P. J., Sekuler, A. B., and Pilz, K. S. (2010). Spatiotemporal properties of apparent motion perception and aging. *J. Vis.* 10, 5.

Roudaia, E., Farber, L. E., Bennett, P. J., and Sekuler, A. B. (2011). The effects of aging on contour discrimination in clutter. *Vision Res.* 51, 1022–1032.

Sanabria, D., Correa, A., Lupiáñez, J., and Spence, C. (2004). Bouncing or streaming? Exploring the influence of auditory cues on the interpretation of ambiguous visual motion. *Exp. Brain Res.* 157, 537–541.

Scholl, B. J., and Pylyshyn, Z. W. (1999). Tracking multiple items through occlusion: clues to visual objecthood. *Cogn. Psychol.* 38, 259–290.

Schutz, M., and Kubovy, M. (2009). Causality and cross-modal integration. *J. Exp. Psychol. Hum. Percept. Perform.* 35, 1791–1810.

Sekuler, A. B., and Palmer, S. E. (1992). Perception of partly occluded objects: a microgenetic analysis. *J. Exp. Psychol. Gen.* 121, 95–111.

Sekuler, A. B., and Sekuler, R. (1999). Collisions between moving visual targets: what controls alternative ways of seeing an ambiguous display? *Perception* 28, 415–432.

Sekuler, R., McLaughlin, C., and Yotsumoto, Y. (2008). Age-related changes in attentional tracking of multiple moving objects. *Perception* 37, 867–876.

Sekuler, R., Sekuler, A. B., and Lau, R. (1997). Sound alters visual motion perception. *Nature* 385, 308.

Senkowski, D., Talsma, D., Herrmann, C. S., and Woldorff, M. G. (2005). Multisensory processing and oscillatory gamma responses: effects of spatial selective attention. *Exp. Brain Res.* 166, 411–426.

Setti, A., Finnigan, S., Sobolewski, R., McLaren, L., Robertson, I. H., Reilly, R. B., et al. (2011). Audiovisual temporal discrimination is less efficient with aging: an event-related potential study. *Neuroreport* 22, 554–558.

Shimojo, S., Scheier, C., Nijhawan, R., Shams, L., Kimitani, Y., and Watanabe, K. (2001). Beyond perceptual modality: auditory effects on visual perception. *Acoust. Sci. Technol.* 22, 61–67.

Soto-Faraco, S., Kingstone, A., and Spence, C. (2003). Multisensory contributions to the perception of motion. *Neuropsychologia* 41, 1847–1862.

Stephen, J. M., Knoefel, J. E., Adair, J., Hart, B., and Aine, C. J. (2010). Aging-related changes in auditory and visual integration measured with MEG. *Neurosci. Lett.* 484, 76–80.

Talsma, D., Doty, T. J., and Woldorff, M. G. (2007). Selective attention and audiovisual integration: is attending to both modalities a prerequisite for early integration? *Cereb. Cortex* 17, 679–690.

Talsma, D., Senkowski, D., Soto-Faraco, S., and Woldorff, M. G. (2010). The multifaceted interplay between attention and multisensory integration. *Trends Cogn. Sci.* 14, 400–410.

The R Project for Statistical Computing. (2012). Available at: http://www.r-project.org

Trick, L. M., Perl, T., and Sethi, N. (2005). Age-related differences in multiple-object tracking. *J. Gerontol. B Psychol. Sci. Soc. Sci.* 60, P102–P105.

Watanabe, K., and Shimojo, S. (1998). Attentional modulation in perception of visual motion events. *Perception* 27, 1041–1054.

Watanabe, K., and Shimojo, S. (2001). When sound affects vision: effects of auditory grouping on visual motion perception. *Psychol. Sci.* 12, 109–116.

Winn, B., Whitaker, D., Elliott, D. B., and Phillips, N. J. (1994). Factors affecting light-adapted pupil size in normal human subjects. *Invest. Ophthalmol. Vis. Sci.* 35, 1132–1137.

Winneke, A. H., and Phillips, N. A. (2011). Does audiovisual

speech offer a fountain of youth for old ears? An event-related brain potential study of age differences in audiovisual speech perception. *Psychol. Aging* 26, 427–438.

Yuval-Greenberg, S., and Deouell, L. Y. (2007). What you see is not (always) what you hear: induced gamma band responses reflect cross-modal interactions in familiar object recognition. *J. Neurosci.* 27, 1090–1096.

Zhou, F., Wong, V., and Sekuler, R. (2007). Multi-sensory integration of spatio-temporal segmentation cues: one plus one does not always equal two. *Exp. Brain Res.* 180, 641–654.

Zvyagintsev, M., Nikolaev, A. R., Sachs, O., and Mathiak, K. (2011). Early attention modulates perceptual interpretation of multisensory stimuli. *Neuroreport* 22, 586–591.

Conflict of Interest Statement: The authors declare that the research was conducted in the absence of any commercial or financial relationships that could be construed as a potential conflict of interest.

Received: 13 January 2013; accepted: 24 April 2013; published online: 23 May 2013.

Citation: Roudaia E, Sekuler AB, Bennett PJ and Sekuler R (2013) Aging and audio-visual and multi-cue integration in motion. Front. Psychol. ***4****:267. doi: 10.3389/fpsyg.2013.00267*

This article was submitted to Frontiers in Perception Science, a specialty of Frontiers in Psychology.